A Statistical Analysis of Rainfall Seasonality Across South Africa

Sarah Jane Roffe

A Thesis submitted in fulfilment of the academic requirements for the degree of Doctor of Philosophy

School of Geography, Archaeology and Environmental Studies

University of the Witwatersrand, Johannesburg

October 2019

DECLARATION

I declare that this thesis is my own, unaided work, except where otherwise acknowledged. It is being submitted for the Degree of Doctor of Philosophy in Science at the University of the Witwatersrand, Johannesburg. It has not been submitted before for any degree or examination at this or any other university.

_____

Sarah Jane Roffe

_____day of_____20_____at_____

ABSTRACT

Straddling the subtropics and mid-latitudes, the climate of South Africa is influenced by the seasonal migration of the Intertropical Convergence Zone, the Antarctic sea ice extent and associated displacement of the Southern Hemisphere Westerlies. As a consequence of this synoptic mechanism, South Africa has a unique rainfall climatology of summer, winter and year-round rainfall zones (SRZ, WRZ and YRZ). Since the first known publication in 1938, much research has attempted to classify the spatial distribution of these rainfall zones. Different methods with different definitions of rainfall seasonality have been applied, and as such the classification of rainfall seasonality is disputed throughout this literature. Unlike research attempting to classify rainfall seasonality, there has been little research investigating how the seasonal characteristics of rainfall have and may possibly change under anthropogenically induced climate change. Across these studies different seasonality metrics have been applied making spatial and cross-study comparisons difficult. This is problematic for South Africa which has a heavy reliance on the seasonal characteristics of rainfall for activities such as agriculture, water resource management and tourism. To address the aforementioned gaps and issues in literature, this research sought to develop a standard approach to quantify, classify and understand rainfall seasonality and the changes thereof. A consistent dataset of daily rainfall and temperature spanning the period of 1987-2016 from 46 weather stations spread across South Africa was applied to objectively test four seasonality metrics which statistically discriminate between SRZ and WRZ conditions. Linear correlation analysis was applied to the annual seasonality quantities to investigate changes in rainfall seasonality. The results of the classification of rainfall seasonality across the four approaches were not fully consistent, further highlighting the necessity of a standard approach. Due to the different applications of seasonality metrics, two standard approaches were proposed. The first metric quantifies climatological seasonality based on the relationship between temperature and rainfall and returns a seasonality score. This method was suggested as it produced the best classification of rainfall seasonality, with the YRZ extending northwest from the southern coast to the Namibian border, spanning the transition between the SRZ and WRZ. The second metric is based on the timing of accumulation of 10% and 90% of daily rainfall representing boundaries for the wet season and was suggested due the societal relevance of this metric for agricultural seasonality. These standard metrics are important for future climatological research across South Africa and are valuable to facilitate development of more accurate climate model forecasts and projections. Few statistically significant (8%) changes were quantified. Although this was the case, the changes quantified demonstrated much agreement across the seasonality metrics and spatially, and were broadly consistent with literature. For the majority of SRZ locations, an increase in SRZ seasonality with a reduction in the wet season duration due to later commencement was quantified, which is consistent with an expansion of the tropics. The results for the WRZ locations predominantly suggest a decrease in WRZ seasonality and a longer wet season duration which coincided with a reduction in rainfall during many winter months; this has been linked to a poleward migration of the Westerlies. For the YRZ locations along the southern coast, an increase in WRZ seasonality consistent with a reduction in the wet season duration was quantified. These quantified changes in the seasonal characteristics of rainfall have implications for crop yields and water supplies across South Africa and are particularly important for developing adaptation strategies to reduce potentially detrimental consequences of climate change.

ACKNOWLEDGEMENTS

Firstly, I would like to thank my supervisor Dr. Jennifer Fitchett for all the guidance, wisdom and support you provided throughout my PhD. You aided me in producing a thesis that I am truly proud of. You constantly encouraged and challenged me, and in doing so you have helped to develop my knowledge and critical thought as well as improve my writing and research skills which has truly helped me grow as an academic. I have really valued all of our meetings, especially because afterwards work always seemed less daunting. I truly appreciate all your efforts in editing and proofreading my work, particularly during recent months. You also provided me with funding to attend the 2018 South African Geographer's Biennial Academic Conference, and for that I am grateful especially because the feedback from my presentation was so helpful in improving the manuscript of the paper we published. You have been a fantastic supervisor, and I don't think I may ever adequately express my appreciation for all that you have done throughout my PhD.

My co-supervisor, Prof. Christopher Curtis, should also be acknowledged. Thank you for always assisting me, and for editing and proofreading my written work. Your feedback on my written work was always helpful especially where my writing was not clear and easy to understand. You were particularly helpful during the process of preparing the manuscript for the publication we produced with Dr. Fitchett.

I gratefully acknowledge the National Research Foundation for financially supporting this research project under grant number 107742. Without this funding I would not have been able to undertake my PhD.

The Society of South African Geographers must also be acknowledged for financial support to attend the 2018 South African Geographer's biennial Academic Conference. This conference provided invaluable exposure to work being undertaken by South African geographers, and the opportunity to meet and interact with South African Geographers.

I thank and acknowledge the South African Weather Services for providing the observational data records used for this research project.

To my friends in the School of Geography, Archaeology and Environmental Studies. I wish to thank you all for your kindness and support. I would also like to acknowledge the friends I have made from the group of students supervised by Dr. Fitchett. Our group meetings were always great for motivation and they both encouraged and stimulated valuable conversations.

I recruited a number of people to edit and proofread my work. Although there was a lot to read, you were all so willing to assist, and your comments have been so helpful to complete my PhD.

My family (my mom, dad, and sister) need to be thanked. Without all of your support I would not be where I am today.

Finally, to my partner Kyle. It is difficult to thank you for all that you have done. In saying this I would like to thank you for, among others, your continuous support and encouragement, for proofreading and editing my work, for always listening to my MANY thoughts on my project, feeding me when I was hungry and too tired to cook, and for forcing me to go outside, to sleep and to take breaks. I promise to do the same while you complete the rest of your MSc and during your PhD. Additionally, your mom should be thanked for her kindness and support.

TABLE OF CONTENTS

DECLARATION ii
ABSTRACT iii
ACKNOWLEDGEMENTS iv
LIST OF FIGURES ix
LIST OF TABLES xiv
LIST OF GENERAL ACRONYMS xvi
LIST OF STATISTICAL ACRONYMS xvii
LIST OF WEATHER STATION ACRONYMS xviii
LIST OF EQUATIONS xx
1. INTRODUCTION 1
1.1 RATIONALE AND CONTRIBUTION TO EXISTING KNOWLEDGE 4
1.2 STUDY AIM, HYPOTHESES AND OBJECTIVES 7
1.3 STRUCTURE OF THIS THESIS 8
2. LITERATURE REVIEW 10
2.1 INTRODUCTION 10
2.2 CLASSIFYING AND MAPPING RAINFALL SEASONALITY IN SOUTH AFRICA: A REVIEW 11
2.3 RAINFALL SEASONALITY SHIFTS AND PROJECTIONS 29
2.3.1 THE USE OF RAINFALL SEASONALITY METRICS TO QUANTIFY CHANGE AND VARIABILITY GLOBALLY 29
2.3.2 SOUTHERN AFRICA 36
2.3.2.1 THE CASE FOR INTERROGATION OF RAINFALL SEASONALITY SHIFTS DURING THE LATE QUATERNARY: LESSONS FROM PALAEO RECORDS 36
2.3.2.2 DRAWING ON RAINFALL SEASONALITY SHIFTS AND VARIABILTY IN THE CONTEMPORARY RECORD 42
2.3.2.3 RAINFALL SEASONALITY PROJECTIONS 49
2.4 SYNOPSIS: RESEARCH GAPS AND AVENUES FOR FUTURE WORK 53
3. STUDY REGION 55
3.1 INTRODUCTION 55
3.2 THE REPUBLIC OF SOUTH AFRICA 55
3.2.1 DESCRIPTIVE GEOGRAPHY: LOCATION AND TOPOGRAPHY 55
3.2.2 CLIMATE AND WEATHER 56
3.2.3 CONCLUSION 69
4. DATA AND METHODOLOGY 70

4.1 INTRODUCTION 70
4.2. RAINFALL AND TEMPERATURE DATA 70
4.2.1 WEATHER STATION SELECTION 71
4.3 INITIAL DATA ANALYSIS 74
4.3.1 BASIC DESCRIPTIVE STATISTICS AND OUTLIERS OF RAINFALL AND TEMPERATURE 75
4.3.2 TRENDS IN RAINFALL AMOUNT FOR THE PERIOD OF 1987-2016 77
4.4 STATISTICAL APPROACH TO QUANTIFYING RAINFALL SEASONALITY ACROSS SOUTH AFRICA 81
4.4.1 CLUSTERING MONTHLY RAINFALL AND VARIABILITY 81
4.4.2 RELATIONSHIP BETWEEN RAINFALL AND TEMPERATURE 84
4.4.3 ONSET, CESSATION AND LENGTH OF THE WET SEASON 89
4.4.4 ACCUMULATION OF RAINFALL 95
4.5 TIME SERIES ANALYSIS ON RAINFALL SEASONALITY FOR THE PERIOD OF 1987-2016 97
4.5.1 LINEAR SHIFTS 98
4.5.2 CHANGE POINT ANALYSIS 99
4.6 CONCLUSION 102
5. RESULTS 103
5.1 INTRODUCTION 103
5.2 ANNUAL RAINFALL CHARACTERISTICS AND TRENDS 103
5.3 MONTHLY RAINFALL CHARACTERISTICS AND TRENDS 113
5.4 QUANTIFYING AND CLASSIFYING RAINFALL SEASONALITY ACROSS SOUTH AFRICA 135
5.4.1 CLUSTERING MONTHLY RAINFALL AND VARIABILITY 135
5.4.2 SEASONALITY SCORES 141
5.4.3 ONSET AND CESSATION DATES OF THE WET SEASON 155
5.4.4 10% AND 90% DATES OF THE WET SEASON 176
5.5 SHIFTS IN RAINFALL SEASONALITY FOR THE PERIOD OF 1987-2016 195
5.6 SYNOPSIS 222
6. DISCUSSION 224
6.1 INTRODUCTION 224
6.2 ANNUAL AND MONTHLY RAINFALL CHARACTERISTICS ACROSS SOUTH AFRICA 224
6.2.1 ANNUAL RAINFALL TOTALS 224
6.2.2 SEASONALITY: MONTHLY RAINFALL TOTALS 230
6.3 CHARACTERISING AND CLASSIFYING RAINFALL SEASONALITY ACROSS SOUTH AFRICA: TOWARDS QUANTIFYING SPATIAL VARIATIONS 235

6.3.1 TOWARDS A STANDARD APPROACH TO QUANTIFY, CHARACTERISE AND CLASSIFY RAINFALL SEASONALITY ACROSS SOUTHERN AFRICA 254
6.4 SHIFTS IN RAINFALL SEASONALITY ACROSS SOUTH AFRICA 262
6.4.1 TRACKING CHANGES IN THE BOUNDARIES OF THE WRZ SINCE THE LGM 262
6.4.2 CONTEMPORARY CHANGES IN RAINFALL SEASONALITY FOR THE PERIOD OF 1987-2016 267
6.4.2.1 TRENDS TOWARDS SRZ: IMPLICATIONS AND RECOMMENDATIONS 270
6.4.2.2 TRENDS TOWARDS WRZ: IMPLICATIONS AND RECOMMENDATIONS 274
6.4.2.3 TRENDS TOWARDS YRZ: IMPLICATIONS AND RECOMMENDATIONS 278
6.5 LIMITATIONS 287
6.5.1 DATA LIMITATIONS 288
6.5.2 STATISTICAL LIMITATIONS 291
6.6 CONTRIBUTION TO KNOWLEDGE 293
6.7 SYNOPSIS 295
7. CONCLUSION 297
7.1 INTRODUCTION 297
7.2 ACHIEVEMENT OF STUDY AIM AND OBJECTIVES 298
7.3 FUTURE RESEARCH TRAJECTORIES 303
7.4 SYNOPSIS AND SIGNIFICANCE OF THE STUDY FINDINGS 307
REFERENCES 310
APPENDIX A: BAR CHARTS ANNUAL RAINFALL TOTALS 339
APPENDIX B: MONTHLY RAINFALL STATISTICS 343
B.1 JANUARY 343
B.2 FEBRUARY 344
B.3 MARCH 345
B.4 APRIL 346
B.5 MAY 347
B.6 JUNE 348
B.7 JULY 349
B.8 AUGUST 350
B.9 SEPTEMBER 351
B.10 OCTOBER 352
B.11 NOVEMBER 353
B.12 DECEMBER 354

B.13 SUMMARY OF THE CHANGE POINTS DETECTED FOR MONTHLY RAINFALL 355
APPENDIX C: CLUSTER ANALYSIS OF MONTHLY RAINFALL, RAIN DAYS AND RESPECTIVE VARIABILITY 356
C.1: MONTHLY RAINFALL AND VARIABILITY 356
C.2: DECADAL MONTHLY RAINFALL AND VARIABILITY 356
C.3: RAIN DAYS AND VARIABILITY 367
APPENDIX D: ANNUAL SEASONALITY SCORES 371
APPENDIX E: ANNUAL ONSET AND CESSATION DATES, LENGTH OF THE WET SEASON AND NUMBER OF RAIN DAYS 376
APPENDIX F: ANNUAL 10% AND 90% DATES, LENGTH OF THE WET SEASON AND NUMBER OF RAIN DAYS 389
APPENDIX G: INDIVIDUAL WEATHER STATION SEASONALTY SHIFTS AND CHANGE POINTS 402
APPENDIX H: DETAILS ON THE SEASONALITY SCORE SHIFTS 411
APPENDIX I: DETAILS ON THE ONSET AND CESSATION DATE SHIFTS 412
I.1 ONSET DATES 412
I.2 CESSATION DATES 413
APPENDIX J: DETAILS ON THE 10% AND 90% DATE SHIFTS 414
J.1 10% DATES 414
J.2 90% DATES 415

LIST OF FIGURES

Figure 2.1: Flow diagram of selected seasonality metrics, input data and output measurements of seasonality which contribute to describing rainfall seasonality. The percentiles of accumulation represents the approaches of Ilesanmi (1972a, b) and Pryor and Schoof (2008). The start and end dates represent the approaches of Dunning *et al.* (2016) and Stern *et al.* (1982). The daily precipitation concentration period represents the approach of Martin-Vide (2004). The Gini index represents the approach of Rajah *et al.* (2014). The Precipitation Concentration Period and Precipitation Concentration Degree represents the approach of Zhang and Qian (2003). The precipitation concentration index represents the approach of Oliver (1980). The seasonality concentration index represents the approach of Fujita (2008). The seasonality index represents the approach of Walsh and Lawler (1981). The dimensionless seasonality index and relative entropy represents the approach of Feng *et al.* (2013). The vector analysis represents the approach of Markham (1970). The relationship between mean monthly rainfall and mean monthly temperature represents the approach of Thackeray and Fitchett (2016)……30

Figure 2.2: Number of publications from 2000-2019 per continent which have investigated rainfall seasonality shifts using seasonality metrics captured under *Figure 2.1*. Data derived from Google Scholar, Science Direct and Web of Knowledge……31

Figure 2.3: Selected locations (Cowling *et al.*, 1999; Parkington *et al.*, 2000; Lim *et al.*, 2016; Thackeray & Fitchett, 2016; Combrink, 2017; Faith *et al.*, 2019) understood to have been characterised by a predominant WRZ regime during the LGM (24,000-18,000 cal. yr BP). The dark blue boundary represents the region estimated to have been under a WRZ regime during the LGM, with the WRZ LGM boundary shown to have progressively reduced to the estimated contemporary WRZ region. The estimated contemporary WRZ boundary represents the area known to demonstrate at least 75% consensus in the classification of WRZ from previous published maps captured under *Figure 2* of *Section 2.2*……38

Figure 3.1: Map of the study region of South Africa indicating the nine provinces and major cities, topography, the surrounding oceans and their respective ocean currents……56

Figure 3.2: Schematic diagram of the synoptic features which influence weather and climate across South Africa during summer (top) and winter (bottom; After: Tyson & Preston-Whyte, 2000; Hart *et al.*, 2010; Reason & Smart, 2015; Lennard, 2019)……62

Figure 4.1: Map of the SAWS weather stations utilised for this study. These weather stations are labelled using the assigned weather station code in *Table 4.1*……74

Figure 5.1: Mean annual rainfall and coefficient of variation for individual weather stations for the period 1987-2016……104

Figure 5.2: Annual rainfall totals and trend for individual weather stations for the period 1987-2016. *P values* are listed only for statistically significant trends. Green (Brown) trendlines represent increasing (decreasing) trends……107

Figure 5.3: Trends in total annual rainfall for individual weather stations for the period 1987-2016. Shaded symbols represent statistically significant trends at the 5% level……111

Figure 5.4: Annual cycles of rainfall for the period of 1987-2016……115

Figure 5.5: Ordinary kriging interpolation of mean monthly rainfall totals for the period of 1987-2016……121

Figure 5.6: Trends in total monthly rainfall for individual weather stations for the period 1987-2016. Shaded symbols indicate statistically significant trends at the 5% level……125

Figure 5.7: Colour coded dendrogram displaying weather stations (code) in groups 1 to 5 based on agglomerative hierarchical clustering of mean monthly rainfall and monthly CV using Ward's minimum variance algorithm and the squared Euclidean distance……136

Figure 5.8: Spatial distribution of homogeneous rainfall groups 1 to 5, from Figure 5.7, based on agglomerative hierarchical clustering of mean monthly rainfall and monthly CV using Ward's minimum variance algorithm and the squared Euclidean distance……137

Figure 5.9: Boxplots representing the annual cycles rainfall for cluster groups 1 to 5. Circles represent outliers……..138

Figure 5.10: Dendrograms of monthly rainfall for groups 1 to 5 based on mean monthly rainfall and monthly CV using Ward's minimum variance algorithm and the squared Euclidean distance. Brown and green represent the dry and wet seasons months respectively……139

Figure 5.11: Spatial distribution of the SRZ and WRZ based on the wet and dry season timing of groups 1 to 5, represented under *Figure 5.10*……140

Figure 5.12: Relationship between sqrt MMT and sqrt MMR for individual weather stations across South Africa. Red, blue and yellow trendlines represent SRZ, WRZ and YRZ classifications respectively……144

Figure 5.13: Boxplots of the CV for individual weather stations grouped as SRZ (red), WRZ (blue) and YRZ (yellow)……149

Figure 5.14: Ordinary kriging interpolation of the total period seasonality scores for the period 1987-2016……151

Figure 5.15: Spatial distribution of the SRZ, WRZ and YRZ using the total period seasonality scores……153

Figure 5.16: Strength of relationship between sqrt transformed MMR and MMT for individual weather stations for the period 1987-2016……154

Figure 5.17: Boxplots displaying the distribution of mean onset and cessation dates, length of the wet season and number of rain days for individual weather stations grouped as SRZ (red), WRZ (blue) and YRZ (yellow)……157

Figure 5.18: Calendar plot of the mean onset and cessation dates, and length of the wet season for weather stations classified as SRZ. This plot is colour coded according to late and long SRZ. Dark red represents long SRZ and light red represents late SRZ……160

Figure 5.19: Bar graph of mean annual rainfall, length of the wet season and number of rain days for weather stations classified as SRZ……162

Figure 5.20: Calendar plot of the mean onset and cessation dates, and length of the wet season for weather stations classified as WRZ. This plot is colour coded according to early, mid and late WRZ, where dark blue represents late WRZ, light blue represents mid WRZ and very light blue represents early WRZ……163

Figure 5.21: Bar graph of mean annual rainfall, length of the wet season and number of rain days for weather stations classified as WRZ……164

Figure 5.22: Calendar plot of the mean onset and cessation dates, and length of the wet season for weather stations classified as YRZ.....165

Figure 5.23: Bar graph of mean annual rainfall, length of the wet season and number of rain days for weather stations classified as YRZ.....166

Figure 5.24: Boxplots displaying the distribution of CV for the mean onset and cessation dates, length of the wet season and number of rain days for individual weather stations grouped as SRZ (red), WRZ (blue) and YRZ (yellow).....167

Figure 5.25: Ordinary kriging interpolation of the mean onset and cessation dates for the period of 1987-2016.....170

Figure 5.26: Ordinary kriging interpolation of the mean length of the wet season and number of rain days for the period of 1987-2016.....173

Figure 5.27: Spatial distribution of the SRZ, WRZ and YRZ classified using the mean onset and cessation dates. ND represents a weather station where no onset and cessation dates were obtained.....174

Figure 5.28: Spatial distribution of weather stations classified as late and long SRZ, early, mid and late WRZ, and YRZ. ND represents a weather station where no onset and cessation dates were obtained.....175

Figure 5.29: Boxplots displaying the distribution of mean 10% and 90% dates, length of the wet season and number of rain days for individual weather stations grouped as SRZ (red), WRZ (blue) and YRZ (yellow)...179

Figure 5.30: Calendar plot of the mean 10% and 90% dates, and length of the wet season for weather stations classified as SRZ. This plot is colour coded according to late and long SRZ, where dark red represents long SRZ and light red represents late SRZ.....181

Figure 5.31: Bar graph of mean annual rainfall, length of the wet season and number of rain days for weather stations classified as SRZ.....183

Figure 5.32: Calendar plot of the mean 10% and 90% dates, and length of the wet season for weather stations classified as WRZ. This plot is colour coded according to late and long WRZ, where dark blue represents long WRZ and light blue represents late WRZ.....184

Figure 5.33: Bar graph of mean annual rainfall, length of the wet season and number of rain days for weather stations classified as WRZ.....185

Figure 5.34: Calendar plot of the mean 10% and 90% dates, and length of the wet season for weather stations classified as YRZ.....186

Figure 5.35: Bar graph of mean annual rainfall, length of the wet season and number of rain days for weather stations classified as YRZ.....187

Figure 5.36: Boxplots displaying the distribution of CV for the mean 10% and 90% dates, length of the wet season and number of rain days for individual weather stations grouped as SRZ (red), WRZ (blue) and YRZ (yellow).....188

Figure 5.37: Ordinary kriging interpolation of the mean 10% and 90% dates for the period of 1987-2016.....190

Figure 5.38: Ordinary kriging interpolation of the mean length of the wet season and the number of rain days for the period of 1987-2016……193

Figure 5.39: Spatial distribution of the SRZ, WRZ and YRZ classified using the mean 10% and 90% dates….194

Figure 5.40: Spatial distribution of weather stations classified as late and long SRZ, late and long WRZ, and YRZ……195

Figure 5.41: Shifts in the seasonality scores from 1987 to 2016 based on extended regression analysis. Lines with arrows represent individual weather station trends, starting from 1987 and ending at 2016. Specific values for each trend are under *Appendix G and H*. Squares represent change in the seasonality scores of less than or equal to +/-0.02. Only weather stations with significant trends at the 5% level were highlighted, whereby the colour corresponds to the classification of each weather station under *Section 5.4.2*. Pale blue, yellow and red represent WRZ, YRZ and SRZ……197

Figure 5.42: Shifts in the onset dates for the period of 1987-2016 based on extended regression analysis. Lines with arrows represent individual weather station trends which start from 1987 and end at 2016, and these specific values are under *Appendix G and I.1*. Squares represent changes of 2 days or less. Statistically significant trends at the 5% level were highlighted, whereby the colour corresponds to the classification of each weather station under *Section 5.4.3*. Pale red and blue represent SRZ and WRZ split at the autumn and spring equinox dates of 21 March and 23 September. Horizontal dotted lines indicate weather stations where onset dates shifted to the next or previous calendar year……198

Figure 5.43: Shifts in the cessation dates for individual weather stations for the period of 1987-2016 based on extended regression analysis. Lines with arrows represent individual weather station trends which start from 1987 and end at 2016. Specific values for each trend are under *Appendix G and H.2*. Squares represent changes of 2 days or less. Weather stations with statistically significant trends at the 5% level were highlighted, whereby the colour corresponds to the classification of each weather station under *Section 5.4.3*. Pale red and blue represent SRZ and WRZ split at the autumn and spring equinox dates of 21 March and 23 September……199

Figure 5.44: Shifts in the 10% dates for individual weather stations for the period of 1987-2016 based on extended regression analysis. Lines with arrows represent individual weather station trends which start from 1987 and end at 2016. Specific values for each trend are under *Appendix G and J.1*. Squares represent changes of 2 days or less. Weather stations with statistically significant trends at the 5% level were highlighted, whereby the colour corresponds to the classification of each weather station under *Section 5.4.4*. Pale red and blue represent SRZ and WRZ split at the autumn and spring equinox dates of 21 March and 23 September……200

Figure 5.45: Shifts in the 90% dates for individual weather stations for the period of 1987-2016 based on extended regression analysis. Lines with arrows represent individual weather station trends which start from 1987 and end at 2016. Specific values for each trend are under *Appendix G and J.2*. Squares represent changes of 2 days or less. Weather stations with statistically significant trends at the 5% level were highlighted, whereby the colour corresponds to the classification of each weather station under *Section 5.4.4*. Pale red and blue represent SRZ and WRZ split at the autumn and spring equinox dates of 21 March and 23 September……201

Figure 5.46: Probability of change in rainfall seasonality indicators for the period of 1987-2016. The direction as well as probability of change are indicated. Green and brown represent positive and negative trends respectively. The different levels of probability are based on de Luis et al. (2011) and categorised as:

exceptionally likely (p <0.01), extremely likely (p <0.05), very likely (p <0.10) and as likely as not (p >0.10). ND represents where no onset and cessation dates were obtained for a PNO. Considering the maps of the length of the wet season and number of rain days, (O) represents these quantities for the onset and cessation dates while (%) is for the percentile-based approach……203

Figure 5.47: Consensus regarding the direction of rainfall seasonality trends across South Africa based on Table 5.9……213

Figure 6.1: Composite map of the consensus on the spatial distribution of rainfall seasonality zones across South Africa (including Lesotho and Swaziland) captured between the statistical approaches, represented in Figures 5.11, 5.15, 5.27 and 5.39, used for this study……237

Figure 6.2: Composite map on the consensus and dispute on the spatial distribution of rainfall seasonality zones across South Africa (including Lesotho and Swaziland) captured between the statistical approaches used for this study and from previous maps of rainfall seasonality represented in *Figure 2* of the published paper under *Section 2.2* of *Chapter 2 (Literature Review)*……252

Figure 6.3: Estimated spatial distribution of rainfall seasonality across South Africa (including Lesotho and Swaziland)……254

Figure 6.4: Map demonstrating the estimated boundary location of the WRZ during the LGM, based on *Figure 2.3*, and presently, based on *Figure 6.3*. Arrows on the contemporary WRZ boundary represent the progressive shift of this boundary under climate change. The study locations are represented on the basis of the total period seasonality scores presented under *Table 5.2*……264

LIST OF TABLES

Table 4.1: Details regarding location (i.e. province, elevation, latitude and longitude), data availability following data cleaning and code of each SAWS weather station utilised for this study. The code of each weather station has been used in text, and as a label on all maps and some graphs. The Köppen-Geiger climate zone codes are as follows in full: BSh – Arid, Steppe, Hot; BSk – Arid, Steppe, Cold; BWh – arid, desert, hot; BWk – arid, desert, cold; Cfa – temperate, without dry season, hot summer; CSa – temperate, dry summer, hot summer; CSb – temperate, dry summer, warm summer; CWa – temperate, dry winter, hot summer; Cwb – temperate, dry winter, warm summer.....73

Table 4.2: Details of the months omitted from analyses for this and following sections.....78

Table 4.3: Details of the months omitted from analyses of the relationship between temperature and rainfall.....86

Table 4.4: Seasonality score class limits for classification of SRZ, YRZ and WRZ.....89

Table 4.5: Onset and cessation date criteria used in agroclimatology research across Africa. These criteria are colour coded, where green represents onset criteria and brown represents cessation criteria.....90

Table 4.6: Criteria used to determine onset and cessation dates of the wet season.....92

Table 5.1: Summary statistics of the annual rainfall totals for the period 1987-2016. Statistically significant trends are indicated by an asterisk (*).....105

Table 5.2: Total period seasonality scores and rainfall zone classification for individual weather stations for the period 1987-2016. A *p value* below 0.05 is statistically significant and is indicated using an asterisk (*). Particularly strong correlations, between sqrt MMR and sqrt MMT, equal to and greater than 0.7 are indicated using a double asterisk. Rainfall zone classifications are highlighted, where red indicates SRZ, blue indicates WRZ and yellow indicates YRZ.....142

Table 5.3: Resulting *r* and *p values* from correlation analyses between total period seasonality scores, latitude, longitude, elevation, strength of relationship and CV. Statistically significant *p values* are denoted using an asterisk (*). Correlations which were not tested are denoted using a hyphen (-).....151

Table 5.4: Mean onset and cessation dates, length of the wet season and number of rain days for individual weather stations for the period 1987-2016. Rainfall zone classifications are highlighted, where red, blue and yellow represent SRZ, WRZ and YRZ respectively. Weather stations which are not highlighted were not classified and captured as ND.....156

Table 5.5: Resulting *r* and *p values* from correlation analyses between mean onset and cessation dates, length of the wet season, number of rain days, latitude, longitude and elevation. Statistically significant *p values* are denoted using an asterisk (*).....171

Table 5.6: Mean 10% and 90% dates, length of the wet season and number of rain days for each individual weather station for the period 1987-2016. Rainfall zone classifications are highlighted, where red, blue and yellow represent classifications of SRZ, WRZ and YRZ respectively.....177

Table 5.7: Resulting *r* and *p values* from correlation analyses between mean 10% and 90% dates, length of the wet season, number of rain days, latitude, longitude and elevation. Statistically significant *p values* are denoted using an asterisk (*).....191

Table 5.8: Stability of the rainfall regimes for each weather station, displaying the number of years classified as the mean classification for the period of 1987-2016, and the percentage stability quantified considering the number of individual years classified as the mean rainfall zone as well as the total number of years classified……209

Table 5.9: Description of the rainfall seasonality shifts across the seasonality scores, onset and cessation dates as well as the wet season length (wet season change description), and the 10% and 90% dates and the length of the wet season (wet season change description). The direction of trends towards a rainfall zone are used to describe these changes. This is highlighted, where red represents a trend towards SRZ conditions, blue towards WRZ conditions and yellow towards YRZ conditions. Statistically significant changes at the 0.05 level are denoted using an asterisk (*) and corresponds to *Figure 5.41-5.45*. The specific details for this table are presented under *Appendix G, H, I, J*……210

Table 6.1: Location specific mean rainfall seasonality classification according to each seasonality metric for the period of 1987-2016. Rainfall zone classifications are highlighted, where red indicates SRZ, blue indicates WRZ and yellow indicates YRZ classifications respectively……238

LIST OF GENERAL ACRONYMS

cal. yr BP: calibrated years before present

CH: Continental High-pressure Cell

DPCI: Daily Precipitation Concentration Index

DSI: Dimensionless Seasonality Index

ENSO: El Niño Southern Oscillation

GCM: Global Circulation Model

IPCC: Intergovernmental Panel for Climate Change

ITCZ: Intertropical Convergence Zone

LGM: Last Glacial Maximum

m.asl: meters above sea level

PCI: Precipitation Concentration Index

RCM: Regional Climate Model

RE: Relative Entropy

SI: Seasonality Index

SIA: South Indian Anticyclone

SAA: South Atlantic Anticyclone

SAM: Southern Annular Mode

SAWB: South African Weather Bureau

SAWS: South African Weather Service

SST: Sea Surface Temperature

SRZ: Summer Rainfall Zone

TTT: Tropical-temperate Trough

WMO: World Meteorological Organization

WRZ: Winter Rainfall Zone

YRZ: Year-round Rainfall Zone

LIST OF STATISTICAL ACRONYMS

CUSUM: Cumulative Sum

CV: Coefficient of Variation

IQR: Interquartile Range

MMT/MMR: Mean Monthly Temperature/Rainfall

ND: No Date

Sqrt: Square-root

$T_{min/max}$: Daily Minimum/Maximum Temperature

LIST OF WEATHER STATION ACRONYMS

ANP: Aliwal-North Plaatkop

BET: Bethal

BEW: Bethlehem Wo (Wo represents a weather station at an airport)

BLW: Bloemfontein Wo

CAG: Cape Agulhas

CED: Cedara

CMU: Cradock-Mun

CTW: Cape Town Wo

CWO: Calvinia Wo

DAW: De Aar Wo

ELW: East London Wo

FRA: Fraserburg

FTN: Frankfort-TNK

JIW: Johannesburg Wo

KWO: Kimberley Wo

LAD: Ladysmith

LAW: Langebaanweg AWS

LEP: Lephalale

MAN: Mandini

MAR: Mara

MRC: Makatini Research Centre

MWO: Mafikeng Wo

NEL: Nelspruit

OTT: Ottosdal

OUD: Oudtshoorn

PAD: Paddock

PEW: Port Elizabeth Wo

PNO: Port Nolloth

POF: Pofadder

PRI: Prieska

PWO: Polokwane Wo

RIV: Riversdale

ROB: Robertson

SHA: Shaleburn

SKU: Skukuza

SUT: Sutherland

SWO: Springbok Wo

TRI: Twee Rivieren

UMW: Umtata Wo

UPW: Upington Wo

VRE: Vredendal

VRY: Vryburg

VWY: Vanwyksvlei

WEL: Welkom

WIL: Willowmore

WTO: Warmbad Towoomba

LIST OF EQUATIONS

Equation 1: Arithmetic Mean

Equation 2: Coefficient of Variation

Equation 3: Median

Equation 4: Quartile One

Equation 5: Quartile Three

Equation 6: Interquartile Range

Equation 7: Upper Data Limit

Equation 8: Lower Data Limit

Equation 9: Pearson Correlation Coefficient

Equation 10: Least Square Linear Regression Line

Equation 11: *Y* Intercept of Least Square Linear Regression Line

Equation 12: Coefficient of *X* for Least Square Linear Regression Line

Equation 13: Ward's Minimum Variance Algorithm

Equation 14: Ordinary Kriging Estimator

Equation 15: Semivariogram Function

Equation 16: Length of Wet Season with Onset and Cessation Dates Following a Calendar Year

Equation 17: Length of Wet Season with Onset and Cessation Dates Not Following a Calendar Year

Equation 18: Cumulative Sum Change Point

Equation 19: Magnitude of Cumulative Sum Change Point

Equation 20: Confidence Level of Cumulative Sum Change Point

Equation 21: Pettitt Test Change Point

Equation 22: Magnitude of Pettitt Test Change Point

Equation 23: Confidence Level of Pettitt Test Change Point

1. INTRODUCTION

South Africa has a unique geographical position at the transition between the subtropical and mid-latitude climatic belts, and as a result of this location the country is characterised by both summer and winter rainfall zones (SRZ and WRZ; Fitchett & Bamford, 2017). It is well-understood that this dichotomy in seasonality is driven by the seasonal migration of the Intertropical Convergence Zone (ITCZ), the Antarctic sea ice extent and the resultant displacement of the Southern Hemisphere Westerlies (Chase *et al.*, 2017; Lennard, 2019). The synoptic climatology behind these rainfall zones is well-understood (Taljaard, 1996; Tyson & Preston-Whyte, 2000; Lennard, 2019). It is well-known that the majority of the country receives primarily convective summer rainfall mainly during the months of October to March, and this is predominantly driven by the southward displacement of the ITCZ and the tropical easterly winds (Favre *et al.*, 2016). During the Southern Hemisphere winter months, the northward displacement of the Westerlies and associated mid-latitude cyclones are primarily responsible for winter rainfall mainly during the months of April to September (Favre *et al.*, 2016). Along the southern coast rainfall is meteorologically complex and is known to show no seasonal structure, with rainfall occurring throughout the year from numerous summer and winter synoptic rain-bearing circulation systems (Engelbrecht *et al.*, 2015). The timing of rainfall across South Africa is particularly important as it dictates activities such as agriculture (Tadross *et al.*, 2009), and tourism (Fitchett *et al.*, 2017a), both of which are important activities contributing to the Gross Domestic Product of South Africa (Statistics South Africa, 2019). Although the timing of rainfall and the synoptic rain-bearing features behind rainfall are well-understood, there is much dispute in quantifying and classifying the rainfall seasonality across South Africa.

Rainfall seasonality is a concept that describes timing, duration and magnitude of wet and dry seasons (Feng *et al.*, 2013). Rainfall seasonality is not only limited to describing these characteristics of the wet and dry season and as such it is considered to be a complex concept as it can be described in many ways (e.g. Dunning *et al.*, 2016; Deng *et al.*, 2019), and it may also include additional metrics, for instance quantifying the length of wet and dry spells (Dunning, 2018). The rainfall seasonality of a location can be both qualitatively and quantitatively defined

(Walsh & Lawler, 1981). A qualitative description of rainfall seasonality may be through the describing the annual cycles of rainfall through quantifying mean monthly rainfall amount across a calendar year (e.g. SAWB, 1957 Landman *et al.*, 2017). In attempting to quantitatively define rainfall seasonality, a plethora of metrics have been proposed, such as analyses of arrival and end dates of wet/dry seasons (e.g. Ileshamni, 1972a; Liebmann *et al.*, 2012; Dunning *et al.*, 2016), precipitation concentration index (PCI; e.g. Oliver, 1980), seasonality index (SI; e.g. Walsh & Lawler, 1981), dimensionless seasonality index and relative entropy (DSI and RE; e.g. Feng *et al.*, 2013), and harmonic analysis (e.g. Schumann & Hofmeyr, 1938), among others. Over South Africa, a number of these metrics, with varying levels of accuracy and usability, have been used to quantify and classify rainfall seasonality since 1938. Across these analyses, it is agreed that the seasonality of rainfall across South Africa is considerably complex particularly due to its latitudinal location in the subtropical and mid-latitude climatic belts (Taljaard, 1996; Chase & Meadows, 2007). It is also agreed that there are three distinct rainfall zones with the SRZ spanning much of the interior and east coast, the WRZ across the southwestern Cape and western coast, and the year-round rainfall zone (YRZ) along the southern coast. However, across different mapped outcomes, the spatial distribution of the classification rainfall seasonality is considerably disputed (e.g. Taljaard & Steyn, 1991; Carr *et al.*, 2006; Schulze & Maharaj, 2007; Cramer & Hoffman, 2015).

As a result of the latitudinal location of South Africa and the resulting complexity of rainfall regimes, it may be suggested that the country is a key location in which to investigate rainfall seasonality (Fitchett & Bamford, 2017). In considering the investigation of rainfall seasonality, it is important to note that similar to all climatic elements it is subject to change and year to year variability (Feng *et al.*, 2013). Globally, numerous studies have highlighted that rainfall seasonality has changed under anthropogenically induced climate change (e.g. Sumner *et al.*, 2001; Pryor & Schoof, 2009; de Luis *et al.*, 2011; Feng *et al.*, 2013; Raziei, 2017; Deng *et al.*, 2019; Sarricolea *et al.*, 2019). It is apparent that many studies exploring change in the seasonality of rainfall across southern Africa have investigated this over seasonal scales (e.g. Hoerling *et al.*, 2006; Thomas *et al.*, 2007; Nel, 2009; Shongwe *et al.*, 2009; Mazvimavi, 2010; MacKellar *et al.*, 2014; Davies *et al.*, 2016; du Plessis & Scholms, 2017; MacFayden *et al.*, 2018). From these investigations it would appear that there is an assumption that changes in rainfall seasonality may be understood through

changing seasonal rainfall amounts (Dunning *et al.*, 2018). Shongwe *et al.* (2009), as an example, identified that a decline in spring (September to November) rainfall totals is associated with a delay in onset of the wet season. Such an assumption is problematic as it disregards the complexity of what rainfall seasonality entails. Certainly, the importance of understanding changes in seasonal rainfall amount are clear both for academic and societal purposes, however, rainfall characteristics may change without necessarily being reflected in changes in seasonal rainfall totals (Pryor & Schoof, 2008). For instance, changes only in the timing of wet season arrival and end dates may not affect calendar season totals or even annual rainfall totals as changes in the wet season timing may in turn be balanced by changes in the intensity or distribution of daily rainfall during that season. Additionally, it has been demonstrated by Van Der Walt and Fitchett (Under Review) that temperature seasonality across South Africa does not follow the strict seasonal brackets which have been typically applied to climate studies (i.e. Summer as December to January, Autumn as February to May, Winter as June to August and Spring as September to November). Moreover, much late Quaternary palaeoclimatological research has highlighted significant shifts in rainfall seasonality zones across southern Africa since the Last Glacial Maximum (LGM; e.g. Chase & Meadows, 2007; Thackeray & Fitchett, 2016; Fitchett & Bamford, 2017; Faith *et al.*, 2018). As a result, under contemporary climate change, which extends the trends of warming since the LGM at a more rapid rate, progressive changes in rainfall seasonality are likely to have occurred (Chase & Meadows, 2007;). Changes in the frequency of key winter and summer rain-bearing synoptic circulation systems have also been detected (Lennard & Hegerl, 2015), and as a result it is very likely that rainfall seasonality across South Africa has changed.

Arguably, changes and variability in the characteristics of rainfall which pertain to the seasonality of rainfall are of more importance for investigations than changes in rainfall amount (Raziei, 2017). For example, information on changes in and variability of the timing and duration of the wet season may inform annual decisions on crop planting dates and the selection of crop types (Tadross *et al.*, 2009), and this may also inform annual water management decisions on when to optimise water storage (Kahinda *et al.*, 2008). In fact, changes in rainfall seasonality have important implications on a number of climate sensitive activities across southern Africa such as conservation (Cramer & Hoffman, 2015; van Wilgen *et al.*, 2016), forestry (Borchert, 1998, Suepa

et al., 2016), health (Briët *et al.*, 2008a, b), and land use planning (Evrard *et al.*, 2010), to name a few. Despite the obvious importance of understanding how rainfall seasonality has changed, this has rarely been analysed using observational records across southern Africa (e.g. Reason *et al.*, 2005; Tadross *et al.*, 2009; van Wilgen *et al.*, 2016; Botai *et al.*, 2018).

To this end, this research project is focused on quantifying rainfall seasonality across South Africa using a number of different methods adopted from literature, where the methods selected are known to be able to differentiate between summer and winter rainfall (Thackeray & Fitchett, 2016). The purpose here is to objectively assess these approaches in the ability to quantify and classify rainfall seasonality across South Africa, to determine a standard climatological seasonality approach. Additionally, this research is also focused on investigating, for the first time, how rainfall seasonality has changed across the full area of South Africa. The specific aim and objectives of this research project are captured later under *Section 1.2*.

1.1 RATIONALE AND CONTRIBUTION TO EXISTING KNOWLEDGE

If temperatures continue to increase at the current rate, the most recent Intergovernmental Panel for Climate Change (IPCC) special report projects, with high confidence, that global temperatures are likely to increase in the order of 1.5°C between 2030 and 2052 (IPCC, 2018). In response to anthropogenically induced climate warming during the 21st century it is expected that the global precipitation field will be altered, although not uniformly (IPCC, 2013, 2018). By the end of the 21st century, under medium to high emission scenarios most global circulation model (GCM) projections generally agree on simulations of rainfall reductions in subtropical arid and semi-arid regions and increased rainfall in equatorial and high-latitude regions (IPCC, 2013, 2018). In particular, this points to southern Africa as being vulnerable to future rainfall reductions, where the most recent IPCC special report highlights southern Africa as a climate change 'hotspot' even under low mitigation scenarios (IPCC, 2018). Regional climate models (RCM), which afford greater detail, project reductions in mean annual rainfall across most parts of southern Africa, where statistically significant reductions in seasonal rainfall amounts have also been projected for some regions (Englebrecht *et al.*, 2009; SAWS, 2017). From the numerous projections of seasonal rainfall amount and characteristics for South Africa there is much evidence which links shifts in summer

and winter rain-bearing synoptic features to an expansion of the tropics as well as a poleward shift of the Southern Hemisphere Westerlies (e.g. Christensen *et al.*, 2007; Engelbrecht *et al.*, 2009; Mahlalela *et al.*, 2018; Sousa *et al.*, 2018). As a result there is much concern surrounding the implications of these changes for the rainfall regimes across South Africa (Engelbrecht *et al.*, 2009). For the WRZ there is much evidence that there may be an increased incidence of drought (e.g. Engelbrecht *et al.*, 2009; Mahlalela *et al.*, 2018; Sousa *et al.*, 2018; Burls *et al.*, 2019), whereas for the SRZ much evidence indicates that this may result in increased uncertainty surrounding the arrival of the first rains and subsequently shorter wet seasons (e.g. Engelbrecht *et al.*, 2009; Shongwe *et al.*, 2009; Dunning *et al.*, 2018).

With such dire rainfall projections, southern Africa as a region with a low adaptive capacity which depends highly on the seasonal characteristics of rainfall is considerably vulnerable to potential future changes and variability in rainfall seasonality (Ziervogel *et al.*, 2014). Indeed, a large number of southern Africans are dependent on the seasonal characteristics of rainfall for crop sowing, irrigation and yields, the replenishment of water supplies for drinking and domestic use, and for renewable hydroelectric energy generation (Mukheibir, 2007; Tadross *et al.*, 2009; Moeletsi *et al.*, 2011; Botai *et al.*, 2017). Beyond this, the seasonality of rainfall over southern Africa has implications for health and conservation management decisions, among others, as the occurrence of malaria is somewhat related to the timing of rainfall (Craig *et al.*, 2004; Briët *et al.*, 2008a, b), and the timing of wet and dry seasons largely determines the timing of fire occurrence (Kraaij *et al.*, 2018). Not only are such sectors and activities vulnerable to future changes and variability in rainfall seasonality, it may be argued that the region of southern Africa has already felt such affects. For example, farmers near Beaufort West in the Western Cape have noted changes in the timing of rainfall where it is reported that in the past rainfall fell between February and May and currently it is reported to fall between September and November (Harrison & Petersen, 2017). It is surprising that there have been few investigations exploring changes in rainfall seasonality across southern Africa. Studies which have been conducted across southern Africa investigating contemporary seasonality changes have typically only been over relatively small spatial scales (e.g.. Reason *et al.*, 2005; Tadross *et al.*, 2005a; 2009; Nel, 2009; Moeletsi *et al.*, 2011; Le Roux, 2015; Mupangwa *et al.*, 2015; Tongwane *et al.*, 2015; van Wilgen *et al.*, 2016) or over time frames

shorter than 30 years (e.g.. Botai *et al.*, 2018). These studies have also used different seasonality metrics, and this makes spatial and cross-study comparisons particularly difficult.

In order to address these issues of comparability, this research aims to determine a standard approach to quantify rainfall seasonality across southern Africa. Not only is a standard metric important for rainfall seasonality, standard metrics have shown importance for quantifying the duration, frequency, intensity and severity of droughts (Botai *et al.*, 2016, 2017), quantifying climate suitability for tourism (Fitchett *et al.*, 2017a) and quantifying vegetation health and productivity (Xulu *et al.*, 2018). Establishing a standard metric to quantify rainfall seasonality for southern Africa which may be applied into future research across the region provides a basis for which to improve the capacity to plan, manage, and adapt to changing in rainfall regimes. From a scientific perspective a standard metric is important to provide information, which is comparable, on the rates of seasonality change, the patterns of variability in seasonal rainfall characteristics, and the drivers and mechanisms of change and variability in rainfall seasonality (Dunning *et al.*, 2016). Since there are few published investigations on rainfall seasonality changes across southern Africa, it can be argued that the development of a standard approach now is at an imperative and key time for the future of climatological research across the region.

Before changes in rainfall characteristics can be investigated, an understanding of the seasonality of rainfall experienced at the ground is important (Herrmann & Mohr, 2011). Since the classification of rainfall seasonality across southern Africa is disputed (Roffe *et al.*, 2019), a standard approach may address this issue as classifications across different studies may then be comparable, avoiding confusion. Thus, this research attempts to address the classification issue by testing statistical approaches to determine a standard climatological seasonality approach as well as activity specific approaches which may be used for large scale classification.

There is plausibly much research which may follow on from this study, where this will be discussed later under *Chapter 7 (Conclusion)*. This is argued here because the standard approach which will be developed in this research project, and later published, offers the potential for much research which may involve new locations and even longer time frames. This in part highlights the

contribution and importance of this research project to climatological knowledge across South Africa, and broadly southern Africa, for both academic and societal purposes.

The innovation of this work surrounds a number of contributions to South African climatological research. Firstly, this is through application of seasonality metrics which are for the first time applied across the full area of South Africa. Secondly, assessing these metrics on the basis of relative value to determine a standard statistical method which may direct future research is a contribution to an improved understanding of rainfall seasonality. Thirdly, seasonality changes have rarely been investigated across South Africa, therefore the contribution is that seasonality changes are explored considering the full area of South Africa for the first time. Finally, the multi-method approach adopted is methodological contribution, as to date contemporary seasonality and the changes thereof have not been investigated this manner.

1.2 STUDY AIM, HYPOTHESES AND OBJECTIVES

To contribute knowledge to the aforementioned gaps in literature, the primary aim of this PhD is to statistically quantify rainfall seasonality and the changes thereof across South Africa. This work is undertaken using daily rainfall and temperature readings from 46 weather stations for the period of 1987-2016. In addressing the primary aim of the study, the hypotheses are that:

1. There is a statistical method that can accurately characterise and classify rainfall seasonality across South Africa;
2. Rainfall seasonality across South Africa has changed during 1987-2016.

To interrogate these hypotheses and to address the aim of this research, the specific objectives of this project are:

1. To investigate the spatiotemporal patterns of rainfall amount for the selection of 46 weather stations over an annual and a monthly scale for the period of 1987-2016;
2. To develop a statistical approach to accurately quantify, characterise and classify the climatological rainfall seasonality of the selection of 46 weather stations using methods, with known application across South Africa, from a diverse range of scientific fields including:

a. Cluster analysis of mean monthly rainfall and variability (Climatology);
b. The relationship between mean monthly temperature and rainfall (Palaeoclimatology);
c. Onset and cessation dates of the wet season (Agroclimatology);
d. Accumulation of minimum (10%) and maximum (90%) rainfall amount (Agroclimatology);

3. To interrogate and understand the contemporary rainfall seasonality characteristics for the selection of weather stations using the statistical approach developed under objective 2;
4. To quantify changes in rainfall seasonality over the period of 1987-2016 for the 46 weather stations.

1.3 STRUCTURE OF THIS THESIS

This thesis has been divided into seven chapters which are structured as follows:

This introductory chapter is followed by the literature review chapter (*Chapter 2*) which is presented in two parts. Part one is presented as a published paper, with no modifications, in the South African Geographical Journal, which focuses on reviewing both the classifications of rainfall seasonality across South Africa as well as the broad range of methodologies used. Part two returns to thesis form and explores key literature investigating rainfall seasonality changes globally as well as across southern Africa. The section covering the current knowledge on rainfall seasonality changes across southern Africa explores this topic through a review of the palaeoclimatology, contemporary climatology and climate modelling knowledge surrounding the research topic. The final section of this literature review covers a synthesis of the literature presented in this chapter by highlighting the existing scientific knowledge to which this study will contribute.

The study site chapter (*Chapter 3*) is presented next. This chapter is aimed at providing a reader with a background on the Republic of South Africa, the study region. In this chapter focus is placed on providing a description of the climate, where specific emphasis is placed on the rainfall

characteristics including, among others, a description on the synoptics, topography and surrounding oceans.

Next, the data and methodology chapter (*Chapter 4*) is presented. The process for the selection of the study weather stations is firstly covered. This is followed by an outline of the methodological procedures undertaken which includes the processes of data cleaning, understanding the general rainfall characteristics, developing a statistical approach and quantifying changes in rainfall seasonality.

The results chapter (*Chapter 5*) which follows presents the results of the annual and monthly rainfall characteristics, the statistical approaches used to quantify rainfall seasonality, and the changes in rainfall seasonality for the study period.

The discussion chapter (*Chapter 6*) explores the results and interpretations in the context of both the aim and objectives presented in this introduction chapter as well as previous literature. This chapter focuses on the development of a standard approach to quantify rainfall seasonality following on from the results of each statistical approach. This is followed by a discussion on the changes in rainfall seasonality and some possible implications thereof. This chapter also presents an overview of the main limitations of this study, and the contribution of the research findings to knowledge on climatology across South Africa.

The conclusion (*Chapter 7*) is the final chapter presented. This chapter reflects on the extent to which the study aim and objectives have been achieved. This chapter also discusses possible avenues for future research following on from this research project. Finally, this chapter reflects on the key findings of this study as well as the significance of these.

2. LITERATURE REVIEW

2.1 INTRODUCTION

Southern Africa occupies a key position within the tropical, subtropical and temperate climate belts, and at the intersection between the Atlantic and Indian Oceans (Fitchett & Bamford, 2017). As a result of this location, the subcontinent hosts a diverse range of rainfall regimes, namely summer, winter and year-round rainfall regimes, and is highly sensitive to perturbations in the Earth's climate system both at regional and global scales (Chase & Meadows, 2007). Using a range of seasonality metrics, there have been numerous attempts to classify rainfall seasonality across South Africa to understand the spatial distribution of these rainfall regimes (e.g. Schumann & Hofmeyr, 1938; Cooke, 1946; Taljaard & Steyn, 1991; Herrmann & Mohr, 2011; Liebmann *et al.*, 2012; Botai *et al.*, 2018). It is well-known that spatially and temporally these rainfall zones have shifted as a result of changes undergone in synoptic-scale atmospheric circulation (Lennard & Hegerl, 2015), where seasonality shifts have been most widely documented within palaeoclimatological work across the region (Fitchett & Bamford, 2017). Notably, much research has been conducted to further understand the synoptic-scale atmospheric circulation systems responsible for rainfall and the changes in as well as variability thereof across or within areas of the SRZ (e.g. Crétat *et al.*, 2012; Pohl *et al.*, 2018), WRZ (e.g. Mahlalela *et al.*, 2018; Sousa *et al.*, 2018) and YRZ (e.g. Engelbrecht *et al.*, 2015; Engelbrecht & Landman, 2016). However, this interest has rarely translated into active research exploring changes in rainfall seasonality within the contemporary record of South Africa (e.g. Tadross *et al.*, 2009; MacKellar *et al.*, 2014; Botai *et al.*, 2018). Furthermore, compared with the Northern Hemisphere where much research exists (e.g. Pryor & Schoof, 2008; Elagib, 2011; Cortesi *et al.*, 2012; Feng *et al.*, 2013; Raziei, 2017; Sarricolea *et al.*, 2019; Zhang *et al.*, 2019), there is a limited understanding on how rainfall seasonality has and may potentially change across southern Africa.

To this end, this literature review chapter explores existing literature surrounding rainfall seasonality both globally and for southern Africa. This literature review is presented in two parts. Part one is presented as a peer-reviewed journal article, with no modifications as published in the South African Geographical Journal (Volume: 101; Issue: 2; Page numbers: 158-174), investigating previous attempts at classifying rainfall seasonality across South Africa, where focus was placed

on reviewing rainfall seasonality classifications and the methodologies used. Part two is in written form and is focused on research regarding rainfall seasonality shifts both globally and across southern Africa. Firstly, this section covers literature regarding the use of rainfall seasonality metrics globally (i.e. excluding southern Africa) with a specific focus on studies exploring change and variability. Next, focus is placed on southern Africa. Acknowledging that there is limited research regarding contemporary rainfall seasonality shifts, the first section covers key literature regarding the methods applied to investigate palaeo rainfall seasonality shifts. Following this, literature regarding shifts and variability in contemporary rainfall seasonality is explored. Under this section, variability and change in rainfall amount is also considered as contemporary rainfall seasonality shifts may also be understood through an understanding of the modifications in rainfall amount. This chapter then explores rainfall amount and seasonality projections. Finally, this chapter concludes by highlighting the research gaps and avenues for future research, which this project aims to contribute knowledge to.

2.2 CLASSIFYING AND MAPPING RAINFALL SEASONALITY IN SOUTH AFRICA: A REVIEW

This section includes an authored paper with no modifications. The details of this publication, including the citation, impact factor, and contribution of each author, are below:

Roffe, S.J., Fitchett, J.M. and Curtis, C.J. (2019) Classifying and mapping rainfall seasonality in South Africa: a review. *South African Geographic Journal, 101*(2): 158-174. DOI: 10.1080/03736245.2019.1573151. Impact factor for 2017: 1.180.

Fitchett J.M (20% contribution) conceptualised the scope of this paper. Roffe S.J (75% contribution) collected, digitised and georeferenced historic maps to produce the map in text. Roffe S.J collated the reviewed research and led the writing of the manuscript, with input from both Fitchett J.M and Curtis C.J (5% contribution) and with valuable contributions from the anonymous reviewers.

SOUTH AFRICAN GEOGRAPHICAL JOURNAL
2019, VOL. 101, NO. 2, 158–174
https://doi.org/10.1080/03736245.2019.1573151

Routledge
Taylor & Francis Group

Check for updates

Classifying and mapping rainfall seasonality in South Africa: a review

S.J. Roffe, J.M. Fitchett and C.J. Curtis

School of Geography, Archaeology and Environmental Studies, University of the Witwatersrand, Johannesburg, South Africa

ABSTRACT

Across South Africa, many activities warrant consistent and predictable rainfall patterns which can be achieved from classification of rainfall seasonality into homogeneous zones. Since the first seasonality map for South Africa which was published in 1938, attempts to classify and map rainfall seasonality for the region has proliferates, with many different approaches adopted. Currently, 59 published maps depicting rainfall seasonality across South Africa are known. Although the dichotomy between the summer and winter rainfall zones is well-reported, classification and mapping of the seasonal rainfall zones remains somewhat arbitrary and relatively inconsistent amongst authors. Amongst these maps, there is a broad consensus that three distinct regions with a relatively homogenous seasonal distribution of rainfall exist, known as: summer, winter and year-round rainfall zones. Much of the country has been classified with at least 75% spatial agreement, while classification for the remainder of the country remains rather disputed. Available classification approaches were interrogated, and it was demonstrated that each approach is associated with limitations affecting the accuracy of these maps. We suggest a rigorously assessed approach, or a set of approaches should be used to classify rainfall zones which may be important in further understanding rainfall seasonality across South Africa.

ARTICLE HISTORY
Received 24 August 2018
Accepted 20 December 2018

KEYWORDS
Rainfall zone classification; winter rainfall zone; summer rainfall zone; year-round rainfall zone; climatology; integrated mapping

Introduction

The variety of rainfall regimes across South Africa complicates the classification of rainfall seasonality. Across South Africa, three rainfall seasonality zones are reported to exist and in literature are termed winter rainfall zone (WRZ), summer rainfall zone (SRZ) and year-round rainfall zone (YRZ) (Tyson & Preston-Whyte, 2000). These rainfall zones exist as a result of the latitudinal location of South Africa (Tyson & Preston-Whyte, 2000), which is between 22° and 34°S, at the intersection between the tropical, subtropical and temperate atmospheric pressure systems (Braun, Bar-Matthews, Ayalon, Zilberman, & Matthews, 2017). The WRZ located in the south-western Cape region receives predominantly frontal induced rainfall, driven by westerly derived mid-latitude cyclones, during April to September (Philippon, Rouault, Richard, & Favre, 2012). The SRZ receives primarily convective rainfall during October to March

CONTACT J.M. Fitchett Jennifer.Fitchett@wits.ac.za School of Geography, Archaeology and Environmental Studies, University of the Witwatersrand, Johannesburg 2000, South Africa

© 2019 The Society of South African Geographers

and is located across the interior and eastern parts of the country (Crétat et al., 2012). The YRZ receives rainfall from both summer and winter rainfall systems and is understood to exist along the southern coast (Engelbrecht, Landman, Englbrecht, & Malherbe, 2015). Across the YRZ, there is no pronounced seasonality and rainfall occurs throughout the year, with small peaks during April and September (Engelbrecht & Landman, 2016). Rainfall seasonality across South Africa is well-documented climatologically, and the general area of each rainfall zone is well-known.

South Africa, as a relatively arid country with an uneven spatial distribution of rainfall and two-thirds of the country receiving less than 500 mm of annual rainfall (King, Mitchell, & Pienaar, 2011), requires accurate representation of rainfall zones experienced on the ground. Such information is invaluable for activities such as rain-fed agriculture and sustainable water resource management across the country. There have been many attempts to identify temporally and spatially homogeneous rainfall zones using a number of rainfall seasonality classifications. Amongst maps on rainfall seasonality, there is little consensus on the position of the geographical boundaries of each rainfall zone. To this end, we explore the different rainfall seasonality classifications to critically review approaches and compare mapping efforts amongst authors to quantify the degree of uncertainty in these maps of rainfall seasonality across South Africa.

Importance of a rainfall seasonality classification and a spatially consistent approach to mapping

A standard definition of rainfall seasonality has not been established, and while this is the case, to describe rainfall seasonality, previous scholars have highlighted the importance of classifications based on measurements on the magnitude, timing and duration of wet and dry seasons (Feng, Porporato, & Rodriguez-Iturbe, 2013; Pascale, Lucarini, Feng, Porporato, & Hasson, 2014; Raziei et al., 2017). Additionally, there are no formally established categories of rainfall seasonality to spatially classify an area (Herrmann & Mohr, 2011). To motivate for the importance of rainfall seasonality classification and spatially consistent mapping, the applicability of these classifications and maps is to be considered. Applicability is not necessarily in decision-making, but rather in meteorological and related research across South Africa.

In climate science, homogenous rainfall regions can be used to explore drivers of rainfall in different regions, and for this task maps of rainfall seasonality are necessary (Tennant & Hewitson, 2002). A quantifiable classification of rainfall seasonality may be used to investigate historical changes in rainfall seasonality under a changing climate (Herrmann & Mohr, 2011; Raziei, 2017), and consistency in the classification of rainfall seasonality is necessary for such a task. In agroclimatology, research on the degree and type of vegetation cover across a region and the timing of key phenophase events benefits considerably from classifications on measurements on the arrival of the wet season and on maps of homogenous rainfall zones (Feng et al., 2013; Raziei, 2017). Application of information regarding the timing of rainfall, obtained from rainfall seasonality classifications, is necessary to quantify climate suitability of tourism destinations using tourism climate indices (Fitchett, Robinson, & Hoogendoorn, 2017). Quantifiable measurements on the year-round temporal distribution of rainfall and timing of flood and drought risk are vital for research concerning sustainable water and soil resource management (Feng et al., 2013; Raziei, 2017).

Review of methodologies to classify and map rainfall seasonality across South Africa

Proliferation of attempts to map rainfall seasonality

To date, at least 60 maps depicting rainfall seasonality across the full area of South Africa have been published, adapted and reused directly (Table 1). There are 19 original maps based on primary data sources of rainfall. These original maps were reused and adapted 13 and 28 times, respectively. These maps have been reused and/or adapted in literature on contemporary and palaeoenvironmental research across South Africa. Maps created by Carr, Thomas, Bateman, Meadows, and Chase (2006), Keen (1971) and Schumann and Hofmeyr (1938) were most frequently reused or adapted. To date, the most recent publication of a rainfall seasonality map was by Botai, Botai, and Adeola (2018) on research regarding the spatio-temporal variability of rainfall concentration. The most recent reuse of a map was Quick et al. (2018) on research regarding changes in climatic zones through time. These maps describing rainfall seasonality are still produced and used, and since these maps are dissimilar, the inconsistencies in the spatial distribution and boundaries of rainfall zones are perpetuated.

The proliferation of rainfall seasonality classification maps for South Africa is clearly apparent in Table 1. In spite of this, there is no evidence of a consistent process of developing methods to classify rainfall seasonality, and maps have typically been prepared without consideration of previous mapping or classification efforts. Most maps have received little/no interrogation in literature. With so many approaches available to create a rainfall seasonality classification, it is surprising that previous classification approaches and maps have not been interrogated. Only Keen (1971) reviewed and interrogated previous maps and classification approaches for his rainfall seasonality classification (Table 1). Additionally, authors which reused or adapted maps have generally done so without questioning those maps.

Classification methods and maps

In any systematic investigation of rainfall seasonality over a large region, especially one which is climatologically heterogeneous, it is essential that the region is divided into a number of smaller homogeneous regions such that each can be treated as a separate entity for application into research (Keen, 1971). This applies to South Africa, where there is remarkable diversity in the total annual rainfall amount and the seasonal distribution of rainfall. Since there are many ways in which rainfall seasonality at a particular location may be characterized, there are many ways of achieving a classification of a region into smaller rainfall regions (Schumann & Hofmeyr, 1938).

For this section of the review, the different approaches that have been applied to create a map of rainfall seasonality across South Africa have been evaluated in terms of their ability to provide a complete description of rainfall seasonality. A complete description captures measurements on the magnitude, timing and duration of wet and dry seasons (Pascale et al., 2014). These maps have typically been created to characterize rainfall seasonality into homogeneous rainfall regions as is experienced on the ground (Herrmann & Mohr, 2011), based on either point weather stations, remote-sensing products or a combination thereof.

Table 1. Literature analysis of published rainfall seasonality classification maps for South Africa, from publications obtained from Web of Science, Scopus, Google Scholar and the University of the Witwatersrand libraries.

Publication	Rainfall data scale	Stations/dataset	Temporal period	Seasonality approach; Interpolation technique	Reused directly	Adapted
Schumann and Hofmeyr (1938)	Mean monthly	72	1906–1935	Harmonic analysis; unknown	South African Weather Bureau (1949); Wellington (1955); South African Weather Bureau (1960); Keen (1971); Van Heerden, Terblanche, and Schulze (1988)	South African Weather Bureau (1972); McGee (1977)
Cooke (1946)	Mean monthly	150	Unknown	Percentage analysis; unknown	Keen (1971)	No record
South African Weather Bureau (1957)	Mean monthly	49	Unknown	Bar chart analysis; none		No record
South African Weather Bureau (1965)	Mean monthly	Unknown	Unknown	Percentage analysis; unknown	Keen (1971); Dyer (1975b)	No record
South African Weather Bureau (1965)	Mean monthly	Unknown	Unknown	Percentage analysis; unknown	Keen (1971)	No record
South African Weather Bureau (1965)	Mean monthly	Unknown	Unknown	Isohyet analysis; unknown	Keen (1971); Dyer (1975b)	No record
Keen (1971)	Mean monthly and annual total	355	1916–1965	Spectral analysis; unknown	No record	Keen and Tyson (1973); Dyer (1975a, 1975b); Tyson (1977); Tyson (1978); Tyson, Dyer, and Mametse (1975); Gillooly (1976); Tyson (1981); Harrison (1984); Harrison (1986); Tyson (1986); Walker (1989)
McGee (1977)	Mean monthly	200	1921–1950	Vector analysis; unknown	No record	Lindesay (1988)
Walsh and Lawler (1981)	Mean monthly and annual total	Unknown	Unknown	Statistical index; unknown	No record	No record
Taljaard and Steyn (1991)	Mean monthly	Unknown	Unknown 60-year period	Descriptive statistics; none	No record	No record
(1) Schulze and Kunz (1997) Updated by (2) Schulze and Maharaj (2007)	Mean monthly	Unknown	1950–1999	Vector analysis; unknown	Kuhlmann, Guo, Veldtman, and Donaldson (2012) reused (2); Botai et al. (2018) reused (1)	Ellery et al. (2016) adapted from (1)

(*Continued*)

Table 1. (Continued).

Publication	Rainfall data scale	Stations/dataset	Temporal period	Seasonality approach; Interpolation technique	Reused directly	Adapted
Carr et al. (2006)	Mean monthly	UNEP GRID data	1951–1980	Percentage analysis; unknown	No record	Chase and Meadows (2007); Gasse, Chalie', Vincens, Williams, and Williamson (2008); Norström, Scott, Partridge, Risberg, and Holmgren (2009); Chase et al. (2012); Mills, Grab, Rea, Carr, and Farrow (2012); Chase et al. (2013); Truc et al. (2013); Stone (2014); Chase et al. (2015); Hannaford, Jones, and Bigg (2015); Chevalier and Chase (2016); Braun et al. (2017); Quick et al. (2018)
Herrmann and Mohr (2011) *Two maps	Monthly satellite derived estimates	Satellite grid cells at 0.25° and 2.5° resolution	Unknown	Remote sensing; N/A	No record	No record
Liebmann et al. (2012)	Daily rainfall	Satellite grid cells at 0.25°	1998–2008	Wet season start and end dates; N/A	No record	No record
Cramer and Hoffman (2015)	Mean monthly	1km^2 resolution interpolated surface	1950–2000	Ratio of winter to summer rainfall; Spline	No record	No record
Dunning et al. (2016)	Daily rainfall	Satellite grid cells at 1°	1998–2013	Wet season start and end dates; N/A	No record	No record
Botai et al. (2018)	Monthly satellite derived estimates	Satellite grid cells at 0.25°	1998–2015	PCI; N/A	No record	No record

Across the world, many approaches to classify rainfall seasonality have been developed and applied. These include harmonic analysis explained by Schuman and Hofmeyr (1938), the seasonality index (SI) developed by Walsh and Lawler (1981), vector analysis developed by Markham (1970), the precipitation concentration index (PCI) developed by Oliver (1980), the precipitation concentration degree and precipitation concentration period developed by Zhang and Qian (2003), the daily precipitation concentration index (DPCI) developed by Martin-Vide (2004), the seasonal concentration index developed by Fujita (2008), the dimensionless SI and relative entropy developed by Feng et al. (2013) and the Gini index (GI) first used for inequality of daily rainfall by Rajah et al. (2014).

Some of these and additional approaches have been applied to classify and map rainfall seasonality across South Africa (Table 1). These methods range from simple approaches, such as bar chart analysis (South African Weather Bureau, 1957), isobar analysis (South African Weather Bureau, 1965), descriptive statistics (Taljaard & Steyn, 1991), percentage analysis (Carr et al., 2006; Cooke, 1946; South African Weather Bureau, 1965) and the ratio of winter to summer rainfall (Cramer & Hoffman, 2015), to more complex approaches such as vector analysis (McGee, 1977; Schulze & Kunz, 1997; Schulze & Maharaj, 2007), SI (Walsh & Lawler, 1981), PCI (Botai et al., 2018), harmonic analysis (Schumann & Hofmeyr, 1938), spectral analysis (Keen, 1971), remote-sensing techniques (Herrmann & Mohr, 2011) and calculation of wet season start and end dates (Dunning, Black, & Allan, 2016; Liebmann et al., 2012).

The first known published map of rainfall seasonality across South Africa was by Schumann and Hofmeyr (1938) using harmonic analysis by fitting sine waves to mean monthly rainfall distribution (Table 1). The final map was drawn using two systems of lines of 'equal phase' and 'equal relative amplitude', which are measures of the period of maximum rainfall and normal rainfall fluctuation during the course of a year respectively. Twenty-three delimited regions representing annual percentage of summer rainfall, during October to March, were mapped, and summer rainfall for region one was 20.2% which increased to 88.1% for region 23 (Schumann & Hofmeyr, 1938). The final classification results provide measurements on the percentage and timing of rainfall, only on a monthly scale. Many regions across South Africa may experience wet seasons which commence not at the start but rather during a month. The magnitude of rainfall across the country is considerably variable, and such variability was not considered by this approach.

Almost a decade later, Cooke (1946) created a rainfall seasonality map, with 16 rainfall regions, using two periods of percentage monthly rainfall (Table 1). The first period was of the months contributing above 10% of annual rainfall and the second of the months contributing below 5% of annual rainfall (Cooke, 1946). The prepared map depicts the duration and timing of the wet season, again only on a monthly scale. Information regarding rainfall magnitude is again unknown.

Starting in 1957, the South African Weather Bureau (SAWB) released a number of maps depicting rainfall seasonality across South Africa. The first was produced by plotting a location-specific classification of yearly rainfall distribution using bar graphs on mean monthly rainfall (South African Weather Bureau, 1957; Table 1). The second map was created using mean monthly rainfall values to calculate isohyet lines of summer rainfall percentage across the country (South African Weather Bureau, 1965; Table 1). The third map was produced using mean monthly rainfall

values to create isohyet lines of seasonal rainfall, where the zero line indicated year-round rainfall, and positive and negative lines represented excess spring and autumn rainfall, respectively (South African Weather Bureau, 1965; Table 1). The fourth map was created by plotting monthly migration of the 50mm isohyet, which provided an incomplete classification of rainfall regimes (South African Weather Bureau, 1965; Table 1). Common amongst these maps is that rainfall seasonality zones have not been delimited into homogeneous zones, which should be treated as separate entities in rainfall discussions on research topics such as water and soil resource management. Additionally, measurements on the duration, timing and magnitude of wet seasons are not evident from these classifications.

Keen (1971) classified rainfall seasonality using spectral analysis, mean monthly and annual total rainfall (Table 1). The spectra of rainfall series were plotted and the classification was developed by analysing the variance of the spectrum of rainfall series and the mean amplitudes of the waves, which constituted various possible rainfall regimes identified as spectral cycle fluctuations (Keen, 1971). By superimposing the spatial distributions of the spectral cycle fluctuations, a map of 18 rainfall regions was created (Keen, 1971). This classification and map described rainfall seasonality with measurements on the duration, timing and magnitude of the wet season on a monthly scale (Keen, 1971). The temporal distribution of rainfall, for example unimodal, bimodal or year-round, was captured using this approach (Keen, 1971).

McGee (1977), Schulz and Kunz (1997) and Schulze and Maharaj (2007) classified rainfall zones across South Africa using vector analysis (Table 1). This approach assumes that mean monthly rainfall values for a location are vector quantities, with a magnitude being monthly rainfall amount and a direction being the month expressed (Markham, 1970; McGee, 1977). The resultant vector is a percentage ranging from zero for rainfall evenly distributed throughout the year to 100 indicating all rainfall fell in 1 month, with a direction representing the period of rainfall (Markham, 1970; McGee, 1977). This approach describes the duration, timing and distribution of rainfall throughout the year; however, a disadvantage of this method is that only one rainfall peak may be identified as only one resultant vector is produced (Oliver, 1984). The southern Cape coast of South Africa experiences a bimodal rainfall distribution, with more than one rainfall peak during the year-round rainfall season. All three maps demonstrated consistency using this rainfall seasonality classification.

Using the SI, mean monthly and annual average rainfall data, Walsh and Lawler (1981) mapped rainfall seasonality across Africa (Table 1). This approach measures the variability of monthly rainfall throughout a year, where the result is the degree of seasonality ranging from zero, for equal monthly rainfall, to 1.83, where rainfall occurs during a single month (Walsh & Lawler, 1981). This value does not demonstrate the timing nor duration of seasonal rainfall, and in South Africa seasonal rainfall occurs during summer and winter. Maps depicting the timing of rainfall are considerably different to this map Walsh and Lawler (1981) produced.

In 1972, the SAWB produced a map of 93 rainfall districts across South Africa. Taljaard and Steyn (1991) calculated mean and total monthly rainfall for each district to group them according to the timing, duration and distribution of rainfall (Table 1). No information regarding the magnitude of rainfall was obtained from this approach.

Using predefined zones incorporated bias into the final rainfall zone boundary locations as these were not calculated but rather boundaries of the rainfall districts.

Carr et al. (2006) used mean monthly rainfall data to create a map with SRZ, WRZ and YRZ areas based on the annual percentage of winter rainfall (Table 1). Areas classified as WRZ, YRZ and SRZ receive above 66%, 33–66% and below 33% of winter rainfall, respectively (Carr et al., 2006). Classification into SRZ, WRZ and YRZ provides some information on the timing and distribution of rainfall, but there is no information regarding the magnitude nor duration of rainfall.

Herrmann and Mohr (2011) produced two maps of rainfall seasonality across Africa based on the relationship between temperature and rainfall, at two different spatial resolutions (Table 1). Non-seasonal humid, arid and single-, dual-, and multiple-wet-season regimes were mapped to describe rainfall seasonality in terms of the timing and distribution of rainfall throughout a year (Herrmann & Mohr, 2011). These maps were created using gridded rainfall from the Tropical Rainfall Measuring Mission Multisatellite Precipitation Analysis (TMPA), at 0.25°, and the Global Precipitation Climatology Project (GPCP), at 2.5°, and the Moderate Resolution Imaging Spectroradiometer land surface temperature product (Herrmann & Mohr, 2011). Grid cells are not purely based on observed rainfall values, but rather a combination of satellite and rain gauge observations (Rana, McGregor, & Renewick, 2015), which may provide more spatially complete datasets of rainfall and arguably more homogeneity over point-based weather stations. The spatial scale of grid cells at 0.25° is equivalent to approximately 27-28km, which provides a better spatial resolution than meteorological stations where the spatial distribution is equivalent to the distance between stations which is not uniform and often larger than the spatial resolution offered by remote-sensing products. Remote-sensing grid cells may provide predefined boundaries along grid cell boundaries. Possibly a better way to determine the location of rainfall zone boundaries may incorporate both remote-sensing products and point-based weather stations.

Dunning et al. (2016) and Liebmann et al. (2012), using GPCP at 2.5° resolution, defined the wet season across Africa using a quantity called the 'anomalous accumulation', which is plotted to determine the start and end dates of rainfall when the accumulation plot increases and decreases, respectively. This was the only approach to classify rainfall seasonality on a daily scale. Additionally, information calculated from this approach adequately describes the timing, duration and magnitude of the wet season.

Cramer and Hoffman (2015) used mean monthly rainfall data obtained from a spline interpolated surface created by Hijmans, Cameron, Parra, Jones, and Jarvis (2005), to create a rainfall seasonality classification based on the ratio of winter (April to September) and summer (October to March) rainfall (Table 1). While this ratio does provide a statistical dichotomy on winter and summer rainfall and some information on the timing of rainfall, there is no information regarding the duration, distribution and magnitude of wet seasons.

The most recent map of rainfall seasonality was created using gridded mean monthly rainfall, of 0.25° from TMPA, and the PCI to classify the temporal distribution of rainfall (Botai et al., 2018). The class limits used were adapted from Oliver (1980) and indicate the distribution as follows: a PCI value less than 10 indicates a uniform rainfall

distribution indicative of year-round rainfall, a PCI value between 10 and 15 indicates a moderate rainfall distribution, a PCI value between 16 and 20 indicates an irregular rainfall distribution and PCI values greater than 20 indicates a strong irregular rainfall distribution indicative of highly seasonal rainfall. Similar to the SI approach, this approach does not depict the timing nor duration of rainfall, and maps are also considerably different to those depicting the timing of rainfall.

One of the main issues associated with most of the approaches used to classify rainfall seasonality across South Africa is related to temporal data scale. Most approaches call for monthly scale data (Table 1), which offers a coarse resolution not accounting for daily scale rainfall variability and is an issue for areas where rainfall seasons start within a month. This scale is problematic as rainfall anomalies may skew monthly averages or totals and create misleading trends, while analysis at a daily scale may account for these anomalies and short rainfall seasons (Keen, 1971; Walsh & Lawler, 1981). The 'anomalous accumulation' quantity is the only approach which considered rainfall on a daily scale, and subsequent maps were on a daily scale. Additionally, the DPCI and GI, approaches with no known published use in South Africa, use daily rainfall values for calculation (Martin-Vide, 2004). Results from these approaches demonstrate the distribution of rainfall throughout a year, where higher and lower values indicate a heterogeneous and homogeneous distribution of rainfall, respectively (Sangüesa et al., 2018). No numerical limits have been developed to indicate seasonal or year-round rainfall from the DPCI and GI results (Martin-Vide, 2004; Rajah et al., 2014; Sangüesa et al., 2018), and the resulting value does not indicate the timing of rainfall. This limits the applicability of these approaches to research activities on topics such as water resource management and agriculture which rely on measurements on the timing of rainfall.

Despite continuous attempts to classify and map the rainfall seasonality across South Africa and the rest of the world, there still does not exist a universally accepted classification nor an objectively assessed ideal statistical approach for constructing one. Even leading climatological organizations, for example the World Meteorological Organisation, have not created a standard rainfall seasonality classification. However, the SI and PCI are the most commonly used approaches (Raziei, 2017). These approaches are associated with issues surrounding input data scale, and both approaches do not demonstrate the timing of rainfall, issues highlighted earlier. By using different approaches, comparisons over time and between different areas are difficult, especially in areas with considerable dispute regarding their classification.

Analysis of rainfall seasonality classification maps

Amongst these maps, there is a broad consensus that South Africa contains a SRZ, a WRZ and a YRZ, yet the geographical boundaries of these zones vary considerably between maps (Figure 1). Across the country, the WRZ is typically shown to cover the western coast, the SRZ is typically shown to cover the interior and eastern parts of the country and the YRZ is typically shown along the southern coast, and this is represented fairly consistently throughout most maps.

Each of the 19 original rainfall seasonality maps was imported into *ArcMap 10.3* and georeferenced to a map of South Africa projected using the WGS84 coordinate system.

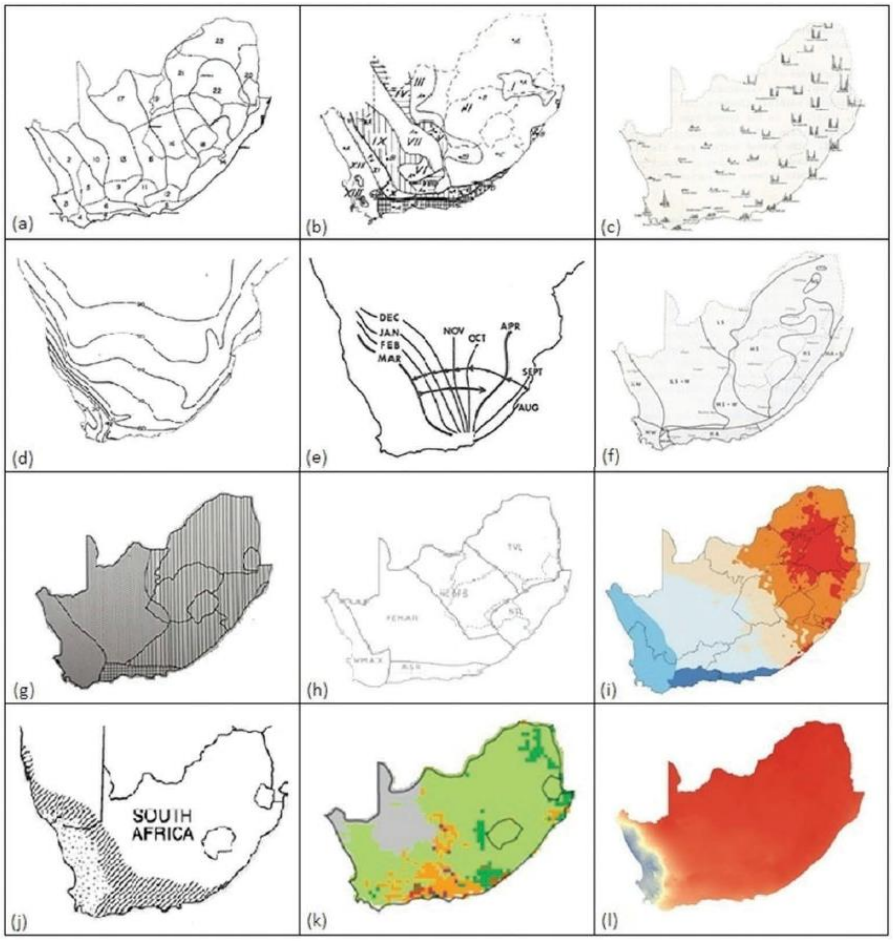


Figure 1. Example of maps depicting rainfall seasonality across South Africa: (a) Schumann and Hofmeyr (1938), (b) Cooke (1946), (c) South African Weather Bureau (1957), (d) South African Weather Bureau (1965), (e) South African Weather Bureau (1965) (f) Keen (1971), (g) McGee (1977), (h) Taljaard and Steyn (1991), (i) Schulze and Kunz (1997), (j) Carr et al. (2006), (k) Herrmann and Mohr (2011) and (l) Cramer and Hoffman (2015).

Once the maps were georeferenced, spatial feature classes were identified which describe consensus/dispute regarding the classification of rainfall zones to create a composite map (Figure 2). From the composite map, it is clear that there are some inconsistencies in these maps classifying rainfall seasonality across South Africa (Figure 2). Only 78% of the country has been classified with at least 75% consensus, leaving the rainfall seasonality classification for the remaining area disputed by at least 25% of authors (Figure 2; Table 2). The landmass located between the SRZ and WRZ, excluding the southern coast of the country, is disputed by at least 50% of authors (Figure 2; Table 2). Within this area, 3% of the country's rainfall seasonality classification is highly disputed as the area has been classified as SRZ, WRZ and

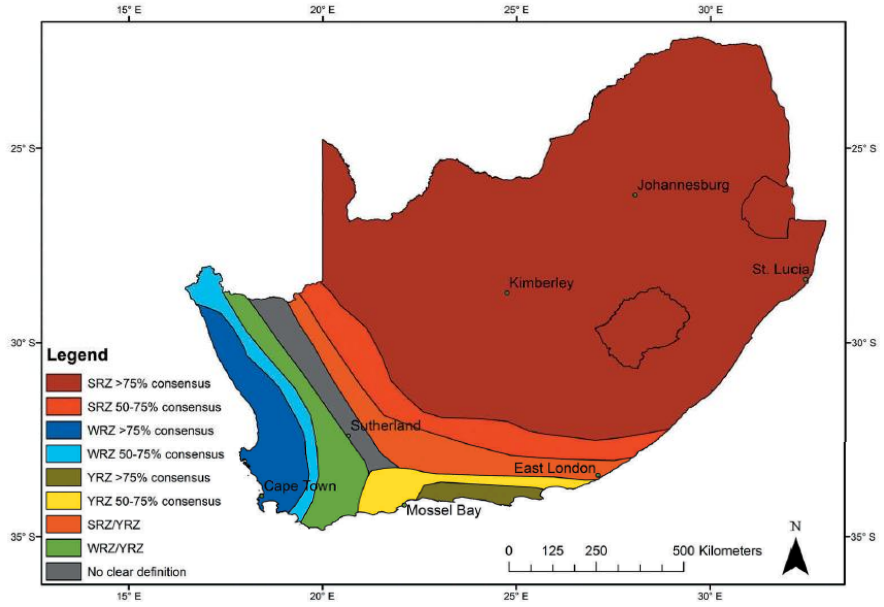


Figure 2. Consensus and dispute between authors on the spatial distribution of rainfall seasonality zones across South Africa. The locations Cape Town, East London, Johannesburg, Kimberley, Mossel Bay, St. Lucia and Sutherland have been labelled for use in Table 2.

Table 2. Portion of South Africa, including Lesotho and Swaziland, classified under each class of consensus/dispute regarding the rainfall seasonality classification in Figure 2.

Class of consensus/dispute	Portion classified (%)
SRZ>75% consensus	73
SRZ 50–75% consensus	6
WRZ>75% consensus	4
WRZ 50–75% consensus	2
YRZ>75% consensus	1
YRZ 50–75% consensus	2
SRZ/YRZ	5
WRZ/SRZ	4
No clear definition	3

YRZ amongst the maps, indicating that there is no clear definition in the classification for this area (Figure 2; Table 2).

The differences in maps appear to represent most clearly the differences in methods used. A range of methods should converge on the same empirical observation, at very least for the extremes of rainfall zones. More than 75% of the maps have converged on the same rainfall seasonality classification for 78% of South Africa, and at least 50% of maps converged on the same rainfall seasonality classification for 88% of the country (Figure 2; Table 2). Between the WRZ and SRZ, there are inconsistencies in the rainfall

seasonality classification. In this highly disputed area, classification approaches may either not have the ability to capture weak signals of rainfall seasonality of the SRZ and WRZ and may capture these as YRZ or classification approaches may capture weak signals of seasonality, or this area is a YRZ and only some methods capture this.

The differences in maps may also represent the differences in temporal periods, different spatial distribution and numbers of stations, different data products and different spatial interpolation methods. Maps would be dissimilar unless the exact same dataset, temporal period and spatial interpolation techniques are used to classify rainfall seasonality using the exact same approach. First, different temporal periods would capture the average rainfall seasonality of a specific period which would not be the same as another period. Second, differences in the spatial distribution and number of stations and data products will cause differences in the final surface of rainfall seasonality which would capture rainfall seasonality specific to the spatial distribution of selected stations and/or data products. Last, differences in spatial distribution may be attributed to the use of different spatial interpolation methods, as no method will display the exact same spatial distribution (Dobesch, Dumolard, & Dyras, 2007). These differences would manifest mostly along boundary locations between rainfall zones, where the classification of rainfall zones is disputed amongst authors (Figure 2).

The differences in maps also appear over time as new maps were published. These differences over time could be a result of different definitions of rainfall seasonality captured by different categories of rainfall regimes, reflecting the time these maps were created. Additionally, the differences could also indicate temporal shifts in seasonality distribution as rainfall seasonality, similar to all climatic elements, is subject to change (Sousa, Blamey, Reason, Ramos, & Trigo, 2018). This does not seem to be the case for the locations mapped in Figure 2, and over time classifications for the same location are similar, and only the classification of Sutherland is considerably disputed amongst the authors (Table 3). Sutherland is located in the highly disputed area between the SRZ and WRZ (Figure 2). Along the eastern coast of the country, as shown by the classification of St. Lucia captured in the maps (Table 3), there are some discrepancies as some authors classified this full coastline area or small parts of the coastline area as a YRZ (Chase, Boom, Carr, Meadows, & Reimer, 2013; Keen, 1971; Walsh & Lawler, 1981).

Conclusions, future developments and research questions regarding rainfall seasonality in South Africa

There have been many attempts to classify rainfall seasonality across South Africa and to create a single map describing the spatial distribution of rainfall seasonality. This study is the first of its kind to review the methods used to classify and map rainfall seasonality across South Africa and to quantify the degree of uncertainty in subsequent maps. Classification and mapping efforts were demonstrated to be inconsistent. The inconsistencies are most apparent at the transition between the WRZ and SRZ, and further work is essential to understand this area. In view of this, an important question to consider is whether a YRZ characterizes the transition between the SRZ and WRZ. It is also important to re-evaluate the spatial distribution of rainfall zones, especially the YRZ which is considered to only occupy the southern coast in literature (Engelbrecht & Landman, 2016; Engelbrecht et al., 2015).

Table 3. Rainfall seasonality classification from the 19 original maps for seven locations mapped in Figure 2. SRZ: summer rainfall zone; WRZ: winter rainfall zone; YRZ: year-round rainfall zone; WS: Wet season. NC: not classified. Only SRZ, WRZ and YRZ have been highlighted.

Publication	Cape Town	East London	Johannesburg	Kimberley	Mossel Bay	St. Lucia	Sutherland
Schumann and Hofmeyr (1938)	WRZ	YRZ	SRZ	SRZ	YRZ	SRZ	YRZ
Cooke (1946)	WRZ	YRZ	SRZ	SRZ	YRZ	SRZ	WRZ
South African Weather Bureau (1957)	WRZ	SRZ	SRZ	SRZ	YRZ	SRZ	WRZ
South African Weather Bureau (1965)	WRZ	SRZ	SRZ	SRZ	YRZ	SRZ	WRZ
South African Weather Bureau (1965)	Autumn	YRZ	Spring	Spring	YRZ	Spring	Autumn
South African Weather Bureau (1965)	NC	SRZ	SRZ	SRZ	NC	SRZ	NC
Keen (1971)	WRZ	YRZ	SRZ	YRZ	YRZ	YRZ	YRZ
McGee (1977)	WRZ	YRZ	SRZ Max: Jan	SRZ Max: Jan	YRZ	SRZ Max: Feb	WRZ
Walsh and Lawler (1981)	Rather seasonal	YRZ	Rather seasonal	Rather seasonal	YRZ	YRZ	Rather seasonal
Taljaard and Steyn (1991)	WRZ	YRZ	SRZ	SRZ	YRZ	SRZ	WRZ
Schulze and Kunz (1997)	WRZ	YRZ	Early-SRZ Max: Dec	Late-SRZ Max: Feb	YRZ	Late-SRZ Max: Feb	WRZ
Carr et al. (2006)	WRZ	YRZ	SRZ	SRZ	YRZ	SRZ	YRZ
Schulze and Maharaj (2007)	WRZ	YRZ	Mid-SRZ Max: Jan	Late-SRZ Max: Feb	YRZ	Mid-SRZ Max: Jan	WRZ
Herrmann and Mohr (2011) *Map one	One WS, unimodal	One WS, bimodal	One WS, unimodal	One WS, unimodal	Two WS, unimodal-unimodal	One WS unimodal	Two WS, unimodal-unimodal
Herrmann and Mohr (2011) *Map two	One WS unimodal	One WS unimodal	One WS unimodal	One WS unimodal	One WS unimodal	One WS unimodal	One WS unimodal
Liebmann et al. (2012)	WRZ	YRZ	SRZ	SRZ	YRZ	SRZ	YRZ
Cramer and Hoffman (2015)	WRZ	SRZ	SRZ	SRZ	SRZ	SRZ	SRZ
Dunning et al. (2016)	WRZ	SRZ	SRZ	SRZ	WRZ	SRZ	WRZ
Botai et al. (2018)	Irregular	Uniform	Irregular	Irregular	Moderate	Moderate	Irregular

The inconsistencies apparent between the maps clearly represent the different classification approaches, which refer to different definitions and categories of rainfall seasonality. Inconsistencies amongst these maps are problematic for application of these maps, for activities such as water resource management and agriculture which require information on consistent and predictable rainfall regimes. A potential way to reduce the issues of inconsistency may be to implement one approach, or a number of approaches, with

established categories to classify and map rainfall seasonality across South Africa. This approach is a consideration of our current research. The aim is that this approach can provide quantifiable measurements on the magnitude, timing, duration and distribution of wet and dry seasons which are considered to provide a complete description of rainfall seasonality. An important feature of this approach should be the ability to qualitatively and quantitatively describe rainfall seasonality for meaningful comparisons across the entire country. This approach should be consistent and based on an objectively and rigorously assessed statistical approach with all information disclosed regarding its calculation and limitations. This approach should be able to quantitatively reflect change over time, which would enable identification of rainfall seasonality trends under a changing climate.

Disclosure statement

No potential conflict of interest was reported by the authors.

Funding

This work was supported by the National Research Foundation (NRF), South Africa under Grant number 107742.

ORCID

S.J. Roffe http://orcid.org/0000-0003-3683-8377
J.M. Fitchett http://orcid.org/0000-0002-0854-1720

References

Botai, C. M., Botai, J. O., & Adeola, A. M. (2018). Spatial distribution of temporal precipitation contrasts in South Africa. *South African Journal of Science*, *114*(7–8), 70–78.

Braun, K., Bar-Matthews, M., Ayalon, A., Zilberman, T., & Matthews, A. (2017). Rainfall isotopic variability at the intersection between the winter and summer rainfall regimes in coastal South Africa (Mossel Bay, Western Cape Province). *South African Journal of Geology*, *120*(3), 323–340.

Carr, A. S., Thomas, D. S. G., Bateman, M. D., Meadows, M. E., & Chase, B. M. (2006). Late Quaternary palaeoenvironments of the winter-rainfall zone of southern Africa: Palynological and sedimentological evidence from the Agulhas Plain. *Palaeogeography, Palaeoclimatology, Palaeoecology*, *239*(1–2), 147–165.

Chase, B. M., Boom, A., Carr, A. S., Meadows, M. E., & Reimer, P. J. (2013). Holocene climate change in southernmost South Africa: Rock hyrax middens record shifts in the southern westerlies. *Quaternary Science Reviews*, *82*, 199–205.

Chase, B. M., Lim, S., Chevalier, M., Boom, A., Carr, A. S., Meadows, M. E., & Reimer, P. J. (2015). Influence of tropical easterlies in southern Africa's winter rainfall zone during the Holocene. *Quaternary Science Reviews*, *107*, 138–148.

Chase, B. M., & Meadows, M. E. (2007). Late Quaternary dynamics of southern Africa's winter rainfall zone. *Earth-Science Reviews*, *84*(3–4), 103–138.

Chase, B. M., Scott, L., Meadows, M. E., Gil-Romera, G., Boom, A., Carr, A. S., … Quick, L. J. (2012). Rock hyrax middens: A palaeoenvironmental archive for southern African drylands. *Quaternary Science Reviews*, *56*, 107–125.

Chevalier, M., & Chase, B. M. (2016). Determining the drivers of long-term aridity variability: A southern African case study. *Journal of Quaternary Science*, *31*(2), 143–151.
Cooke, H. B. S. (1946). Some observations on rainfall distribution in South Africa. *South African Geographical Journal*, *28*(1), 34–38.
Cramer, M. D., & Hoffman, M. T. (2015). The consequences of precipitation seasonality for Mediterranean-ecosystem vegetation of South Africa. *PloS one*, *10*(12), e0144512.
Crétat, J., Richard, Y., Pohl, B., Rouault, M., Reason, C., & Fauchereau, N. (2012). Recurrent daily rainfall patterns over South Africa and associated dynamics during the core of the austral summer. *International Journal of Climatology*, *32*(2), 261–273.
Dobesch, H., Dumolard, P., & Dyras, I. (2007). *Spatial interpolation for climate data: The use of GIS in climatology and meteorology*. Great Britain: ISTE Ltd.
Dunning, C. M., Black, E. C. L., & Allan, R. P. (2016). The onset and cessation of seasonal rainfall over Africa. *Journal of Geophysical Research: Atmospheres*, *121*(11), 405–411.
Dyer, T. G. J. (1975a). Solar activity and rainfall variation over southern Africa. *South African Journal of Science*, *71*(12), 369–372.
Dyer, T. G. J. (1975b). *Secular variation in South African rainfall* (Unpublished doctoral dissertation). University of the Witwatersrand, Johannesburg.
Ellery, W. N., Grenfell, S. E., Grenfell, M. C., Powell, R., Kotze, D., Marren, P., & Knight, J. (2016). Wetlands in southern Africa. In J. Knight & S. Grab (Eds.), *Quaternary environmental change in southern Africa: Physical and human dimensions* (pp. 188–202). Cambridge: Cambridge University Press.
Engelbrecht, C. J., & Landman, W. A. (2016). Interannual variability of seasonal rainfall over the Cape south coast of South Africa and synoptic type association. *Climate Dynamics*, *47*(1–2), 295–313.
Engelbrecht, C. J., Landman, W. A., Engelbrecht, F. A., & Malherbe, J. (2015). A synoptic decomposition of rainfall over the Cape south coast of South Africa. *Climate Dynamics*, *44* (9–10), 2589–2607.
Feng, X., Porporato, A., & Rodriguez-Iturbe, I. (2013). Changes in rainfall seasonality in the tropics. *Nature Climate Change*, *3*(9), 811–815.
Fitchett, J. M., Robinson, D., & Hoogendoorn, G. (2017). Climate suitability for tourism in South Africa. *Journal of Sustainable Tourism*, *25*(6), 851–867.
Fujita, K. (2008). Effect of precipitation seasonality on climatic sensitivity of glacier mass balance. *Earth and Planetary Science Letters*, *276*(1–2), 14–19.
Gasse, F., Chalie´, F., Vincens, A., Williams, M. A. J., & Williamson, D. (2008). Climatic patterns in equatorial and southern Africa from 30,000 to 10,000 years ago reconstructed from terrestrial and near-shore proxy data. *Quaternary Science Reviews*, *27*(25–26), 2316–2340.
Gillooly, J. F. (1976). Dendroclimatology in South Africa. *South African Forestry Journal*, *98*(1), 64–65.
Hannaford, M. J., Jones, J. M., & Bigg, G. R. (2015). Early-nineteenth-century southern African precipitation reconstructions from ships' logbooks. *Holocene*, *25*(2), 379–390.
Harrison, M. S. J. (1984). A generalised classification of South African summer rain-bearing synoptic systems. *Journal of Climatology*, *4*(5), 547–560.
Harrison, M. S. J. (1986). *A synoptic climatology of South African rainfall variations* (Unpublished doctoral dissertation). University of the Witwatersrand, Johannesburg.
Herrmann, S. M., & Mohr, K. I. (2011). A continental-scale classification of rainfall seasonality regimes in Africa based on gridded precipitation and land surface temperature products. *Journal of Applied Meteorology and Climatology*, *50*(12), 2504–2513.
Hijmans, R. J., Cameron, S. E., Parra, J. L., Jones, P. G., & Jarvis, A. (2005). Very high resolution interpolated climate surfaces for global land areas. *International Journal of Climatology*, *25* (15), 1965–1978.
Keen, C. S. (1971). *Rainfall spectra and the delimitation of rainfall regimes in South Africa.* (Unpublished master's thesis). University of the Witwatersrand, Johannesburg.

Keen, C. S., & Tyson, P. D. (1973). Seasonality of South African rainfall: A note on its regional delimitation using spectral analysis. *Archiv für Meteorologie, Geophysik und Bioklimatologie, Serie B*, *21*(2–3), 207–214.

King, J., Mitchell, S., & Pienaar, H. (2011). Water supply and demand. In J. King & H. Pienaar (Eds.), *Sustainable use of South Africa's inland waters* (pp. 1–16). Pretoria: Water Research Commission.

Kuhlmann, M., Guo, D., Veldtman, R., & Donaldson, J. (2012). Consequences of warming up a hotspot: Species range shifts within a centre of bee diversity. *Diversity and Distributions*, *18* (9), 885–897.

Liebmann, B., Bladé, I., Kiladis, G. N., Carvalho, L. M., Senay, G. B., Allured, S., … Funk, C. (2012). Seasonality of African precipitation from 1996 to 2009. *Journal of Climate*, *25*(12), 4304–4322.

Lindesay, J. A. (1988). South African rainfall, the Southern Oscillation and a Southern Hemisphere semi-annual cycle. *Journal of Climatology*, *8*(1), 17–30.

Markham, C. G. (1970). Seasonality of precipitation in the United States. *Annals of the Association of American Geographers*, *60*(3), 593–597.

Martin-Vide, J. (2004). Spatial distribution of a daily precipitation concentration index in peninsular Spain. *International Journal of Climatology*, *24*(8), 959–971.

McGee, O. S. (1977). The determination of rainfall seasons in South Africa using Markham's technique. *South African Geographer*, *5*, 390–396.

Mills, S. C., Grab, S. W., Rea, B. R., Carr, S. J., & Farrow, A. (2012). Shifting westerlies and precipitation patterns during the Late Pleistocene in southern Africa determined using glacier reconstruction and mass balance modelling. *Quaternary Science Reviews*, *55*, 145–159.

Norström, E., Scott, L., Partridge, T. C., Risberg, J., & Holmgren, K. (2009). Reconstruction of environmental and climate changes at Braamhoek wetland, eastern escarpment South Africa, during the last 16,000 years with emphasis on the Pleistocene–Holocene transition. *Palaeogeography, Palaeoclimatology, Palaeoecology*, *271*(3–4), 240–258.

Oliver, J. (1984). *Delimitation and analysis of homogeneous rainfall regions in the South-Eastern Traansvaal* (Unpublished master's thesis). University of Johannesburg, Johannesburg.

Oliver, J. E. (1980). Monthly precipitation distribution: A comparative index. *The Professional Geographer*, *32*(3), 300–309.

Pascale, S., Lucarini, V., Feng, X., Porporato, A., & Hasson, S. (2014). Analysis of rainfall seasonality from observations and climate models. *Climate Dynamics*, *44*(11–12), 3281–3301.

Philippon, N., Rouault, M., Richard, Y., & Favre, A. (2012). The influence of ENSO on winter rainfall in South Africa. *International Journal of Climatology*, *32*(15), 2333–2347.

Quick, L. J., Chase, B. M., Wündsch, M., Kristen, K. L., Chevalier, M., Mäusbacher, R., … Haverzettl, T. (2018). A high-resolution record of Holocene climate and vegetation dynamics from the southern Cape coast of South Africa: Pollen and microcharcoal evidence from Eilandvlei. *Journal of Quaternary Science*, *33*, 1–14.

Rajah, K., O'Leary, T., Turner, A., Petrakis, G., Leonard, M., & Westra, S. (2014). Changes to the temporal distribution of daily precipitation. *Geophysical Research Letters*, *41*(24), 8887–8894.

Rana, S., McGregor, J., & Renwick, J. (2015). Precipitation Seasonality over the Indian subcontinent: An evaluation of gauge, reanalyses, and satellite retrievals. *Journal of Hydrometeorology*, *16*(2), 631–651.

Raziei, T. (2017). An analysis of daily and monthly precipitation seasonality and regimes in Iran and the associated changes in 1951–2014. *Theoretical and Applied Climatology*, *130*, 1–22.

Sangüesa, C., Pizarro, R., Ibañez, A., Pino, J., Rivera, D., García-Chevesich, P., & Ingram, B. (2018). Spatial and temporal analysis of rainfall concentration using the Gini index and PCI. *Water*, *10*(2), 112.

Schulze, R. E., & Kunz, R. P. (1997) Rainfall seasonality. In R. E. Schulze, M. Maharaj, S. D. Lynch, B. J. Howe, & B. Melvil-Thompson (Ed.), *South African atlas of agrohydrology and –climatology WRC report TT82/96* (pp. 39–40). Pretoria: Water Research Commission.

Schulze, R. E., & Maharaj, M. (2007). Rainfall seasonality. In R. E. Schulze (Ed.), *South African atlas of climatology and agrohydrology WRC report 1489/1/06* (pp. 39–40). Pretoria: Water Research Commission.

Schumann, T. E. W., & Hofmeyr, W. L. (1938). The partition of a region in rainfall districts: With special reference to South Africa. *Quarterly Journal of the Royal Meteorological Society*, *64*(276), 484–488.

Sousa, P. M., Blamey, R., Reason, C., Ramos, A. M., & Trigo, R. M. (2018). The "Day Zero" Cape Town drought and the poleward migration of moisture corridors. *Environmental Research Letters*. doi:10.1088/1748-9326/aaebc7

South African Weather Bureau. (1949). *District rainfall for the union of South Africa*. (W.B. 6). Pretoria: Government Printer.

South African Weather Bureau. (1957). *Climate of South Africa*. Part 4, Rainfall maps (W.B. 22). Pretoria: Government Printer.

South African Weather Bureau. (1960). *Climate of South Africa*. Part 5, District rainfall (W.B. 23). Pretoria: Government Printer.

South African Weather Bureau. (1965). *Climate of South Africa*. Part 8, General Survey (W.B. 28). Pretoria: Government Printer.

South African Weather Bureau. (1972). *Climate of South Africa*. Part 10, General Survey (W.B. 35). Pretoria: Government Printer.

Stone, A. E. (2014). Last Glacial Maximum conditions in southern Africa: Are we any closer to understanding the climate of this time period? *Progress in Physical Geography*, *38*(5), 519–542.

Taljaard, J. J., & Steyn, P. C. L. (1991) *Relationship between atmospheric circulation and rainfall in the South African region* (Technical Paper No. 24). Pretoria: Government Print.

Tennant, W. J., & Hewitson, B. C. (2002). Intra-seasonal rainfall characteristics and their importance to the seasonal prediction problem. *International Journal of Climatology*, *22*(9), 1033–1048.

Truc, L., Chevalier, M., Favier, C., Cheddadi, R., Meadows, M. E., Scott, L., … Chase, B. M. (2013). Quantification of climate change for the last 20,000 years from Wonderkrater, South Africa: Implications for the long-term dynamics of the Intertropical Convergence Zone. *Palaeogeography, Palaeoclimatology, Palaeoecology*, *386*, 575–587.

Tyson, P. D. (1977). The enigma of changing world climates. *South African Geographical Journal*, *59*(2), 77–116.

Tyson, P. D. (1978). Rainfall changes over South Africa during the period of the meteorological record. In M. J. A. Werger (Ed.), *Biogeography and ecology of Southern Africa* (pp. 55–69). Australia: The Hague.

Tyson, P. D. (1981). Atmospheric circulation variations and the occurrence of extended wet and dry spells over Southern Africa. *Journal of Climatology*, *1*(2), 115–130.

Tyson, P. D. (1986). *Climatic change and variability in Southern Africa*. Cape Town: Oxford University Press.

Tyson, P. D., Dyer, T. G. J., & Mametse, M. N. (1975). Secular changes in South African rainfall: 1880 to 1972. *Quarterly Journal of the Royal Meteorological Society*, *101*(430), 817–833.

Tyson, P. D., & Preston-Whyte, R. A. (2000). *The weather and climate of Southern Africa*. Cape Town: Oxford University Press Southern Africa.

Van Heerden, J., Terblanche, D. E., & Schulze, G. C. (1988). The southern oscillation and South African summer rainfall. *International Journal of Climatology*, *8*(6), 577–597.

Walker, N. D. (1989). *Seas surface temperature-rainfall relationships and associated ocean-atmosphere coupling mechanisms in the southern African region*. (Unpublished doctoral dissertation). University of Cape Town, Cape Town.

Walsh, R. P. D., & Lawler, D. M. (1981). Rainfall seasonality: Description, spatial patterns and change through time (British Isles, Africa). *Weather*, *36*(7), 201–208.

Wellington, J. H. (1955). *Southern Africa: A geographical study*. Volume 1: Physical Geography. Cambridge: Cambridge University Press.

Zhang, L. J., & Qian, Y. F. (2003). Annual distribution features of precipitation in China and their interannual variations. *Acta Meteorologica Sinica*, *17*(2), 146–163.

2.3 RAINFALL SEASONALITY SHIFTS AND PROJECTIONS

2.3.1 THE USE OF RAINFALL SEASONALITY METRICS TO QUANTIFY CHANGE AND VARIABILITY GLOBALLY

Climate change has not only altered the overall magnitude of rainfall but also its seasonal distribution and inter-annual variability worldwide (IPCC, 2013, 2018). As previously noted, literature has produced a confounding number of metrics to quantify rainfall seasonality (Figure 2.1). In investigations regarding inter-annual variability and long-term time series trends of rainfall seasonality, many of these metrics have been applied globally (Figure 2.2), either across or for areas within the tropics (e.g. Feng *et al.*, 2013), Europe (e.g. Cortesi *et al.*, 2012; Coscarelli & Caloiero, 2012; Vyshkvarkova & Voskresenkaya, 2014), Asia (e.g. Tao *et al.*, 2018; Deng *et al.*, 2019; Zhang *et al.*, 2019), the Middle East (e.g. Mathbout, 2015; Yeşilırmak & Atatanır 2016; Raziei, 2017), North America (e.g. Pryor & Schoof, 2008; Pal *et al.*, 2013; Gitau, 2016), South America (e.g. Vélez *et al.*, 2018; Meseguer-Ruiz *et al.*, 2019; Sarricolea *et al.*, 2019), and Africa (e.g. Adelekan & Adegebo, 2014; Ezenwaji *et al.*, 2017; Salhi *et al.*, 2019). In recent years numerous seasonality metrics have been developed (e.g. Zhang & Qian, 2003; Martin-vide *et al.*, 2004; Liebmann *et al.*, 2012; Feng *et al.*, 2013), and as such there has been an increasing number of studies which have investigated shifts in rainfall seasonality particularly since 2010 (Figure 2.2). However, given the concerns surrounding changes (Pascale *et al.*, 2016; IPCC, 2018), under anthropogenically induced climate change, in the seasonal characteristics of rainfall, there are still relatively few studies regarding rainfall seasonality shifts highlighting a need for continued research (Figure 2.2). Commonly applied metrics to quantify rainfall seasonality shifts in this body of literature include the DSI and RE, Daily Precipitation Concentration Index (DPCI), PCI, onset and cessation dates, and SI, metrics previously noted under *Section 2.2* (Figure 2.1). Recently, seasonality metrics have been incorporated into climate modelling endeavors in order to produce projections on more than just rainfall amount and to assess the performance of climate models in simulating rainfall (e.g Dunning *et al.*, 2016, 2018; Li *et al.*, 2016; ul Hasson, 2016; Kumi & Abiodun, 2018).

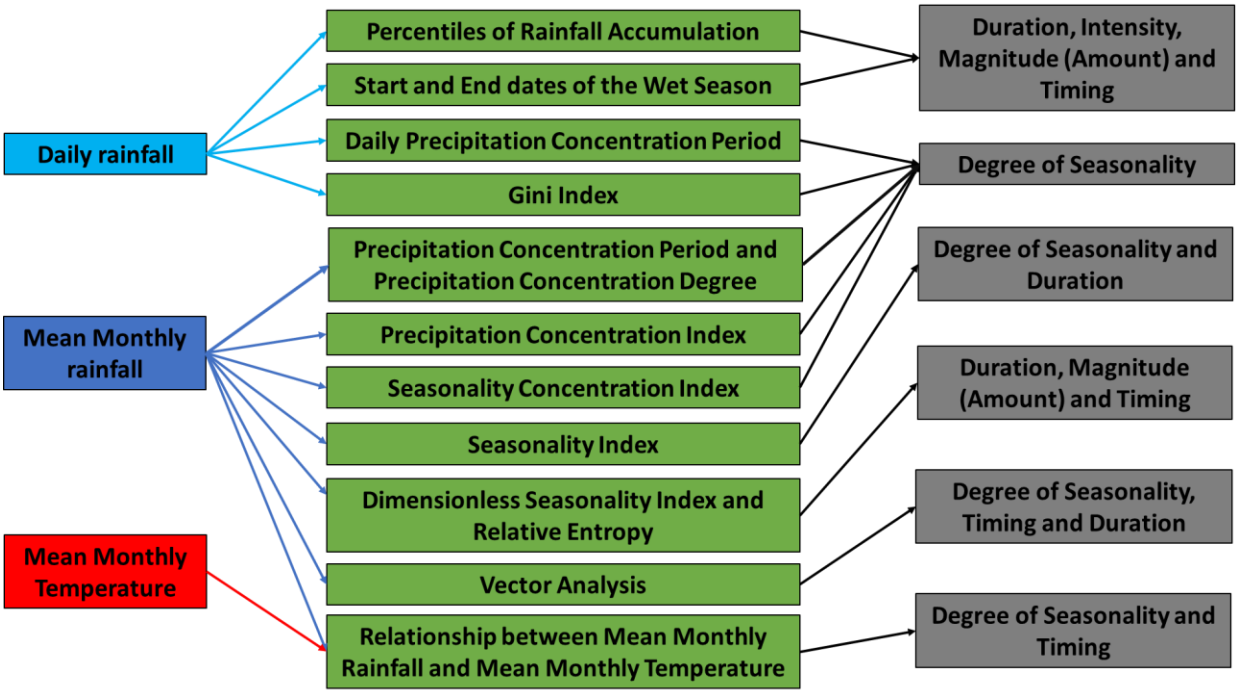


Figure 2.1: Flow diagram of selected seasonality metrics, input data and output measurements of seasonality which contribute to describing rainfall seasonality. The percentiles of accumulation represents the approaches of Ilesanmi (1972a, b) and Pryor and Schoof (2008). The start and end dates represent the approaches of Dunning *et al.* (2016) and Stern *et al.* (1982). The daily precipitation concentration period represents the approach of Martin-Vide (2004). The Gini index represents the approach of Rajah *et al.* (2014). The Precipitation Concentration Period and Precipitation Concentration Degree representes the approach of Zhang and Qian (2003). The precipitation concentration index represents the approach of Oliver (1980). The seasonality concentration index represents the approach of Fujita (2008). The seasonality index represents the approach of Walsh and Lawler (1981). The dimensionless seasonality index and relative entropy represents the approach of Feng *et al.* (2013). The vector analysis represents the approach of Markham (1970). The relationship between mean monthly rainfall and mean monthly temperature represents the approach of Thackeray and Fitchett (2016).

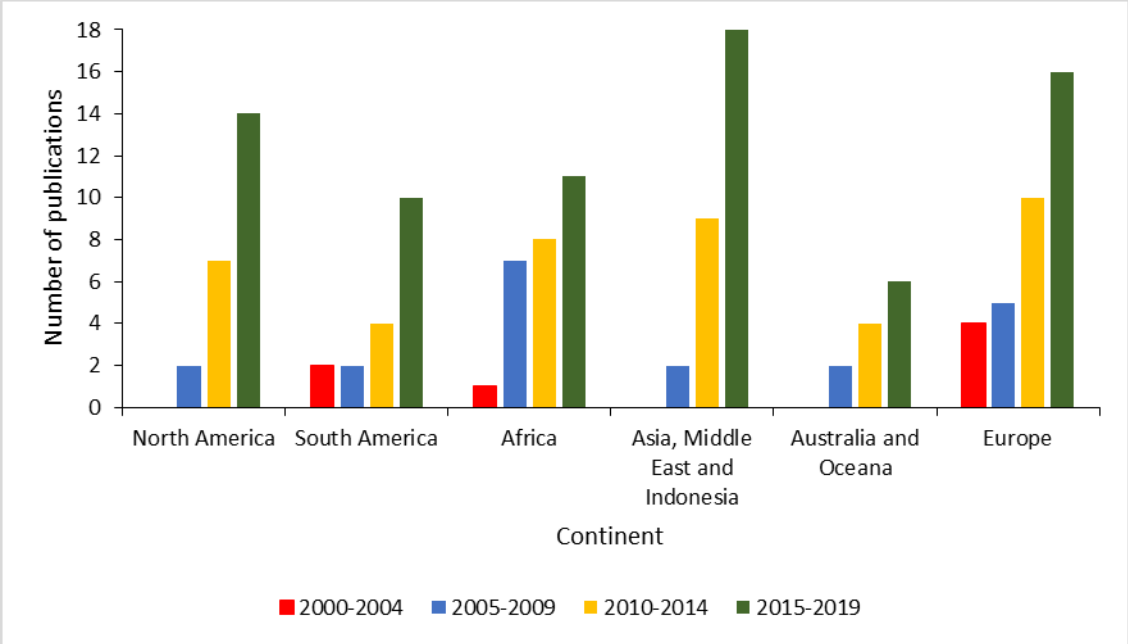


Figure 2.2: Number of publications from 2000-2019 per continent which have investigated rainfall seasonality shifts using seasonality metrics captured under *Figure 2.1*. Data derived from Google Scholar, Science Direct and Web of Knowledge.

Investigations regarding rainfall seasonality are considered to be particularly important as it has been reported that statistics on annual, seasonal and monthly rainfall amount do not provide enough information on rainfall in general (Feng *et al.*, 2013; Ma & Zhou, 2015). However, Feng *et al.* (2013) note that changes in monthly and annual rainfall amount are particularly useful when considering agreement with trends in seasonality metrics. This is because rainfall changes are considerably complex, and to understand rainfall modifications it is important to capture all aspects of change and variability over multiple temporal scales (Feng *et al.*, 2013; Pascale *et al.*, 2015, 2016; Raziei, 2017). For instance, changes in the annual distribution (i.e. seasonality) of rainfall have been noted as a consequence of changes in rainfall amount (over monthly to annual scales), and also without changes in rainfall amount (e.g. Pryor & Schoof, 2008; de Luis *et al.*, 2011; Cortesi *et al.*, 2012; Feng *et al.*, 2013; Ma & Zhou, 2015; Huang *et al.*, 2018; Deng *et al.*, 2019).

Studies considering historical shifts, for temporal periods of up to 100 years, in rainfall seasonality have typically used either rain gauge, reanalyses or satellite derived products of rainfall over daily or monthly scales. Although most studies note many statistically insignificant trends, from these

studies it is evident that there have been significant changes in rainfall seasonality globally. For example, using the PCI for the period of 1946-2005 de Luis *et al.* (2011) note a general, statistically insignificant increase in annual rainfall seasonality across Spain, and over a seasonal scale a statistically significant increasing trend in wet season rainfall seasonality was particularly noted to contribute to the annual change. In China, as an example, Tao *et al.* (2018) note a general increase in rainfall seasonality using the SI, where this increase was statistically related, particularly for the statistically significant areas, to an increase in the frequency of extreme rainfall. In Senegal, Camberlin and Diop (2003) note a decrease in the duration of the wet season as a result of delayed onset dates.

Across most of these studies it is typically highlighted that rainfall seasonality may be considerably variable from year to year and that any trends in rainfall seasonality are rather complex, where these are not likely to be caused by one single factor and are probably related to, among others: global to local scale atmospheric circulation patterns, sea surface temperature (SST) anomalies, rising temperatures, greenhouse gas concentrations as well as local geographical factors (e.g. de Luis *et al.*, 2010a; Feng *et al.*, 2013; Deng *et al.*, 2019; Zhang *et al.*, 2019). This highlights that any trends and variability in rainfall seasonality are particularly location dependent. As an example, Ma and Zhou (2015) suggest that regional drivers of trends and variability in rainfall seasonality across China include, among others, land use change, irrigation, urbanisation, and natural internal climate variability. Similarly, Raziei (2017) highlights that in Iran topography may either enhance or reduce the influence of regional scale drivers of rainfall seasonality change and variability. Additionally, Zhang *et al.* (2019) note the role of latitude, longitude, altitude and the teleconnections with large scale circulation patterns (including El Niño Southern Oscillation (ENSO), the Pacific Decadal Oscillation, the Arctic Oscillation, the Indian Ocean Dipole and the North Atlantic Oscillation) in change and variability of annual PCI. Despite the vast knowledge on the drivers behind rainfall seasonality changes and variability, many studies do not highlight the drivers behind changes observed, particularly because so many statistically insignificant trends are detected which are assumed to represent no change, and hence many studies conclude there and do not explore further (e.g. Livada & Asimakopoulos, 2005; Elagib, 2011; Cortesi *et al.*, 2012; Coscarelli & Caloiero, 2012; Gitau, 2016; Suepa *et al.*, 2016; Bari *et al.*, 2017; Sharma & Singh, 2017; Huang *et al.*, 2018;

Sangüesa *et al.*, 2018; Salhi *et al.*, 2019). However, it may be that there are changes instead in the inter-annual variability of rainfall seasonality (e.g. Camberlin & Diop, 2003; Lana *et al.*, 2004; de Luis *et al.*, 2011; Feng *et al.*, 2013; Mathbout, 2015; Raziei, 2017), or over a longer temporal period there may be a stronger signature of change (e.g. de Luis *et al.*, 2011). Several studies have also detected abrupt shifts, especially from the 1970s, in rainfall seasonality which are noted to indicate changes in inter-annual variability (e.g. Gong & Ho, 2002; Camberlin & Diop, 2003; Mathbout, 2015). Considering the variability of rainfall seasonality for the period of 1930-2002, Feng *et al.* (2013) quantify an increased variability in conjunction with changing seasonality trends which is suggested to have contributed to an increasing uncertainty in the timing of rainfall across the tropics.

Indeed, there has been an increase in the number of studies incorporating seasonality metrics in climate modelling research (e.g. Li *et al.*, 2006; Rauscher *et al.*, 2007; Biasutti & Sobel, 2009; Pryor & Schoof, 2008; Guenang & Kamga, 2012; Polson *et al.*, 2013; Pascale *et al.*, 2015, 2016; Demirel & Moradkhani, 2016; Dunning *et al.*, 2016, 2018; Li *et al.*, 2016; ul Hasson, 2016; Kumi & Abiodun, 2018); seasonality metrics which have been incorporated in these studies include DSI and RE, SI, and various metrics on the timing of start and end dates of the wet season. It has been suggested by many that accurate and reliable identification of rainfall seasonality regimes, using seasonality metrics, is necessary to assess the performance of both GCMs and RCMs in simulating current climate and in projecting future climate (e.g. Rauscher *et al.*, 2006; Pascale *et al.*, 2015; Demirel & Moradkhani, 2016; Li *et al.*, 2016). Studies exploring modifications in the seasonal cycle of rainfall, note that subtropical arid and semi-arid regions are expected to get drier, whereas wet equatorial and high latitude regions are expected to get wetter (Chou *et al.*, 2013; IPCC, 2013), which is likely to influence rainfall seasonality. This is projected as a consequence of a widening of the Hadley cell (Seidel *et al.*, 2008; IPCC, 2013, 2018), and a consequent poleward tendency of the subtropics as well as tropical and extra tropical storm tracks (IPCC, 2013, 2018; Tamarin-Brodsky & Kaspi, 2017).

In considering global rainfall seasonality trends, both projected and observed, it is widely agreed that the seasonality of rainfall has and will exhibit marked changes (e.g. Pryor & Schoof, 2008; Cortesi *et al.*, 2012; Feng *et al.*, 2013; Li *et al.*, 2016; Pascale *et al.*, 2016; Raziei, 2017; Dunning *et*

al., 2018; Deng *et al.*, 2019; Sarricolea *et al.*, 2019). Across the various studies, globally or smaller regions thereof, which have used different seasonality metrics for different temporal periods, there is much spatial agreement in the direction of change tending towards increasingly seasonal rainfall across most regions, as will be discussed in the paragraphs below. The magnitude of change is not consistent across these studies; however, although not impossible it is difficult to compare the magnitude of seasonality across different metrics, even without considering changes (Raziei, 2017). This is due to the fact that different seasonality metrics through quantification capture different definitions and different characteristics of rainfall seasonality (Feng *et al.*, 2013; Raziei *et al.*, 2017; Roffe *et al.*, 2019).

To consider the agreement in seasonality trends globally, the direction of change is thus considered here for some studies across the world. Where the direction of change does not agree, this may be attributed to the fact that different metrics of rainfall seasonality have been used, and this may also be due to differences in the spatial and temporal characteristics of input datasets (Li *et al.*, 2016; Raziei, 2017; Deng *et al.*, 2019). Over a global scale for instance, the studies of Li *et al.* (2016) and Pascale *et al.* (2016) display remarkably different results. Li *et al.* (2016) note a predominant decrease, with scattered regions of increasing trends in SI for the period 1948-2005, while Pascale *et al.* (2016) mainly project (2080-2100) increasing RE implying an increase in the seasonality of rainfall also with some decreasing trends RE trends, projected across high latitudes (>50° N and S), which are suggestive of an increase in the number of wet months.

Across the tropics using the DSI Feng *et al.* (2013) quantify a complex pattern of seasonality changes in seasonality for the period of 1930-2002, where this is somewhat consistent with the observed results presented by Li *et al.* (2016) and the projected trends across the African tropics presented by Dunning *et al.* (2018) based on start and end dates of the wet season. The pattern of change Feng *et al.* (2013) documented across the tropics is also relatively consistent with some of the model ensembles from Pascale *et al.* (2016).

Across Europe using the DPCI for the period of 1971-2010, Cortesi *et al.* (2012) detected predominantly increasing trends with some smaller regions of decreasing trends across western Europe, where an increase is indicative of an increase in the degree of seasonality with rain days

tending towards being concentrated in a shorter temporal period. Similarly, Vyshkvarkova and Voskresenkaya (2014) detect reductions in PCI across Ukraine for the period of 1961-1990. In agreement with the results of Cortesi *et al.* (2012), Pascale *et al.* (2016) project an increase in RE across the entire Europe region, while Li *et al.* (2016) quantify increasing trends in SI mainly across western Europe and decreasing trends across the eastern regions. Similar to the results of Cortesi *et al.* (2012) across Greece, Italy, Portugal and Spain, the results of Sumner *et al.* (2001), Livada and Asimakopoulos (2005), Cannarozzo *et al.* (2006), and de Luis *et al.* (2010a, 2011) using either SI or PCI quantify mainly increases in the degree of seasonality.

Across Asia, the results for the trends in seasonality using either RE and DSI, PCI, and the start and end dates of the wet season also display much agreement (e.g. Cook & Buckley, 2009; Li *et al.*, 2011; Guhathakurta & Saji, 2013; Nair *et al.*, 2014; Luo & Zhang, 2015; Ma & Zhou, 2015; Li *et al.*, 2016; Pascale *et al.*, 2016; Suepa *et al.*, 2016; ul Hasson, 2016; Bari *et al.*, 2017; Huang *et al.*, 2018; Sahany *et al.*, 2018; Tao *et al.*, 2018; Deng *et al.*, 2019; Zhang *et al.*, 2019), however, this is not as strong as that displayed across Europe. Across Asia there is a predominant signal of increasing seasonality, while some of these studies have also detected small regions of decreasing trends in seasonality mainly across countries such as India (e.g. Guhathakurta & Saji, 2013; Sahany *et al.*, 2018) and China (Ma & Zhou, 2015; Deng *et al.*, 2019; Zhang *et al.*, 2019). A few studies have been conducted in the Middle East, yielding much agreement in trends which are indicative of increasing seasonality across a number of metrics including DPCI, SI, RE and DSI, PCI and precipitation concentration period and degree (e.g. Mathbout, 2015; Li *et al.*, 2016; Pacale *et al.*, 2016; Yeşilırmak & Atatanır 2016; Raziei, 2017).

Across North America, the projected results of Pascale *et al.* (2016) and observed results of Li *et al.* (2016) are in complete disagreement, where Li *et al.* (2016) quantified increasing trends for SI in the northern regions and decreasing trends across the southern regions. Additionally, the results of Pal *et al.* (2013), and Pryor and Schoof (2008) were also contrasting using different seasonality metrics. Using SI Pryor and Schoof (2008) quantified mainly increasing trends, while Pal *et al.* (2013) using start and end dates of the wet season note trends towards a longer wet season. The majority of studies across South America using PCI, SI, and RE and DSI display much agreement where there are predominantly increasing, observed and projected, trends with

smaller regions of decreasing trends mainly in the northern regions of the continent (e.g. Feng *et al.*, 2013; Li *et al.*, 2016; Pascale *et al.*, 2016; Sangüesa *et al.*, 2018; Vélez *et al.*, 2018; Meseguer-Ruiz *et al.*, 2019; Sarricolea *et al.*, 2019).

Lastly, across Africa there is also much agreement in the trends projected and observed using metrics such as SI, DSI and RE, PCI and the start and end dates of the wet season, where there is again a dominant trend towards an increase in the degree of seasonality with smaller regions mainly across central Africa displaying decreasing trends (e.g. Hulme, 1992; Oladipo & Kyari, 1993; Bello, 1998; Tarhule & Woo, 1998; Camberlin & Diop, 2003; Odekunle & Adejuwon, 2007; Kniveton *et al.*, 2009; Elagib, 2011; Feng *et al.*, 2013; Adelekan & Adegebo, 2014; Li *et al.*, 2016; Pascale *et al.*, 2016; Ezenwaji *et al.*, 2017; Dunning *et al.*, 2018; Salhi *et al.*, 2019).

2.3.2 SOUTHERN AFRICA

2.3.2.1 THE CASE FOR INTERROGATION OF RAINFALL SEASONALITY SHIFTS DURING THE LATE QUATERNARY: LESSONS FROM PALAEO RECORDS

There have been considerable efforts to investigate rainfall seasonality and the shifts thereof across southern Africa for the late Quaternary (e.g. Chase and Meadows, 2007; Norström *et al.*, 2009, 2014; Finné *et al.*, 2010; Stager *et al.*, 2012, 2013; Chase *et al.*, 2013, 2015, 2017; Truc *et al.*, 2013; Chevalier & Chase, 2015; Fitchett *et al.*, 2016, 2017b; Thackeray and Fitchett, 2016; Fitchett and Bamford, 2017; Chase & Quick, 2018; Faith *et al.*, 2019). Most studies exploring rainfall seasonality, particularly focusing on the shifts in rainfall zones, across the subcontinent have been based on either or a combination of proxy records of biomarkers, geomorphology, pollen, phytoliths, sediment properties, diatoms, coccoliths, micromammalian fossils, microcharcoal, and stable isotopes of carbon and nitrogen (e.g. Mills *et al.*, 2012; Chase *et al.*, 2013; Cordova, 2013; Fitchett *et al.*, 2016, 2017b; Thackeray & Fitchett, 2016; Weiser *et al.*, 2016; Fitchett & Bamford, 2017; Hahn *et al.*, 2017). Some attempts to reconstruct rainfall seasonality for the late Quaternary have incorporated or been based solely on climate modelling (e.g. Barrable *et al.*, 1998; Mills *et al.*, 2012; Engelbrecht *et al.*, Under Review). The studies exploring rainfall zone shifts have been particularly useful in investigations regarding the dynamics of the ITCZ and Southern Hemisphere Westerlies, which have been identified as underlying drivers of synoptic

scale and essentially rainfall seasonality shifts throughout the late Quaternary periods (Fitchett & Bamford, 2017).

Key to understanding the dynamics of the ITCZ and Westerlies have been the conceptual models developed during the early years of Quaternary research across southern Africa (e.g. Van Zinderen Bakker, 1976; Tyson, 1986; Cockroft *et al.*, 1987; Chase & Meadows, 2007; Fitchett & Bamford, 2017; Fitchett *et al.*, 2017c; Neumann & Scott, 2018). These early conceptual models are, to an extent, based on the contemporary seasonal dynamic between the ITCZ and Westerlies (Chase & Meadows, 2007). Based on these models it has been hypothesised that during glacial and neoglacial periods, expansion of Antarctic sea ice extent would have caused the polar high-pressure cell to expand, resulting in the Westerlies being displaced equatorward, and due to diminished equatorial heating the Hadley cell would have contracted (Van Zinderen Bakker, 1976; Cockroft *et al.*, 1987; Barrable *et al.*, 1998; Stuut *et al.*, 2004; Chase & Meadows, 2007; Fitchett *et al.*, 2017c; Neumann & Scott, 2018). This would have influenced the climate over southern Africa through frontal rainfall which may have occurred both more frequently and with greater intensity, thereby increasing the spatial extent of the WRZ (Van Zinderen Bakker, 1976; Cockroft *et al.*, 1987; Barrable *et al.*, 1998; Stuut *et al.*, 2004; Chase & Meadows, 2007; Fitchett *et al.*, 2017c). Considering interglacial periods, the opposite is hypothesised where reduced Antarctic sea ice extent would have resulted in contraction of the polar high-pressure cell, a poleward displacement of the Westerlies, and due to increased equatorial heating the Hadley cell would have expanded with a resultant southward displacement of the ITCZ and associated tropical easterlies (Van Zinderen Bakker, 1976; Cockroft *et al.*, 1987; Barrable *et al.*, 1998; Stuut *et al.*, 2004; Chase & Meadows, 2007; Stager *et al.*, 2012; Chase *et al.*, 2015; Fitchett *et al.*, 2017c; Neumann & Scott, 2018). This would have influenced the subcontinent through more frequent and more intense convective rainfall, and hence the extent of the SRZ would have been larger (Van Zinderen Bakker, 1976; Cockroft *et al.*, 1987; Barrable *et al.*, 1998; Stuut *et al.*, 2004; Chase & Meadows, 2007; Stager *et al.*, 2012; Chase *et al.*, 2015; Fitchett *et al.*, 2017c). Since the LGM and during the Holocene, an interglacial period, the WRZ has reduced in size (Fitchett & Bamford, 2017), where agreement on the contemporary spatial extent of the WRZ is largely restricted to the southwestern Cape and western coast (Figure 2.3).

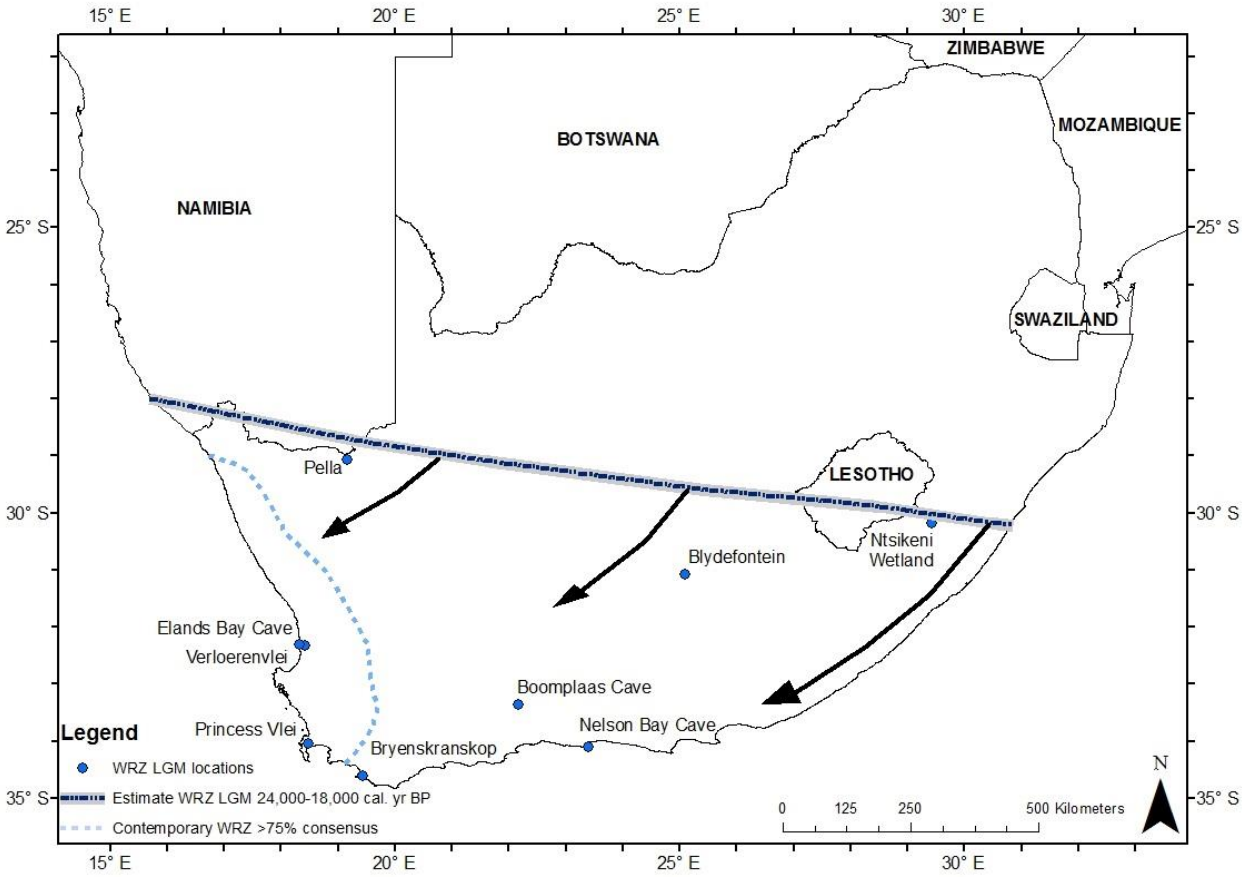


Figure 2.3: Selected locations (Cowling *et al.*, 1999; Parkington *et al.*, 2000; Lim *et al.*, 2016; Thackeray & Fitchett, 2016; Combrink, 2017; Faith *et al.*, 2019) understood to have been characterised by a predominant WRZ regime during the LGM (24,000-18,000 cal. yr BP). The dark blue boundary represents the region estimated to have been under a WRZ regime during the LGM, with the WRZ LGM boundary shown to have progressively reduced to the estimated contemporary WRZ region. The estimated contemporary WRZ boundary represents the area known to demonstrate at least 75% consensus in the classification of WRZ from previous published maps captured under *Figure 2* of *Section 2.2*.

Recent studies investigating the extent of rainfall zones have led to some consensus that during the late Pleistocene and Holocene, the WRZ extent fluctuated and expanded in both northerly and easterly directions (e.g. Carr *et al.*, 2006; Chase & Meadows, 2007; Norström *et al.*, 2009, 2014; Mill *et al.*, 2012; Stager *et al.*, 2012; Thackeray & Fitchett, 2016; Fitchett & Bamford, 2017; Faith *et al.*, 2019; Figure 2.3), however, the geographic extent of this has not been fully quantified (Fitchett and Bamford, 2017). This is partly because of the difficulties in obtaining direct information pertaining to rainfall seasonality, as proxies instead reflect broader fluctuations in total annual precipitation which is not necessarily a reflection of seasonality and rather a reflection

of moisture (Chase & Meadows, 2007; Chase *et al.*, 2015, 2017 Engelbrecht *et al.*, Under Review). Few locations have been confidently captured as WRZ for the LGM (Figure 2.3). Through these locations an estimated extent of the WRZ may be drawn (Figure 2.3), where this particularly highlights that there may have been a greater shift in the eastern extent of the WRZ. Through dynamic downscaling, Engelbrecht *et al.* (Under review) similarly quantify relatively no change in the northern extent (i.e. quantified during the LGM at ~22-23°S and ~23°S presently) and a larger shift in the eastern extent (i.e. quantified during the LGM at ~22-24°E and ~20°E presently) of the WRZ.

The earliest attempt to reconstruct the WRZ was during 1976, where Van Zinderen Bakker suggested that the WRZ extend north to ~24°S and east into the Free State. Later Van Zinderen Bakker (1983) suggested that the WRZ did not extend that far north. Additionally, Cockroft *et al.* (1987) suggest that in the western parts of the country the WRZ extended up to ~25°S and in the eastern regions up to ~30°S. More recently, Fitchett and Bamford (2017) argue a northward shift in the extent of the Westerlies to ~28°S during the Pleistocene-Holocene transition, and hence it is also suggested that the WRZ would not have extended further north than ~28°S. Neumann and Scott (2018) recently suggest that the WRZ may have only extended north to southern Namibia. Pollen, diatom and phytolith records as well as palaeogeomorphological evidence of periglacial features for the Pleistocene from Nörstrom *et al.* (2009, 2014), at Braamhoek wetland in the Free State, and Mills *et al.* (2012), in the Lesotho highlands of eastern Lesotho, confirm a greater influence and increased intensity of mid-latitude cyclones associated with a northward shift of the Westerlies. When considering the smallest extent of the WRZ, there are no records from the contemporary southwestern Cape WRZ which suggest that this region was influenced by SRZ conditions at any point during the late Pleistocene or Holocene or even earlier (Chase & Meadows, 2007; Fitchett & Bamford, 2017). Pollen, microcharcoal, and stable carbon and nitrogen isotope records extracted from a hyrax midden at Swartruggens Mountains in the Western Cape provide evidence that fluctuations in the easterly wave are linked to variability in summer rainfall, and essentially the SRZ extent (Chase *et al.*, 2015). Additionally, diatom records from Lake Sibaya in KwaZulu-Natal (Stager *et al.*, 2013), and pollen records from Wonderkrater spring mound in Limpopo (Truc *et al.*, 2013), have been used to investigate the role of ITCZ shifts in SRZ variability

since the LGM. There is, however, still ongoing debate regarding the nature and extent of the shifts in the position of the Southern Hemisphere Westerlies and the ITCZ (Fitchett *et al.*, 2017c), where it is held that investigation into the rainfall seasonality zone shifts provide crucial evidence for synoptic scale shifts (e.g. Carr *et al.*, 2006; Chase *et al.*, 2017; Fitchett & Bamford, 2017).

Work during recent years has highlighted that although applicable broadly, the conceptual model hypotheses fail to explain climatic dynamics over smaller temporal and spatial scales (e.g. Norström *et al.*, 2009, 2014; Chase *et al.*, 2013, 2015, 2017; Stone, 2014; Fitchett *et al.*, 2016, 2017b; Chase & Quick, 2018; Faith *et al.*, 2019). These studies highlight the heterogeneity of moisture records on precipitation amount and records on seasonality, where these records are particularly location specific (Fitchett & Bamford, 2017). Over local scales there is consensus that synoptic scale changes are related to dynamics in the Agulhas and Benguela currents, and also to topographic variability (e.g. Carr et al., 2006; Norström *et al.*, 2009, 2014; Chase *et al.*, 2013, 2015, 2017; Chevalier & Chase, 2015; Fitchett *et al.*, 2016, 2017b; Chase & Quick, 2018; Faith *et al.*, 2019). For instance, Fitchett *et al.* (2017b) note delays in wet and dry periods when comparing moisture inferences from their study to those from lower altitude Drakensberg sites, at Braamhoek (Norström *et al.*, 2009, 2014; Finné *et al.*, 2010) and Mahwaqa Mountain (Neumann *et al.*, 2014). These differences are attributed to the influence of the Great Escarpment in inducing orographic rainfall (Fitchett *et al.*, 2017b), a feature also known to strongly govern the spatial variability in contemporary rainfall distribution by controlling the transfer of moist air from the Indian Ocean (Tyson & Preston-Whyte, 2000).

Efforts to reconstruct rainfall seasonality and the shifts thereof have mainly been based on pollen records (e.g. Scott & Nyakale, 2002; Norstöm *et al.*, 2009, 2014; Neumann *et al.*, 2014; Fitchett *et al.*, 2016, 2017b), being the most commonly used proxy across southern Africa (Fitchett & Bamford, 2017; Knight & Fitchett, 2019; Fitchett, 2019a). Rainfall seasonality reconstructions based on pollen records have followed a number of avenues. Studies have reconstructed vegetation patterns to detect periods when pollen specific to WRZ flora are evident in records from locations in the contemporary SRZ (e.g. Scott *et al.*, 2004; Neumann *et al.*, 2014). Many studies have applied the fossil pollen ratio of Asteraceae: Poaceae to detect shifts in the strength of rainfall seasonality (e.g. Norström *et al.*, 2009, 2014; Fitchett *et al.*, 2016, 2017b); most of these

studies based on this ratio have adopted a multi-proxy approach using proxies such as diatoms, phytoliths and sediment properties to validate the shifts detected in the pollen records. Studies have also used probability density functions and principal component analysis to compare contemporary vegetation distributions and fossil pollen records to investigate shifts in the dominant tropical and temperate rain-bearing synoptics (e.g. Truc *et al.*, 2013; Chevalier & Chase, 2015). Recently more studies investigating rainfall seasonality shifts have been based on diatom records, again mainly to corroborate pollen reconstructions of rainfall seasonality dynamics (e.g. Finné *et al.*, 2010; Stager *et al.*, 2012; Fitchett *et al.*, 2016, 2017b). Hyrax middens containing stable isotopes of carbon and nitrogen have also been used to infer shifts in rainfall seasonality (Chase *et al.*, 2015). Although these approaches to investigate rainfall seasonality shifts have been invaluable in understanding and reconstructing past rainfall seasonality and the shifts thereof, few of these approaches have been objectively assessed on their accuracy in discriminating between contemporary SRZ and WRZ conditions (Fitchett & Bamford, 2017), which is key to understanding seasonality shifts since the LGM, or even earlier, to present (Thackeray & Fitchett, 2016).

More recently efforts to reconstruct rainfall seasonality have focused on assessing these approaches used to investigate rainfall seasonality. Fitchett and Bamford (2017) focused on objectively assessing the ability of the commonly used Asteraceae: Poaceae pollen ratio, developed by Coetzee (1967), in discriminating between SRZ and WRZ conditions across southern Africa for the last ~20,000 cal. yr BP, where it was confirmed that this ratio accurately discriminates between SRZ and WRZ conditions. Thackeray and Fitchett (2016) quantified rainfall seasonality shifts from ~80,000 cal. yr BP to present using fossil rodent distributions, from Boomplaas cave in the Western Cape, in comparison to their contemporary distributions and climatic regimes. To quantify contemporary rainfall regimes Thackeray and Fitchett (2016) developed a seasonality metric based on the relationship between temperature and rainfall (Figure 2.1), and through testing this metric on meteorological records in the SRZ, WRZ and YRZ it was demonstrated that this index statistically discriminates between WRZ and SRZ conditions in the contemporary record. However, even though this approach has been tested for its use in the contemporary record, it is yet to be objectively assessed across the entire region of southern Africa (Fitchett & Bamford, 2017). Given this, debates surrounding late Quaternary research will therefore benefit from

efforts to explore rainfall seasonality across southern Africa using instrumental records (Fitchett & Bamford, 2017). Such efforts will also be important for climate modelling to understand synoptic circulation changes, where the specifics remain largely unresolved for southern Africa (Fletcher & Moreno, 2012). This is particularly important given the concern that there may be a greater incidence of drought in the WRZ with a reduction in the spatial extent, and for the SRZ there may be an increase in seasonality which may result in a higher amount of summer rainfall possibly having resultant effects on the intensity of rainfall (Christensen *et al.*, 2007; Engelbrecht *et al.*, 2009; Fitchett *et al.*, 2017c; Engelbrecht *et al.*, Under Review; Figure 2.3). Since the YRZ is influenced by atmospheric circulation and weather processes affecting both the SRZ and the WRZ, it is more difficult to interpret changes as they may either positively correlate with the SRZ (given the expected tropical circulation changes noted under *Sections 2.3.1 and 2.3.2.3*) or changes may be inversely correlated or not even correlated at all (Tyson & Preston-Whyte, 2000). Compared to late Quaternary investigations into rainfall seasonality shifts across southern Africa, few studies have explored contemporary rainfall seasonality changes. Studies which have explored contemporary seasonality shifts are discussed under the section of the literature review which follows.

2.3.2.2 DRAWING ON RAINFALL SEASONALITY SHIFTS AND VARIABILTY IN THE CONTEMPORARY RECORD

Within southern Africa, rainfall variability and changes are considerably complex and are strongly influenced by the Great Escarpment, creating an inland plateau, and the surrounding cold Benguela current of the Atlantic Ocean and warm Agulhas Current of the Indian Ocean (Fauchereau *et al.*, 2003; Jury, 2013, 2018). Although rainfall trends over the subcontinent show little coherence given the large spatial and temporal variability, notable changes have been detected (Jury, 2013, 2018). Against the background of spatially and temporally heterogeneous trends in rainfall across the subcontinent, knowledge on these trends are crucial for agriculture, water resource management and tourism, amongst other rainfall dependent activities, especially to develop adaptation strategies (Mphale *et al.*, 2014; Jury, 2018). It is known that changes in rainfall regimes will be most felt in arid and semi-arid regions of the world (Herrmann & Mohr,

2011; Feng *et al.*, 2013; IPCC, 2013), which includes most of southern Africa (Knight & Holmes, 2018). Despite this and the highly seasonal and diverse rainfall regimes evident across southern Africa, there remain only a few studies which have investigated trends and variability in rainfall seasonality characteristics for the contemporary record (e.g. Reason *et al.*, 2005; Tadross *et al.*, 2005a, 2007, 2009; Nel, 2009; Moeletsi *et al.*, 2011; Mupangwa *et al.*, 2011; Le Roux, 2015; Tongwane *et al.*, 2015; van Wilgen *et al.*, 2016; Lipsett, 2017; Botai *et al.*, 2018). For the purpose of this section of the literature review the studies on rainfall trends and variability across southern Africa will be structured into two main parts: 1) the studies which investigate trends and variability in terms of rainfall amount and seasonality characteristics, and 2) the studies which explore drivers behind the changes and variability in rainfall amount and seasonality characteristics. Although trends in rainfall amount are reported, the main focus of this section regards the trends in rainfall seasonality characteristics where the drivers of year-to-year variability in rainfall are also captured, but briefly, given that this is important to consider when exploring long-term trends in rainfall amount and seasonality (Fauchereau *et al.*, 2003; Tadross *et al.*, 2009).

Given that rainfall amount and seasonality across southern Africa have high spatial and temporal variability, studies exploring changes based on surface observations and/or gridded data products have observed few statistically significant and spatially coherent trends (e.g. Jury, 2013; MacKellar *et al.*, 2014; Kruger & Nxumalo, 2017; Jury, 2018). From numerous studies, it is suggested that across southern Africa inter-annual variability has increased since the 1970's, further contributing to quantifying few statistically significant and spatially coherent trends (e.g. Richard *et al.*, 2001; Fauchereau *et al.*, 2003; Tadross *et al.*, 2009; Phillipon *et al.*, 2012; Jury, 2013; Dieppois *et al.*, 2016). These inconsistencies can also be attributed to data quality and studies capturing different time frames and locations, where inconsistencies are not likely due to methodological differences (MacKellar *et al.*, 2014; Kruger & Nxumalo, 2017). On an annual scale, rainfall trends are known to be considerably heterogeneous in terms of direction and magnitude (Jury, 2013, 2018), however, results from the observed records of rainfall from Kruger (2006), MacKellar *et al.* (2014) and Kruger and Nxumalo (2017) are largely consistent, presenting predominantly decreasing trends in the eastern parts of the country and increasing trends in the western part of the country.

Trends in rainfall amount have also been detected over a seasonal scale, where seasonal groupings are typically as summer (December to February), autumn (March to May), winter (June to August) and spring (September to November). Trends in rainfall amount over this scale are also notably heterogeneous, however, some spatial patterns may be noted. Again, considering the studies across South Africa of MacKellar *et al.* (2014) and Kruger and Nxumalo (2017), trends for summer rainfall are somewhat consistent where increasing trends were mostly evident with some decreasing trends particularly across the eastern parts of the country. However, during winter the trends in rainfall amount were less consistent. Kruger and Nxumalo (2017) note increasing trends across the western parts of the country and decreasing trends in the eastern parts of the country, while MacKellar *et al.* (2014) note predominantly decreasing trends. During the transitional seasons of spring and autumn the trends between these studies were somewhat consistent, where predominantly increasing trends were quantified for spring and for autumn decreasing trends were quantified (MacKellar *et al.*, 2014; Kruger & Nxumalo, 2017). Although for spring rainfall totals, most of the resulting trends from both MacKellar *et al.* (2014) and Kruger and Nxumalo (2017) suggest a deceasing trend across the eastern parts of the country.

Some studies noting trends particularly during the transitional seasons have postulated that these are evidence for changes in rainfall seasonality (e.g. Hoerling *et al.*, 2006; Thomas *et al.*, 2007; Nel, 2009; Mazvimavi, 2010; Davis *et al.*, 2016; du Plessis & Scholms, 2017; Nicholson *et al.*, 2018; MacFayden *et al.*, 2018); for example, across the Western Cape for the period of ~1900-2014 an increase in October and a decrease in November rainfall amount along the southern coast portion is suggested to point towards an earlier onset date, whereas an increase in September and a decrease in October rainfall amount is suggested to indicate an earlier end date within the Mediterranean portion of South Africa. Additionally, in the Namaqualand for the period 1901-2009, Davis *et al.* (2016) detect no statistically significant changes in rainfall amount during any season, suggesting this is indicative of no seasonality changes. Although likely to be true, such analyses on rainfall amount offer no quantitative assessment on how rainfall seasonality may be changing. One would expect changing onset and cessation dates to be related to changes in rainfall amount at the beginning and end of the wet season (Dunning *et al.*, 2018), but to assume this may be overlooking the complexity of rainfall.

Over recent years studies have investigated aspects of the wet and dry seasons which may contribute to a complete description of rainfall seasonality, where the following attributes of rainfall seasonality have been captured: onset and cessation dates including wet season duration and rain days (e.g. Tadross *et al.*, 2005a, 2009; Kniveton *et al.*, 2009; Moeletsi *et al.*, 2011; Tongwane *et al.*, 2015; Kabanda & Nenwiini, 2016; Lipsett, 2017), PCI (e.g. Nel, 2009; Botai *et al.*, 2018), SI (e.g. Tongwane *et al.*, 2015; van Wilgen *et al.*, 2016), rainfall percentiles (e.g. van Wilgen *et al.*, 2016), duration of wet and dry spells (e.g. Usman & Reason, 2004; Kruger, 2006; Zengeni *et al.*, 2016; Kruger & Nxumalo, 2017), and the occurrence of heavy to extreme rainfall events or changes in rainfall intensity (e.g. Mason *et al.*, 1999; Easterling *et al.*, 2000; Groisman *et al.*, 2005; Kruger 2006; New *et al.*, 2006; Lumsden *et al.*, 2009; Roy & Rouault, 2013; Kruger & Nxumalo, 2017; Burls *et al.*, 2019).

Across most of these studies, changes in rainfall seasonality characteristics have been detected but again few statistically significant trends are evident. Botai *et al.* (2018) explore change in PCI (see PCI under *Section 2.2*), for the period 1998-2015 across South Africa. Although the magnitudes of trends were small, ranging between -0.02 to 0.20.yr^{-1}, and no trends were statistically significant there was spatial consistency in trends where most of the country displayed an increase in the degree of seasonality (Botai *et al.*, 2018). Using PCI for the period 1921-2000 across the eastern Drakensberg, Nel (2009) also detect an increase in seasonality where two locations demonstrated statistically significant trends. Across the northeastern parts of southern Africa for the period 1960-2005, a shift towards later onset and earlier cessation of the wet season was mostly evident with an overall decrease in the duration of the wet season by up to 1d.yr^{-1} coinciding with an increase in the mean dry spell length, during the wet season, due to fewer rain days (Tadross *et al.*, 2009). Very few statistically significant trends were identified, and this was attributed to very high inter-annual variability (Tadross *et al.*, 2009). Similarly, in northeast South Africa Kabanda and Nenwiini (2016) note high variability in rainfall seasonality characteristics, and a statistically significant shortening of the wet season was evident due to later onset and earlier cessation. Trends quantified using SI (see SI under *Section 2.2*), and dates of accumulation of 25 and 75% rainfall amount in various national parks across South Africa were not statistically significant and it was suggested that rainfall regimes were stable for the period of 1960-2010 (van

Wilgen *et al.*, 2016). Rainfall regimes were, however, characterised by high levels of inter-annual variability (van Wilgen *et al.*, 2016). Considering extreme rainfall, Roy and Rouault (2013) attribute the considerably strong positive trends in extreme rainfall across the eastern Drakensberg and adjacent coastal areas to the orographic effect of the Drakensberg Mountains and increasing moisture from the warming Agulhas current. Across South Africa, Kruger and Nxumalo (2017) demonstrate predominantly an increase in extreme daily rainfall, and across the eastern half of the country an increase in the frequency of dry spells with no change in mean annual rainfall amount which may possibly be attributed to a change in the annual distribution of rainfall. From these studies it is evident that elements of rainfall seasonality have changed across southern Africa, however, this review also highlights that there is insufficient literature exploring rainfall seasonality changes.

Throughout the studies which investigate rainfall seasonality, over different temporal periods using different methods, there is some agreement regarding changes in the seasonality of rainfall. However, all the rainfall seasonality quantities had high inter-annual variability, and hence this may be the reason for low levels of statistical significance evident across previous studies. Important to note is that since rainfall across southern Africa is characterised by high year-to-year variability, it is not surprising that rainfall seasonality characteristics are also characterised by high variability (Herrmann & Mohr, 2011). Analysis of the stability of rainfall regimes across Africa highlights that rainfall regimes across South Africa (including Lesotho and Swaziland) are particularly unstable compared to neighboring countries to the north (Herrmann & Mohr, 2011). In particular, the highest level of variability in the seasonality across southern Africa was found across the transition zone between the SRZ and WRZ. This study also highlights that any changes in seasonality captured using the seasonality approach based on temperature and rainfall applied, which is discussed under *Section 2.2*, are a consequence of rainfall regime shifts given that mean monthly temperatures are relatively stable from year-to-year (Herrmann & Mohr, 2011). Lennard and Hegerl (2015) note that changes in the seasonality of rainfall at Cape Town and Johannesburg can be related to synoptic circulation changes, namely mid-latitude cyclones and convective synoptic systems. During the period of 1979-2009 they detect an increase in the frequency of key summer circulation modes and a decrease of key winter circulation modes (Lennar & Hegerl,

2015). Similarly, Burls *et al.* (2019) detect changes in the South Atlantic Anticyclone (SAA) and frontal systems, which are linked to a poleward expansion of the Hadley cell. These changes are postulated to suppress orographic rainfall in the southwestern Cape, where this was corroborated by an observed reduction in the number of rain days associated with a decrease in the duration of rainfall events associated with frontal systems (Burls *et al.*, 2019). The results of these studies provide evidence that synoptic circulation changes are taking place, where this has also been highlighted by Mphale *et al.* (2014), and such changes are likely to result in a shift in the boundary between the SRZ and WRZ across southern Africa (Knight & Holmes, 2018). The patterns of rainfall and its seasonality are a direct consequence of synoptic circulation patterns, and hence changes in circulation patterns directly influence rainfall seasonality (Nicholson, 2000). Over recent years literature has highlighted progressive changes in Southern Hemisphere climatic belts through changes in the strength of these belts, and expansion of the tropics and poleward deviation of the subtropical and temperate climatic belts (e.g. Biastoch *et al.*, 2009; Mahlobo *et al.*, 2018; Sousa *et al.*, 2018; Mahlalela *et al.*, 2018; Burls *et al.*, 2019).

Notable, as already mentioned, were the high levels of variability in rainfall seasonality characteristics investigated across studies. Few studies have investigated the drivers of variability in rainfall seasonality characteristics (e.g. Tadross *et al.*, 2005a; 2009; Usman & Reason, 2004; Reason *et al.*, 2005; Moeletsi *et al.*, 2011). In the Free State, for the period of 1950-2008, Moeletsi *et al.* (2011) find no clear pattern between onset date and the positive and negative phases of ENSO. However, earlier and later cessation dates were strongly correlated to El Niño and La Niña years respectively. Additionally, they note a shorter than normal wet season during El Niño years and a longer than normal wet season during La Niña years (Moeletsi *et al.*, 2011). Across most of southern Africa it was found that dry spell frequencies are usually highest during El Niño events and lowest during La Niña (Usman & Reason, 2004). Similarly, Reason *et al.* (2005) find a strong correlation between dry spell frequencies and ENSO via changes in regional circulation patterns over Limpopo for the period 1979-2002. Here they also recommend the use of dry spell frequencies and other rainfall seasonality characteristics in seasonal forecasting and projecting efforts for the SRZ (Reason *et al.*, 2005), where Mahlalela *et al.* (2018), for example, note the lack of forecasting skill in the South African Weather Service (SAWS) seasonal forecasting models for

the WRZ due to complex topography and highly variable surrounding oceans. Reason *et al.* (2005) also find a relationship evident between ENSO and onset of the wet season. Typically, late onset was associated with El Niño events and early onset was associated with La Niña (Reason *et al.*, 2005). However, this association was not particularly strong and two strong El Niño events were associated with early onset (Reason *et al.*, 2005). It was highlighted that a different definition for onset date may have produced a different relationship with ENSO (Reason *et al.*, 2005). On this point, across the northeastern parts of southern Africa Tadross *et al.* (2009) find that three different onset definitions did produce a different relationship with ENSO. Given this, it may be important to create standard methods based on standard definitions to quantify rainfall seasonality, for large scale spatial comparisons, in order to characterise the mechanisms responsible for variability, which is particularly important to inform decision making on for example agriculture and water resource management. Arguably very little is understood regarding the variability of rainfall seasonality parameters (e.g. Reason *et al.*, 2005; Tadross *et al.*, 2009; Ratnam *et al.*, 2018), where studies across southern Africa have predominantly investigated anomalies in seasonal rainfall totals.

Although not fully understood, the mechanisms behind variability in total seasonal rainfall are well documented in the exhaustive body of literature for southern Africa (e.g. Nicholson, 2000; Reason & Jagadheesha, 2005; Reason & Rouault, 2005; Blamey & Reason, 2007; Fauchereau *et al.*, 2009; Kane, 2009; Pohl *et al.*, 2010; Ambrosino *et al.*, 2011; Crétat *et al.*, 2012; Phillippon *et al.*, 2012; Weldon & Reason, 2014; Engelbrecht & Landman, 2016; Dieppois *et al.*, 2016; Pohl *et al.*, 2018). A wide range of factors, over numerous time scales, are suggested to contribute to summer and winter rainfall variability across the subcontinent (Nicholson, 2000; Nicholson *et al.*, 2018). Summer rainfall variability is known to be primarily associated with the ENSO and Indian Ocean SSTs (e.g. Reason, 2001; Fauchereau *et al.*, 2009; Ambrosino *et al.*, 2011; Crétat *et al.*, 2012; Dieppois *et al.*, 2016; Nicholson *et al.*, 2018). A number of other mechanisms have been suggested to contribute to summer rainfall variability, and these include Quasi-biennial and -triennial oscillations (Kane, 2009), Madden-Julian oscillation (Pohl *et al.*, 2007; Fauchereau *et al.*, 2009; Pohl *et al.*, 2010), and the Atlantic oscillation and South Atlantic SSTs (Reason & Jagadheesha, 2005; Pohl *et al.*, 2010), among others. ENSO, being the most prominent driver, affects are nonlinear

although below average summer rainfall is noted during El Niño years and above average summer rainfall is noted during La Niña years (Fauchereau *et al.*, 2009; Dieppois *et al.*, 2016). Winter rainfall variability is thought to be predominantly related to the Southern Annular Mode (SAM, also known as the Antarctic Oscillation; e.g. Reason & Rouault, 2005; Dieppois *et al.*, 2016; Mahlalela *et al.*, 2018); although a range of other factors have also been highlighted to contribute to this variability, including anomalies in South Atlantic SSTs and sea ice in the region of the Southern Ocean bordering the Atlantic (Reason *et al.*, 2002; Reason & Jagadheesha, 2005; Blamey & Reason, 2007), and ENSO (Reason *et al.*, 2002; Philippon *et al.*, 2012). SAM, being the most prominent driver, is associated with above normal winter rainfall during a negative phase and below normal rainfall during the positive phase (Reason & Rouault, 2005). A study by Engelbrecht and Landman (2016) linked rainfall variability within the YRZ along the southern Cape coast to both ENSO and the SAM.

2.3.2.3 RAINFALL SEASONALITY PROJECTIONS

RCMs which are either empirically or dynamically downscaled from GCMs are typically used to provide a range of scenarios on future climate change across southern Africa (e.g. Tadross *et al.*, 2005b, 2009, 2011; Hewitson & Crane, 2006; Engelbrecht *et al.*, 2009; Shongwe *et al.*, 2009; MacKellar *et al.*, 2014; Davis *et al.*, 2017; SAWS, 2017; Archer *et al.*, 2018). Temperatures are reliably projected with GCMs and RCMs similarly projecting increases of 1-3°C by approximately 2060, and it is estimated that the central interior areas will experience the greatest temperature increases of up to 5°C by 2099 for the Representative Concentration Pathway 8.5 emission scenario (Tadross *et al.*, 2011; MacKellar *et al.*, 2014; Archer *et al.*, 2018). Conversely, projected rainfall changes are associated with much uncertainty, and especially is there low confidence in areas with complex topography for example (e.g. Lennard & Hegerl, 2015; Dedekind *et al.*, 2016; Munday & Washington, 2018). Even so these projections provide important information on how rainfall may change across the subcontinent and understanding this is key to developing successful adaptation strategies for agriculture and water resource management amongst other rainfall dependent activities (Tadross *et al.*, 2009). Notably, it is projected that mid-latitude and subtropical arid and semi-arid regions, of which most of southern Africa comprises such regions, will likely experience less precipitation (Christensen *et al.*, 2007; IPCC, 2013, 2018).

On the topic of rainfall seasonality projections, there is a rudimentary understanding of how these characteristics may change in the future, owing to the lack of application of rainfall seasonality metrics in modelling endeavors. Few studies have produced projections on rainfall seasonality characteristics for southern Africa, where these studies used GCMs which of course are typically over larger spatial scales (i.e. Globally or across Africa) possibly masking out spatial and temporal variability in rainfall (e.g. Li *et al.*, 2016; Pascale *et al.*, 2016; Dunning *et al.*, 2018). Instead RCM modelling studies for southern Africa have typically focused on projecting changes in rainfall amount over annual and seasonal scales (e.g. Tadross *et al.*, 2005b, 2009; Hewitson & Crane, 2006; Engelbrecht *et al.*, 2009; Shongwe *et al.*, 2009; Engelbrecht *et al.*, 2013; Pohl *et al.*, 2017; Mahlalela *et al.*, 2018), where the findings of these studies are summarised in the next paragraph.

Seasonal shifts in rainfall can be expected in the future (Christensen *et al.*, 2007). Projections developed for the period 2070-2079 using two RCMs suggest a statistically significant decrease in rainfall for October to December for the western parts of southern Africa, whereas in the eastern parts of the subcontinent a statistically significant increase in rainfall was projected for January to March (Tadross *et al.*, 2005b). Similar results are obtained using the empirical downscaling technique, where Hewitson and Crane (2006) project a statistically significant increase in summer rainfall from December to February over the central and eastern plateau, with the largest increase to the east of the Drakensberg Mountain range. Very little change is projected for the southwestern Cape where slight drying is expected during summer, and during winter (June to August) a slight decrease in frontal rainfall is projected (Hewitson & Crane, 2006). Across the northeastern parts of southern Africa, for the period of 2046-2065, Tadross *et al.* (2009) project no statistically significant changes in summer (December to February) and winter (June to August) rainfall amount. A statistically significant decrease in spring rainfall evident for most of this area is suggested to be consistent with later onset dates from the observed trends for the period of 1960-2005 (Tadross *et al.*, 2009). Additionally, it is noted that the increase in autumn rainfall (September to November) projected does not correspond to the earlier cessation dates from the observed trends (Tadross *et al.*, 2009).

Engelbrecht *et al.* (2009) explore projected (2070-2100) changes in annual and seasonal rainfall totals through analysing the drivers of these changes, namely changes in atmospheric circulation.

The annual rainfall total changes projected are small, with annual rainfall along the western coast and southwestern Cape projected to significantly decrease by approximately 10-20% (Engelbrecht *et al.*, 2009). Spring rainfall amount is projected to decrease across the northeastern parts of South Africa, Mozambique, Botswana and Zimbabwe, and this is linked to a decrease in moisture from the Indian Ocean and enhanced anticyclonic circulation (Engelbrecht *et al.*, 2009). Similarly, Shongwe *et al.* (2009) project a statistically significant decrease in rainfall from September to November for the period 2051-2200. This decline was linked to a delay in onset of the wet season and together with the projected decline in autumn rainfall a reduction in the duration of the wet season was postulated (Shongwe *et al.*, 2009). For summer (December to February), Engelbrecht *et al.* (2009) project widening, larger than for winter and spring, of the tropical belt and a poleward deviation of the subtropical high-pressure belt. This projection is associated with a statistically significant increase in rainfall amount over the northeastern parts of southern Africa and a decrease in the western parts of the subcontinent (Engelbrecht *et al.*, 2009). Shongwe *et al.* (2009) similarly, for the period of 2051-2200, project a statistically significant increase in summer rainfall over the eastern parts of the subcontinent, and in the central areas a statistically significant increase in the severity of droughts. Over the northeastern area of South Africa and over Botswana a statistically significant decrease in autumn (March to May) rainfall was projected and this was again linked to a poleward deviation of the subtropical high-pressure belt (Engelbrecht *et al.*, 2009). During winter the subtropical high-pressure belt is projected to intensify leading to a further poleward displacement of the frontal rain bands to the south (Engelbrecht *et al.*, 2009). Similarly, two studies across the southwestern Cape link drought conditions during 2015-2017 to a poleward deviation of the Westerlies (Mahlalela *et al.*, 2018; Sousa *et al.*, 2018); and Mahlalela *et al.* (2018) project, for the period of 2040-2060, an increase in the frequency of prolonged dry conditions during winter which was linked to the SAM shifting to a more positive phase. Here it is suggested that there is agreement with much other research projecting expansion of the Hadley circulation (tropics) leading to a poleward shift of the subtropical high-pressure belt (Mahlalela *et al.*, 2018). Archer *et al.* (2018) link the projected changes in rainfall over southern Africa to a widening of the tropical belt with a poleward deviation of the subtropics and the Westerlies. Projecting similar

dynamics in atmospheric circulation, Pohl *et al.* (2017) and Engelbrecht *et al.* (2013) additionally project an increase in extreme rainfall events over much of southern Africa.

These RCM studies provide relatively similar signals of future rainfall and atmospheric circulation changes, but the magnitude of these changes differs considerably and hence only the direction of change was reported (Davis *et al.*, 2017). Projections on rainfall amount from these studies are typically over a seasonal scale. Through a comparison between observed trends in onset and cessation dates and modelled trends in seasonal rainfall amount, Tadross *et al.* (2009) note that it is difficult to compare rainfall amount changes to statistics on wet season changes, and the importance of incorporating quantitative metrics of seasonal rainfall characteristics in RCM projections across southern Africa is also highlighted. Similar to studies globally, few studies across southern Africa offer quantitative projections on future rainfall seasonality characteristics. There is, however, a growing number of studies on this topic. Pascale *et al.* (2016) use the DSI and RE, noted under *Section 2.2*, to provide quantitative projections for the period of 2006-2100 on rainfall seasonality changes globally, and for southern Africa the increase in seasonality projected is evident from an increase in the number of dry months and a shortening of the wet season. Over Africa, Dunning *et al.* (2018) applied a modified version of the metric created by Liebmann *et al.* (2012), described under *Section 2.2*. Over southern Africa, predominantly later onset dates, earlier cessation dates, a shorter duration of the wet season and a decrease in wet season rainfall amount were projected for the period of 2080-2099 (Dunning *et al.*, 2018). Additionally, Shongwe *et al.* (2015) evaluate the ability of the Coordinated Regional Downscaling Experiment RCMs in simulating the timing of onset and cessation dates across the eastern half of southern Africa using the method Liebmann *et al.* (2012) developed. The model was demonstrated to adequately capture the timing of the wet season (Shongwe *et al.*, 2015), however, no projections on rainfall seasonality characteristics were reported. Even Favre *et al.* (2016) using cluster analysis of monthly rainfall amount for the period of 1998-2006 simulated rainfall seasonality across southern Africa, although projections on how the seasonal characteristic of rainfall may change were not reported. Hence, there has been much effort recently to investigate rainfall seasonality to evaluate simulations of rainfall regimes (e.g. Shongwe *et al.*, 2015; Engelbrecht *et al.*, 2016; Favre *et al.*, 2016; Pascale *et al.*, 2016), and the metrics used in this project may be useful to understand how

rainfall seasonality has changed across southern Africa and how it may be projected to change. This could be especially important to refine RCMs to improve rainfall projections over the subcontinent to allow for better preparedness for the unfortunate droughts projected in the Western Cape (Mahlalela *et al.*, 2018; Sousa *et al.*, 2018), and the general reductions in the duration of the wet season projected across most other regions of the subcontinent (Christensen *et al.*, 2007; Dunning *et al.*, 2018). Additionally, objectively assessed metrics on rainfall seasonality may also be useful for seasonal forecasting of onset and cessation dates (Mahlalela *et al.*, 2018; Phakula *et al.*, 2018; Ratnam *et al.*, 2018).

2.4 SYNOPSIS: RESEARCH GAPS AND AVENUES FOR FUTURE WORK

The complexity of rainfall regimes as well as the societal importance of the seasonal characteristics of rainfall for numerous climate sensitive activities (e.g. agricultural crop and livestock production, sustainable water resource management, forestry, disaster risk management, wild fire management, ecosystem management) across South Africa highlights the importance of continued research investigating rainfall seasonality (Botai *et al.*, 2018). Complexity in rainfall regimes across southern Africa is also captured within the palaeoclimatological record, where recent research has highlighted a need for continued research in the contemporary record to contribute to better understand the extent to which rainfall seasonality has changed since the LGM (Thackeray & Fitchett, 2016). Additionally, most climate change projections point to an expansion of the Hadley circulation and a consequent poleward shift of the Westerlies which is likely to have an immense and dire influence on southern African rainfall both in terms of rainfall amount and seasonality (IPCC, 2013; Favre *et al.*, 2016), thereby further stressing a need for continued research on rainfall seasonality.

In considering the need for continued research, the confounding number of seasonality metrics which have been developed both in literature globally and for southern Africa highlight the need for a standard approach to direct future research endeavors in quantifying and characterising rainfall seasonality across southern Africa. The recent use of rainfall seasonality metrics in assessing the ability of climate models in simulating rainfall seasonality and in producing

projections globally highlights an avenue of future research across southern Africa, where a standard approach to quantifying rainfall seasonality may be applied in order to improve model projections and to also produce projections on the seasonal characteristics of rainfall (Shongwe *et al.*, 2015). An objectively tested set of methods may also be particularly useful for corroboration of trends detected in rainfall seasonality (Raziei, 2017); of which there is limited research across southern Africa. Additionally, there is a call for application of methods used to infer rainfall seasonality from proxy records in contemporary attempts to quantify rainfall seasonality (Fitchett & Bamford, 2017).

3. STUDY REGION

3.1 INTRODUCTION

This study is focused on exploring the rainfall seasonality characteristics and the changes thereof using 46 weather stations, spanning the period of 1987-2016, spread across the Republic of South Africa. A discussion on the data used, collection of data and the locations of the project weather stations can be found under *Chapter 4 (Data and Methodology)*. What follows in this chapter is a description of the geographic location and topographic characteristics, and contemporary climate of the study region. The discussion on the contemporary climate is the main focus of this chapter, where the key focus here is on the wide range of synoptic features which contribute to rainfall across South Africa.

3.2 THE REPUBLIC OF SOUTH AFRICA

3.2.1 DESCRIPTIVE GEOGRAPHY: LOCATION AND TOPOGRAPHY

South Africa is the southernmost country of Africa and is located between the coordinates of 22-35°S and 16-33°E covering a terrestrial area of 1,220,000km^2 (Figure 3.1; Landman *et al.*, 2017; Lennard, 2019). The country is bordered by six neighbouring countries which include Botswana, Lesotho, Mozambique, Namibia, Swaziland and Zimbabwe (Figure 3.1). To the south and southeast the country is bordered by the Indian Ocean which hosts the warm Agulhas Current which flows southwards along the coast, whereas to the west the country is bordered by the Atlantic Ocean which hosts the cold Benguela Current which flows northwards along the coast (Figure 3.1). The topography across South Africa is considerably complex and is characterised predominantly by a mountainous escarpment (i.e. the Great Escarpment) which separates the coastal plain from a high-lying interior plateau (Figure 3.1; Grab & Knight, 2018); the influence of both the surrounding oceans and topography on the climate of South Africa will be discussed under the section which follows. The coastal regions of the country are generally situated below 500m.asl (Figure 3.1). The Great Escarpment extends through eastern Limpopo, eastern Mpumalanga, western Swaziland, the border of KwaZulu-Natal and Lesotho, northern Eastern Cape, northern Western Cape and western Northern Cape, and is highest in the eastern parts of the country where it reaches over

3,000m in some regions, particularly in the Maloti Mountains of Lesotho (Figure 3.1; Grab & Knight, 2018). The inland plateau is situated at a height of approximately 500m.asl in the western regions and 2,000m.asl in the eastern regions (Figure 3.1). Also contributing to the complex topography of South Africa are the Cape Fold Mountains which are located within the southwestern Cape and along the southern coast, reaching heights of approximately 1,000-2,500m.asl (Figure 3.1; Grab & Knight, 2018).

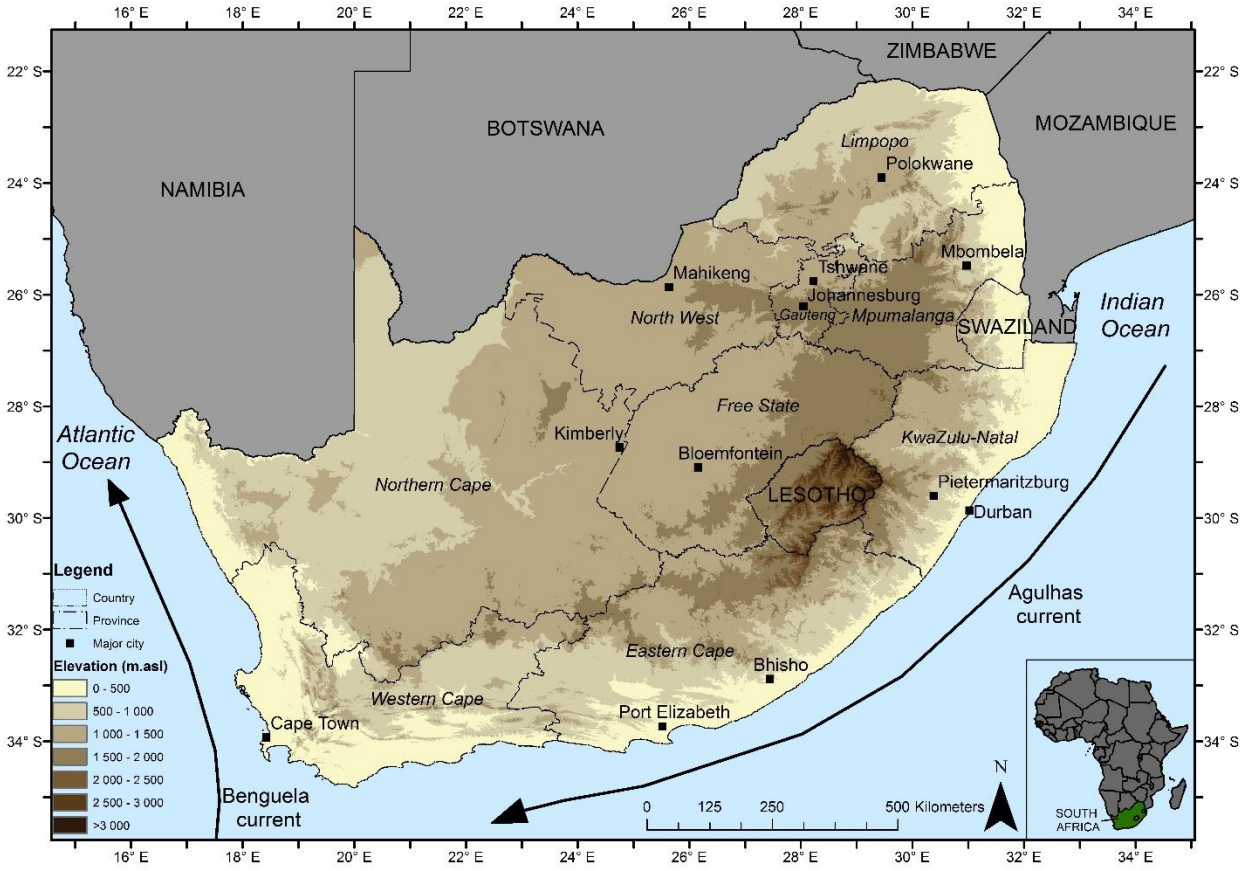


Figure 3.1: Map of the study region of South Africa indicating the nine provinces and major cities, topography, the surrounding oceans and their respective ocean currents.

3.2.2 CLIMATE AND WEATHER

The climate and weather characteristics across South Africa are well documented (e.g. Taljaard, 1996; Tyson & Preston-Whyte, 2000; Landman *et al.*, 2017; Lennard, 2019). Climate across South

Africa can be generalised to range from being warm, wet and humid in the east to being hot, dry and arid in the west (Landman *et al.*, 2017; Botai *et al.*, 2018; Lennard, 2019). As a result of South Africa's latitudinal location mainly in the subtropics, the country is influenced by the seasonal migration of ITCZ and Southern Hemisphere Westerlies, and as such seasonality is known to play an important role in the climate of the country (Tyson & Preston-Whyte, 2000; Chase & Meadows, 2007; Jury, 2013). For instance, temperatures across the country are characteristically warmer during summer and cooler during winter (Landman *et al.*, 2017). Additionally, over most of the country rainfall occurs during summer, in the southwestern Cape and along the western coast rainfall occurs during winter, and along the southern coast rainfall occurs throughout the year (Schulze & Maharaj, 2007; Lennard & Hegerl, 2015). In general, the weather and climate of South Africa are spatially and temporally variable over numerous scales and owe their characteristics to the latitudinal location, topography and surrounding oceans (Taljaard, 1996; Nicholson, 2000; Tyson & Preston-Whyte, 2000; Landman *et al.*, 2017; Jury, 2018; Lennard, 2019). Although these physical controls on South African climate are discussed separately below, it is important to note that these controls are not in isolation but interact with one another.

Due to South Africa's latitudinal location predominantly in the subtropics it is affected by circulation systems prevailing in the tropical, subtropical and temperate climatic belts, where these will be discussed later in this section (Tyson & Preston-Whyte, 2000; Braun *et al.*, 2017). First, the topographic controls on the latitudinally determined climate need to be discussed as the topography of South Africa affects regional climate in a number of ways. In general, as altitude increases from the coast up the escarpment, temperatures decrease with height (Landman *et al.*, 2017). As such, winter snowfall in the highest parts of the Drakensberg and Maloti Mountains is common especially when cold fronts persist (Grab, 1997; Mills *et al.*, 2012). The occurrence of mid-latitude cyclones and cold cored cut-off low pressure systems during winter also bring snow across the highest parts of the Cape Fold Mountains (Cowling *et al.*, 2009). Although temperature follows a decreasing trend with altitude, it should be noted that the surrounding oceans moderate seasonal temperature variations and as a result winters across the coastal plains, for instance, are milder than those across the inland plateau (Landman *et al.*, 2017).

Besides the effect on temperatures, the topography of the country particularly influences rainfall and the associated synoptic systems. The escarpment affects both westerly flow in the mid-latitudes during winter as well as easterly flow in the subtropics during summer (Lennard, 2019). During each season a respective low-pressure trough forms on the leeward side of the escarpment (Lennard, 2019). These troughs form on the westerly and easterly waves and will be discussed later. Over the eastern escarpment, moist air from the Indian Ocean and the warm Agulhas current is forced to rise resulting in orographic rainfall and high annual rainfall totals (Favre *et al.*, 2016; Landman *et al.*, 2017). Similarly, over the southern coast and southwestern Cape, annual rainfall totals are relatively high due to the Cape Fold Mountains forcing moist frontal air to rise (Engelbrecht *et al.*, 2015; Favre *et al.*, 2016; Landman *et al.*, 2017). Additionally, it should be noted that the interior elevated plateau receives significantly less rainfall than it would if it were at sea level and if there were no escarpment, and this is due to the influence of the steep escarpment slopes which in general act as barriers blocking the flow of moisture into the interior (Favre *et al.*, 2016; Landman *et al.*, 2017). The eastern escarpment interacts with the descending limbs of the Hadley and Ferrel cells of the tricellular circulation system, where during summer it facilitates the flow of moisture into the interior of the country and in winter it restricts moisture into the interior (Tyson & Preston-Whyte, 2000; Favre *et al.*, 2016). Here, the descending limbs of the Hadley and Ferrel cells bring about the subtropical high-pressure systems which cause air to subside, resulting in characteristically clear skies as well as subsidence inversion layers over the interior of the country (Tyson & Preston-Whyte, 2000). During summer the base of these inversion layers is at approximately 3000m over the interior thus facilitating moisture flow from the warm Agulhas current of the Indian Ocean, whereas during winter the base of these inversion layers is at approximately 1750m which is below the escarpment and thus moisture flow is restricted into the interior (Tyson & Preston-Whyte, 2000). Finally, the escarpment is also responsible for the formation of coastal low-pressure systems, and this will be discussed later in this section (Reason & Jury, 1990).

The surrounding oceans, as already noted, largely influence the climate of South Africa in a number of ways and these can be considered to be local, through the influence of ocean currents, and remote, through the influence of teleconnections (Landman *et al.*, 2017; Lennard, 2019). First, it

should be highlighted that the presence of the warm Agulhas and cold Benguela currents contribute to the general spatial pattern of rainfall across South Africa, where rainfall mostly decreases as you move west from the east coast over the plateau (Jury, 2013; Favre *et al.*, 2016); for additional discussions on the annual rainfall characteristics across the country refer to *Chapter 5 (Results) Section 5.2* and *Chapter 6 (Discussion) Section 6.2*. During summer, moisture and energy from the Agulhas current is transported inland by the easterly winds and is critical for rainfall over the interior of the country (Nicholson, 2000; Favre *et al.*, 2016). The semi-arid and arid conditions in the western parts of the country result from the occurrence of subsidence from the descending limbs of the Hadley and Ferrel cells, the presence of the cold, dry air due to the cold Benguela current and upwelling along the western coast (Tyson & Preston-Whyte, 2000; Chase *et al.*, 2015; Lennard, 2019).

The climate of South Africa, as previously noted under *Chapter 2 (Literature Review) Section 2.3.2.2*, is impacted by numerous large scale teleconnections which modulate South African rainfall, of which some of the most commonly known are the ENSO, the SAM and SST variability in the south Indian and south Atlantic Oceans (Crétat *et al.*, 2012; Dieppois *et al.*, 2015, 2016; Pohl *et al.*, 2018). Of these the ENSO is known to have the strongest influence on South Africa rainfall, especially at the inter-annual timescale (Dieppois *et al.*, 2015, 2016; Landman *et al.*, 2017; Crétat *et al.*, 2019). ENSO has a large influence on global weather systems and is a coupled ocean-atmosphere phenomenon which occurs approximately every 2-8 years (Dieppois *et al.*, 2015, 2016; Landman *et al.*, 2017; Pohl *et al.*, 2018). This phenomenon refers to a SST oscillation in the equatorial Pacific Ocean which involves prolonged warming or cooling of SSTs, where the warm phase is referred to as El Niño and the cold phase is referred to as La Niña (Landman *et al.*, 2017; Lennard, 2019). Generally, anomalously warm equatorial Pacific SSTs (El Niño) are associated with below average summer rainfall and anomalously cold equatorial Pacific SSTs (La Niña) are associated with above average summer rainfall (Dieppois *et al.*, 2015, 2016; Pohl *et al.*, 2018). This relationship does not always hold, for instance the very strong 1997/98 El Niño event produced normal rainfall totals and did not result in drought conditions as expected (Richard *et al.*, 2001). Additionally, Philippon *et al.* (2012) detected a relationship between ENSO and winter rainfall, such

that El Niño events are associated with high seasonal rainfall amounts and longer wet spells with La Niña events showing the opposite.

The SAM is the principal mode of atmospheric variability in the mid-latitudes and high latitudes in the Southern Hemisphere and is known as a prominent driver of winter rainfall variability across South Africa (Thompson & Wallace, 2000; Reason & Rouault, 2005; Mahlalela *et al.*, 2018; Lennard, 2019). The SAM is defined as an oscillation in atmospheric pressure between the Antarctic region and the mid-latitudes (Reason & Rouault, 2005). A positive phase in the SAM is characterised by anomalously high pressure over the mid-latitudes and anomalously low pressure over Antarctica, whereas a negative phase is characterised by anomalously high pressure over Antarctica and anomalously low pressure over the mid-latitudes (Reason & Rouault, 2005; Mahlalela *et al.*, 2018). Both of these phases are associated with variability in the location of the Southern Hemisphere Westerlies storm track, such that during the positive phase the storm track is shifted poleward typically resulting in subsequently less winter rainfall over the WRZ of South Africa (Reason & Rouault, 2005; Gillett *et al.*, 2006). During the negative phase typically wetter winters in the WRZ are associated with the equatorward shift of the Westerlies storm track (Reason & Rouault, 2005; Gillett *et al.*, 2006).

To a lesser extent and at a more regional scale, SST variability in the south Indian and south Atlantic Oceans is known to be modulated with inter-annual rainfall fluctuations (Crétat *et al.*, 2012). South Atlantic SSTs are known to partially influence moisture fluxes between the south Atlantic Ocean and the western coast regions of South Africa (Reason *et al.*, 2002; Reason & Jagadheesha, 2005). Wet winters tend to coincide with SSTs which are anomalously warm in the southwest Atlantic and southeast Atlantic and cool in the central south Atlantic (Reason *et al.*, 2002; Reason & Jagadheesha, 2005). SST variability in the south Indian Ocean is known to influence rainfall variability to a greater extent than SST variability in the south Atlantic, where this is because the Indian Ocean is a major source of moisture for rainfall across South Africa (Crétat *et al.*, 2012; Lennard, 2019). SST variability in the Indian Ocean is often referred to as the Indian Ocean Dipole (Lennard, 2019). Wetter conditions over central and eastern South Africa are known to be associated with positive SST anomalies in the southwest Indian Ocean (Reason, 2001, 2002; Crétat *et al.*, 2012).

As a result of South Africa's latitudinal location, there are three dominant controls, namely the tropical, subtropical and temperate controls, on the climate of the county (Tyson & Preston-Whyte, 2000). Given that South Africa is predominantly located in the subtropics, the descending limbs of the Hadley and Ferrel cells particularly influence the climate and as a result the mean circulation throughout the year is anticyclonic (Taljaard, 1996; Tyson & Preston-Whyte, 2000; Dyson & van Heerden, 2002; Lennard, 2019). The tropical and temperate controls are seen during the summer and winter months respectively and are a function of the movement of the ITCZ and the Westerlies (Lennard, 2019; Figure 3.2). These three controls are together responsible for the general climate dichotomy between SRZ and WRZ across South Africa (Lennard & Hegerl, 2015; Chase *et al.*, 2017; Fitchett & Bamford, 2017). This is because each of these controls is associated with particular synoptic circulation features which in turn display specific weather characteristics (Harrison, 1984; Taljaard, 1996; Lennard & Hegerl, 2015; Figure 3.2). Below, these synoptic circulation features which are associated with South African rainfall patterns are briefly discussed, generally following the order of tropical, subtropical and temperate synoptic circulation features. Throughout the following paragraphs it is highlighted that rainfall can vary across different regions of South Africa in terms of the underlying synoptic circulation features behind rainfall.

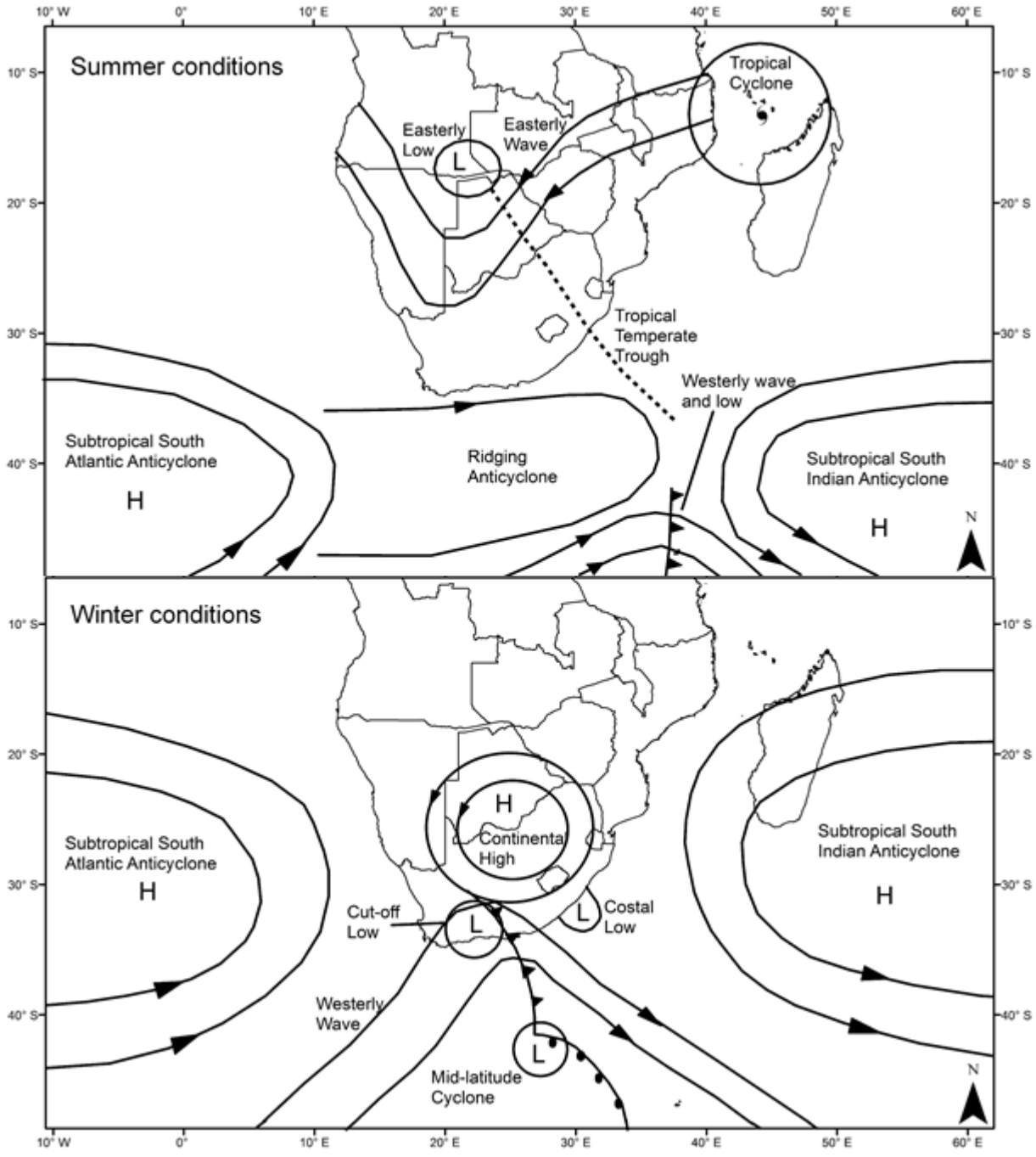


Figure 3.2: Schematic diagram of the synoptic features which influence weather and climate across South Africa during summer (top) and winter (bottom; After: Tyson & Preston-Whyte, 2000; Hart *et al.*, 2010; Blamey & Reason, 2013; Reason & Smart, 2015; Lennard, 2019).

As previously noted, the tropical control on weather and climate across South Africa is only evident during the summer months, where it is associated with the southward migration of the ITCZ (Tyson

& Preston-Whyte, 2000). Over Africa the ITCZ displays a tilde-like shape (~), and during summer over the Southern Hemisphere this shape is most pronounced (Tyson & Preston-Whyte, 2000; Nicholson, 2018). During the Southern Hemisphere summer months, the ITCZ reaches approximately ~17°S over the eastern parts of southern Africa (Taljaard, 1994; Nicholson, 2000, 2018; Tyson & Preston-Whyte, 2000). During this time there is an arm of convergence off the ITCZ, known as the Congo Air Boundary, approximately extending west from Zambia through to northern Namibia and the Atlantic Ocean (Taljaard, 1994; Nicholson, 2000, 2018). Together with moisture from the Indian Ocean and warm Agulhas current, the ITCZ and Congo Air Boundary are important sources of moisture for convective summer rainfall across the eastern and central parts of South Africa (Munday & Washington, 2017). Associated with the southward progression of the ITCZ are the easterly waves and lows (Taljaard, 1996; Tyson & Preston-Whyte, 2000; Munday & Washington, 2017; Lennard, 2019; Figure 3.2).

The main tropical controls on South African rainfall are exerted through the easterly waves and associated lows predominantly during the summer months of the year (Taljaard, 1996; Tyson & Preston-Whyte, 2000; Lennard & Hegerl, 2015; Lennard, 2019; Figure 3.2). The easterly wave is a barotropic semi-stationary wave which is associated with warm, humid easterly winds between the ITCZ and the subtropical high-pressure belt (Taljaard, 1996; Tyson & Preston-Whyte, 2000; Dyson & van Heerden, 2002; Lennard & Hegerl, 2015; Lennard, 2019). Flowing from east to west, the easterly wave advects warm, moist air from the warm Agulhas current of the Indian Ocean to the interior of the country, and thus is an important control on summer rainfall over the eastern and interior parts of the country (Tyson & Preston-Whyte, 2000; Dyson & van Heerden, 2002; Lennard, 2019). Associated with the easterly wave is a closed low-pressure system which forms over the interior of the country (Taljaard, 1996; Tyson & Preston-Whyte, 2000; Lennard & Hegerl, 2015; Lennard, 2019; Figure 3.2). This associated low pressure system is a thermal low which causes convergence and uplift at the surface and along the escarpment bringing about convective rainfall across the interior and eastern parts of the country, rarely influencing the western coast region (Tyson & Preston-Whyte, 2000; Dyson & van Heerden, 2002; Lennard & Hegerl, 2015; Lennard, 2019). Convective rainfall from these associated lows may last for a few hours or up to a few days and this may bring rainfall across large areas of the eastern and central regions of the

country (Tyson & Preston-Whyte, 2000; Lennard, 2019). Copious amounts of convective rainfall from these systems may result in wide-spread flooding events (Dyson & van Heerden, 2002; Engelbrecht *et al.*, 2013). Thunderstorms are the main mesoscale convective phenomenon during the summer months which typically occur during the afternoon and early evening lasting for a few hours (Tyson & Preston-Whyte, 2000; Blamey & Reason, 2009). Individual single-cell storms general only influence small regions while large-scale composite storms such as squall line storms affect much larger regions (Tyson & Preston-Whyte, 2000; Blamey & Reason, 2009). Recently on 5 March 2019, severe thunderstorm activity led to localised flooding across numerous parts of the Limpopo, Gauteng, Mpumalanga and North West provinces (Kahla, 2019).

Tropical cyclones are also part of the tropical controls on South African rainfall (Tyson & Preston-Whyte, 2000; Figure 3.2). These systems, depending on size and intensity (i.e. the category), are known to contribute to rainfall in the northeastern parts of the country and sometimes along the eastern coastline where inland penetration is blocked by the escarpment (Tyson & Preston-Whyte, 2000; Malherbe *et al.*, 2012; Fitchett, 2018). Tropical cyclones are warm-cored cyclonic disturbances which mainly occur during December to April, may have a diameter of up to 2000km, and typically have a lifespan, from development to dissipation, of a few days (Tyson & Preston-Whyte, 2000; Fitchett & Grab, 2014; Lennard, 2019). Tropical cyclones are associated with strong winds as well as copious rainfall which typically leads to wide-spread flooding (Malherbe *et al.*, 2012; Fitchett & Grab, 2014). This year (2019) alone, two tropical cyclones namely Idai (March), which straddled category 2 and 3, and Kenneth (April), which was a category 4, had devastating impacts which reached the northeastern parts of South Africa causing much flooding (Fitchett, 2019b, 2019c).

The subtropical control on South African weather and climate is through a belt, spanning approximately 20-40°S, of semi-permanent subtropical anticyclones (i.e. high-pressure systems) known as the South Indian Anticyclone (SIA), the Continental High-pressure cell (CH) and the SAA (Taljaard, 1996; Tyson & Preston-Whyte, 2000; Cherchi *et al.*, 2018; Figure 3.2). Variations in the latitudinal and longitudinal position and intensity of these high-pressure systems play an important role in the spatial and temporal distribution of rainfall across South Africa (Dyson & van Heerden, 2002). These anticyclones are a function of the descending limbs of the Hadley and Ferrel

cells and are associated with strong subsidence, relatively clear sunny skies and little or no rainfall (Taljaard, 1996; Tyson & Preston-Whyte 2000; Dyson & van Heerden, 2002; Lennard, 2019). The CH dominates the weather over the interior during winter, and during summer the CH is relatively absent over the interior, however, during the summer months the CH migrates south and dominates weather in the southwestern and southern parts of the country (Tyson & Preston-Whyte, 2000; Lennard, 2019; Figure 3.2). During winter this band of high-pressure cells, particularly the CH, is associated with the presence of subsidence inversion layers which may last for approximately four days, and as already noted these inversion layers restrict the flow of moisture into the interior (Cosijn & Tyson, 1996; Tyson & Preston-Whyte, 2000). Together with the SIA and SAA, the CH migrates south during summer due to the seasonal migration of the ITCZ (Tyson & Preston-Whyte, 2000; Lennard, 2019). During winter the SIA and SAA are located relatively adjacent to the CH, and during summer the SIA and SAA migrate south by approximately 6° (Tyson & Preston-Whyte, 2000). During the summer months these weather systems are positioned offshore of the country and over the eastern parts of the country, where the winds associated with SIA assist to facilitate moisture flow into the interior which contribute to rainfall (Tyson & Preston-Whyte, 2000; Lennard, 2019; Figure 3.2). Additionally, associated with the SAA are ridging anticyclones which contribute considerably (~46%) to annual orographic rainfall across the southern coast with a peak contribution during the spring months, where these systems also contribute to orographic rainfall over the eastern escarpment (Jury & Levey, 1993; Engelbrecht *et al.*, 2015; Ndarana *et al.*, 2018; Figure 3.2). Ridging anticyclones occur south of the country and form (i.e. break off) from the SAA when it ridges eastwards as it interacts with the westerly wave (Tyson & Preston-Whyte, 2000; Ndarana *et al.*, 2018; Lennard, 2019). These ridging anticyclones flow towards the SIA and are eventually absorbed by the SIA (Tyson & Preston-Whyte, 2000; Ndarana *et al.*, 2018).

The temperate control on South African rainfall as previously noted occurs during the winter months for the Southern Hemisphere, where this is associated with the northward migration of the ITCZ, subtropical high-pressure belt and the mid-latitude Westerlies (Tyson & Preston-Whyte, 2000). The temperate control on South African rainfall is associated with the equatorward movement of the circumpolar Westerlies and is exerted through travelling perturbations from the

Westerlies, where the specific synoptic circulation systems include the westerly wave, cold fronts mainly associated with mid-latitude cyclones, coastal lows and berg winds, cut-off lows, and ridging anticyclones (Tyson & Preston-Whyte, 2000; Reason *et al.*, 2002; Singleton & Reason, 2007; Philippon *et al.*, 2012; Favre *et al.*, 2013; Mahlalela *et al.*, 2018; Sousa *et al.*, 2018; Lennard, 2019; Figure 3.2). These temperate systems are typically confined to the southwestern Cape and southern coast due to the presence of topographic barriers and as previously noted this is important for orographic rainfall (Philippon *et al.*, 2012). Recently, Blamey *et al.* (2018) quantified that atmospheric rivers influencing the west coast contribute between 15-60% of total winter rainfall across the southwestern Cape.

During the winter months, the westerly wave, which has a periodicity of 2-8 days, is located further north (Taljaard, 1996; Tyson & Preston-Whyte, 2000; Lennard, 2019; Figure 3.2). During the winter months the rear of westerly wave trough is typically located over the Western Cape where this is associated with surface convergence and uplift, and clouds with rainfall (Taljaard, 1996; Tyson & Preston-Whyte, 2000; Lennard, 2019). Conversely, ahead of this trough, which is typically located over the interior and eastern parts of the country, there is subsistence and associated clear skies, where the presence of the escarpment typically blocks the influence of rainfall from the westerly wave in the interior (Tyson & Preston-Whyte, 2000; Lennard, 2019). Associated with the westerly wave are cold fronts (i.e. mid-latitude cyclones or frontal systems) and cut-off lows which form as closed low pressure systems (Tyson & Preston-Whyte, 2000; Philippon *et al.*, 2012; Lennard & Hegerl, 2015; Lennard, 2019; Figure 3.2).

Mid-latitude cyclones occur throughout the year, however, their cold front arms only reach the southern and interior regions of the country during the winter months (Taljaard, 1996; Tyson & Preston-Whyte, 2000; Figure 3.2). Mid-latitude cyclones are cold-cored low-pressure systems which move from west to east, particularly influencing weather by contributing to rainfall across the south-western and southern regions of the country, however, when particularly strong these may also influence weather across the interior (Taljaard, 1996; Tyson & Preston-Whyte, 2000; Lennard, 2019; Figure 3.2). These systems are baroclinically unstable disturbances which originate in the Westerlies and have a lifetime of approximately three to five days, reaching maturity in approximately 24-hours, during which time these systems may travel up to 10,000km (Tyson &

Preston-Whyte, 2000). Mid-latitude cyclones particularly contribute the majority of rainfall in the southwestern Cape (Reason *et al.*, 2002; Lennard & Hegerl, 2015; Mahlalela *et al.*, 2018; Sousa *et al.*, 2018); Lennard and Hegerl (2015) quantified that mid-latitude cyclones contributed up to two thirds of wet days at Cape Town for the period 1980-2009. If the core of these systems is particularly deep, then there may be associated extreme rainfall and gale force winds (Taljaard, 1996; Lennard & Hegerl, 2015).

Passing frontal systems may lead to the formation of cut-off lows, where these form in the upper and middle atmosphere on the equatorward side of frontal systems when a closed low detaches from the frontal system (Tyson & Preston-Whyte, 2000; Singleton & Reason, 2007; Favre *et al.*, 2013; Figure 3.2). These systems occur throughout the year but exert a maximum contribution to rainfall across South Africa during the autumn and spring months (Singleton & Reason, 2007; Favre *et al.*, 2013). The occurrence of rainfall from these systems depends on the amount of moisture in the atmosphere, where rainfall typically occurs along the southern and eastern coastline and when these systems are particularly strong rainfall may occur in the western interior across the transition region between the SRZ and WRZ (Tyson & Preston-Whyte, 2000; Singleton & Reason, 2007; Favre *et al.*, 2013; Engelbrecht *et al.*, 2015; Lennard, 2019). These systems contribute to most of the winter rainfall across the SRZ regions (Taljaard, 1996; Tyson & Preston-Whyte, 2000). When these systems are particularly deep and remain relatively stationary, they may be associated with particularly heavy 24-hour rainfall totals which may result in widespread flooding (Singleton & Reason, 2007; Favre *et al.*, 2013; Engelbrecht *et al.*, 2015). According to Singleton and Reason (2007) and Engelbrecht *et al.* (2015) the most rainfall that has been recorded from a single cut-off low occurred during September 1987, where the three-day rainfall total associated with this system exceeded 900mm along the KwaZulu-Natal coastline.

The final temperate control on South African rainfall discussed here is the coastal low (Figure 3.2). The coastal low is a shallow mesoscale disturbance in the atmosphere, and the influence of these features is confined to the coastal and adjacent areas (Reason & Jury, 1990; Tyson & Preston-Whyte, 2000). Without the presence of the escarpment confining the coastal regions, these systems would not form (Reason & Jury, 1990; Tyson & Preston-Whyte, 2000). These systems form on the windward side of the escarpment on the western coast of the country as a frontal system

approaches the Western Cape and as air descends due to the presence a subsidence inversion layer, which traps these systems along the coast (Reason & Jury, 1990; Tyson & Preston-Whyte, 2000; Lennard, 2019). These systems occur most commonly during late winter and early spring and are mostly associated with mist and fine drizzle as well as hot, dry berg winds (Reason & Jury, 1990; Tyson & Preston-Whyte, 2000; Lennard, 2019). Following formation, these systems travel south to the southwestern Cape and thereafter travel eastward along the coastline where they generally dissipate over Mozambique as the landscape is flat with no escarpment to trap the system (Reason & Jury, 1990; Tyson & Preston-Whyte, 2000; Lennard, 2019).

Finally, it is possible for tropical (e.g. easterly wave and easterly low) and mid-latitude (e.g. westerly wave, cold front and cut-off low) weather systems to combine and form composite synoptic scale cloud bands, typically orientated from northwest to southeast, known as Tropical-temperate troughs (TTT; Harrison, 1984; Taljaard, 1996; Tyson & Preston-Whyte, 2000; Hart *et al.*, 2010, 2013; Blamey & Reason, 2013; Ratna *et al.*, 2013; Macron *et al.*, 2014; Figure 3.2). TTT systems typically last between three to seven days and are known to contribute substantially to summer rainfall across large parts of the country (Harrison, 1984; Taljaard, 1996; Hart *et al.*, 2010, 2013; Blamey & Reason, 2013; Ratna *et al.*, 2013; Macron *et al.*, 2014); where Hart *et al.* (2013) quantified that these systems contribute between 30-60% of rainfall during the months of October to March. These systems are also known to contribute to summer rainfall across the southern coast (Hart *et al.*, 2013; Engelbrecht *et al.*, 2015), and they are known to be associated with a high proportion of heavy rainfall (Hart *et al.*, 2010, 2013). For instance, Hart *et al.* (2013) identified a total of 52 extreme rainfall events during 1979-1999 and found that 30 of these events were associated with TTTs. Additionally, Lindesay and Jury (1991) attributed the TTT as the weather system responsible for heavy rainfall over the interior of the country during February 1988. Mesoscale convective thunderstorms may form within TTTs bringing rainfall to the central and eastern parts of the country (Hart *et al.*, 2010, 2013; Blamey & Reason, 2013; Ratna *et al.*, 2013; Macron *et al.*, 2014).

3.2.3 CONCLUSION

Due to the latitudinal location of South Africa, the country is characterised by a complex rainfall climatology comprised of tropical, subtropical and temperate synoptic features. The surrounding oceans and complex regional topography of the country additionally contribute to the complex rainfall regimes of the SRZ, WRZ and YRZ. This highlights that South Africa is a key location in which to investigate rainfall regimes through testing numerous methods on the ability to characterise and quantify the seasonality of rainfall. Located at the intersection between the subtropical and temperate climate belts, South Africa is particularly vulnerable to changing dynamics in global circulation. This thus highlights that the county is a key region to explore how rainfall regimes may have potentially changed under the influence of anthropogenically induced climate change, a topic which has received little attention in the literature.

4. DATA AND METHODOLOGY

4.1 INTRODUCTION

This chapter outlines the data and the methodological procedure followed in analyses of data for this study. Many standard methods have been developed for analyses of rainfall data, for the purpose of comparison and for reproducible results. Unless otherwise stated, throughout this chapter standard methods have been used. This chapter begins with a description of the data required, the selection of weather stations and identification of the temporal period for this study. This is followed by a description of the initial data analysis whereby data were analysed to understand the general rainfall characteristics, to identify outliers in the rainfall and temperature datasets and to quantify trends in rainfall amount over the study period. Next, the process undertaken for developing a standard statistical approach to quantify and classify rainfall seasonality across South Africa has been described. Finally, using this statistical approach the process undertaken to quantify the shifts in rainfall seasonality has been described.

4.2. RAINFALL AND TEMPERATURE DATA

To quantify rainfall seasonality and the shifts over time, climate data including daily rainfall total in millimeters (mm) and daily minimum (T_{min}) and maximum (T_{max}) temperature in degree Celsius (°C) have been obtained from the SAWS. The rainfall data obtained from SAWS is a measurement of rainfall accumulated over a 24-hour period that is measured at 08h00 South African Standard Time (SAWS, 2018). Rainfall measured between 08h00 South African Standard Time yesterday and 08h00 South African Standard Time today is recorded as rainfall for yesterday's date (SAWS, 2018). The temperature readings obtained are the highest and lowest temperature readings recorded over a 24-hour period.

Data sourcing was limited to the selection of weather stations offered by SAWS for a number of reasons. Firstly, SAWS is an accredited meteorological organization run by the South African government and a member of the World Meteorological Organisation (WMO), therefore consistency and accuracy in the datasets is ensured for the user (SAWS, 2019a, b). Secondly, having one data source ensures further consistency in the results presented under *Chapter 5 (Results)*. Finally, measured meterological data were favoured as these provide more accurate

measurements compared to global reanalyses datasets (e.g. ERA-40, NCEP-R1, and MERRA). Moreover, Zhang *et al.* (2013) assess the performance of eight global reanalyses datasets across southern Africa through a comparison with observed records, and find a number of inconsistencies across all of the reanalyses datasets assessed.

4.2.1 WEATHER STATION SELECTION

The SAWS offer 174 weather stations in their current climate database for South Africa (SAWS, 2019a). All of these weather stations were assessed for use in this study, where the selected weather stations are required to be spatially representative of rainfall across the country. Weather stations were selected for inclusion in this study on the basis of two criteria which are discussed below:

Firstly, a weather station required at least 30 years of both rainfall and temperature data. As the number of years for which readings are available increases then the influence of incorrect or inaccurate readings diminishes (Arguez & Vose, 2011). Additionally, the WMO standards require a minimum of 30 years of data for a study on climate (WMO, 2000). There were 62 weather stations which met this requirement. Many of these weather stations contain data starting from and even prior to the 1960's and 1970's. However, for some of these weather stations, data were not available or contained many gaps prior to 1987 (Botai *et al.*, 2015). Hence, the year of 1987 was selected as the start of the temporal period for this study, to obtain the same time frame across all the weather stations. This year was also selected to include as many SAWS weather stations as possible for near complete coverage of the South African landmass. Notably, in the Northern Cape and Lowveld region of the country, the spatial coverage of weather stations is low and is limited to populated areas (Tennant & Hewitson, 2002). Additionally, a collection of as many weather stations as possible was required as rainfall is highly variable in space (Nicholson, 2000; MacKellar *et al.*, 2014), and as a result rainfall seasonality may also demonstrate high spatial heterogeneity. The year of 2016 was used as the final year for this study. This time frame provides 30 years of data available for statistical analyses.

Secondly, a weather station was selected only if it contained at least 90% of rainfall, T_{max} and T_{min} data for the period 1987-2016 following the data cleaning process, discussed under *Section 4.3.1* (Dyson, 2009; Moeletsi & Walker, 2012; MacKellar *et al.*, 2014; Kruger & Nxumalo, 2017). A level of 90% was selected as a study assessing different methods to determine rainfall seasonality will benefit from near complete datasets. Forty-six weather stations met this requirement. Therefore, the sample for this study includes these 46 weather stations (Table 4.1). The selected weather stations are generally well-distributed across South Africa, across all the provinces of the country (Figure 4.1).

Table 4.1: Details regarding location (i.e. province, elevation, latitude and longitude), data availability following data cleaning and code of each SAWS weather station utilised for this study. The code of each weather station has been used in text, and as a label on all maps and some graphs. The Köppen-Geiger climate zone codes are as follows in full: BSh – Arid, Steppe, Hot; BSk – Arid, Steppe, Cold; BWh – arid, desert, hot; BWk – arid, desert, cold; Cfa – temperate, without dry season, hot summer; CSa – temperate, dry summer, hot summer; CSb – temperate, dry summer, warm summer; CWa – temperate, dry winter, hot summer; Cwb – temperate, dry winter, warm summer (Engelbrecht & Engelbrecht, 2016).

Weather station name	Köppen-Geiger climate zone	Code	Province	Elevation (m.asl)	Latitude (°S)	Longitude (°E)	Data availability (%)		
							Rainfall	T_{max}	T_{min}
Aliwal-North Plaatkop	BSk	ANP	Eastern Cape	1353	30.80	26.88	97.1	97.0	96.4
Bethal	CWb	BET	Mpumalanga	1690	26.46	29.46	96.3	96.3	96.1
Bethlehem Wo	CWb	BEW	Free State	1650	28.25	28.33	100.0	100.0	100.0
Bloemfontein Wo	BSk	BLW	Free State	1352	29.10	26.30	99.9	99.9	99.9
Calvinia Wo	BWk	CWO	Northern Cape	973	31.48	19.76	99.9	99.8	99.8
Cape Agulhas	CSb	CAG	Western Cape	9	34.83	20.01	99.9	99.8	98.5
Cape Town Wo	CSa	CTW	Western Cape	45	33.97	18.60	100.0	100.0	100.0
Cedara	CWb	CED	KwaZulu-Natal	1066	29.54	30.24	99.9	99.8	99.8
Cradock-Mun	BSk	CMU	Eastern Cape	940	32.17	25.63	99.9	99.7	99.4
De Aar Wo	BWk	DAW	Northern Cape	1266	30.65	24.02	99.9	99.5	99.6
East London Wo	Cfa	ELW	Eastern Cape	127	33.03	27.83	99.2	99.5	99.5
Frankfort–TNK	CWb	FTN	Free State	1532	27.70	28.49	99.0	98.8	98.7
Fraserburg	BWk	FRA	Northern Cape	1266	31.92	21.51	99.6	99.0	99.0
Johannesburg INT Wo	CWb	JIW	Gauteng	1706	26.13	28.23	99.9	100.0	100.0
Kimberley Wo	BSh	KWO	Northern Cape	1201	28.80	24.77	99.9	99.9	99.9
Ladysmith	CWa	LAD	KwaZulu-Natal	1006	28.58	29.75	97.3	95.3	95.3
Langebaanweg AWS	BSk	LAW	Western Cape	34	32.97	18.16	99.5	99.6	99.5
Lephalale	BSh	LEP	Limpopo	848	23.68	27.71	98.9	97.9	97.6
Mafikeng Wo	BSh	MWO	North West	1282	25.80	25.54	99.6	99.3	99.3
Makatini Research Centre	BSh	MRC	KwaZulu-Natal	64	27.39	32.18	99.3	98.6	98.3
Mandini	Cfa	MAN	KwaZulu-Natal	87	29.16	31.40	99.3	99.0	98.4
Mara	BSh	MAR	Limpopo	899	23.14	29.56	98.8	98.8	98.7
Nelspruit	CWa	NEL	Mpumalanga	810	25.50	30.91	92.8	92.9	92.6
Ottosdal	BSk	OTT	North West	1504	26.82	26.02	98.5	97.4	97.4
Oudtshoorn	BSk	OUD	Western Cape	409	33.57	22.22	98.3	96.6	96.6
Paddock	Cfa	PAD	KwaZulu-Natal	496	30.82	30.22	99.6	99.0	99.0
Pofadder	BWh	POF	Northern Cape	990	29.12	19.39	99.0	99.0	99.0
Polokwane Wo	BSh	PWO	Limpopo	1238	23.86	29.45	99.4	99.4	99.4
Port Elizabeth Wo	BSh	PEW	Eastern Cape	59	33.98	25.60	99.9	99.8	99.8
Port Nolloth	BWk	PNO	Northern Cape	13	29.25	16.87	99.6	97.7	97.9
Prieska	BWh	PRI	Northern Cape	967	29.67	22.74	96.7	98.0	97.9
Riversdale	BSk	RIV	Western Cape	172	34.10	21.25	100.0	99.5	99.5
Robertson	BSk	ROB	Western Cape	173	33.83	19.90	99.9	99.8	99.8
Shaleburn	CWb	SHA	KwaZulu-Natal	1618	29.80	29.35	99.7	98.3	99.0
Skukuza	BSh	SKU	Mpumalanga	269	24.99	31.59	99.3	99.0	99.0
Springbok Wo	BWk	SWO	Northern Cape	1021	29.67	17.88	98.3	98.0	98.0
Sutherland	BSk	SUT	Northern Cape	1462	32.38	20.67	98.4	97.5	97.5
Twee Rivieren	BWh	TRI	Northern Cape	889	26.47	20.61	99.6	99.2	99.2
Umtata Wo	Cfa	UMW	Eastern Cape	709	31.53	28.67	98.8	98.6	98.5
Upington Wo	BWh	UPW	Northern Cape	833	28.43	21.27	100.0	100.0	100.0
Vanwyksvlei	BWh	VWY	Northern Cape	965	30.35	21.82	97.4	99.3	99.3
Vredendal	BWk	VRE	Western Cape	36	31.67	18.50	99.7	99.6	99.6
Vryburg	BSh	VRY	North West	1251	26.95	24.65	99.2	98.9	98.9
Warmbad Towoomba	BSh	WTO	Limpopo	1142	24.90	28.32	98.5	99.2	99.2
Welkom	BSk	WEL	Free State	1342	27.99	26.70	97.3	97.7	97.7
Willowmore	BSk	WIL	Eastern Cape	839	33.30	23.48	98.9	97.6	97.8

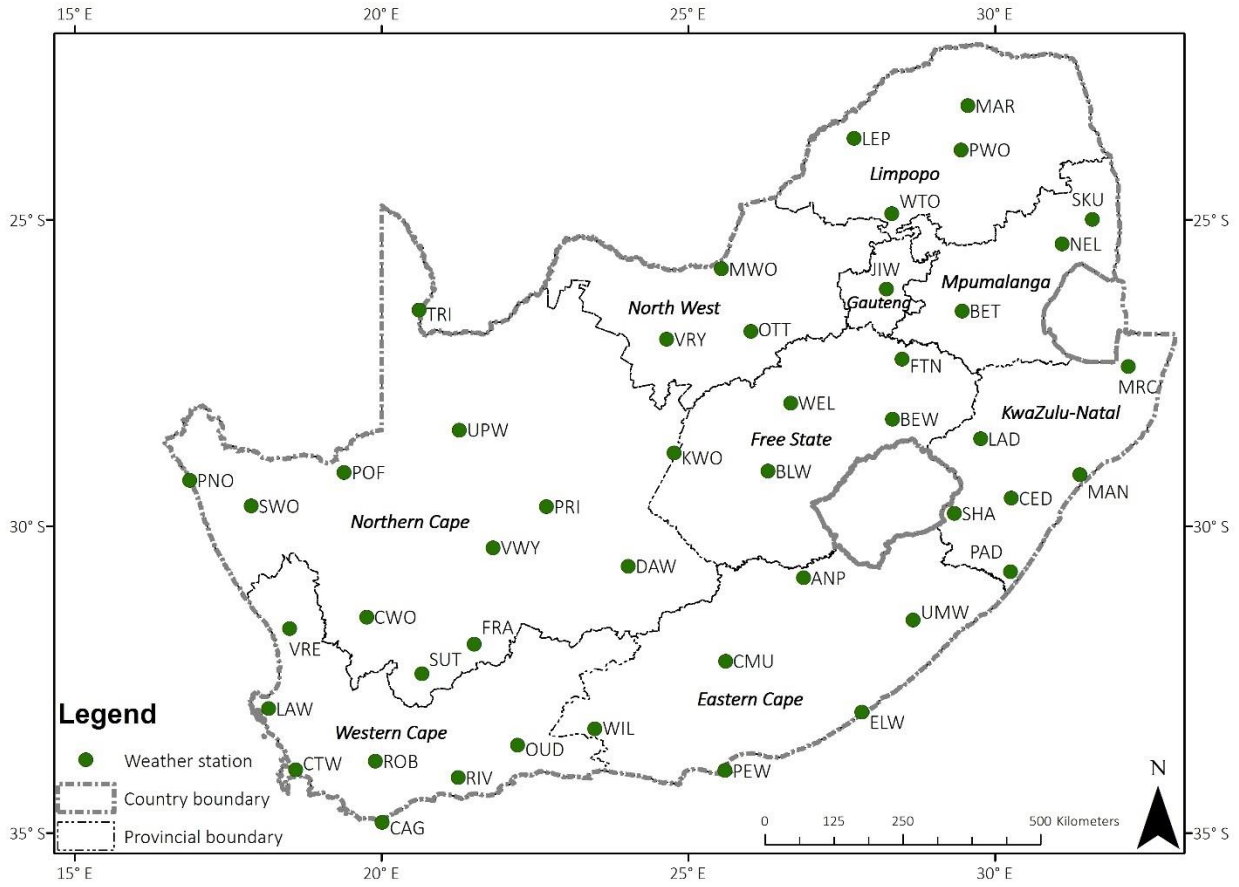


Figure 4.2: Map of the SAWS weather stations utilised for this study. These weather stations are labelled using the assigned weather station code in Table 4.1.

4.3 INITIAL DATA ANALYSIS

An initial data analysis was performed on the rainfall, T_{max} and T_{min} datasets for each of the selected weather stations. The main purpose of this task was to firstly calculate the basic descriptive statistics of each dataset to describe the annual and monthly rainfall characteristics, and to identify outliers in the rainfall, T_{max} and T_{min} datasets over the 30-year period of 1987-2016. Following this, linear trends as well as the magnitude and statistical significance of these trends were calculated for the rainfall datasets.

4.3.1 BASIC DESCRIPTIVE STATISTICS AND OUTLIERS OF RAINFALL AND TEMPERATURE

The procedures described below were undertaken to determine the mean and distribution of data over the 30-year study period. This task was undertaken with the main purpose to calculate the distribution of each dataset and to identify outliers. The basic statistics of each variable were calculated over monthly and annual temporal scales.

To quantify mean conditions in the datasets, the arithmetic mean was calculated using the following equation:

$$\bar{x} = \frac{1}{n}\sum_{i=1}^{n} x_i \text{ (Equation 1)}$$

(Burt *et al.*, 2009).

where x_i is the ith observation and n is the number of observations.

Mean rainfall over the various temporal scales was calculated using total monthly and annual total rainfall recorded over the study period (Kruger, 2006; Kruger & Nxumalo, 2017). Rainfall totals instead of mean values were used due to the high variability in daily rainfall amount (Kruger, 2006; Kruger & Nxumalo, 2017). To determine spatial patterns in the monthly rainfall totals, mean monthly rainfall totals were mapped through ordinary kriging interpolation using the process of kriging and semivariogram selection described under *Section 4.4.2*. The following semivariograms were used per month for kriging: circular (January, February, March and December), exponential (April, May, August and September), rational quadratic (June), j-bessel (July), spherical (October) and k-bessel (November). For this section, mean conditions of T_{max} and T_{min} were only used for the purpose of identifying outliers in these datasets, and later T_{max} and T_{min} were used in the analyses described under *Section 4.4.2*.

Whilst the mean provides information of the central tendency of a dataset, it does not convey any information regarding the variability of data over the study period (Burt *et al.*, 2009; Underhill & Bradfield, 2009). The relative variability of the rainfall data was calculated over annual and monthly scales using the ratio of the standard deviation (σ) to the mean, which is known as the coefficient of variation (CV; Hare 1983). CV is used to classify the degree of variability of rainfall events as low (CV <20%), moderate (20% < CV <30%), and high (CV >30%; Hare 1983) and is calculated as follows:

$$CV = \frac{\sigma}{\bar{x}} \times 100 \text{ (Equation 2)}$$

(Burt *et al.*, 2009).

Additionally, variability of data was determined by calculating the spread of the dataset over the study period (Burt *et al.*, 2009; Underhill & Bradfield, 2009). This analysis of variability for each dataset was calculated through analysis of the 'five number summary' which is comprised of the median, quartile one and three, the interquartile range (IQR) and the upper and lower fences using the following equations:

$$Median = \frac{n+1}{2} \text{ (Equation 3);}$$

$$Quartile\ 1 = \frac{n+1}{4} \text{ (Equation 4);}$$

$$Quartile\ 3 = \frac{3}{4}(n+1) \text{ (Equation 5);}$$

$$IQR = Q3 - Q1 \text{ (Equation 6);}$$

$$Upper\ fence = Q3 + 1.5(IQR) \text{ (Equation 7); } and$$

$$Lower\ fence = Q1 - 1.5(IQR) \text{ (Equation 8)}$$

(Underhill & Bradfield, 2009).

Using the 'five number summary', histograms and the method Dyson (2009) employed, outliers and erroneous values for rainfall, T_{max} and T_{min} of each weather station were identified (WMO, 2006). The presence of outliers in a dataset may easily affect the accuracy of results generated. Outliers refer to values which differ significantly to the bulk of the observations (Burt *et al.*, 2009). Outliers may represent genuine, naturally anomalous observations, but they may potentially result from error in data collection or recording, and as such it is necessary to investigate outliers.

Values larger or smaller than the upper and lower fences were identified as outliers (Moeletsi & Walker, 2012; Bekele *et al.*, 2017). Outliers were identified over daily, monthly and annual time scales. Through a comparison analysis, outliers across all temporal scales were investigated to discriminate between true erroneous values and naturally anomalous values (Dyson, 2009; Bekele

et al., 2017). Outliers were compared to surrounding weather stations, newspaper reports archived in the William Cullen at the University of the Witwatersrand, SAWS technical papers, monthly reports and daily weather bulletin books, and online flood archives, for example the Dartmouth Flood Observatory active archive of large floods globally (Dartmouth Flood Observatory, 2018). Outliers representing true erroneous values were deleted and remained omitted from the data analyses to avoid identification of misleading trends (Dyson, 2009). Outliers representing genuine values were recorded as anomalous values. Moeletsi and Walker (2012) suggest that a minimum of two and a maximum of 5 surrounding weather stations within a 50km radius are required for accurate estimation of missing and omitted data values. Not all weather stations had a minimum of two surrounding weather stations within a 50km radius, therefore no missing or deleted values were estimated.

Additional errors were also investigated throughout the rainfall datasets. The raw rainfall data obtained from SAWS include possible errors which are marked either by an "E" representing an error, "A" or "B" indicating that no rainfall reading was taken on the day but that any rainfall that did occur is included in the accumulation total at the end of the period, and "C" representing a rainfall value accumulated over more than one day. These possible errors were omitted from the statistical analyses. Next, accumulated days not highlighted in the raw datasets were also investigated (Dyson, 2009). These days were identified when there was missing data for one or more days followed by a day reporting a high rainfall value. A high rainfall value here represents the 99th percentile of daily rainfall specific to each weather station (Dyson, 2009). This value was deleted if after a comparison analysis, as above, it was classified as an outlier. Finally, mistakes from human error were also investigated. These were entries with an extra digit, where a rainfall reading may have been recorded as 120mm instead of 12mm as an example. These high values were typically picked up as outliers in the dataset and after a comparison analysis, the high value was changed or deleted if it was in fact an outlier.

4.3.2 TRENDS IN RAINFALL AMOUNT FOR THE PERIOD OF 1987-2016

Changes in the seasonality of rainfall may be associated with a combination of changes in mean annual amount and/or monthly distribution of rainfall (Pryor & Schoof, 2008; Feng *et al.*, 2013).

Hence, a study regarding the changes in rainfall seasonality over time requires a time series analysis of annual and monthly rainfall amount (Feng *et al.*, 2013). An analysis of the trends in monthly rainfall amount is also particularly important in providing a complete description of the shifts in rainfall seasonality (Feng *et al.*, 2013). Trends in total rainfall amount were calculated over monthly and annual temporal scales over the 30-year study period 1987-2016.

Rainfall varies considerably in space and time, and this results in trend calculations being sensitive to the location and temporal period of the observations (MacKellar *et al.*, 2014; Kruger & Nxumalo, 2017). Hence, rainfall trends were calculated individually for each weather station as the changes for each location are not likely to be equal (MacKellar *et al.*, 2014). Since the purpose of this study is mainly to assess four methods which statistically quantify and classify rainfall seasonality and it is not focused specifically on rainfall trends, only linear time trends in rainfall data were calculated.

For the purpose of trend analysis, the following analyses described below were performed. Some weather stations were missing an entire month of rainfall data or there were too few rainfall readings to accurately represent the month of interest. These months were omitted from the analysis of monthly rainfall totals (Table 4.2). For the annual totals, the months with either no data or too few rainfall readings (i.e. less than two weeks) may alter the annual rainfall totals and are important to note (Feng *et al.*, 2013; Table 4.2). Additionally, no annual totals were calculated for years with more than two months missing (Feng *et al.*, 2013; Table 4.2).

Table 4.2: Details of the months omitted from analyses for this and following sections.

Weather station	Months omitted from analyses
Aliwal-North Plaatkop	August 1989
Bethal	March to December 2016
East London Wo	October 2014
Fraserburg	June 1993
Ladysmith	May 2016
Mafikeng Wo	July 1991
Makatini Research Centre	December 2008; January 2009
Nelspruit	March to June 1993; November 2012
Oudtshoorn	April 2005; July 2005
Prieska	December 1992; February 1993
Springbok Wo	January to June 1987
Sutherland	April 1994; March to May 2015
Vanwyksvlei	January 1990
Welkom	June 1992

Correlation analysis was undertaken to determine the strength and direction of rainfall trends over the study period 1987-2016 (Burt *et al.*, 2009; Nel, 2009). The purpose of a correlation analysis is to determine whether a relationship exists between a dependent (y) and an independent (x) variable (Burt *et al.*, 2009; Underhill & Bradfield, 2009), and for the purpose of this study monthly total or annual total rainfall were dependent variables and time in years was the independent variable (Burt *et al.*, 2009; Underhill & Bradfield, 2009). The Pearson correlation coefficient was calculated using the following equation:

$$r = \left| \frac{\sum(x_i - \bar{x})(y_i - \bar{y})}{\sum \sqrt{x_i - \bar{x})^2 \sum (y_i - \bar{y})^2} \right|$$ (Equation 9)

(Underhill & Bradfield, 2009).

Resulting *r values* range between -1 and +1, and values closer to -1 or +1 represent a stronger relationship between the dependent and independent variable and that there has been a consistent change in the dependent variable of the time period (Burt *et al.*, 2009; Underhill & Bradfield, 2009). An *r value* tending towards 0 indicates a weak relationship between the dependent and independent variables and suggests either no clear pattern in the data over the time period or that there has been little or no change (Burt *et al.*, 2009; Underhill & Bradfield, 2009). For the purpose of this study, the absolute *r value* is reported for comparison of the trends. This is the case for all *r values* reported throughout this study, unless otherwise stated. Once a relationship between rainfall and time has been calculated, the magnitude and direction of this trend is to be determined.

To determine the magnitude of change in rainfall over time, the rate of change over the 30-year study period was calculated through regression analysis (Burt *et al.*, 2009; Kruger & Nxumalo, 2017). A line of best-fit was fit to quantify the linear rate of change of the dependent variable rainfall over monthly and annual time scales. A linear trend line will quantify the trend demonstrating either an increasing or decreasing trend in rainfall. Important to note is that rainfall changes may be both linear and non-linear and other trend analyses should be applied for future studies (Nel, 2009; MacKellar *et al.*, 2014; Kruger & Nxumalo, 2017; MacFayden *et al.*, 2018). The best-fit line for the data was calculated using the following equation:

$$y = mx + c \text{ (Equation 10)}$$

(Manly, 2009).

where *m* is the coefficient of *x* and *c* is the *y* intercept, and they are determined using the following equations:

$$c = \frac{\sum xy - \frac{\sum x \sum y}{n}}{\sum x^2 - \frac{(\sum x)^2}{n}} \text{ (Equation 11)}$$

$$m = \frac{\sum y - b \sum x}{n} \text{ (Equation 12)}$$

(Manly, 2009).

Only the results of *a* are reported for the linear regression analysis. This is reported as a rate of change per year and for rainfall amount the results are presented as a millimeter change per year ($mm.year^{-1}$). This result will also indicate the direction of linear change through either a negative or positive *a value*. A negative value indicates a decline in rainfall over the study period 1987-2016, while a positive result indicates an increase in rainfall over this period. Having calculated the magnitude and direction of rainfall trends, it is important to determine the statistical significance of the rainfall trends (Burt *et al.*, 2009; Underhill & Bradfield, 2009).

To determine the degree of statistical significance, the *p value* of each trend was determined. The *p value* ranges from 0 to 1 and is a measure of the probability that trends are occurring by chance as a result of random sampling or are an accurate reflection of the data over the study period (Burt *et al.*, 2009; Manly, 2009; Underhill & Bradfield, 2009). The *p value* tests the null hypothesis which states that there is no trend (Manly, 2009), and in particular that rainfall over the period 1987-2016 remained unchanged. A *p value* of less than 0.05, selected for this study, indicates strong evidence against the H_0, which indicates that the rainfall trend is statistically significant, and that rainfall has changed over the study period (Burt *et al.*, 2009; Manly, 2009; Underhill & Bradfield, 2009; MacKellar *et al.*, 2014).

4.4 STATISTICAL APPROACH TO QUANTIFYING RAINFALL SEASONALITY ACROSS SOUTH AFRICA

To quantify rainfall seasonality, there are a number of statistical approaches which have been developed; and these have been described under *Section 2.2* of the literature review. To develop a statistical approach specific to South Africa, approaches from the main body of literature regarding rainfall seasonality classification have been assessed on accuracy and usability under *Section 2.2*. From this assessment of approaches used across South Africa and globally, no single metric on rainfall seasonality had the ability to completely describe this concept (Roffe *et al.*, 2019). To completely describe rainfall seasonality across a region, scholars have emphasised the importance of quantifiable measurements on the duration of wet and dry season, their timing and their magnitude and intensity (Feng *et al.*, 2013; Pascale *et al.*, 2015, 2016). Using this set of criteria, a combination of approaches to classify rainfall seasonality, used across South Africa, were selected for use in this study. These approaches were further analysed for application across South Africa and were only included in the sections below if such an approach discriminates between summer and winter rainfall (Thackeray & Fitchett, 2016). Four approaches, which are described in detail below, were selected to create a statistical approach which can be used to quantify, classify and completely describe rainfall seasonality across South Africa.

4.4.1 CLUSTERING MONTHLY RAINFALL AND VARIABILITY

To determine homogeneous rainfall seasonality regions based on monthly rainfall amount, cluster analysis has been widely applied globally (e.g. Lyra *et al.*, 2014; Awan *et al.*, 2015; Teodoro *et al.*, 2016; Dehghan *et al.*, 2017; Huang *et al.*, 2017; Lin *et al.*, 2017; Rau *et al.*, 2017; Singh *et al.*, 2017; Fazel *et al.*, 2018; Forestieri *et al.*, 2018; Raziei, 2018; Crétat *et al.*, 2019). Cluster analysis has also been applied widely in climate science across South Africa or portions of the country for delineating homogeneous rainfall regions on the basis of, among others, rainfall amount and onset dates, for a range of purposes such as identifying climate drivers (e.g. Tennant & Hewitson, 2002; Rouault & Richard, 2003; Shongwe *et al.*, 2009; Crétat *et al.*, 2012; Favre *et al.*, 2016; Mahlalela *et al.*, 2018; Phakula *et al.*, 2018; Burl *et al.*, 2019). Cluster analysis is a statistical technique used to partition groups of a set of entities according to the similarity and differences between these

entities (Lin *et al.*, 2017; Fazel *et al.*, 2018; Crétat *et al.*, 2019). In recent studies, both hierarchical and nonhierarchical cluster analysis methods have commonly been used. Hierarchical cluster analysis methods include agglomerative hierarchical clustering, and nonhierarchical cluster analysis methods include k-means cluster analysis amongst others.

For the purpose of this study, agglomerative hierarchical clustering using Ward's minimum variance algorithm and the squared Euclidean distance to quantify dissimilarity is utilised (Ward, 1963; Unal *et al.*, 2003; Lyra *et al.*, 2014; Awan *et al.*, 2015; Teodoro *et al.*, 2016; Singh *et al.*, 2017; Crétat *et al.*, 2019). The Ward's minimum variance algorithm considers the sum of squares within groups *W*, which is calculated using the homogeneity within groups and the heterogeneity outside the group, according to the following equation:

$$W = \sum_{i=1}^{n} x_i^2 - \frac{1}{n}(\sum x_i)^2 \text{ (Equation 13)}$$

(Ward, 1963).

where n is the number of elements and x_i is the ith element of the group (Ward, 1963). This agglomerative hierarchical clustering method was utilised as it minimizes the within group variance at each stage of merging, and it optimizes an objective statistic (Tennant & Hewitson, 2002). Finally, the optimal number of clusters was determined by finding the level at which the within group similarity is maximized and the between group similarity is minimized (Lyra *et al.*, 2014; Brito *et al.*, 2016; Singh *et al.*, 2017).

Employing this method, the methodological process carried out by Lyra *et al.* (2014) and Teodoro *et al.* (2016) has been followed to group weather stations on the basis of mean monthly rainfall amount and its spatial and temporal variability (i.e. CV). In addition to clustering on the basis of mean monthly rainfall and its CV, weather stations were also clustered on the basis of the number of rain days and the respective CV. Although not commonly used as a seasonality indicator in comparison to the distribution of mean monthly rainfall, previous scholars have demonstrated that the annual distribution of rain days can be used to represent the seasonality of rainfall

(Odekunle, 2006; Amekudzi *et al.*, 2015). For this process, a rain day was defined as 0.1mm, as this is the minimum amount of rainfall recorded in the SAWS datasets.

Based on the results from Lyra *et al.* (2014) and Teodoro *et al.* (2016), this method demonstrates the ability to classify the mean rainfall seasonality across a large geographic region, and this method also provides information on the length of both the dry and wet season which are important measurements towards a complete description of rainfall seasonality. Firstly, the data were subject to standardisation as a *z score* to produce values which are comparable (Lyra *et al.*, 2014; Kassambara, 2017). Next, the mean monthly rainfall totals or mean rain days and the respective CV for each month were used to create groups of weather stations with similar patterns of monthly rainfall (Lyra *et al.*, 2014; Awan *et al.*, 2015; Teodoro *et al.*, 2016). Following this, within each group of weather stations, mean monthly rainfall totals or mean rain days and the respective monthly CV for weather stations were grouped to identify the months with similar rainfall amount or rain days and the respective variability (Lyra *et al.*, 2014; Teodoro *et al.*, 2016). This step was followed to define the wet and dry season across the cluster groups (Lyra *et al.*, 2014; Teodoro *et al.*, 2016). In R, the cluster, vegan and rioja packages were utilised in conjunction to compute these groupings (Kaufman & Rousseeuw, 2009). These packages were used in combination to create groupings using agglomerative hierarchical clustering, Ward's minimum variance algorithm and the squared Euclidean distance, where groupings were not constrained by nearest neighbour (Lyra *et al.*, 2014; Awan *et al.*, 2015; Teodoro *et al.*, 2016).

To determine the optimal number of clusters, silhouette plots and a scree plot were created (Kaufman & Rousseeuw, 2009; Lyra *et al.*, 2014; Corporal-Lodangcoa & Leslie, 2017). The results of the silhouette plots were the main determinants for the optimal number of groups. Silhouette plots were created for all possible group numbers to determine the optimal number of groups (Kaufman & Rousseeuw, 2009). These plots represent the silhouette width which is a measure of the average distance of each object and all other objects in the group, compared to the same measure for the nearest group (Kaufman & Rousseeuw, 2009). A silhouette plot with values closest to 1 suggests an optimal number of groups, while negative values suggest that samples are currently in the wrong group, and values close to 0 suggest that samples may fall between groups (Kaufman & Rousseeuw, 2009). To group the weather stations firstly on mean monthly rainfall

(and mean monthly rain days) and CV, silhouette plots were created for two to 10 groups. To determine the wet and dry season durations within each of the weather station groups silhouette plots were created for one to four groups, to potentially account for a year long wet season for one group and to account for up to two transitions seasons between the wet and dry seasons with four groups (Lyra *et al.*, 2014). Additionally, the structure of the cluster dendrogram and sudden changes in a scree plot were also used to determine the appropriate number of clusters (Wilks, 1995; Griffith & Amrhein, 1997; Lyra *et al.*, 2014).

Furthermore, the results of the cluster analysis solution for the optimal number of clusters of each cluster solution were further validated using the cophenetic correlation coefficient (Kaufman & Rousseeuw, 2009; Corporal-Lodangcoa & Leslie, 2017). The cophenetic correlation coefficient measures the correlation between the original pairwise distance matrix and the cophenetic distance matrix of the dendrogram, and hence it is a measure of how well the dendrogram represents dissimilarities amongst observations (Saraçli *et al.*, 2013). Resulting values closer to 1 represent a high-quality cluster analysis solution (Saraçli *et al.*, 2013).

The resulting mean monthly rainfall and mean rain day groups may be spatially represented through grouping the resulting cluster groups as SRZ, WRZ and YRZ. For the purpose of this section, these groupings of were based on the resulting wet and dry season length which were determined through clustering. A group was classified as YRZ if the wet season, containing contiguous rainfall, was at least nine months in length. Groups with less than nine months of contiguous rainfall with the summer solstice (21-22 December), and not the winter solstice (20-22 June), during the wet season were classified as SRZ (Keen & Tyson, 1973; NOAA, 2018). Groups with less than nine months of contiguous rainfall with the winter solstice and not the summer solstice during the wet season during the wet season were classified as WRZ (Keen & Tyson, 1973).

4.4.2 RELATIONSHIP BETWEEN RAINFALL AND TEMPERATURE

Based on the relationship between mean monthly rainfall (MMR) and mean monthly temperature (MMT), Thackeray and Fitchett (2016) developed a seasonality metric. From this relationship, summer and winter rainfall are statistically segregated where summer rainfall is characterised by

a positive relationship and winter rainfall is characterised by a negative, inverse relationship (Thackeray & Fitchett, 2016). This relationship is quantified using the *m-coefficient* derived from the standard least squared linear regression equation:

$$y=mx+c \quad \text{(Equation 10)}$$

(Burt *et al.*, 2009).

In this equation *y* refers to the square-root (sqrt) transformed MMR values and *x* refers to the sqrt transformed MMT values (Thackeray & Fitchett, 2016). Data are sqrt transformed to reduce the skewness in the distribution of the datasets to improve the assumptions of normality, and to produce values which are more comparable for the linear relationship (McCune *et al.*, 2002; Erdin *et al.*, 2012). The resulting *m-coefficient* from the linear relationship provides a rainfall seasonality score and will from now onwards be referred to as a seasonality score. Towards providing a complete description of rainfall seasonality, the seasonality score provides a measure on the timing and degree of seasonality. Positive seasonality scores are associated with summer rainfall regimes and higher values indicate a stronger degree of seasonality (Thackeray & Fitchett, 2016). Negative seasonality scores are associated with winter rainfall and higher negative values indicate a stronger degree of seasonality (Thackeray & Fitchett, 2016). A seasonality score of 0 would indicate the hypothetical situation of equivalent year-round rainfall (Thackeray & Fitchett, 2016).

To quantify the seasonality scores for the weather stations, daily temperature and daily rainfall were used to calculate MMT and MMR values (Thackeray & Fitchett, 2016). This and all mean quantities were calculated using the arithmetic mean described under *Section 4.3.1*. Daily mean temperature was obtained by calculating the mean of the daily T_{max} and T_{min}. Daily mean temperature values were omitted and regarded as missing when either a T_{max} or T_{min} reading was missing. Some weather stations were missing an entire month of rainfall or temperature data or both, or there were too few data points (i.e. less than two weeks of data) to accurately represent the month of interest, and as a result these months were omitted from this analysis (Feng *et al.*, 2013; Table 4.3). Years with more than two months missing were also omitted from this analysis (Feng *et al.*, 2013; Table 4.3).

Table 4.3: Details of the months omitted from analyses of the relationship between temperature and rainfall.

Weather station name	Months omitted from analyses
Aliwal-North Plaatkop	August 1989
Bethal	March to December 2016
East London Wo	October 2014
Fraserburg	June 1993; September 2004
Ladysmith	February to June 2003; May 2016
Mafikeng Wo	July 1991
Makatini Research Centre	December 2008; January 2009; May 2012
Mandini	June 1987
Nelspruit	March to June 1993; November 2012
Oudtshoorn	April to July 2005
Prieska	December 1992; February 1993
Springbok Wo	January to June 1987
Sutherland	April 1994; March to May 2015
Vanwyksvlei	January 1990
Welkom	June 1992

The resulting MMT and MMR values were used to determine the relationship of the sqrt transformed MMT and sqrt transformed MMR over an annual scale and for the entire period of 1987-2016 for each of the weather stations (Table 4.1). Calculation of the annual seasonality scores accounts for the year to year variability in rainfall seasonality. Both the annual and total period seasonality scores were calculated using the aforementioned standard least squared linear regression equation (Thackeray & Fitchett, 2016).

The total period seasonality scores were further described by the *p* and *r values*. The *r value* represents the strength of the relationship between MMR and MMT, and was calculated using the Pearson correlation coefficient equation, as previously described under *Section 4.3.2*. The resulting *r values* are again reported as an absolute value ranging between 0 and 1. The statistical significance of each relationship was calculated at a level of 95% and a *p value* less than 0.05 is statistically significant (MacKellar *et al.*, 2014).

The seasonality scores for the period of 1987-2016 have now been calculated at single point locations. However, this only provides a location specific classification which is not easily applicable for decision-making and research regarding activities such as water resource management, which requires information on the spatial variability and distribution of rainfall regimes across a catchment (Adikhary *et al.*, 2015; Yang *et al.*, 2015). Spatial interpolation can be

used to develop an estimated continuous surface from measured point locations, which can be used to provide information on the seasonality scores at unmeasured locations.

There are a number of interpolation techniques that have been used for the purpose of mapping environmental variables, and these can be grouped into deterministic and geostatistical interpolation methods (Adhikary *et al.*, 2015). Deterministic methods include inverse distance weighting, spline and nearest neighbour among others (Li & Heap, 2014). Geostatistical methods include kriging methods which are ordinary, simple and universal kriging among others (Li & Heap, 2014). For the purpose of rainfall mapping both deterministic and geostatistical methods have been employed. Amongst studies comparing spatial interpolation methods to estimate the spatial distribution of rainfall, kriging has typically outperformed alternative spatial interpolation methods (e.g. Coulibaly *et al.*, 2007; Di Piazza *et al.*, 2011; Ly *et al.*, 2011; Adikhary *et al.*, 2015; Kisaka *et al.*, 2015; Xu *et al.*, 2015; Yang *et al.*, 2015).

Kriging is typically preferred as it is an exact interpolator which generates an estimate that is the same as the observed value at a measured location, and it is a stochastic interpolation method which incorporates the concept of randomness while also providing measures of error for the estimated surface (Li & Heap, 2014). Amongst the numerous studies using kriging for univariate samples, simple and ordinary kriging have typically been employed (e.g. Bargaoui & Chebbi, 2009; Di Piazza *et al.*, 2011; Sun *et al.*, 2015; Xu *et al.*, 2015; Frazier *et al.*, 2016). In a review on spatial interpolation methods, Li and Heap (2014) recommended ordinary over simple kriging, because ordinary kriging allows one to account for local variation of the mean, and ordinary kriging estimates are suggested to better follow the data than simple kriging estimates. For the purpose of mapping rainfall seasonality for this study, ordinary kriging has been utilised from the *geostatistical analyst* extension on *ArcMap 10.3.1*. The ordinary kriging estimator is expressed as:

$$\hat{z}(x_0) = \sum_{i=1}^{n} w_i z(x_i) \quad \text{(Equation 14)}$$

(Li & Heap, 2014).

where $\hat{z}(x_0)$ refers to the estimated value of $\hat{z}$ at the point of interest x_0, $z(x_i)$ refers to z the observed value at sample point x_i, w_i is the weight assigned to the sample point and n represents the number of sample points used for observation (Li & Heap, 2014). One ordinary kriging map

will be created using the seasonality scores of the weather stations for the entire period of 1987-2016.

Kriging interpolation relies on the appropriate selection of a semivariogram model that defines the spatial structure of the observed data (Adhikary *et al.*, 2015). The semivariogram is a mathematical function which is fitted to the data points and defines the variability of data under the effect of separation distance between data points (Ly *et al.*, 2011; Verworn & Haberlandt, 2011; Adhikary *et al.*, 2015). A semivariogram is fitted to the observed data based on the distance and direction of two data points and once a proper semivariogram is selected, ordinary kriging can be employed for the missing data estimation to create a continuous raster surface displaying rainfall seasonality (Adhikary *et al.*, 2015). The semivariogram function is expressed as:

$$\hat{\gamma}(h) = \frac{1}{2N(h)}\sum_{i=1}^{N(h)}(Z(x_i) - z(x_i + h))^2 \text{(Equation 15)}$$

(Adhikary *et al.*, 2015).

where *N(h)* is the number of pairs of data locations at a lag distance *h* apart, x_i and $(x_i + h)$ represent observed data point locations separated by a distance *h*, and $z(x_i)$ and $z(x_i + h)$ indicate data values *z* observed at the corresponding locations x_i and $(x_i + h)$, respectively (Adhikary *et al.*, 2015).

ArcMap 10.3.1 offer 11 types of semivariogram models which can be fitted to the observed total period seasonality scores. These semivariogram models include the: circular, spherical, tetraspherical, pentaspherical, exponential, gaussian, rational quadratic, hole effect, k-bessel, j-bessel and stable semivariogram. The choice of semivariogram for interpolation should not be arbitrary and must be based on the available observed total period seasonality scores (Leung & Law, 2002; Ly *et al.*, 2011; Adhikary *et al.*, 2015). For ordinary kriging interpolation of rainfall, the exponential, gaussian and spherical semivariogram models are most widely used (Adhikary *et al.*, 2015).

To select an appropriate semivariogram for the observed total period seasonality scores, the following procedure was undertaken. First, each of the available semivariogram options on *ArcMap* were considered and if a nugget value of zero was not obtained, the semivariogram was not selected or the lowest possible nugget value was selected (Leung & Law, 2002; Ly *et al.*, 2011).

A nugget value indicates the behaviour of the semivariogram at the origin, and a value of zero indicates that the semivariogram model intercepts the y-axis at zero indicating that the observed and model values are the same value (Leung & Law, 2002). Lastly, measurements on the prediction error associated with fitting the semivariogram were used for the selection of the final semivariogram model for ordinary kriging interpolation of the seasonality scores (Obrośląk & Dorozhynskyy, 2017). The results from the *geostatistical analyst* provide measurements of these prediction errors, and these measurements include: mean, root mean square, mean standardized, root mean square standardized and mean standard error. A semivariogram with the smallest error measurements was selected to interpolate the individual weather stations total period seasonality scores. The final semivariogram model selected to interpolate the total period seasonality scores was the exponential semivariogram model.

The seasonality scores for the individual weather stations may additionally be spatially represented through grouping of the scores into SRZ, WRZ and YRZ. For the purpose of this study, class limits have been developed to classify a weather station across South Africa into these respective rainfall zones (Table 4.4). These class limits were developed considering the strength of observed seasonality scores, where stronger scores tending away from zero indicate a higher degree of seasonality and unevenly distributed rainfall with a clear wet season, and scores tending towards zero indicate a lower degree of seasonality and more evenly distributed rainfall (Thackeray & Fitchett, 2016).

Table 4.4: Seasonality score class limits for classification of SRZ, YRZ and WRZ.

Rainfall zone classification	Seasonality score class limit
SRZ	Seasonality score > 0.30
YRZ	0.30 ≥ Seasonality score ≥ -0.30
WRZ	-0.30 > seasonality score

4.4.3 ONSET, CESSATION AND LENGTH OF THE WET SEASON

Onset and cessation dates of the wet season are commonly used measures of rainfall seasonality in agricultural applications, marking the time at which the rainfall distribution has become adequate for crop development, and the time beyond which the rainfall distribution may no longer sustain crop growth, respectively (Odekunle *et al.*, 2005; Amekudzi *et al.*, 2015). These dates are

used to describe the timing and length of the wet season and can therefore be used to describe rainfall seasonality. Numerous methods have been developed to determine onset and cessation dates to describe the wet season. For the purpose of this section, onset and cessation criteria which are determined only using rainfall data are considered (Table 4.5). Many different sets of criteria have been developed to determine onset and cessation dates to describe the growing season of specific crops for specific regions (Stern *et al.*, 1982; Kniveton *et al.*, 2009; Table 4.5). These criteria have for a prolonged time been used across Africa, and in particular South Africa, and were developed for the purpose of determining optimal planting time by ensuring sufficient soil moisture for crop germination and development (Stern *et al.*, 1982; Kniveton *et al.*, 2009; Moeletsi & Walker, 2012). In South Africa, these criteria have been applied extensively for rainfed maize cultivation (e.g. Reason *et al.*, 2005; Tadross *et al.*, 2005a, 2007, 2009; Moeletsi *et al.*, 2011, 2013; Moeletsi & Walker, 2012; Husak *et al.*, 2013; Tongwane & Moeletsi, 2015; Tshililo, 2017). The suitability of such criteria across the full area of South Africa has never been tested. Since these criteria are still regularly used (Table 4.5), a set of criteria most frequently used in literature will be tested across South Africa.

Table 4.5: Onset and cessation date criteria used in agroclimatology research across Africa. These criteria are colour coded, where green represents onset criteria and brown represents cessation criteria.

Publication	Location	Onset and cessation date criteria
Ati *et al.* (2002)	Northern Nigeria	First day of a three-day period, after 1 May, where at least 20mm of rainfall accumulated, and no dry spell during the subsequent 30 days exceeds seven days. Sixth day of a ten-day period where at least 25mm of rainfall accumulated, and no dry spell during the subsequent 30 days exceeds seven days.
Raes *et al.* (2004)	Zimbabwe	First day of a seven-day period when cumulative rainfall exceeds 25mm. First day of a 15-day period where at least 40mm of rainfall accumulated.
Reason *et al.* (2005)	Limpopo, South Africa	First day of a ten-day period with at least 25mm rainfall followed by a 20-day period with at least 20mm rainfall.
Tadross *et al.* (2005a)	Zimbabwe and north eastern South Africa	Last day of ten-day period with at least 25mm rainfall followed by a 20-day period with at least 20mm rainfall.
Tadross *et al.* (2007)	Southern Africa	First day after 1 August when at least 25mm of rainfall accumulated during a ten-day period without ten consecutive dry days (rainfall <2mm) occurring during the following 20 days. First day of a four-day period where at least 45mm of rainfall accumulated. First day, from 1 February, of three consecutive ten-day periods with less than 20mm accumulated rainfall.

Ati *et al.* (2008)	Kano, Nigeria	First day of a ten-day period in which rainfall accumulated to more than 25mm and no dry spell longer than ten days occurs within the next 30 days.
Hachigonta *et al.* (2008)	Zambia	Last day of a ten-day period where at least 25mm of rainfall has accumulated and at least 20mm of rainfall has accumulated in the subsequent 20 days.
Tadross *et al.* (2009)	Southeast Africa	First day after 1 August when at least 25mm of rainfall accumulated during a ten-day period without ten consecutive dry days (rainfall <2mm) occurring during the following 20 days. First day of a four-day period where at least 45mm of rainfall accumulated. First day after 1 February of three consecutive ten-day periods with less than 20mm accumulated rainfall.
Marteau *et al.* (2011)	Southwest Niger	First day of a three-day period, after 15 April, with at least 20mm of rainfall, without any ten-day dry spell (<1mm) following.
Moeletsi *et al.* (2011)	Free State, South Africa	Last day starting from July, where at least 25mm of rainfall has accumulated over the previous ten days and at least 20mm has accumulated in the subsequent 20 days. Last day starting from 1 December where a cumulative of 25mm of rainfall occurs over ten days.
Mupangwa *et al.* (2011)	Southern Zimbabwe	First day after 1 October when rainfall accumulated over one to three days is at least 20mm, and no dry spell of more than 10 days occurs during the 30 days which follow. Last day before 30 June that accumulates at least 10mm rainfall.
Moeletsi & Walker (2012)	Free State, South Africa	The last day in which at least 25mm of rainfall has accumulated during the previous ten days and at least 20mm rainfall accumulated in the subsequent 20 days. Last day of ten-day period in which at least 25mm rainfall accumulated.
Husak *et al.* (2013)	Sub-Saharan Africa	First day of a ten-day period with at least 25mm of accumulated rainfall, followed by two ten-day periods with at least 20mm of rainfall.
Moeletsi *et al.* (2013)	Free State, South Africa	Last day starting from 1 July, where at least 25mm of rainfall has accumulated over the previous ten days and at least 20mm has accumulated in the subsequent 20 days. Last day of ten-day period in which at least 25mm rainfall accumulated.
Adelekan & Adegebo (2014)	Ibadan, Nigeria	The first day of a five-day period with at least 25mm of rainfall, where the start day and at least two other days receive more than 0.25mm of rainfall. No dry period of seven or more days should occur in the subsequent 30 days. The last day of a five-day period with less than 25mm of rainfall, where three days of this period receive less than 5mm rainfall. This period is followed by a dry period of at least seven days.
Ngetich *et al.* (2014)	Kenyan highlands	The first wet day of a three to five-day period with at least 25mm of accumulated rainfall for the semi-humid region and 30mm accumulated the humid region.
Tongwane & Moeletsi (2015)	Northern Lowlands of Lesotho	First day of rainfall (≥1mm) after 1 September when rainfall accumulated to at least 20mm during at least two days of a three-day period with no dry spell of more than ten days during the following 30 days.
Sobowale *et al.* (2016)	Southwest Nigeria	Either a seven-day period with at least 25mm rainfall or a ten-day period with at least 30mm of rainfall.
Bekele *et al.* (2017)	Sinana District, South Eastern Ethiopia	First day of a three-day period with at least 20mm of accumulated rainfall, and no dry spell greater than ten days occurs during the subsequent 30 days.
Tshililo (2017)	Luvuvhu river catchment,	First day after 1 October when accumulated rainfall in ten days is at least 25mm. First day after 1 February of three consecutive ten-day periods with less than 25mm rainfall during each period.

	Limpopo, South Africa	
Byakatonda *et al.* (2018)	Botswana	Accumulation of at least 25mm during a ten-day period with no dry spell of more than ten days during 30 days which follow. Seventh day of a dry spell exceeding 10 days.
Kumi & Abiodun (2018)	West Africa	The first day of a five-day period with at least 25mm rainfall, where no dry spell greater than seven days occurs during the subsequent 30 days.

The onset and cessation dates for this study were calculated using a combination of criteria used across Africa (Table 4.6). Eight different onset criteria were identified, and those criteria used more than five times were adapted for use in this study (Table 4.6). Four different cessation criteria were identified, and those criteria used more than three times were adapted for use in this study (Table 4.6). It is known that these criteria are region specific (Liebmann *et al.*, 2012), but since they may be used to describe the wet season on a daily scale, they were used to determine the suitability of such criteria across the entire country. Additionally, the 'dry spell' criteria (which are required to ensure enough soil water is available for crop germination) have not been used, as this study focuses on climatological rather than agricultural seasonality. Hence, three criteria were identified to determine onset dates, while two criteria were identified to determine cessation dates (Table 4.6).

Table 4.6: Criteria used to determine onset and cessation dates of the wet season.

Date	Criteria adapted from literature
Onset date	1. First day of rainfall for a period of ten days where at least 25mm of rainfall has accumulated. 2. Last day of rainfall for a period of ten days where at least 25mm of rainfall has accumulated. 3. First day of rainfall for a period of three days where at least 20mm of rainfall has accumulated during two of the three days.
Cessation date	1. Last day of rainfall for the last ten-day period of rainfall where at least 25mm of rainfall has accumulated. 2. First day of three consecutive ten day periods where accumulated rainfall during each period is below 20mm.

For the purpose of this analysis, a rain day is defined as a day with a total accumulation of 0.1mm of rainfall. A rain day in previous studies has been defined either meteorologically as 0.1mm (Burls *et al.*, 2019), 0.2mm (Tyson & Preston-Whyte, 2000) and 0.85mm (Mupangwa *et al.*, 2011), or agriculturally for the purpose of sustaining crop development as 0.1mm (Nandargi & Mulye, 2012;

Bekele *et al.*, 2017; Kumi & Abiodun, 2018), 0.85mm (Ngetich *et al.*, 2014), 1mm (Reason *et al.*, 2005; Marteau *et al.*, 2011; Byakatonda *et al.*, 2018), 2mm (Tadross *et al.*, 2007, 2009) and 5mm (Mupangwa *et al.*, 2011; Tshililo, 2017). A rain day of 0.1mm was adopted for this study as this is the minimum amount of rainfall recorded in the datasets obtained from the SAWS, and by using this value all rainfall within the wet season is considered for this analysis.

The onset and cessation dates were determined annually as the Julian day (JD) and for the total period (i.e. mean) of 1987-2016 for each of the 46 weather stations. Important to note are the months with missing data (Table 4.2), as this may potentially influence the accuracy of onset and cessation dates for a certain year or no dates may be obtained. For the purpose of defining the climatological year, onset dates were quantified from the month following the month of mean minimum rainfall quantified under *Section 4.3.1*, and for locations with no clearly defined uni-modal wet season (e.g. PEW: Port Elizabeth Wo) the quantification of dates was from January to ensure meaningful dates were obtained (Liebmann *et al.*, 2012; Feng *et al.*, 2013; Dunning *et al.*, 2016). Since three and two criteria were used to determine the onset and cessation dates respectively, the latest date was taken as the annual onset and cessation dates. By doing this, each criterion agrees that the wet season has either begun or ended. No date (ND) was captured for a criterion for which no date was obtained, and if all criteria did not produce an onset or cessation date. Additionally, if a classification of ND was captured for an onset date then no cessation date was captured. To determine the onset and cessation dates for the total period, the mean of the annual JDs was quantified using the arithmetic mean equation as described under *Section 4.3.1*. The mean JDs were converted to a date for a normal year with 365 days. The mean onset and cessation dates were only calculated from years which contained both onset and cessation dates describing the full wet season.

To further describe the wet season using onset and cessation dates, scholars have quantified the length of the wet season in days and the total number of rain days (Tadross *et al.*, 2009; Moeletsi & Walker, 2012; Tshililo, 2017). This information was calculated for all weather stations, and only for the years where both an onset and cessation date were obtained. To determine the number of rain days during the wet season, all rain days with above 0.1mm of rainfall were considered. To determine the length of the wet season for weather stations with onset dates during January or

later, the onset date in JDs was subtracted from the cessation date in JDs and one was added, where the equation is:

$$Length\ of\ the\ wet\ season = cessation - onset + 1 \text{ (Equation 16)}$$

(Amekudzi *et al.*, 2015).

The length of the wet season for the remaining weather stations with onset dates before 31 December was determined by subtracting the onset date of the rains in JDs from 365 for normal years or 366 for leap years and adding one plus the JD of the cessation date, where the equation is:

$$Length\ of\ the\ wet\ season = 365\ or\ 366 - onset + cessation + 1 \text{ (Equation 17)}$$

(Moeletsi & Walker, 2012).

Together the onset and cessation dates, the length of the wet season and the number of rain days provide measurements on the timing and duration of the wet and dry season on a daily scale. These quantities are important with regard to providing a complete description of rainfall seasonality.

Similar to the previous approach outlined in *Section 4.4.2*, ordinary kriging has been used for the purpose of interpolating the onset and cessation dates and the respective wet season length and number of rain days. The mean JDs and number of days were used for interpolation. The choice of semivariogram was based on the observed mean onset and cessation dates, mean length of the wet season and mean number of rain days following the same procedure captured under *Section 4.4.2*. For the mean onset dates and the mean length of the wet season, the exponential semivariogram was selected, whereas the tetraspherical semivariogram was selected for the cessation dates and the spherical semivariogram was selected for the number of rain days. These semivariogram models displayed a zero-nugget value and the smallest prediction error values for the observed data points respectively.

The mean onset and cessation dates were used to group the weather stations employing known rainfall classifications in literature for South Africa, where SRZ is typically classified as between

October to March, WRZ is typically classified as between April to September and YRZ is typically classified as rainfall throughout the year (Tyson and Preston-Whyte, 2000; Philippon *et al.*, 2012; Crétat *et al.*, 2012). Building on this, the weather stations were grouped as SRZ, WRZ and YRZ assuming three main rainfall zones. Firstly, weather stations were classified as YRZ if they contained less than three months of no contiguous rainfall (i.e. more than 9 months contiguous rainfall). Next weather stations were classified as SRZ or WRZ. A weather station with less than 9 months of contiguous rainfall with the summer solstice, and not the winter solstice, during the wet season was classified as SRZ. A weather station with less than 9 months of contiguous rainfall with the winter solstice, and not the summer solstice, during the wet season was classified as WRZ.

Following this the rainfall zones were further grouped to gain a classification of a higher resolution than just the SRZ and WRZ, as in literature these are captured as heterogeneous regions (e.g. Favre *et al.*, 2016). Both the SRZ and WRZ were further described as early, late, mid or long (Keen & Tyson, 1973). A classification of early SRZ was given if the spring equinox (22-23 September) and the summer solstice occurs during the wet season (NOAA, 2018). A classification of late SRZ was given if the summer solstice and autumn equinox (20-21 March) occur during the wet season (NOAA, 2018), whereas a classification of mid SRZ was given when only the summer solstice, and not the equinoxes, occur during the wet season. A classification of long SRZ was given if the spring equinox and autumn equinox occur during the wet season. A classification of early WRZ was given if the autumn equinox and winter solstice occur during the wet season. A classification of late WRZ was given if the winter solstice and spring equinox occur during the wet season. A classification of mid WRZ was given if the winter solstice, and not the equinoxes, occur during the wet season, and a classification of long WRZ was given if the autumn equinox, winter solstice and spring equinox occur during the wet season.

4.4.4 ACCUMULATION OF RAINFALL

The timing of accumulation of minimum (10th percentile) and maximum (90th percentile) rainfall together can be used to represent the boundaries of the wet season (Pryor & Schoof, 2008; van Wilgen *et al.*, 2016). To determine the timing of these boundaries, as onset and cessation dates of the wet season, scholars across Africa have typically applied an approach proposed by Ilesanmi

(1972a, b) which is termed the percentage mean cumulative rainfall (e.g. Odekunle, 2004, 2006; Odekunle *et al.*, 2005; Camberlain *et al.*, 2009; Guenang & Kamga, 2012; Recha *et al.*, 2012; Amekudzi *et al.*, 2015). This approach, similar to the previous approach described under *Section 4.4.3*, is an approach which relies on rainfall data alone (Amekudzi *et al.*, 2015). Scholars who have applied this approach have argued that it is a relatively objective approach which can be applied across a region as it depends on local rainfall amount (Amekudzi *et al.*, 2015). For this reason, the suitability of this approach to determine onset and cessation dates of the wet season will for the first time be tested across South Africa. The onset and cessation dates of the wet season for this section will, for the purpose of discriminating between this and the previous section, be referred to as the 10% and 90% dates of the wet season.

The 10% and 90% dates for this study were determined, annually as the JD per year and for the total period (i.e. mean) of 1987-2016, using an adapted version of the percentage mean cumulative rainfall approach (Ilesanmi, 1972a, b). Important to note are the months with missing rainfall values (Table 4.2), as these may potentially influence the accuracy of the 10% and 90% dates for a certain year or as a result no dates may be obtained. The first step of this approach is to quantify mean daily rainfall in five-day intervals (Ilesanmi, 1972a, b). Since this study requires a high temporal resolution at a daily scale, this step has not been included. Starting from the month following the month of mean minimum rainfall amount (Liebmann *et al.*, 2012; Feng *et al.*, 2013), daily rainfall amounts were converted to a percentage of total annual rainfall amount (Ilesanmi, 1972a, b). The 10% and 90% dates were captured when 10 and 90% of daily rainfall (i.e. ≥0.1mm) accumulated respectively. For locations which do not demonstrate a uni-modal wet season (e.g. RIV: Riversdale), the climatological year was taken from January to ensure meaningful dates were obtained (Liebmann *et al.*, 2012; Dunning *et al.*, 2016), similar to the previous *Section 4.4.3*. Ilesanmi (1972a, b), captured onset dates at 7-8%, and for this study a level of 10% was instead selected. Since rainfall is known to occur outside of the main wet season, a level of 10% was selected to account for 80% of rainfall during the main wet season and 20% of rainfall occurring outside of the main wet season (Pryor & Schoof, 2008). Additionally, as further justification for the use of 10% and 90%, using a consistent and objective methodology Liebmann *et al.* (2012) found

that over much of the African continent, approximately 80% of annual rainfall occurs during the wet season.

To determine the mean 10% and 90% dates for the total period of 1987-2016, the mean of the annual JDs was quantified using the arithmetic mean equation as described under *Section 4.3.1*. The mean JDs were converted to a 10% and 90% date for a normal year with 365 days. For this section, similar to *Section 4.4.3*, a rain day is defined as 0.1mm. The length of the wet season and number of rain days, as described under *Section 4.4.3*, has also been quantified. Together the 10% and 90% dates, the length of the wet season and the number of rain days provide measurements on the timing and duration of the wet and dry season on a daily scale, and these quantities are important with regard to completely describing rainfall seasonality.

Similar to the previous two approaches, ordinary kriging has been used for the purpose of interpolating the mean 10% and 90% dates. The mean JDs were used for interpolation, and the choice of semivariogram was based on the observed 10% and 90% dates following the same process employed under *Section 4.4.2*. For the mean 10% dates, the spherical semivariogram was employed, whereas for the 90% dates, length of the wet season and the number of rain days the circular semivariogram was employed. These semivariograms displayed a zero-nugget value and the smallest prediction error values for the observed data points respectively and were selected to interpolate these dates.

The mean 10% and 90% dates were also used to classify the weather stations as SRZ, WRZ and YRZ, employing the exact process reported under *Section 4.4.3*. Additionally, the weather stations classified as SRZ and WRZ were grouped as early, late, mid or long following the procedure reported under *Section 4.4.3*.

4.5 TIME SERIES ANALYSIS ON RAINFALL SEASONALITY FOR THE PERIOD OF 1987-2016

Having quantified rainfall seasonality for each of the weather stations, it is possible to investigate the shifts and variability in rainfall seasonality for the study period of 1987-2016. The statistical analysis undertaken and described for this section includes an investigation on the linear shifts

and change points. This process was performed using the annual seasonality quantified for each approach (i.e. under *Section 4.4.2*, *4.4.3* and *4.4.4*) for each weather station.

4.5.1 LINEAR SHIFTS

To quantify the linear shifts in the rainfall seasonality characteristics defined for each approach, the least square linear regression model, described under *Section 4.3.2*, was applied across each individual weather station, similar to prior studies on rainfall seasonality shifts (e.g. Pryor & Schoof, 2008; Feng *et al.*, 2013; Guhathakurta & Saji, 2013; Pal *et al.*, 2013; MacKellar *et al.*, 2015; Kruger & Nxumalo, 2017). Shifts in the following metrics were quantified for each individual weather station: annual and monthly rainfall totals, annual seasonality scores, annual onset and cessation dates and their respective length of the wet season and number of rain days and the annual 10% and 90% dates as well as their respective length of the wet season and number of rain days. Using all of these measurements, a complete description of rainfall seasonality shifts across South Africa was quantified for the period of 1987-2016 (Feng *et al.*, 2013; Pascale *et al.*, 2015, 2016).

Shifts in annual and monthly rainfall totals were calculated according to *Section 4.3.2* using the least squares linear regression model. For this section, the least squares linear regression model was also used to quantify the shifts in seasonality for each weather station using the annual measurements of rainfall seasonality from each statistical approach under *Section 4.4* (i.e. excluding *Section 4.4.1*). Important to note are the months with missing data (Table 4.2, 4.3), as these may influence the number of annual seasonality measurements. Using the standard least squares linear regression model, *y* refers to the annual measurements of the rainfall seasonality metric and *x* refers to the year. The shifts in rainfall seasonality are represented by the resulting *m-coefficient* and are a measure of the shift in the rainfall seasonality metric per year. These shifts are further described by the absolute *r value* and the *p value* as described under *Section 4.3.2*.

For the seasonality scores, only the shifts in the annual seasonality scores were quantified. A positive shift is associated with either a decreasing strength of WRZ conditions or an increasing strength of SRZ conditions and a negative shift is associated with either a decreasing strength of SRZ conditions or an increasing strength of WRZ conditions. These shifts are represented as a shift in the seasonality score per year.

For both the onset and cessation dates, and 10% and 90% dates, shifts in these dates and the respective wet season length and number of rain days were quantified. Shifts in the dates are represented by a shift in the JD per year, and as days per year for the length of the wet season and for the number of rain days. A positive change for onset and cessation dates, and 10% and 90% dates represents later dates during the study period, while a negative shift represents earlier dates during the study period. A positive and negative shift in the length of the wet season and number of rain days demonstrates a progressive increase or decrease in these quantities.

4.5.2 CHANGE POINT ANALYSIS

Through quantification of linear shifts in rainfall seasonality, a general trend for the time period of interest is be obtained. For a climatic element such as rainfall, and in particular rainfall seasonality, there is considerable temporal variability which has been heightened by anthropogenic climate change (Nicholson, 2000; Tyson *et al.*, 2002; Fauchereau *et al.*, 2003; Feng *et al.*, 2013; Dieppois *et al.*, 2016). Quantification only of linear trends may not provide information on this variability. In an attempt to quantify and understand rainfall variability, numerous scholars have applied change point analysis techniques to detect abrupt shifts in the mean and variance of rainfall amount (e.g. Chu *et al.*, 2012; Gocic & Trajkovic, 2013; Guerreiro *et al.*, 2014; Rahmani *et al.*, 2015; Mathbout, 2015; Lee & Kim, 2016; Akinsanola & Ogunjobi, 2017; Arif *et al.*, 2017; Sharma & Singh, 2017; Palaniswami & Muthiah, 2018). Amongst scholars quantifying change points in rainfall amount, the most widely used method of change point detection is the cumulative sum (CUSUM) in conjunction with bootstrapping, and the Pettitt or t-test test (Guerreiro *et al.*, 2014).

Change points represent abrupt shifts in climatic systems (Beaulieu *et al.*, 2012; Guerreiro *et al.*, 2014; Mathbout, 2015). Contrary to slow changes that translate into trends, change points in rainfall seasonality may be related to regime shifts in synoptics for instance (Guerreiro *et al.*, 2014). To test the null hypothesis that data are homogeneous and no change has occurred during the period of 1987-2016, both the CUSUM in conjunction with bootstrapping, and the Pettitt test were employed (Guerreiro *et al.*, 2014; Rahmani *et al.*, 2015; Mathbout, 2015). Both tests were employed as they are non-parametric tests (with no assumptions on the distribution of the datasets) used to detect change in the mean at an unknown point in time (WMO, 2000). Change

points obtained from these tests may represent a point where the direction of a trend has changed, from positive to negative vice versa, or a point at which the direction of the trend remained the same and the strength of a trend has changed becoming stronger or weaker. Following Guerreiro *et al.* (2014) and Rahmani *et al.* (2015), only statistically significant change points were included in the results, and where both tests provided statistically significant change points at different times then the later year was selected as the change point to be more reliable.

Change points were tested for in the following datasets: the annual and monthly rainfall totals, annual seasonality scores, annual onset and cessation dates and their respective length of the wet season and number of rain days and the annual 10% and 90% dates as well as their respective length of the wet season and number of rain days, for each individual weather station. The Pettitt and CUSUM tests were applied using the R trend and change point packages.

Using the CUSUM method, a change point may be determined, using the following equation:

$$S_i = S_{i-1} + (x_i - \bar{x}) \text{ (Equation 18)}$$

(Taylor, 2000).

where S_i represents the CUSUM, $S_0 = 0$ (i.e. S_{i-1}), x_i is the ith observation and $\bar{x}$ is the mean, as described under *Section 4.3.1* (Taylor, 2000). The CUSUM values are then graphically represented, and a sudden change in the direction of the CUSUM values indicates an abrupt shift in the mean (Taylor, 2000; Gocic & Trajkovic, 2013; Rahmani *et al.*, 2015). Any change point detected is reported as the year during which the change occurred. Once the change point is (or multiple change points are) detected, the magnitude of change may be quantified. To determine the magnitude of change, the following equation was used:

$$S_{diff} = S_{max} - S_{min} \text{ (Equation 19)}$$

(Taylor, 2000).

Once the magnitude of change has been quantified, the statistical confidence of this change may be determined using bootstrapping analysis (Guerreiro *et al.*, 2014; Mathbout, 2015). For the purpose of bootstrap analysis with replacement, 10000 bootstrap samples were created through

random reordering of the original *n* values which are denoted as $x_1^0, x_2^0, \ldots, x_n^0$ (Efron, 1982; Gocic & Trajkovic, 2013; Rahmani *et al.*, 2015). Bootstrap resampling has been used as it draws samples from the observed data to draw conclusions about the population of interest (Efron, 1982). Additionally, bootstrapping is a non-parametric statistical method with no assumptions regarding the dataset, and it provides a more robust estimation of the variance of the distribution of the dataset (Efron, 1982; Herbert, 2016). Based on this bootstrap sample, the CUSUM and S_{diff}^0 were calculated, and it was noted when $S_{diff}^0 < S_{diff}$ (Taylor, 2000; Gocic & Trajkovic, 2013; Rahmani *et al.*, 2015). To quantify the confidence level, the following equation was used:

$$Cl = \frac{X}{n} \times 100\% \text{ (Equation 20)}$$

(Taylor, 2000).

where *X* represents the number of times when $S_{diff}^0 < S_{diff}$ and *n* is the number of bootstrap samples. A confidence level of 95%, representing a *p value* of less than 0.05, was used to determine if a change occurred (Taylor, 2000; Gocic & Trajkovic, 2013; Rahmani *et al.*, 2015). If the desired confidence level is achieved, then the change point occurred during the year when the maximum or minimum S_{diff} was obtained. The year following the year in which the change occurred was reported for both the CUSUM and Pettitt test which follows.

Using the Pettitt test, a change point is identified as the year a change occurred. To calculate the change point, the U_k variable was calculated using the following equation:

$$U_k = 2\sum_{i=1}^{k} Ry_i - k(n+1) \text{ (Equation 21)}$$

(Pettitt, 1979).

where Ry_i is the rank of the *i*th observation when the values $y_1, y_2, \ldots, y_n$ in the series are arranged in ascending order. The statistical change point statistic is then defined as:

$$K = \max_{1 \le k \le n} |U_k| \text{ (Equation 22)}$$

(Pettitt, 1979).

A change point in the series occurs when U_k achieves a maximum value of K. The change point is statistically significant if $K>K_a$. The critical value K_a is calculated using the following equation:

$$K_a = [-ln\alpha(n^3 + n^2)/6]^{1/2} \quad \text{(Equation 23)}$$

(Pettitt, 1979).

A change point was only accepted for a *p value* (α) of less than 0.05.

4.6 CONCLUSION

Data for this project was sourced from the SAWS climate database, whereby 46 weathers stations were determined to contain a sufficient data availability for the purpose of addressing the objectives developed under *Section 1.2* of *Chapter 1 (Introduction)*. Data were cleaned and errors were explored to ensure accuracy of the datasets. Monthly and annual rainfall characteristics were quantified in order to determine the reliability of the data and appropriateness of the weather station locations. Standard statistical methods were applied to facilitate reproducibility of the results and for broad comparisons with literature. In developing a standard statistical seasonality approach, metrics which have previously been applied in literature were explored under *Section 2.2* of *Chapter 2 (Literature Review)* in order to test metrics which are known to statistically discriminate between summer and winter rainfall conditions, a requirement Thackeray and Fitchett (2016) highlight as being important for modelling South African rainfall seasonality. Finally, to investigate the changes in seasonality, all the metrics which quantify annual seasonality were applied in order to facilitate corroboration of the trends detected.

5. RESULTS

5.1 INTRODUCTION

This study involves the use of daily rainfall and temperature readings from 46 weather stations distributed across South Africa for the period of 1987-2016, for the purpose of statistically quantifying rainfall seasonality and the shifts thereof. This chapter presents the results of these analyses, starting with a description of the general annual and monthly rainfall characteristics and trends. Next, the results are presented individually for each statistical approach with a description on the spatial and temporal rainfall seasonality characteristics captured by each approach. Finally, the results on the changes in rainfall seasonality for the study period are presented, whereby the results from each method are integrated for a more accurate and comprehensive description on these changes. The interpretation of these results is presented in *Chapter 6 (Discussion)*.

5.2 ANNUAL RAINFALL CHARACTERISTICS AND TRENDS

Mean annual rainfall displays a large range from 72.4mm at Port Nolloth (PNO), located along the western coast, to 1,099.6mm at Paddock (PAD), located along the eastern coast (Figure 5.1; Table 5.1). Mean annual rainfall progressively increases from east to west (Figure 5.1). The relationship between longitude and mean annual rainfall is statistically significant ($r = 0.79$, $p < 0.0001$), and hence, the lowest mean annual rainfall is at Port Nolloth (PNO), Pofadder (POF), Vredendal (VRE), Fraserburg (FRA), and Vanwyksvlei (VWY) in the Northern Cape, and these are all below 200mm with a range from 72.4mm (PNO) and 197.9mm (VWY; Figure 5.1; Table 5.1). The highest mean annual rainfall is at East London Wo (ELW), Cedara (CED), Mandini (MAN), Shaleburn (SHA), and Paddock (PAD) in KwaZulu-Natal and the Eastern Cape, and these are all above 800mm with range from 839.3mm (ELW) to 1,099.6mm (PAD; Figure 5.1; Table 5.1). High mean annual rainfall evident along the eastern escarpment is mostly due to orographic rainfall and this is especially evident at SHA and PAD (Figure 5.1; Landman *et al.*, 2017). Additionally, there are regions of relatively high mean annual rainfall in the southwestern Cape and along the southern coast which are also associated with orographic rainfall, and this is evident at CAG (Cape Agulhas), CTW (Cape Town Wo), PEW (Port Elizabeth Wo) and RIV (Riversdale) where mean annual rainfall ranges between 400-600mm (Figure 5.1; Landman *et al.*, 2017). Considering the correlation of mean annual rainfall with latitude and elevation, there were no statistically significant relationships evident.

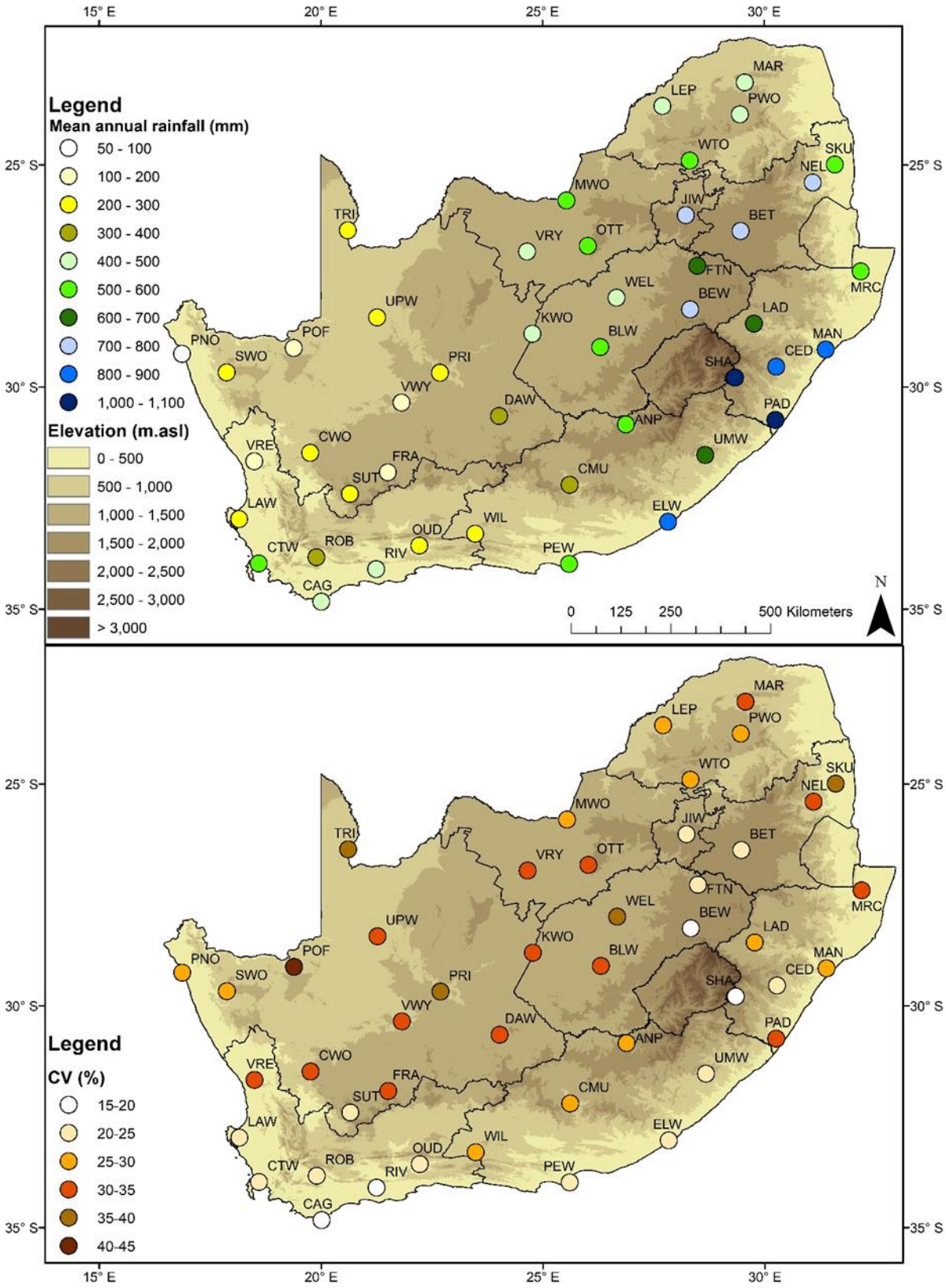


Figure 5.1: Mean annual rainfall and coefficient of variation for individual weather stations for the period 1987-2016.

Table 5.2: Summary statistics of the annual rainfall totals for the period 1987-2016. Statistically significant trends are indicated by an asterisk (*).

Location	Mean annual rainfall (mm)	Range	CV (%)	Sample size (n)	Change over time (mm.year^{-1})	Strength of trend (r)
Aliwal-North Plaatkop	552.0	629.5	29.2	30	0.09	0.004
Bethal	742.7	679.3	23.5	29	-1.13	0.05
Bethlehem Wo	718.9	509.8	18.8	30	-2.62	0.17
Bloemfontein Wo	555.5	803.8	33.3	30	-6.14	0.29
Calvinia Wo	206.3	284.5	31.1	30	-1.02	0.14
Cape Agulhas	453.0	401.5	19.4	30	-3.34	0.33
Cape Town Wo	524.2	358.3	21.4	30	-5.54	*0.43
Cedara	843.3	928.6	22.3	30	-11.71	*0.54
Cradock-Mun	356.5	346.0	25.2	30	1.84	0.18
De Aar Wo	341.5	482.8	31.7	30	-2.12	0.17
East London Wo	839.3	675.1	20.9	30	-1.09	0.05
Frankfort-TNK	653.6	687.9	24.9	30	-3.25	0.17
Fraserburg	196.5	263.6	31.5	30	0.12	0.02
Johannesburg INT Wo	752.4	619.1	21.7	30	-1.73	0.09
Kimberley Wo	421.7	602.2	34.0	30	-2.52	0.15
Ladysmith	669.5	696.2	25.4	30	-7.10	*0.36
Langebaanweg AWS	261.9	268.6	23.5	30	-1.89	0.27
Lephalale	404.5	449.6	26.5	30	-2.06	0.17
Mafikeng Wo	525.2	582.5	26.8	30	-6.89	*0.42
Makatini Research Centre	584.6	769.4	33.8	30	-11.15	*0.49
Mandini	854.6	1236.3	29.3	30	-13.17	*0.46
Mara	435.4	610.2	30.0	30	-0.81	0.05
Nelspruit	721.4	1091.1	33.4	29	2.24	0.08
Ottosdal	554.5	740.8	31.5	30	-5.32	0.26
Oudtshoorn	243.6	206.0	20.8	30	0.82	0.14
Paddock	1099.6	1446.3	31.6	30	-12.15	0.30
Pofadder	121.7	207.9	44.4	30	-0.68	0.11
Polokwane Wo	484.3	682.7	28.3	30	-0.22	0.01
Port Elizabeth Wo	595.5	632.0	24.6	30	3.20	0.20
Port Nolloth	72.4	83.7	29.6	30	0.29	0.12
Prieska	226.4	319.0	37.7	30	-0.25	0.02
Riversdale	481.2	375.3	18.3	30	1.66	0.16
Robertson	332.0	282.7	22.4	30	1.79	0.21
Shaleburn	1052.7	847.7	17.2	30	-5.71	0.27
Skukuza	573.5	964.2	36.2	30	-1.77	0.07
Springbok Wo	221.7	253.3	27.9	29	-0.39	0.05
Sutherland	262.9	249.6	21.3	29	1.34	0.20
Twee Rivieren	213.3	318.0	35.0	30	2.28	0.26
Umtata Wo	682.1	533.5	21.5	30	-1.56	0.09
Upington Wo	214.0	294.3	34.5	30	3.08	*0.36
Vanwyksvlei	197.9	287.5	33.4	30	-1.49	0.19
Vredendal	157.4	200.3	31.2	30	-0.43	0.08
Vryburg	470.4	663.7	34.3	30	-5.45	0.29
Warmbad Towoomba	597.5	616.7	26.8	30	-3.05	0.17
Welkom	429.2	727.1	37.5	30	-10.32	*0.56
Willowmore	279.6	291.0	25.5	30	0.83	0.10

The year to year annual rainfall totals are considerably variable at individual weather stations, and this is especially highlighted at Pofadder, Prieska, Skukuza, Twee Rivieren and Welkom located in the Free State, the Northern Cape and Mpumalanga (Figure 5.1). At these weather stations CV values describing inter-annual variability in annual rainfall totals are particularly high and range between 35.0% (TRI) and 44.4% (POF; Table 5.1; Figure 5.1). Compared to mean annual total rainfalls the range in minimum and maximum rainfall totals are high (Table 5.1), highlighting the variable nature of rainfall across the country. The maximum and minimum range in annual totals across the country are evident at Port Nolloth (83.7mm) and Paddock (1446.3mm) within Northern Cape and KwaZulu-Natal respectively (Table 5.1). The CV values across the weather stations range between 17.2% at Shaleburn and 44.4% Pofadder, again within KwaZulu-Natal and the Northern Cape respectively (Table 5.1; Figure 5.1). There are 42 weather stations with CV >20%, which suggests there was at least a moderate inter-annual variability in the annual rainfall totals for most of the weather stations during the study period (Table 5.1; Figure 5.1). Of these, 19 weather stations have a high inter-annual variability, above 30% (Table 5.1; Figure 5.1). When considering all the weather stations, there is a weak yet statistically significant relationship ($r = -0.38$; $p = 0.010$) between the CV and mean annual rainfall totals, where weather stations with smaller mean annual rainfall totals typically displayed a higher level of variability compared to those with larger mean annual rainfall totals (Table 5.1; Figure 5.1). Similarly, the correlation between CV and latitude was calculated to be weak but statistically significant ($r = -0.38$, $p = 0.009$), where weather stations at a larger latitude typically have lower inter-annual variability (Figure 5.1). The relationship between CV and longitude as well as elevation is statistically insignificant and thus not reported.

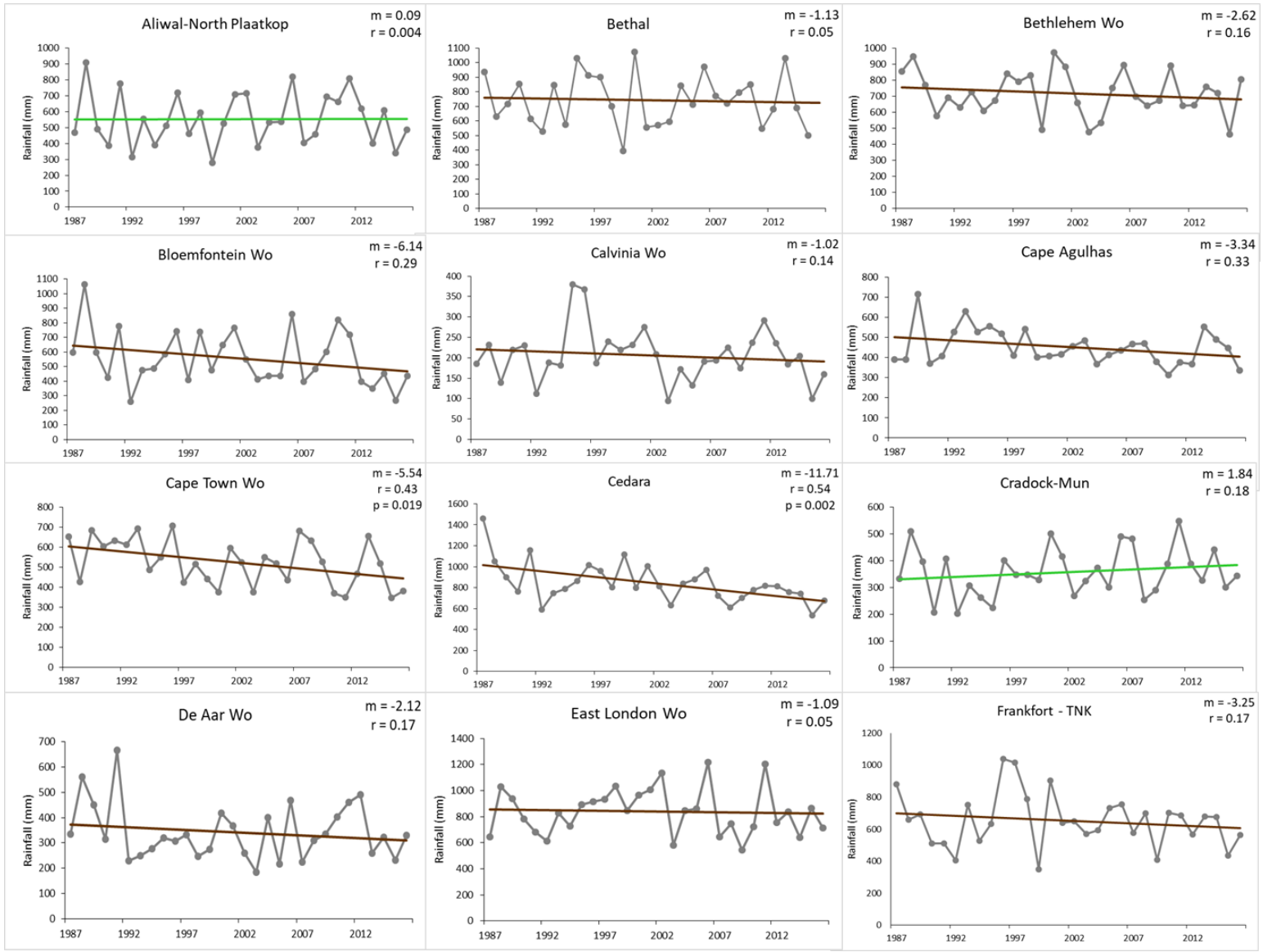


Figure 5.2: Annual rainfall totals and trend for individual weather stations for the period 1987-2016. *P values* are listed only for statistically significant trends. Green (Brown) trendlines represent increasing (decreasing) trends.

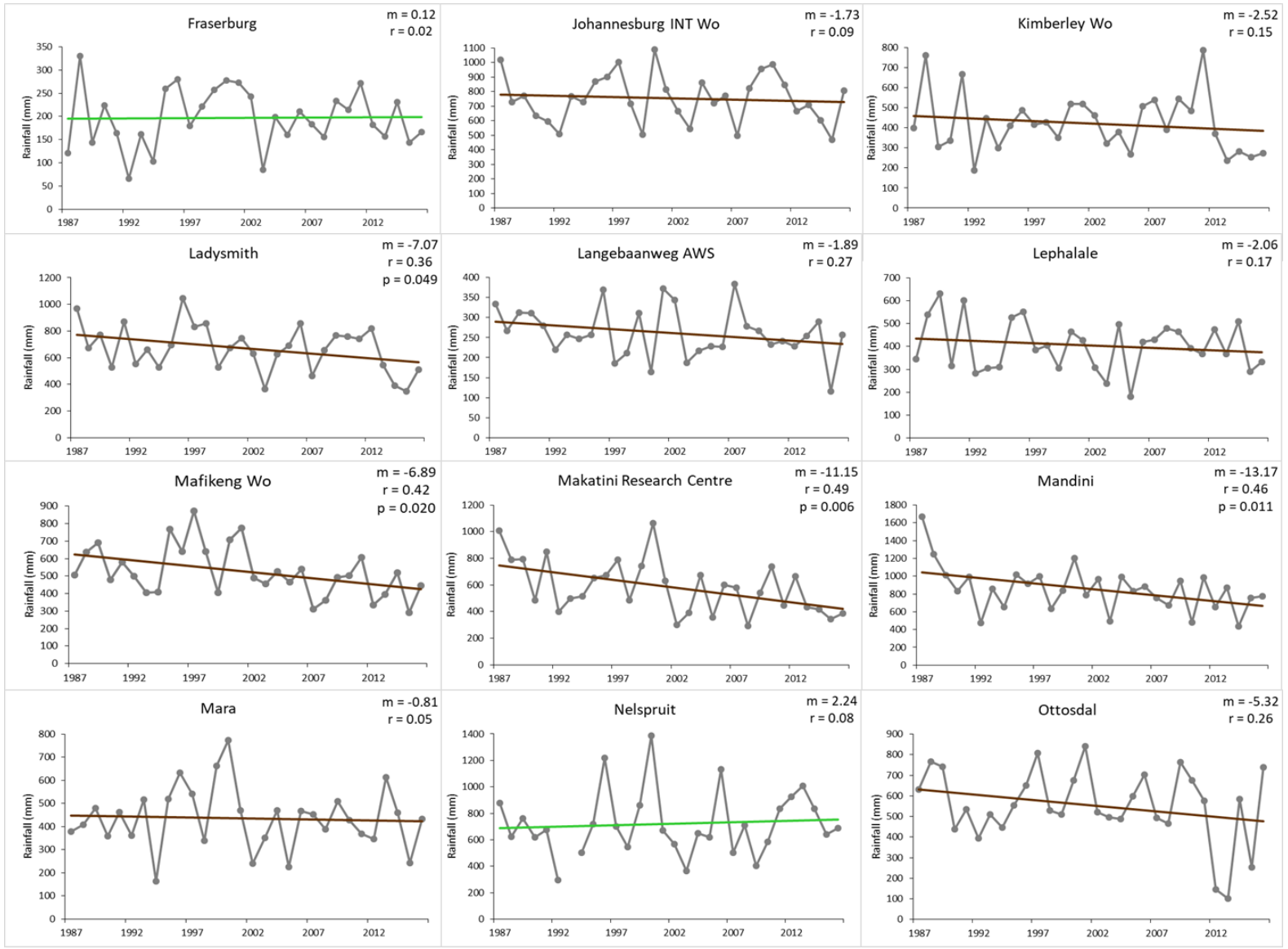


Figure 5.2 continued: Annual rainfall totals and trend for individual weather stations for the period 1987-2016. *P values* are listed only for statistically significant trends. Green (Brown) trendlines represent increasing (decreasing) trends.

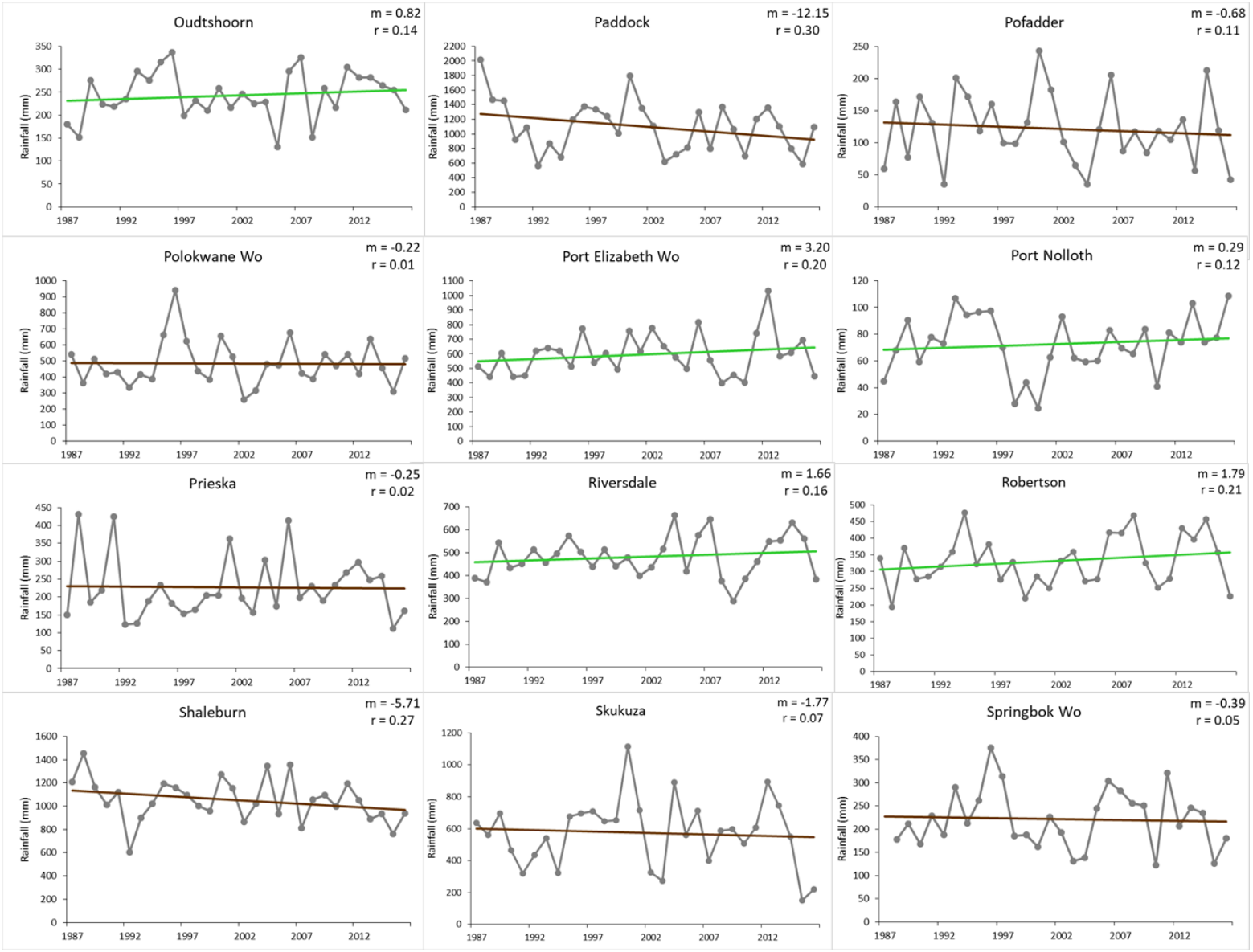


Figure 5.2 continued: Annual rainfall totals and trend for individual weather stations for the period 1987-2016. *P values* are listed only for statistically significant trends. Green (Brown) trendlines represent increasing (decreasing) trends.

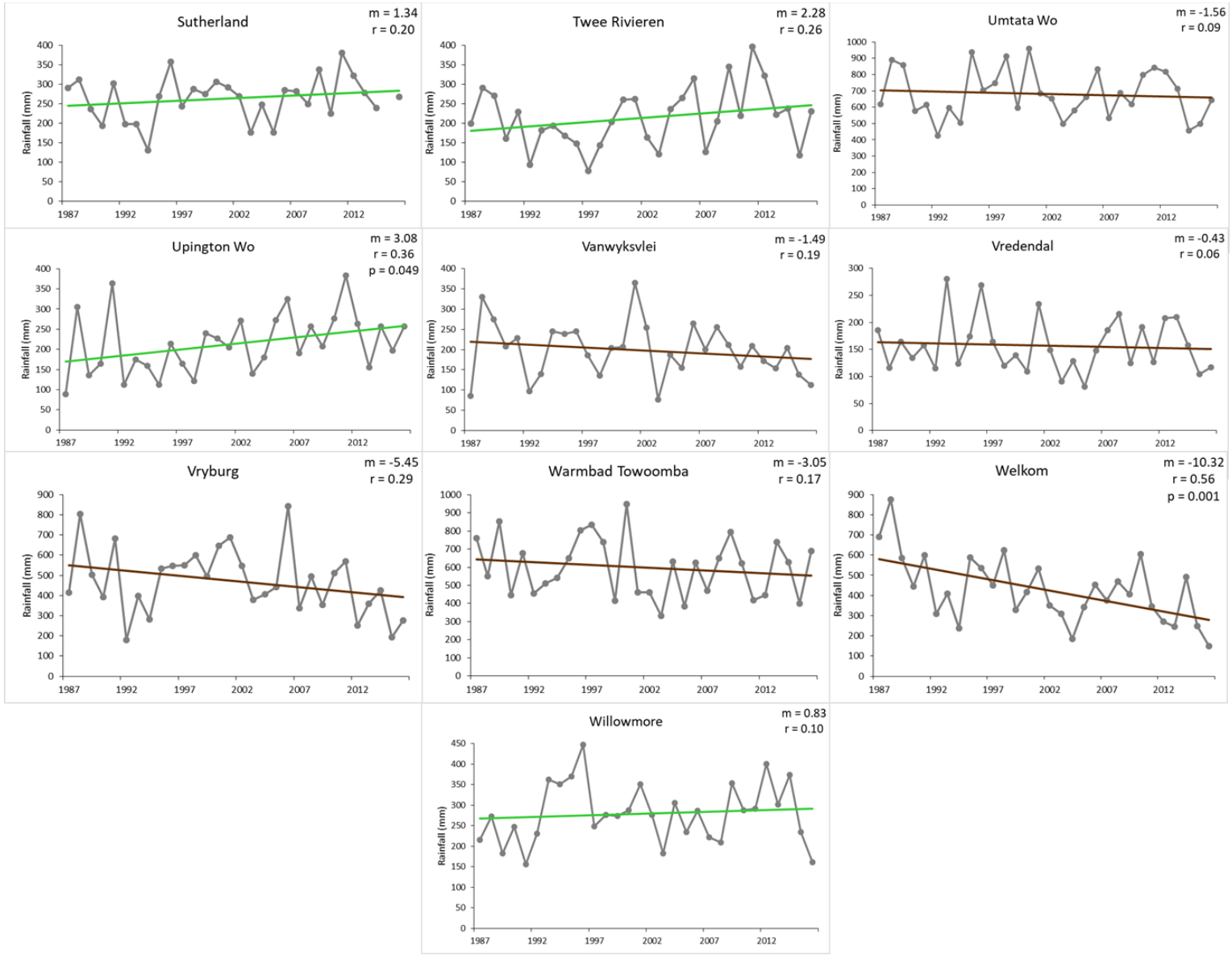


Figure 5.2 continued: Annual rainfall totals and trend for individual weather stations for the period 1987-2016. *P values* are listed only for statistically significant trends. Green (Brown) trendlines represent increasing (decreasing) trends.

All of the weather stations displayed shifts in the annual rainfall totals during the study period (Table 5.1; Figure 5.2, 5.3). Most of these changes in annual rainfall amount were statistically insignificant (Table 5.1), which may suggest that annual rainfall did not necessarily change at most locations or that any changes which occurred were considerably small. The year to year variability in the annual rainfall totals at most weather stations was quantified as moderate (Table 5.1), at the least, and this is a reason behind quantifying few statistically significant trends. Most of the trends in annual rainfall amount were characterised by very weak *r values*, where the *r values* calculated were below 0.30 for 36 weather stations (Table 5.1). Although many of the time series trends were not statistically significant, it is necessary to quantify annual rainfall time series trends as over a longer time period a trend may continue along the same trajectory and become statistically significant. Statistically significant trends were quantified for eight weather stations, of which seven are decreasing trends, located mostly across the eastern half of the country within the Free State, KwaZulu-Natal and North West provinces (Table 5.1; Figure 5.3).

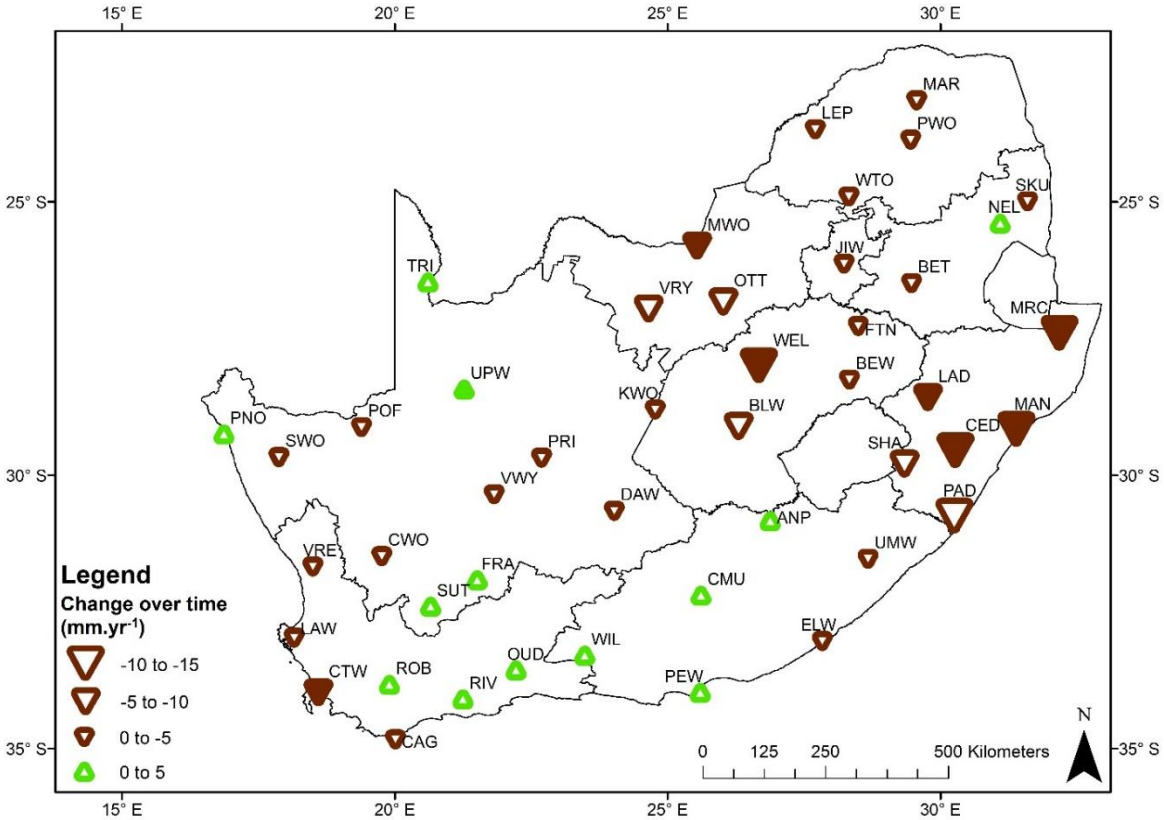


Figure 5.3: Trends in total annual rainfall for individual weather stations for the period 1987-2016. Shaded symbols represent statistically significant trends at the 5% level.

Considering the negative trends first, there were 33 weather stations with tentative trends towards drier conditions (Figure 5.3; Table 5.1). These weather stations are mostly located across the eastern parts of the country and along the western interior and western coastline (Figure 5.3). The range in these trends is between -0.22mm.yr^{-1} at PWO, located within Limpopo, to -13.17mm.yr^{-1} at MAN within KwaZulu-Natal (Table 5.1; Figure 5.3). The greatest reductions in rainfall per year are evident amongst the weather stations in KwaZulu-Natal, North West and Free State, where most of the statistically significant trends were located and where most of the trends were relatively high, ranging between -5.0 and -15.0mm.yr^{-1} (Figure 5.3). The statistically significant decreasing trends include: CED (-11.71mm.yr^{-1}, r = 0.54, p = 0.002), LAD (-7.10mm.yr^{-1}, r = 0.36, p = 0.049), MWO (-6.89mm.yr^{-1}, r = 0.42, p = 0.020), MRC (-11.15mm.yr^{-1}, r = 0.49, p = 0.006), MAN (-13.17mm.yr^{-1}, r = 0.46, p = 0.011) and WEL (-10.32mm.yr^{-1}, r = 0.56, p = 0.001; Table 5.1; Figure 5.3). These are weather stations which are considerably important to monitor for future rainfall changes. In this area, BLW, OTT, PAD, SHA and VRY have *r values* quantified between 0.21 and 0.30, and over a longer time period these locations may demonstrate statistically significant reductions in annual rainfall (Table 5.1; Figure 5.3). Located in the southwestern Cape, CTW also exhibited a statistically significant reduction in annual rainfall (-5.54mm.yr^{-1}, r = 0.36, p = 0.019; Table 5.1; Figure 5.3). In this area, the *r values* calculated for the trends at CAG (r = 0.33) and LAW (r = 0.27) were relatively strong, and hence monitoring at these locations is also important (Table 5.1; Figure 5.3). When considering change points, only CED (2007; p = 0.030), MWO (2002; p = 0.043) and MRC (2002; p = 0.016), all of which displayed statistically significant decreasing trends, had change points detected using the Pettitt test. From the year reported until 2016 for CED (Before 2007: m = -9.96, r = 0.30, p = 0.200; From 2007: m = -4.82, r = 0.16, p = 0.653) and MRC (Before 2002: m = -2.61, r = 0.06, p = 0.833; From 2002: m = -1.08, r = 0.03, p = 0.906), the decreasing trend in rainfall was smaller than prior to the change point. Conversely, MWO (Before 2002: m = 10.89, r = 0.33, p = 0.229; From 2002: m = -5.40, r = 0.26, p = 0.345) had an increasing trend prior to the change point and a decreasing trend following the change point, highlighting that the overall trend is strongly influenced by the trend from the change point year. These change points are important for management and adaptation plans and thus the direction and rate are important to note.

When considering the positive trends in annual rainfall totals, only thirteen weather stations demonstrated an increasing trend for mean annual rainfall during the study period (Figure 5.3). These tentative increasing trends range between 0.09mm.yr^{-1} at ANP and 3.20mm.yr^{-1} at PEW both of which are located within the Eastern Cape (Table 5.1; Figure 5.3). The weather stations which demonstrate an increase in annual rainfall are mostly located along the southern coastline and the adjacent interior, and some are also scattered in the northeastern and northwestern parts of the country (Figure 5.3). Only the trend at UPW was quantified as statistically significant (3.08mm.yr^{-1}, r = 0.36, p = 0.049; Table 5.1; Figure 5.3). At PEW, ROB, SUT and TRI, the calculated *r values* were relatively high ranging between 0.20 and 0.26 (Table 5.1), and since these locations are surrounded by locations with increasing trends it is worthwhile noting these trends especially for monitoring purposes (Figure 5.3). No change points were detected amongst the weather stations with increasing trends.

Across the weather stations, the changes in annual rainfall demonstrate relatively strong spatial consistency, however, the trends quantified for locations including NEL and PNO are not consistent with surrounding location trend directions (Figure 5.3). Additional weather stations in regions surrounding these locations may reflect similar patterns or over longer temporal periods the trends for PNO and NEL may reflect similar trends to surrounding locations. These may also reflect local scale trends, where the proximity to the Atlantic Ocean may influence the trend of PNO. At NEL the adajacent escarpment regions may influence the direction of trend given the strong control topography has on moisture dispersal across the country (Favre *et al.*, 2016). Indeed this would be an important consideration for the monthly trends considered in the following section.

5.3 MONTHLY RAINFALL CHARACTERISTICS AND TRENDS

According to Feng *et al.* (2013) the seasonality of rainfall may be qualitatively described through analysing the monthly rainfall climatology, where this may provide information on the magnitude, timing and duration of wet and dry seasons. In considering this, the annual cycles of mean monthly rainfall for each individual weather station, presented as Figure 5.4, may be used to robustly

classify rainfall seasonality. Details of the respective descriptive statistics used for Figure 5.4 and elsewhere in this section are presented under Appendix B and more specifically under Appendix B.1 to B.13. The annual cycles of rainfall vary in terms of the timing and magnitude of wetter and drier periods across the weather stations, and this depicts location specific cycles of annual rainfall (Figure 5.4). However, when considering the timing of wetter and drier periods across the project weather stations there are also many similarities (Figure 5.4). As a result, each location can be classified into one of the three main rainfall zones (i.e. SRZ, WRZ and YRZ). Locations which display distinct wetter and drier periods (i.e. uni-modal seasonality) may be classified as either SRZ or WRZ depending on the timing of the wetter and drier periods. Locations which display no clear seasonal structure with relatively equable monthly rainfall totals may be classified as YRZ.

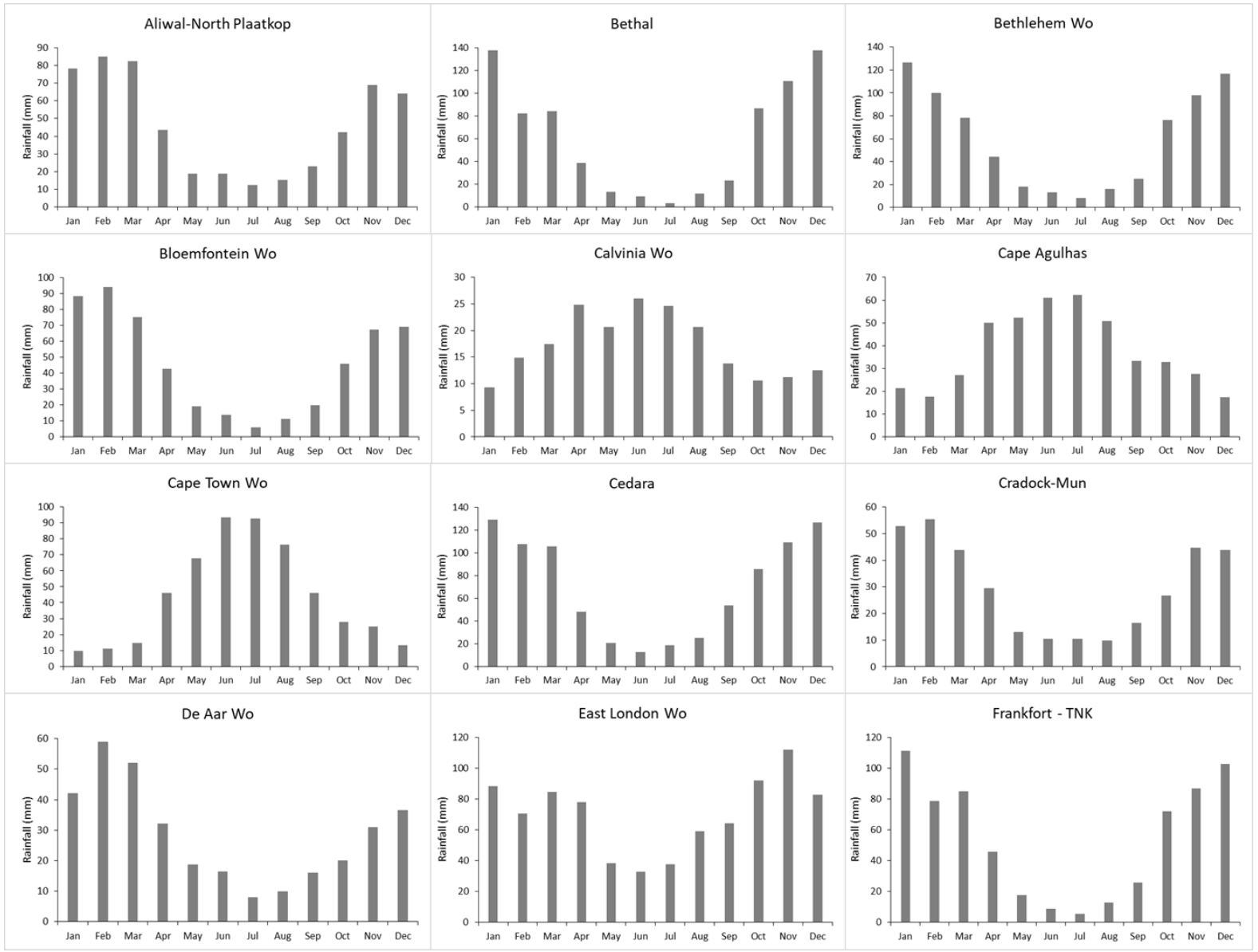


Figure 5.4: Annual cycles of rainfall for the period of 1987-2016.

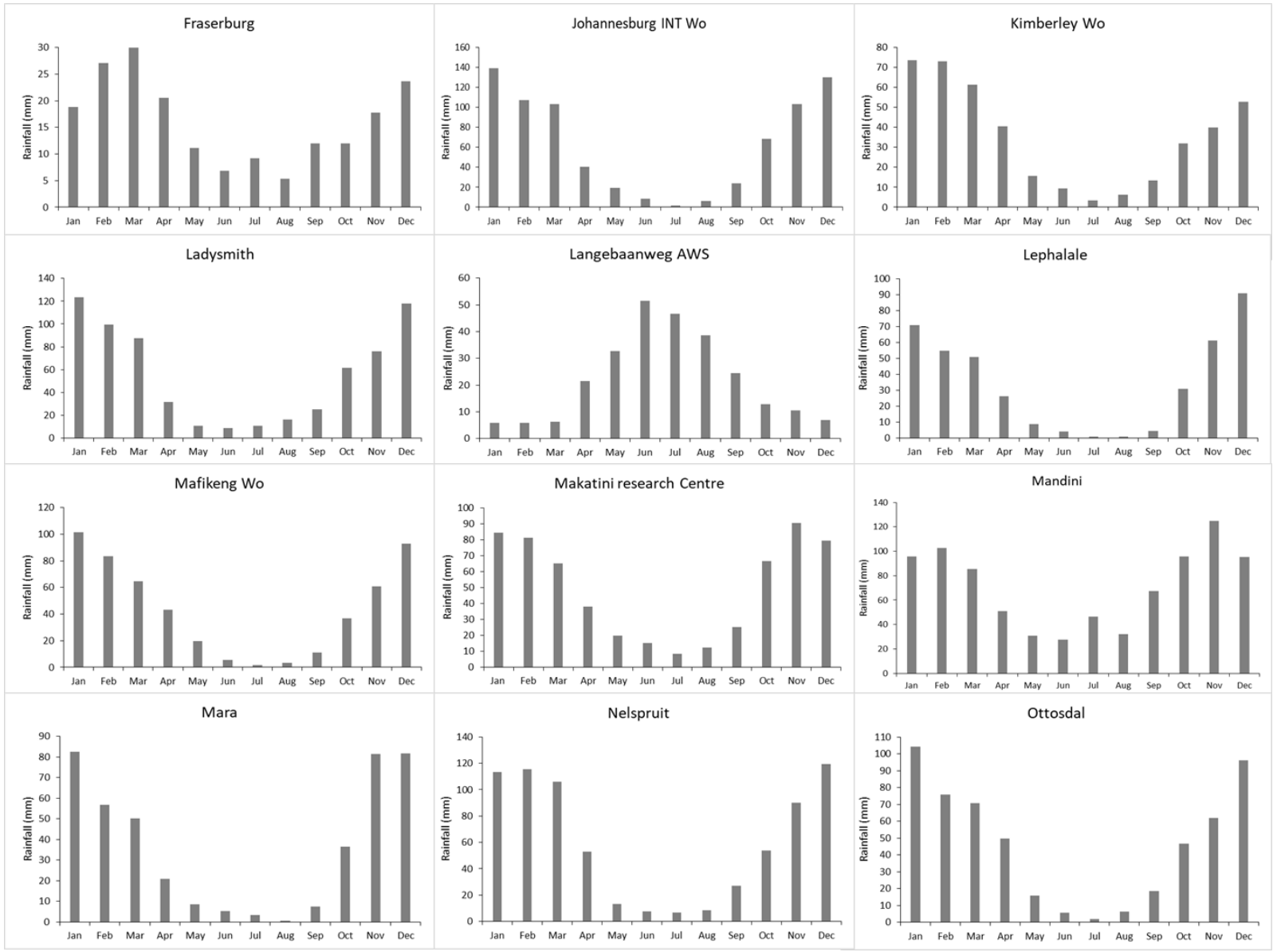


Figure 5.4 continued: Annual cycles of rainfall for the period of 1987-2016.

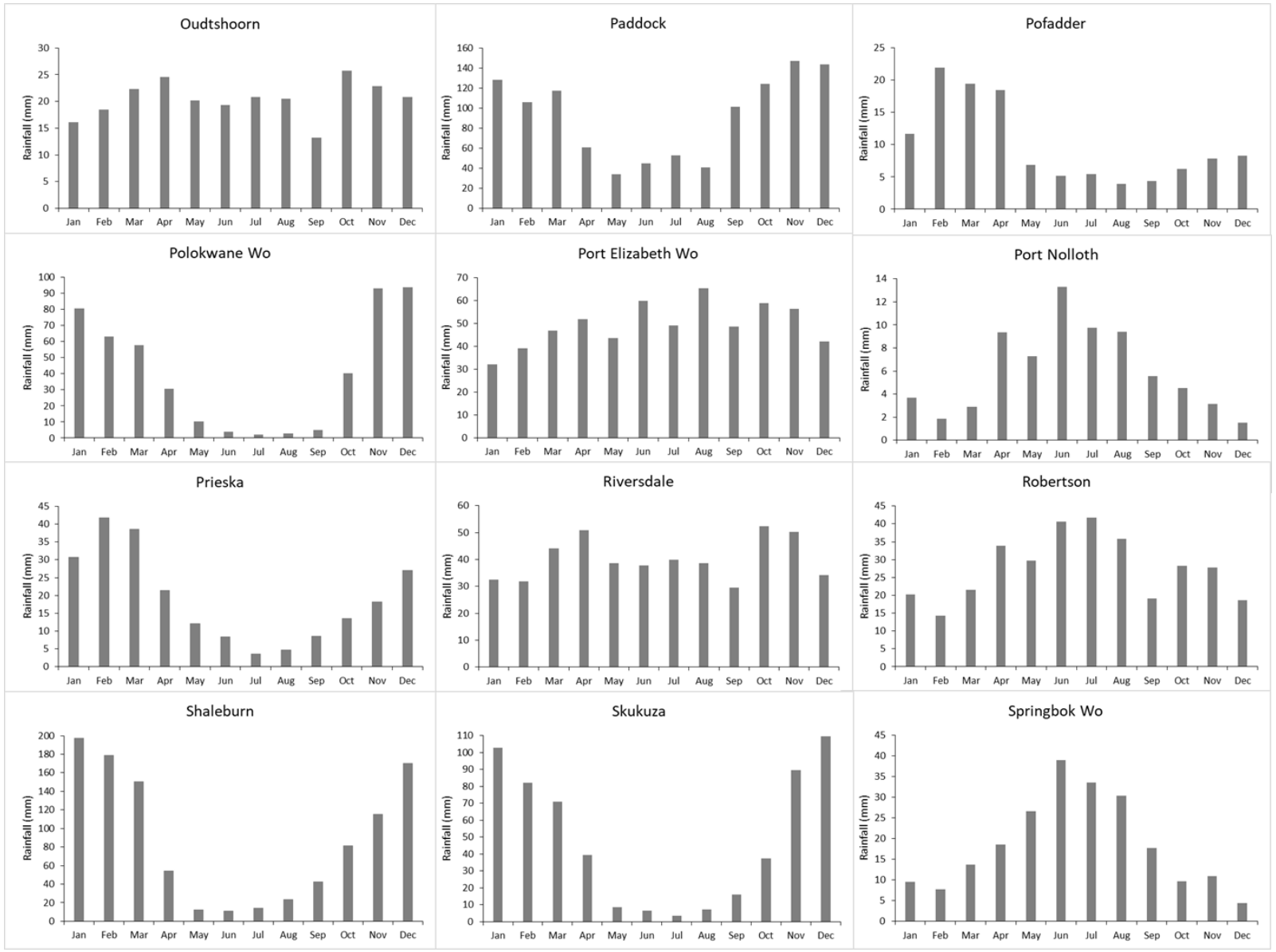


Figure 5.4 continued: Annual cycles of rainfall for the period of 1987-2016.

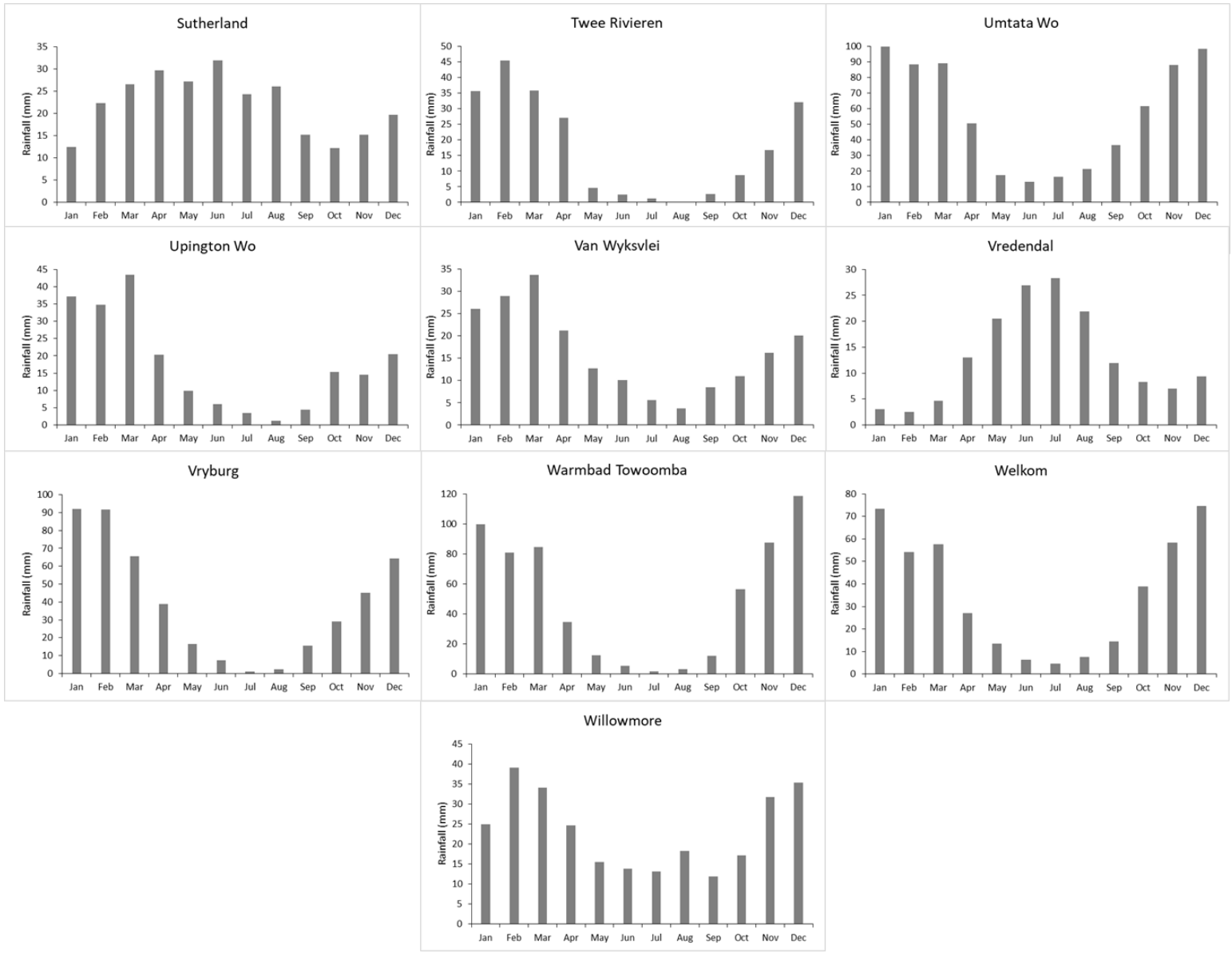


Figure 5.4 continued: Annual cycles of rainfall for the period of 1987-2016.

Of the 46 weather stations, there are 34 which reveal higher mean monthly rainfall totals during the summer months of the year from September/October or even later, through to March/April (Figure 5.4). These weather stations are mostly located within the eastern, central and northern regions of the country. Along the eastern coast, at Cedara, East London Wo, Mandini, Paddock, Shaleburn and Umtata Wo, higher monthly rainfall totals are evident from as early as August/September through to April (Figure 5.4). Within the Northern Cape, at locations including Pofadder, Twee Rivieren, Upington Wo and Vanwyksvlei, higher monthly rainfall totals are evident only from as late as December/January (Figure 5.4). The remaining locations, within the central and north eastern parts of the country, which display SRZ conditions demonstrate higher monthly rainfall totals from October/November (Figure 5.4). Following March/April across the 34 SRZ locations, mean monthly rainfall totals are considerably lower compared to the wetter months, where there is a distinct drier period during April/May through to the months where rainfall begins to increase, namely August/September/October/November/December (Figure 5.4). The drier periods across all the SRZ locations, as expected, display different intensities (Figure 5.4). Locations including East London Wo, Mandini, Paddock and Willowmore, located in the south and eastern parts of the country, have a drier period which is less noticeable compared to the wetter period of these locations and to the drier period across other SRZ locations (Figure 5.4). At Lephalale, Mara, Polokwane Wo, Skukuza, Twee Rivieren and Warmbad Towoomba, within the northern parts of the country, the drier period is particularly marked where rainfall is considerably low compared to the wetter period and there are even some months with zero rainfall (Figure 5.4).

Calvinia Wo, Cape Town Wo, Cape Agulhas, Langebaanweg AWS, Port Nolloth, Robertson, Springbok Wo, Sutherland and Vredendal located within the southwestern Cape and along the western coast and adjacent areas, receive higher rainfall during the winter months of the year, particularly from April to September (Figure 5.4). At Cape Town Wo, Langebaanweg AWS, Port Nolloth, Springbok Wo and Vredendal rainfall totals during the drier months are considerably low compared to the remainder of the year (Figure 5.4). Conversely, Calvinia Wo, Cape Agulhas, Robertson and Sutherland demonstrate relatively higher monthly rainfall during the drier period (Figure 5.4). At Robertson and Sutherland, in particular, the annual cycles of rainfall are relatively similar to Oudtshoorn, Riversdale and Port Elizabeth Wo, but there is a distinct rainfall peak during

the winter months of the year (Figure 5.4). Oudtshoorn, Riversdale and Port Elizabeth Wo receive rainfall throughout the year and demonstrate aseasonal, year-round rainfall characteristics (Figure 5.4). At these locations, mean monthly rainfall totals throughout the year are relatively equable (Figure 5.4).

When considering the annual rainfall cycles at individual weather stations, groupings into SRZ, WRZ and YRZ were evident. In considering these rainfall zones, the spatial distribution of rainfall totals for each month also reveal patterns in the timing of rainfall across the country, and SRZ, WRZ and YRZ conditions are evident amongst the maps presented in Figure 5.5. Monthly rainfall gradually increases from August/September along the eastern coast to cover the entire eastern half and western interior of the country by November/December, where monthly rainfall totals across this area range between 10 and 200mm (Figure 5.5). From March/April, rainfall across the eastern half and western interior of the country begins to decrease considerably, and from May this area of the country is relatively dry (Figure 5.5). During May to September most of the country which receives rainfall during the summer months remains considerably dry with mean monthly rainfall totals consistently below 30mm, and for many locations in the northern parts and western interior of the country monthly rainfall totals are below 10mm (Figure 5.5). Throughout the year the western coast and adjacent areas of the country remain relatively dry with fluctuations in the amount of monthly rainfall, where during April to September rainfall totals are highest and typically range between 10 and 90mm (Figure 5.5). From April, mean monthly rainfall totals across the southwestern Cape gradually increase, where rainfall totals are above 30mm throughout April to September (Figure 5.5). During this time rainfall along the western coast is consistently above 10mm, whereas during the remainder of the year rainfall is below 10mm (Figure 5.5). Along the southern coast rainfall remains relatively consistent throughout the year, where mean monthly rainfall totals range between 10 and 70mm (Figure 5.5).

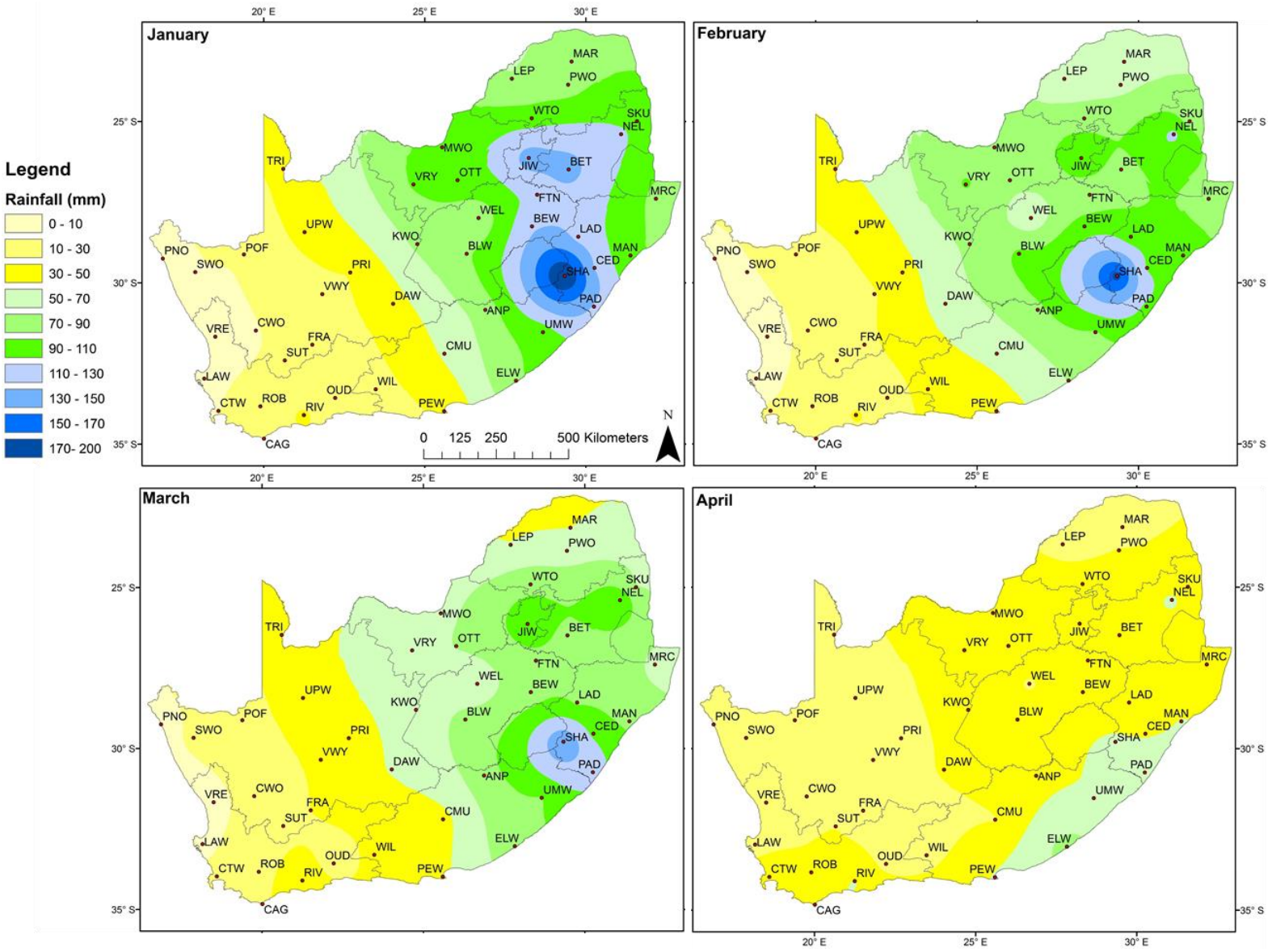


Figure 5.5: Ordinary kriging interpolation of mean monthly rainfall totals for the period of 1987-2016.

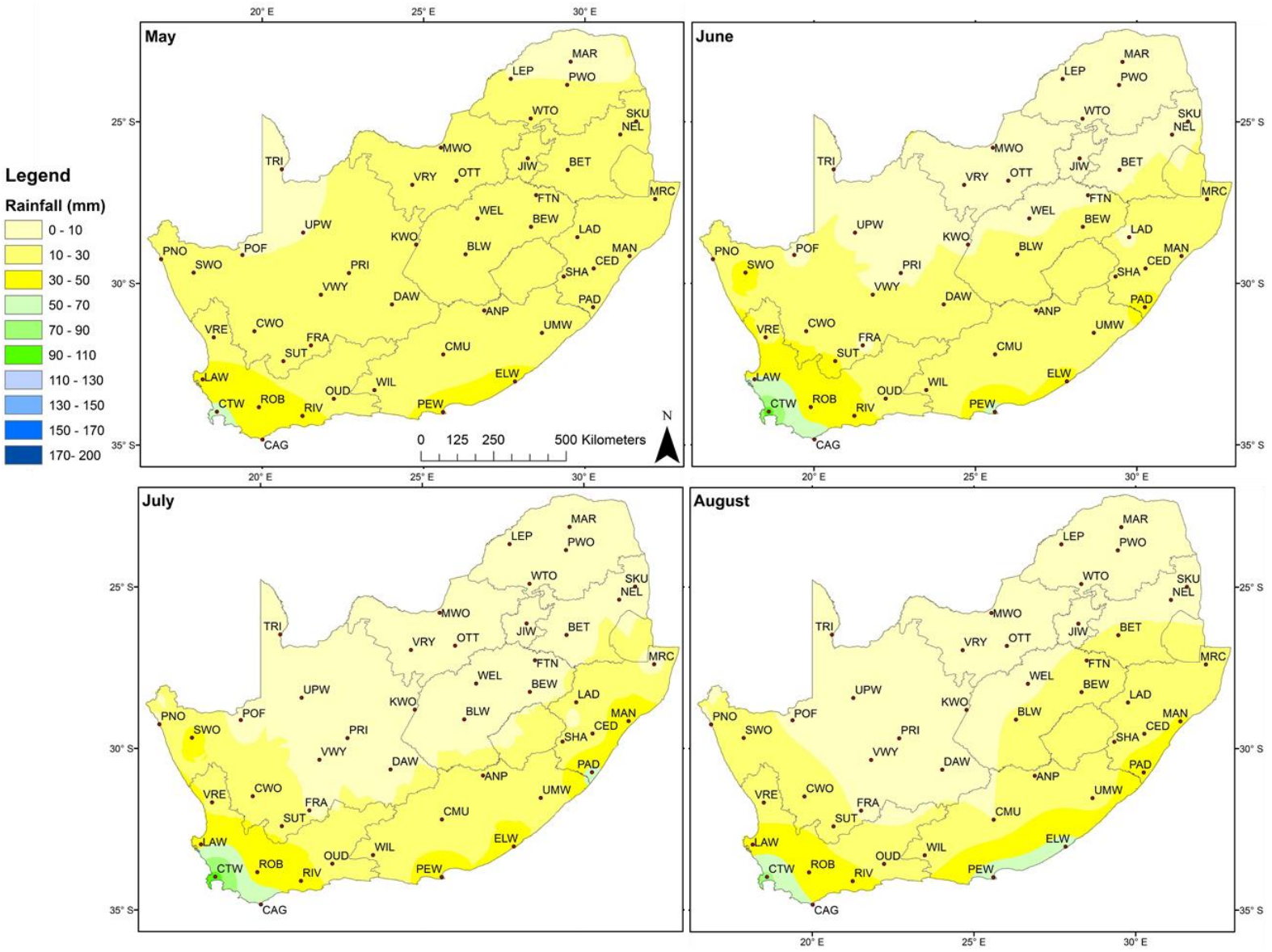


Figure 5.5 continued: Ordinary kriging interpolation of mean monthly rainfall totals for the period of 1987-2016.

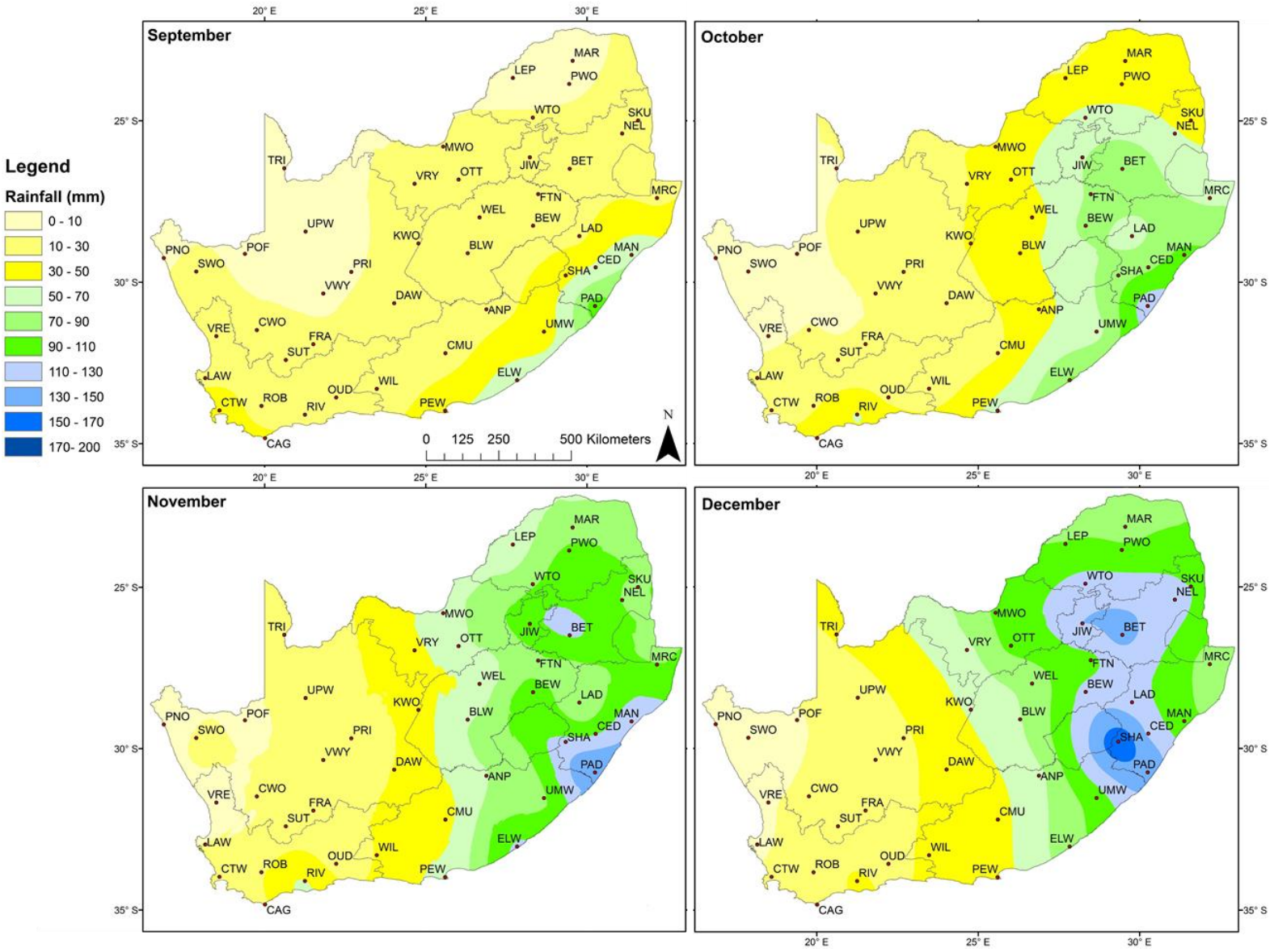


Figure 5.5 continued: Ordinary kriging interpolation of mean monthly rainfall totals for the period of 1987-2016.

Considering the annual cycles of rainfall, a study exploring rainfall seasonality and the shifts thereof benefits considerably from quantifying shifts in monthly rainfall amount. Across the country, each weather station demonstrated shifts, of varied magnitude and statistical strength, in the monthly rainfall totals (Figure 5.6; Appendix B). Spatial patterns are evident and are documented for each individual calendar month in the paragraphs which follow below Figure 5.6. Only 42 statistically significant time series trends were quantified for the entire period of 1987-2016, and this equates to approximately 8% of the trends quantified (Figure 5.6; Appendix B). An additional four statistically significant trends were evident when considering the change points (Appendix B.13). Since there were few statistically significant trends quantified, this may suggest that there were typically no or very few changes in monthly rainfall amount during the study period (Appendix B; Figure 5.6). Considering this, the shifts quantified may also suggest tentative trends in rainfall amount, and over a longer temporal period may become statistically significant. Hence, these trends are important to quantify, especially since this information may be used to corroborate the shifts in rainfall seasonality which are explored later under *Section 5.5*. Having captured very few statistically significant trends may be associated with the high levels of variability across all monthly rainfall totals for each weather station (Appendix B). The lowest CV quantified was 27.4% which is evident at SHA for the January rainfall totals (Appendix B). The remaining CV values for all locations across all months were above 30%, demonstrating that the monthly rainfall totals are highly variable from year to year (Appendix B). For each month the maximum CV value quantified was larger than 100%, where the largest CV value was evident at Twee Rivieren for the August rainfall totals (CV = 538.5%; Appendix B). Additionally, a total of 39 statistically significant change points were detected from 1991 to 2014 (Appendix B.13). Since there are change points throughout most of the study period, this may reflect that monthly rainfall totals were considerably variable, and that there was no change in the inter-annual variability of monthly rainfall amount during the study period (Appendix B.13), which additionally was not investigated here.

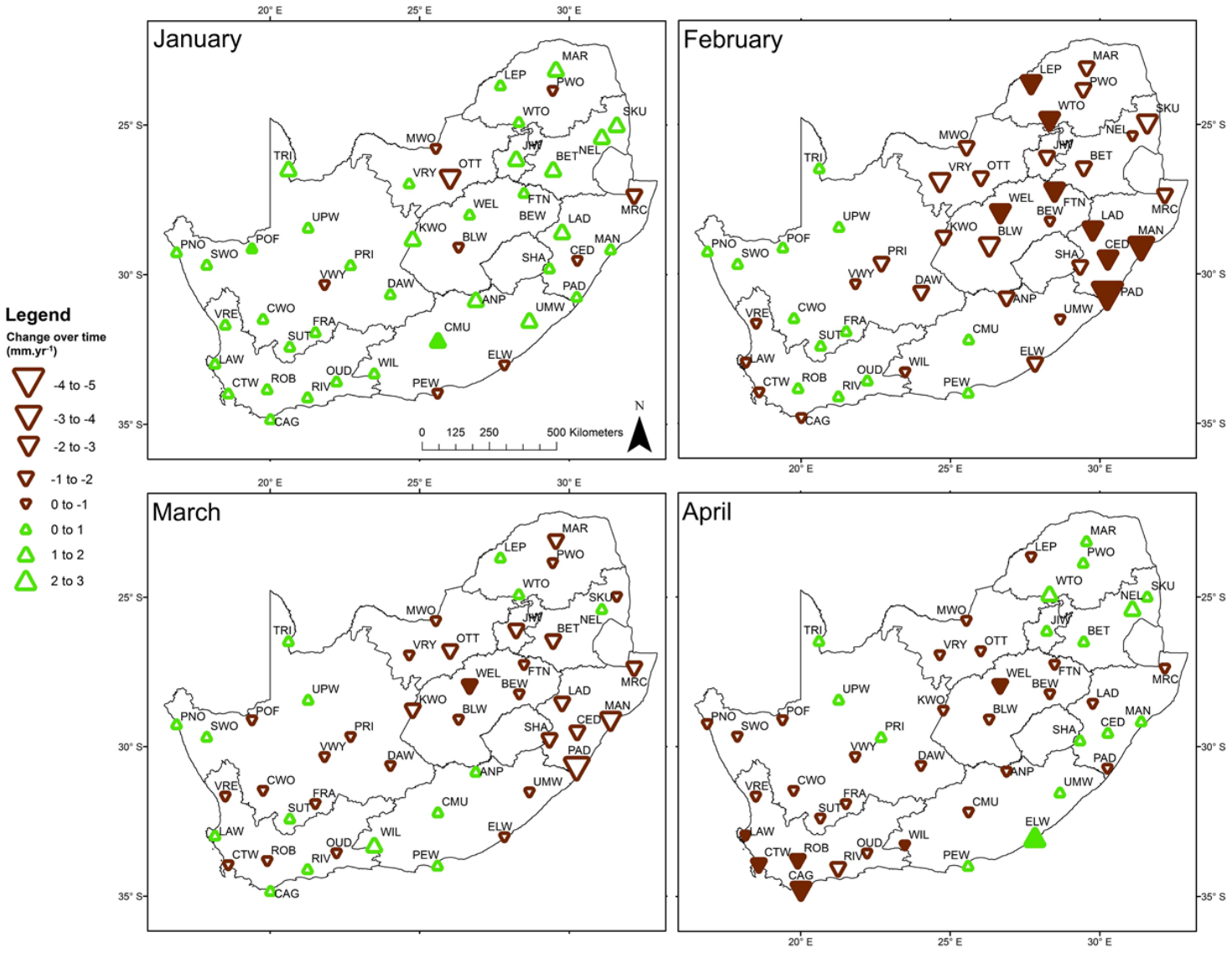


Figure 5.6: Trends in total monthly rainfall for individual weather stations for the period 1987-2016. Shaded symbols indicate statistically significant trends at the 5% level.

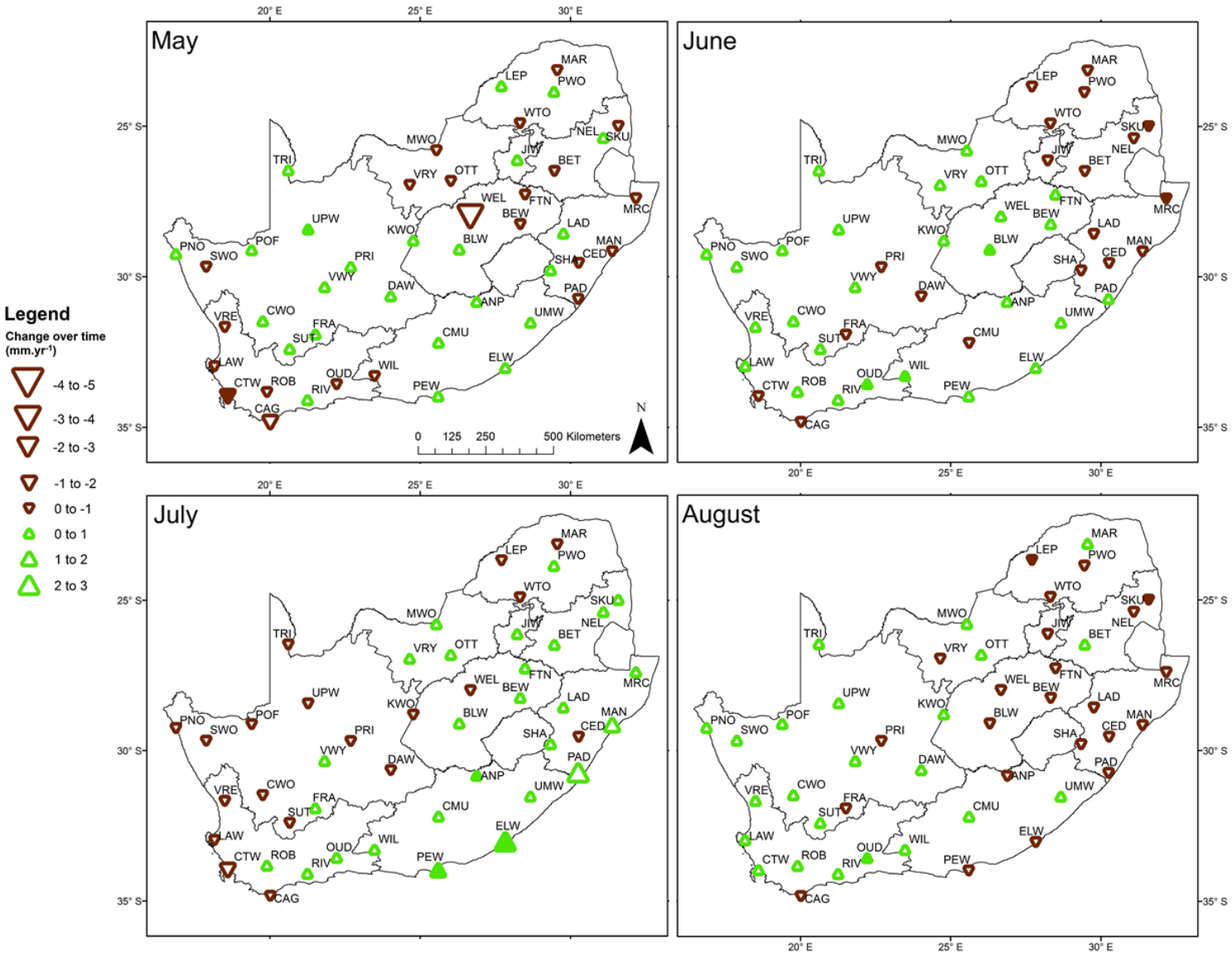


Figure 5.6 continued: Trends in total monthly rainfall for individual weather stations for the period 1987-2016. Shaded symbols indicate statistically significant trends at the 5% level.

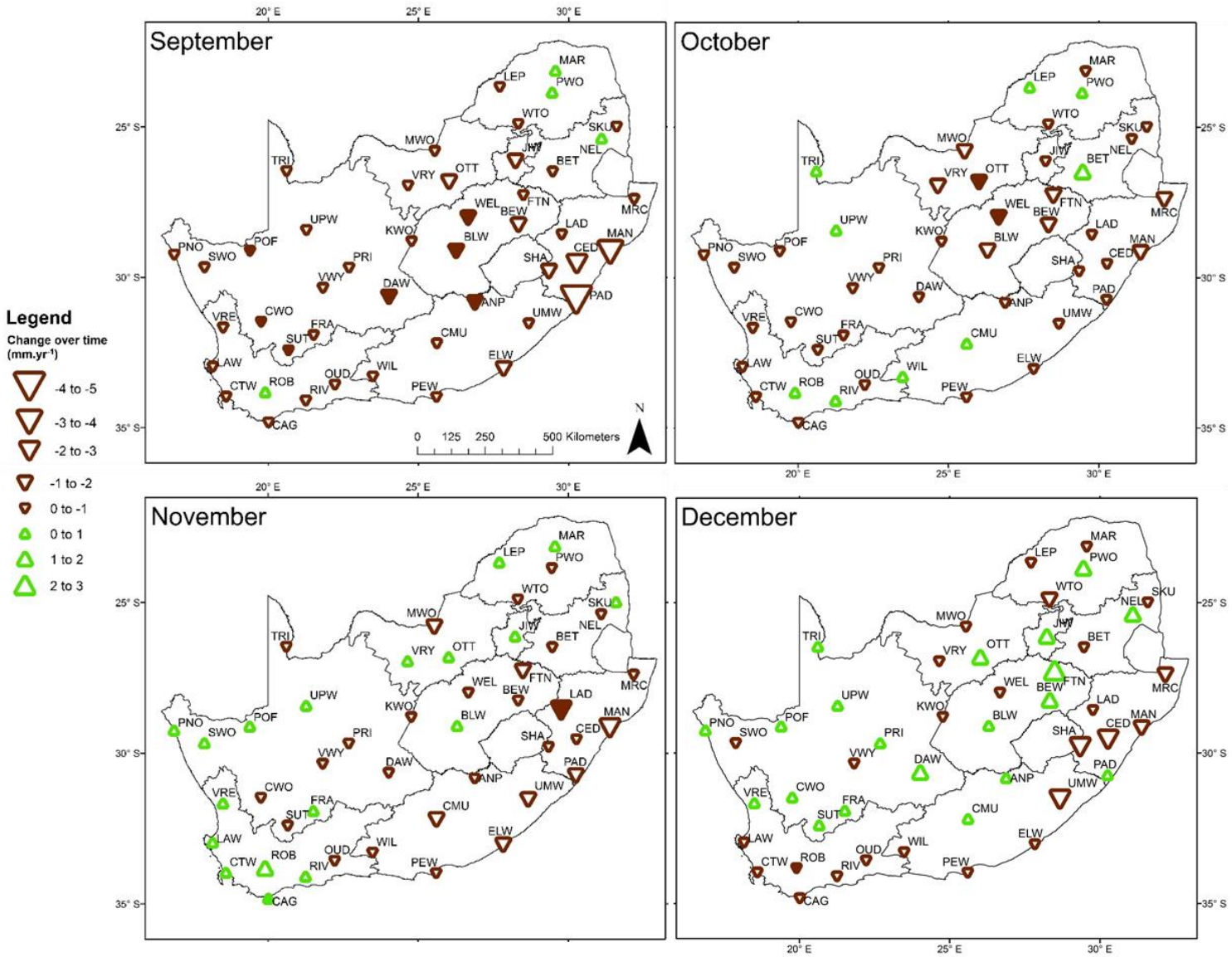


Figure 5.6 continued: Trends in total monthly rainfall for individual weather stations for the period 1987-2016. Shaded symbols indicate statistically significant trends at the 5% level.

Of 46 weather stations, 37 demonstrate an increase in January rainfall totals as the study period progressed (Figure 5.6). These increasing trends are quantified to range between 0.05mm.yr^{-1} at VRE, along the western coast, to 2.16mm.yr^{-1} at BEW within the Free State (Appendix B.1). CMU (1.44mm.yr^{-1}, r = 0.39, p = 0.036), within the Eastern Cape, and POF (0.59mm.yr^{-1}, r = 0.37, p = 0.043), within the Northern Cape, were the only weather stations which demonstrated statistically significant trends (Figure 5.6; Appendix B.1). Scattered amongst the positive trends, mostly in the eastern half of the country, are very few negative trends which range between -0.10mm.yr^{-1} at BLW, within the Free State, to -2.45mm.yr^{-1} at OTT within the North West (Figure 5.6; Appendix B.1). Change points were detected at ELW and PEW, where both locations are along the southern coast and both demonstrated weak negative trends for the entire study period (Appendix B.13; Figure 5.6). Prior to 2012 rainfall at ELW was increasing, and following 2012 rainfall was instead decreasing (Appendix B.13). Two change points were detected for PEW, where rainfall before, between and after the change points was consistently increasing at varying magnitudes (Appendix B.13).

There were 33 locations, across the southwestern Cape and the central and eastern parts of the country which displayed a decrease in rainfall during February (Figure 5.6). These decreasing trends were quantified to range between -0.01mm.yr^{-1} at VRE, along the western coast, and -4.86mm.yr^{-1} at PAD within KwaZulu-Natal (Figure 5.6; Appendix B.2). Statistically significant negative trends are evident at eight locations including CED (-2.30mm.yr^{-1}, r = 0.44, p = 0.015), FTN (-2.37mm.yr^{-1}, r = 0.44, p = 0.015), LAD (-2.93mm.yr^{-1}, r = 0.46, p = 0.009), LEP (-2.00mm.yr^{-1}, r = 0.38, p = 0.040), MAN (-3.36mm.yr^{-1}, r = 0.37, p = 0.045), PAD (-4.86mm.yr^{-1}, r = 0.46, p = 0.011), WEL (-2.69mm.yr^{-1}, r = 0.48, p = 0.005) and WTO (-2.73mm.yr^{-1}, r = 0.42, p = 0.022), all located within the Free State, KwaZulu-Natal and Limpopo (Figure 5.6; Appendix B.2). Weather stations located in these provinces as well as in the North West, Northern Cape and Eastern Cape also predominantly demonstrated trends towards reduced February rainfall totals. Across the western half of the country, increases in the February rainfall totals ranged between 0.07mm.yr^{-1} at PEW and POF to 0.96 mm.yr^{-1} CMU (Figure 5.6; Appendix B.2). These locations are mostly located in the western half of the Northern Cape and the eastern half of the Western Cape. Only

BET, located in Mpumalanga, demonstrated a change point during February, whereby prior to 2007 rainfall was increasing and from 2007 rainfall was decreasing (Appendix B.13).

Considering the March rainfall totals, there were 31 locations with decreasing trends, where there were negative trends within each province and especially in the northeastern part of the country (Figure 5.6). These trends were quantified to range between -0.0004mm.yr^{-1} at PRI, in the Northern Cape, and -3.04 mm.yr^{-1} at PAD in KwaZulu-Natal (Appendix B.3). Only WEL (-1.94mm.yr^{-1}, r = 0.40, p = 0.015) within the Free State demonstrated a statistically significant trend (Figure 5.6; Appendix B.3). Some weather stations across the western half and in the northeastern part of the country demonstrated increasing trends which range from 0.01mm.yr^{-1} at LEP, within Limpopo, to 1.05mm.yr^{-1} at WIL within the Eastern Cape (Figure 5.6; Appendix B.3). MAN and SHA, within KwaZulu-Natal, and VRY, within North West, all displayed an overall negative trend in March rainfall totals and displayed statistically significant change points (Appendix B.13; Figure 5.6). At VRY from 1992 there was a negative trend detected following a positive trend (Appendix B.13). From 1997 at MAN a positive trend with a smaller magnitude than the prior negative trend was detected (Appendix B.13). From 2008 a larger and statistically stronger negative trend was evident at SHA (Appendix B.13).

Amongst the weather stations located within the western, central and northern parts of the country there was dominant decline in April rainfall which was evident across 30 weather stations (Figure 5.6). This was quantified to range between -0.04mm.yr^{-1} at LAD and DAW, within KwaZulu-Natal and the Northern Cape, to -2.31mm.yr^{-1} at CAG within the Western Cape (Appendix B.4). Within the southwestern Cape and the Eastern Cape, statistically significant reductions in rainfall during the April months were evident at: CAG (-2.31mm.yr^{-1}, r = 0.49, p = 0.006), CTW (1.60mm.yr^{-1}, r = 0.37, p = 0.044), LAW (-0.82mm.yr^{-1}, r = 0.39, p = 0.035), ROB (-1.07mm.yr^{-1}, r = 0.39, p = 0.034) and WIL (-0.92mm.yr^{-1}, r = 0.37, p = 0.043; Figure 5.6; Appendix B.4). Additionally, WEL (-1.55mm.yr^{-1}, r = 0.44, p = 0.009), within the Free State, also demonstrated a statistically significant negative trend (Figure 5.6; Appendix B.4). Locations within the north, eastern and northwestern parts of the country and along the eastern coast display increasing trends (Figure 5.6), and these range between 0.07mm.yr^{-1} at UPW, in the Northern Cape, to 2.80mm.yr^{-1} at ELW within the Eastern Cape (Appendix B.4). ELW was the only weather station with a statistically significant

increasing trend (r = 0.45, p = 0.043; Figure 5.6; Appendix B.4). Seven change points were detected for the April rainfall totals (Appendix B.13). The earliest change points were detected at FTN and MWO, within the Free State and North West, and from 1991 increasing trends smaller than prior to 1991 were detected (Appendix B.13). At ELW, within the Eastern Cape, there was change in the trajectory of the rainfall trend evident from 1995 (Appendix B.13). Prior to 1995 April rainfall totals were increasing, and following 1995 a decreasing trend was quantified (Appendix B.13). CAG and VRE, located in the Western Cape, both have negative trends quantified prior to the change points detected, and following 2007 the magnitude of the decreasing trend at CAG was smaller than prior to 2007 and at VRE rainfall totals were increasing following 2008 (Appendix B.13).

There were 22 increasing and 24 decreasing trends quantified for the May rainfall totals (Appendix B.13). The locations which displayed decreasing trends were concentrated within the southwestern and northeastern parts of the country (Figure 5.6). The reductions in rainfall totals were quantified to range between -0.02mm.yr^{-1} at OUD, within the Western Cape, and -3.41mm.yr^{-1} at WEL within the Free State (Figure 5.6; Appendix B.5). Only the trend at CTW (-1.35mm.yr^{-1}, r = 0.38, p = 0.039) was statistically significant (Figure 5.6; Appendix B.5). Evident across the entire country were increasing trends, although these were mostly within the Northern and Eastern Cape (Figure 5.6; Appendix B.5). These trends range between 0.02mm.yr^{-1} at LEP, within Limpopo, and 0.79mm.yr^{-1} at SUT within the Northern Cape (Appendix B.5; Figure 5.6). Only UPW (0.63mm.yr^{-1}, r = 0.39, p = 0.031), within the Northern Cape, displayed a statistically significant increasing trend (Figure 5.6; Appendix B.5). Three change points were detected during 1995 and 1996 (Appendix B.13). Prior to 1995 an increasing trend was quantified for WTO, and after 1995 a statistically significant decreasing trend was evident (-1.84mm.yr^{-1}, r = 0.61, p = 0.002; Appendix B.13). From 1996 there was a change in the magnitude of the trends evident at LAD, located in KwaZulu-Natal, and at PEW located in the Eastern Cape (Appendix B.13). At PEW prior to 1996 there was a statistically significant increasing trend (3.03mm.yr^{-1}, r = 0.72, p = 0.029), and from 1996 a decreasing trend was detected (Appendix B.13). At LAD a decreasing trend was detected prior to and from the change point at 1996, and from 1996 a statistically significant decreasing trend was quantified (-1.72mm.yr^{-1}, r = 0.58, p = 0.007; Appendix B.13).

For June the weather stations predominantly indicate increasing trends, however, in the northeastern, southwestern and central parts of the country some negative trends in rainfall amount were evident across 19 locations (Figure 5.6). The increasing trends detected were concentrated within the Eastern Cape, Free State, Northern Cape, North West and Western Cape (Figure 5.6). These trends were quantified to range from 0.04mm.yr^{-1} at UMW, within the Eastern Cape, to 0.84mm.yr^{-1} at RIV within the Western Cape (Appendix B.6). Statistically significant increasing trends were evident at BLW (0.67mm.yr^{-1}, r = 0.34, p = 0.042), within the Free State, and at OUD (0.64mm.yr^{-1}, r = 0.45, p = 0.013) as well as WIL (0.61mm.yr^{-1}, r = 0.42, p = 0.019) both along the southern coast (Figure 5.6; Appendix B.6). The decreasing trends detected were mostly concentrated within Gauteng, KwaZulu-Natal, Limpopo and Mpumalanga, and were quantified to range between -0.03mm.yr^{-1} at PRI, within the Northern Cape, to -0.98mm.yr^{-1} at CTW within the Western Cape (Appendix B.6; Figure 5.6). Statistically significant increasing trends were evident at MRC (-0.90mm.yr^{-1}, r = 0.42, p = 0.019), within KwaZulu-Natal, and SKU within Mpumalanga (-0.53mm.yr^{-1}, r = 0.44, p = 0.015; Figure 5.6; Appendix B.6). Nine change points were detected for the June rainfall totals (Appendix B.13). These change points were evident at locations within the Eastern and Western Cape. The earliest change points were detected from 1993 at OUD and RIV, and for both locations a second change point was detected from 2005 for RIV and 2009 for OUD (Appendix B.13). Two change points were also detected at ROB, and these were during 1998 and 2009 (Appendix B.13). For RIV and ROB the trends before, between and from the change points were positive with varying magnitudes (Appendix B.13). From the change point during 2009 OUD demonstrated a decrease in June rainfall totals, whereas the trends before 2009 were increasing (Appendix B.13). From 2007, rainfall totals at VRE were decreasing at a smaller rate than prior to 2007 (Appendix B.13). From 2008 rainfall totals at ANP and WIL were decreasing at a rate larger than that prior to 2008 (Appendix B.13).

Weather stations within the eastern and southern parts of the country predominantly indicate an increase in the July rainfall totals (Figure 5.6), and were quantified to range between 0.01mm.yr^{-1} at PWO, within Limpopo, and 2.69mm.yr^{-1} at PAD within KwaZulu-Natal (Appendix B.7). Located within the Eastern Cape, ANP (0.72mm.yr^{-1}, r = 0.39, p = 0.038), ELW (2.23mm.yr^{-1}, r = 0.39, p = 0.016) and PEW (1.91mm.yr^{-1}, r = 0.38, p = 0.038) demonstrated statistically significant increasing

trends (Figure 5.6; Appendix B.7). Across the southwestern, western and northern parts of the country there were 27 locations with shifts towards lower July rainfall totals, and were quantified to range between -0.01mm.yr^{-1} at DAW and WTO, within Limpopo and the Northern Cape, to -1.36mm.yr^{-1} at CTW within the Western Cape (Figure 5.6; Appendix B.7). No statistically significant change points were detected for the July rainfall totals (Appendix B.13).

Across the western, southern and northern parts of the country, weather stations mostly display trends towards increasing August rainfall totals (Figure 5.6). Increasing trends are evident at 23 weather stations, and were quantified to range from 0.01mm.yr^{-1} at TRI, within the Northern Cape, to 0.75mm.yr^{-1} at OUD within the Western Cape (Figure 5.6; Appendix B.8). Only OUD ($r = 0.39$, $p = 0.034$) demonstrated a statistically significant increasing trend (Figure 5.6; Appendix B.8). There were decreasing trends across all the provinces, however, the majority of locations with decreasing trends were concentrated within the eastern half of the country (Figure 5.6). These decreasing trends were quantified to range between -0.02mm.yr^{-1} at PRI and VRY, located in the Northern Cape and North West, to -0.83mm.yr^{-1} at MAN within KwaZulu-Natal (Appendix B.8). Located within Limpopo and Mpumalanga respectively, LEP (-0.12mm.yr^{-1}, $r = 0.42$, $p = 0.022$) and SKU (-0.54mm.yr^{-1}, $r = 0.41$, $p = 0.023$) demonstrated statistically significant trends towards drier conditions (Figure 5.6; Appendix B.8). Between 2001 and 2004, change points were detected in the August rainfall totals at CED, FRA, OUD and RIV (Appendix B.13). OUD and RIV are located within the Western Cape, and FRA is located directly north of these locations (Figure 5.6). CED on the other hand is located within KwaZulu-Natal (Figure 5.6). At CED, rainfall totals were decreasing at a smaller rate from 2001 than prior to 2001, whereas at RIV rainfall totals were decreasing at a larger rate than prior to 2001 (Appendix B.13). At OUD rainfall totals were increasing prior to the change point and from 2002 there was a decreasing trend (Appendix B.13). At FRA, rainfall totals were increasing at a smaller rate from 2004 when compared to the trend prior to 2004 (Appendix B.13).

It is evident that across the entire country rainfall totals were predominantly decreasing during September, where there were only four locations which demonstrated increasing trends (Figure 5.6). The decreasing trends were quantified to range between -0.0002mm.yr^{-1} at SKU, located within Mpumalanga, and -4.74mm.yr^{-1} at PAD within KwaZulu-Natal (Appendix B.9). Within the

central parts of the country, ANP (-1.52mm.yr^{-1}, r = 0.46, p = 0.009), BLW (-1.56mm.yr^{-1}, r = 0.39, p = 0.033), CWO (-0.70mm.yr^{-1}, r = 0.38, p = 0.037), DAW (-1.17mm.yr^{-1}, r = 0.42, p = 0.020), POF (-0.34mm.yr^{-1}, r = 0.44, p = 0.014), SUT (-0.96mm.yr^{-1}, r = 0.48, p = 0.006) and WEL (-1.32mm.yr^{-1}, r = 0.37, p = 0.047) all displayed statistically significant negative trends (Figure 5.6; Appendix B.9). Only MAR, PWO and SKU in the northeastern parts of the country and ROB within the southwestern Cape demonstrated increasing trends (Figure 5.6), and were quantified to range between 0.03mm.yr^{-1} at PWO and 0.27mm.yr^{-1} at MAR (Appendix B.9). Only MAR demonstrated a change point, where prior to 1996 a decreasing trend was quantified and from 1996 an increasing trend was evident (Appendix B.13).

Trends towards drier conditions during October were evident across all the provinces (Figure 5.6). Only nine weather stations located within the Eastern Cape, Limpopo, Northern Cape, Mpumalanga and Western Cape demonstrated trends towards higher October rainfall totals (Figure 5.6), and quantified these trends range between 0.02mm.yr^{-1} at UPW, within the Northern Cape, and 1.09mm.yr^{-1} at BET within Mpumalanga (Appendix B.10). The decreasing trends range between -0.04mm.yr^{-1} at FRA, within the Northern Cape, and -1.83mm.yr^{-1} at WEL located within the Free State (Appendix B.10). Located within the Free State and North West, only OTT (-1.82mm.yr^{-1}, r = 0.41, p = 0.026) and WEL (r = 0.42, p = 0.025) demonstrated statistically significant trends (Figure 5.6; Appendix B.10). Only OTT and VRY, both located in the North West, demonstrated change points for the October rainfall totals (Appendix B.13). Prior to 2004 rainfall totals were increasing at VRY, whereas from 2004 a decreasing trend was evident (Appendix B.13). Prior to and from 2010 rainfall totals were increasing at OTT, where the increasing trend was larger from 2010 (Appendix B.13).

Across the western coast, southwestern Cape and northern parts of the country there were 18 weather stations which demonstrated increasing trends for the November monthly rainfall totals (Figure 5.6). These increasing trends were quantified to range between 0.02mm.yr^{-1} at POF, in the Northern Cape, to 1.20mm.yr^{-1} at ROB within the Western Cape (Figure 5.6; Appendix B.11). Only CAG (0.95mm.yr^{-1}; r = 0.38, p = 0.037), located within the Western Cape, demonstrated a statistically significant increasing trend (Figure 5.6; Appendix B.11). Spanning across the entire country weather stations demonstrated decreasing trends which range between -0.08mm.yr^{-1} at

OUD, within the Western Cape, to -2.14mm.yr^{-1} at MAN within KwaZulu-Natal (Appendix B.11). LAD (-2.09mm.yr^{-1}, r = 0.40, p = 0.025), located within KwaZulu-Natal, was the only weather station which demonstrated a statistically significant decreasing trend (Figure 5.6; Appendix B.11). A statistically significant change point was only detected at SKU located in Mpumalanga (Figure 5.6; Appendix B.13). Prior to 1992 there was an increasing trend and from 1992 a statistically significant decreasing trend was detected (-5.64mm.yr^{-1}, r = 0.54, p = 0.013; Appendix B.13).

Scattered throughout the country, both increasing and decreasing trends in the December rainfall totals were evident across the weather stations (Figure 5.6). There were 26 decreasing trends evident, and these were quantified to range from -0.08mm.yr^{-1} at LAW, located in the Western Cape, to -2.68mm.yr^{-1} at CED located in KwaZulu-Natal (Appendix B.12). Only ROB (-0.79mm.yr^{-1}, r = 0.39, p = 0.034), located in the Western Cape, demonstrated a statistically significant decreasing trend (Figure 5.6; Appendix B.12). At most of the interior locations, trends towards wetter conditions are evident (Figure 5.6), and these trends were quantified to range between 0.02mm.year^{-1} at FRA, in the Northern Cape, and 2.08mm.year^{-1} at FTN within the Free State (Appendix B.12). Statistically significant change points were detected at CED, FRA, MRC, MAR and SWO during 1994 to 2008 (Appendix B.13). CED and MRC are located in KwaZulu-Natal, MAR is located in Limpopo, and FRA and SWO are located in the Northern Cape (Figure 5.6). Prior to 1994 there was an increasing trend at MAR, and from 1994 an increasing trend was also evident but at a greater rate (Appendix B.13). Prior to 1995 at FRA rainfall was decreasing, and from 1995 rainfall was decreasing but at a smaller rate (Appendix B.13). Prior to 2000 rainfall was increasing at SWO, and from 2000 an increase was still evident but at a smaller rate than the trend prior to 2000 (Appendix B.13). Rainfall totals were increasing prior to 2002 at CED, whereas from 2002 rainfall totals were decreasing (Appendix B.13). At MRC from 2008 there was a larger increasing trend evident when compared to the trend rate prior to 2008 (Appendix B.13).

5.4 QUANTIFYING AND CLASSIFYING RAINFALL SEASONALITY ACROSS SOUTH AFRICA

5.4.1 CLUSTERING MONTHLY RAINFALL AND VARIABILITY

Given that the climatology of monthly rainfall is often referred to when considering rainfall seasonality, the results presented under this section mainly regard the cluster analysis process of mean monthly rainfall and the associated CV. The results of the decadal mean monthly rainfall and rain day clustering are presented under *Appendix C*, and will be refered to where necessary within the following paragrpahs.

Agglomerative hierarchical clustering using Ward's minimum variance algorithm separates the weather stations into five groups on the basis of mean monthly rainfall and variability (Figure 5.7; Appendix C.1). Five groups were determined as the optimal number of classes, where the average silhouette width was quantified to 0.29 (Appendix C.1), whereas four cluster groups are suggested as the optimal number of clusters on the basis of the mean monthly rain days (Appendix C.3) The silhouette width of 0.29 is relatively low and close to zero. This may indicate that too few locations were used to compile the cluster solution and that rainfall across South Africa may be too complex to group using this method as some weather stations may fall between groups or are incorrectly grouped. The silhouette width quantified for three and four groups was 0.22, and for any other number of groups the silhouette width was less than 0.20 (Appendix C.1). The cophenetic coefficient was quantified to 0.6020, which is relatively lower that the cluster strength of 0.6272 associated with the mean rain days cluster solution (Appendix C.3). A value closer to 1 represents a high-quality cluster solution, and hence this cluster solution has a relatively moderate strength.

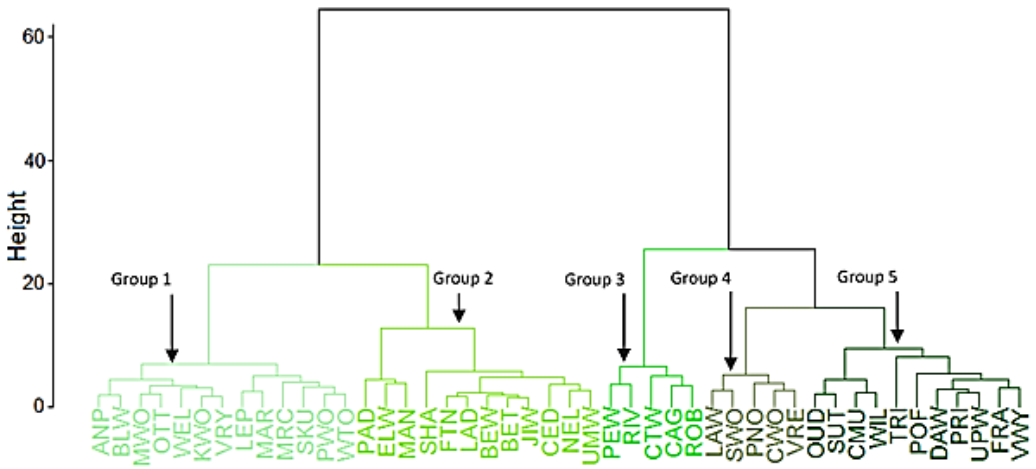


Figure 5.7: Colour coded dendrogram displaying weather stations (code) in groups 1 to 5 based on agglomerative hierarchical clustering of mean monthly rainfall and monthly CV using Ward's minimum variance algorithm and the squared Euclidean distance.

Group 1 weather stations are located in the northern and some central parts of the country, and represent a region across the plateau of South Africa with a steppe (subtropical) climate (Figure 5.8, 5.9; Engelbrecht & Engelbrecht, 2016). Group 2 weather stations are located across the eastern coast and span north up to BET, JIW and NEL, located in Gauteng and Mpumalanga (Figure 5.8). The locations are characterised by a wetter temperate climate with locations in the interior plateau as well as along regions east of the escarpment (Figure 5.8, 5.9; Engelbrecht & Engelbrecht, 2016). Group 3 weather stations include PEW, along the southern coast, and weather stations located in the southwestern Cape (Figure 5.8). The group 3 locations are south of the Cape Folded mountains and are characterised by an oceanic, temperate climate and are relatively dry (Figure 5.8, 5.9; Engelbrecht & Engelbrecht, 2016). Notably, additional weather stations located along the southern coast between PEW and the rest of group 3 may have resulted in continuation of this group within this area (Figure 5.8). Group 4 weather stations are located along the western coast and the adjacent inland area, and appear to be bound by the western edges of the escarpment being characterised by an oceanic, arid, desert climate (Figure 5.8, 5.9; Engelbrecht & Engelbrecht, 2016). Group 5 weather stations are located across the western interior plateau, and are characterised by an arid desert climate (Figure 5.8, 5.9; Engelbrecht & Engelbrecht, 2016).

Interestingly, the spatial distribution of these cluster zones reflects aridity zones as presented by Landman *et al.* (2017) and biome regions as presented by Rutherford *et al.* (2006).

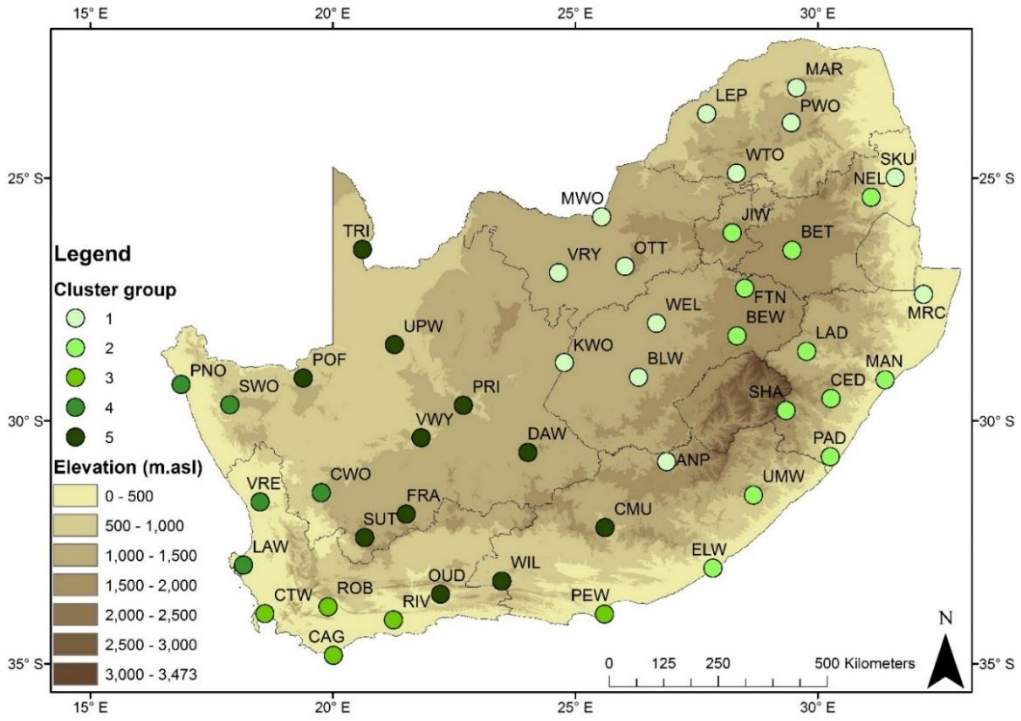


Figure 5.8: Spatial distribution of homogeneous rainfall groups 1 to 5, from Figure 5.7, based on agglomerative hierarchical clustering of mean monthly rainfall and monthly CV using Ward's minimum variance algorithm and the squared Euclidean distance.

For weather stations in group 1, the monthly rainfall distribution indicates that rainfall gradually increases from September to November where rainfall totals remain relatively high until February when rainfall gradually decreases (Figure 5.9). Group 2 rainfall totals display a similar pattern, however, after March rainfall considerably decreases (Figure 5.9). Monthly rainfall totals across group 2 are relatively higher than for group 1 (Figure 5.9). Group 5 also reflects summer rainfall with monthly rainfall totals relatively lower than for groups 1 and 2 (Figure 5.9). For the group 5 locations, rainfall totals gradually increase from September to December and following this they remain relatively high until they begin to decrease following March (Figure 5.9). Groups 3 and 4 represent winter rainfall conditions (Figure 5.9). Weather stations in group 3 have relatively higher monthly rainfall totals than for those in group 4 (Figure 5.9). Group 3 weather stations display a

dry season, between September and March, which receives a considerable amount of rainfall (Figure 5.9). Group 4 weather stations also have a dry season between September and March, but rainfall totals during these months are considerably low compared to the wet season rainfall totals (Figure 5.9). Indeed, the seasonal structure across the rain day box plots reflects similar patterns thus complimenting these boxplots (Appendix C.3; Figure 5.9).

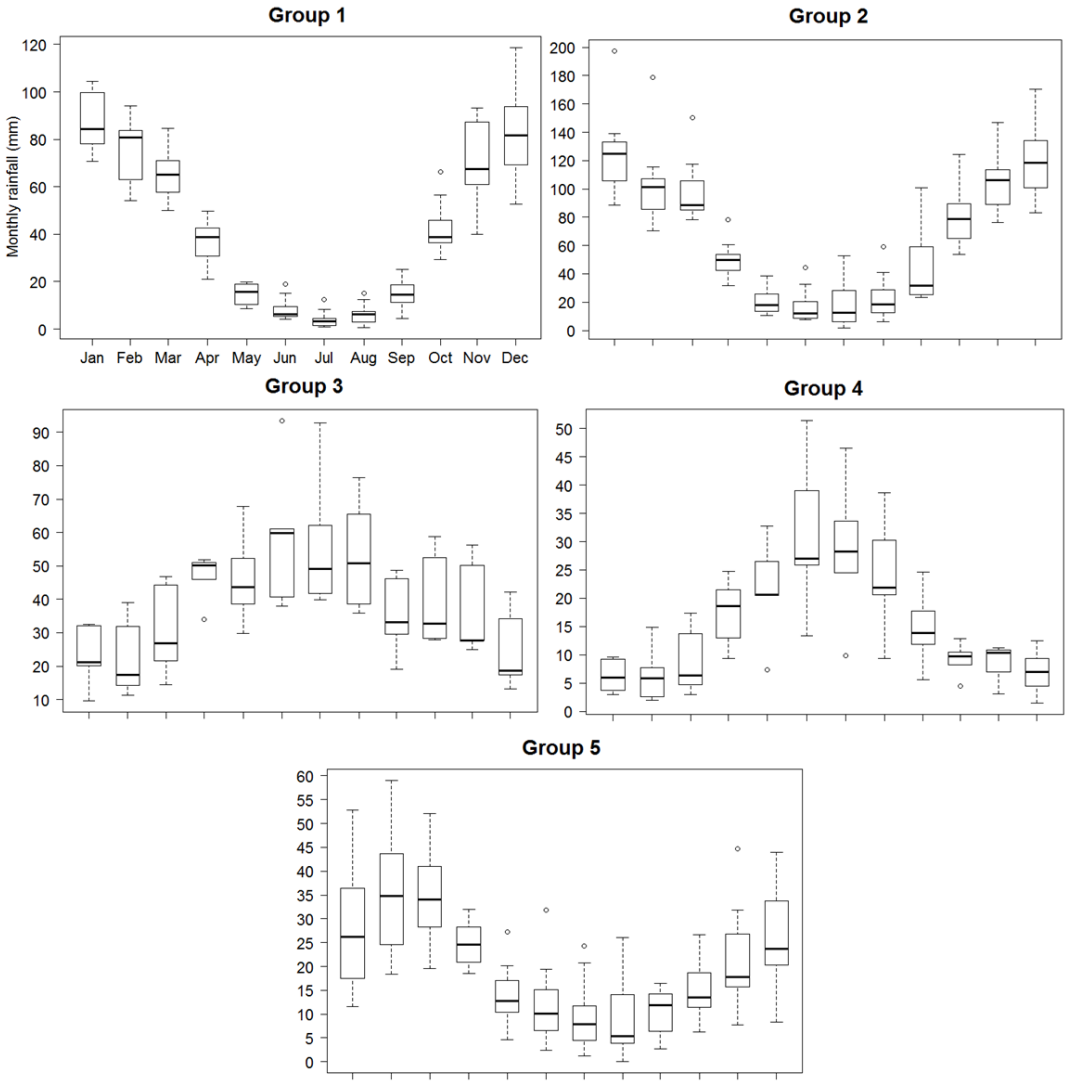


Figure 5.9: Boxplots representing the annual cycles rainfall for cluster groups 1 to 5. Circles represent outliers.

Based on the highest average silhouette values, agglomerative hierarchical clustering using Ward's minimum variance algorithm separates each group (i.e. groups 1 to 5 in Figure 5.8) into two

distinct dry and wet seasons (Figure 5.10; Appendix C.1). The wet season for group 1 and 2 occurs during October to April (Figure 5.10). For these groups, the dry season spans a period of approximately five months (Figure 5.10). Group 3 and 4 weather stations have an approximately four month long wet season which occurs during May to August (Figure 5.10). The wet season amongst group 5 weather stations spans December to April and is approximately 5 months long (Figure 5.10). Again, the wet and dry season lengths are similarly reflected across the rain day and decadal seasonal dendrograms complimenting these dendrograms in that wet and dry seasons were only clustered and through similar wet and dry season durations (Figure 5.10; Appendix C.2, C.3).

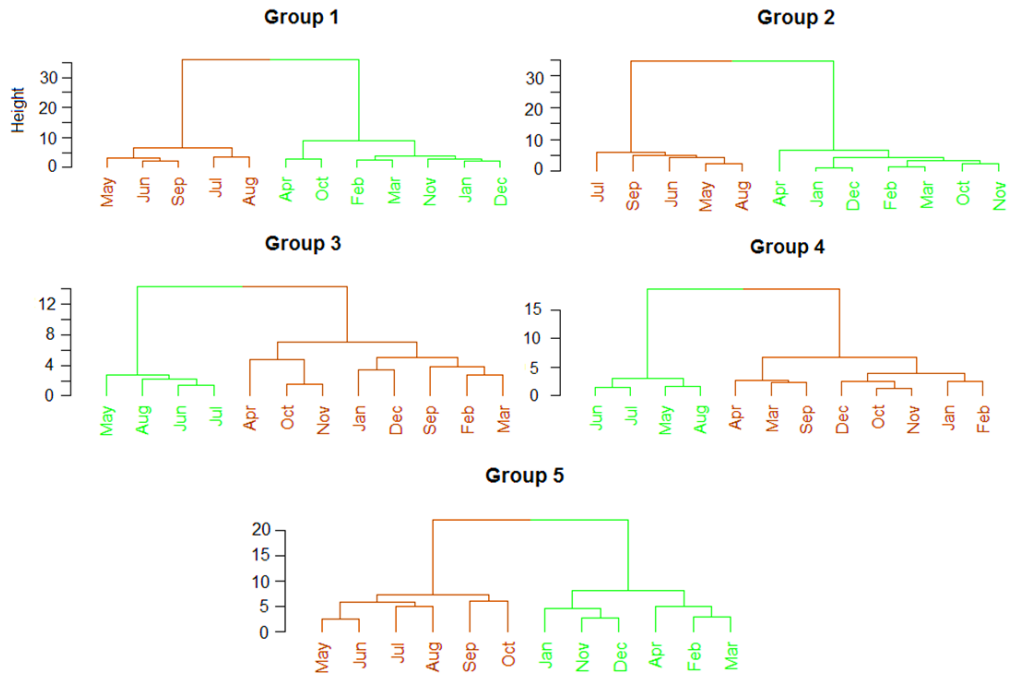


Figure 5.10: Dendrograms of monthly rainfall for groups 1 to 5 based on mean monthly rainfall and monthly CV using Ward's minimum variance algorithm and the squared Euclidean distance. Brown and green represent the dry and wet seasons months respectively.

Using this method, only the SRZ and WRZ were captured (Figure 5. 11). Of the 46 weather stations 36 were classified as SRZ, where these locations are evident across the central, eastern and northern areas of South Africa (Figure 5.11). Weather stations along the western coast and adjacent areas were classified as WRZ, and PEW located along the southern coast was also

classified as WRZ (Figure 5.11). Additional weather stations along the southern coast, west of PEW, may as previously mentioned display WRZ conditions across this area or the YRZ known to occur along the southern coast may have been classified (Figure 5.11). Similarly, no YRZ is classified from the results of the cluster analysis process of the mean monthly rain days as well as the decadal cluster analyses outputs (Appendix C.2, C.3). Notably, there is variability in the classifications of locations particularly at the transition between the SRZ and WRZ defined using the mean monthly rainfall and rain day cluster groupings (Figure 5.11; Appendix C.3). SUT, OUD and WIL are classified as SRZ in Figure 5.11 and as WRZ on the basis of the mean monthly rain days (Appendix C.3). PNO is classified as WRZ using the mean monthly rainfall clustering and as SRZ using the mean monthly rain day clustering (Appendix C.3). Interestingly, clustering mean monthly rainfall per decade also reflects heightened variability in the classifications of locations at the transition between the SRZ and WRZ, thus highlighting that seasonality varies considerably at the SRZ and WRZ transition (Appendix C.2).

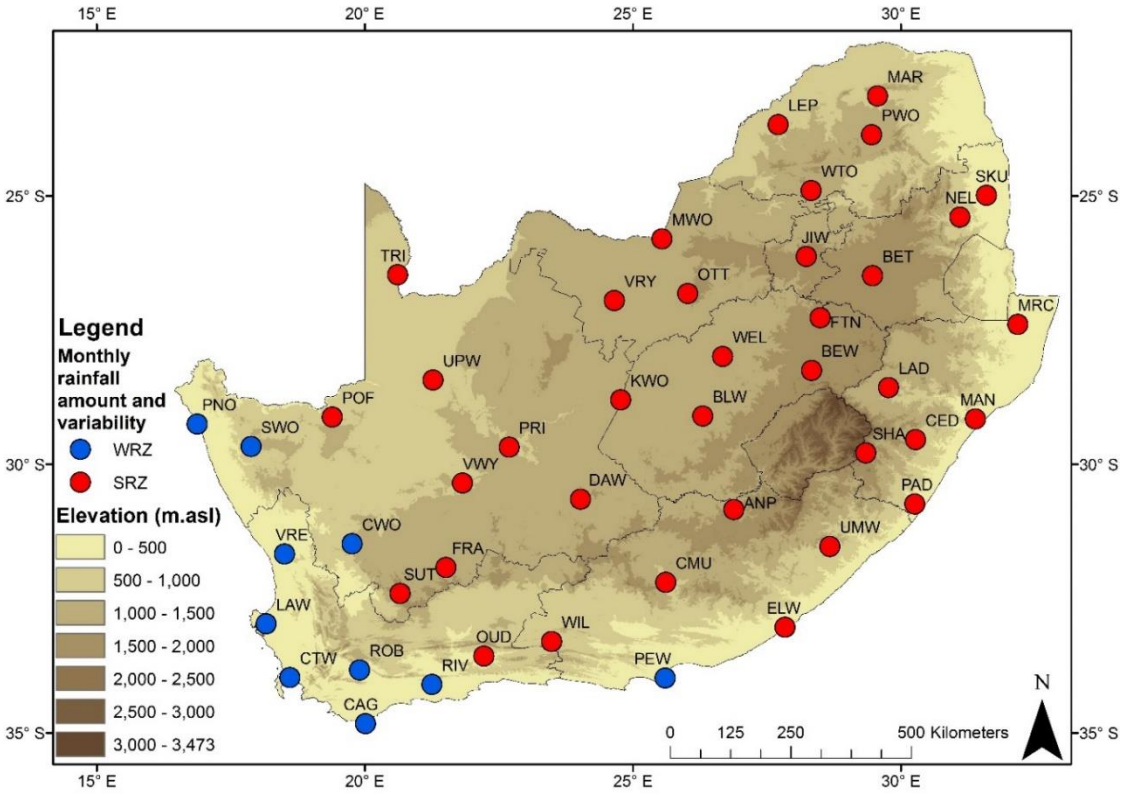


Figure 5.11: Spatial distribution of the SRZ and WRZ based on the wet and dry season timing of groups 1 to 5, represented under *Figure 5.10*.

5.4.2 SEASONALITY SCORES

The seasonality scores for the period of 1987-2016 were quantified across South Africa, both annually and for the entire period (Table 5.2; Appendix D). The total period seasonality scores range between -1.04 at Cape Town Wo, within the Western Cape, to 1.59 at Nelspruit within Mpumalanga (Table 5.2). The seasonality scores statistically segregate summer and winter rainfall, and since there are 34 weather stations characterised by positive seasonality scores this indicates that most of the country experiences a dominant summer rainfall regime (Table 5.2). Variation in the magnitude and sign of seasonality scores indicates that there are varying degrees of seasonality across the country, and this was used to group these weather stations as SRZ, WRZ and YRZ (Table 5.2). Seasonality scores tending towards zero, equal to and between -0.30 and 0.30, reflect YRZ conditions, and this is particularly highlighted by the scores quantified for Oudtshoorn (-0.05) and Riversdale (-0.08) located along the southern coast (Table 5.2). At these two weather stations, rainfall is relatively evenly distributed throughout the year with slightly more rainfall during the winter months. Particularly high negative seasonality scores were quantified in the southwestern Cape for Cape Agulhas (-0.75) and Cape Town Wo (-1.04), and this indicates particularly strong winter seasonality with relatively high winter rainfall amounts at these locations (Table 5.2). The high positive seasonality scores quantified for Johannesburg INT Wo (1.24) and Nelspruit (1.59), located within the northeastern parts of the country, reflect particularly strong summer rainfall conditions with relatively high summer rainfall amounts (Table 5.2). These particularly strong positive or negative seasonality scores indicate that rainfall is mostly confined to the summer or winter months of the year, respectively.

Table 5.2: Total period seasonality scores and rainfall zone classification for individual weather stations for the period 1987-2016. A *p value* below 0.05 is statistically significant and is indicated using an asterisk (*). Particularly strong correlations, between sqrt MMR and sqrt MMT, equal to and greater than 0.7 are indicated using a double asterisk. Rainfall zone classifications are highlighted, where red indicates SRZ, blue indicates WRZ and yellow indicates YRZ.

Location	Seasonality score	Statistical strength of relationship (r)	Statistical significance (p)
Aliwal-North Plaatkop	0.48	0.53	*<0.0001
Bethal	1.09	**0.70	*<0.0001
Bethlehem Wo	0.82	0.69	*<0.0001
Bloemfontein Wo	0.58	0.59	*<0.0001
Calvinia Wo	-0.21	0.30	*<0.0001
Cape Agulhas	-0.75	0.54	*<0.0001
Cape Town Wo	-1.04	**0.76	*<0.0001
Cedara	0.88	0.57	*<0.0001
Cradock-Mun	0.50	0.53	*<0.0001
De Aar Wo	0.32	0.39	*<0.0001
East London Wo	0.59	0.25	*<0.0001
Frankfort – TNK	0.77	0.68	*<0.0001
Fraserburg	0.15	0.27	*<0.0001
Johannesburg INT Wo	1.24	**0.70	*<0.0001
Kimberley Wo	0.56	0.57	*<0.0001
Ladysmith	0.99	0.64	*<0.0001
Langebaanweg AWS	-0.74	**0.71	*<0.0001
Lephalale	0.96	0.64	*<0.0001
Mafikeng Wo	0.93	0.65	*<0.0001
Makatini Research Centre	1.08	0.54	*<0.0001
Mandini	0.93	0.38	*<0.0001
Mara	1.03	0.62	*<0.0001
Nelspruit	1.59	0.66	*<0.0001
Ottosdal	0.82	0.62	*<0.0001
Oudtshoorn	-0.05	0.07	0.1600
Paddock	0.81	0.27	*<0.0001
Pofadder	0.13	0.20	*0.0001
Polokwane Wo	1.14	0.67	*<0.0001
Port Elizabeth Wo	-0.27	0.19	*0.0003
Port Nolloth	-0.37	0.29	*<0.0001
Prieska	0.31	0.40	*<0.0001
Riversdale	-0.08	0.08	0.1240
Robertson	-0.33	0.39	*<0.0001
Shaleburn	1.20	**0.78	*<0.0001
Skukuza	1.13	0.62	*<0.0001
Springbok Wo	-0.50	0.56	*<0.0001
Sutherland	-0.10	0.17	*0.0010
Twee Rivieren	0.49	0.61	*<0.0001
Umtata Wo	1.02	0.62	*<0.0001
Upington Wo	0.40	0.50	*<0.0001
Vanwyksvlei	0.22	0.33	*<0.0001
Vredendal	-0.55	0.60	*<0.0001
Vryburg	0.73	0.65	*<0.0001
Warmbad Towoomba	1.09	0.67	*<0.0001
Welkom	0.63	0.55	*<0.0001
Willowmore	0.23	0.29	*<0.0001

Seasonality scores greater than 0.30 were classified as SRZ, and these scores are evident for weather stations within the eastern and northern parts of the country (Table 5.2; Figure 5.12). The seasonality scores for weather stations classified as SRZ range between 0.31 at Prieska and 1.59 at Nelspruit (Table 5.2; Figure 5.12). Particularly strong SRZ seasonality scores were evident across the northeastern parts of the country, where the strongest seasonality scores were evident at Nelspruit (1.59, r = 0.66, p <0.0001), Johannesburg INT Wo (1.24, r = 0.70, p <0.0001) and Shaleburn (1.21, r = 0.78, p <0.0001; Table 5.2; Figure 5.12). At these weather stations, and especially for weather stations with a score greater than 0.80, the particularly high scores are driven by the numerous months with zero rainfall outside of the wet season and the high rainfall values during the wet season, evident from the clustering of points for considerably high MMT and high MMR values (Figure 5.12). These weather stations are also associated with a moderate to strong strength of relationship, which is above 0.50, between MMT and MMR highlighting that rainfall is considerably higher during the summer months (Table 5.2; Figure 5.12). SRZ weather stations with weaker seasonality scores are located mostly within the central and southern parts of the country, where the weakest SRZ seasonality scores were quantified for Prieska (0.31, r = 0.40, p <0.0001), De Aar Wo (0.32, r = 0.39, p <0.0001), Upington Wo (0.40, r = 0.50, p <0.0001), Aliwal-North Plaatkop (0.48, r = 0.53, p <0.0001) and Twee Rivieren (0.49, r = 0.61, p <0.0001; Table 5.2; Figure 5.12). At these weather stations, the low seasonality scores are driven by the relatively low variation along the trendline, relatively high MMR when MMT is high, the numerous months with zero rainfall and the relatively weak to moderate relationship strength between MMR and MMT (Figure 5.12). At these locations rainfall is higher during the summer months when compared to the winter months, however, summer rainfall is still relatively low compared to the locations with particularly strong SRZ seasonality scores above 0.80 (Figure 5.12).

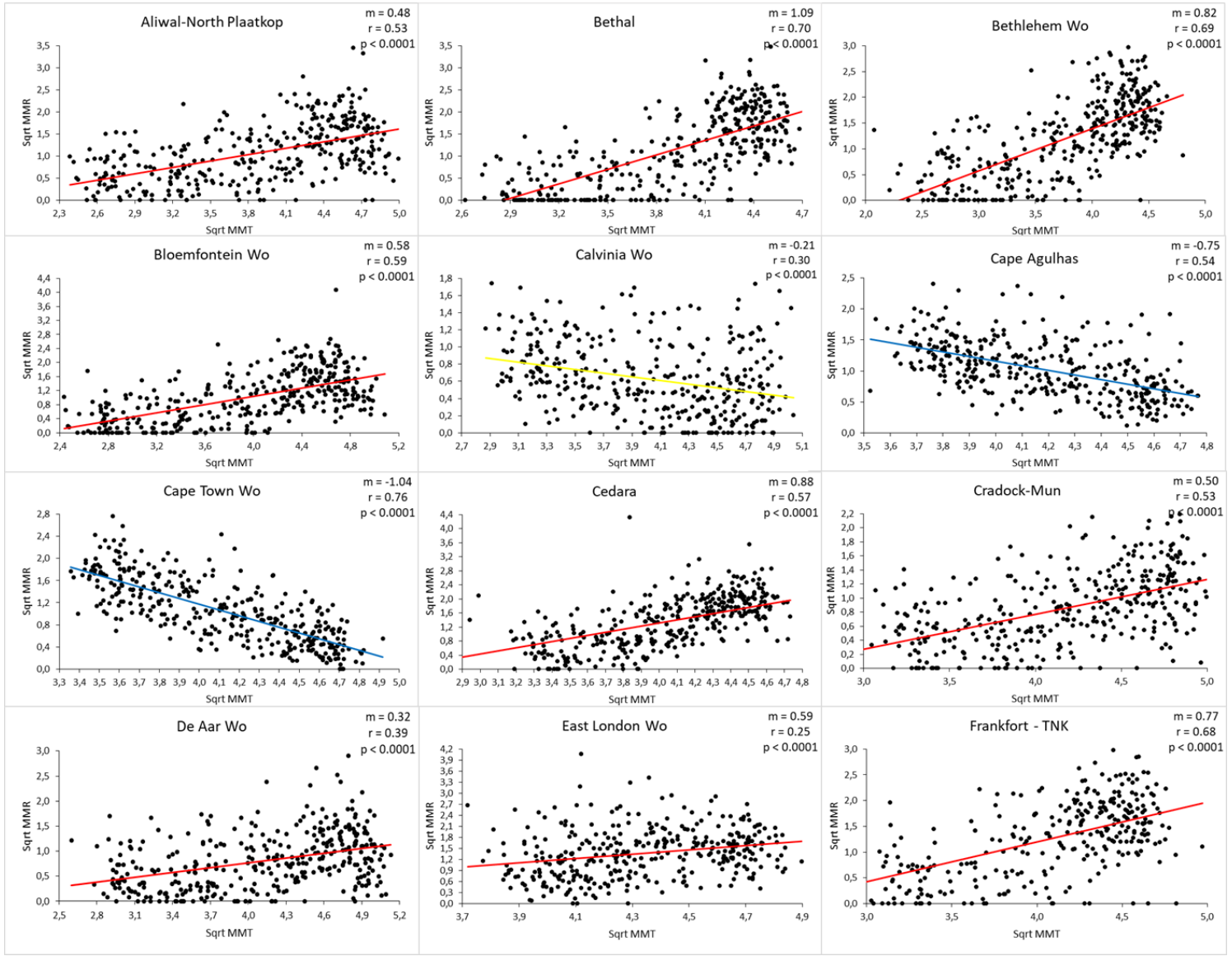


Figure 5.12: Relationship between sqrt MMT and sqrt MMR for individual weather stations across South Africa. Red, blue and yellow trendlines represent SRZ, WRZ and YRZ classifications respectively.

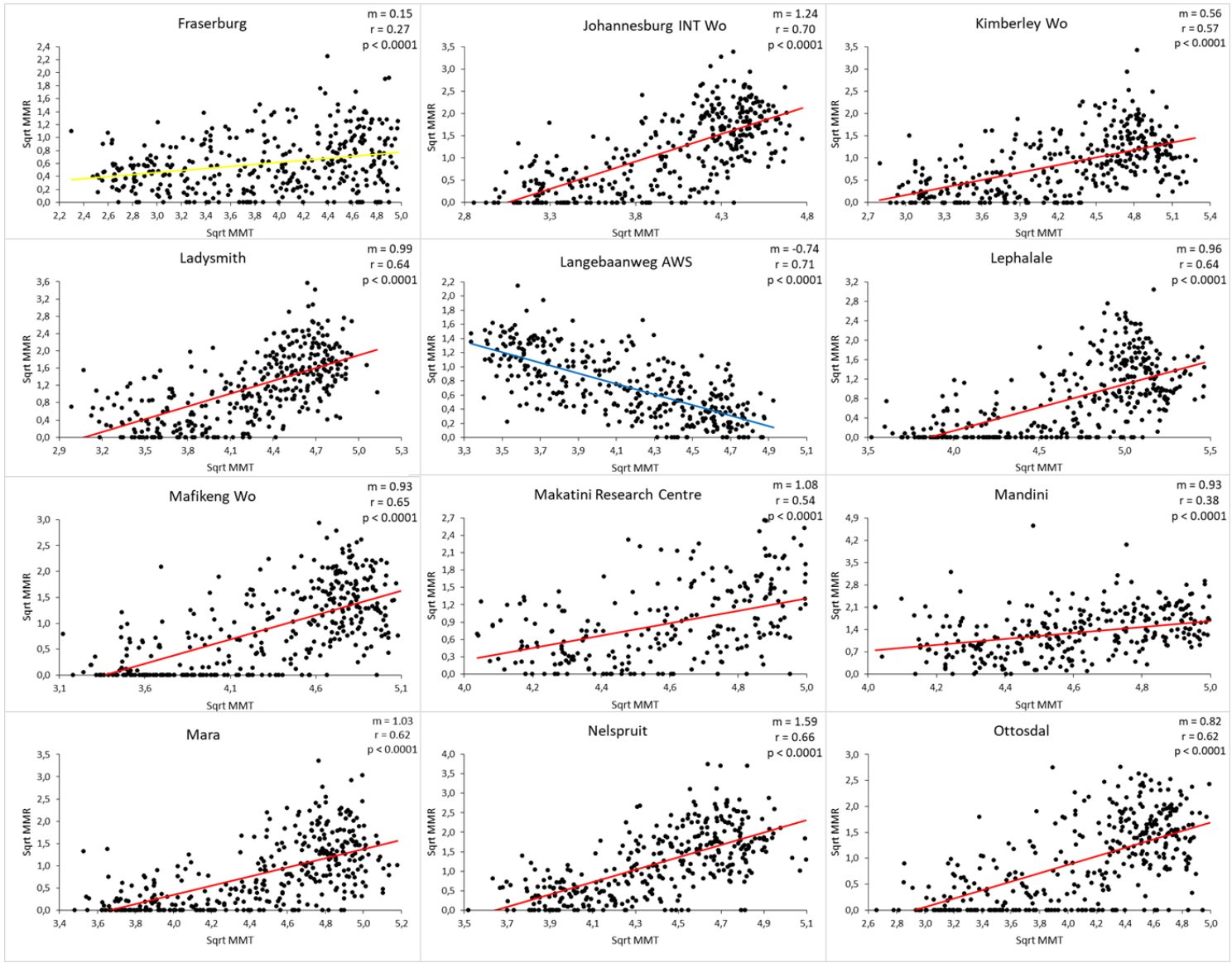


Figure 5.12 continued: Relationship between sqrt MMT and sqrt MMR for individual weather stations across South Africa. Red, blue and yellow trendlines represent SRZ, WRZ and YRZ classifications respectively.

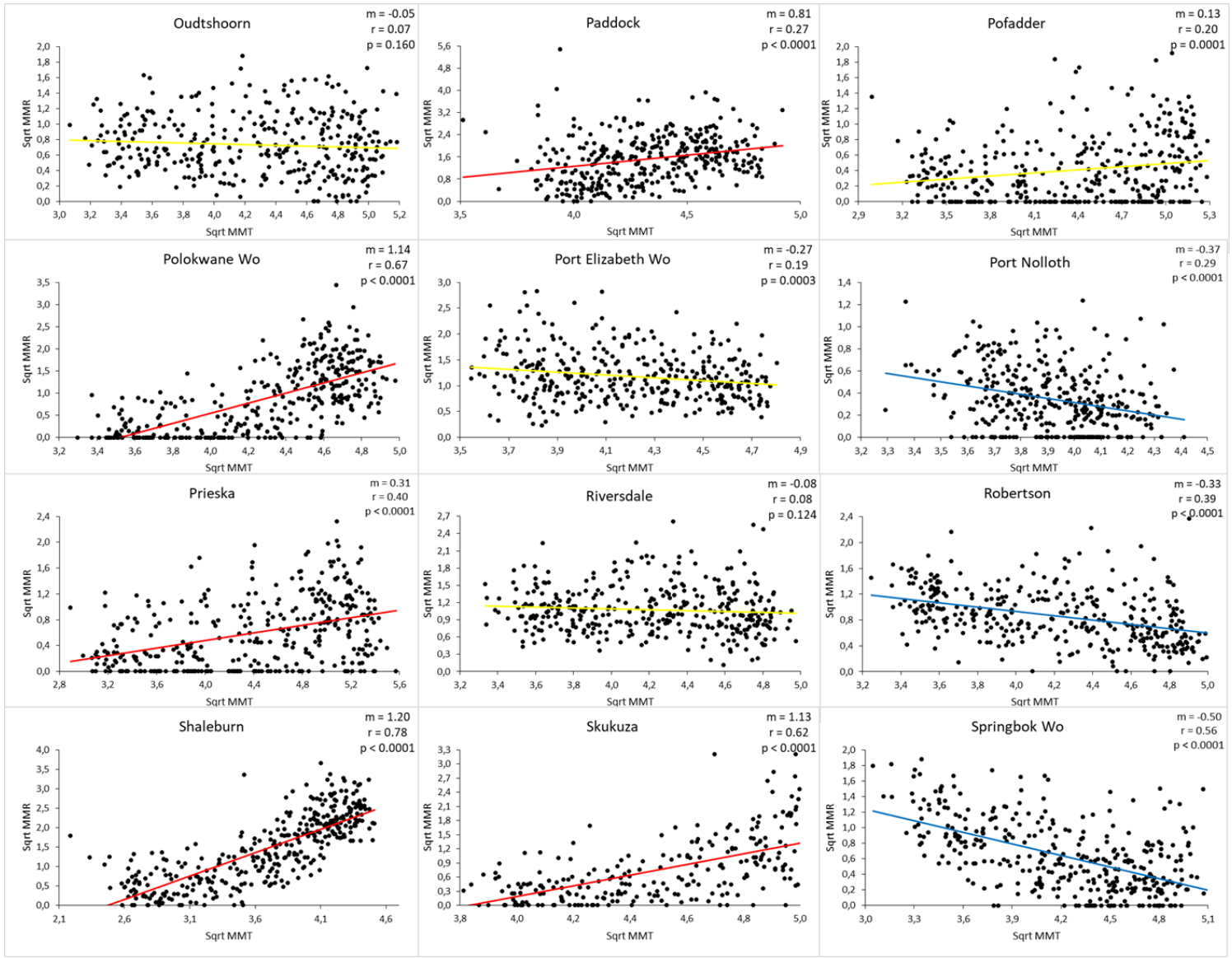


Figure 5.12 continued: Relationship between sqrt MMT and sqrt MMR for individual weather stations across South Africa. Red, blue and yellow trendlines represent SRZ, WRZ and YRZ classifications respectively.

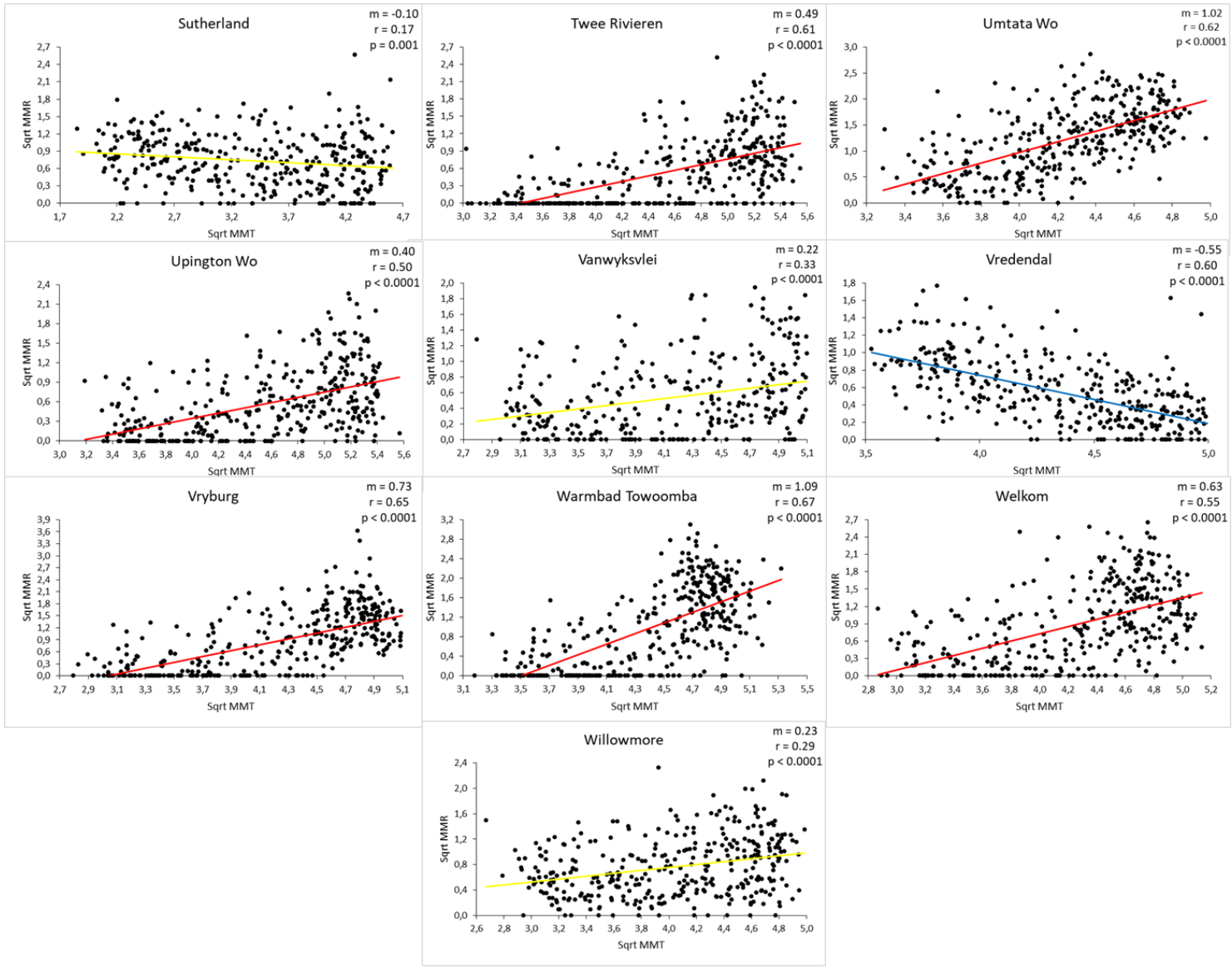


Figure 5.12 continued: Relationship between sqrt MMT and sqrt MMR for individual weather stations across South Africa. Red, blue and yellow trendlines represent SRZ, WRZ and YRZ classifications respectively.

Weather stations with seasonality scores below -0.30 were classified as WRZ and are located across the southwestern Cape and the western coast (Table 5.2; Figure 5.12). Particularly strong WRZ seasonality scores were evident at Cape Town Wo (-1.04, r = 0.76, p <0.0001), Cape Agulhas (-0.75, r = 0.54, p <0.0001) and Langebaanweg AWS (-0.74, r = 0.71, p <0.0001; Table 5.2; Figure 5.12). These large seasonality scores are driven by considerably high MMR when MMT is low, relatively low variation along the trendline and the moderate to strong inverse relationship between MMT and MMR (Figure 5.12). The strong seasonality scores at these locations highlights that rainfall is higher during the winter months compared to locations with lower WRZ scores (Figure 5.12). Port Nolloth (-0.37, r = 0.29, p <0.0001) and Robertson (-0.33, r = 0.39, p <0.0001) are characterised by weak WRZ seasonality scores (Table 5.2; Figure 5.12). This score is driven by the relatively high MMR when MMT is low, considerable variation along the trendline, and for Port Nolloth this is also due to the numerous months without rainfall (Figure 5.12).

Weather stations with seasonality scores ranging from 0.30 to -0.30 were classified as YRZ and are mostly located along the southern coast and interior north, up to the border between South Africa and Namibia (Table 5.2; Figure 5.12). Slightly positive scores depict YRZ conditions with relatively more summer rainfall and are in the eastern parts of the YRZ, while slightly negative scores depict YRZ with relatively more winter rainfall and are in the western parts of the YRZ (Figure 5.12; Table 5.2). At these weather stations the strength of relationship, below 0.30, between MMT and MMR is characterised as very weak (Table 5.2; Figure 5.12). The weak seasonality scores characterising these weather stations are driven by the considerable variation along the trendline and the relatively even spread of MMR for all MMT values (Figure 5.12). Oudtshoorn, Riversdale, Port Elizabeth Wo, located across the southern coast, display no or very few months with zero rainfall, whereas the remaining YRZ locations within the interior, including Calvinia Wo, Fraserburg, Vanwyksvlei, Pofadder, Sutherland and Willowmore, have numerous months with zero rainfall and when rainfall does occur it is very low resulting in relatively equal monthly rainfall totals throughout the year, hence the low scores (Figure 5.12). When considering the annual seasonality scores, the weather stations classified as YRZ have very high inter-annual variability compared to SRZ and WRZ locations (Figure 5.13). In particular, Oudtshoorn and Riversdale are characterised by extremely high inter-annual variability at 551.1% and 443.1% respectively. These high levels of

variability may explain why these are the only locations not characterised by a statistically significant relationship between MMT and MMR (Table 5.2).

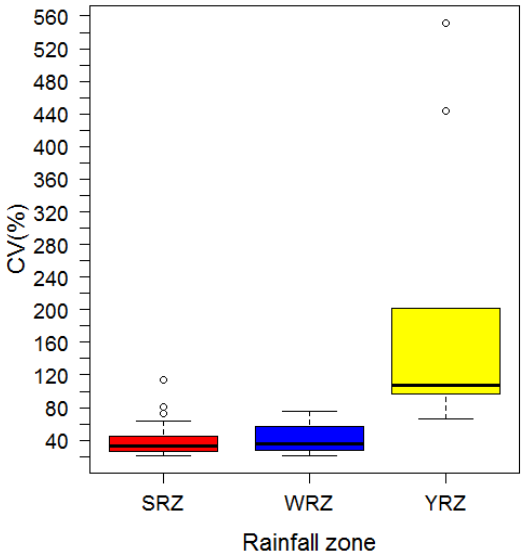


Figure 5.13: Boxplots of the CV for individual weather stations grouped as SRZ (red), WRZ (blue) and YRZ (yellow).

Inter-annual variability for the seasonality scores ranges between 21.4% at Cape Town Wo, located within the Western Cape, to 551.1% at Oudtshoorn located along the southern coast (Figure 5.13). Since all the weather stations were quantified with CV >20% this indicates that there was at least a moderate inter-annual variability in the annual seasonality scores (Figure 5.13). Out of 46 locations there are 34 with CV >30%, suggesting high inter-annual variability in the seasonality scores across most of the weather stations (Figure 5.13). CV across the SRZ locations ranges from 21.5% at Polokwane Wo, located in Limpopo, to 114.5% at East London Wo within the Eastern Cape (Figure 5.13). Out of 30 SRZ locations, 20 were quantified with an inter-annual variability of at least 30%. Cradock-Mun, De Aar Wo, East London Wo, Mandini, Paddock and Prieska were characterised with CV >50%, where all of these locations are within the Eastern and Northern Cape, and KwaZulu-Natal. These locations are located relatively close to the weather stations classified as YRZ, all of which have particularly high levels of variability (Figure 5.13). Inter-annual variability in the seasonality scores across the WRZ locations range from 21.4% at Cape Town Wo, within the southwestern Cape, to 76.0% at Port Nolloth along the northern parts of the western

coastline (Figure 5.13). Cape Agulhas, Port Nolloth, Robertson, Springbok Wo and Vredendal, locations adjacent to the YRZ within the Northern and Western Cape, were characterised by CV >30%. CV values across the YRZ were all particularly high and range from 66.1% at Fraserburg, located in the Northern Cape, to 551.1% at Oudtshoorn along the southern coast (Figure 5.13).

There are notable patterns evident in the spatial distribution of the total period seasonality scores (Figure 5.14). Variation in the strength and sign of the seasonality scores follows a potential east-west as well as a north-south gradient, where strong relationships are evident (Figure 5.14; Table 5.3). Along the east-west gradient seasonality scores increase from negative scores tending away from zero to scores tending towards zero and to positive scores tending away from zero as longitude increases ($r = 0.89$, $p < 0.0001$; Figure 5.14; Table 5.3). Along the north-south gradient seasonality scores decrease from positive scores tending away from zero towards scores tending towards zero and to negative scores tending away from zero as latitude increases ($r = -0.74$, $p < 0.0001$; Figure 5.14; Table 5.3). The seasonality scores, as previously mentioned, range between -1.04 and 1.59 (Table 5.1; Figure 5.14). Across the southwestern Cape there are particularly strong WRZ conditions evident from the large negative scores, and moving north and east these negative scores tend towards zero (Figure 5.14). Across the western interior, the YRZ is represented by the -0.30 to 0 and 0 to 0.30 classes in the western and eastern parts of the YRZ respectively (Figure 5.14). When considering the -0.30 to 0 class, especially along the southern coast, there are notable issues (Figure 5.14). Additional weather stations along the coast to the south of WIL may display a continuation of the -0.30 to 0 class (Figure 5.14). Additionally, when considering the spatial distribution of the seasonality scores, it is also important to note that inter-annual variability in the seasonality scores are spatially associated with latitude ($r = 0.47$, $p = 0.001$; Table 5.3), where locations further south typically have higher inter-annual variability in the seasonality scores. Even though this relationship is statistically significant, it is considered as relatively weak given the *r value* ($r = -0.29$; $p = 0.048$; Table 5.3). Although weak, this relationship indicates that inter-annual variability increases when seasonality scores tend towards zero, and this again highlights that at YRZ locations there is high inter-annual variability in the annual seasonality scores (Figure 5.13). This is also evident with a moderate to strong strength of relationship when considering the

positive (r = -0.64, p <0.0001) and negative scores (r = 0.72, p = 0.0009) as separate winter and summer rainfall regimes (Table 5.3).

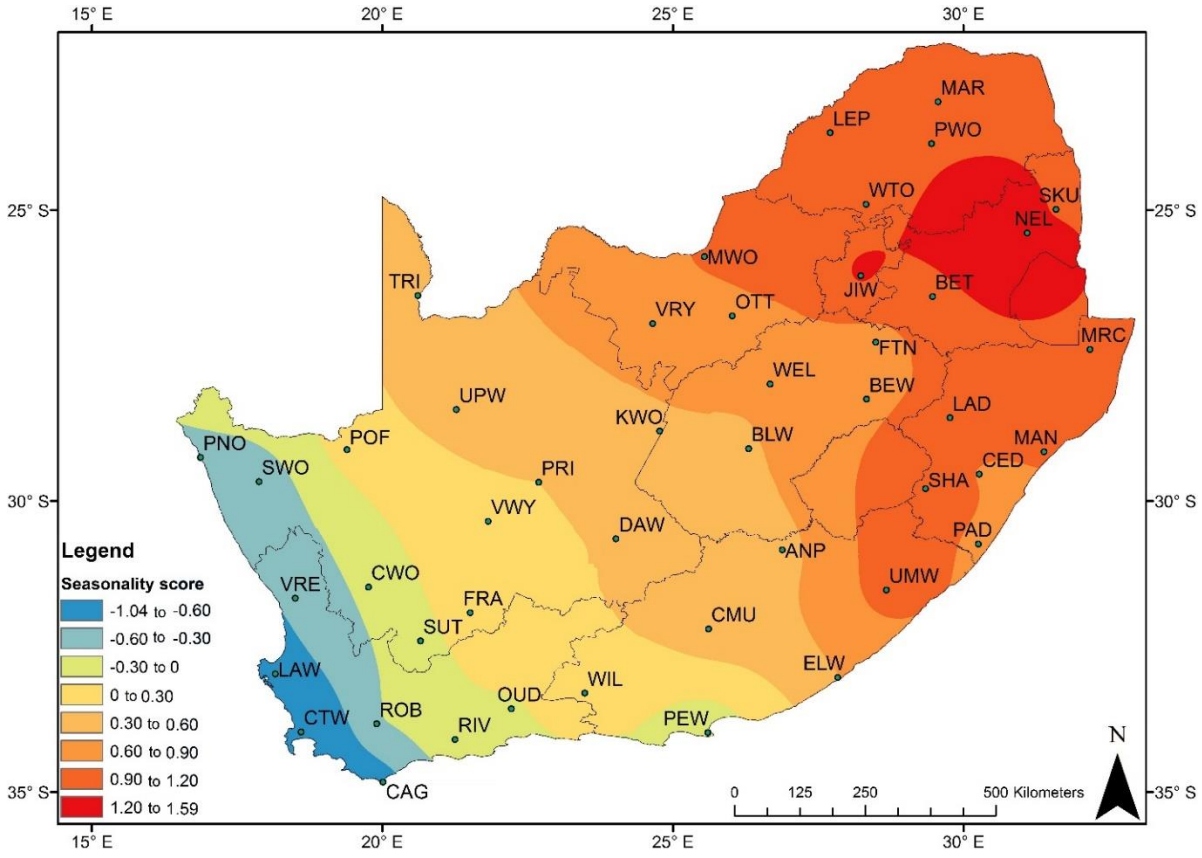


Figure 5.14: Ordinary kriging interpolation of the total period seasonality scores for the period 1987-2016.

Table 5.3: Resulting *r* and *p values* from correlation analyses between total period seasonality scores, latitude, longitude, elevation, strength of relationship and CV. Statistically significant *p values* are denoted using an asterisk (*). Correlations which were not tested are denoted using a hyphen (-).

Variables	Latitude (°)	Longitude (°)	Elevation (m.asl)	Strength of relationship (r)	CV (%)
All seasonality scores	-0.74 (*< 0.0001)	0.89 (*< 0.0001)	0.50 (*0.0004)	0.40 (*0.006)	-0.29 (*0.048)
Positive seasonality scores	-0.60 (*0.0002)	0.83 (*<0.0001)	-0.017 (0.922)	0.72 (*<0.0001)	-0.64 (*<0.0001)
Negative seasonality scores	-0.10 (0.749)	0.49 (0.107)	0.45 (0.144)	-0.94 (*<0.0001)	0.72 (*0.0009)
CV (%)	0.47 (*0.001)	-0.23 (0.117)	-0.28 (0.059)	-0.74 (*< 0.0001)	-
Strength of relationship (r)	-0.56 (*<0.0001)	0.36 (*0.015)	0.34 (*0.021)	-	-

The spatial distribution of the location specific classifications for each weather station highlights, as previously mentioned, that the majority of the country receives summer rainfall (Figure 5.15). Along the southern coast and north towards the border between South Africa and Namibia, weather stations were classified as YRZ (Figure 5.15). Weather stations along the southwestern Cape and western coast were classified as WRZ (Figure 5.15). Considering the topography across the country, there is a moderate association between elevation and the seasonality scores ($r = 0.50$, $p = 0.0004$; Table 5.3; Figure 5.15). Since this relationship is characterised by a moderate *r value* of 0.50, it is suggested that topography does not necessarily govern the spatial patterns of the seasonality scores as latitude and longitude does (Table 5.3; Deng *et al.*, 2019; Zhang *et al.*, 2019). Hence, this is also highlighted given that this relationship is not statistically significant when considering the positive and negative seasonality scores separately, given that they represent different rainfall regimes (Table 5.3). This relationship with elevation may instead indicate that topography provides orographic boundaries for the rainfall zones, as topographic barriers play an important role in moisture dispersal across South Africa (Singleton & Reason, 2007; Lennard, 2019). This is highlighted particularly for the WRZ which is constrained by the Cape Fold Mountains in the Western Cape as well as the Great Escarpment in the Northern Cape directly adjacent to SWO (Figure 5.15). Notably, within the YRZ the Cape Fold Mountains also act as a topographic barrier. For instance, there are very few months with no rainfall at OUD, RIV and PEW potentially due to orographic rainfall as these locations are south of the Cape Fold Mountains (Singleton & Reason, 2007), while the YRZ locations to the north of the mountains have numerous months with zero rainfall (Figure 5.12).

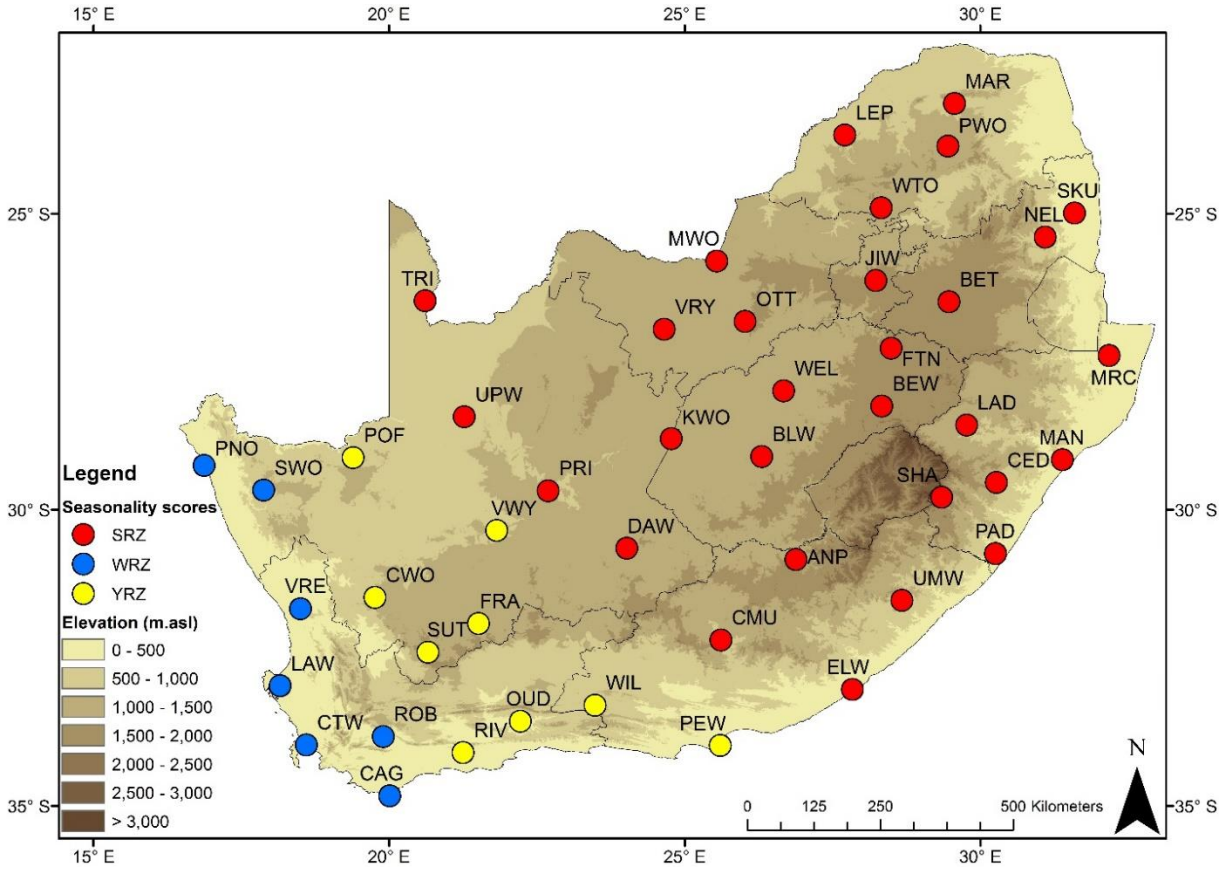


Figure 5.15: Spatial distribution of the SRZ, WRZ and YRZ using the total period seasonality scores.

The resulting Pearson correlation coefficient, *r values*, which characterise the relationship between MMR and MMT display spatial patterns across South Africa (Figure 5.16). When considering the correlation between latitude and the strength of the relationship between MMT and MMR, there is a moderate association which is statistically significant indicating that there is a general decrease in relationship strength as latitude increases ($r = -0.56$, $p < 0.0001$; Figure 5.16; Table 5.3). A statistically significant, yet weak relationship is also evident between longitude and the strength of this relationship ($r = 0.36$, $p = 0.015$; Table 5.3), where an increase in longitude is somewhat associated with an increase in the strength of relationship (Figure 5.16). A relationship is also evident when considering the correlation individually between the strength of relationship and the positive ($r = 0.72$, $p < 0.0001$) and negative ($r = -0.94$, $p < 0.0001$) scores (Table 5.3). Hence, these relationships suggest that high SRZ and WRZ seasonality scores are associated with a higher relationship strength between MMR and MMT. The strongest relationship strengths are evident

within the southwestern Cape at LAW and CTW, and within the northeastern parts of the country at BET, JIW and SHA (Figure 5.16). For weather stations classified as YRZ, located along the southern coast and north towards the South Africa and Namibia border, weak and very weak relationships are evident between MMT and MMR (Figure 5.16). It should also be noted here that there was a statistically significant relationship between elevation and the strength of relationship ($r = 0.34$, $p = 0.021$; Table 5.3), however, this relationship only highlights the role topography plays in moisture dispersal and topography does not necessarily govern the spatial distribution of the strength of relationship (Deng *et al.*, 2019; Zhang *et al.*, 2019). As with the spatial distribution of the seasonality scores, it is important to note that a general decrease in the strength of the relationship is associated with an increase in the inter-annual variability of the seasonality scores ($r = -0.74$, $p < 0.0001$; Table 5.3).

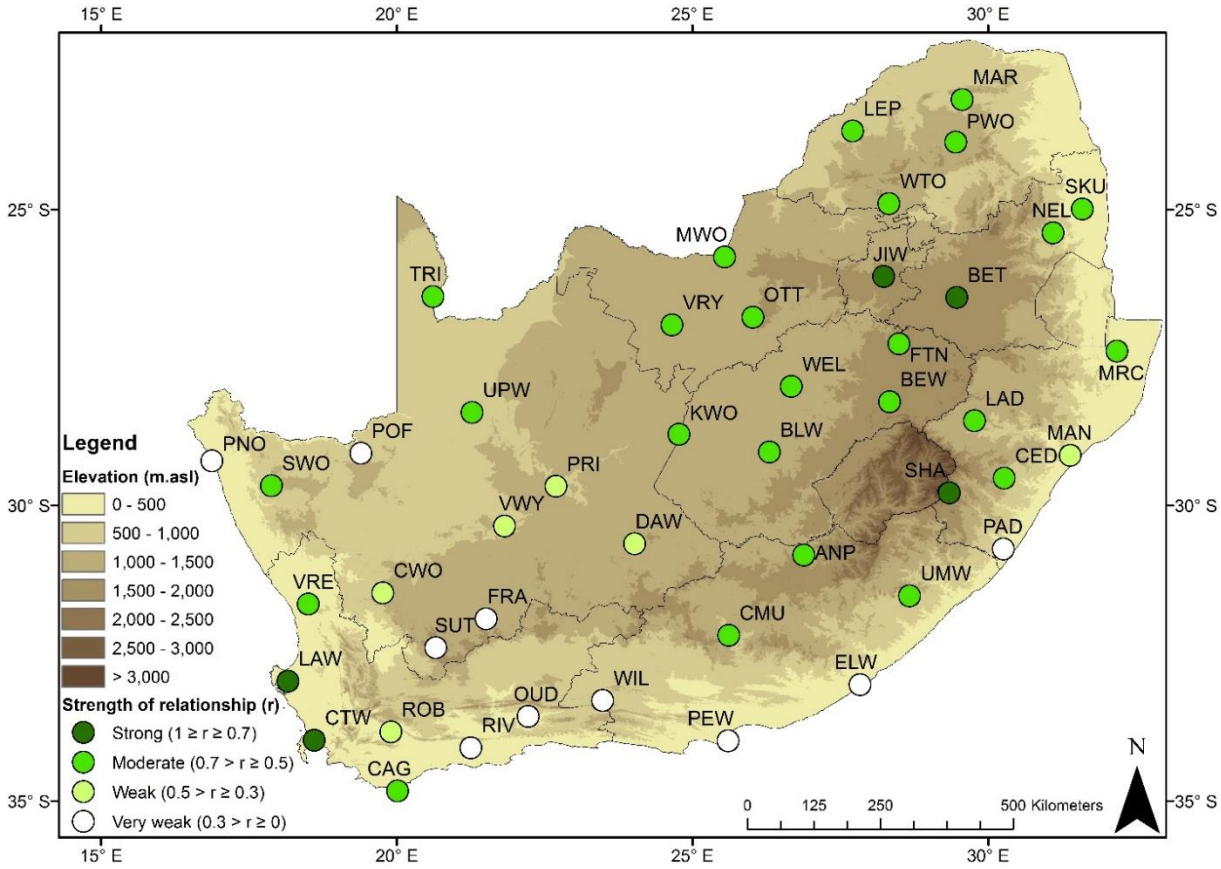


Figure 5.16: Strength of relationship between sqrt transformed MMR and MMT for individual weather stations for the period 1987-2016.

5.4.3 ONSET AND CESSATION DATES OF THE WET SEASON

Onset and cessation dates were quantified for the period of 1987-2016 for each weather station (Table 5.4; Appendix E). No onset and cessation dates were quantified for Port Nolloth, located along the northern part of the western coast, as daily rainfall totals were considerably lower than the onset and cessation date criteria described under *Section 4.4.3* (Table 5.4; Appendix E). There are 34 locations classified as SRZ, where SRZ conditions are most distinct for weather stations with onset dates from September to early December and cessation dates from the end of March through to the beginning of May (Table 5.4). Along the eastern coast at Paddock and East London Wo the SRZ wet season commences particularly early, during August, whereas in the Northern Cape at Twee Rivieren and Pofadder onset of the wet season starts as late as January (Table 5.4). At Pofadder and Twee Rivieren the wet season does occur with the summer solstice during the wet season, but since the wet season spans the summer months and cessation is at a similar time to other SRZ weather stations these two locations were classified as SRZ for the purpose of this study (Table 5.4). Weather stations with onset dates between March and June, and cessation dates during August to October reflect WRZ conditions, and this was evident for weather stations such as Cape Town Wo and Cape Agulhas (Table 5.4). Along the southern coast at Oudtshoorn, Port Elizabeth Wo and Riversdale onset of the wet season occurs during late February to early March and cessation occurs during late November to early December, clearly representing year-round rainfall conditions (Table 5.4).

Table 5.4: Mean onset and cessation dates, length of the wet season and number of rain days for individual weather stations for the period 1987-2016. Rainfall zone classifications are highlighted, where red, blue and yellow represent SRZ, WRZ and YRZ respectively. Weather stations which are not highlighted were not classified and captured as ND.

Location	Mean Onset date	Julian day (JD)	Mean Cessation date	Julian day (JD)	Number of years of onset and cessation dates	Mean length of the wet season (days)	Mean number of rain days
Aliwal-North Plaatkop	28-Oct	301	4-May	124	29	189	63
Bethal	8-Oct	281	22-Apr	112	28	197	70
Bethlehem Wo	16-Oct	289	27-Apr	117	29	194	78
Bloemfontein Wo	1-Nov	305	21-Apr	111	29	172	57
Calvinia Wo	8-Apr	98	7-Sep	250	15	153	31
Cape Agulhas	23-Apr	113	10-Oct	283	30	171	61
Cape Town Wo	20-Apr	110	26-Sep	269	30	160	59
Cedara	17-Sep	260	21-Apr	111	29	217	123
Cradock-Mun	16-Nov	320	7-Apr	97	29	143	37
De Aar Wo	5-Nov	309	4-May	124	28	181	39
East London Wo	28-Aug	240	7-May	127	29	253	97
Frankfort-TNK	25-Oct	298	24-Apr	114	29	182	69
Fraserburg	13-Dec	347	20-Apr	110	21	129	23
Johannesburg INT Wo	17-Oct	290	23-Apr	113	29	189	76
Kimberley Wo	12-Nov	316	22-Apr	112	29	163	47
Ladysmith	29-Sep	272	15-Apr	105	29	199	74
Langebaanweg AWS	2-Jun	153	11-Sep	254	23	102	34
Lephalale	19-Nov	323	28-Mar	87	29	130	37
Mafikeng Wo	7-Nov	311	20-Apr	110	29	165	52
Makatini Research Centre	16-Oct	289	28-Apr	118	29	195	56
Mandini	7-Sep	250	29-Apr	119	29	235	96
Mara	10-Nov	314	26-Mar	85	29	137	37
Nelspruit	20-Oct	293	22-Apr	112	29	184	74
Ottosdal	28-Oct	301	15-Apr	105	29	170	55
Oudtshoorn	3-Mar	62	23-Nov	327	14	266	49
Paddock	25-Aug	237	29-Apr	119	29	248	114
Pofadder	29-Jan	394	7-Apr	97	8	69	10
Polokwane Wo	8-Nov	312	3-Apr	93	29	147	43
Port Elizabeth Wo	24-Feb	55	9-Dec	343	27	289	83
Port Nolloth	ND	ND	ND	ND	0	ND	ND
Prieska	16-Dec	350	27-Apr	117	21	133	25
Riversdale	4-Mar	63	25-Nov	329	24	267	79
Robertson	7-May	127	5-Oct	278	25	152	37
Shaleburn	21-Sep	264	20-Apr	110	29	212	128
Skukuza	18-Oct	291	15-Apr	105	29	180	56
Springbok Wo	3-May	123	16-Sep	259	22	137	25
Sutherland	18-Mar	77	16-Sep	259	18	183	39
Twee Rivieren	1-Jan	366	7-Apr	97	22	97	19
Umtata Wo	22-Sep	265	30-Apr	120	29	221	88
Upington Wo	19-Dec	353	9-Apr	99	19	112	23
Vanwyksvlei	22-Dec	356	25-Apr	115	19	125	23
Vredendal	4-Jun	155	28-Aug	240	6	86	25
Vryburg	17-Nov	321	21-Apr	111	29	156	43
Warmbad Towoomba	22-Oct	295	18-Apr	108	29	179	55
Welkom	3-Nov	307	6-Apr	96	28	155	48
Willowmore	5-Dec	339	6-May	126	26	153	28

Mean onset dates for the SRZ range between 25 August (JD: 237) at Paddock to 29 January (JD: 394 i.e. 394-365=29) at Pofadder (Table 5.4; Figure 5.17). Compared to WRZ onset dates, which range between 18 March (JD: 77) at Sutherland and 4 June (JD: 155) at Vredendal, the SRZ onset dates have a larger temporal spread (Figure 5.17). For the mean cessation dates the spread in dates across the SRZ and WRZ are relatively similar, spanning a period of approximately three months (Figure 5.17). The SRZ dates range between 26 March (JD: 85) at Mara and 7 May (JD: 127) at East London Wo (Table 5.4; Figure 5.17). WRZ dates range between 28 August (JD: 240) at Vredendal and 10 October (JD: 283) at Cape Agulhas (Table 5.4; Figure 5.17). Considering the large temporal range in the SRZ onset dates and the small range in the cessation dates, a large range of 69 days at Pofadder to 253 days East London Wo for the mean length of the wet season is expected (Figure 5.17; Table 5.4). The small range in the length of the wet season across the WRZ stations is also expected given the relatively low temporal range in both the onset and cessation dates (Figure 5.17). On the other hand, the YRZ onset dates range from 24 February (JD: 55) at Port Elizabeth Wo and 4 March (JD: 63) at Riversdale (Table 5.4; Figure 5.17). The cessation dates range between 23 November (JD: 327) at Oudtshoorn and 9 December (JD: 343) at Port Elizabeth Wo (Table 5.4; Figure 5.17). Considering that the length of the mean wet season for the YRZ locations was an average of 274 days, the number of rain days across these locations is considerably low, with an average of 71 rain days, compared to the number of rain days across the SRZ and WRZ which was highest at Shaleburn (128 days) and Cape Agulhas (61 days; Table 5.4; Figure 5.17).

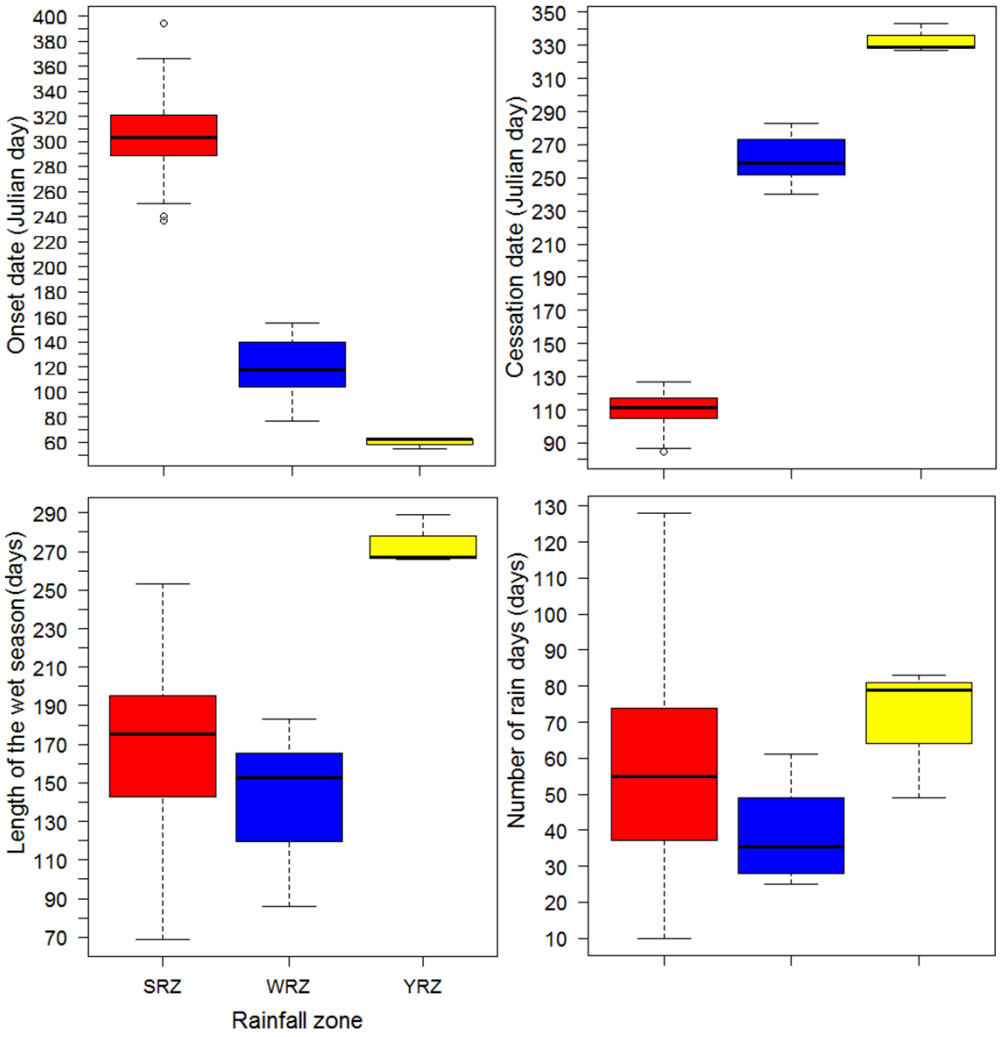


Figure 5.17: Boxplots displaying the distribution of mean onset and cessation dates, length of the wet season and number of rain days for individual weather stations grouped as SRZ (red), WRZ (blue) and YRZ (yellow).

Starting with the SRZ, the patterns across the locations within each rainfall zone were explored (Figure 5.18). As previously mentioned, the mean onset dates amongst the SRZ have a relatively long temporal range from 25 August at PAD, within KwaZulu-Natal, to 29 January at POF within the Northern Cape (Table 5.4). The mean cessation dates range between 29 March at MAR, within Limpopo, and 7 May at ELW within the Eastern Cape (Table 5.4). The range in the mean length of the wet season is from 69 days at POF to 253 days at ELW (Table 5.4). Across these locations earlier onset dates are typically accompanied by a relatively long wet season length, and this is evident given the small range in the mean cessation dates across the SRZ (Figure 5.18). This pattern is particularly highlighted by early onset and a relatively long wet season at CED, ELW, MAN, PAD,

SHA and UMW, all located within the eastern parts of KwaZulu-Natal and the Eastern Cape (Figure 5.18). These weather stations experience a dry season of approximately four to five months which is shorter than the wet season (Figure 5.18). POF and TRI, located in the Northern Cape, have considerably late onset dates and as a result the length of the wet season is also particularly short, much shorter than the dry season which is approximately eight months in length (Figure 5.18). There were 20 SRZ locations, within the northeastern and central interior of the country, with mean onset dates quantified during October and November, and at these locations the wet and dry seasons are of a relatively similar length (Table 5.4; Figure 5.18).

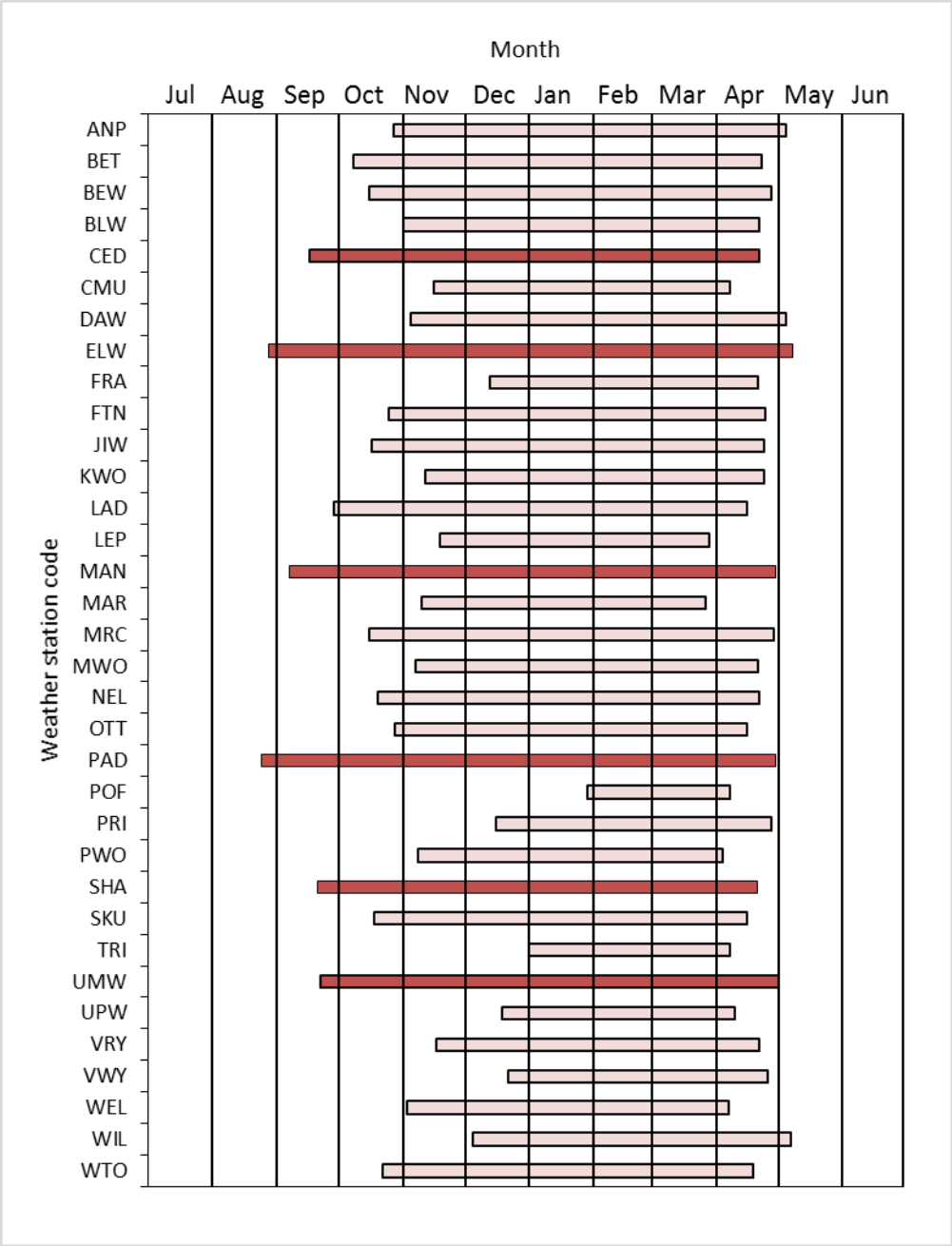


Figure 5.18: Calendar plot of the mean onset and cessation dates, and length of the wet season for weather stations classified as SRZ. This plot is colour coded according to late and long SRZ. Dark red represents long SRZ and light red represents late SRZ.

Amongst the weather stations classified as SRZ, there are also patterns in mean annual rainfall, the mean length of the wet season and the mean number of rain days (Figure 5.19). As previously mentioned, the mean wet season length across the SRZ locations ranges from 69 at POF, within the Northern Cape, to 253 days at ELW within the Eastern Cape (Figure 5.19; Table 5.4). Again, the mean number of rain days across these locations ranges between 10 days at POF and 128 days at SHA within KwaZulu-Natal (Table 5.4), and the mean annual rainfall range is from 121.7mm at POF and 1099.6 at PAD, within KwaZulu-Natal (Table 5.1). Apparent from Figure 5.19 is that locations with higher annual rainfall typically experience a relatively longer length of the wet season and a higher number of rain days. Additionally, locations with lower annual rainfall typically experience a relatively shorter wet season length and a lower number of rain days (Figure 5.19). This pattern is particularly evident at CED, ELW, MAN, PAD, SHA and UMW which are all located within the eastern parts of KwaZulu-Natal and Eastern Cape (Figure 5.19). Similarly, locations within the Northern Cape and North West including FRA, PRI, POF, TRI, UPW and VWY with lower annual rainfall typically experience a relatively shorter length of the wet season with fewer rain days (Figure 5.19).

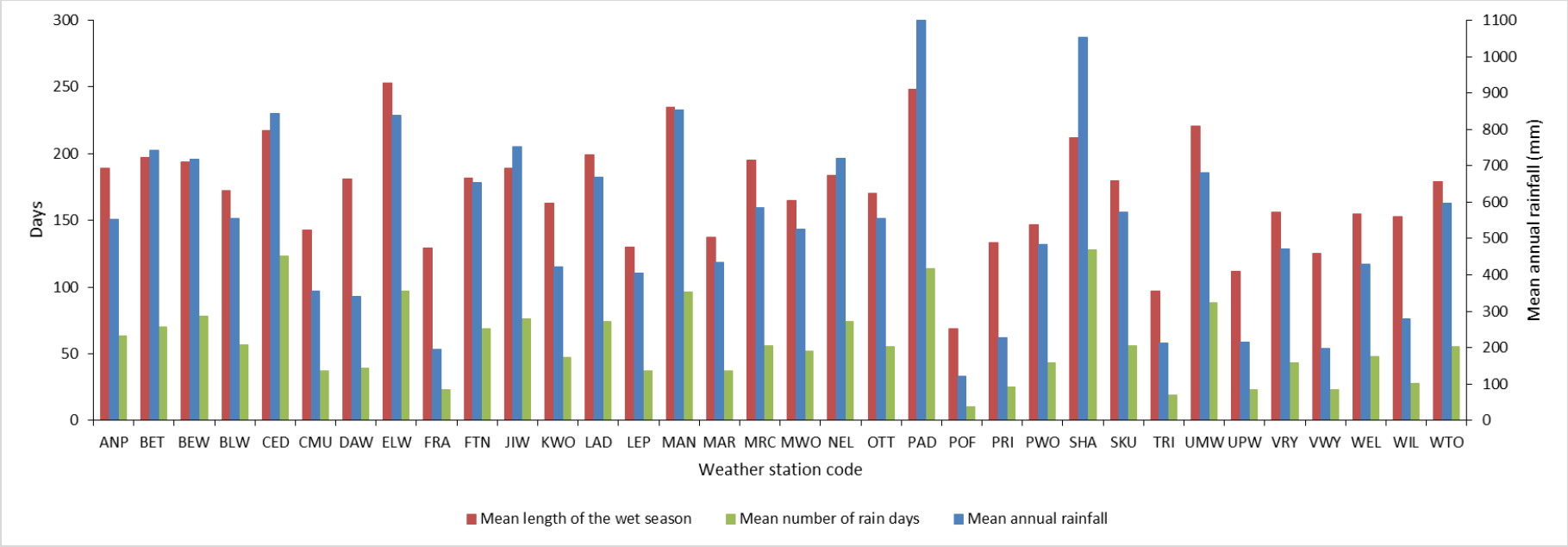


Figure 5.19: Bar graph of mean annual rainfall, length of the wet season and number of rain days for weather stations classified as SRZ.

Unlike the SRZ weather stations, there are no distinct temporal patterns amongst the WRZ weather stations which are located within the southwestern Cape, and along the western coast and adjacent regions (Figure 5.20). Mean onset dates, as previously mentioned, range from 18 March at SUT to 4 June at VRE, and mean cessation dates range from 28 August at VRE to 10 October at CAG (Table 5.4; Figure 5.20). Again, the mean length of the wet season across the WRZ ranges between 86 to 183 days at VRE and SUT respectively (Table 5.4; Figure 5.20). SUT was classified as early WRZ and compared to CAG, CTW and ROB, all classified as late WRZ, the length of the wet seasons across these locations are similar (Figure 5.20). The mean length of the wet season across these locations is also a similar length to the dry season (Figure 5.20) CWO, LAW, SWO and VRE were all classified as mid WRZ (Figure 5.20). CWO has the earliest mean onset date, while VRE has the latest mean onset date (Figure 5.20). VRE also experiences the shortest wet season of these locations which is of a relatively similar length to LAW, and hence the dry season at these locations is considerably longer than the wet season (Figure 5.20). At CWO and SWO the dry season is of a relatively similar length to the wet season (Figure 5.20).

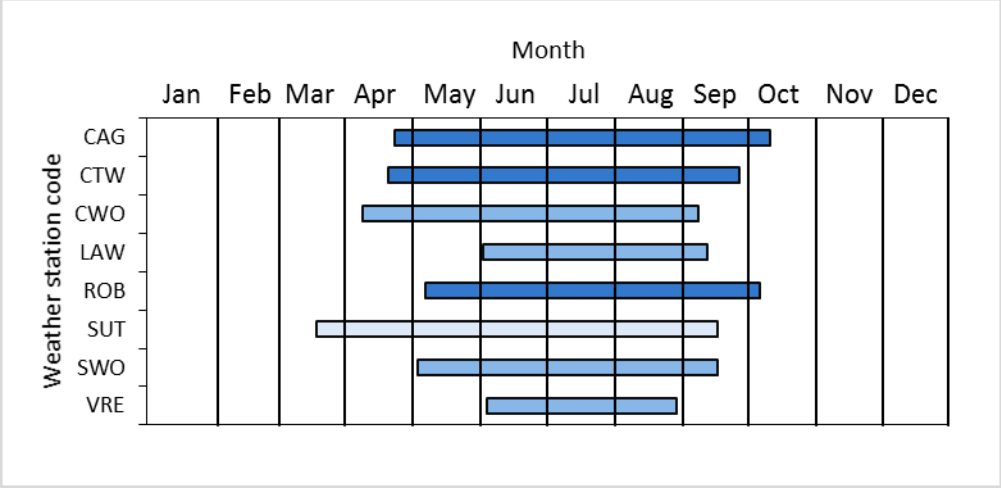


Figure 5.20: Calendar plot of the mean onset and cessation dates, and length of the wet season for weather stations classified as WRZ. This plot is colour coded according to early, mid and late WRZ, where dark blue represents late WRZ, light blue represents mid WRZ and very light blue represents early WRZ.

Across the locations classified as WRZ, the mean length of the wet season ranges from 86 days at VRE to 183 days at SUT with a range of 25 to 61 rain days again at VRE and SUT respectively (Table

5.4; Figure 5.21). Mean annual rainfall across the WRZ locations ranges from 157.4mm at VRE to 524.2mm at CTW (Table 5.1; Figure 5.21). Again, there is also no distinct pattern evident in mean annual rainfall, the length of the wet season and the number of rain days (Figure 5.21). CAG and CTW both have relatively high mean annual rainfall, a relatively long wet season and a relatively higher number of rain days (Figure 5.21). SUT has a similar wet season length to CAG and CTW, but SUT has relatively low annual rainfall and a low number of rain days (Figure 5.21). ROB, classified as late WRZ with CAG and CTW, has a similar wet season length but receives less rainfall during fewer days (Figure 5.21). Across the mid WRZ locations CWO has the longest wet season, which is a similar length to ROB, however, CWO receives less rainfall and has fewer rain days spread across the wet season (Figure 5.21). VRE has the shortest wet season with considerably low annual rainfall and a similar number of rain days as SWO (Figure 5.21).

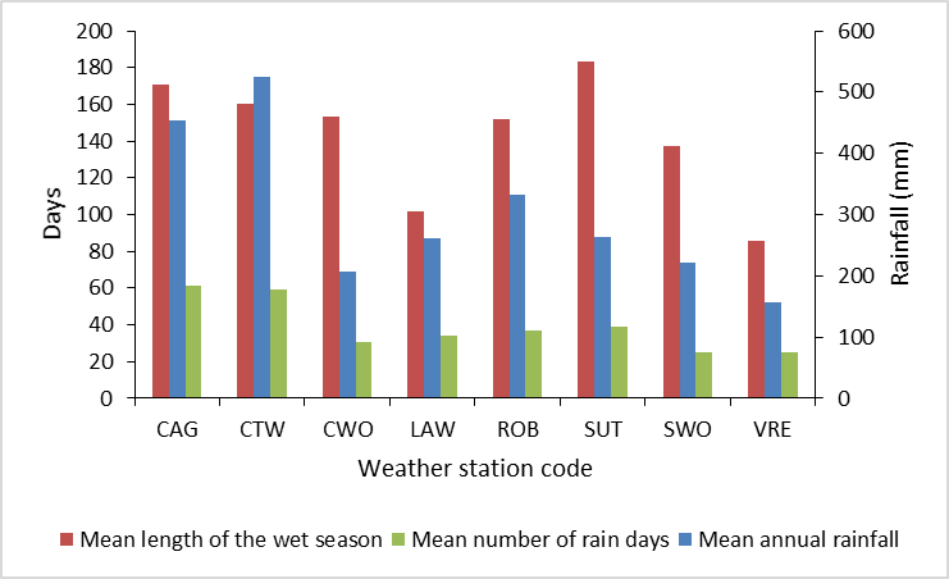


Figure 5.21: Bar graph of mean annual rainfall, length of the wet season and number of rain days for weather stations classified as WRZ.

The mean onset and cessation dates across the weather stations classified as YRZ, located along the southern coast, have an annual wet season to some extent (Figure 5.22). The earliest mean onset date is 24 February evident at PEW and the latest mean cessation date is 9 December also evident at PEW (Figure 5.22; Table 5.4). The longest wet season amongst these weather stations

is again observed at PEW and is 289 days (Figure 5.22). RIV and OUD have similar onset and cessation dates during early March and late December (Figure 5.22). The wet season length at these locations is also similar and is approximately 20 days shorter than at PEW (Figure 5.22).

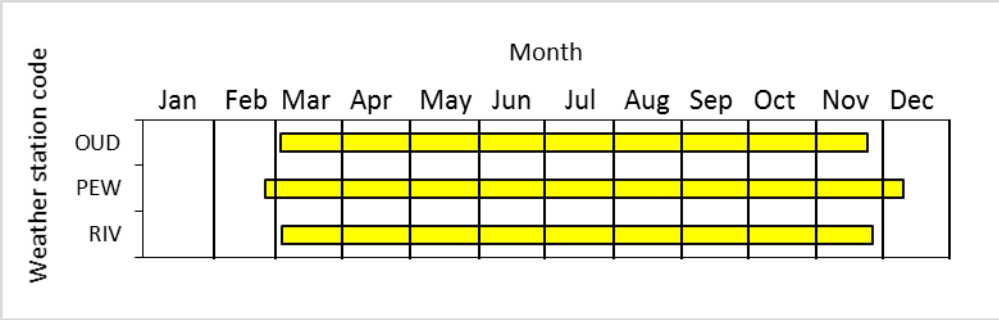


Figure 5.22: Calendar plot of the mean onset and cessation dates, and length of the wet season for weather stations classified as YRZ.

The weather stations classified as YRZ have a year-round wet season which equates to between 266 to 289 days at OUD and PEW respectively, with an average of between 49 (OUD) and 83 (PEW) rain days at each location (Figures 5.23; Table 5.4). OUD with the lowest mean annual rainfall experiences a relatively low number of rain days as compared to RIV (79 days) and PEW (Figure 5.23; Table 5.4). PEW and RIV experience a relatively similar wet season length and number of rain days, however, PEW (595.5mm) receives higher mean annual rainfall than RIV (481.2mm), indicating that relatively higher daily rainfall occurs at PEW during the wet season (Figure 5.4; Table 5.1).

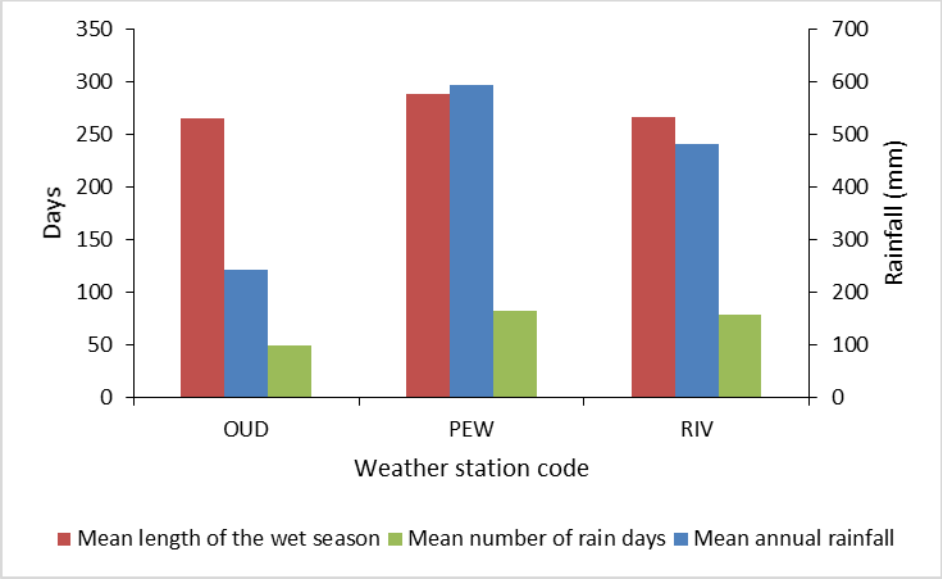


Figure 5.23: Bar graph of mean annual rainfall, length of the wet season and number of rain days for weather stations classified as YRZ.

There are also patterns evident in the inter-annual variability, quantified as CV, amongst the weather stations across the SRZ, WRZ and YRZ (Figure 5.24). YRZ locations have low inter-annual variability, below 20%, in the cessation dates, length of the wet season and number of rain days, however, there is considerable inter-annual variability in the YRZ onset dates, which ranges from 53.0 to 63.3% at Riversdale and Port Elizabeth Wo respectively (Figure 5.24). Amongst the SRZ there is relatively low to moderate variability, ranging from 7.3% at Mara to 16.5% at De Aar Wo, in the onset dates (Figure 5.24). There is a low to high level of inter-annual variability across the SRZ cessation dates, length of the wet season and number of rain days, ranging from 14.9 to 75.5% (Figure 5.24). Out of 34 SRZ locations there were 15 locations with high inter-annual variability above 30% for the cessation dates, where Welkom and Mara displayed a particularly high level of 50.1 and 50.8% respectively. There were 14 locations with high inter-annual variability, CV >30%, for the wet season length, where Upington Wo and Pofadder located in the Northern Cape had particularly high variability of 53.0 and 75.5% respectively. There were 18 locations with CV >30% in the number of rain days, and particularly high levels were evident at Fraserburg (46.3%), Twee Rivieren (46.1%), and Upington Wo (48.8%) again located in the Northern Cape. Conversely to the SRZ locations, the WRZ locations have a relatively higher level of inter-annual variability in the

onset dates than for the cessation dates (Figure 5.24). The highest levels of variability in the onset dates range from 42.5 to 49.0% and are evident at Cape Agulhas, Springbok Wo, Calvinia Wo and Sutherland, located within the central parts of the WRZ. For the cessation dates, only Sutherland (CV = 20.8%) had CV >20%. There was a moderate to high level of inter-annual variability in the length of wet season across the WRZ locations (Figure 5.24), and this was highest at Springbok Wo (39.9%) and Langebaanweg AWS (35.9%). All the WRZ locations had CV >20% for the number of rain days (Figure 5.24), and at Sutherland this level was particularly high at 44.2%.

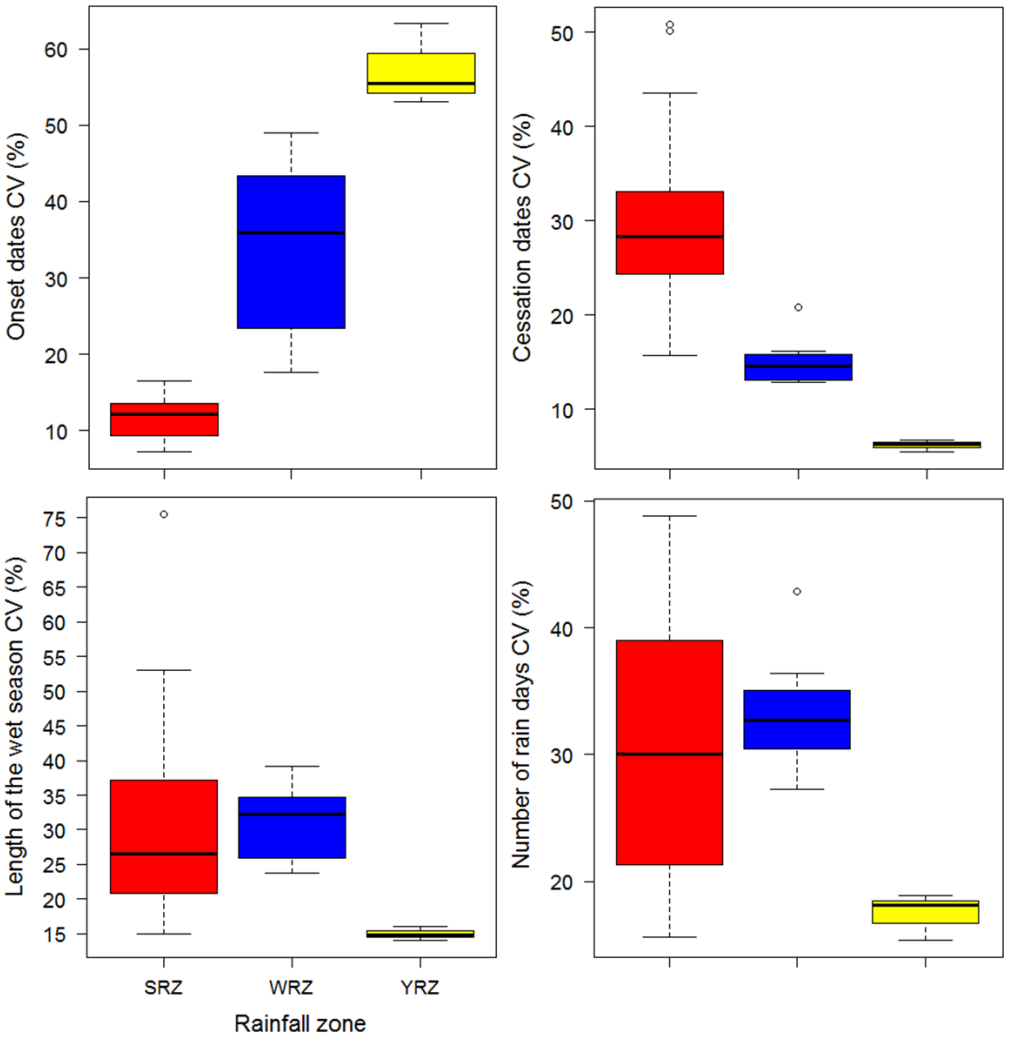


Figure 5.24: Boxplots displaying the distribution of CV for the mean onset and cessation dates, length of the wet season and number of rain days for individual weather stations grouped as SRZ (red), WRZ (blue) and YRZ (yellow).

To gain a full understanding of rainfall seasonality across South Africa through the onset and cessation dates approach, an understanding of the spatial patterns is necessary, and this may be understood through spatial interpolation. There are spatial patterns evident across the interpolated map on the mean onset dates (Figure 5.25). Within the SRZ, along a relatively east-west gradient, the onset dates range between 1 August and 31 January (Figure 5.25; Table 5.5). This relationship is somewhat evident when considering all onset dates, and although statistically significant this relationship is considered weak ($r = 0.40$; $p = 0.007$; Table 5.5). However, when considering only the SRZ onset dates it is apparent that there is a considerably strong relationship between onset and longitude ($r = -0.84$, $p = 0.0001$; Table 5.5), where this relationship highlights that the progression of SRZ onset dates is from east to west (Figure 5.25). The earliest SRZ onset dates are between 1 and 31 August and are observed along the eastern coast at PAD and ELW (Figure 5.25). Between these two weather stations, onset dates occur between 1 and 30 September, however, additional weather stations along this area of coastline may instead display a different pattern in the onset dates (Figure 5.25). The latest SRZ onset dates are evident across the northwestern parts of the country where POF and TRI are located (Figure 5.25). The YRZ weather stations OUD, PEW and RIV have onset dates between 1 and 28 February, however, the portion of the southern coastline between these weather stations does not display onset dates during this time (Figure 5.25), where additional weather stations may display a more continuous distribution of the 1 to 31 March class (Figure 5.25). Mean onset dates across the WRZ range between 1 April and 31 June (Figure 5.25), and the relationship between WRZ onset and longitude, being statistically significant, highlights the progression of winter rains ($r = -0.70$, $p = 0.033$; Table 5.5). North of the western coast, where PNO is located and a confirmed WRZ (Figure 2 in published paper under *Section 2.2 Chapter 2*), the onset dates range between 1 and 30 June (Figure 5.25). Had PNO been classified, this area may have had a similar or earlier onset date (Figure 5.25). Between the SRZ and WRZ onset dates, the range in onset dates is between 1 July and 31 October (Figure 5.25). Additional weather stations between these locations may instead display onset dates ranging from January at POF through to March, April and May when winter rainfall commences (Figure 5.25). Considering latitude, there is also a moderate association where onset dates were typically earlier in the southern parts of the country ($r = -0.63$, $p = 0.0007$; Table 5.5;

Figure 5.25). Given that latitude and the onset dates demonstrate the strongest association, then latitude is suggested to play a larger role in governing the spatial distribution across all the locations for the onset dates (Deng *et al.*, 2019; Zhang *et al.*, 2019). However, it is important not to forget the associations of latitude and longitude individually for the onset dates of the SRZ and WRZ locations, as these were statistically significant when considering longitude (Table 5.5). There is also moderate association with elevation and the onset dates ($r = 0.51$, $p = 0.0004$; Table 5.5; Figure 5.25), and this relationship may be used to highlight that topographic barriers such as the Cape Fold Mountain range along the southern coast and the eastern Escarpment in KwaZulu-Natal do play a role in the spatial distribution of onset dates as a result of moisture dispersal (Sene *et al.*, 1998; Singleton & Reason, 2007; Lennard, 2019). Additionally, when considering the spatial distribution of the onset dates, it is important to note that inter-annual variability in these dates is suggested to increase as latitude increases ($r = 0.63$, $p < 0.0001$; Table 5.5). There is also an association with longitude and elevation and inter-annual variability in the onset dates, where this relationship highlights that there was typically greater inter-annual variability in the WRZ and YRZ onset dates (Table 5.5; Figure 5.25).

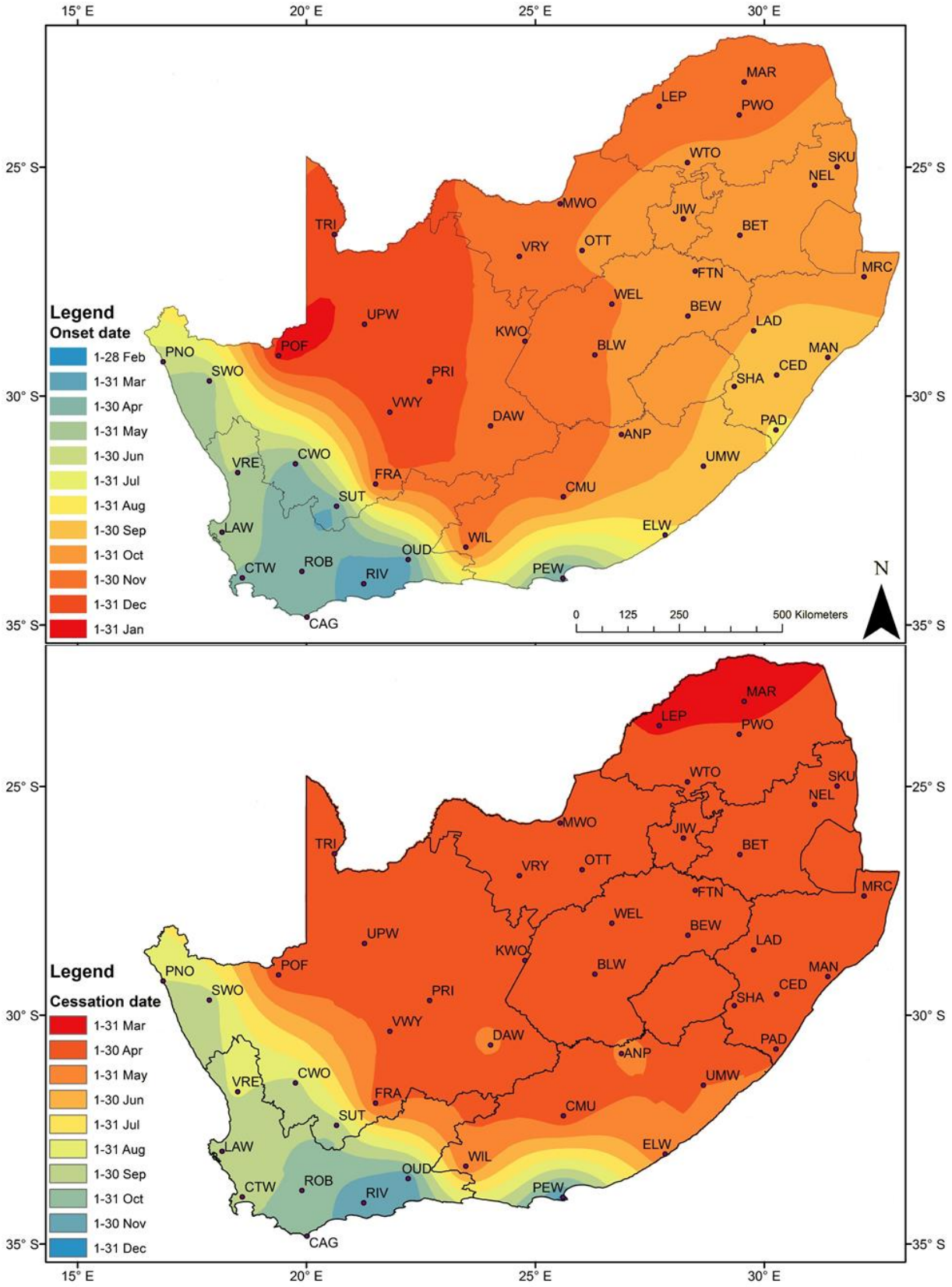


Figure 5.25: Ordinary kriging interpolation of the mean onset and cessation dates for the period of 1987-2016.

Table 5.5: Resulting *r* and *p values* from correlation analyses between mean onset and cessation dates, length of the wet season, number of rain days, latitude, longitude and elevation. Statistically significant *p values* are denoted using an asterisk (*).

Variables	Latitude (°)	Longitude (°)	Elevation (m.asl)
Onset date (Julian day)	-0.63 (*<0.0001)	0.40 (*0.007)	0.51 (*0.0004)
SRZ onset date (Julian day)	-0.08 (0.640)	-0.84 (*0.0001)	-
WRZ onset date (Julian day)	-0.05 (0.896)	-0.71 (*0.033)	-
Cessation date (Julian day)	0.70 (*<0.0001)	-0.60 (*<0.0001)	-0.54 (*0.0001)
SRZ cessation date (Julian day)	0.62 (*0.0001)	0.10 (0.549)	-
WRZ cessation date (Julian day)	0.70 (*0.037)	0.39 (0.295)	-
Length of the wet season (days)	0.25 (0.104)	0.49 (*0.001)	-0.15 (0.311)
Number of rain days	0.05 (0.735)	0.64 (*<0.0001)	-0.02 (0.893)
Onset CV (%)	0.64 (*<0.0001)	-0.47 (*0.0008)	-0.39 (*0.007)
Cessation CV (%)	-0.57 (*<0.0001)	0.31 (0.032)	0.38 (*0.008)
Length of the wet season CV (%)	-0.06 (0.677)	-0.50 (*0.0004)	0.09 (0.552)
Number of rain days CV (%)	-0.09 (0.530)	-0.46 (*0.001)	0.09 (0.551)

There are also spatial patterns evident for the mean cessation dates (Figure 5.25). There is a potential east-west gradient in the cessation dates, and this relationship is of moderate strength and is statistically significant ($r = -0.60$, $p < 0.0001$; Table 5.5). Additionally, there was a strong association between latitude ($r = 0.70$, $p < 0.0001$), where a north-south gradient is evident (Table 5.5). There was also a moderate association when considering elevation, and this relationship highlights the role topography plays in terms of moisture dispersal ($r = -0.54$, $p = 0.0001$; Table 5.5; Figure 5.25). Considering these relationships, especially the statistical strength, it is important to note that latitude plays the greatest role in governing the spatial distribution of the cessation dates, and this is additionally highlighted by the statistically significant relationships between latitude and both the SRZ and WRZ onset dates (Table 5.5; Deng *et al.*, 2019; Zhang *et al.*, 2019). The earliest cessation dates are from 1 to 31 March and are within the northeast of the country, and moving south cessation dates are later (Figure 5.25). For most of the SRZ locations, cessation is evident during 1 to 30 April (Figure 5.25). Closer to the transition between WRZ, YRZ and SRZ weather stations, the cessation dates range from 1 May to 30 June (Figure 5.25). Between these rainfall zones the temporal gradient of the cessation dates is less steep than the gradient for the onset dates (Figure 5.25). Along the southwestern Cape and southern coast, cessation dates range from 1 October to 31 December (Figure 5.25). The portion of coast between OUD and PEW may

display a more continuous pattern for the 1 to 30 November class with data from additional weather stations (Figure 5.25). WRZ locations along part of the western coast and the southwestern Cape had cessation dates between 1 August and 31 October (Figure 5.25). Had PNO been classified, this area may have a mean cessation date between 1 and 30 September (Figure 5.25). Considering the spatial distribution of the cessation dates, it is also important to note that inter-annual variability in these dates is moderately associated with latitude ($r = -0.50$, $p = 0.0004$) and there is a weak but significant association with elevation ($r = 0.31$, $p = 0.016$; Table 5.5).

For the mean length of the wet season there is a weak spatial association with longitude ($r = 0.49$, $p = 0.0001$; Table 5.5). This is evident from the interpolated map on the length of the wet season, where weather stations along the eastern and southern coast have a longer wet season and weather stations in the north western and western parts of the country have a particularly short wet season (Figure 5.26). Considering this, there is also somewhat of an east-west gradient in the inter-annual variability of the length of the wet season, where WRZ locations and SRZ locations within the western interior of the country typically have higher levels of inter-annual variability ($r = -0.50$, $p = 0.0001$; Table 5.5; Figure 5.26).

For the number of rain days during the wet season, there is a moderate and statistically significant spatial association with longitude ($r = 0.64$, $p < 0.0001$), where weather stations along the western coast typically experience fewer rain days, and locations in the eastern regions typically have a higher number of rain days (Table 5.5; Figure 5.26). Additionally, there is also an association with longitude ($r = -0.46$, $p = 0.001$) and inter-annual variability across the weather stations for the number of rain days, where weather stations across the western parts of the country exhibit a higher level of inter-annual variability in the number of rain days (Table 5.5).

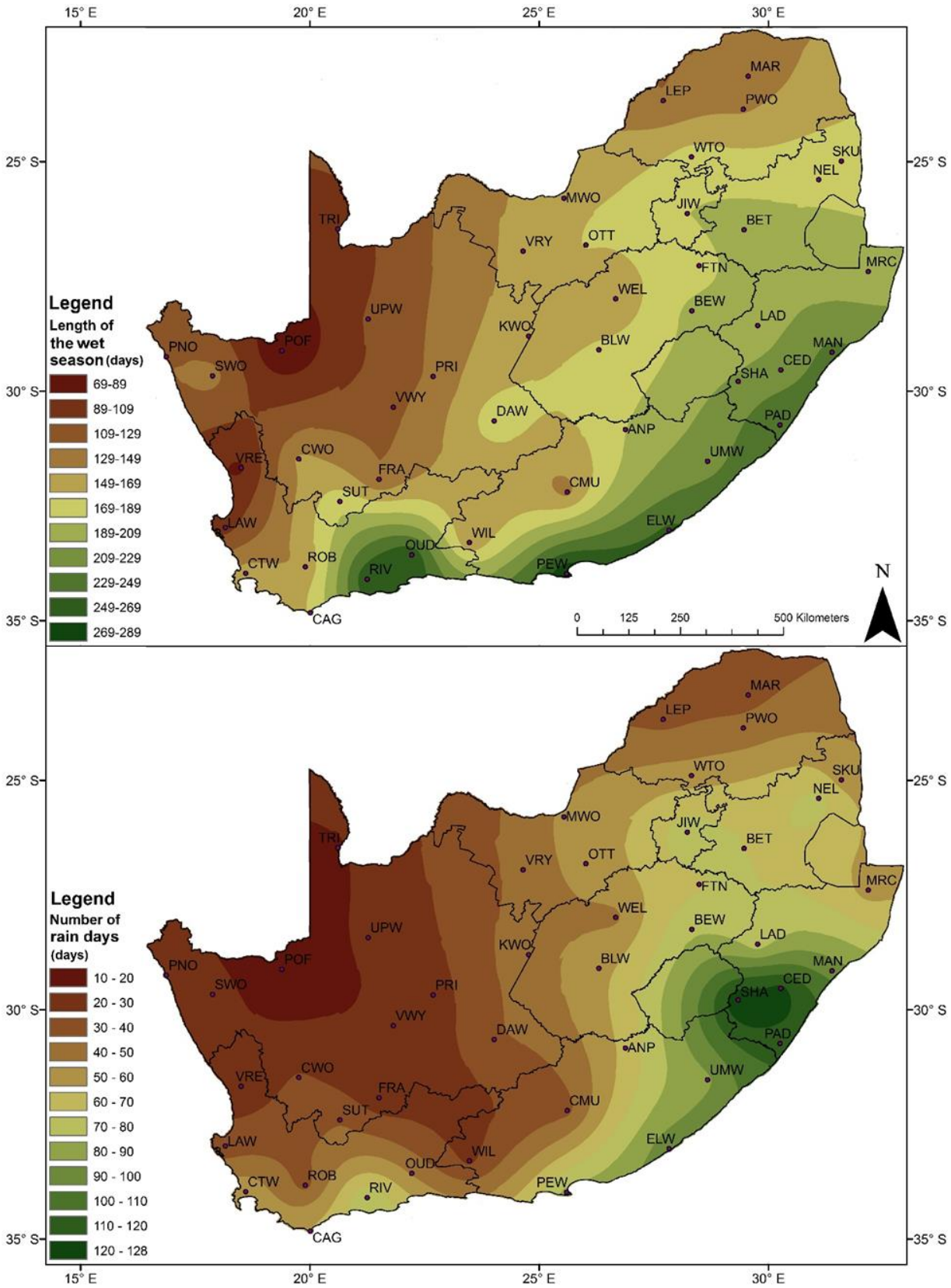


Figure 5.26: Ordinary kriging interpolation of the mean length of the wet season and number of rain days for the period of 1987-2016.

The spatial distribution of the location specific classifications for each weather station, as previously mentioned, highlights that most of the country receives summer rainfall (Figure 5.27). Along the southern coast, south of the Cape Fold Mountains, weather stations were classified as YRZ (Figure 5.27). Weather stations within the southwestern Cape and along the western coast were classified as WRZ (Figure 5.27). As previously mentioned, PNO was not classified as no onset and cessation dates were obtained for this weather station (Figure 5.27).

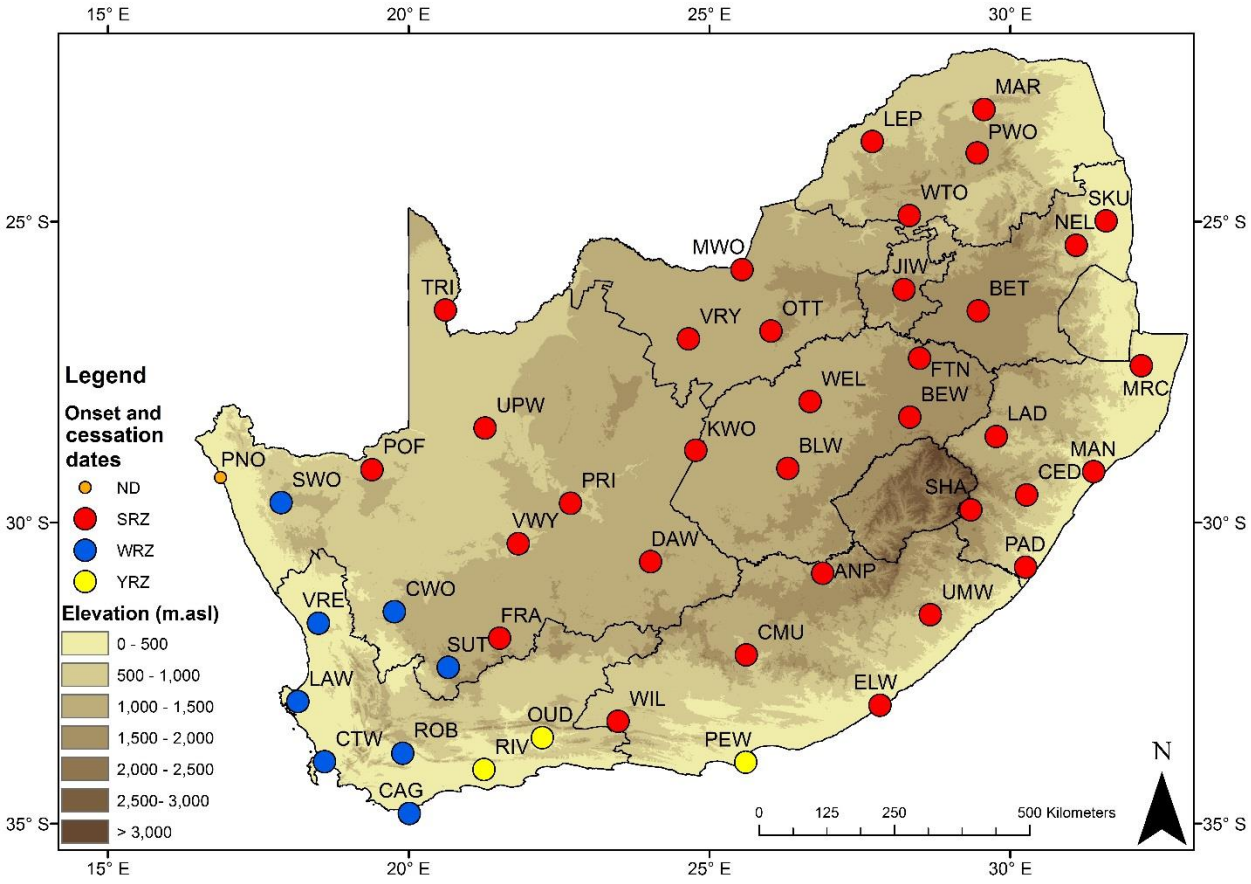


Figure 5.27: Spatial distribution of the SRZ, WRZ and YRZ classified using the mean onset and cessation dates. ND represents a weather station where no onset and cessation dates were obtained.

The mean onset and cessation dates were further classified into late and long SRZ, early, mid and late WRZ, and YRZ (Figure 5.28). Weather stations along the eastern coast, to the southeast of the Great Escarpment, were classified as long SRZ, whereas late SRZ conditions were evident at inland SRZ weather stations (Figure 5.28). SUT closer to the SRZ and WRZ boundary was classified as early

WRZ (Figure 5.28). Weather stations in the southwestern Cape were classified as late WRZ, whereas weather stations to the north of the late WRZ were classified as mid WRZ (Figure 5.28). As already mentioned, PNO was not classified but given this, PNO can potentially be classified as arid since rainfall was too low to identify onset or cessation dates using the criteria discussed under *Section 4.4.3* (Figure 5.28). Additionally, along the southern coast the weather stations classified as YRZ were not further classified (Figure 5.28).

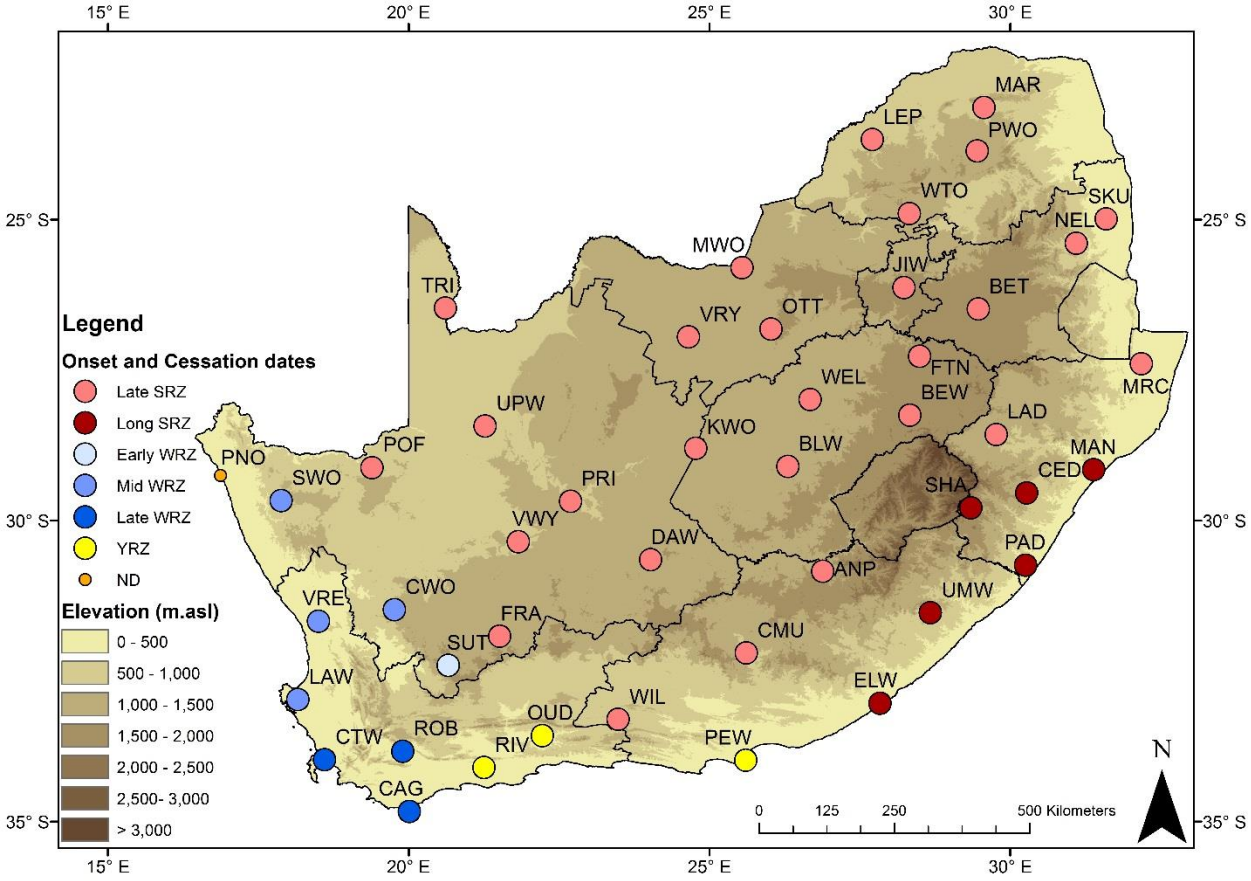


Figure 5.28: Spatial distribution of weather stations classified as late and long SRZ, early, mid and late WRZ, and YRZ. ND represents a weather station where no onset and cessation dates were obtained.

5.4.4 10% AND 90% DATES OF THE WET SEASON

Annual and mean 10% and 90% dates were quantified and classified as SRZ, WRZ and YRZ for each weather station for the period of 1987-2016 (Table 5.6; Appendix F). Weather stations with 10% dates during September through to early December, and 90% dates between March and early June portray SRZ conditions and are evident across the central, eastern and northern areas of the country (Table 5.6). Of the 46 weather stations 33 were classified as SRZ confirming that the majority of the country receives summer rainfall, where SRZ conditions are highlighted at weather stations such as Paddock and Pofadder located in KwaZulu-Natal and the Northern Cape respectively (Table 5.6). Weather stations with 10% dates during March and April and 90% dates during September to November reflect WRZ conditions (Table 5.6). WRZ conditions were evident at weather stations within the Northern and Western Cape at locations such as Sutherland and Vredendal (Table 5.6). At Oudtshoorn, Port Elizabeth Wo and Riversdale, along the southern coast, 10% dates were quantified during February and 90% dates were during November, representing year-round rainfall conditions (Table 5.6). At Willowmore also along the southern coast, the mean 10% (22 November) and 90% (11 July) dates only span a period of approximately eight months, but because both the summer and winter solstice occur during this wet season period, this location was classified as YRZ (Table 5.6).

Table 5.6: Mean 10% and 90% dates, length of the wet season and number of rain days for each individual weather station for the period 1987-2016. Rainfall zone classifications are highlighted, where red, blue and yellow represent classifications of SRZ, WRZ and YRZ respectively.

Location	Mean 10% date	Julian day (JD)	Mean 90% date	Julian day (JD)	Mean length of the wet season (days)	Mean number of rain days
Aliwal-North Plaatkop	25-Oct	298	25-Apr	115	183	61
Bethal	20-Oct	293	30-Mar	89	162	62
Bethlehem Wo	20-Oct	293	10-Apr	110	173	72
Bloemfontein Wo	24-Oct	297	19-Apr	109	178	57
Calvinia Wo	8-Mar	67	7-Oct	280	214	41
Cape Agulhas	17-Mar	76	25-Oct	298	223	77
Cape Town Wo	17-Apr	107	12-Oct	285	179	66
Cedara	24-Sep	267	29-Mar	88	187	111
Cradock-Mun	27-Oct	300	13-May	133	199	48
De Aar Wo	24-Oct	297	8-May	128	197	41
East London Wo	8-Sep	251	18-Apr	108	223	88
Frankfort-TNK	21-Oct	294	11-Apr	101	173	66
Fraserburg	21-Nov	325	13-Jun	164	205	31
Johannesburg INT Wo	27-Oct	300	1-Apr	91	157	67
Kimberley Wo	29-Oct	302	16-Apr	106	170	47
Ladysmith	14-Oct	287	26-Mar	85	164	67
Langebaanweg AWS	13-Apr	103	6-Oct	279	177	53
Lephalale	9-Nov	313	27-Mar	86	139	39
Mafikeng Wo	4-Nov	308	10-Apr	100	158	51
Makatini Research Centre	17-Oct	290	9-Apr	99	175	53
Mandini	14-Sep	257	8-Apr	98	207	89
Mara	3-Nov	307	23-Mar	82	141	39
Nelspruit	25-Oct	298	2-Apr	92	160	66
Ottosdal	28-Oct	301	31-Mar	90	155	53
Oudtshoorn	24-Feb	55	13-Nov	317	263	52
Paddock	1-Sep	244	26-Mar	85	207	101
Pofadder	2-Dec	336	7-Jun	158	188	19
Polokwane Wo	2-Nov	306	30-Mar	89	149	44
Port Elizabeth Wo	24-Feb	55	16-Nov	320	266	77
Port Nolloth	7-Apr	97	8-Oct	281	185	28
Prieska	7-Nov	311	4-May	124	179	28
Riversdale	17-Feb	48	13-Nov	317	270	81
Robertson	9-Mar	68	7-Nov	311	244	53
Shaleburn	14-Oct	287	23-Mar	82	161	108
Skukuza	27-Oct	300	27-Mar	86	152	50
Springbok Wo	28-Mar	87	30-Sep	273	187	32
Sutherland	3-Mar	62	23-Oct	296	235	47
Twee Rivieren	23-Nov	327	16-Apr	106	145	23
Umtata Wo	2-Oct	275	5-Apr	95	186	80
Upington Wo	13-Nov	317	1-May	121	170	27
Vanwyksvlei	16-Nov	320	20-May	140	186	28
Vredendal	21-Apr	111	8-Oct	281	171	39
Vryburg	6-Nov	310	10-Apr	100	156	44
Warmbad Towoomba	27-Oct	300	29-Mar	88	154	50
Welkom	25-Oct	298	7-Apr	97	165	51
Willowmore	22-Nov	326	11-Jul	192	232	42

Across the SRZ within the central, eastern and northeastern regions of the country, mean 10% dates range over approximately three months, from 1 September (JD: 244) at Paddock to 2 December (JD: 336) at Pofadder (Table 5.6; Figure 5.29). The 90% dates for the SRZ have a slightly shorter temporal range of about two and a half months from 23 March (JD: 82) at Mara and Shaleburn to 13 June (JD: 164) at Fraserburg (Table 5.6; Figure 5.29). The range in WRZ, across the southwestern Cape and western coastline, 10% dates is short, spanning one month, from 3 March (JD: 62) at Sutherland to 21 April (JD: 111) at Vredendal (Table 5.6; Figure 5.29). The 90% dates for the WRZ range from 30 September (JD: 273) at Springbok Wo to 7 November (JD: 311) at Robertson (Table 5.6; Figure 5.29). The 10% dates for the YRZ, along the southern coast, also range over approximately three months from Willowmore at 22 November (JD: 326) to Oudtshoorn and Port Elizabeth Wo at 24 February (JD: 55; Table 5.6; Figure 5.29). The 90% dates across the YRZ also have a large range from 11 July (JD: 192) at Willowmore to 16 November (JD: 320) at Port Elizabeth Wo (Table 5.6; Figure 5.29). Considering the length of the wet season and number of rain days amongst the three rainfall zones, WRZ and YRZ weather stations typically have a relatively long wet season but fewer rain days compared to the relatively shorter length and high number of rain days across some of the SRZ weather stations, especially including East London Wo, Mandini, Paddock, Shaleburn and Cedara which are located within the eastern parts of KwaZulu-Natal and Eastern Cape (Table 5.6; Figure 5.29).

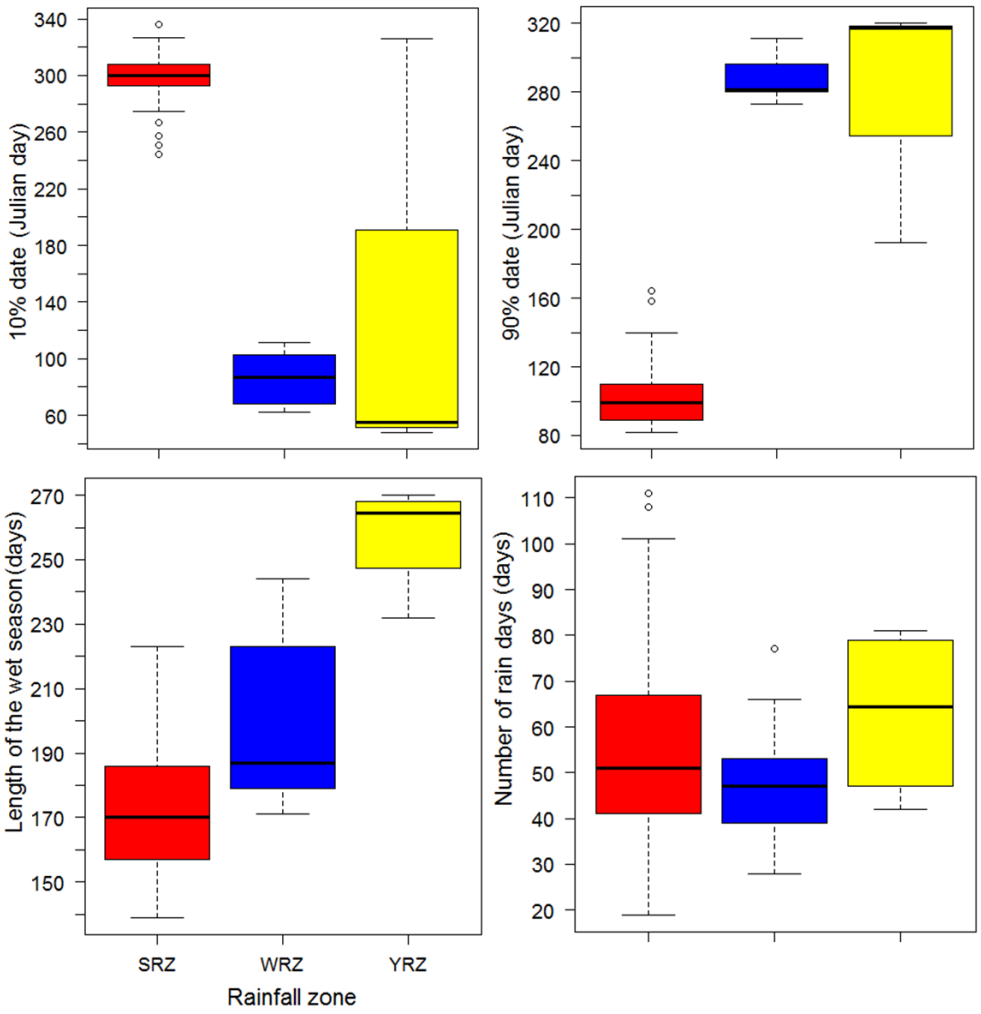


Figure 5.29: Boxplots displaying the distribution of mean 10% and 90% dates, length of the wet season and number of rain days for individual weather stations grouped as SRZ (red), WRZ (blue) and YRZ (yellow).

Considering the SRZ first, there are some patterns present in the mean 10% and 90% dates, and the wet season length (Figure 5.30). The mean length of the wet season across the SRZ locations ranges between 139 days at LEP, located within Limpopo, to 223 days at ELW within the Eastern Cape (Table 5.6; Figure 5.30). Along the eastern coast CED, ELW, MAN and PAD were classified as long SRZ and have early 10% dates with a considerably long wet season length ranging between 187 and 223 days (Table 5.6; Figure 5.30). At these locations the length of the wet season is slightly longer than that of the dry season (Figure 5.30). The remaining weather stations were all classified as late SRZ, and unlike the long SRZ locations there were relatively few temporal patterns (Figure 5.30). At the late SRZ locations the dry season is either a similar length to the wet season or slightly

longer or shorter (Figure 5.30). The wet season is shortest for LEP, MAR, PWO and TRI, located in Limpopo and Northern Cape, where the range is 139 to 149 days (Table 5.6; Figure 5.30). The longest wet season lengths were evident at CMU, DAW, FRA and POF, located across the central western parts of the country, and at these locations the wet season length ranges from 188 to 205 days (Table 5.6; Figure 5.30). Across the late SRZ weather stations, 10% dates were observed during October and November and 90% dates ranged from March to June (Figure 5.30). The earliest 10% dates for the late SRZ locations were evident from 2 to 17 October at LAD, MRC, SHA and UMW within KwaZulu-Natal and the Eastern Cape (Table 5.6; Figure 5.30). Within the Northern Cape FRA, POF, TRI and VWY had the latest 10% dates, from 16 November to 2 December, amongst the late SRZ locations (Figure 5.30). FRA, POF and VWY also had the latest 90% dates, whereas TRI with a late 10% date has a 90% date at a relatively earlier time to these locations (Figure 5.30). The earliest 90% dates were evident at 23 to 27 March at LEP, LAD, MAR, SHA and SKU located in KwaZulu-Natal, Limpopo and Mpumalanga (Table 5.6; Figure 5.30).

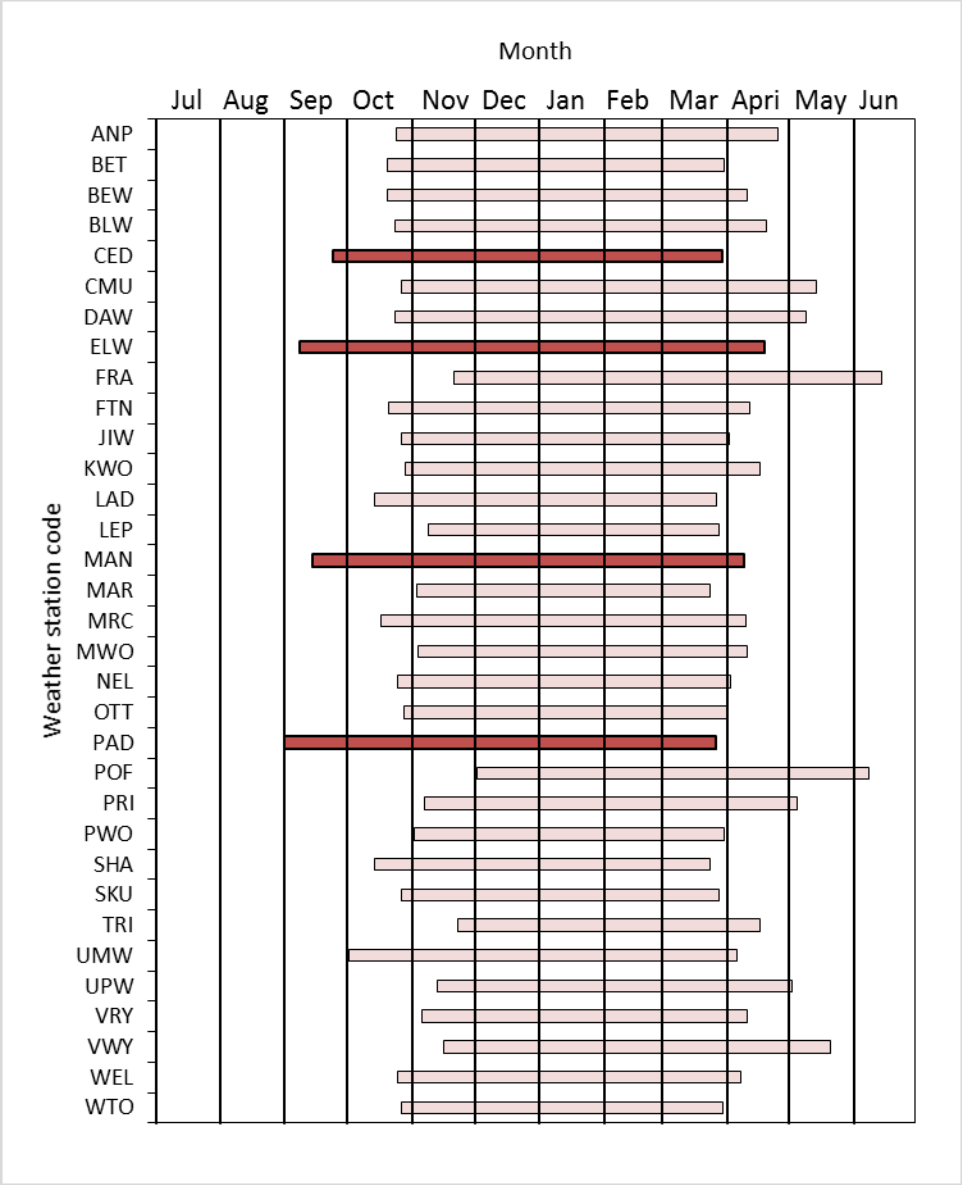


Figure 5.30: Calendar plot of the mean 10% and 90% dates, and length of the wet season for weather stations classified as SRZ. This plot is colour coded according to late and long SRZ, where dark red represents long SRZ and light red represents late SRZ.

Across the SRZ locations there are some patterns in mean annual rainfall, the length of the wet season and the number of rain days (Figure 5.31). Mean annual rainfall across these SRZ locations has a particularly large range from 121.7mm at POF, in the Northern Cape, to 1099.6mm at PAD in KwaZulu-Natal (Table 5.1; Figure 5.31). The wet season length across the SRZ locations ranges from 139 days at LEP, within Limpopo, to 223 days at ELW within the Eastern Cape (Table 5.6; Figure 5.31). POF has the lowest number of rain days which is 19 days, and CED, within KwaZulu-

Natal, has the highest number of rain days which is 111 days (Table 5.6; Figure 5.31). Typically, locations with higher mean annual rainfall have a relatively longer wet season and a higher number of annual rain days, as is evident across CED, ELW, MAN and PAD which are located along the eastern coast (Figure 5.31). SHA within KwaZulu-Natal, however, has particularly high annual rainfall with a relatively short wet season of 161 days and a relatively high number of rain days (108 days), and this may indicate that there are relatively few dry days during the wet season (Figure 5.31). Some locations with particularly low mean annual rainfall also have relatively long wet seasons, and this is evident at FRA, POF with a low number of rain days during the wet season (Figure 5.31). This may indicate that there are numerous no rain days between the rain days at these locations.

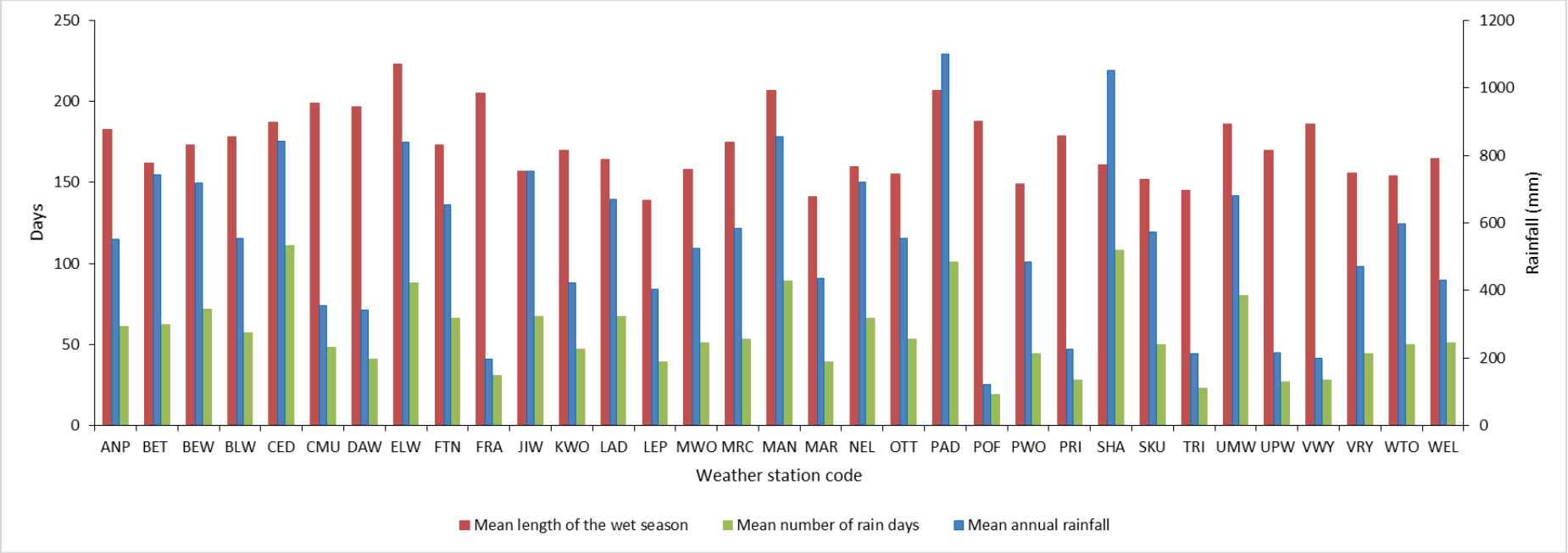


Figure 5.31: Bar graph of mean annual rainfall, length of the wet season and number of rain days for weather stations classified as SRZ.

The locations classified as WRZ display 10% dates from 3 March (SUT) to 21 April (VRE), and are located across the southwestern Cape, and western coast and adjacent regions (Table 5.6; Figure 5.32). The 90% dates range from 30 September (SWO) to 7 November (ROB; Table 5.6; Figure 5.32). The length of the wet season ranges from 171 days at VRE to 244 days at ROB (Table 5.6; Figure 5.32). Across the WRZ locations, earlier 10% dates were typically accompanied by later 90% dates and a longer wet season, and this was evident at CAG, CWO, ROB and SUT which were classified as long WRZ (Figure 5.32). Later 10% dates were also typically accompanied by relatively earlier 90% dates and this was evident at CTW, LAW, PNO, SWO and VRE which were classified as late WRZ (Figure 5.32).

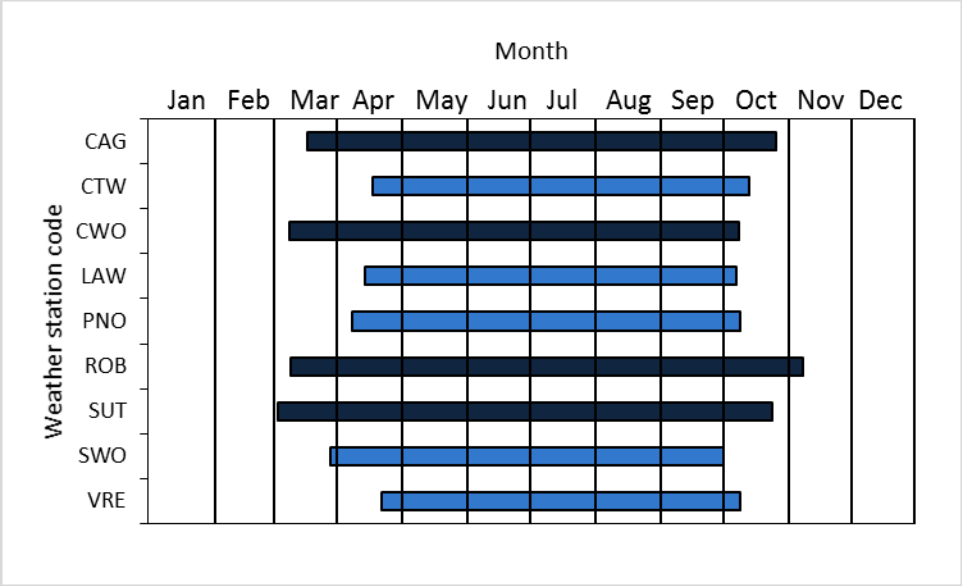


Figure 5.32: Calendar plot of the mean 10% and 90% dates, and length of the wet season for weather stations classified as WRZ. This plot is colour coded according to late and long WRZ, where dark blue represents long WRZ and light blue represents late WRZ.

There are no distinct patterns when considering mean annual rainfall, the length of the wet season and the number of rain days for the WRZ weather stations (Figure 5.33). Mean annual rainfall across these locations ranges from 72.4mm at PNO to 524.2mm at CTW (Table 5.1; Figure 5.33). The wet season, as previously mentioned, is longest at ROB (244 days) and shortest at VRE (171 days; Table 5.6; Figure 5.33). CAG (77 days) receives the highest number of rain days, whereas

PNO (28 days) receives the lowest number of rain days (Table 5.6; Figure 5.33). CAG, CWO, ROB and SUT were classified as long WRZ (Figure 5.33). Across these locations, CWO, ROB and SUT display similar patterns with relatively similar annual rainfall, length of the wet season and number of rain days (Figure 5.33). CAG does not display a similar pattern to these locations, as CAG has considerably higher mean annual rainfall and more rain days during the wet season (Figure 5.33). At CTW mean annual rainfall and the number of rain days are also particularly high, but the wet season is relatively short (Figure 5.33). This indicates that at CTW there may be relatively higher daily rainfall during the wet season. Within the group of mid WRZ, LAW, SWO and VRE display similar patterns, whereas PNO, part of this group, experiences a similar wet season length to these locations but annual rainfall and the number of rain days are considerably lower at PNO (Figure 5.33). This may indicate that between rain days there are numerous no rain days at PNO.

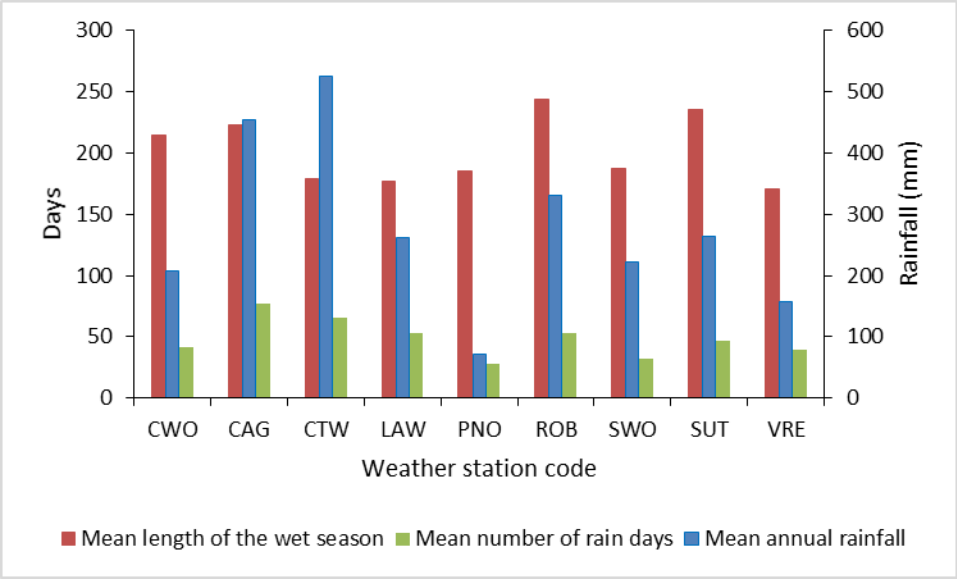


Figure 5.33: Bar graph of mean annual rainfall, length of the wet season and number of rain days for weather stations classified as WRZ.

Across the southern coast YRZ weather stations, OUD, PEW and RIV displayed relatively similar 10% and 90% dates (Figure 5.34). The 10% dates at these locations range between 17 and 24 February, and the 90% dates range between 13 and 16 November (Table 5.6; Figure 5.34). The wet season at these locations spans a period of 263 days at OUD to 270 days at RIV (Table 5.6;

Figure 5.34). At WIL, 10% dates occur when the wet season at OUD, PEW and RIV typically ends (Figure 5.34). The wet season spans a period of approximately 232 days at WIL from 22 November until 11 July which indicates YRZ conditions as this temporal period encompasses both the winter and summer solstice (Figure 5.34).

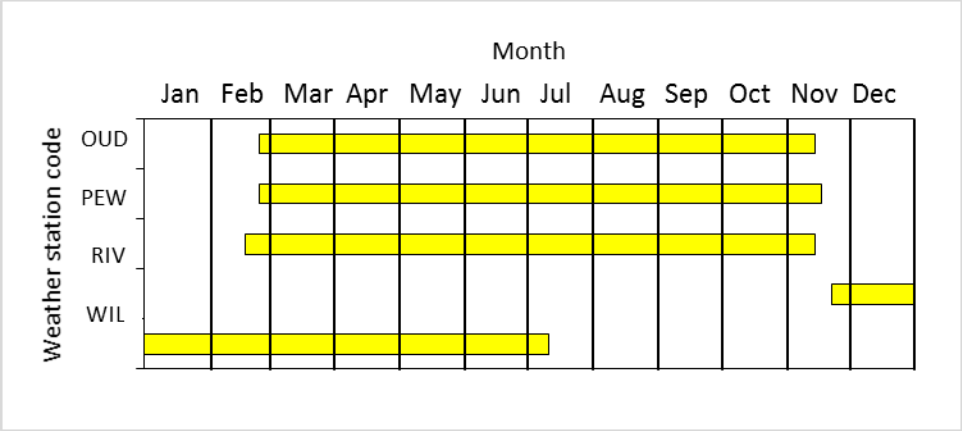


Figure 5.34: Calendar plot of the mean 10% and 90% dates, and length of the wet season for weather stations classified as YRZ.

There are some patterns evident in the mean annual rainfall, length of the wet season and number of rain days across the YRZ locations (Figure 5.35). WIL, as previously mentioned, has the shortest wet season, whereas at OUD, PEW and RIV the wet season is a similar length of approximately 266 days (Figure 5.35). OUD and WIL both have relatively low annual rainfall of 243.6mm and 279.6mm (Table 5.1), and a similar number of rain days during the wet season (OUD: 52, WIL: 42; Table 5.6; Figure 5.35). Since WIL has a shorter wet season and a lower number of rain days than OUD this may indicate that at WIL there is typically higher daily rainfall than for OUD (Table 5.1; Figure 5.35). PEW and RIV, both with relatively high annual rainfall have a relatively high number of rain days compared to OUD and WIL (Figure 5.35; Table 5.1). PEW receives higher annual rainfall than RIV, but they receive a similar number of rain days possibly indicating that PEW may receive higher daily rainfall (Figure 5.35).

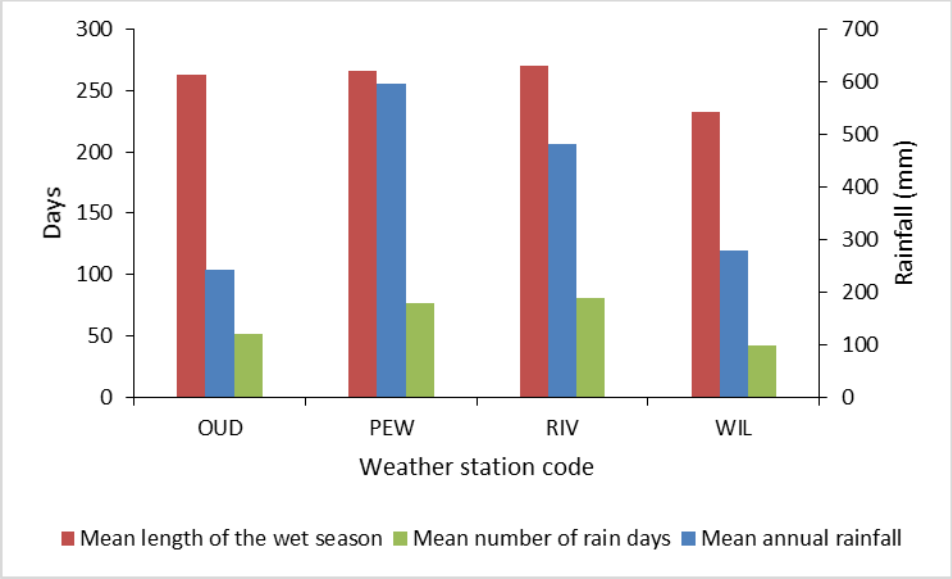


Figure 5.35: Bar graph of mean annual rainfall, length of the wet season and number of rain days for weather stations classified as YRZ.

An understanding of rainfall seasonality across South Africa as described by the 10% and 90% dates is not complete without considering the inter-annual variability across these dates for individual locations. For the 10% dates, both the WRZ and YRZ have relatively high inter-annual variability, whereas the inter-annual variability is low across the SRZ weather stations (Figure 5.36). Inter-annual variability in the 10% dates was above 20% for all WRZ locations, and at Sutherland CV was particularly high at 56.6% (Figure 5.36). Willowmore (7.9%) had particularly low inter-annual variability for the 10% dates, whereas Oudtshoorn, Port Elizabeth Wo and Riversdale had particularly high CV which ranges between 42.9 to 46.2% (Figure 5.36). WRZ and YRZ locations display low inter-annual variability (CV <20%) in the 90% dates (Figure 5.36). WIL, classified as YRZ, had a moderate level of inter-annual variability at 22.3% (Figure 5.36). Inter-annual variability for SRZ locations for the 90% dates ranges between 12.4% at Shaleburn and 43.9% at Mara, where Bethlehem Wo, Cradock-Mun, Frankfort TNK, Mandini, Ottosdal and Welkom had CV >30% (Figure 5.36). YRZ locations had relatively low levels of inter-annual variability in the wet season length, where WIL was the only location with CV >20% (Figure 5.36). CV values for the wet season length across the WRZ were all below 30%, where locations including Langebaanweg AWS, Port Nolloth, Springbok Wo and Vredendal along the western coast had CV >20% (Figure 5.36). Inter-annual

variability quantified for the wet season length across the SRZ locations ranges between 13.4% and 38.7%, and only Prieska and Pofadder within the Northern Cape had CV >30% (Figure 5.36). Inter-annual variability in the number of rain days was relatively similar across the rainfall zones, where Fraserburg, Pofadder, Port Nolloth, Sutherland and Twee Rivieren located in the Northern Cape had CV >30% (Figure 5.36). At Port Nolloth CV was particularly high at 59.0% (Figure 5.36).

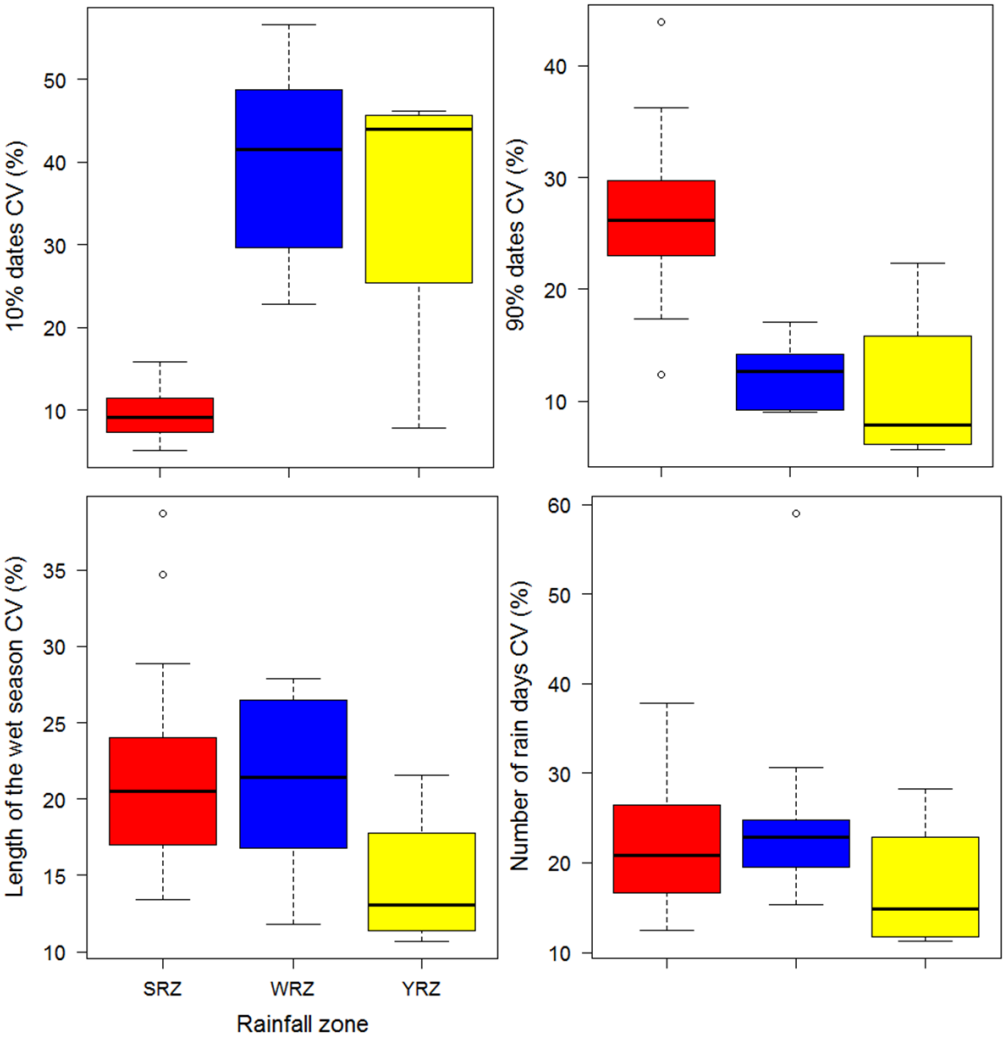


Figure 5.36: Boxplots displaying the distribution of CV for the mean 10% and 90% dates, length of the wet season and number of rain days for individual weather stations grouped as SRZ (red), WRZ (blue) and YRZ (yellow).

To gain a full understanding of rainfall seasonality according to the 10% and 90% dates, again the spatial distribution across South Africa is also important to consider. Concentrating first on the

10% dates, it is evident that there are spatial patterns across South Africa (Figure 5.37). The earliest 10% dates are at OUD, PEW and RIV (Figure 5.37), however, additional weather stations between OUD and RIV, and PEW may instead indicate that rainfall across the southern coast has 10% dates between 1 and 28 February instead of the range between 1 March and 31 October (Figure 5.37). Additional weather stations between the SRZ and WRZ may also display a different spatial pattern (Figure 5.37). WRZ 10% dates occur during March and April, with later dates further north and west, where the latest dates are evident mostly along the western coast (Figure 5.37). This progression of rainfall is highlighted by the relationships evident between the WRZ 10% dates as well as longitude and latitude (Table 5.7). The earliest SRZ 10% dates are evident along the eastern coast, and further inland the 10% dates are gradually later, where these dates are latest across the northern parts of the country and along the boundary between the SRZ and WRZ (Figure 5.37). The progression of rains into the SRZ from the east to west is highlighted by the relationship between the 10% dates and longitude ($r = -0.70$, $p = 0.0001$; Table 5.7). These patterns are additionally somewhat highlighted by the statistically significant, although moderate association between all 10% dates and latitude ($r = -0.64$, $p < 0.0001$), longitude ($r = 0.58$, $p < 0.0001$) and elevation ($r = 0.56$, $p < 0.0001$; Table 5.7). These relationships potentially highlight that along the coastal regions, 10% dates are typically earliest (Figure 5.37). Considering these dates, it is important to highlight that latitude plays the greatest role in governing the spatial distribution of the 10% dates given that the *r value* is strongest (Table 5.7; Deng *et al.*, 2019; Zhang *et al.*, 2019). There is also a spatial association between the inter-annual variability in the 10% dates at individual weather stations and latitude ($r = 0.63$, $p < 0.0001$), longitude ($r = -0.65$, $p < 0.0001$) and elevation ($r = -0.42$, $p = 0.003$), which indicates that the WRZ and YRZ 10% dates were associated with relatively higher levels of variability compared to SRZ locations (Table 5.7; Figure 5.36).

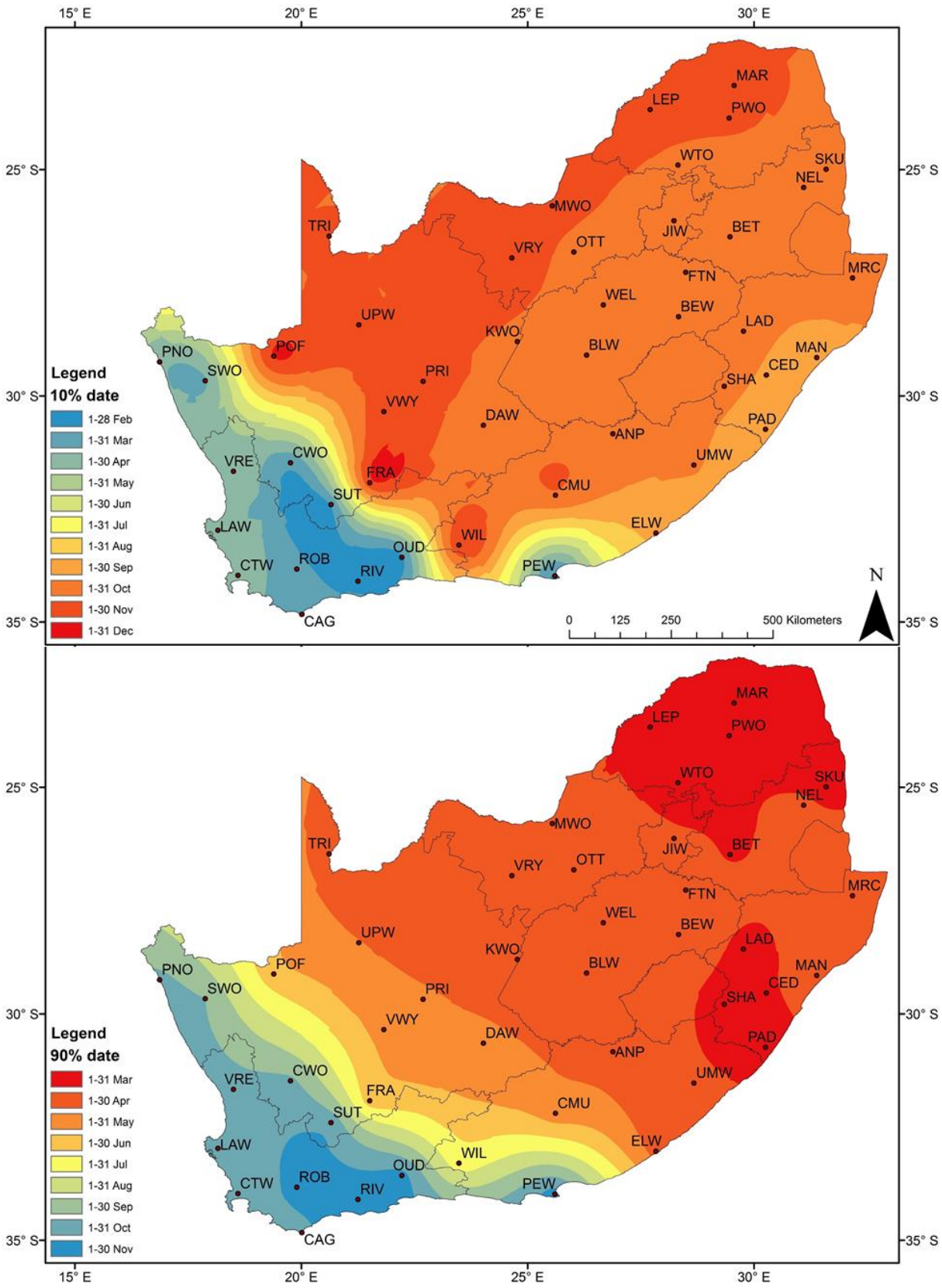


Figure 5.37: Ordinary kriging interpolation of the mean 10% and 90% dates for the period of 1987-2016.

Table 5.7: Resulting *r* and *p values* from correlation analyses between mean 10% and 90% dates, length of the wet season, number of rain days, latitude, longitude and elevation. Statistically significant *p values* are denoted using an asterisk (*).

Variables	Latitude (°)	Longitude (°)	Elevation (m.asl)
10% date (Julian day)	-0.64 (*<0.0001)	0.58 (*<0.0001)	0.56 (*<0.0001)
SRZ 10% dates (Julian day)	-0.24 (0.170)	-0.70 (*0.0001)	-
WRZ 10% dates (Julian day)	-0.15 (0.651)	-0.76 (*0.011)	-
90% date (Julian day)	0.72 (*<0.0001)	-0.77 (*<0.0001)	-0.54 (*0.0001)
SRZ 90% dates (Julian day)	0.60 (*0.0001)	-0.71 (*<0.0001)	-
WRZ 90% dates (Julian day)	0.66 (*0.039)	0.69 (*0.028)	-
Length of the wet season (days)	0.83 (*<0.0001)	-0.35 (*0.018)	-0.44 (*0.003)
Number of rain days	0.22 (0.143)	0.53 (*0.0002)	-0.09 (0.543)
10% CV (%)	0.63 (*<0.0001)	-0.65 (*<0.0001)	-0.42 (*0.003)
90% CV (%)	-0.63 (*<0.0001)	0.46 (*0.001)	0.50 (*0.0005)
Length of the wet season CV (%)	-0.24 (0.105)	-0.35 (*0.017)	0.17 (0.254)
Number of rain days CV (%)	-0.16 (0.286)	-0.41 (*0.005)	-0.02 (0.900)

There are also spatial patterns evident for the 90% dates across South Africa (Figure 5.37). The earliest 90% dates are evident in the northeastern part of the country and at CED, LAD, PAD and SHA in KwaZulu-Natal (Figure 5.37). Moving west across the SRZ, 90% dates are later and the latest dates range between 1 and 30 June (Figure 5.37), where this is particularly highlighted by the statistically significant relationship between the 90% dates and longitude ($r = -0.71$, $p > 0.0001$; Table 5.7). Between the SRZ and WRZ, there is a relatively steep temporal gradient which is between 1 July and 31 August (Figure 5.37). Additional weather stations may display a different pattern in this area. The earliest WRZ 90% dates are between 1 and 30 September at SWO and moving west and south 90% dates are earlier (Figure 5.37). Considering the WRZ 90% separately, it is apparent that there is a statistically significant relationship between both longitude and latitude (Table 5.9), where these relationships may highlight the withdrawal of WRZ rainfall according to the 90% dates. Along the southern coast, 90% dates are expected between 1 and 30 November, but this is not evident and an additional weather station below WIL may display continuation of this class (Figure 5.36). It is evident that across the country, there is a spatial association between the 90% dates and latitude ($r = 0.72$, $p < 0.0001$), longitude ($r = -0.77$, $p < 0.0001$) and elevation ($r = -0.54$, $p < 0.0001$; Table 5.7; Figure 5.37). This indicates that with an increase in latitude 90% dates are later and with a decrease in longitude 90% dates are also

typically later (Figure 5.37). The association with elevation is more complex and since this association is of a moderate strength, then it is suggested that elevation does not govern the spatial distribution of the 90% dates as latitude and longitude do (Deng *et al.*, 2019; Zhang *et al.*, 2019). There are also spatial patterns in the inter-annual variability across the weather stations, as is evident from the association between latitude ($r = -0.63$, $p < 0.0001$), longitude ($r = 0.46$, $p = 0.001$) and elevation ($r = 0.50$, $p = 0.0005$) indicating that inland weather stations demonstrated relatively higher variability in the cessation dates (Table 5.7).

Spatial patterns are also evident considering the length of the wet season, where weather stations along the southern coast experience the longest wet season (Figure 5.38). Moving north, the length of the wet season gradually decreases, where LEP, MAR, PWO and TRI, in the northern parts of the country, have the shortest wet seasons (Figure 5.38). Hence, the association between the length of the wet season and latitude ($r = 0.83$, $p < 0.0001$), longitude ($r = -0.31$, $p = 0.018$) and elevation ($r = -0.44$, $p = 0.003$) is statistically significant and this association is especially strong when considering latitude (Table 5.7). Even the level of inter-annual variability in the length of the wet season and the association between longitude is statistically significant ($r = -0.35$, $p = 0.017$; Table 5.7). This indicates that central and western locations typically display higher inter-annual variability in the wet season length.

Across the country, weather stations in the eastern parts and along the southern coast of the country experience a higher number of rain days relative to other weather stations (Figure 5.38). This spatial pattern is highlighted by the statistically significant association quantified between longitude and the number of rain days ($r = 0.53$, $p = 0.0002$; Table 5.7). Along this east-west gradient, there is also an association with inter-annual variability in the number of rain days ($r = -0.41$, $p = 0.005$; Table 5.7), where locations within the western parts of the country are associated with relatively higher inter-annual variability in the number of rain days during the wet season.

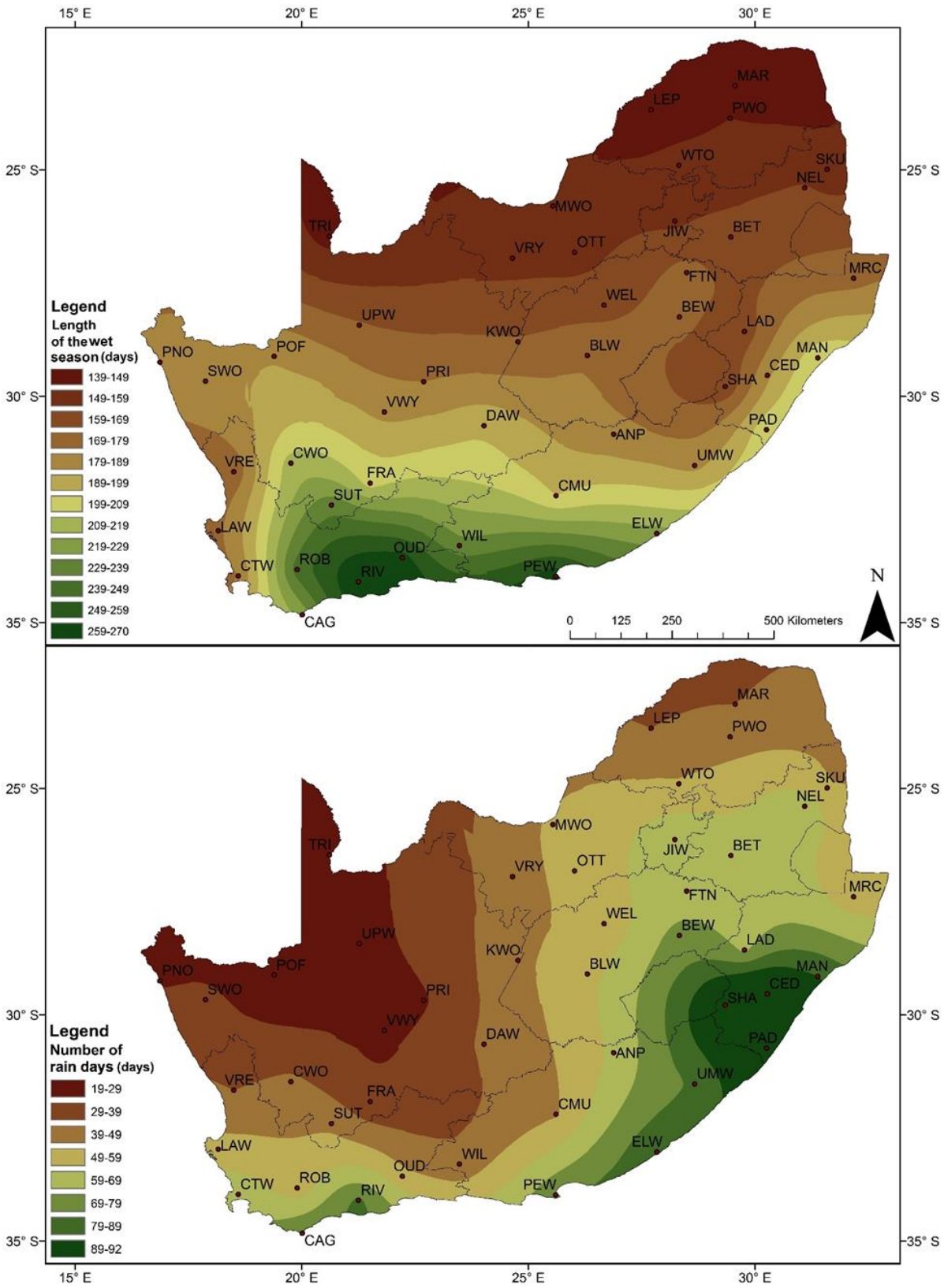


Figure 5.38: Ordinary kriging interpolation of the mean length of the wet season and the number of rain days for the period of 1987-2016.

Considering the spatial distribution of the location specific classifications, it is evident that most of the country receives summer rainfall, where 33 locations were classified as SRZ (Figure 5.39). The SRZ covers the western interior and the eastern half of the country (Figure 5.39). Along the southern coast, bound by the Cape Fold Mountain range, weather stations were classified as YRZ (Figure 5.39). Weather stations within the southwestern Cape and along the western coast as well as adjacent areas were classified as WRZ (Figure 5.39).

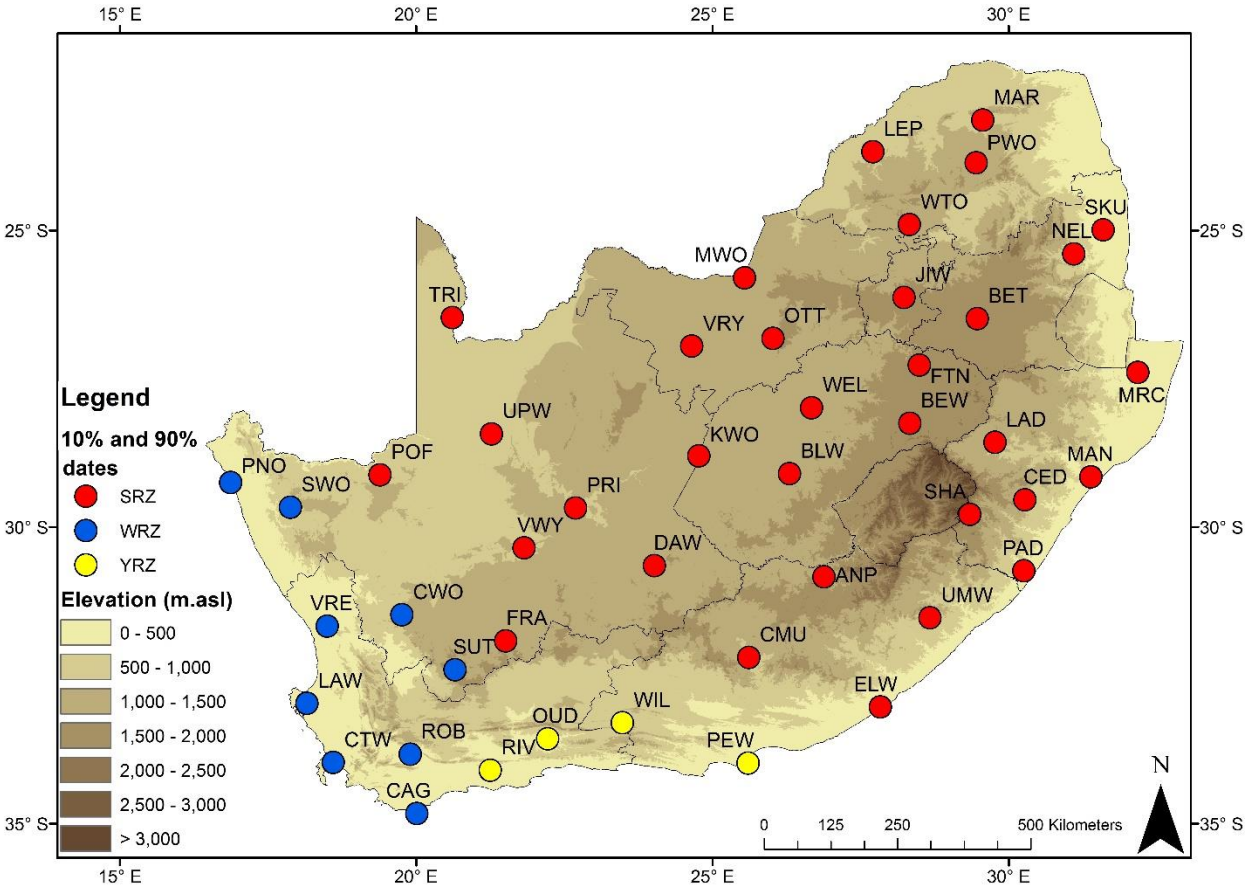


Figure 5.39: Spatial distribution of the SRZ, WRZ and YRZ classified using the mean 10% and 90% dates.

The mean 10% and 90% dates were further classified into late and long SRZ, late and long WRZ, and YRZ (Figure 5.40). Most locations along the eastern coast, mostly to the southeast of the Great Escarpment, including CED, ELW, MAN and PAD, display long SRZ conditions (Figure 5.40). Late SRZ conditions were evident at inland SRZ weather stations (Figure 5.40). CAG, CWO, ROB and SUT

at the intersection between the three rainfall zones were classified as long WRZ (Figure 5.40). Weather stations along the western coast were classified as late WRZ (Figure 5.40). Again, the YRZ locations along the southern coast were not further classified (Figure 5.40).

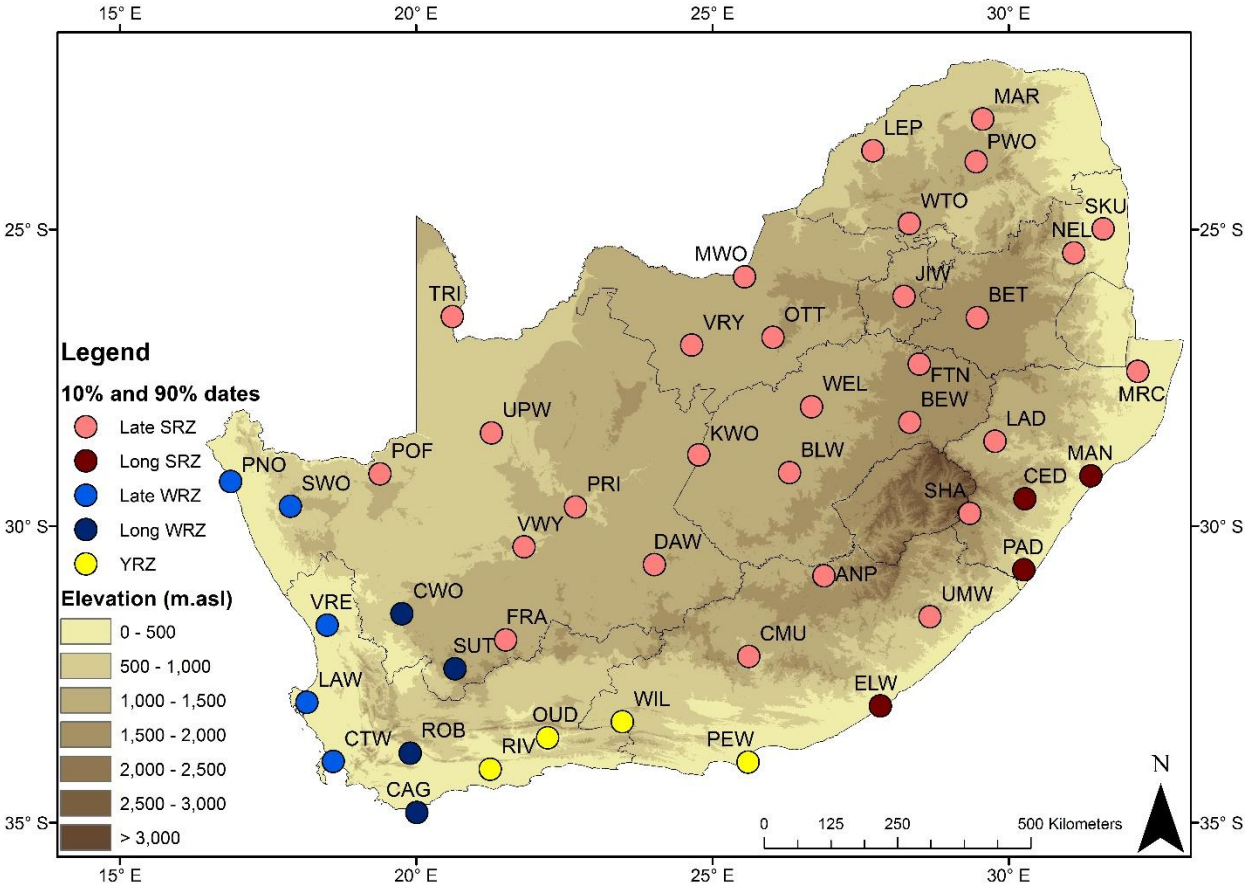


Figure 5.40: Spatial distribution of weather stations classified as late and long SRZ, late and long WRZ, and YRZ.

5.5 SHIFTS IN RAINFALL SEASONALITY FOR THE PERIOD OF 1987-2016

Shifts in the seasonality of rainfall across South Africa were quantified across all weather stations using the annual rainfall seasonality quantities from the metrics investigated under *Sections 5.4.2, 5.4.3, and 5.4.4*. Most of these changes were small and were not statistically significant, where 31% of these trends were quantified with considerably weak *r values* of less than 0.10 (Appendix G). This may suggest that no changes occurred at most of weather stations (Appendix G). Approximately 11% (45 trends) of these trends had a *p value* smaller than 0.10 (Appendix G), which

means that there was a very high possibility that these trends did not occur by chance. Only 8% of the trends quantified were statistically significant, where there were 32 statistically significant trends with 17 of these quantified for the 10% and 90% dates, and the respective length of the wet season and number of rain days (Appendix G). There were two statistically significant trends for the seasonality scores, four for the onset dates, three for the cessation dates, one for the 10% dates, and four across the 90% dates (Appendix G). Considering all the trends calculated across each weather station, there were 23 locations with at least one statistically significant trend in all the quantities tested for changes (Appendix G; Figure 5.41, 5.42, 5.43, 5.44, 5.45). This equates to half of the sample of weather stations, which suggests that across South Africa components of rainfall seasonality have changed at many locations and it is important to continue monitoring over longer time periods. BEW, LAW, OTT, PNO and WEL displayed more than one statistically significant trend in all the quantities, while there was one statistically significant trend at the remaining 18 weather stations (Appendix G). Although only a small portion of trends were statistically significant, all trends were recorded. The trends which have relatively large rates of change but are not statistically significant, although with low *p values*, and demonstrate relatively strong *r values* may suggest tentative trends which over a longer time period may become stronger and possibly statistically significant (Appendix G). Such a location would include LAD, located within KwaZulu-Natal, which has relatively large rates of change, strong *r values* and low *p values* for the cessation dates and associated wet season duration and number of rain days (Appendix G). In this case, as with the statistically significant trends, these trends are important to record and continuously monitor. Change points were also included in this section to identify any changes in magnitude and/or direction of trends (Appendix G). Few change points were detected, with 11 change points during the first half of the study (prior to 2002), and 17 change points during the second half of the study; where 12 change points, four each, were detected during 2001, 2007 and 2008 (Appendix G).

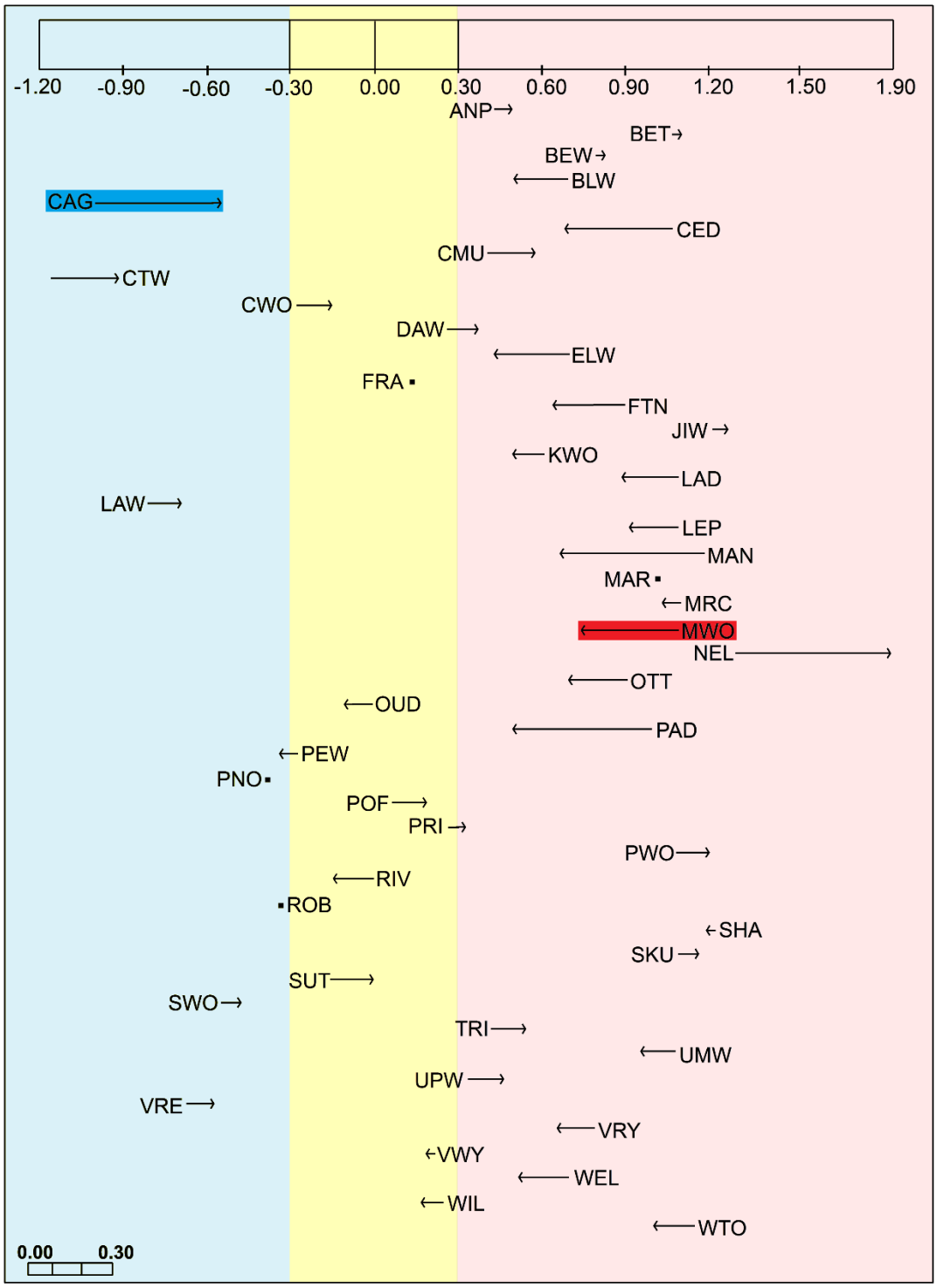


Figure 5.41: Shifts in the seasonality scores from 1987 to 2016 based on extended regression analysis. Lines with arrows represent individual weather station trends, starting from 1987 and ending at 2016. Specific values for each trend are under *Appendix G and H*. Squares represent change in the seasonality scores of less than or equal to +/- 0.02. Only weather stations with significant trends at the 5% level were highlighted, whereby the colour corresponds to the classification of each weather station under *Section 5.4.2*. Pale blue, yellow and red represent WRZ, YRZ and SRZ.

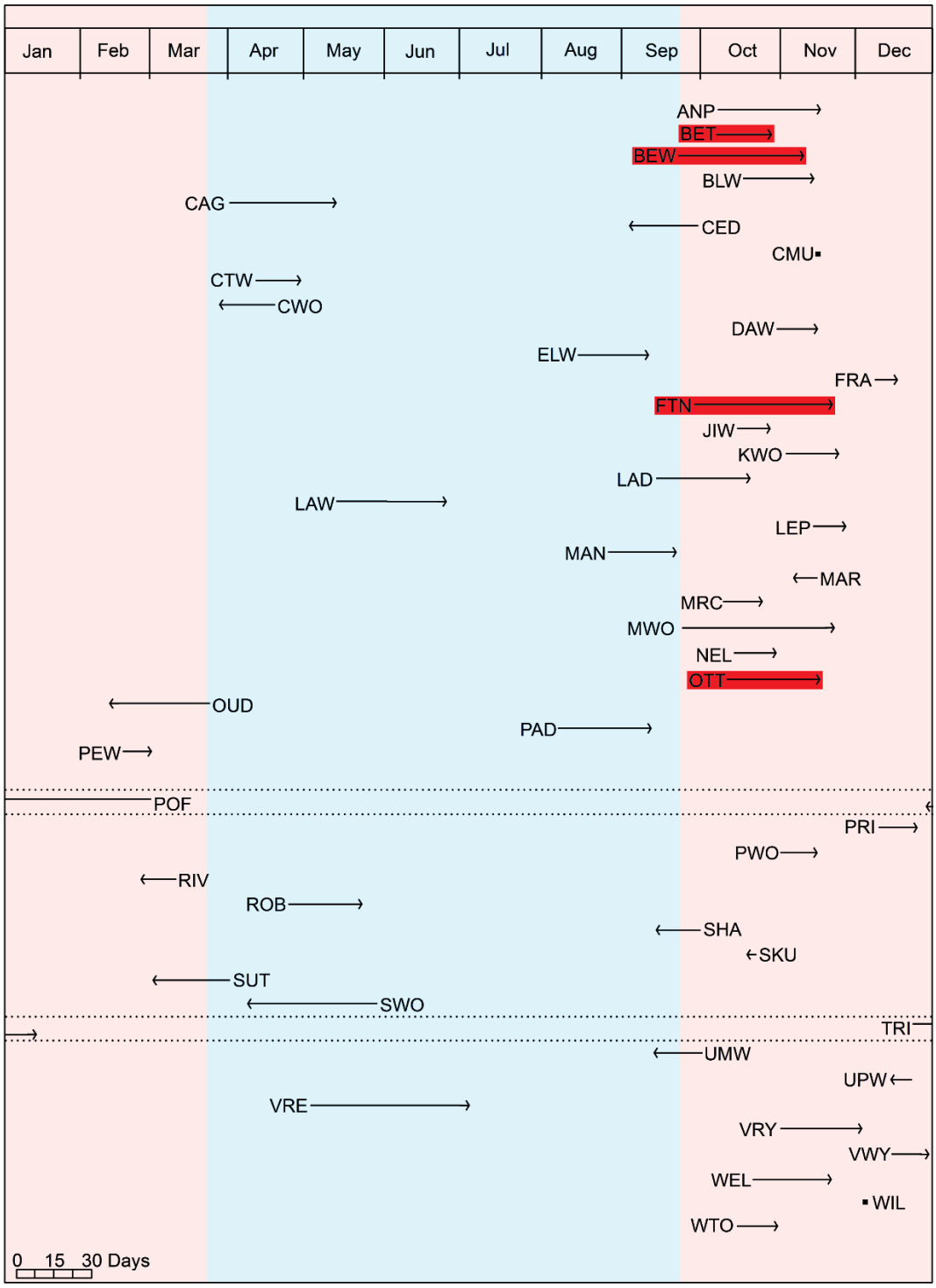


Figure 5.42: Shifts in the onset dates for the period of 1987-2016 based on extended regression analysis. Lines with arrows represent individual weather station trends which start from 1987 and end at 2016, and these specific values are under *Appendix G* and *I.1*. Squares represent changes of 2 days or less. Statistically significant trends at the 5% level were highlighted, whereby the colour corresponds to the classification of each weather station under *Section 5.4.3*. Pale red and blue represent SRZ and WRZ split at the autumn and spring equinox dates of 21 March and 23 September. Horizontal dotted lines indicate weather stations where onset dates shifted to the next or previous calendar year.

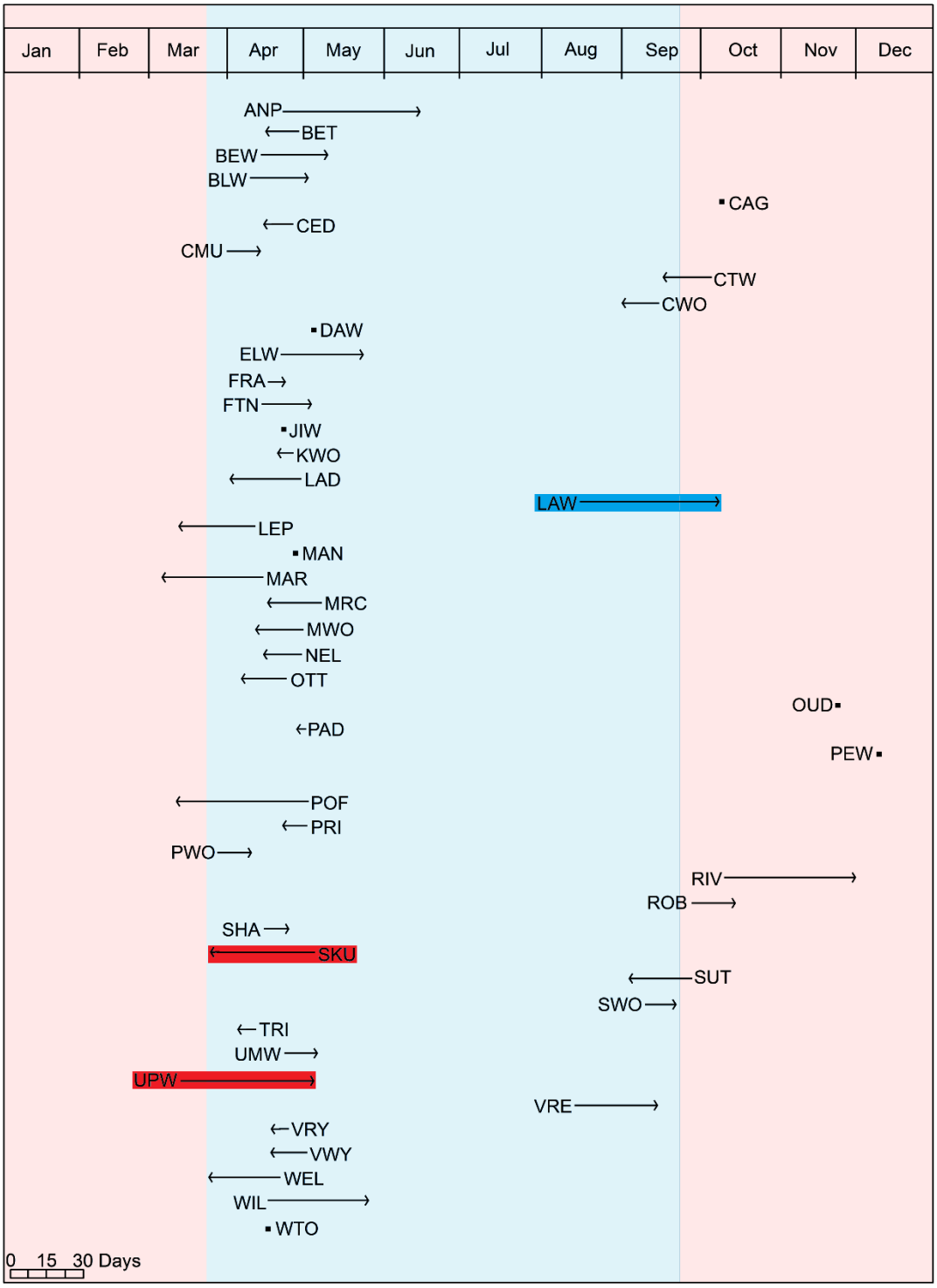


Figure 5.43: Shifts in the cessation dates for individual weather stations for the period of 1987-2016 based on extended regression analysis. Lines with arrows represent individual weather station trends which start from 1987 and end at 2016. Specific values for each trend are under *Appendix G and I.2*. Squares represent changes of 2 days or less. Weather stations with statistically significant trends at the 5% level were highlighted, whereby the colour corresponds to the classification of each weather station under *Section 5.4.3*. Pale red and blue represent SRZ and WRZ split at the autumn and spring equinox dates of 21 March and 23 September.

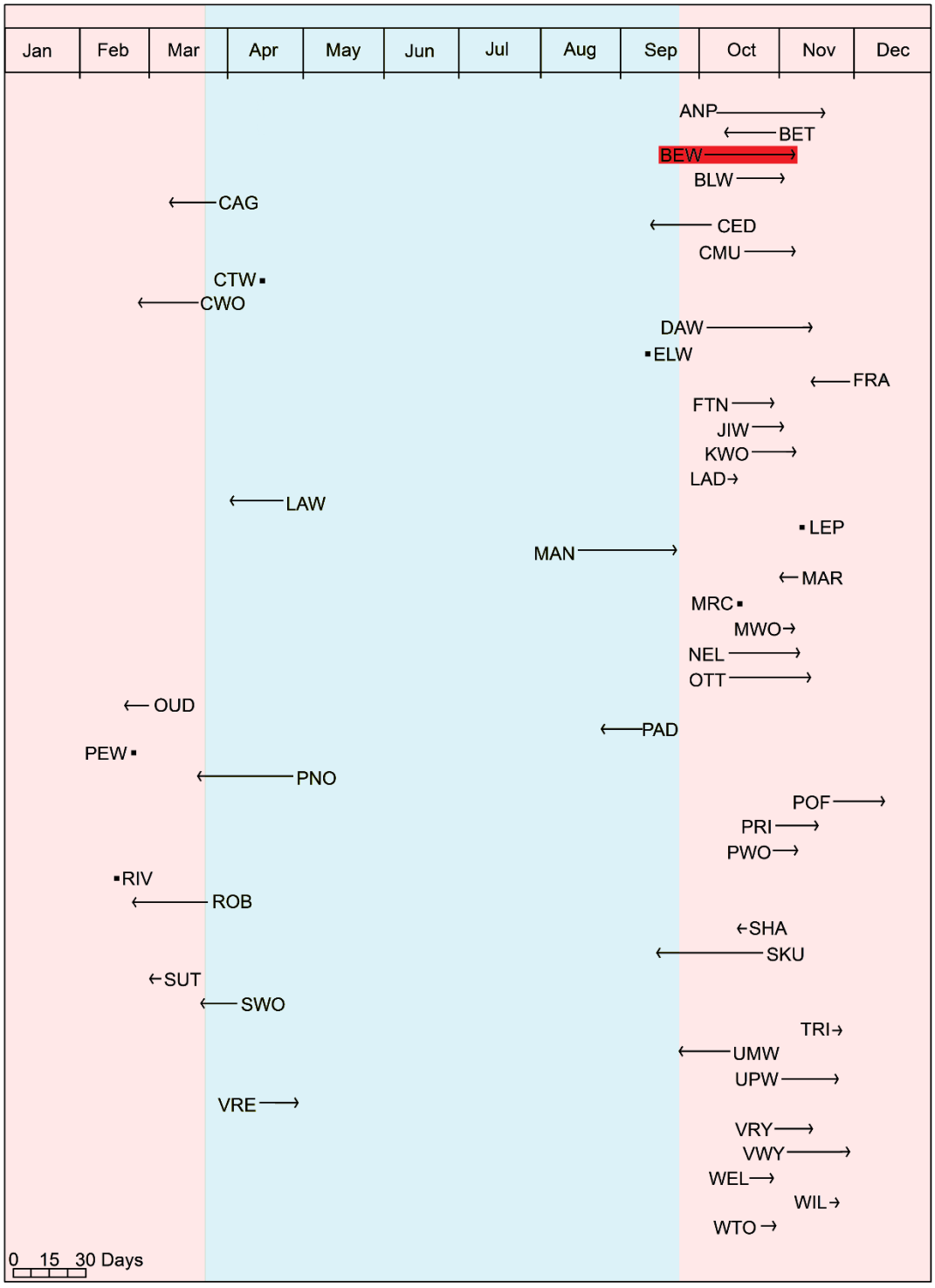


Figure 5.44: Shifts in the 10% dates for individual weather stations for the period of 1987-2016 based on extended regression analysis. Lines with arrows represent individual weather station trends which start from 1987 and end at 2016. Specific values for each trend are under *Appendix G* and *J.1*. Squares represent changes of 2 days or less. Weather stations with statistically significant trends at the 5% level were highlighted, whereby the colour corresponds to the classification of each weather station under *Section 5.4.4*. Pale red and blue represent SRZ and WRZ split at the autumn and spring equinox dates of 21 March and 23 September.

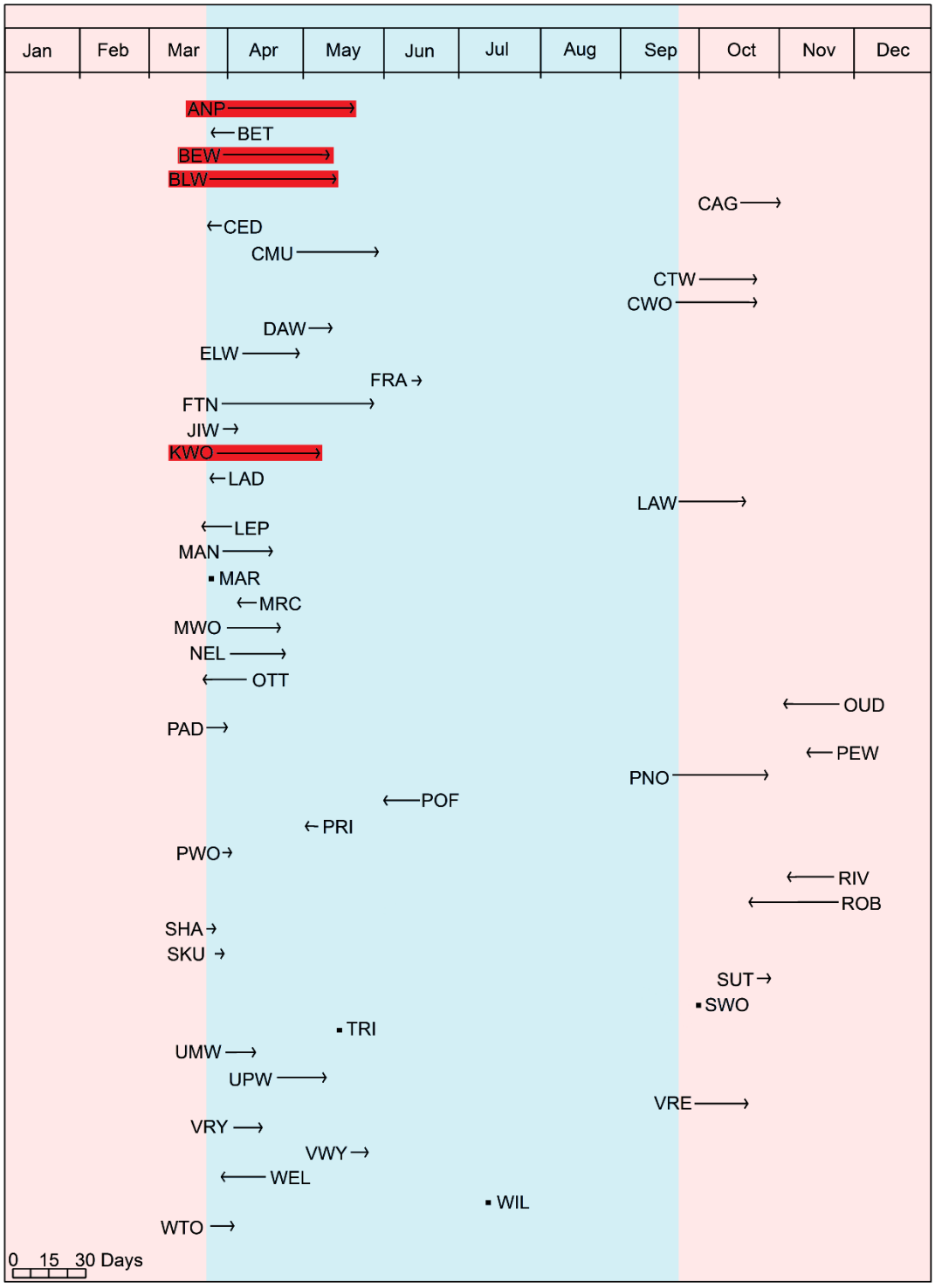


Figure 5.45: Shifts in the 90% dates for individual weather stations for the period of 1987-2016 based on extended regression analysis. Lines with arrows represent individual weather station trends which start from 1987 and end at 2016. Specific values for each trend are under *Appendix G* and *J.2*. Squares represent changes of 2 days or less. Weather stations with statistically significant trends at the 5% level were highlighted, whereby the colour corresponds to the classification of each weather station under *Section 5.4.4*. Pale red and blue represent SRZ and WRZ split at the autumn and spring equinox dates of 21 March and 23 September.

Considering the changes recorded using each individual statistical approach, there are patterns evident from Figures 5.41 to 5.45, where the seasonality scores will be discussed first. Spatially, there are also patterns in the trends for the seasonality scores (Figure 5.46). Almost all of the trends were classed 'as likely as not' which means that the *p values* at these locations were greater than 0.10 and thus there is a high possibility that these trends were detected by chance (Figure 5.46). Of the 46 weather stations, there are 23 locations which demonstrate a shift towards aseasonal conditions, where this was evident across 17 out of 30 SRZ locations and six out of seven WRZ locations (Figure 5.41). The SRZ locations which demonstrate a shift towards weaker seasonality and aseasonal, namely YRZ, conditions are concentrated along the eastern coastal regions and scattered with the Free State, Limpopo and North West, where MWO was the only location which demonstrated a statistically significant trend ($-0.0112.yr^{-1}$, $r = 0.37$, $p = 0.047$; Appendix G; Figure 5.41, 5.46). The WRZ locations are concentrated along the southwestern Cape and western coast (i.e. CAG, CTW, LAW, PNO, SWO and VRE) and were all classified with negative seasonality scores, and as a result an increasing trend in seasonality would essentially result in rainfall which is less seasonal (Figure 5.46). This trend was statistically significant at CAG ($-0.0119.yr^{-1}$, $r = 0.38$, $p = 0.036$; Appendix G; Figure 5.41, 5.46). Only ROB, of the WRZ locations, demonstrated a shift towards stronger WRZ conditions (Figure 5.41). ROB is located near to YRZ locations along the southern coast and within the interior, including OUD, PEW, RIV, VWY and WIL, which also displayed a shift towards WRZ conditions (Figure 5.41, 5.46). These locations with shifts towards WRZ conditions essentially represent where rainfall may be tending towards becoming increasingly seasonal. The remaining YRZ locations instead display a shift towards increasingly seasonal SRZ conditions (Figure 5.41, 5.46). Additionally, the remaining 13 SRZ locations within the northeastern regions of the country all displayed trends towards increasingly seasonal SRZ conditions (Figure 5.41, 5.46).

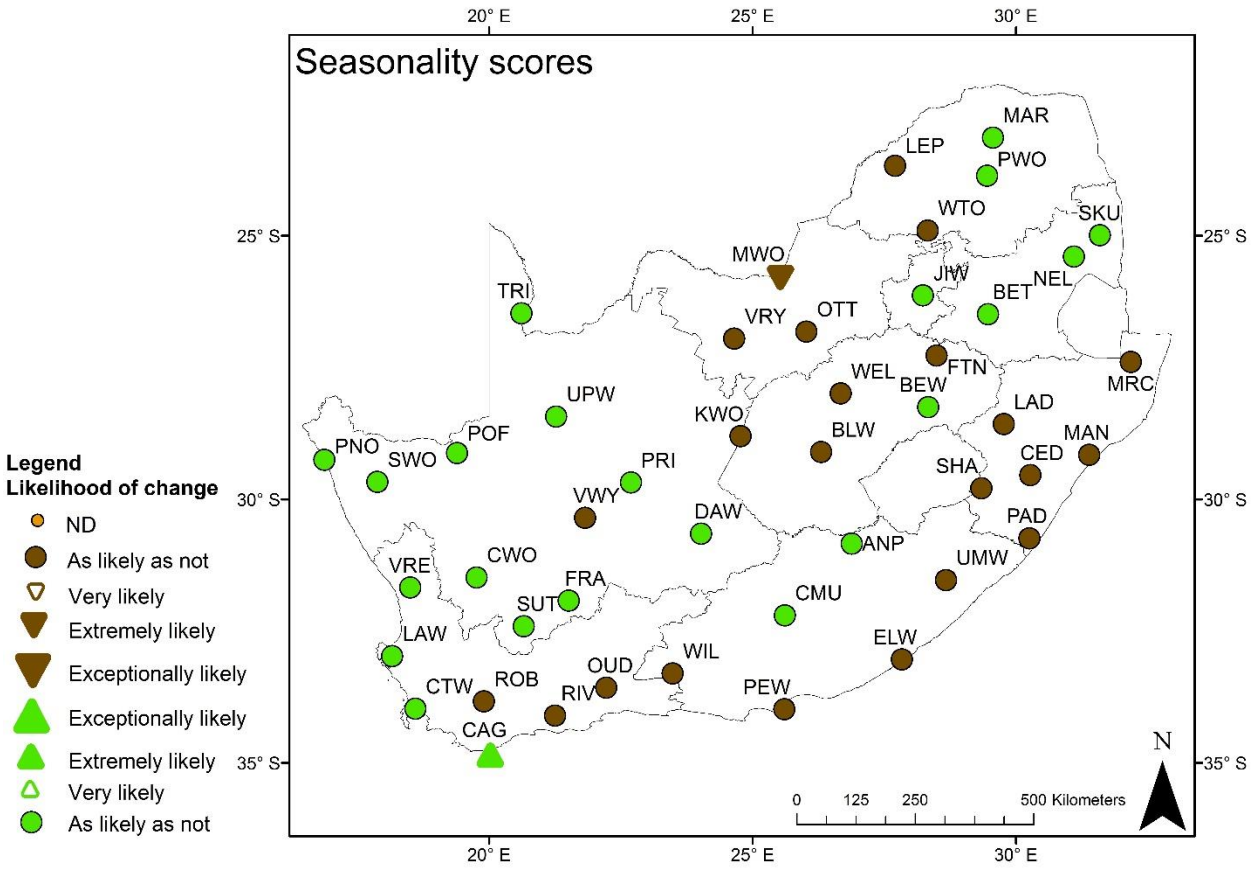


Figure 5.46: Probability of change in rainfall seasonality indicators for the period of 1987-2016. The direction as well as probability of change are indicated. Green and brown represent positive and negative trends respectively. The different levels of probability are based on de Luis et al. (2011) and categorised as: exceptionally likely ($p < 0.01$), extremely likely ($p < 0.05$), very likely ($p < 0.10$) and as likely as not ($p > 0.10$). ND represents where no onset and cessation dates were obtained for a PNO. Considering the maps of the length of the wet season and number of rain days, (O) represents these quantities for the onset and cessation dates while (%) is for the percentile-based approach.

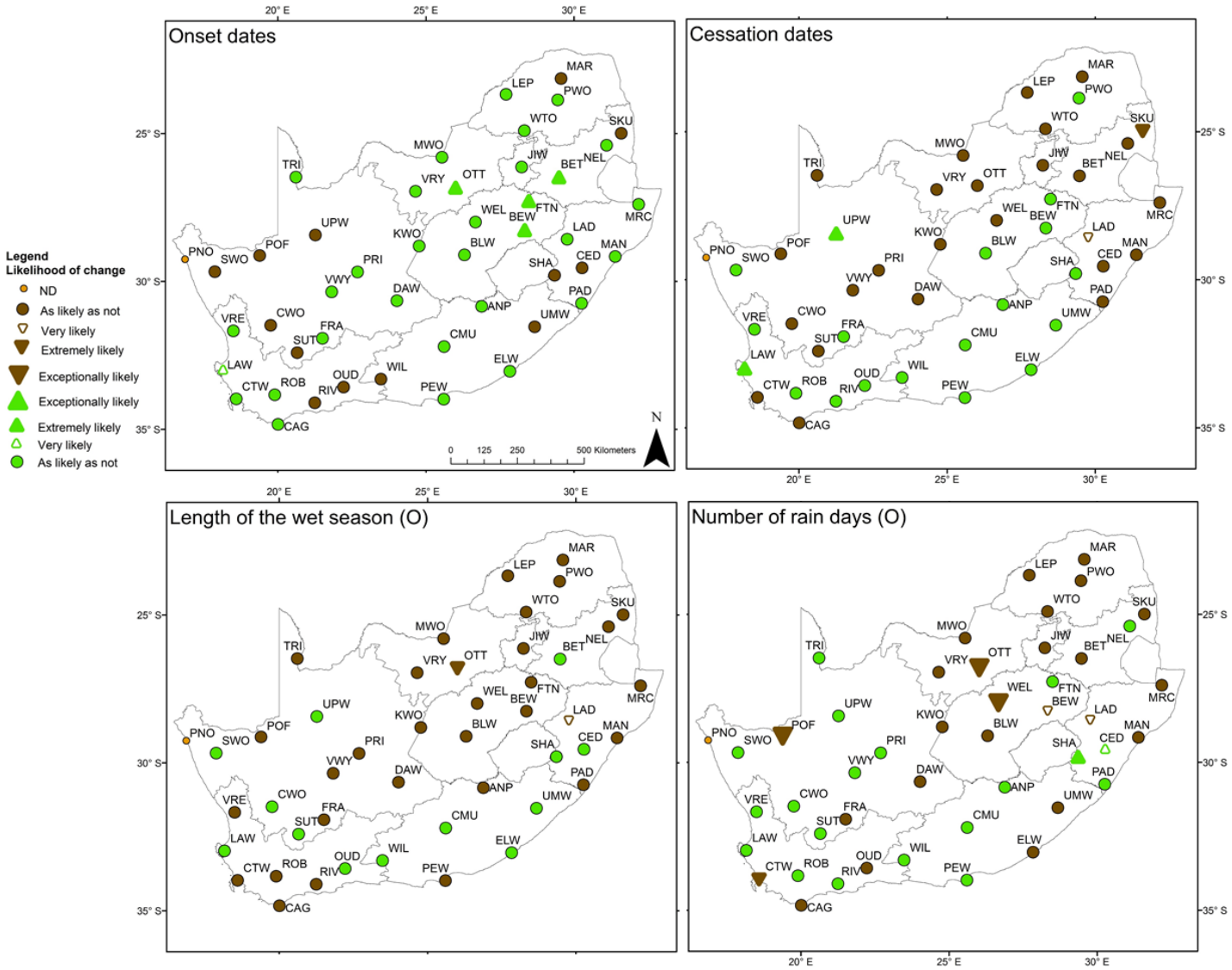


Figure 5.46: Probability of change in rainfall seasonality indicators for the period of 1987-2016. The direction as well as probability of change are indicated. Green and brown represent positive and negative trends respectively. The different levels of probability are based on de Luis et al. (2011) and categorised as: exceptionally likely ($p < 0.01$), extremely likely ($p < 0.05$), very likely ($p < 0.10$) and as likely as not ($p > 0.10$). ND represents where no onset and cessation dates were obtained for a PNO. Considering the maps of the length of the wet season and number of rain days, (O) represents these quantities for the onset and cessation dates while (%) is for the percentile-based approach.

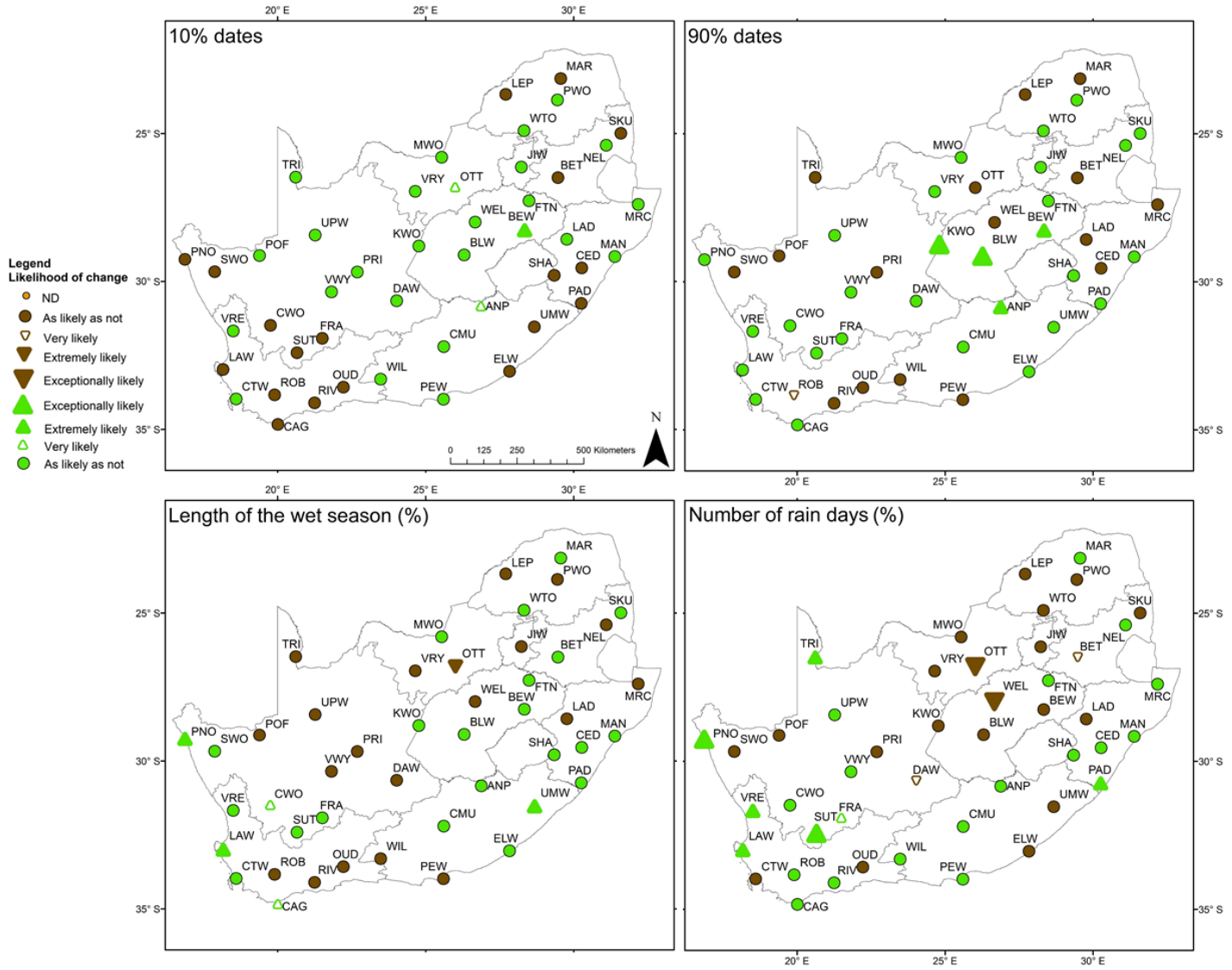


Figure 5.46: Probability of change in rainfall seasonality indicators for the period of 1987-2016. The direction as well as probability of change are indicated. Green and brown represent positive and negative trends respectively. The different levels of probability are based on de Luis et al. (2011) and categorised as: exceptionally likely ($p < 0.01$), extremely likely ($p < 0.05$), very likely ($p < 0.10$) and as likely as not ($p > 0.10$). ND represents where no onset and cessation dates were obtained for a PNO. Considering the maps of the length of the wet season and number of rain days, (O) represents these quantities for the onset and cessation dates while (%) is for the percentile-based approach.

Considering the changes in the onset and cessation dates as well as the length of the wet season, most of these were characterised by *p values* >0.10 (Figure 5.46). For the onset dates, 26 out of 34 SRZ locations demonstrated a shift towards later onset dates (Figure 5.42, 5.46). These trends were statistically significant with an extremely high probability at BET (r = 0.41, p = 0.030), BEW (1.59d.yr^{-1}, r = 0.44, p = 0.017), FTN (1.85d.yr^{-1}, r = 0.37, p = 0.045) and OTT (1.30d.yr^{-1}, r = 0.40, p = 0.037), located within Mpumalanga, the Free State and North West (Appendix G; Figure 5.46). CED, MAR, POF, SHA, SKU, UMW, UPW and WIL demonstrated a shift towards earlier onset dates (Figure 5.42), where these are located in the Eastern and Northern Cape, KwaZulu-Natal, Limpopo, and Mpumalanga (Figure 5.46). The WRZ locations, across the southwestern Cape and western coast, mostly demonstrate shifts towards later onset dates, and WRZ locations with trends towards earlier onset dates (i.e. CWO, SUT and SWO) are located within the Northern Cape (Figure 5.42, 5.46). All of the trends for the WRZ locations had *p values* >0.10, and only the trend at LAW (p = 0.067) was detected with a very high possibility that this trend was not quantified by chance (Figure 5.46). Across the southern coast, where locations are classified as YRZ, PEW displayed a shift towards earlier onset dates, while onset dates were shifting later at OUD and RIV (Figure 5.42, 5.46). For the cessation dates there are 22 SRZ locations which demonstrate a shift towards earlier dates, and this was statistically significant at SKU (-1.50d.yr^{-1}, r = 0.44, p = 0.017; Appendix G), within Mpumalanga, and there was a high possibility of the trend at LAD (p = 0.0083), within KwaZulu-Natal (Appendix G; Figure 5.43, 5.46). The remaining SRZ locations with a shift towards later cessation dates are located within the Eastern Cape, Free State, KwaZulu-Natal, Limpopo and Northern Cape, where this was statistically significant at UPW (1.72d.yr^{-1}, r = 0.47, p = 0.045; Appendix G; Figure 5.43, 5.46). There are four WRZ locations, located within the central and northern WRZ, which demonstrate a shift towards later cessation dates, with a statistically significant trend quantified for LAW (1.72d.yr^{-1}, r = 0.41, p = 0.049; Figure 5.43, 5.46). The YRZ locations (i.e. OUD, PEW and RIV) along the southern coast all demonstrate a shift towards later cessation dates (Figure 5.43). Across all 46 weather stations, 13 locations demonstrated a tentative shift towards a longer wet season, and these are located in the Eastern Cape, KwaZulu-Natal, Mpumalanga, the Northern Cape and the Western Cape (Figure 5.46). The remaining trends

were suggestive of a shorter duration of the wet season, and this was statistically significant at OTT (-1.88d.yr^{-1}, r = 0.37, p = 0.049) and very likely at LAD (p = 0.065; Appendix G; Figure 5.46).

Similar to the onset dates, the SRZ locations mostly display a shift towards later 10% dates, and this was statistically significant at BEW (1.11d.yr^{-1}, r = 0.39, p = 0.039) and very likely at ANP (p = 0.096) and OTT (p = 0.078; Appendix G; Figure 5.44, 5.46). There are ten SRZ locations (i.e. BET, CED, ELW, FRA, LEP, MAR, PAD, SHA, SKU and UMW) which had trends displaying earlier 10% dates, and these are concentrated along the eastern coast as well as Limpopo, the Northern Cape and Mpumalanga (Figure 5.44, 5.46). Seven WRZ locations had trends towards earlier 10% dates, and these are located in the northern and central WRZ area (Figure 5.44, 5.46). Only CTW and VRE, of the WRZ locations, had trends towards later 10% dates (Figure 5.44, 5.46). Locations in the eastern part of the YRZ, including OUD and RIV, demonstrate trends towards earlier 10% dates, whereas PEW and WIL demonstrated a shift towards later 10% dates (Figure 5.44, 5.46). Eleven SRZ locations (i.e. BET, CED, LAD, LEP, MAR, MRC, OTT, PRI, POF, TRI and WEL), located within the Free State, KwaZulu-Natal, Limpopo, North West, the Northern Cape and Mpumalanga, had trends towards earlier 90% dates (Figure 5.45, 5.46). The remaining 23 locations all displayed shifts towards later 90% dates, and statistically significant trends were evident at ANP (1.61d.yr^{-1}, r = 0.42, p = 0.025), BEW (1.48d.yr^{-1}, r = 0.38, p = 0.040), BLW (1.76d.yr^{-1}, r = 0.50, p = 0.006) and KWO (1.47d.yr^{-1}, r = 0.49, p = 0.007; Appendix G; Figure 5.45, 5.46). Six WRZ locations displayed trends towards later 90% dates, and these are mostly located in the northern and southern areas of the WRZ (Figure 5.45, 5.46). Only ROB and SWO had trends towards earlier 90% dates, and at ROB (p = 0.097) this trend was very likely (Appendix G; Figure 5.45, 5.46). All YRZ locations along the southern coast display a shift towards earlier 90% dates (Figure 5.45, 5.46). The majority of trends for the duration of the wet season are suggestive of longer wet seasons, and this was statistically significant at LAW (1.62d.yr^{-1}, r = 0.36, p = 0.048), PNO (2.59d.yr^{-1}, r = 0.45, p = 0.014) and UMW (1.11d.yr^{-1}, r = 0.37, p = 0.048) and very likely at CAG (p = 0.070) and CWO (p = 0.069) locations within the Eastern, Northern and Western Cape provinces (Appendix G; Figure 5.46). Twenty locations demonstrated trends towards a shorter wet season, and this was statistically significant at OTT (-1.77d.yr^{-1}, r = 0.38, p = 0.047; Appendix G; Figure 5.46). All of the YRZ locations along the southern coast and ROB directly adjacent to these had trends displaying a shorter wet

season, and the remaining twenty locations were spread across Gauteng, Free State, KwaZulu-Natal, Limpopo, Mpumalanga, North West and the Northern Cape (Figure 5.46).

Having discussed the spatial patterns for the trends across the individual seasonality metrics, it also important to, prior to discussing the trends in conjunction, discuss the stability of the rainfall regimes classified. Most locations demonstrated relatively high stability, mostly above 80% (Table 5.8), indicating that at least 80% of the years classified were the same as the mean classification. Notable is that relatively low stability may be indicative of relatively high inter-annual variability, and possibly a greater chance of regime shifts from WRZ to YRZ, or vice versa, or from SRZ to YRZ, or vice versa. Locations across the transition region between the SRZ and WRZ demonstrate relatively low stability in the rainfall regimes classified using each rainfall seasonality metric (Table 5.8). This is evident at locations such as DAW, PRI, PEW, RIV, ROB and WIL (Table 5.8). The lowest stability in the seasonality scores was quantified for PEW (37%; Table 5.8), along the southern coast. The classified annual regimes straddled the classification of SRZ, WRZ and YRZ, where PEW was classified as YRZ for 37% of the study period (Table 5.8; Appendix D). Similarly, locations such as ELW, MAN, OUD, PAD, PNO and RIV were classified as SRZ, WRZ and YRZ during the study period. This jump between an annual classification of SRZ, WRZ and YRZ was only evident for these locations using the seasonality scores. For the onset and cessation dates and 10% and 90% dates approaches locations only switched between SRZ and YRZ or WRZ and YRZ. The highest stability for the seasonality scores was evident at locations in the northeastern parts of the SRZ and the southwestern parts of the WRZ, which are the extremes of these rainfall zones (Table 5.8). OUD, PEW and ROB, along the southern coast, demonstrated the lowest stability in the classification of the rainfall regimes using the onset and cessation dates approach, where these locations straddled between the classification of WRZ and YRZ (Table 5.8). The highest stability in the onset and cessation dates classification was again evident at locations in the northeastern parts of the SRZ and the southwestern parts of the WRZ (Table 5.8). OUD, PEW and RIV, located along the southern coast, switched between the classification of WRZ and YRZ and demonstrated the lowest stability in the classification of the rainfall regimes using the 10% and 90% dates approach (Table 5.8). The highest stability considering the 10% and 90% dates approach was again evident at locations in the northeastern parts of the SRZ and the southwestern parts of the WRZ (Table 5.8).

Table 5.8: Stability of the rainfall regimes for each weather station, displaying the number of years classified as the mean classification for the period of 1987-2016, and the percentage stability quantified considering the number of individual years classified as the mean rainfall zone as well as the total number of years classified.

	Seasonality scores		Onset and cessation dates		10% and 90% dates	
Location	Number of years as mean classification	Stability (%)	Number of years as mean classification	Stability (%)	Number of years as mean classification	Stability (%)
ANP	23	77	26	90	26	90
BET	29	100	27	96	28	100
BEW	30	100	27	93	27	93
BLW	26	87	28	97	28	97
CAG	29	97	29	97	28	93
CED	28	93	29	100	29	100
CMU	24	80	27	93	24	83
CTW	30	100	30	100	29	97
CWO	19	63	15	100	26	87
DAW	18	60	23	82	26	90
ELW	21	70	24	83	29	100
FRA	24	80	20	95	18	62
FTN	29	97	28	97	28	97
JIW	30	100	29	100	29	100
KWO	28	93	28	97	28	97
LAD	29	100	29	100	29	100
LAW	30	100	23	100	29	97
LEP	30	100	29	100	29	100
MAN	27	90	26	90	29	100
MAR	30	100	27	93	28	97
MRC	30	100	24	83	29	100
MWO	30	100	27	93	29	100
NEL	29	100	29	100	29	100
OTT	29	97	29	100	29	100
OUD	26	90	8	57	16	53
PAD	23	77	26	90	29	100
PEW	11	37	19	70	18	60
PNO	20	67	0	0	29	97
POF	25	83	8	100	19	66
PRI	18	60	17	81	24	83
PWO	30	100	28	97	29	100
RIV	18	60	13	54	20	67
ROB	16	53	25	100	17	57
SHA	30	100	29	100	29	100
SKU	30	100	28	97	29	100
SUT	24	83	15	79	19	63
SWO	26	90	21	95	27	93
TRI	26	90	20	95	28	97
UMW	29	97	26	90	29	100
UPW	25	83	18	95	23	79
VRE	26	87	6	100	29	97
VRY	29	97	29	100	29	100
VWY	21	70	15	79	19	66
WEL	28	93	26	93	29	100
WIL	16	53	21	81	22	76
WTO	30	100	28	97	29	100

Having quantified shifts in rainfall seasonality using numerous statistical methods, it is important to consider the agreement across these approaches (Figure 5.47; Table 5.9). This is especially important for corroboration of these shifts, where these may also be further corroborated by considering the shifts in monthly rainfall amount which will be discussed under *Chapter 6 (Discussion)*. The trajectory of the changes quantified using each approach for each weather station is captured in Table 5.9, and agreement amongst the approaches for individual locations is captured in Figure 5.47. There are 16 locations which demonstrate agreement in the trajectory of change across all three approaches, and the remaining 30 locations demonstrate agreement between two of the three approaches (Figure 5.47). Over a longer temporal period there may turn out to be a higher level of agreement across the approaches. Weather stations with complete agreement across all three approaches are located in the Eastern Cape, Gauteng, KwaZulu-Natal, Limpopo, Mpumalanga, the Northern Cape and the Western Cape (Figure 5.47). With additional weather stations there may have been more spatial patterns evident (Figure 5.47). Notably, there are already spatial patterns evident (Figure 5.47). Concentrated across the eastern coast, southwestern Cape and western coast, and scattered in the eastern interior, there are numerous locations where there was agreement between at least two approaches for tentative shifts towards aseasonal, year-round rainfall conditions (Figure 5.47). Along the southern coast, there was agreement for rainfall regimes tentatively tending towards WRZ conditions (Figure 5.47). Within the interior, it is evident that the majority of locations demonstrated tentative shifts towards SRZ conditions (Figure 5.47).

Table 5.9: Description of the rainfall seasonality shifts across the seasonality scores, onset and cessation dates as well as the wet season length (wet season change description), and the 10% and 90% dates and the length of the wet season (wet season change description). The direction of trends towards a rainfall zone are used to describe these changes. This is highlighted, where red represents a trend towards SRZ conditions, blue towards WRZ conditions and yellow towards YRZ conditions. Statistically significant changes at the 0.05 level are denoted using an asterisk (*) and corresponds to *Figure 5.41-5.45*. The specific details for this table are presented under *Appendix G, H, I and J*.

Location	Seasonality scores	Onset date	Cessation dates	Wet season change description	10% dates	90% dates	Wet season change description
ANP	SRZ	Later onset	Later cessation	Shorter SRZ	Later 10%	Later 90%*	Longer SRZ, YRZ
BET	SRZ	Later onset*	Earlier cessation	Longer SRZ, YRZ	Earlier 10%	Earlier 90%	Longer SRZ, YRZ

BEW	SRZ	Later onset*	Later cessation	Shorter SRZ	Later 10%*	Later 90%*	Longer SRZ, YRZ
BLW	YRZ	Later onset	Later cessation	Shorter SRZ	Later 10%	Later 90%*	Longer SRZ, YRZ
CAG	YRZ*	Later onset	Earlier cessation	Shorter WRZ	Earlier 10%	Later 90%	Longer WRZ, YRZ
CED	YRZ	Earlier onset	Earlier cessation	Longer SRZ, YRZ	Earlier 10%	Earlier 90%	Longer SRZ, YRZ
CMU	SRZ	Later onset	Later cessation	Longer SRZ, YRZ	Later 10%	Later 90%	Longer SRZ, YRZ
CTW	YRZ	Later onset	Earlier cessation	Shorter WRZ	Later 10%	Later 90%	Longer WRZ, YRZ
CWO	SRZ	Earlier onset	Earlier cessation	Longer WRZ, YRZ	Earlier 10%	Later 90%	Longer WRZ, YRZ
DAW	SRZ	Later onset	Earlier cessation	Shorter SRZ	Later 10%	Later 90%	Shorter SRZ
ELW	YRZ	Later onset	Later cessation	Longer SRZ, YRZ	Earlier 10%	Later 90%	Longer SRZ, YRZ
FRA	SRZ	Later onset	Later cessation	Shorter SRZ	Earlier 10%	Later 90%	Longer SRZ, YRZ
FTN	YRZ	Later onset*	Later cessation	Shorter SRZ	Later 10%	Later 90%	Longer SRZ, YRZ
JIW	SRZ	Later onset	Earlier cessation	Shorter SRZ	Later 10%	Later 90%	Shorter SRZ
KWO	YRZ	Later onset	Earlier cessation	Shorter SRZ	Later 10%	Later 90%*	Longer SRZ, YRZ
LAD	YRZ	Later onset	Earlier cessation	Shorter SRZ	Later 10%	Earlier 90%	Shorter SRZ
LAW	YRZ	Later onset	Later cessation*	Longer WRZ, YRZ	Earlier 10%	Later 90%	Longer WRZ, YRZ*
LEP	YRZ	Later onset	Earlier cessation	Shorter SRZ	Earlier 10%	Earlier 90%	Shorter SRZ
MAN	YRZ	Later onset	Earlier cessation	Shorter SRZ	Later 10%	Later 90%	Longer SRZ, YRZ
MAR	SRZ	Earlier onset	Earlier cessation	Shorter SRZ	Earlier 10%	Earlier 90%	Longer SRZ, YRZ
MRC	YRZ	Later onset	Earlier cessation	Shorter SRZ	Later 10%	Earlier 90%	Shorter SRZ
MWO	YRZ*	Later onset	Earlier cessation	Shorter SRZ	Later 10%	Later 90%	Longer SRZ, YRZ
NEL	SRZ	Later onset	Earlier cessation	Shorter SRZ	Later 10%	Later 90%	Shorter SRZ
OTT	YRZ	Later onset*	Earlier cessation	Shorter SRZ*	Later 10%	Earlier 90%	Shorter SRZ*
OUD	WRZ	Earlier onset	Later cessation	Longer YRZ	Earlier 10%	Earlier 90%	Shorter YRZ, WRZ
PAD	YRZ	Later onset	Earlier cessation	Shorter SRZ	Earlier 10%	Later 90%	Longer SRZ, YRZ
PEW	WRZ	Later onset	Later cessation	Shorter YRZ, to WRZ	Later 10%	Earlier 90%	Shorter YRZ, WRZ
PNO	YRZ	ND	ND	ND	Earlier 10%	Later 90%	Longer WRZ, YRZ*
POF	SRZ	Earlier onset	Earlier cessation	Shorter SRZ	Later 10%	Earlier 90%	Shorter SRZ
PRI	SRZ	Later onset	Earlier cessation	Shorter SRZ	Later 10%	Earlier 90%	Shorter SRZ
PWO	SRZ	Later onset	Later cessation	Shorter SRZ	Later 10%	Later 90%	Shorter SRZ

RIV	WRZ	Earlier onset	Later cessation	Shorter YRZ, to WRZ	Earlier 10%	Earlier 90%	Shorter YRZ, WRZ
ROB	WRZ	Later onset	Later cessation	Shorter WRZ	Earlier 10%	Earlier 90%	Shorter WRZ
SHA	YRZ	Earlier onset	Later cessation	Longer SRZ, YRZ	Earlier 10%	Later 90%	Longer SRZ, YRZ
SKU	SRZ	Earlier onset	Earlier cessation*	Shorter SRZ	Earlier 10%	Later 90%	Longer SRZ, YRZ
SUT	SRZ	Earlier onset	Earlier cessation	Longer WRZ, YRZ	Earlier 10%	Later 90%	Longer WRZ, YRZ
SWO	YRZ	Earlier onset	Later cessation	Longer WRZ, YRZ	Earlier 10%	Earlier 90%	Longer WRZ, YRZ
TRI	SRZ	Later onset	Earlier cessation	Shorter SRZ	Later 10%	Earlier 90%	Shorter SRZ
UMW	YRZ	Earlier onset	Later cessation	Longer SRZ, YRZ	Earlier 10%	Later 90%	Longer SRZ, YRZ*
UPW	SRZ	Earlier onset	Later cessation*	Longer SRZ, YRZ	Later 10%	Later 90%	Shorter SRZ
VRE	YRZ	Later onset	Later cessation	Shorter WRZ	Later 10%	Later 90%	Longer WRZ, YRZ
VRY	YRZ	Later onset	Earlier cessation	Shorter SRZ	Later 10%	Later 90%	Shorter SRZ
VWY	WRZ	Later onset	Earlier cessation	Shorter SRZ	Later 10%	Later 90%	Shorter SRZ
WEL	YRZ	Later onset	Earlier cessation	Shorter SRZ	Later 10%	Earlier 90%	Shorter SRZ
WIL	WRZ	Earlier onset	Later cessation	Longer SRZ, YRZ	Later 10%	Earlier 90%	Shorter YRZ, WRZ
WTO	YRZ	Later onset	Earlier cessation	Shorter SRZ	Later 10%	Later 90%	Longer SRZ, YRZ

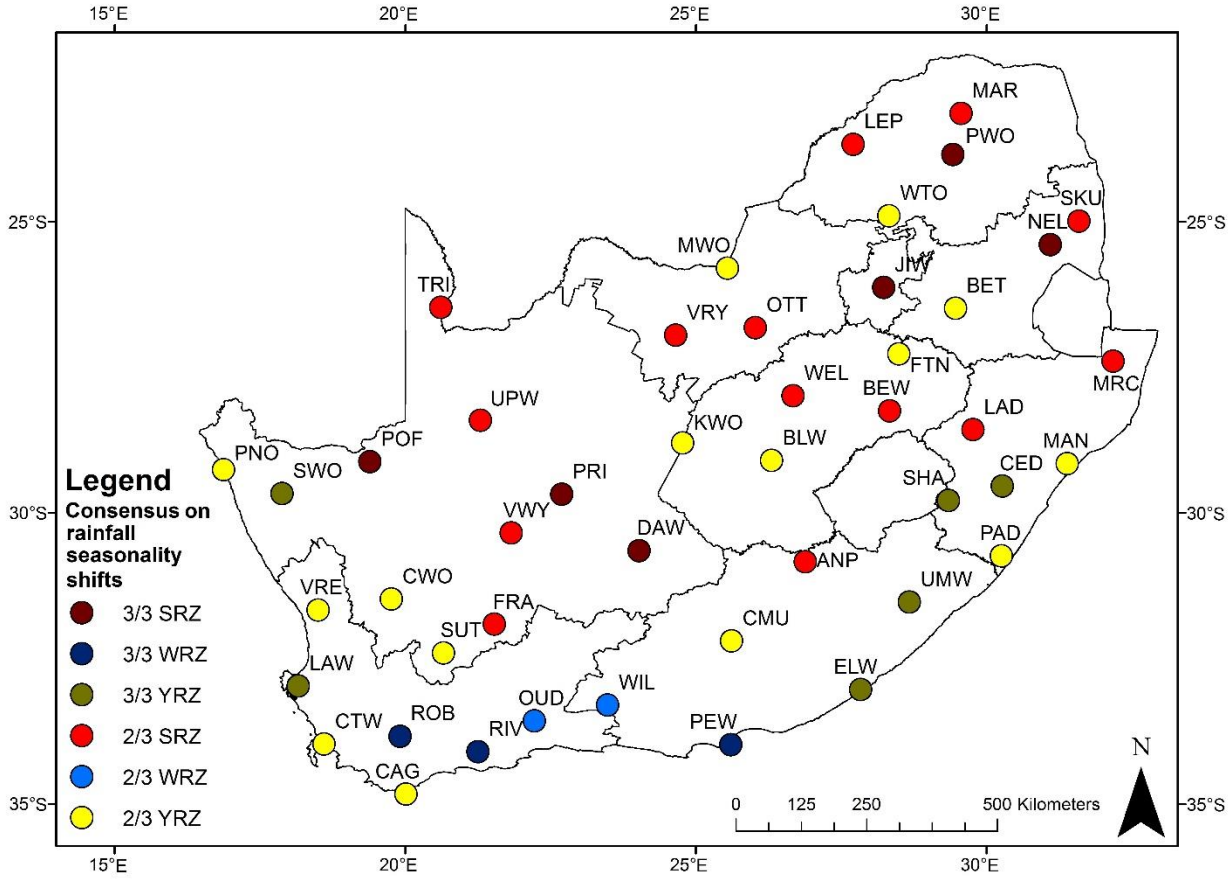


Figure 5.47: Consensus regarding the direction of rainfall seasonality trends across South Africa based on Table 5.9.

Having highlighted the changes observed using each approach as well as the spatial patterns of these changes, it is also important to highlight the statistically significant changes across the weather stations, noting these for single locations. Statistically significant changes reject the null hypothesis, where the null hypothesis suggests that no changes occurred. Hence, a statistically significant change is suggested to be statistical 'fact' and the chance that this change was observed by accident is less than that of the *p value*. Given this, it is important to highlight the locations which demonstrate statistically significant changes in rainfall seasonality. As mentioned earlier in this section, there are 23 out 46 locations with at least one statistically significant trend quantified (Appendix G). These locations are discussed in the paragraphs which follow, where the locations with two or more statistically significant trends are explored first.

OTT, located in the North West, displayed five statistically significant trends for the onset dates (1.30d.yr^{-1}, r = 0.40, p = 0.037) and for both methods considering the length of the wet season (O: -1.88d.yr^{-1}, r = 0.37, p = 0.049; %: -1.77d.yr^{-1}, r = 0.38, p = 0.047), and the number of rain days (O: -1.10d.yr^{-1}, r = 0.52, p = 0.004; %: -0.94d.yr^{-1}, r = 0.52, p = 0.004; Appendix G, I, J). The onset dates shifted towards occurring later in the year, where this was also evident across the 10% dates, with a very high possibility that this trend was not detected by chance (p = 0.078; Appendix G; Figure 5.42, 5.44; 5.46). The onset and 10% dates trends were quantified at a similar magnitude with both dates moving from early October to early November (Figure 5.42, 5.44; Appendix I, J). For these dates an extended linear regression analysis suggests that if these trends persist it is estimated that between 2046 and 2054 the summer solstice may no longer occur during the wet season (Appendix I, J). Both the cessation and 90% dates displayed trends towards occurring earlier during the year (Figure 5.43, 5.45, 5.46), thus demonstrating a decrease in the length of the wet season which was statistically significant across both methods (Appendix G; Figure 5.46). On the other hand, the seasonality scores demonstrated a statistically insignificant shift towards a lower degree of summer seasonality (Figure 5.41, 5.46; Appendix H), which may suggest a change towards less summer rainfall. Hence, there was only agreement amongst the approaches of onset and cessation dates and the 10% and 90% dates (Table 5.9; Figure 5.47).

At BEW, located in the Free State, the changes calculated in the onset (1.59d.yr^{-1}, r = 0.44, p = 0.017) and 10% (1.11d.yr^{-1}, r = 0.39, p = 0.039) dates were statistically significant suggesting later dates (Appendix G; Figure 5.42, 5.44, 5.46). If these changes persist it is estimated that by 2059, for the 10% dates, the summer solstice may no longer occur during the wet season (Appendix I, J). There was a statistically significant shift in 90% dates (1.48d.yr^{-1}, r = 0.38, p = 0.040; Appendix G; Figure 5.45, 5.46), suggesting later occurrence of this date, and this was also evident for the cessation dates although at a smaller, statistically insignificant rate (Appendix I, J; Figure 5.43, 5.45, 5.46). Since the magnitude of change for the onset dates was considerably larger than for the cessation dates, this method suggested a decrease in the length of the wet season (-0.72d.yr^{-1}) whereas an increase in the length was suggested for the percentile-based approach (0.36d.yr^{-1}; Appendix G; Figure 5.46). A decrease in the length of the wet season here demonstrates stronger summer rainfall conditions with the wet season more concentrated around the summer solstice.

The seasonality scores demonstrated a very weak statistically insignificant increasing trend over the study period indicating a move towards a higher degree of summer rainfall seasonality (Figure 5.41, 5.46; Appendix H). Hence, agreement in the suggested change was between seasonality scores and the onset and cessation dates approach (Table 5.9; Figure 5.47).

At LAW, located in the Western Cape, the cessation dates demonstrated a statistically significant shift from mid August to early October, and if this trend persists it is estimated that the summer solstice may occur during the wet season by 2061 (1.72d.yr^{-1}, r = 0.41, p = 0.049; Figure 5.43, 5.46; Appendix G, I). The 90% dates also displayed a shift towards occurring later during the year (Figure 5.45, 5.46; Appendix J). The trend quantified for onset dates suggest a considerably large, very likely shift of 1.38d.yr^{-1} (r = 0.39, p = 0.067) moving from early May to late June, where it is estimated that if this trend persists in 2016 the winter solstice may no longer occur during the wet season (Figure 5.42, 5.46; Appendix G, I). This was already evident by the late onset date of 4 July in 2014 (Appendix E). The shift in onset had a very high possibility that this trend was not detected by chance (p = 0.067), and with additional years of data, this trend may have been statistically significant (Appendix G; Figure 5.46). Although the onset dates are suggested to occur later, the length of the wet season for this and the percentile-based approaches suggest an increase, potentially indicating a shift towards YRZ conditions (Figure 5.46; Appendix G, I, J). This shift towards a longer wet season (1.62d.yr^{1}, r = 0.36, p = 0.048) was only statistically significant for the percentile-based approach, and there was also a statistically significant increase in the number of rain days (0.45d.yr^{-1}, r = 0.38, p = 0.039; Figure 5.46; Appendix G). On the other hand, the trend quantified for seasonality scores suggest a decrease in the degree winter seasonality (Figure 5.41, 5.46; Appendix H), moving towards YRZ conditions where a reduction in winter rainfall may also be expected. The shifts in rainfall seasonality at LAW demonstrated agreement across all the approaches (Table 5.9; Figure 5.47).

At PNO, within the Northern Cape, the shifts quantified for the wet season length (2.59d.yr^{-1}, r = 0.45, p = 0.014) and number of rain days (1.41d.yr^{-1}, r = 0.75, p < 0.0001), for the percentile-based approach, were statistically significant (Figure 5.46; Appendix G). Considering the trend calculated for the length of the wet season, an increase is suggested which may indicate a shift towards YRZ conditions (Figure 5.46; Appendix G). This is evident from an earlier 10% date and a later 90% date

(Figure 5.44, 5.45, 5.46). Since no onset and cessation dates were obtained for this location, only the shifts in the seasonality scores may be used for comparative purposes. The seasonality scores demonstrated an increase, however, this relationship ($r = 0.01$, $p = 0.946$) is very weak suggesting very little or no change in the seasonality scores (Figure 5.41, 5.46; Appendix G). Although weak, the change in seasonality scores suggests a shift towards YRZ conditions from a reduction in the degree of winter seasonality (Figure 5.41, 5.46). Hence, there is agreement across these two approaches (Table 5.9; Figure 5.47).

WEL, located in the Free State, only demonstrated two statistically significant shifts towards a decrease in rain days (O: $-0.96 d.yr^{-1}$, $r = 0.48$, $p = 0.009$; %: $-0.86 d.yr^{-1}$, $r = 0.60$, $p = 0.001$; Appendix G; Figure 5.46). Since shifts in the rain days do not describe shifts in rainfall seasonality without considering other measurements and no other quantities demonstrated statistically significant changes, the shifts at WEL will not be explored in detail. Any statistically significant shifts, and the general shifts in the number of rain days are presented under Appendix G and Figure 5.46 and will be considered further under the next *Chapter 6 (Discussion)*. Next, the individual weather stations which demonstrated one statistically significant trend in all other quantities, excluding the number of rain days, were considered. This includes ten locations across the country (Appendix G).

For ANP, located in the Eastern Cape, the trend quantified for the 90% dates was statistically significant, where this trend suggests a shift towards later dates at a rate of $1.61 d.yr^{-1}$ ($r = 0.42$, $p = 0.025$; Appendix G; Figure 5.45, 5.46). If this trend persists it is estimated that by 2037 the winter solstice may occur during the wet season (Appendix J). However, there were already three years following and including 2008 where the winter solstice occurred during the wet season dates (Appendix F). The cessation dates, although split by numerous change points, also demonstrated a shift towards occurring later (Appendix G). If this trend persists, it is estimated that the winter solstice will occur during the wet season by 2017, and similar to the 90% dates this occurred during the study period (Appendix F). Both the onset and 10% dates displayed a shift towards dates moving from October to November, and with additional years of monitoring the 10% dates may come to demonstrate a statistically significant trend (Figure 5.42, 5.44, 5.46). The trends calculated for the 10% and 90% dates display a shift towards a longer wet season (Figure 5.46; Appendix G, J). For the onset and cessation dates a shift towards a shorter wet season was evident

(Figure 5.46; Appendix G, I). Similarly, the shift quantified for the seasonality scores suggested an increase in the degree of summer seasonality and potentially a shift towards more rainfall concentrated during the summer months (Figure 5.41, 5.46; Appendix H). Hence, agreement in the direction of change is evident across the onset and cessation dates and the seasonality scores (Figure 5.47; Table 5.9).

For BET, within Mpumalanga, a statistically significant shift towards earlier onset dates was quantified (-1.67d.yr^{-1}, r = 0.41, p = 0.030; Figure 5.42, 5.46; Appendix G). However, a change point was detected for this trend, where the trend from and prior to 2005 suggested later onset dates (Appendix G; Figure 5.43). When considering this change point, the trajectory of the shifts in onset and 10% disagree (Appendix I, J; Figure 5.42, 5.44, 5.46). Both the trends quantified for the cessation and 90% dates suggest that these dates were tending towards occurring earlier in the year (Figure 5.43, 5.45, 5.46; Appendix I, J). When considering shifts for the length of the wet season of each method, the percentile-based approach suggests a longer wet season with the onset and cessation dates suggesting a similar shift at a larger rate (Appendix G; Figure 5.46). The suggested trend, although very weak considering the *r* and *p values*, in the annual seasonality scores indicates a shift towards increasing summer seasonality which may indicate a shift towards more summer rainfall (Figure 5.41, 5.46; Appendix G, H). Agreement in the direction of change is thus demonstrated between the percentile-based approach and for the onset and cessation dates (Table 5.9; Figure 5.47).

At BLW, located in the Free State, the shift towards later 90% dates was statistically significant (1.76d.yr^{-1}, r = 0.50, p = 0.006; Appendix G; Figure 5.45, 5.46). If this trend persists, it is estimated that by 2037 the winter solstice may occur during the wet season (Appendix J). The trend calculated for cessation dates also suggested a shift towards later dates, although the rate of change was considerably lower at 0.77d.yr^{-1} and this trend was not statistically significant (Figure 5.43, 5.46; Appendix I). Both the trends quantified for the onset and 10% dates suggested a shift towards occurring later (Figure 5.42, 5.44, 5.46; Appendix I, J). The trend quantified for the percentile-based approach suggested an increase in the length of the wet season, whereas for the onset and cessation dates a reduction in the wet season duration was quantified (Figure 5.46; Appendix G). A shift towards a lower degree of summer seasonality was demonstrated (Figure

5.41, 5.46), and this shift together with those for the percentile-based approach may suggest a shift towards YRZ conditions with a reduction in summer rainfall expected (Appendix H, I; Table 5.9; Figure 5.47).

For CAG, within the Western Cape, the annual seasonality scores demonstrated a statistically significant shift (0.0119, r = 0.38, p = 0.036) which indicates a trend towards increased YRZ conditions, lower winter seasonality as well as a reduction in winter rainfall (Figure 5.41, 5.46; Appendix G, H). If this trend persists, it is estimated that by 2035 YRZ conditions may occur at CAG (Appendix H), where YRZ conditions were quantified for 2014 (Appendix D). The trend quantified for onset dates demonstrated a shift towards occurring later, whereas the 10% dates are suggested to have shifted earlier (Figure 5.42, 5.44, 5.46). A very weak *r value* was quantified for the cessation dates suggesting earlier dates, whereas the 90% dates shifted towards occurring later (Figure 5.43, 5.45, 5.46; Appendix G, I, J). The tentative trend towards an increase in the duration for the wet season occurred with a very high probability (p = 0.070) for the percentile-based approach, and a decrease in the duration for the onset and cessation dates (Figure 5.46). When considering the agreement amongst these methods, the shifts in the percentile-based approach and seasonality scores demonstrated agreement (Table 5.9; Figure 5.47).

The onset dates at FTN, within the Free State, shifted from late September to late November, and this change was statistically significant (1.85d.yr^{-1}, r = 0.37, p = 0.045; Appendix G, I; Figure 5.42, 5.46). Similarly, the trend quantified for 10% dates also suggested a shift towards occurring later during the year (Appendix J; Figure 5.44). Both the trends calculated for the cessation and 90% dates demonstrated a shift towards later dates (Figure 5.43, 5.45, 5.46; Appendix I, J). For the percentile-based approach a shift towards a longer wet season was evident, whereas a shift towards a shorter wet season was evident for the onset and cessation dates (Appendix G; Figure 5.46). A decrease in the seasonality scores suggests a shift towards a lower degree of summer seasonality and potentially YRZ conditions (Figure 5.41, 5.46; Appendix H). Hence, there is agreement between the seasonality score and percentile shifts at FTN, and this disagrees with the onset, a statistically significant trend, and cessation date shifts collectively (Table 5.9; Figure 5.47).

At KWO, located in the Northern Cape, the trend calculated for 90% dates demonstrated a statistically significant shift towards occurring later (1.47d.yr^{-1}, r = 0.49, p = 0.007; Appendix G, J; Figure 5.45, 5.46). Conversely, the cessation dates displayed a shift towards occurring earlier, but an *r value* of 0.07 and a *p value* of 0.700 may suggest little to no change occurred (Appendix G, I; Figure 4.43, 5.46). Both the trends quantified for the onset and 10% dates suggest a shift towards occurring later (Figure 5.42, 5.44, 5.46; Appendix G, H, I). The trajectory of shifts for the onset and cessation dates suggest a shorter wet season length, however, a considerably weak *r value* and a low *p value* was quantified (Figure 5.46; Appendix G). The trends quantified for the 10% and 90% dates suggest an increase in the wet season length with a relatively stronger *r value* and higher *p value* for this time series trend (Figure 5.46; Appendix G). The trend quantified for the seasonality scores suggests a decrease in the degree of summer seasonality (Figure 5.41, 5.46; Appendix H), and as a result there is agreement between the percentile-based approach and the seasonality scores (Table 5.9; Figure 5.47).

The seasonality scores at MWO, within the North West, demonstrated a statistically significant shift towards lower seasonality scores (-0.0112.yr^{-1}, r = 0.37, p = 0.047; Appendix G, H; Figure 5.41, 5.46). This shift suggests a change towards YRZ conditions and a reduction in the degree of summer seasonality. The trends for the onset and 10% dates suggest a shift towards occurring later during the year, with a considerably weak shift demonstrated for the 10% dates (Figure 5.42, 5.44, 5.46; Appendix I, J). The 90% and cessation dates disagreed on the trajectory of change with a later date suggested for the 90% dates and an earlier date for the cessation dates (Figure 5.43, 5.45, 5.46; Appendix I, J). Hence, the trajectory of change for the length of the wet season was also disagreed upon, and the percentile approach suggested an increase and the onset and cessation date approach suggested a decrease (Appendix G; Figure 5.46). Agreement is evident between the seasonality scores and the percentile-based approach (Table 5.9; Figure 5.47).

The trend calculated for cessation dates at SKU, within Mpumalanga, was statistically significant (-1.50d.yr^{-1}, r = 0.44, p = 0.017) suggesting a shift from early May to late March (Figure 5.43, 5.46; Appendix G, I). The 90% dates were suggested to shift later during the year, however, this shift was quantified with a very high *p value* of 0.657 indicating little to no change (Appendix G, J; Figure 5.45, 5.46). The shifts quantified for the onset dates, 10% dates and the seasonality scores also

demonstrated *p values* above 0.10 suggesting little to no change amongst these quantities (Appendix G). However, the onset and 10% dates both demonstrated a shift towards occurring later during the year (Figure 5.42, 5.44, 5.46; Appendix I, J). The 10% dates also demonstrated a change point, where after 2012 there was a shift towards earlier dates at a larger rate of -11.9d.yr^{-1} (r = 0.73, p = 0.272; Appendix J). An increase in the wet season duration was quantified for the percentile-based approach, whereas a reduction was quantified for the onset and cessation dates (Figure 5.46). When considering the trajectory of these changes, there was agreement between the seasonality scores and the onset and cessation date quantities (Appendix G, H, I; Table 5.9), suggesting a shift towards a shorter summer wet season and an increase in the degree of summer seasonality with a potential increase in summer rainfall (Figure 5.41, 5.46, 5.47).

At UMW, within the Eastern Cape, the length of the wet season for the percentile-based approach was calculated as a statistically significant increasing trend (1.11d.yr^{-1}, r = 0.37, p = 0.048; Figure 5.46; Appendix G). An increase in the length was also demonstrated for the onset and cessation dates approach (Figure 5.46; Appendix G). Both of these shifts displayed change points, at 2001 and 2003 for the onset and cessation dates and the percentile approach respectively, whereby the shift prior to and after the change points were negative for both approaches (Appendix G). The trend quantified for onset and 10% dates suggests a shift from occurring during October to September (Figure 5.42, 5.44, 5.46; Appendix I, J). Similarly, the trends calculated for cessation and 90% dates demonstrated agreement in a shift towards earlier dates (Figure 5.43, 5.45, 5.46). The shifts for both approaches suggest an increase in the length of the wet season (Appendix I, H; Figure 5.46). When considering the seasonality scores, there is agreement amongst all approaches suggesting a shift towards YRZ conditions (Table 5.9; Figure 5.47).

The trend quantified for the cessation dates at UPW, located in the Northern Cape, indicates a statistically significant (1.72d.yr^{-1}, r = 0.47, p = 0.045) shift towards occurring later during the year (Figure 5.43, 5.46; Appendix G). If this trend persists, it is estimated that by 2034 the winter solstice may occur during the wet season (Appendix I). Similarly, the shift quantified for the 90% dates suggests a shift towards later dates (Figure 5.45, 5.46; Appendix G, I). There is disagreement amongst the onset and 10% dates, whereby the onset and 10% dates display a shift towards earlier and later dates respectively (Appendix G, I, J; Figure 5.42, 5.44, 5.46). The shifts in the length of

the wet season for both approaches were split by change points (Appendix G). These shifts also demonstrated disagreement whereby the trends for the onset and cessation dates suggest an increase in the wet season length, whereas for the 10% and 90% dates a decrease is suggested (Appendix G; Figure 5.46). The shift quantified for seasonality scores suggests an increase and essentially a shift towards stronger summer seasonality (Appendix G, I; Figure 5.41). The shifts quantified at UPW demonstrate agreement when considering the changes in the seasonality scores and for the percentile-based approach for a shorter wet season duration (Table 5.9; Figure 5.47).

Having considered in detail the locations which display statistically significant shifts, it is suggested that continuous monitoring occurs at these weather stations as it was demonstrated that there was considerable agreement amongst the suggested trajectory of change across all the approaches (Table 5.9; Figure 5.47). Not only is it important to monitor these locations, but continuous monitoring of the locations which demonstrated relatively high *r values* above 0.30 and *p values* below 0.10 is also important as tentative shifts may be suggested from the direction and magnitude of these trends (Appendix G; Figure 5.46, 5.47). Over a longer temporal period these shifts may be quantified as statistically significant. Additionally, it is also important to consider the locations which demonstrated regime shifts during the study period as well as those which may occur within the next century (Appendix H, I, J). A regime shift from one rainfall zone to another may be associated with considerable rainfall changes with implications on activities dependent on rainfall, including agriculture and water resource management. Considering the seasonality scores, DAW, PEW and PRI, located in the Eastern and Northern Cape, demonstrated rainfall zone shifts during the study period (Figure 5.41; Appendix H). For the onset dates, LAW, PRI, VRE and VWY, in the Northern and Western Cape, demonstrated regime shifts, whereby during the study period it was quantified that the summer or winter solstice no longer occurred during the wet season (Figure 5.42; Appendix I). No regime shifts occurred during the study period for the cessation, 10% and 90% dates (Figure 5.43, 5.44, 5.45). Additionally, weather stations which demonstrated statistically significant shifts in the number of rain days are also important to monitor, especially with monthly rainfall amount to consider a complete description of the changes in rainfall seasonality (Figure 5.46). Finally, although less important, is monitoring of the

weather stations which demonstrated a very low chance of change (i.e. as likely as not) having occurred in the rainfall seasonality metrics (Figure 5.46). It may be useful to consider these over a longer temporal period to confidently determine if no change has occurred. Notably, most of the trends had a particularly low possibility of occurrence and as a result this highlights that additional monitoring of rainfall regimes is imperative, across the entire country using additional weather stations over longer temporal periods (Figure 5.46).

5.6 SYNOPSIS

The results from the statistical analyses on the rainfall characteristics and rainfall seasonality for the period of 1987-2016 across South Africa are presented in this chapter. Mean annual rainfall totals are spatially and temporally variable. Analysis of the trends in annual rainfall amount suggests there was a shift towards drier conditions across most of the country, and especially across the eastern half of the country where eight locations had statistically significant trends.

There are distinct spatial patterns in mean monthly rainfall across the country. The timing of wetter and drier periods provides a robust classification of rainfall seasonality which may be used for more of a qualitative description on rainfall amount and timing across the SRZ, WRZ and YRZ. Even though there was little change evident for monthly rainfall amount, the trajectory and magnitude of the changes may be used to further understand the shifts in rainfall seasonality captured under *Section 5.5*. Across weather stations with summer rainfall conditions there was generally a shift towards lower rainfall. This was particularly highlighted in the February and September rainfall totals where the most statistically significant trends were also observed. There are, however, notable increases in monthly rainfall amount observed across these weather stations during the months of January, April, July and December. The locations which display winter rainfall conditions had notable trends towards drier conditions during April, May, July, September and October. At these locations there were also shifts towards higher monthly rainfall amount during January, August and November. For the locations along the southern coast with year-round rainfall, there was a general trend towards drier conditions, although during June, July and August there were notable increases in monthly rainfall amount.

Following this rainfall seasonality was statistically quantified and classified across the country. Each of the approaches used, both quantitatively and qualitatively described different components which together provide a complete description of rainfall seasonality. The seasonality scores quantify the magnitude/degree of seasonality and timing of rainfall over a monthly scale. The approaches on the onset and cessation dates, and 10% and 90% dates provide quantities for the timing and duration of the wet season over a daily scale. The number of rain days considered in conjunction with monthly rainfall amount may provide information on the intensity of rainfall. The approach on clustering monthly rainfall amount and variability provided qualitative information on the duration and timing of the wet season.

There were notable spatial patterns in rainfall seasonality, and these were highlighted across all the approaches through statistically significant associations between latitude and longitude, in particular. Noteworthy is the high agreement in the classification of SRZ, WRZ and YRZ across the country. As expected, the extremes of the rainfall zones were classified with agreement amongst all the approaches. At the transition between the SRZ and WRZ there was a relatively moderate agreement with particularly low agreement at Sutherland. Across this transition area between the rainfall zones there was also considerably high inter-annual variability which was displayed across all the approaches which quantified components of rainfall seasonality.

Considering the complete description of rainfall seasonality, the shifts covered under *Section 5.5* provide a comprehensive description on how rainfall seasonality has changed across the weather stations. This section highlights how complex rainfall seasonality is, and how shifts in rainfall seasonality are location specific, but spatial patterns may be drawn from these shifts. Amongst all the methods, there was a relatively high level of agreement. There was agreement across all approaches at 16 locations indicating high confidence in the direction of change at these locations. As suggested earlier in this section, a complete understanding on the rainfall seasonality shifts across the country may be more comprehensive when considering the shifts in monthly rainfall amount. This will be discussed in the following *Chapter 6 (Discussion)*, where the results from this chapter will be analysed in the context of the wider literature surrounding this research topic.

6. DISCUSSION

6.1 INTRODUCTION

Through objectively testing four statistical methods to quantify and classify rainfall seasonality, this study aims to determine a standard statistical approach which can be applied in future research to characterise rainfall seasonality across South Africa. In addition to this, this study also aims to explore how rainfall seasonality has changed using 46 weather stations (i.e. the exact weather stations used for testing the statistical methods), for which data spans the temporal period of 1987-2016 and which are spread across the entire country. The need for this research is highlighted by the current research gaps which have been identified under *Chapter 2 (Literature Review)*. Within the context of existing literature, this chapter presents the interpretations, implications and limitations of the results captured under *Chapter 4 (Results)*. Firstly, interpretations of the annual and monthly rainfall characteristics are presented and discussed through a comparison with previous studies across South Africa, in order to determine the reliability and appropriateness of the selected weather stations in objectively testing the seasonality metrics. Next, the characteristics and classifications of rainfall seasonality are described using the results from each statistical approach and are discussed through comparison between the approaches and literature to provide clarification on the classification of rainfall seasonality. Furthermore, the approaches used to describe rainfall seasonality are evaluated in terms of relative value and a complete description to propose a standard approach which is specifically suited to understand the complex rainfall regimes across South Africa. This is followed by a discussion on the shifts in rainfall seasonality considering this in the context of palaeoclimatology and contemporary climatology, where the implications of the results will also be considered. Finally, the limitations associated with this research are critically explored.

6.2 ANNUAL AND MONTHLY RAINFALL CHARACTERISTICS ACROSS SOUTH AFRICA

6.2.1 ANNUAL RAINFALL TOTALS

It is commonly cited that mean annual rainfall across South Africa displays high spatial variability, and broadly follows a west-east gradient (cf. Lynch, 2004; Engelbrecht & Landman, 2012; Schulze,

2012; Hart *et al.*, 2013; Favre *et al.*, 2016; Landman *et al.*, 2017). For this study, a statistically significant relationship was quantified between longitude and mean annual rainfall amount ($r = 0.79$, $p < 0.0001$). This confirms that the mean annual rainfall patterns quantified across the weather stations follow a similar gradient to that reported in literature, of low annual rainfall totals along the western coast gradually increasing with increasing longitude to high annual rainfall totals along the eastern coast. Higher rainfall totals in the eastern half of the country, and particularly across the eastern coast regions, are attributed to convective and/or orographic rainfall (i.e. mainly along the eastern coast) fueled by moisture which principally originates from the warm Agulhas current of the western boundary of the Indian Ocean and is advected inland by easterly winds (Nicholson, 2000; Engelbrecht & Landman, 2012; Favre *et al.*, 2016; Landman *et al.*, 2017). Lower mean annual rainfall totals within the central interior plateau of the country are due to the fact that the eastern escarpment acts to block the advection of warm, moist air into the interior (Figure 5.1; Mills *et al.*, 2012; Favre *et al.*, 2016; Landman *et al.*, 2017). Lower mean annual rainfall totals across the western half of the country, and particularly along the western coast regions, are linked to the atmospheric stability induced by subtropical subsistence (i.e. through the South Atlantic high-pressure system) and cold SSTs associated with the Benguela current which forms the eastern boundary current of the South Atlantic Ocean, and the induced coastal upwelling (Favre *et al.*, 2016). There is additionally consistency between the results of this study and with literature, in that relatively high mean annual rainfall totals were captured across small regions along the southern coast and in the southwestern Cape (Figure 5.1; cf. Lynch, 2004; Engelbrecht & Landman, 2012; Hart *et al.*, 2013; Landman *et al.*, 2017). Rainfall across these regions is attributed to orographic rainfall mostly from moist frontal air, and additionally along the southern coast rainfall is also associated with warm moist air from the Agulhas current of the Indian Ocean (Engelbrecht *et al.*, 2015; Favre *et al.*, 2016; Landman *et al.*, 2017). In literature relatively high mean annual rainfall totals are also captured along the eastern escarpment in the Limpopo and Mpumalanga provinces (cf. Nicholson, 2000; Lynch, 2004; Engelbrecht & Landman, 2012; Hart *et al.*, 2013; Landman *et al.*, 2017), however, this was not necessarily captured given the relatively low spatial resolution of the sample of weather stations (Figure 5.1).

Prior to considering the patterns in annual rainfall across smaller regions, it is important to briefly consider the spatial patterns in CV of annual rainfall (Figure 5.1). The statistically significant inverse relationship ($r = -0.38$; $p = 0.010$) between inter-annual variability (captured as CV) and mean annual rainfall amount are consistent both spatially and in magnitude with the results presented by Schulze (2012). The map Schulze (2012) presents demonstrates that relatively higher CV is spatially associated with regions of relatively low mean annual rainfall, and vice versa, and this is similarly reflected in Figure 5.1. This spatial pattern appears to broadly reflect the spatial extent of the summer and winter rain-bearing synoptics. The northwestern regions of the country generally demonstrate the highest CV levels, and it is known that these regions represent the marginal area for the summer and winter rain-bearing features (Taljaard, 1996; Nicholson, 2000; Favre *et al.*, 2016). Additionally, coastal locations at lower elevations generally demonstrate relatively low CV (Figure 5.1). This would potentially be as a result of the Great escarpment control on moisture dispersal, as this topographic barrier promotes orographic rainfall (Landman *et al.*, 2017). It is notable that the sample of weather stations are broadly representative of the year-to-year variability in annual rainfall, demonstrating additional consistency with literature on the annual rainfall characteristics of South Africa.

Along the eastern coast, considering locations in KwaZulu-Natal and the Eastern Cape (i.e. CED: Cedara, ELW: East London Wo, LAD: Ladysmith, MAN: Mandini, MRC: Makatini Research Centre, PAD: Paddock, SHA: Shaleburn and UMW: Umtata Wo; Figure 5.1), the range in mean annual rainfall is commonly cited as 400-1,200mm (Lynch, 2004), 600-1,100mm (Hart *et al.*, 2013), and 600-1,500mm (Landman *et al.*, 2017). The ranges in literature are broadly similar with some differences in the minimum and maximum of the range, and this may be attributed to capturing different temporal periods and different spatial characteristics of the input data (MacKellar *et al.*, 2014). A range of 500-1,100mm was captured for this study (Figure 5.1), which is broadly consistent with the ranges captured in literature. Small regions of particularly high mean annual rainfall are captured, in literature, directly along the eastern escarpment on the border of KwaZulu-Natal and Lesotho and directly along regions of the coastline (cf. Lynch, 2004; Hart *et al.*, 2013; Landman *et al.*, 2017). Such regions of high mean annual rainfall are captured by PAD (1,099.6mm) and SHA (1,052.7mm; Figure 5.1; Table 5.1), and the ranges are again broadly

consistent with the ranges reported by Lynch (2004), Hart *et al.* (2013) and Landman *et al.* (2017). The value of mean annual rainfall quantified for SHA is, however, inconsistent with the range of 1,250-1,500mm reported by Landman *et al.* (2017); this is attributed to the temporal period differences, where the period captured by Landman *et al.* (2017) has not been reported. The lowest mean annual rainfall totals for this region are captured where LAD and MRC are located (Lynch, 2004; Hart *et al.*, 2013; Landman *et al.*, 2017). The ranges are again broadly consistent, with the mean annual rainfall entirely consistent for LAD, and for MRC the range of 600-700mm reported by Hart *et al.* (2013) and Landman *et al.* (2017) is larger than the mean of 584.6mm (Table 5.1). This would again relate to the temporal periods captured, of which Hart *et al.* (2013) captures the period of 1979-1999. When considering the remaining weather stations in this region, it is apparent that the mean annual rainfall quantified is considerably consistent with the results of Lynch (2004), Hart *et al.* (2013) and Landman *et al.* (2017).

Within the eastern part of the central interior of the country, considering weather stations located in the Eastern Cape, Free State, Gauteng, Limpopo, Mpumalanga and North West (i.e. ANP: Aliwal-North Plaatkop; BET: Bethal, BEW: Bethlehem Wo, BLW: Bloemfontein Wo, FTN: Frankfort-TNK, JIW: Johannesburg INT Wo, LEP: Lephalale, MAR: Mara, MWO: Mafikeng Wo, NEL: Nelspruit, OTT: Ottosdal, PWO: Polokwane Wo, SKU: Skukuza, VRY: Vryburg, WEL: Welkom, and WTO: Warmbad Towoomba; Figure 5.1), the ranges of 200-1,200mm (Lynch, 2004), 300-1,100mm (Hart *et al.*, 2013), and 300-1,250mm (Landman *et al.*, 2017) are reported in literature. The range of 400-800mm was reported for this study and this is somewhat inconsistent with the ranges reported in literature (Figure 5.1). This is because of the spatial distribution of the weather stations, where fewer weather stations were used in this study compared to the literature (Lynch, 2004; Hart *et al.*, 2013; Landman *et al.*, 2017). No weather stations were included for the far northern regions of Limpopo and in the northwestern region of North West which accounts for why the minimum of the range quantified for this study is larger than that reported in literature. Additionally, it has also been noted that relatively no locations were captured across the eastern escarpment spanning through Limpopo and Mpumalanga which accounts for why the maximum of the range reported here is much lower than that of literature, as these studies had a higher spatial resolution (Lynch, 2004; Hart *et al.*, 2013; Landman *et al.*, 2017). NEL was captured in the eastern escarpment

region of Mpumalanga, and it is notable that the range of 700-800mm is lower than the ranges of 800-900mm reported by Hart *et al.* (2013) and 800-1000mm reported by Lynch (2004) and Landman *et al.* (2017; Figure 5.1). The mean of 721.4mm quantified for NEL is not considerably lower than the ranges captured in literature (Table 5.1), but the ranges in literature across different temporal periods are very similar. This inconsistency may then point to the data availability for NEL, where this weather station was demonstrated to contain the lowest data availability, following data cleaning, for daily rainfall (92.8%; Table 4.1). The remaining locations in this region were all consistent with the ranges reported in literature.

The ranges of <100-400mm (Lynch, 2004), <100-500mm (Hart *et al.*, 2013), and <50-500mm (Landman *et al.*, 2017) are captured for across the Northern Cape, northern and eastern region of the Western Cape and northwestern region of the Eastern Cape (i.e. CMU: Cradock-Mun, CWO: Calvinia Wo, DAW: De Aar Wo, FRA: Fraserburg, KWO: Kimberly Wo, OUD: Oudtshoorn, PNO: Port Nolloth, POF: Pofadder, PRI: Prieska, SUT: Sutherland, SWO: Springbok Wo, TRI: Twee Rivieren, UPW: Upington Wo; VRE: Vredendal, VWY: Vanwyksvlei, and WIL: Willowmore ; Figure 5.1). The range of 50-500mm quantified for this study is considerably consistent with literature (Figure 5.1). Consistent across literature and the results of this study is that the far northwestern region along the western coast of the Northern Cape is characterised by the lowest mean annual rainfall totals (Figure 5.1). PNO is located in this region and receives an average of 72.4mm where this value is consistent with what is reported in literature (Table 5.1; Lynch, 2004; Hart *et al.*, 2013; Landman *et al.*, 2017). Interestingly, the relatively higher mean annual rainfall total for SWO (221.7mm) is similarly captured in literature (Table 5.1; Lynch, 2004; Hart *et al.*, 2013; Landman *et al.*, 2017), and this may be attributed to orographic rainfall (Davis *et al.*, 2016). Most of the mean annual rainfall totals for the locations in this region are consistent with literature, and only the mean annual rainfall totals at POF, TRI and UPW demonstrate slight inconsistencies (Figure 5.1; Lynch, 2004; Hart *et al.*, 2013; Landman *et al.*, 2017). At POF, mean annual rainfall equates to 121.7mm, which is grouped in the range of 100-200mm for this study (Table 5.1; Figure 5.1). This is consistent with Landman *et al.* (2017) and Hart *et al.* (2013), whereas this range is higher than the range of 0-100mm captured by Lynch (2004). For TRI and UPW, Lynch (2004), Hart *et al.* (2013) and Landman *et al.* (2017) capture a range of 100-200mm which is slightly lower than the amount of

213.3mm (TRI) and 214.0mm (UPW) captured in the range of 200-300mm (Table 5.1; Figure 5.1). These inconsistencies are only slight in magnitude and this may be attributed to a different temporal period captured for this study.

Across the southwestern Cape and southern coast (i.e. CAG: Cape Agulhas, CTW: Cape Town Wo, LAW: Langebaanweg AWS, PEW: Port Elizabeth Wo, RIV: Riversdale, and ROB: Robertson), the ranges of 200-1,200mm (Lynch, 2004), 300-1,100mm (Hart *et al.*, 2013) and 300-1,500mm (Landman *et al.*, 2017) are captured. For this study a range 200-600mm was captured, where the maximum is considerably lower than that captured in literature (Figure 5.1). This is because of the low spatial resolution of the weather stations, where very few locations are captured across the Cape Fold Mountains (Figure 5.1). Very few locations were captured in this region given that only SAWS weather stations were used and due to the requirements for weather station selection (See *Section 4.2.1* of *Data and Methodology Chapter 4*). When considering the individual locations, it is evident that there is considerable agreement with literature (e.g. Lynch, 2004; Hart *et al.*, 2013; Landman *et al.*, 2017), however, the results of LAW are somewhat inconsistent with the range captured by Landman *et al.* (2017). A range of 200-300mm was captured for LAW (261.9mm) for this study (Figure 5.1; Table 5.1), whereas Landman *et al.* (2017) quantify a range of 300-400m. This is only a slight difference and this may be attributed to different temporal periods captured.

It is evident that the mean annual rainfall totals quantified across the weather stations are considerably consistent with literature, and where differences in magnitude are reported these were only small. Small differences in magnitude would inevitably occur, and as noted in this section this would be attributed to the period over which the data were analysed, and the locations of the weather stations from which data were obtained or the gridded products used (MacKellar *et al.*, 2014). The data temporal period would play a notable role in the differences in magnitude given that rainfall across South Africa is known to be inherently characterised by inter-annual variability (Nicholson, 2000; Fauchereau *et al.*, 2003; MacKellar *et al.*, 2014). Further factors that may play a role include data quality and quality-control measures (MacKellar *et al.*, 2014). Since the differences were small, this further highlights that the data obtained from the SAWS for these weather stations is accurate in magnitude. The broad spatial patterns of mean annual rainfall captured in this study were consistent with literature, thus highlighting that the

sample of weather stations closely represent the true annual rainfall patterns across South Africa. On this basis, these weather stations are argued to be appropriate to address objectives two to four, stated under *Section 1.2* of *Chapter 1 (Introduction)*, where the subsequent section further discusses the appropriateness of these weather stations on the basis of representing the known summer, winter and year-round rainfall regimes across South Africa through the annual cycles of rainfall. It is important to demonstrate the appropriateness and representativeness of the sample of weather stations given that this sample was used to test the seasonality metrics in classifying and quantifying rainfall seasonality across the country.

6.2.2 SEASONALITY: MONTHLY RAINFALL TOTALS

According to Cooke (1946) and Favre *et al.* (2016), the annual cycles of rainfall across South Africa can be described either as uni-modal with a distinct wet season during the summer or winter months, or as aseasonal with no distinct seasonal structure to rainfall. It is noteworthy that under *Section 5.3* of *Chapter 5 (Results)*, the resulting annual cycles of rainfall presented under Figure 5.4 reveal these patterns of seasonal winter or summer rainfall, or aseasonal annual rainfall. The results of these annual cycles of rainfall are very consistent in terms of the timing of rainfall across the country, and broadly these results are consistent with the resulting annual rainfall cycles presented in previous studies which have been conducted drawing on different temporal periods and using different observational datasets (Figure 5.4; cf. Taljaard, 1996; Rouault & Richard, 2003; Engelbrecht *et al.*, 2009, 2015; Liebmann *et al.*, 2012; Philippon *et al.*, 2012; Favre *et al.*, 2016; Lennard & Hegerl, 2015; Maraschin, 2016; du Plessis & Schloms, 2017; Landman *et al.*, 2017; Phakula *et al.*, 2018). In considering the accuracy of the annual cycles of rainfall quantified for each weather station, and in determining the representativeness of the sample of weather stations on the basis of the magnitude and spatial distribution, the results of Figure 5.4 and Figure 5.5 will be discussed in terms of the locations which demonstrated SRZ, WRZ and YRZ conditions. Since these conditions are already broadly evident in the sample of weather stations it is apparent that the sample is representative of rainfall regimes across South Africa, however, the accuracy of the sample is important to confirm the appropriateness of the weather stations in addressing the remaining objectives two to four. In considering the spatial distribution of the mean monthly

rainfall totals, the maps in Figure 5.5 are compared to the maps of mean monthly rainfall totals created by Cooke (1946). Before this is done it should be highlighted that the interpolated maps presented in this project are not as detailed given that fewer weather stations were utilised compared to the 400 weather stations applied in Cooke (1946). However, there are remarkable similarities between the maps presented in this project and the maps presented in Cooke (1946).

Across the sample of weather stations, 34 locations spread across the central and eastern parts of South Africa clearly represent SRZ conditions, where this includes weather stations such as Bethlehem Wo (BEW), Johannesburg INT Wo (JIW), Ladysmith (LAD), Mafikeng Wo (MWO), Nelspruit (NEL), Polokwane Wo (PWO), Umtata Wo (UMW) and Upington Wo (UPW; Figure 5.4, 5.5). Landman *et al.* (2017) quantified the annual cycles of rainfall for a number of weather stations across the central and eastern parts of the country, where these are either exact locations included in this study or locations near to the study weather stations. It is not surprising that the results from Landman *et al.* (2017) compare almost exactly with the weather stations used in this project. Landman *et al.* (2017) similarly quantify the mean annual rainfall cycles for Bloemfontein Wo (BLW), Cradock-Mun (CMU), MWO, NEL, PWO, UMW and UPW (Figure 5.4). The resulting mean annual rainfall cycles at these locations only differ slightly for BLW, NEL and UPW, where the maximum mean monthly rainfall for BLW is slightly higher than Landman *et al.* (2017) with the maximum slightly lower at NEL, and for UPW the minimum of this study is slightly lower and the maximum is also slightly higher (Figure 5.4). There are only small differences in magnitude between exact weather stations, and this would be due to different temporal periods, although the temporal period captured by Landman *et al.* (2017) is unknown. Across the weather stations representative of SRZ conditions, relatively higher monthly rainfall totals are quantified for the months of October to March, (Figure 5.4, 5.5), where the summer season rainfall first starts along the eastern coast before spreading west, deeper into the interior (Figure 5.5). This is consistent with maps of mean monthly rainfall created by Cooke (1946) as well as the map of the cluster groupings developed by Phakula *et al.* (2018). It is evident that mean monthly rainfall totals along the eastern coast begin to increase gradually from August, and again the maps presented by Cooke (1946) demonstrate this. The magnitude of mean monthly rainfall, quantified for this study, during the months of October to March ranges between 10-200mm (Figure 5.5), and is relatively similar

to the range of 12 to >130mm which Cooke (1946) reports. Convective rainfall mainly occurs during these months where this is mainly induced through the semi-stationary subtropical easterly wave which is displaced south due to the southward seasonal migration of the ITCZ (Taljaard, 1996; Tyson & Preston-Whyte, 2000; Engelbrecht *et al.*, 2009; Lennard & Hegerl, 2015). TTTs also contribute to a substantial amount of summer rainfall (Taljaard, 1996; Hart *et al.*, 2010, 2013; Ratna *et al.*, 2013; Macron *et al.*, 2014), and ridging high pressure systems as well as cut-off low pressure systems are known to contribute to rainfall along the eastern coast during August and September (Taljaard, 1996; Singleton & Reason, 2007; Favre *et al.*, 2013). It is notable that peak summer rainfall for this study occurred mainly during December to February, where Cooke (1946) and Favre *et al.* (2016) similarly report this. During the remaining months of the year (i.e. April to September), the eastern half of the country receives little to no rainfall which is attributed to subtropical high pressure systems which are displaced north due to the seasonal migration of the ITCZ and the seasonal expansion of Antarctic sea ice (Taljaard, 1996; Tyson & Preston-Whyte, 2000; Engelbrecht *et al.*, 2009; Lennard & Hegerl, 2015). Mean monthly rainfall during April to September ranges between 0-90mm (Figure 5.5), where Cooke (1946) reports a similar range of 0-100mm and similarly demonstrates that mean monthly rainfall totals throughout these months are consistently highest across the eastern coast.

There are nine locations spread across the southwestern Cape and western coastline which represent WRZ conditions, where this is evident at locations such as Calvinia Wo (CWO), Cape Agulhas (CAG), Cape Town Wo (CTW) and Port Nolloth (PNO; Figure 5.4). During the months of April to September higher mean monthly rainfall results from temperate weather systems (i.e. cold fronts associated with mid-latitude cyclones and cut-off lows) which are displaced further north with the Southern Hemisphere Westerlies as a result of the seasonal migration of the ITCZ north of the equator and the seasonal expansion of the Antarctic sea ice (Taljaard, 1996; Reason *et al.*, 2002; Reason & Rouault, 2005; Singleton & Reason, 2007; Lennard & Hegerl, 2015). In considering the mean annual cycles of rainfall, in literature it is evident that the contribution of rainfall during the summer months is relatively high for locations such as CAG, CWO, ROB (Robertson) and SUT (Sutherland) compared to other locations (i.e. CTW, LAW: Langebaanweg AWS, PNO, SWO: Springbok Wo, VRE: Vredendal) which also demonstrate winter rainfall

conditions (Figure 5.4; Rouault & Richard, 2003; Philippon *et al.*, 2012). It is expected that these locations with more summer rainfall are located further east, closer to locations which receive rainfall during the summer months (Figure 5.5). Of the winter rainfall locations used for this project which Landman *et al.* (2017) similarly capture (i.e. CTW and SWO), it is evident that the annual cycles of rainfall are consistent. The magnitude of 10-30mm of rainfall during the summer months and 40-90mm of rainfall during the winter months at CTW compares exactly with the results presented by Landman *et al.* (2017; Figure 5.4). The results at SWO are consistent between this study and Landman *et al.* (2017), however, the magnitude demonstrates some inconsistencies. The range of 5-10mm during the summer months is consistent, however, during the winter months the June maximum presented by Landman *et al.* (2017) is slightly lower at 30mm compared to the 38mm captured for this study (Figure 5.4). In considering the spatial distribution of mean annual rainfall totals throughout the year, it is evident that the patterns presented for the southwestern Cape and western coast compare very well to the results presented by Cooke (1946). During the months of April to September mean monthly rainfall totals quantified by Cooke (1946) range between 12-102mm, and are almost exactly the same as the range of 10-90mm quantified for this study (Figure 5.4). The highest mean monthly rainfall totals in this region are evident in the southwestern Cape, which Cooke (1946) similarly note. Additionally, it is reported that winter rainfall is highest during the months of May to July (Cooke, 1946; Favre *et al.*, 2016), and this is similarly captured in the results of this study (Figure 5.4, 5.5). During the months of October to March, the southwestern Cape and western coast regions are particularly dry, compared to the wetter months of April to September, with mean monthly rainfall totals consistently below 30mm in the southwestern Cape and below 10mm along the western coast (Figure 5.5). During these months Cooke (1946) quantified mean monthly rainfall totals below 52mm in the southwestern Cape and below 12mm along the western coast which is very consistent with the results of this study (Figure 5.5).

Three locations spread along the southern coast represent aseasonal (year-round rainfall) conditions, where these include Oudtshoorn (OUD), Port Elizabeth Wo (PEW) and Riversdale (RIV; Figure 5.4, 5.5). Mean monthly rainfall, which is mainly orographic at these locations, in literature is known to be relatively consistent throughout the year which is similarly demonstrated in the

results of this project (Figure 5.4, 5.5; Taljaard, 1996; Engelbrecht *et al.*, 2015). Through dynamic modelling mean monthly rainfall along the southern coast has been attributed to the occurrence of winter and summer rain-bearing systems namely cold fronts, ridging high pressure systems, TTTs and cut-off lows (Figure 5.5; Engelbrecht *et al.*, 2015). The annual cycles of rainfall quantified under Figure 5.4 are broadly consistent with the results captured by Rouault and Richard (2003), Engelbrecht *et al.* (2015) and Landman *et al.* (2017). These studies highlight that during the spring and autumn months there are slight peaks in mean monthly rainfall amount, and this is similarly captured by the results of OUD, PEW and RIV (Figure 5.4). It is notable that there are slight differences when considering the magnitude of mean monthly rainfall of these locations in comparison to Engelbrecht *et al.* (2015) and Landman *et al.* (2017). Since different temporal periods were captured, slight differences would inevitably occur, and additionally in comparing these results with Engelbrecht *et al.* (2015) this would occur because the annual cycles of rainfall presented in their study was an amalgamation of numerous weather stations across the different regions they defined. In considering the spatial distribution of rainfall along the southern coast, it is evident that mean monthly rainfall totals consistently range between 10-50mm throughout the year (Figure 5.5), and Cooke (1946) also demonstrated a similar consistent range of 12-50mm. However, the patterns presented in Figure 5.5 only broadly compare to Cooke (1946) given the low density of weather stations, for this study, along the southern coast.

It has now been further demonstrated that the sample of weather stations, on the basis of the annual cycles of rainfall, is representative of the rainfall regimes known to occur across South Africa due to the considerable consistency with literature. Small differences in the magnitude and spatial patterns of mean monthly rainfall are evident, and similar to the differences reported for mean annual rainfall it is expected that such differences would occur. Again this is attributed to the spatial and temporal characteristics of the dataset, among others (MacKellar *et al.*, 2014). This consistency again highlights that the data obtained from SAWS are accurate. The sample of weather stations thus represents closely the true mean monthly rainfall patterns across South Africa; this thus confirms that the weather stations are appropriate to test the statistical methods to address objective two to four of this research project, where the results of this are discussed in the subsequent sections of this chapter. Demonstrating consistency with literature in the annual

cycles of rainfall is important to confirm the validity of the results discussed in the following section. The way in which each metric models the known SRZ, WRZ and YRZ can thus be assessed given that the rainfall datasets for the project weather stations are demonstrated to be accurate, especially in terms of the timing, magnitude and the spatial distribution of mean monthly rainfall amount.

6.3 CHARACTERISING AND CLASSIFYING RAINFALL SEASONALITY ACROSS SOUTH AFRICA: TOWARDS QUANTIFYING SPATIAL VARIATIONS

According to Hattie and Cooksey (1984), a useful statistical method for classification into known groups must be proven to be valid and needs to be reproducible. As such, to model and gain a comprehensive understanding of the nature of rainfall seasonality across South Africa demands a statistical method that is both applicable and accurate across the entire country (Thackeray & Fitchett, 2016). The most important feature of a method to accurately model rainfall seasonality across South Africa is the ability to reliably discriminate between SRZ and WRZ conditions (Thackeray & Fitchett, 2016; Fitchett & Bamford, 2017), where this is especially important at the transition zone between these rainfall zones. In order to characterise and classify the seasonality of rainfall across South Africa, four different statistical approaches were applied using the same datasets (i.e. the same rainfall dataset with quantification of the seasonality scores additionally requiring temperature data) from 46 weather stations which span the period of 1987-2016. Since the same datasets per location were used and only the methods differed, the results are spatially comparable and may be used to assess the spatial variability of the seasonality of rainfall across the methods (Oliver, 1984; Raziei, 2017; Figure 6.1). For the purpose of this current section, the methods used in this study will first be verified in terms of why each method inherently assesses seasonality and then the methods will be compared in terms of how each classified and characterised the SRZ, WRZ and YRZ, rainfall zones which are already confirmed to exist across South Africa (cf. Taljaard & Steyn, 1991; Chase & Meadows, 2007; Schulze & Maharaj, 2007; Liebmann *et al.*, 2012; Engelbrecht *et al.*, 2015; Favre *et al.*, 2016).

In verifying the inherent ability of each method in characterising and classifying rainfall seasonality it should be highlighted that there is no standard definition of rainfall seasonality (Roffe *et al.*, 2019). This is because rainfall seasonality is a complex concept which is comprised of a number of components (e.g. the timing, duration, magnitude and intensity of wet and dry seasons; Walsh & Lawler, 1981; Feng *et al.*, 2013; Pascale *et al.*, 2015, 2016; Dunning *et al.*, 2016; Deng *et al.*, 2019). As a result, the definition of rainfall seasonality will be dependent on the method applied. In saying this, each method used for this research project was adopted from the literature based on methods which are known to successfully quantify rainfall seasonality, where each method was partly selected based on its contribution to quantitatively describing some or all the components which completely describe rainfall seasonality. The successful application of the metrics (i.e. the metrics applied in this research project) in literature thus verifies that these methods inherently assess rainfall seasonality, where the specific contribution of each method to describing rainfall seasonality is discussed under *Section 6.3.1* which follows. In applying these metrics to characterise and classify rainfall seasonality across South Africa it is not enough to verify these as rainfall seasonality metrics. This is because the variety of rainfall regimes (i.e. SRZ, WRZ and YRZ) contribute to a considerably complex rainfall climatology across South Africa. As such, these methods must be verified in their ability to characterise and classify rainfall seasonality across South Africa. Consistency in terms of the spatial distribution of SRZ, WRZ and YRZ with previous maps in literature highlights that these approaches are accurate, where this will be discussed in detail throughout this section. The agreement of the output of these approaches captured in Figure 6.1 is another reason behind why these methods are verified. As expected, these methods classify the extremes of the rainfall zones with much agreement, and the transition between the SRZ, WRZ and YRZ are classified with much dispute (Figure 6.1; Roffe *et al.*, 2019). It is notable that the classification of rainfall seasonality between the four methods are consistent for locations, among others, such as Cape Town Wo (CTW; WRZ), Johannesburg INT Wo (JIW; SRZ) and Port Elizabeth Wo (PEW; YRZ) which are locations not contested on their seasonality classification (See Figure 2 of published paper under *Section 2.2* of *Chapter 2*; Figure 6.1; Table 6.1; Taljaard & Steyn, 1991; Carr *et al.*, 2006; Schulze & Maharaj, 2007). Although, it must be noted that the cluster-based approach did not classify a YRZ and thus the accuracy of this approach is questionable due

to a number of reasons discussed later in this section (Table 6.1). It is thus verified that each method accurately quantifies rainfall seasonality across South Africa. Having confirmed the value of each approach in modelling seasonality across South Africa, now the outputs of each approach will be assessed by comparing these between methods and with literature classifying rainfall seasonality across parts or the entire area of South Africa.

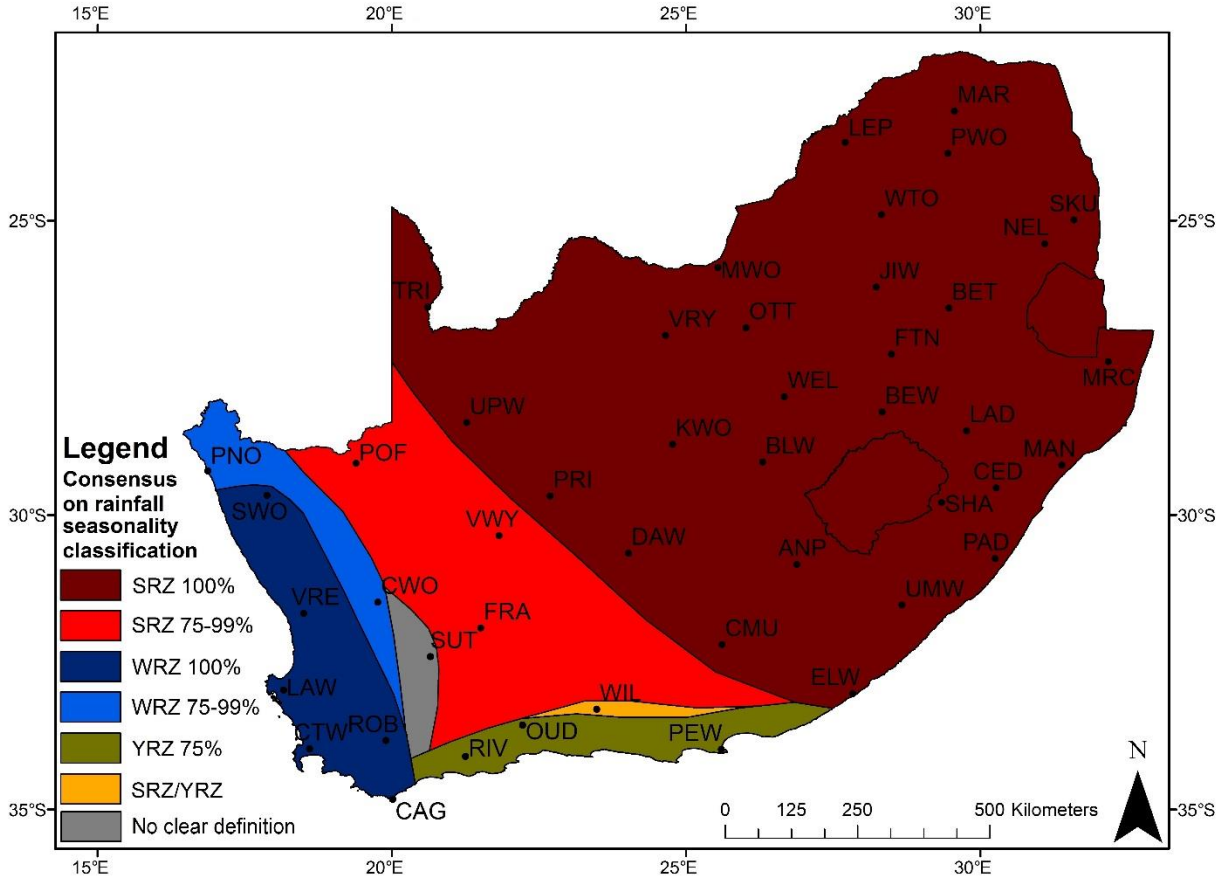


Figure 6.1: Composite map of the consensus on the spatial distribution of rainfall seasonality zones across South Africa (including Lesotho and Swaziland) captured between the statistical approaches, represented in *Figures 5.11, 5.15, 5.27 and 5.39*, used for this study.

Table 6.1: Location specific mean rainfall seasonality classification according to each seasonality metric for the period of 1987-2016. Rainfall zone classifications are highlighted, where red indicates SRZ, blue indicates WRZ and yellow indicates YRZ classifications respectively.

Location	Cluster-based approach	Seasonality Score	Onset and cessation dates	Percentile-based approach
ANP	SRZ	SRZ	SRZ	SRZ
BET	SRZ	SRZ	SRZ	SRZ
BEW	SRZ	SRZ	SRZ	SRZ
BLW	SRZ	SRZ	SRZ	SRZ
CWO	WRZ	YRZ	WRZ	WRZ
CAG	WRZ	WRZ	WRZ	WRZ
CTW	WRZ	WRZ	WRZ	WRZ
CED	SRZ	SRZ	SRZ	SRZ
CMU	SRZ	SRZ	SRZ	SRZ
DAW	SRZ	SRZ	SRZ	SRZ
ELW	SRZ	SRZ	SRZ	SRZ
FTN	SRZ	SRZ	SRZ	SRZ
FRA	SRZ	YRZ	SRZ	SRZ
JIW	SRZ	SRZ	SRZ	SRZ
KWO	SRZ	SRZ	SRZ	SRZ
LAD	SRZ	SRZ	SRZ	SRZ
LAW	WRZ	WRZ	WRZ	WRZ
LEP	SRZ	SRZ	SRZ	SRZ
MWO	SRZ	SRZ	SRZ	SRZ
MRC	SRZ	SRZ	SRZ	SRZ
MAN	SRZ	SRZ	SRZ	SRZ
MAR	SRZ	SRZ	SRZ	SRZ
NEL	SRZ	SRZ	SRZ	SRZ
OTT	SRZ	SRZ	SRZ	SRZ
OUD	SRZ	YRZ	YRZ	YRZ
PAD	SRZ	SRZ	SRZ	SRZ
POF	SRZ	YRZ	SRZ	SRZ
PWO	SRZ	SRZ	SRZ	SRZ
PEW	WRZ	YRZ	YRZ	YRZ
PNO	WRZ	WRZ	ND	WRZ
PRI	SRZ	SRZ	SRZ	SRZ
RIV	WRZ	YRZ	YRZ	YRZ
ROB	WRZ	WRZ	WRZ	WRZ
SHA	SRZ	SRZ	SRZ	SRZ
SKU	SRZ	SRZ	SRZ	SRZ
SWO	WRZ	WRZ	WRZ	WRZ
SUT	SRZ	YRZ	WRZ	WRZ
TRI	SRZ	SRZ	SRZ	SRZ
UMW	SRZ	SRZ	SRZ	SRZ
UPW	SRZ	SRZ	SRZ	SRZ
VWY	SRZ	YRZ	SRZ	SRZ
VRE	WRZ	WRZ	WRZ	WRZ
VRY	SRZ	SRZ	SRZ	SRZ
WTO	SRZ	SRZ	SRZ	SRZ
WEL	SRZ	SRZ	SRZ	SRZ
WIL	SRZ	YRZ	SRZ	YRZ

It is verified that most of South Africa receives rainfall during the summer months of the year as 70% of the country has been classified as SRZ with agreement across all four approaches (Figure 6.1). This area (SRZ 100% agreement) represents the extremes of the SRZ which is expected to, without dispute, be classified as SRZ across all the approaches (Figure 6.1; Table 6.1). This is a region which is classified with strong agreement in literature (See *Literature Review Chapter 2 Section 2.2*), which further confirms that the classification of SRZ across this region is accurate. In this zone of 100% agreement, particularly in the northeastern parts of this zone, it is evident that the classification of SRZ was particularly stable across all of the approaches, as annually these locations were classified as SRZ for more than 90% of the study period (Table 5.8). Herrmann and Mohr (2011) also quantified relatively high stability of approximately 50-90% in the annual classification of the single wet season regimes across the northeastern parts of South Africa.

Considering the regions of SRZ 100% and SRZ 75-99% which covers 85% of the area of South Africa (Figure 6.1), both the approaches of the onset and 10% dates accurately demonstrate the movement of the seasonal wave of contiguous convective summer rainfall, which is known to begin along the eastern coast and expand westwards to the interior of the country (Figure 5.25, 5.37; e.g. SAWB, 1965; Taljaard, 1996; Liebmann *et al.*, 2012; Favre *et al.*, 2016). The spatial distribution of the onset and 10% dates are thus broadly consistent with published maps, conducted over different temporal periods and using different observational datasets, on the start dates of the wet season (e.g. Liebmann *et al.*, 2012; Dunning *et al.*, 2016). The dates of the beginning of the wet season differ between these approaches, where the mean onset dates obtained were typically later than the mean 10% dates (Table 5.4, 5.6; Figure 5.25, 5.37). The differences in the dates are entirely attributed to the dissimilar definitions used to define the onset and 10% date of the wet season (Tadross *et al.*, 2009; Boyard-Micheau *et al.*, 2013); differences in the cessation and 90% dates should also be noted as a result of different definitions. Similarly, the cessation and 90% dates accurately quantify withdrawal of the SRZ wet season, as these dates display a spatial distribution which is consistent with published maps on the withdrawal of the wet season (Figure 5.25, 5.37; e.g. Liebmann *et al.*, 2012; Dunning *et al.*, 2016). The maps presented in this study (Figure 5.25, 5.37), and in literature (e.g. Liebmann *et al.*, 2012; Dunning *et al.*, 2016) demonstrate that the summer wet season typically ends first in the northern parts of Limpopo

before ending across the remaining interior and eastern areas of the country. The spatial distribution of the start (i.e. onset and 10% dates) and end (i.e. cessation and 90% dates) dates highlight that the SRZ is a heterogeneous rainfall zone, where heterogeneity has previously been noted in both contemporary climatology (cf. Rouault & Richard, 2003; Favre *et al.*, 2016) and palaeoclimatology (cf. Chevalier & Chase, 2015; Chase & Quick, 2018) investigations on the SRZ. This heterogeneity is largely, although not only, because a number of different synoptic circulation features contribute to rainfall across the SRZ (Taljaard, 1996; Tyson & Preston-Whyte, 2000). For instance, earlier start dates along the eastern coast from ELW (East London Wo) to MAN (Mandini) are largely attributed to cut-off lows (Singleton & Reason, 2007; Favre *et al.*, 2013), ridging anticyclones (Ndarana *et al.*, 2018) and moisture influx from the warm Agulhas current of the Indian Ocean (Taljaard, 1996; Lee-Thorp *et al.*, 1999; Rouault *et al.*, 2002; Favre *et al.*, 2016). The later start dates in the interior regions of the country are largely attributed to tropical rain-bearing systems which influence South Africa when the ITCZ migrates south of the equator during the Southern Hemisphere summer months (Taljaard, 1996; Nicholson, 2000, 2018; Tyson & Preston-Whyte, 2000; Favre *et al.*, 2016).

The output of the cluster-based approach also demonstrates that the SRZ is heterogeneous (Figure 5.8). From the results of the annual rainfall cycles of the cluster groups one, two and five, it is evident that seasonal rainfall across the SRZ shifts from east to west (Figure 5.8, 5.9; Favre *et al.*, 2016; Rouault & Richard, 2003). The seasonality scores also accurately quantify seasonality in the SRZ, where the seasonality scores correctly show that most of the country receives summer rainfall. Most importantly these scores highlight heterogeneity in the degree of seasonality across the SRZ (Figure 5.14). Heterogeneity is highlighted both by the seasonality scores quantified as well as the strength of relationship between MMT and MMR, where locations in the northeastern parts of the country would be expected to be characterised by the strongest seasonality scores and relationships given the strong seasonal characteristics of rainfall across this region of the country (Figure 5.14, 5.16; Favre *et al.*, 2016; Thackeray & Fitchett, 2016; Botai *et al.*, 2018). It is notable that there is the highest level of agreement between published maps in the northeastern parts of the country (See Figure 2 of published paper *Section 2.2* of *Literature Review Chapter 2*), and this is where the extremes of the rainfall zones occur and where the degree of seasonality has

been shown to be strongest and more pronounced (e.g. Schumann & Hofmeyr, 1938; Rouault & Richard, 2003; Liebmann *et al.*, 2012; Favre *et al.*, 2016; Thackeray & Fitchett, 2016; Botai *et al.*, 2018). Heterogeneity in degree of seasonality is also captured by the length of the wet season, for the onset and cessation dates and percentile-based approach, where a shorter wet season reflects more pronounced seasonality thus confirming that there is a higher degree of seasonality in the northeastern parts of the SRZ (Figure 5.25, 5.37).

It is evident that there is more dispute in the classification of the SRZ moving closer to the transition between the SRZ and WRZ (Figure 6.1). In comparing the two rainfall seasonality classification maps developed by Herrmann and Mohr (2011), similar discrepancies across the transition between these rainfall zones is noted. Disagreement in the classification of SRZ is captured in Figure 6.1 by the region classified as SRZ 75-99% agreement which represents that three of the four approaches agree on the classification of this region. This area covers 15% of the country, where the locations (i.e. FRA: Fraserburg, POF: Pofadder, and VWY: Vanwyksvlei) in this region were classified as SRZ three times, and as YRZ once using the seasonality scores (Table 6.1; Figure 5.11, 5.15, 5.27, 5.39). It is interesting that a comparison of the classification of rainfall seasonality across published maps yielded similar results, where the seasonality classification of western central interior region (i.e. the transition between the SRZ and WRZ) was also disputed (See Figure 2 *Literature Review Chapter 2 Section 2.2*). Notably, most of the maps in literature classified this region (i.e. SRZ 75-99%) as SRZ (See *Literature Review Chapter 2 Section 2.2*; e.g. Schumann & Hofmeyr, 1938; McGee, 1977; Taljaard & Steyn, 1991; Schulze & Maharaj, 2007), which is similarly reflected in the outputs of the seasonality metrics applied in this study. Indeed, the dispute in this region highlights that the classification of seasonality at the transition between the SRZ and WRZ would rely heavily on the way in which seasonality is defined by the metric applied, more so than the extremes of the SRZ and WRZ. This is because the way seasonality is defined is metric specific (Raziei, 2017), and seasonality at the transition zone is not as pronounced as seasonality for the extremes of rainfall zones.

Considering the seasonality scores at FRA, POF and VWY, these locations were characterised by a weak or very weak positive relationship between MMT and MMR (Figure 5.16), and the total period seasonality scores quantified for these locations were particularly weak and positive (FRA

= 0.15; POF = 0.13; VWY = 0.22; Figure 5.12, 5.14, 5.16; Table 5.2). The seasonality scores highlight that although classified as YRZ these locations received more summer rainfall during the study period (Thackeray & Fitchett, 2016). However, even though rainfall received during the summer months is relatively higher than for the rest of the year (Figure 5.4), rainfall during these months is still particularly low and this points to relatively equable rainfall throughout the year which by definition would resemble the YRZ category of the seasonality scores (Thackeray & Fitchett, 2016). On the other hand, using the remaining three approaches both a wet and dry season would have been classified and it is not surprising that the results display summer rainfall conditions given that the annual cycles of rainfall for these locations (i.e. FRA, POF and VWY) do distinctly display a uni-modal regime (Figure 5.4; 5.11, 5.27, 5.39). Additionally, the requirement to start from the month following that of minimum mean monthly rainfall for uni-modal regimes using the onset and cessation dates and percentile-based approach would result in a classification of SRZ for these locations. Similarly, seasonality metrics which define the climatological year from the month following minimum rainfall reflect SRZ conditions in this region (e.g. Liebmann *et al.*, 2012; Dunning *et al.*, 2016).

The dispute in the classification across FRA, POF and VWY may be attributed to the fact that these weather stations are located closer to where the boundary between the SRZ and WRZ would be expected to occur (Figure 6.1). This boundary would vary annually, where the spatial extent of both summer and winter rain-bearing synoptic features would play a large role in dictating the extent of the annual boundary, given that the seasonality of rainfall is a direct consequence of prevailing circulation patterns (Nicholson, 2000; Favre *et al.*, 2016). The annual boundary location between the SRZ and WRZ would thus largely depend on the prevailing atmospheric conditions, where the phases of ENSO and SAM for instance would also play an important role in dictating this boundary location (Nicholson, 2000; Dieppois *et al.*, 2016). Previous investigations regarding rainfall seasonality across South Africa have highlighted the instability of rainfall regimes particularly at the transition between the SRZ and WRZ, where it has been demonstrated that the seasonality of rainfall switches considerably from year to year (cf. Nicholson, 2000; Herrmann & Mohr, 2011; Favre *et al.*, 2016). Herrmann and Mohr (2011) quantified approximately 0-40% stability in rainfall regimes across the western central interior of the country, where the annual

and mean rainfall regime classification were the same for up to 40% of the period of 1998-2010. A closer look at the annual classifications of FRA, POF and VWY highlights that there was instability in the regimes, and this is particularly apparent when considering the stability of the seasonality scores and the percentile-based approach (Table 5.8). Notably, locations closer to the boundary (e.g. CMU: Cradock-Mun, DAW: De Aar Wo, ELW: East London Wo, PRI: Prieska, TRI: Twee Riviren, and UPW: Upington Wo) between the classes of SRZ 100% and SRZ 75-99% also displayed relatively low stability in the annual rainfall regimes (Table 5.8).

It is verified that the southwestern Cape and western coastline of South Africa receive predominantly winter rainfall, where this is demonstrated by the WRZ 100% agreement class which covers 7% of the country (Figure 6.1; Table 6.1). This region represents the extremes of the WRZ, where all four approaches agreed on the classification of these locations as WRZ, as expected given that the extremes, with more pronounced seasonality, would rely less on the way in which a metric defines seasonality (Table 6.1; Figure 5.11, 5.15, 5.27, 5.39; Roffe *et al.*, 2019). It is evident that the rainfall regimes across this region, particularly in the southwestern Cape (e.g. CAG: Cape Aguhlas, CTW: Cape Town Wo, and LAW: Langebaanweg AWS) were relatively stable as the annual classification converged on WRZ for at least 90% of the study period (Table 5.8). Relatively high stability, above 50%, of the rainfall regimes in this region was also captured by Herrmann and Mohr (2011). However, further away from the extremes of the WRZ and closer to the boundaries of this region there was relatively low stability in the regimes as is evident at ROB (Robertson), SWO (Springbok Wo) and VRE (Vredendal; Table 5.8), where a similar pattern is also demonstrated in the rainfall regime stability map created by Herrmann and Mohr (2011). Similar to locations such as CMU, DAW, ELW, PRI, TRI and UPW, the relatively low stability in the rainfall regimes at these weather stations would be related to the fact that the locations are relatively close to where the average boundary between the SRZ and WRZ would be expected occur. As such, the annual classification of these locations would similarly depend on the prevailing atmospheric conditions (Nicholson, 2000), as well as the way in which a metric defines rainfall seasonality (Raziei, 2017).

In considering the WRZ 100% and the WRZ 75-99% classes (Figure 6.1), although quantified with slightly different dates due to different definitions of the start of the wet season, the spatial pattern of the onset and 10% dates are broadly consistent with literature (e.g. Liebmann *et al.*,

2012; Dunning *et al.*, 2016). These dates display the progression of the start of the winter rainfall season from March in the eastern parts of the WRZ to May in the western and northern parts (Figure 5.25, 5.37). This is consistent with the known passage of frontal winter rain-bearing synoptics circulation features, namely cold fronts associated with mid-latitude cyclones (Taljaard, 1996; Tyson & Preston-Whyte, 2000; Favre *et al.*, 2016; Lennard & Hegerl, 2015). Similarly, the spatial pattern of the cessation and 90% dates are also consistent with published literature (e.g. Liebmann *et al.*, 2012; Dunning *et al.*, 2016), where the wet season ceases first in the eastern part of the WRZ and last in the western part (Figure 5.25, 5.37). In considering the onset and cessation dates and percentile-based approach, it is again not surprising that these locations (i.e. WRZ 100% and WRZ 75-99% locations) were classified as WRZ given that the annual cycles of rainfall clearly depict a uni-modal regime with a winter peak (Figure 5.4). The seasonality scores quantified for the WRZ are highest in the southwestern Cape at locations such as CAG, CTW and LAW (Figure 5.14), which is broadly consistent with published literature noting the strongest and most pronounced WRZ conditions here (e.g. Rouault & Richard, 2003; Philippon *et al.*, 2012; Mahlalela *et al.*, 2018). Additionally, the strength of relationship between MMR and MMT similarly demonstrates this, where a relatively high strength of relationship was evident for these locations with CTW and LAW, in particular, demonstrating the strongest relationship (Figure 5.12, 5.16). The cluster-based approach also highlights heterogeneity in the WRZ in terms of rainfall amount where the northern part of the WRZ has relatively lower rainfall than the southern part, and this is again consistent with literature (Keen, 1971; Rouault & Richard, 2003; Philippon *et al.*, 2012; Mahlalela *et al.*, 2018). The confirmed area of the WRZ is known to cover a small region with most authors capturing this zone across the southwestern Cape and western coast as was captured for this study (cf. Keen, 1971; Taljaard & Steyn, 1991; Schulze & Kunz, 1997; Chase & Meadows, 2007; Liebmann *et al.*, 2012; Cramer & Hoffman, 2015). The spatial extent of the WRZ, as with the SRZ, is likely to differ from year to year and is again dictated by the passage of winter and summer rain-bearing synoptic circulation features (Nicholson, 2000; Favre *et al.*, 2016). Additionally, the spatial extent of the WRZ appears to be bound by the western edges of the Great Escarpment. This is most apparent for the seasonality scores (Figure 5.15), and notably the western edges of the Great Escarpment have previously been suggested as a topographic barrier of the WRZ (Ackerly *et al.*,

2014; Favre *et al.*, 2016). The extent of the WRZ 100% classified in this study could have extended up to PNO (Port Nolloth) and possibly to the border between Namibia (Figure 6.1), as PNO was classified as WRZ using the cluster-based approach, the seasonality scores and the 10% and 90% dates (Table 6.1; Figure 5.11, 5.15, 5.39). Since rainfall is particularly low at PNO, this location could not be classified using the onset and cessation dates and as a result this station occupies the class of WRZ 75-99% agreement (Figure 6.1).

CWO (Calvinia Wo) also occupies the region classified as WRZ 75-99% (Figure 6.1). CWO was classified as YRZ using the seasonality scores and as WRZ using the remaining approaches (Table 6.1; Figure 5.11, 5.15, 5.27, 5.39). Considering the cluster-based, onset and cessation dates and percentile-based approach, it is not surprising that the classification of CWO using these methods converged on WRZ (Table 6.1). The output of all of these methods would generally result in a wet and dry season being defined, and since the annual cycles of rainfall at CWO demonstrate a winter peak, this would likely result in the classification of WRZ (Figure 5.4). Although classified as YRZ, the total period seasonality score quantified for CWO was -0.21 which highlights that this location predominantly receives winter rainfall (Table 5.2; Figure 5.12, 5.14). The mean annual cycle of rainfall at CWO displays a uni-modal structure with a winter peak, however, there is a considerable amount of summer rainfall which highlights that rainfall at CWO lacks a distinct seasonal structure (Figure 5.4). The weak inverse relationship between MMT and MMR for the seasonality scores further highlights that CWO lacks a distinct seasonal structure when compared to a location such as CTW (Figure 5.12). Moreover, the high level of inter-annual variability, for the annual seasonality scores, at 96.2% demonstrates that there is instability in the rainfall regimes at CWO (Figure 5.13). It is also apparent that the rainfall regimes at CWO were particularly unstable using the seasonality scores and the percentile-based approach (Table 5.8). Nicholson (2000) specifically note instability in the seasonality regimes at CWO suggesting that rainfall seasonality at this location may switch between summer and winter conditions. Given the requirement of starting from the month following minimum rainfall for the onset and cessation dates and percentile-based approach, it can be argued that these approaches would not detect variability between SRZ and WRZ conditions. On the other hand, the seasonality scores would be able to detect this, however, this was not detected for the study period where the classification of CWO rather straddled

between WRZ and YRZ conditions (Appendix D). This highlights the value of the seasonality scores approach particularly at the transition zone between the rainfall zones. Furthermore, Herrmann and Mohr (2011) quantify up to 30% stability in the regimes across the location CWO occupies. Noting this, the annual seasonality at CWO would be dependent on the prevailing atmospheric circulation of both summer and winter rain-bearing systems as well as the phases of climate drivers such as ENSO and the SAM (Nicholson, 2000; Favre *et al.*, 2016; Lennard & Hegerl, 2015; Dieppois *et al.*, 2016), where the classification of CWO would depend on the seasonality metric applied. In assessing previous seasonality maps, it is notable that the classification of rainfall seasonality across the region CWO occupies similarly ranged between WRZ and YRZ (See Figure 2 *Literature Review Chapter 2 Section 2.2*).

The classification of the YRZ was associated with the most dispute across the four methods applied to quantify rainfall seasonality in this study (Figure 6.1; Table 6.1). Three of the four approaches agreed on the location of the YRZ along the southern coast (Figure 6.1). It should, however, be noted that the cluster-based approach did not classify a YRZ, possibly because there were few locations along the southern coast to compile the cluster solution with YRZ as a class (Figure 5.11; Appendix C.3). The spatial extent of the YRZ differed between the three remaining approaches (Figure 5.15, 5.27, 5.39). The YRZ classified by both the percentile-based and the onset and cessation dates approaches were restricted to the southern coast, however, Willowmore (WIL) was included in the YRZ using the percentile-based approach and excluded using the onset and cessation dates approach (Figure 5.27, 5.39). Using the onset and cessation dates and percentile-based approach, it is expected that locations such as Oudtshoorn (OUD), Port Elizabeth Wo (PEW) and Riversdale (RIV) would be classified as YRZ given the assumption that the climatological year starts from January for locations which lack a distinct uni-modal seasonal structure (Figure 5.4), and as such it is not surprising that the YRZ classified using these approaches was restricted to the southern coast. In literature the YRZ is mainly classified along the southern coast where it is suggested that the northern boundary is restricted by the Cape Fold mountain range (e.g. Cooke, 1946; McGee, 1977; Taljaard & Steyn, 1991; Schulze & Maharaj, 2007; Engelbrecht *et al.*, 2015). In published literature on the YRZ along the southern coast, this zone is highlighted as being heterogeneous with some locations receiving slightly more winter rainfall and others receiving

slightly more summer rainfall (e.g. Engelbrecht *et al.*, 2015). Using the seasonality scores, the YRZ was classified as the transition zone between the SRZ and WRZ, where it extended from the southern coast into the central interior and up to the border between South Africa and Namibia (Figure 5.15). Some previous classifications in literature have also classified the YRZ to extend north from the southern coast either to parts of the central interior or up to the Namibia border (e.g. Schumann & Hofmeyr, 1938; SAWB, 1965; Carr *et al.*, 2006; Chase & Meadows, 2007; Cordova, 2013). The YRZ captured using the seasonality scores may be defined as the transition zone between the SRZ and WRZ, where the seasonality scores were tending towards zero and the weak/very weak strength of relationship between MMR and MMT at these locations highlights the lack of a distinct seasonal structure to rainfall (Figure 5.12, 5.14, 5.16). Additionally, the YRZ classified using the seasonality scores is a heterogeneous rainfall zone (Figure 5.14). Similarly, Cordova (2013) classified the YRZ using the vector analysis approach and also noted heterogeneity, which he attributed to the Cape Fold mountain range. At locations in the northern parts and north of the mountain range (i.e. CWO: Calvinia Wo, FRA: Fraserburg, POF: Pofadder, SUT: Sutherland, VWY: Vanwyksvlei, WIL: Willowmore), annual rainfall appears to have somewhat of a seasonal structure, although compared to the extremes of the SRZ and WRZ the seasonal structure is not as distinct, especially when comparing the drier months (Figure 5.4, 5.14, 5.15). At locations south of the mountain range (i.e. OUD, PEW, RIV), there is no marked seasonal structure to annual rainfall (Figure 5.4, 5.14, 5.15). It is also evident that the locations which are located in the region between the confirmed SRZ and WRZ and classified as YRZ using the seasonality score were associated with particularly high instability in the annual rainfall regimes (Table 5.8). When considering only the seasonality scores, it is apparent that these locations are also associated with particularly high inter-annual variability (Figure 5.13). Both Nicholson (2000) and Herrmann and Mohr (2011) also highlight the instability of rainfall regimes at the transition between the SRZ and WRZ. The dispute in the classification of the YRZ makes it difficult to provide a clear classification of this rainfall zone and to determine the boundary, particularly because the outcome of the YRZ classification is considerably dependent on the methodology used.

South of the region classified as SRZ 75-99% and north of the region classified as YRZ 75% is an area classified as SRZ/YRZ (Figure 6.1; Table 6.1). This area contains the weather station WIL

(Willowmore) which was classified as SRZ twice, using the cluster-based and onset and cessation dates approaches (Figure 5.11, 5.27), and as YRZ twice, using the seasonality scores and percentile-based approach (Figure 5.15, 5.39). The cluster-based approach, as previously noted, did not classify a YRZ and since the annual cycle of rainfall at WIL displays a peak during the summer months of the year then it is not surprising that this location was classified as SRZ using this approach (Figure 5.4, 5.11). The seasonality score quantified for WIL was 0.23, where this slightly positive score highlights that WIL received more summer rainfall during the study period (Figure 5.12, 5.14; Table 5.2; Thackeray & Fitchett, 2016). Using the onset and cessation dates approach, WIL was characterised by a relatively long wet season with a mean cessation date of 6 May which is slightly later than most SRZ locations which were typically during March and April (Table 5.4). Although WIL has been classified as SRZ using onset and cessation dates, for 42% of the study period cessation dates were during May to August, which is particularly late compared to other SRZ locations (Figure 5.18; Appendix E). Since the mean wet season duration quantified using the percentile-based approach occurred with both the summer and winter solstice and was approximately eight months long WIL was classified as YRZ (Table 5.6). However, the classification of WIL may also be suggested as long SRZ given that the wet season duration was shorter than nine months and the timing of the 10% and 90% dates were similar to other SRZ locations (Figure 5.34, 5.31). Hence, the classification of WIL as YRZ or SRZ using this method is entirely dependent on the definition used to classify the SRZ and YRZ. Should the YRZ be restricted only to the southern coast, the dispute in the classification of WIL may highlight that this location is either considerably close to the boundary between the SRZ/YRZ or this location may characterise the boundary location between the SRZ and YRZ. As previously noted, numerous authors (e.g. Cooke, 1946; McGee, 1977; Taljaard & Steyn, 1991; Schulze & Maharaj, 2007; Engelbrecht *et al.*, 2015) have suggested that the YRZ is bound by the Cape Fold mountain range. Given this, it may be expected that WIL, which is bound by the Cape Fold Mountain Range, would have been classified as YRZ across all of the approaches. However, WIL is located in the northern parts of this mountain range closer to the SRZ, and the annual cycle of rainfall at WIL demonstrates predominantly more summer rainfall still with a substantial amount of winter rainfall (Figure 5.4). Thus, the complexity in the topography surrounding WIL may add complexity to the rainfall regimes of WIL, and this

may be a reason for the difficulty in classifying this location as either SRZ or YRZ. Complexity in the classification of WIL may also be attributed to the relatively low stability of the rainfall regimes captured across the methods (Table 5.8). Herrmann and Mohr (2011) quantified only up to 10% stability in the rainfall seasonality classification across the area WIL encompasses.

Of the zones classified in Figure 6.1, the final zone covered here is that of no clear definition. SUT (Sutherland) is the only weather station which occupies this zone, and was classified as SRZ once using the cluster-based approach (Figure 5.11), twice as WRZ using the onset and cessation dates and the percentile-based approach (Figure 5.27, 5.39) and once as YRZ using the seasonality scores (Figure 5.15; Table 6.1). SUT was characterised by a total period seasonality score of -0.10 which highlights that although SUT has relatively equable rainfall throughout the year, there was slightly more winter rainfall during the study period (Figure 5.12). The very weak *r value* of 0.17 highlights that the rainfall regime at SUT has almost no distinct seasonality (Figure 5.12). Both the onset and cessation dates and the percentile-based approaches quantified a relatively long mean wet season length of approximately seven to eight months (Table 5.4, 5.6). A wet season with a duration of at least nine months is required for a location to be classified as YRZ using the percentile-based and onset and cessation dates approaches. SUT appeared to mostly straddle the classification of WRZ and YRZ, during the study period, where the classification of SRZ using the cluster-based approach is questionable. The reason for this is that the strength of the cluster solution was, at best, relatively moderate. Since SUT has a complex seasonal structure, it may have been that SUT was incorrectly classified especially because no YRZ was classified using the cluster-based approach. Under *Chapter 2 (Literature Review) Section 2.2* SUT was also highlighted as a location with considerable dispute regarding the classification of rainfall seasonality. Here SUT was also classified as no clear definition due to this location having been classified as SRZ, WRZ and YRZ in previous maps, as a result providing no definitive classification of SUT. The disputed classification of SUT highlights how complex the rainfall regimes are at the transition between the SRZ and WRZ, because arguably annual rainfall at SUT is characterised by both summer and winter rainfall synoptic systems (Nicholson, 2000). However, the contribution of these synoptic systems will vary annually, and this is highlighted by the relatively low stability in the rainfall regimes at SUT (Table 5.8). Additionally, this is highlighted by the particularly high level of variability, at 173.7%, in the

annual seasonality scores at SUT (Figure 5.13). Since the classification of SUT is considerably disputed here (Figure 6.1; Table 6.1) and in literature (See Figure 2 *Literature Review Chapter 2 Section 2.2*), this highlights that the rainfall seasonality characterisation and classification locations such as SUT (i.e. located at the transition zone between rainfall zones) would rely considerably on the way in which a metric defines rainfall seasonality (Raziei, 2017). The continued dispute at SUT thus highlights the need for a standard seasonality metric to define rainfall seasonality across South Africa.

From the outputs of each method it is evident that the sample of weather stations contained locations from all of the rainfall zones known to occur across South Africa, where this highlights that these weather stations were appropriate to have tested the different seasonality metrics. Arguably, all the methods applied in this study were well-suited for classification of the SRZ and WRZ, especially for the extremes of these rainfall zones. However, when considering the classification closer to where the boundaries would potentially occur and along the southern coast it is evident that the classification of rainfall zones is somewhat disputed (Figure 6.1). The transition between winter and summer rainfall has, in literature, been demonstrated to be the most difficult area to characterise in terms of seasonality (See Figure 2 *Literature Review Chapter 2 Section 2.2*). With the same dataset per location, it is apparent that there will always be dispute when classifying the seasonality of rainfall using different methods, units of scale (i.e. daily and monthly) and class limits (Raziei, 2017). The results of the outputs of the seasonality metrics highlight that classification of the rainfall seasonality of a location, especially for those closer to the boundaries between the rainfall zones, will always be dependent on the way in which seasonality is defined by the metric used. However, in an attempt to provide consensus on the classification of rainfall seasonality across South Africa, it is argued here that the seasonality scores provide the most accurate classification. The most important reason behind this is that the seasonality scores provide the best and most valuable classification of the transition zone between the SRZ and WRZ, where the class limits developed were to account for this transition zone. Additionally, the possible range of seasonality scores accounts for all degrees of seasonality while statistically defining the timing of rainfall, and these scores are spatially and temporally comparable. In light of this, it may be important to reconsider the YRZ and how it is defined, and

it should be noted that this is not to discredit any previous classifications or investigations on the YRZ as these are particularly important in understanding the YRZ. Hence, on the basis of the seasonality scores, the YRZ should be reconsidered and possibly even termed the transition rainfall zone, although YRZ will still be used for the remainder of this thesis. This transition zone is thus the area of South Africa where both summer and winter rain-bearing systems contribute to rainfall in this region. The YRZ may also be considered as two rainfall zones as the Cape Fold Mountain belt is a topographic barrier which splits this rainfall zone into two, being the northern and southern YRZ. It is important to note that the map on the classification of the seasonality scores presented under Figure 5.15 is not a new classification map. This is because the paucity of weather stations used for this study do not allow for accurate demarcation of the average boundary locations between the SRZ, WRZ and YRZ.

With the additional classifications from this study considered with classifications from literature (See Figure 2 of *Literature Review Chapter 2 Section 2.2*), there is still considerable dispute at the transition between the rainfall zones (Figure 6.2). The dispute in the classification presented in Figure 6.2 is relatively similar to that presented as Figure 2 under *Section 2.2* of *Chapter 2 (Literature Review)*. Additionally added to the map presented as Figure 6.2, and not in the previous map, is the class of 100% consensus. This class is captured only for the SRZ and WRZ, and it represents the region where there is absolutely no dispute across the maps presented in this project as well as published maps (Figure 6.2). Interestingly, there is not 100% consensus in the classification of YRZ across the southern coast (Figure 6.2). Although the southern coast is mostly classified as YRZ across previous maps (e.g. Engelbrecht *et al.*, 2015), some metric outputs did not classify a YRZ (e.g. Figure 5.11, Cramer and Hoffman, 2015) leading to the classification of YRZ >75% (Figure 6.2). It would appear that the no clear definition zone has reduced in size from covering 3% of the country to 1% (See Figure 2 of *Literature Review Chapter 2 Section 2.2*; Figure 6.2). However, this only as a result of the additional classifications from this approach, and this does not mean that there is less or more consensus in the classification between the SRZ and WRZ. The current map presented as Figure 6.2 serves to highlight that there is in fact still difficulty in comparing classifications of rainfall seasonality using different methods and that there may always be dispute especially near the boundaries of rainfall zones. The dispute highlighted across the

maps is important to note and it should also be used to suggest that no method may be accepted at face value and that the use of more than one method may be beneficial. However, as previously mentioned, there may always be dispute when classifying rainfall seasonality across South Africa using different methods. As a result, it may be best to instead focus on a standard method which may be used specifically to quantify climatological rainfall seasonality to focus on further understanding the rainfall zones which characterise South Africa. This is important to avoid confusion and to create comparable results between different studies on rainfall seasonality. The standard method, discussed in the subsequent section, is suggested in part to address the dispute in the classification of rainfall seasonality particularly at the transition between the SRZ and WRZ.

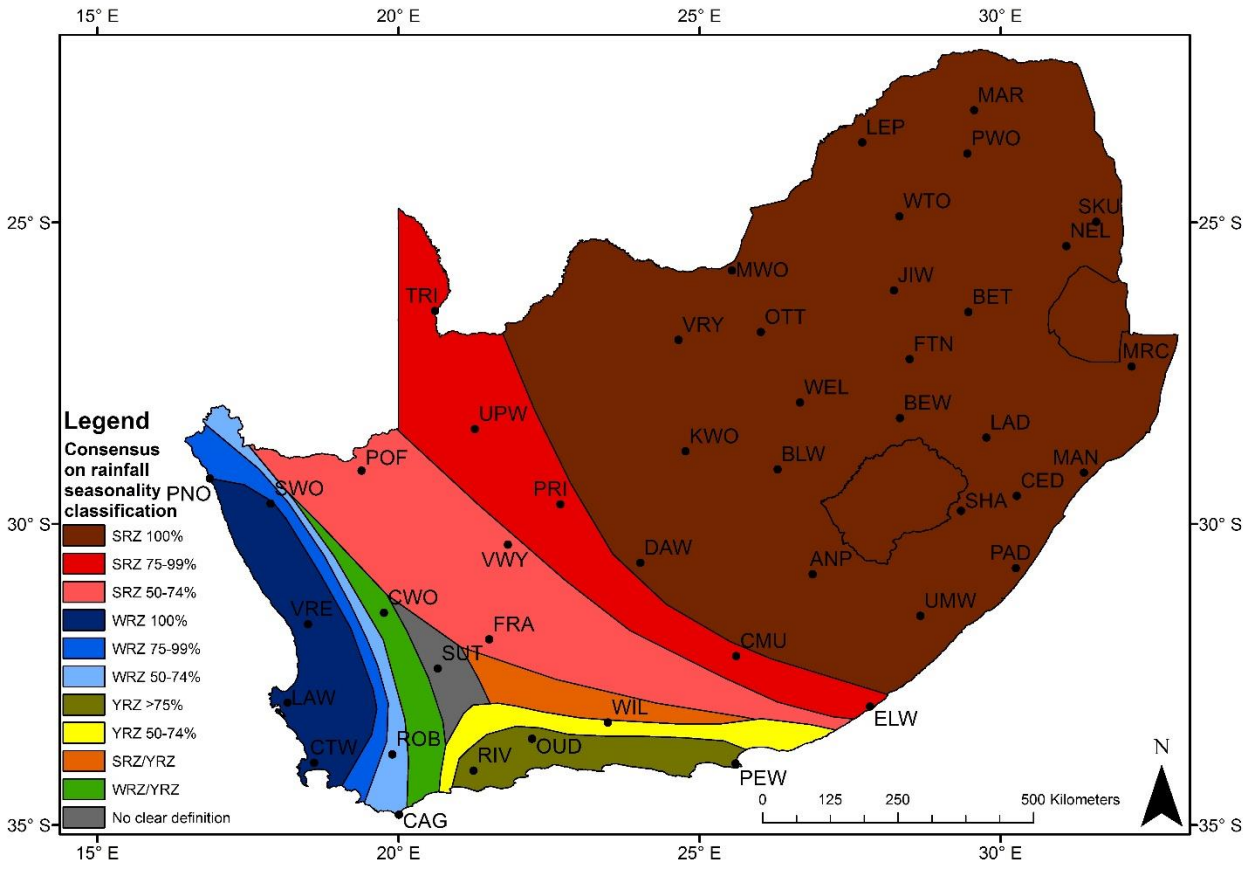


Figure 6.2: Composite map on the consensus and dispute on the spatial distribution of rainfall seasonality zones across South Africa (including Lesotho and Swaziland) captured between the statistical approaches used for this study and from previous maps of rainfall seasonality represented in *Figure 2* of the published paper under *Section 2.2 of Chapter 2 (Literature Review)*.

In an attempt to address the disputed classification of rainfall seasonality across South Africa, the map presented under Figure 6.3 was developed. This map mainly relies on the seasonality scores. However, since the classified weather stations are so sparsely distributed across the country, boundaries estimated on the basis of the seasonality score map presented as Figure 5.15 would not be accurate. In order to demarcate boundaries which are relatively accurate, all the maps used to produce Figure 6.2 were considered. Thus the boundaries of the SRZ and WRZ represent closely the boundaries of SRZ 75-99% and WRZ 50-74% (Figure 6.2, 6.3). Additionally, the YRZ has been classified as the transition zone between the SRZ and WRZ on the basis of the output of the seasonality scores, whereby north and south of the Cape Fold Mountains are treated as different rainfall regimes (Figure 6.3). As previously discussed, locations north of the Cape Fold Mountains demonstrate slight seasonality, while locations to the south demonstrate aseasonal conditions (Figure 6.3). As such, the map presented as Figure 6.3 may be considered as a new classification map, although it is important to note that this is only a tentative classification and there may be discrepancies closer to the boundaries.

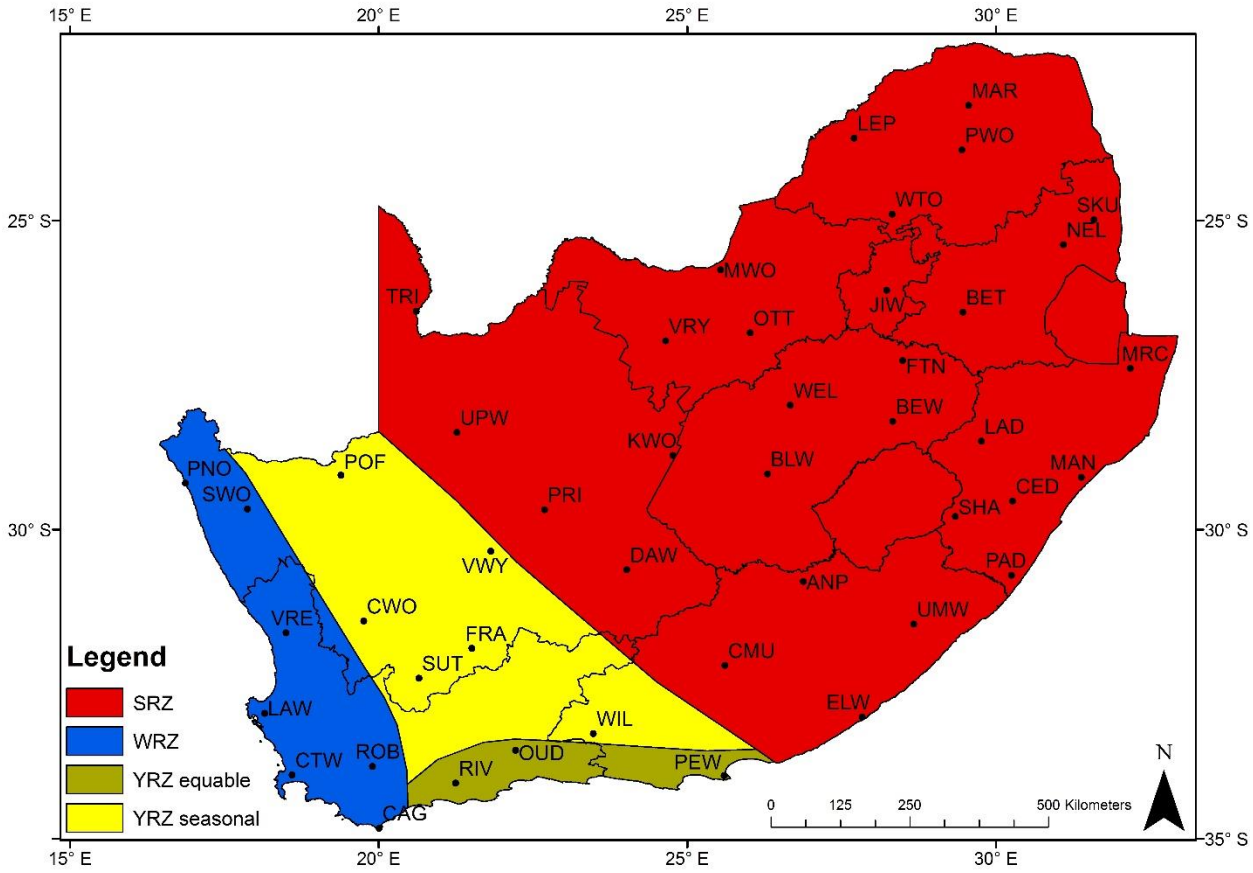


Figure 6.3: Estimated spatial distribution of rainfall seasonality across South Africa (including Lesotho and Swaziland).

6.3.1 TOWARDS A STANDARD APPROACH TO QUANTIFY, CHARACTERISE AND CLASSIFY RAINFALL SEASONALITY ACROSS SOUTHERN AFRICA

Dispute in the classification across the four methods applied in this study emphasises that even with the same datasets per location, the classification of rainfall seasonality may always be disputed across different methods (Figure 6.1). Similarly, across Iran five seasonality metrics were applied to the same temporally constrained dataset per location, and from the results of this study it is evident that the output of the metrics did not converge on the same classification of rainfall seasonality (Raziei, 2017). Given the dispute across the methods and the need for continued research, a standard method to quantify rainfall seasonality is necessary. The standard method presented here is thus to be used to give direction to future research which may be informed by the suggested avenues for future research that are highlighted by the results obtained from this

study and which are discussed under *Chapter 7 (Conclusion)*. The standard approach here is suggested for use across southern Africa, considering the nature of rainfall regimes and accurate representation of these, and is in two parts with two standard methods recommended. The metric selected for use (i.e. between either the first or second standard approach or both) will depend on the scientific end being pursued. In considering the approaches, the first standard method only considers the approaches used in this study. This is not to discredit any previous methods applied in literature, but rather to reflect on a method from this research project which may be best suited to quantify rainfall seasonality across the entire region of southern Africa. The second method considers all rainfall seasonality metrics which have been captured in *Chapter 2 (Literature Review) section 2.2*, where activity specific approaches are also highlighted with the main focus to completely describe the complex concept that is rainfall seasonality. The main purpose of the standard metrics is to characterise the current seasonality and its variability, where the metric can also be used to relate seasonality to wider scale mechanisms and drivers (Dunning *et al.*, 2016). Important to note is that these standard methods are suggested as a consistent methodology particularly for comparison purposes, spatially, temporally and across different studies.

In considering the first standard method it is suggested that the approach on the ratio of temperature to rainfall returning seasonality scores, developed by Thackeray and Fitchett (2016) and described under *Section 4.4.2* of *Chapter 4 (Data and Methodology)*, be applied. This method produced the best classification of rainfall seasonality, where it can be suggested that the seasonality scores were the most accurate in classifying the complex YRZ/transition zone between the SRZ and WRZ (Figure 5.14, 5.15). A distinction should be made between the different types of seasonality (e.g. agricultural and climatological seasonality), with application of the seasonality scores approach mainly to explore climatological seasonality, where the reasons behind this will be highlighted throughout this section. First, it should be noted that the main reason behind suggesting this as a standard approach is that one quantified value on rainfall seasonality is obtained which is the seasonality score. This seasonality score statistically discriminates between summer and winter rainfall conditions which is particularly important when modelling rainfall seasonality across southern Africa (Thackeray & Fitchett, 2016; Fitchett & Bamford, 2017). This seasonality score is also considerably easy to quantify using observational records provided that

at least one calendar year of measurements is available for both rainfall and temperature (See *Chapter 4 Section 4.4.2*). Interestingly, the ratio of temperature to rainfall is one of few seasonality metrics which consider temperature for quantification, the only others being metrics used by Herrmann and Mohr (2011) and Cramer and Hoffman (2015). The metric used by Herrmann and Mohr (2011) does not distinguish between summer and winter rainfall, whereas the metric used by Cramer and Hoffman (2015) did not quantify YRZ conditions across the southern coast, a region in literature well-known for aseasonal rainfall conditions (e.g. Engelbrecht *et al.*, 2015). Additionally, this seasonality score provides invaluable information on rainfall seasonality (See *Chapter 5 Section 5.4.2*), and application of this approach is not limited to contemporary rainfall seasonality as shown by previous application of this approach in the palaeoclimatology record (e.g. Thackeray & Fitchett, 2016). An approach applicable over long temporal scales, particularly over 1,000 years and more, is particularly important in understanding the dynamic nature of rainfall seasonality and the drivers (Fitchett & Bamford, 2017). As a standard approach, there are numerous strengths and some limitations associated with this approach, where these will be reflected on, in the paragraphs which follow, by considering all four approaches applied in this study.

Liebmann *et al.* (2012) note the importance of a consistent and objective method to quantify rainfall seasonality. In considering this, the seasonality scores approach recommended here is consistent in that the score obtained is spatially and temporally comparable as it shows differences in the strength and sign of seasonality across South Africa over a north-south and east-west gradient (Figure 5.14; Table 5.3; Walsh & Lawler, 1981; Thackeray & Fitchett, 2016), and objective in that this method is robust and with few assumptions (Deng *et al.*, 2019). There are especially few assumptions when compared to the methods quantifying the onset and cessation dates as well as the 10% and 90% dates, where the main assumptions associated with these two approaches used in this study include: 1) thresholds defining a rain day as well as the start and end dates of the wet season, and 2) the start of the 12-month climatological year being from the month following the mean month of minimum rainfall and for locations with no clear seasonal structure the starting month is from January (Odekunle, 2006; Liebmann *et al.*, 2012; Boyard-Micheau *et al.*, 2013; Feng *et al.*, 2013; Dunning *et al.*, 2016; Deng *et al.*, 2019). Concerning the seasonality scores,

the most important assumption which mainly influences the classification of rainfall seasonality is that of the boundaries attributed to the SRZ, WRZ and YRZ (Table 4.4). This assumption should not influence the quantified seasonality score, however, in considering the boundaries it should be noted that these were not objectively tested and there may still be some uncertainty. Hence, it is recommended that future research test these boundaries in both the palaeo and contemporary record, possibly following the method of Fitchett and Bamford (2017). Noting this, it can be argued that the boundaries for the seasonality scores are robust since any score obtained can be placed in a category of SRZ, WRZ and YRZ, whereas this is not the case for the remaining approaches given the temporal variability in the dates of the wet season commencement and withdrawal. For instance, a proviso classification was attributed to Pofadder and Twee Rivieren (See Table 5.4 of *Section 5.4.3 of Chapter 5*) where these were classified as SRZ since the mean wet season was during the summer months but the summer solstice did not occur during this period, and Willowmore (See Table 5.6 of *Section 5.4.4 of Chapter 5*) was classified as YRZ given that the mean wet season length dates contain both the winter and summer solstice dates, however, without spanning a period of at least nine months.

An important feature of a method to model rainfall seasonality is the ability to accurately detect change and intra-annual variability (Feng *et al.*, 2013; Herrmann & Mohr, 2011; Dunning *et al.*, 2016; Fitchett & Bamford, 2017; Deng *et al.*, 2019). This is important because rainfall is inherently characterised by variability and as a result the seasonal characteristics of rainfall are also intrinsically characterised by variability (Tadross *et al.*, 2009; Feng *et al.*, 2013; Deng *et al.*, 2019; Zhang *et al.*, 2019). Excluding the cluster-based approach, where only a mean classification is obtained, each of the methods applied in this study demonstrated capability in quantifying change and variability through the ability to quantify annual seasonality characteristics (*Chapter 5 Section 5.5*). It can be argued that the changes detected across all the methods were accurate for the study period of 1987-2016 as it is expected that the changes may not always agree spatially and across different methods especially over shorter temporal periods where naturally occurring variations in climate can greatly affect the calculation of trends (de Luis *et al.*, 2000; MacKellar *et al.*, 2014; Raziei, 2017; Appendix G; Table 5.8). Noting this, there was a high level of agreement both spatially and across the different methods which would confirm the accuracy of most of the

trends (Table 5.9; Figure 5.47), where this will be discussed later under *Section 6.4*. In considering the reliability of the trends quantified, it should be noted that the accuracy of the changes detected in the onset and cessation dates are questionable for some locations. This is especially for locations along the western coast, within the western central interior and along the southern coast where dates were not quantified for each year, mostly due to low rainfall totals (Table 5.4). Additionally, for locations with no clear wet season, for example Port Elizabeth Wo among other locations along the southern coast (Figure 5.4), additional measures, as noted earlier, had to be taken to ensure meaningful dates were obtained for both the onset and cessation dates and percentile-based approaches (See *Section 4.4.3* *and* *4.4.4* of *Chapter 4 Data and Methodology*). Liebmann *et al.* (2012) and Dunning (2018) similarly noted such limited performance across the southern coast in the method of onset and cessation dates they applied. As a result, this may influence the accuracy of both the dates and the trends quantified, not only for the onset and cessation dates but also for the percentile-based approach, for locations with no clear wet season. Hence, these limitations would point towards application of the seasonality scores approach especially in quantifying seasonality across the YRZ, where scores were quantified annually with no need for any additional measures. Additionally, it can also be argued that each method accurately quantified variability as the patterns observed were as expected (Figure 5.13, 5.24, 5.36; Table 5.8). For instance, locations classified as YRZ, using the seasonality scores approach, were characterised by the lowest strength of relationship, the highest CV levels as well as the greatest instability in regimes (Figure 5.13, 5.16; Table 5.8), where this would be expected given that this region is the marginal area between the winter and summer rainfall regimes (Nicholson, 2000). Since similar patterns of variability and instability in regimes were quantified for the onset and cessation dates, and percentile-based approach, then it may be suggested that these patterns are also accurate (Figure 5.24, 5.36; Table 5.8).

To contribute to a complete description of rainfall seasonality the quantified seasonality score provides information on the timing of rainfall as well as the degree of seasonality (Feng *et al.*, 2013; Pascale *et al.*, 2015, 2016), although this is only on a monthly scale. It is notable that none of the seasonality metrics applied in this project and in literature contribute to completely describing rainfall seasonality (Roffe *et al.*, 2019), however, the onset and cessation dates, 10%

and 90% dates and cluster-based approaches provide a more complete description of rainfall seasonality. This information is obtained over a monthly scale using the cluster-based approach, where the boundaries of the wet and dry seasons contribute to the timing and duration components, and rainfall amount during these seasons contributes to the magnitude component (*Chapter 5 Section 5.4.1*; Feng *et al.*, 2013; Pascale *et al.*, 2015, 2016). Of the four approaches, the onset and cessation dates and 10% and 90% dates are more valuable for a complete description where this information is quantified over a daily scale affording application of these approaches for agricultural seasonality as an example (Dunning *et al.*, 2016, 2018). Dates for the start and end of the wet season and quantification of the wet season duration contribute to the components on the timing and duration for both the dry and wet seasons (*Chapter 5 (Results) Section 5.4.3*, *5.4.4*; Liebmann *et al.*, 2012; Dunning *et al.*, 2016). Although not quantified for this study, which focused on the seasonal boundaries of the wet and dry season instead, total rainfall amount during the wet and dry season contributes to the magnitude component and the rainfall rate (total wet or dry season rainfall amount/number of rain days) contributes to quantifying the intensity of rainfall (Liebmann *et al.*, 2012; Pascale *et al.*, 2015). Additionally, the length of wet/dry spells during the wet/dry season may be quantified (Reason *et al.*, 2005; Usman & Reason, 2004; Moeletsi *et al.*, 2011). Although not a quantitative measure of the degree of seasonality, as for the seasonality scores, the duration of the wet season for these approaches may provide a relative measure of the degree of seasonality. For instance, a shorter wet season duration at JIW (Johannesburg Wo), within Gauteng, than at PAD (Paddock), along the eastern coast, highlights that rainfall at JIW is more seasonal than for PAD. For a study focused on obtaining a complete description of rainfall seasonality it would be necessary to consider the methods on the onset and cessation dates and 10% and 90% dates. The 10% and 90%, however, have more value across the entire region of southern Africa as this method depends on the actually rainfall amount of a location and not an arbitrary threshold as for the onset and cessation dates. Moreover, using the onset and cessation dates and percentile-based approach, the wet season of a location can also be further classified into early, late, mid or long wet season categories, or any other categories the user defines, which are valuable to compare the wet season across locations within the SRZ and WRZ. Similarly Hermann and Mohr (2011) defined eight seasonality classes (e.g. single wet season bimodal and

single wet season multimodal) across Africa, where these may be of value in comparing the structure of wet seasons. Across Africa, both Liebmann *et al.* (2012) and Dunning *et al.* (2016) apply harmonic analysis to identify regions which have one or two wet seasons per year which may be valuable in investigations across the southern coast, especially when considering more than the second and first harmonic. Across Australia, rainfall seasonality has also been classified in additional seasonality classes of more than just summer and winter rainfall, where the dry season was used to define regions which have summer rainfall with dry winter months as well as regions which have summer rainfall with low rainfall during the winter months, as an example (Gaffney, 1971).

As previously noted, application of the seasonality scores approach alone may be somewhat limited, especially for some rainfall dependent activities across southern Africa such as agriculture and water resource management. For such activities it would be more societally relevant and valuable to additionally obtain measurements which provide a more complete description, for instance start and end dates of the wet season (Reason *et al.*, 2005; Tadross *et al.*, 2009; Feng *et al.*, 2013; Pascale *et al.*, 2015), and as such it is recommended that multiple approaches be applied. For these activities the seasonality scores approach may be used in conjunction with other approaches which provide a more complete description, where this may contribute to a second standard approach along with other statistical approaches applied from literature. There are a confounding number of seasonality approaches which have been produced in literature (e.g. Raziei, 2017; See *Chapter 2 Section 2.2 Figure 2*), and as a result it is difficult to suggest which would be most accurately applied across southern Africa. Across Iran Raziei (2017) compared most of the known seasonality metrics, noted under *Section 2.2 of Chapter 2 (Literature Review)*, by standardising the indices as a *z-score*, and through correlation analysis it was concluded that the approaches may be used interchangeably since the lowest *r value* was 0.84, which is considered to represent a strong relationship. However, most of these metrics do not statistically discriminate between SRZ and WRZ conditions, through defining the timing of rainfall, and thus should not be applied across southern Africa (Figure 2.1). In considering this, the methods tested in this project as well as methods in literature, and in the context of rainfall dependent activities across southern Africa (i.e. water resource management, tourism, and agriculture among others), it may be argued

that the most widely applicable seasonality approach to obtain a more complete description of rainfall seasonality, in conjunction with the seasonality scores approach, would include some form of the commencement and withdrawal dates of the wet season. This is because these methods discriminate between summer and winter rainfall and these are some of few methods which consider rainfall seasonality over a daily scale (Figure 2.1). The percentile-based method may thus be widely applied across southern Africa to quantify seasonality for activity specific applications. Although, as already mentioned, this approach is only somewhat suitable across the YRZ. This excludes application of the onset and cessation dates as the results from this study would suggest that this approach is not widely applicable across the southern Africa region, owing to areas where rainfall is particularly low. In considering the use of the percentile-based approach in the context of contrasting high and low daily to annual scale rainfall totals South Africa, it is important to note the strengths of this approach as this approach is not sensitive to very low rainfall as the percentile quantification is relative to the rainfall amount of a location (Guenang & Kamga, 2012; Amekudzi *et al.*, 2015). It is notable that the wet season duration and the seasonality scores are relatively strongly related statistically, similar to Raziei (2017), for predominantly winter regimes ($r = 0.71$, $p = 0.0061$), characterised by negative seasonality scores, and predominantly summer regimes ($r = 0.54$, $p = 0.0008$), characterised by positive seasonality scores, thus highlighting that these two methods may be applied together. Although the percentile-based approach is suggested as a second standard approach for application it is important to highlight that it may not be entirely suitable for agriculture as this method does not take into account 'false onset' (i.e. a heavy rainfall event followed by a prolonged dry period at the beginning of the wet season), but it is suitable for other activities sensitive to rainfall regime changes such as water resource management and conservation. Since the anomalous accumulation approach, developed by Liebmann *et al.* (2012) and adapted by Dunning *et al.* (2016) accounts for 'false onset', then it is suggested that this approach is well-suited to agricultural activities and it may especially be useful for seasonal forecasting efforts (Shongwe *et al.*, 2015), of which there have been many developments across South Africa (e.g. Ratnam *et al.*, 2018). It is important to note the limitations of this methodology in that it struggles to quantify seasonality for locations with very low rainfall and with year-round rainfall without additional measures (Dunning, 2018).

6.4 SHIFTS IN RAINFALL SEASONALITY ACROSS SOUTH AFRICA

From the results presented under *Section 5.5 of Chapter 5 (Results)*, there is ample evidence that for the period of 1987-2016 rainfall seasonality across some of the selected weather stations has undoubtedly changed. The sections which follow presents the interpretation of these results both in the context of palaeoclimatology and contemporary climatology research exploring rainfall seasonality shifts across South Africa.

6.4.1 TRACKING CHANGES IN THE BOUNDARIES OF THE WRZ SINCE THE LGM

During the LGM, which for ease of comparison may be conservatively dated to 24,000-18,000 cal. yr BP (Chase & Meadows, 2007), it is well-understood that the latitudinal extent of the Southern Hemisphere Westerlies extended further north than at present (e.g. Carr *et al.*, 2006; Chase & Meadows, 2007; Norström *et al.*, 2009, 2014; Mills *et al.*, 2012; Stager *et al.*, 2012; Thackeray & Fitchett, 2016; Fitchett & Bamford, 2017; Neumann & Scott, 2018; Faith *et al.*, 2019). Although there is ample evidence to support this shift, the geographic limits of this shift in extent are still debated (see *Chapter 2 Literature Review Section 2.3.2.1*; Chase & Meadows, 2007; Fitchett *et al.*, 2017c). Central to this debate is that during the LGM the Westerlies would have extended further north due to expansion of Antarctic sea ice extent and the polar high-pressure cells, with diminished equatorial heating resulting in contraction of the Hadley cell (Chase & Meadows, 2007). The result of this would mean that a greater proportion of cold front arms from frontal systems, originating in the Westerlies, would penetrate into the interior regions of southern Africa which would have resulted in an expanded WRZ (Chase & Meadows, 2007). Accurate quantification of the spatial extent of the WRZ during the LGM, and the dynamics of the WRZ since the LGM to present, would facilitate an improved understanding of the heterogeneity in late Quaternary moisture records for southern Africa (Fitchett & Bamford, 2017). This would also facilitate an improved understanding of the contemporary record, where a connection between contemporary and palaeo rainfall seasonality reconstructions may be pertinent to understanding the dynamics of seasonality and of the rainfall zones across southern Africa.

On the basis of locations understood to represent WRZ conditions during the LGM (Figure 2.3; See *Section 2.3.2.1* of *Chapter 2 Literature Review*), a tentative boundary line for the LGM WRZ has been developed (Figure 6.4). The sites used to develop this boundary were predominantly based on fossil pollen evidence (Figure 2.3; See *Section 2.3.2.1* of *Chapter 2 Literature Review*). On this same map (Figure 6.4), a tentative boundary line of the contemporary WRZ has been drawn, based on the outputs of the metrics (mainly the seasonality scores) used in this study as well as on the consensus across published seasonality maps (Figure 6.2, 6.3). Similarly, Chase and Meadows (2007) and Engelbrecht *et al.* (Under Review) developed maps pertaining to the location of the WRZ boundary location during the LGM. The maps presented by Chase and Meadows are based on the early conceptual models of van Zinderen Bakker (1967, 1976), Heine (1982) and Cockcroft *et al.* (1987). The eight maps presented by Engelbrecht *et al.* (Under Review) are based on dynamic downscaling of the LGM climate, where the percentage of rainfall amount (i.e. WRZ > 66% of rainfall during April to September, SRZ > 66% of rainfall during October to March, and YRZ 33-66% of rainfall during April to September; Chase & Meadows, 2007) was used to delineate boundaries of the SRZ, WRZ and YRZ. The boundaries of the LGM WRZ across the map presented as Figure 6.4, and the maps of Chase and Meadows (2007) as well as Engelbrecht *et al.* (Under Review) are all broadly similar depicting that the WRZ extent during the LGM was larger in both a northerly and an easterly direction. The northern extent of the LGM WRZ boundary, at ~28°S presented under Figure 6.4 is smaller than ~22-23°S quantified by Engelbrecht *et al.* (Under Review), ~23°S reconstructed by Chase and Meadows (2007) on the basis of Van Zinderen Bakker (1967, 1976), and ~22°S reconstructed by Chase and Meadows (2007) on the basis of Cockroft *et al.* (1987). The northern extent of the LGM WRZ boundary presented under Figure 6.4 is, however, relatively similar to the ~30°S boundary reconstructed by Chase and Meadows (2007) on the basis of Heine (1982). The eastern extent of the LGM WRZ boundary was determined as ~30°E (Figure 6.4). This is larger than the extent of 22-24°E quantified by Engelbrecht *et al.* (Under Review) and the ~25°E reconstructed by Chase and Meadows from Van Zinderen Bakker (1967, 1976). The extent presented under Figure 6.4 is smaller than the extent of ~33°E reconstructed by Chase and Meadows from Cockroft *et al.* (1987). Again, the eastern extent is relatively similar to ~28°E reconstructed by Chase and Meadows from Heine (1982). The dispute across these

reconstructions of the WRZ LGM extent highlights the need for a standard approach to quantify rainfall seasonality in the palaeorecord. Since the ratio of temperature to rainfall returning seasonality scores has been successfully applied to the palaeorecord (e.g. Thackeray & Fitchett, 2016) and has now been demonstrated to accurately quantify contemporary rainfall seasonality across South Africa, then it may be argued that the continued use of this approach will be invaluable for future research pertaining to rainfall seasonality.

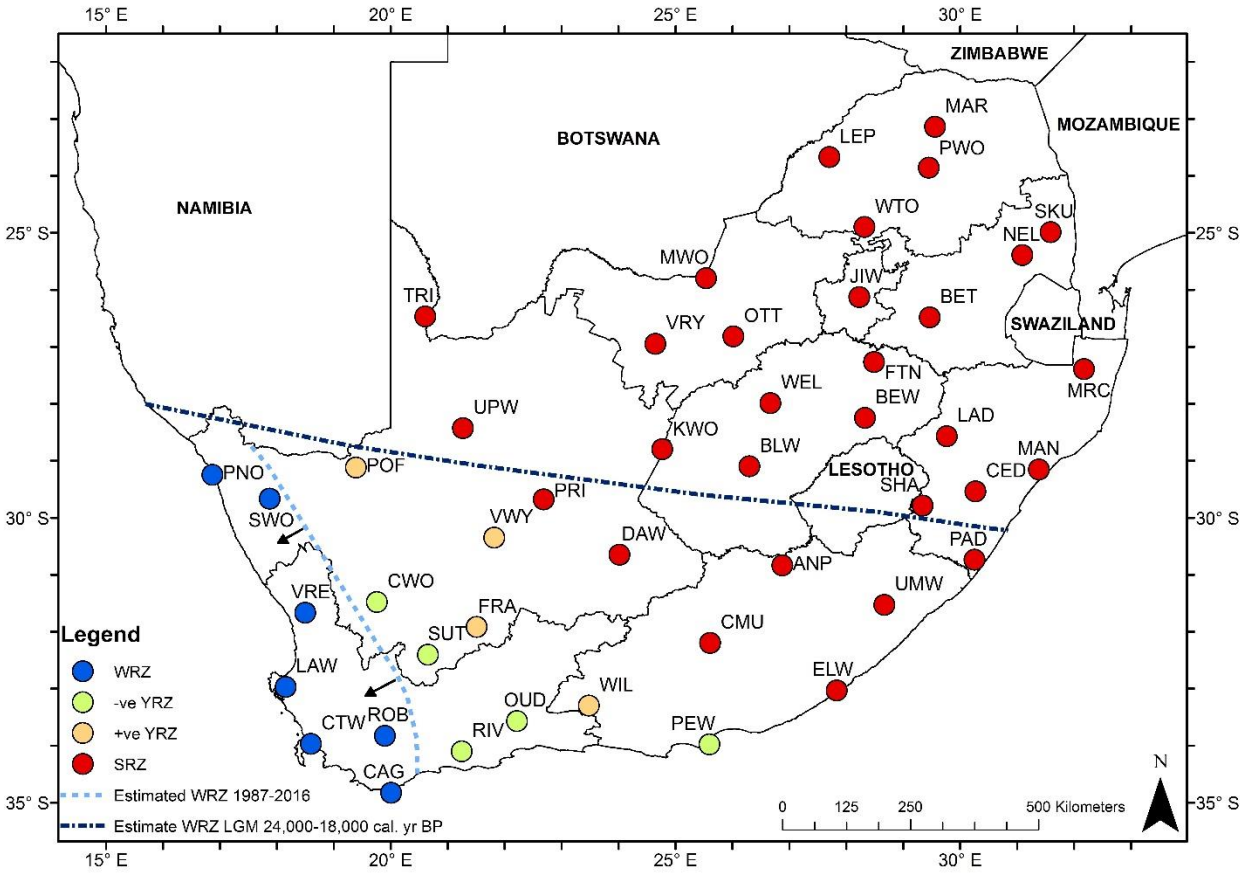


Figure 6.4: Map demonstrating the estimated boundary location of the WRZ during the LGM, based on *Figure 2.3*, and presently, based on *Figure 6.3*. Arrows on the contemporary WRZ boundary represent the progressive shift of this boundary under climate change. The study locations are represented on the basis of the total period seasonality scores presented under *Table 5.2*.

From the two boundaries estimated for Figure 6.4, it is apparent that the extent of the WRZ has shifted considerably since the LGM. The two boundaries plotted, although using different methods, are comparable as both methods rely on a measure of the relationship between

temperature and rainfall (Fitchett & Bamford, 2017). As previously mentioned, the WRZ LGM boundary is mainly based on pollen records using the ratio of fossil pollen ratio Asteraceae to Poaceae, while the contemporary boundary mainly relies on the seasonality scores (Figure 6.4). Fitchett & Bamford (2017) highlight that these two methods should be used in conjunction to quantify shifts in the Westerlies, where this is appropriate given that the seasonality scores method is suggested as the best method to quantify contemporary climatological seasonality across South Africa (see *Section 6.3 and 6.3.1*). In considering the changing extent of the WRZ, as expected the WRZ extent has declined considerably since the LGM (Figure 6.4). The most notable change in the WRZ is in the eastern extent, where it is estimated that the boundary shifted up to ~1,100km along the southern coast (Figure 6.4). Since the LGM, it is argued that the Hadley cell would have expanded, although the latitudinal extent would have varied, and as a result of this expansion as well as a reduction in Antarctic sea ice, increased convective summer rainfall would occur across southern Africa (Chase *et al.*, 2015, 2017; Engelbrecht *et al.*, Under Review). Additionally, there would have also been a reduction in the frequency of cold front arms from frontal systems reaching the interior of southern Africa (Chase *et al.*, 2015, 2017). Change in the relative dominance of tropical and temperate systems would have contributed to changes in the extent of both the SRZ and WRZ (Chase *et al.*, 2017). It would appear that there has been little to no change in the northern extent of the WRZ boundary (Figure 6.4), although it should be highlighted that the northern extent of the contemporary WRZ remains unknown given that no meteorological records from the southwest of Namibia were used in this research project. Notably, Engelbrecht *et al.* (Under Review) also demonstrate little to no change in the northern extent of the resulting LGM and contemporary WRZ boundaries, while noting a change of ~2-4° in the eastern extent. In considering the contemporary boundary locations between the WRZ and YRZ, and the SRZ and YRZ (Figure 6.4), it should be noted that the boundary locations did not necessarily shift in extent when comparing the seasonality scores at the beginning and end of the study period of 1987-2016 (Figure 6.4; Appendix G). This is expected because changes in seasonality would be small over a thirty year period given that changes in synoptic circulation would drive these changes (Nicholson, 2000; Lennard & Hegerl, 2015; Fitchett & Bamford, 2017).

Although, the problem of quantifying the spatial extent of rainfall zones is still noteworthy, this study contributes to a continued effort to quantitatively determine the changing extent of the rainfall zone boundaries. The changing extent of the WRZ evident from Figure 6.4 conceptually confirms evidence from palaeoclimatology and climate modelling research which argues that a poleward displacement of the Westerlies would likely result in increasing aridity and a reduction in the WRZ across South Africa (Christensen & Hewitson, 2007; Engelbrecht *et al.*, 2009; Stager *et al.*, 2012; Favre *et al.*, 2016; Mahlalela *et al.*, 2018; Engelbrecht *et al.*, Under Review). This is similarly demonstrated by the resulting agreement of trends towards YRZ conditions for locations including CAG (Cape Agulhas), CTW (Cape Town Wo), LAW (Langebaanweg AWS), PNO (Port Nolloth), SWO (Springbok Wo) and VRE (Vredendal; Figure 5.47), and this is mainly due to a tentative reduction in rainfall during the winter months (Figure 5.6). An expansion of the Hadley cell and a consequent poleward displacement of both the subtropical high pressure belt (also with an increase in intensity) and Southern Hemisphere Westerlies would promote a reduction in winter rainfall, where Engelbrecht *et al.* (2009) project that this may result in a statistically significant reduction of 10-40% of winter rainfall for the period of 2070-2100. If the changes in the seasonality scores for the WRZ locations (i.e. CAG, CTW, LAW, PNO, SWO and VRE) persist it is estimated that these locations will all experience a year-round rainfall regime by 2112, considering the trends quantified for the seasonality scores (Appendix H). This highlights the pertinence of developing and, more importantly, implementing adaptation strategies for activities such as agriculture, tourism and water resource management within the WRZ (Sousa *et al.*, 2018).

Acknowledging the changes in the seasonality scores across the WRZ, the general tendency towards aseasonal conditions reflected in the seasonality score trends across 23 of the study locations should also be highlighted (Figure 5.41). Thackeray (1988) investigates a 40,000 year record of palaeo temp and rainfall at Wonderwerk in Limpopo, and demonstrate a link between warmer and drier conditions throughout much of this record. It may be postulated that these findings in conjunction with the shifts towards aseasonal conditions across most weather stations may reflect that the predicted future increases in temperatures across South Africa may be associated with drier conditions (e.g. MacKellar *et al.*, 2014, Archer *et al.*, 2018, IPCC, 2018). These aseasonal trends may thus be interpreted through a reduction in rainfall amount given the reliance

of this method on measurements of MMR. With an increase in monthly temperature and a decrease in monthly rainfall, the gradient (i.e. the seasonality score) of the trendline quantifying the relationship between sqrt MMR and sqrt MMT would decrease and tend towards zero (i.e. towards aseasonal conditions). This thus highlights that there should be concern that future increases in temperature may potentially be associated with drier conditions which would surely influence rainfall sensitive activities (e.g. agriculture and water resource management) across the country, and broadly across southern Africa.

6.4.2 CONTEMPORARY CHANGES IN RAINFALL SEASONALITY FOR THE PERIOD OF 1987-2016

Changes in rainfall seasonality for the period of 1987-2016 across South Africa have been quantified and are expressed in terms of the timing, duration and magnitude of rainfall (See *Chapter 5 Section 5.2, 5.3 and 5.5*). This temporal period coincides with the most recent decades where anthropogenically induced climate change has been more evident (IPCC, 2007, 2013, 2018). Agreement, discussed in the sections below, with projected trends for some of the observed trends quantified would suggest that these trends are representative of how rainfall regimes may change under anthropogenically induced climate change (Zhao, 1993; de Luis *et al.*, 2000; MacKellar *et al.*, 2014; Pascale *et al.*, 2016; van Wilgen *et al.*, 2016); and this highlights a need for further monitoring, with additional weather stations and a longer temporal period, especially because projections for rainfall across South Africa are particularly dire (Engelbrecht *et al.*, 2009; IPCC, 2018). Moreover, the burden of climate change is already being experienced across parts of South Africa. For instance, Sousa *et al.* (2018) posit that changing patterns in WRZ seasonality, linked to a poleward displacement of the subtropics and Westerlies, are a cause of the 2015-2017 drought experienced in Cape Town.

Under this section all trends quantified are discussed in conjunction, for the following metrics: annual and monthly rainfall amount; seasonality scores; onset and cessation dates, the wet season duration and number of rain days; and 10% and 90% dates, the wet season duration and number of rain days (See *Chapter 5 Section 5.2, 5.3 and 5.5*). The trend analyses for this period revealed

only 8% (i.e. 83 statistically significant trends out of 1012 trends quantified) of statistically significant trends in all of these quantities indicating that rainfall amount and the seasonal characteristics of rainfall have not necessarily changed during the study period. The statistically significant trends are particularly important to note for devising location specific adaptation strategies. This is the case for a location such as OTT (Ottosdal), located in the North West, which demonstrated statistically significant trends for the onset dates, wet season duration (for both the onset and cessation dates and percentile-based approaches) and number of rain days (for both the onset and cessation dates and percentile-based approaches; Appendix G). In general, there is also a relatively low probability that the changes were quantified by chance for the study period (Figure 5.46). The lack of statistically significant trends was expected and may be attributed to the relatively short time frame of 1987-2016 analysed. This does not imply static rainfall regimes, and instead these regimes would have been subject to year to year variability which would create statistical noise obscuring the trends (Fauceherau *et al.*, 2003; Pryor & Schoof, 2008; MacKellar *et al.*, 2014; Davies *et al.*, 2016; Gitau, 2016). This is also confirmed by the change points which are indicative of relatively high levels of variability (Appendix G; Mphale *et al.*, 2014; Mazvimavi, 2010), where the drivers behind these are beyond the scope of this project and only the changes in the magnitude and direction of trends were considered for the change points. All of the trends quantified, whether statistically significant or not, are considered for this section of the discussion, where the focus is particularly on the direction and probability of change during the study period (Table 5.9; Figure 5.48). Noteworthy, is the high level of agreement in the direction of change across the three approaches (i.e. seasonality scores, onset and cessation dates, and 10% and 90% dates) used to quantify trends, where at 16 locations there was agreement across all three approaches and at the remaining 30 locations there was agreement between two of the three seasonality approaches (Figure 5.47; Table 5.9). Using different seasonality metrics across Iran, Raziei (2017) similarly noted both agreement and disagreement in the direction of trends, and hence it was expected that there would not be complete agreement across all the metrics for all locations.

By comparing the shifts quantified using the numerous metrics applied in this project, a comprehensive understanding of changes in rainfall seasonality may be obtained, where this is

also important for corroboration of the trends. For corroboration purposes, it is also important to compare the trends quantified in this study to previous investigations, across South Africa, regarding rainfall characteristics. In noting this, it is expected that there may be both agreement and disagreement between the results of this study and previous investigations due to different metrics, temporal periods and scales (e.g. monthly and seasonal) and different weather stations (MacKellar *et al.*, 2014; Raziei, 2017); highlighting a need for continued monitoring in all instances, especially with additional weather stations over longer temporal periods. Although considerable caution must be placed on the results from this study, they strongly suggest that irrespective of whether overall rainfall amounts are increasing or decreasing, the distribution of rainfall throughout the year may be changing quite markedly and these changes could have marked implications on continued farming and water resource management, among other climate sensitive activities, across the region. Hence, even if past rainfall regime trends are not indicative of future tendencies, the results discussed here are particularly valuable as there have notably been few investigations exploring rainfall regime trends across South Africa (See *Literature Review Section 2.3.2.2 Chapter 2*). While exploring the trends quantified in this study, some of the possible implications on climate sensitive activities/sectors across South Africa, such as agriculture, water resource management, conservation, and tourism among others, are also explored to highlight that the time to implement plans to cope with climate change across South Africa is now, and to also contribute to helping policy makers devise robust strategies for adaptation to changing rainfall regimes. While exploring the changes in seasonality, it should also be noted that this section considers some of the large scale global atmospheric circulation mechanisms and synoptic mechanisms driving these changes, however, this is only broad and will not be detailed as again this is beyond the scope of the research project. This is important as a consideration for future research and will be discussed later under *Chapter 7 (Conclusion) Section 7.3* (Pal *et al.*, 2013). In considering the changes in rainfall seasonality, these would be related to global atmospheric circulation, synoptic circulation and local/regional factors (i.e. SSTs, topography, land use/cover and irrigation among others) which affect rainfall trends (Taljaard, 1996; de Luis *et al.*, 2011; Pal *et al.*, 2013; Lennard & Hegerl, 2015; Ma & Zhou, 2015). Finally, for this discussion section the trends are presented in terms of agreement in the direction of trend presented under Table 5.9

of *Chapter 5 (Results) Section 5.5*, and hence the sections which follow regard the trends towards SRZ, WRZ and YRZ conditions separately. Since climate is not expected to change uniformly across South Africa (Hewitson & Crane, 2006), it is not surprising that the seasonality shifts quantified differ spatially.

6.4.2.1 TRENDS TOWARDS SRZ: IMPLICATIONS AND RECOMMENDATIONS

Across most regions in SRZ of southern Africa, it is widely reported that the degree of seasonality is increasing (Nel, 2009; Pascale *et al.*, 2016; van Wilgen *et al.*, 2016; Botai *et al.*, 2018), and that the wet season duration is decreasing particularly due to later start and earlier withdrawal of the wet season (Kniveton *et al.*, 2009; Shongwe *et al.*, 2009; Tadross *et al.*, 2009; Tongwane *et al.*, 2015; Kabanda & Nenwiini, 2016; Dunning *et al.*, 2018). There were 20 locations (ANP: Aliwal-North Plaatkop; BEW: Bethlehem Wo; DAW: De Aar Wo; FRA: Fraserburg; JIW: Johannesburg INT Wo; LAD: Ladysmith; LEP: Lephalale; MAR: Mara; MRC: Makatini Research Centre; NEL: Nelspruit; OTT: Ottosdal; POF: Pofadder; PRI: Prieska; PWO: Polokwane Wo; SKU: Skukuza; TRI: Twee Riviren; UPW: Upington Wo; VRY: Vryburg; VWY: Vanwyksvlei; WEL: Welkom), across the central and eastern interior of South Africa with the direction of change for the study period tentatively suggesting a trend towards stronger SRZ conditions, where there was agreement in the direction of these trends between two or three of the seasonality metrics (Figure 5.47; Table 5.9). At these locations, most (i.e. 13 out of 20 locations) of the trends in seasonality scores tentatively shifted towards becoming more positive which is indicative of an increase in the degree of seasonality (Figure 5.41, 5.46; Appendix H). Similarly, the predominant reduction in the duration of the wet season for the onset and cessation dates (i.e. 19 out of 20 locations) and percentile-based approach (i.e. 15 out of 20 locations) is also indicative of increasingly seasonal conditions (Figure 5.46; Appendix G). Notably, the reduction in the wet season was generally coupled by later onset and 10% dates (i.e. 16 out of 20 locations for both the onset and 10% dates; Figure 5.46; Appendix I1, J1), and earlier cessation dates (i.e. 13 out of 20 locations; Figure 5.46; Appendix I2). On the other hand there were generally trends towards later 90% dates (i.e. 11 out of 20 locations; Figure 5.46; Appendix J2). There were few statistically significant trends across the weather stations, with statistically significant trends evident at: ANP for later 90% dates; BEW for later onset, 10% and

cessation dates; OTT for later onset dates and a shorter wet season for both the onset and cessations dates and percentile-based approach; SKU for earlier cessation dates; and at UPW for later cessation dates (Figure 5.46; Appendix G; Table 5.9). Additionally, trends with a very high possibility that these were not detected by chance, due to *p values* <0.10, were evident at: LAD for later cessation dates as well as a reduction in the length of the wet season for the onset and cessation dates; and at both ANP and OTT for later 10% dates (Figure 5.46). The trends in seasonality were typically coupled with a reduction in annual rainfall, which was statistically significant at LAD, MRC and WEL, although a statistically significant increase was quantified for UPW (Figure 5.3). Additionally, during the wet season months these seasonality trends mainly occurred with a reduction in monthly rainfall totals, with particularly strong and numerous statistically significant trends, as well as high spatial consistency during the months of February, March, October and September (Figure 5.6). The tentative reductions in monthly rainfall amount were coupled mainly with the tentative reductions in the number of rain days during the wet season for both the onset and cessation date (i.e. 14 out of 20 locations) and percentile-based (i.e. 12 out of 20 locations) approaches, where some statistically significant reductions in the number of rain days were evident at OTT, POF and WEL (Figure 5.46). When considering all of these trends it is apparent that these are suggestive of increasingly seasonal conditions coupled with an overall reduction in rainfall both during the year and during the wet season months.

The tentative trends towards stronger SRZ conditions across the eastern and central interior of the country are consistent with observational evidence of the Hadley cell expanding particularly since the 1970s (Johanson & Fu, 2009; Nguyen *et al.*, 2015), and with projected evidence of the continued expansion of the Hadley cell and consequent poleward deviation of the subtropical high pressure belt (Lu *et al.*, 2007; Seidel *et al.*, 2008; Engelbrecht *et al.*, 2009; Nguyen *et al.*, 2013; Mahlobo *et al.*, 2018), where this has previously been linked to a reduction in the duration of the summer rainfall season across southern Africa (Christensen & Hewitson, 2007; Shongwe *et al.*, 2009; Dunning *et al.*, 2018). Across this region, Dunning *et al.* (2018) project, for the end of this century, a reduction in the duration of the wet season of up to ~14 days, where this trend was statistically significant in the northeastern parts of South Africa. This reduction is evident due to later onset dates and earlier cessation dates (Dunning *et al.*, 2018). This is consistent with the

majority of trends for the onset and cessation date and percentile-based approaches quantified in this region, where the largest reductions in the length of the wet season were quantified as -2.12d.yr^{-1} for LAD (using onset and cessation dates) and -1.77d.yr^{-1} for OTT (using percentile-based approach; Appendix G). For this region, Dunning *et al.* (2018) additionally project mostly a reduction in wet season rainfall of up to 60mm, albeit with some small increasing trends, up to 10mm projected for regions over Lesotho, western KwaZulu-Natal, southern Free State and northeastern Eastern Cape. The projected results presented by Dunning *et al.* (2018) are considerably consistent with the results of this study. Additionally, Pascale *et al.* (2016) project a statistically significant increase across the central regions of South Africa, for the period of 2070-2100, in RE which implies an increase in the number of dry months. Across the northeastern parts of southern Africa, Tadross *et al.* (2009) similarly detect a reduction in the length of the wet season with later onset and earlier cessation dates. At Mapungubwe and the Kruger National Park, van Wilgen *et al.* (2016) detect an increase in seasonality, using SI, with a longer dry season. Lipsett (2017) similarly detect reductions in the wet season duration across most of the weather stations (located in and surround the Kruger National Park) investigated for the period of 1907-2015, and it is notable that locations with shorter temporal periods (1971-2015) demonstrate larger reductions in the duration of the wet season. Additionally, Botai *et al.* (2018) quantify a dominant increase in the degree of seasonality using the PCI approach. It is notable that the trends quantified for the period of 1998-2015 by Botai *et al.* (2018) have a considerably low magnitude of up to 0.18.yr^{-1}, which is consistent with the low magnitude, of up to 0.02.yr^{-1} for NEL, of trends quantified for seasonality scores (Appendix G).

The reductions in annual rainfall detected across the locations which are tending towards stronger SRZ conditions are relatively consistent with the observed trends reported by MacKellar *et al.* (2014) and Kruger and Nxumalo (2017), and these trends were also broadly consistent with the decreasing trends projected by Engelbrecht *et al.* (2009) for 2070-2100. For this study reductions in annual rainfall of up to 15mm.yr^{-1} are broadly consistent with the reductions of >10mm.dec^{-1} for the period of 1921-2015 which were reported by Kruger and Nxumalo (2017), where the larger reductions for this study may highlight that trends towards reduced annual rainfall may have been more pronounced during the most recent decades. The reductions in rainfall during the autumn

and spring months reported by MacKellar *et al.* (2014) and Kruger and Nxumalo (2017) are largely consistent with the monthly rainfall trends quantified for the autumn and spring months, where this is additionally consistent with trends towards a shorter duration of the wet season. Similarly, Engelbrecht *et al.* (2009) project reductions in rainfall during the autumn and spring months. Interestingly, the increasing trends quantified and projected for the summer months are not consistent with results of this study (Engelbrecht *et al.*, 2009; MacKellar *et al.*, 2014; Kruger & Nxumalo, 2017). Both MacKellar *et al.* (2014) and Kruger and Nxumalo (2017) similarly postulate that an increase in rainfall during the summer months coupled with a reduction in the number of rain days during these months may point to an increase in the intensity of rain events. Although the reduction in the number of rain days is consistent with MacKellar *et al.* (2014) and Kruger and Nxumalo (2017), the dominant reduction in rainfall during the summer months (except for January) does not suggest an increase in the intensity of rain events (Figure 5.6). Since rainfall amount during the wet season and wet season rate (i.e. rainfall per day during the wet season) were not investigated, it is necessary for future research to consider this as this may provide more conclusive evidence on rainfall intensity during the wet season.

Indeed, there is considerable consistency between the results of this study and previous studies. This would confirm the trends towards increased summer rainfall seasonality and a reduction in the wet season duration. Given the considerable agreement for the results of this study compared to previous studies, it is important to consider some possible implications which may be associated with an increase in the degree of seasonality, an increase in the length of the dry season, and a potential reduction in rainfall amount both during the year and during the wet season. These tentative trends may particularly influence agricultural activities across the interior of the country, where agriculture in this region consists of commercial and subsistence farming of livestock, such as cattle and sheep and crops, including forestry, fruits, maize, sunflower and wheat (van Huyssteen *et al.*, 2018; du Preez *et al.*, 2019). A longer dry season with a potential reduction in rainfall during the wet season and a possible increase in dry spells would be detrimental to agriculture, where this would result in a shorter growing season particularly influencing crop germination possibly due to reduced soil moisture, also influencing crop yields as crops may not reach full maturity in turn influencing food security (Reason *et al.*, 2005; Usman & Reason, 2004;

Tadross *et al.*, 2009; Bekele *et al.*, 2017; Dunning *et al.*, 2018). A reduction in the wet season length with reduced wet season rainfall may be detrimental for water resource management, where this may particularly influence water supply for regions such as Gauteng, which is highly populated and the main water source being the Vaal dam reached its lowest during the 2015/2016 hydrological year (Mukheibir, 2008; Botai *et al.*, 2018). These tentative shifts in rainfall regimes across the interior may also influence air pollution deposition and dispersion patterns and general air quality, especially across the Mpumalanga Highveld where most of the coal fired power plants are situated (Leung & Gustafson, 2005; Thambiran & Padayachi, 2017; Hu *et al.*, 2019). These changes in rainfall regimes may also be detrimental for biomes in the interior region, which include the savanna, grassland and Nama-karoo biomes (Finch & Meadows, 2019). Particularly for the grassland regions, a reduced wet season duration with less rainfall may result in expansion of the savanna biome, where this may be detrimental for land carrying capacities which may influence both agriculture and game park tourism (van Wilgen *et al.*, 2016; Elser & Archer, 2018; Finch & Meadows, 2019). An increase in the length of the dry season may also influence fire risk, rainwater harvesting and malaria, as examples, in these regions (Craig *et al.*, 2004; Briët *et al.*, 2008a,b; Kahinda *et al.*, 2008; van Wilgen *et al.*, 2016; Strydom & Savage, 2016; Botai *et al.*, 2018). Possible mitigation strategies and recommendations for the implications of these tentative trends may, among others, include diversifying crop types to include a range of drought resistant crops (e.g. sorghum instead of maize or drought resistant genetically modified crop varieties of commonly grown crops; Moeletsi *et al.*, 2012) which both germinate and grow to completion quicker, removal of invasive species which influence biome distributions and fire frequencies, additional monitoring of rainfall regimes, and improvement of both water resource management and health care practices (Craig *et al.*, 2004; Tadross *et al.*, 2009; van Wilgen *et al.*, 2016; Turton, 2018; Knight, 2019; Sutherland & Mazeka, 2019).

6.4.2.2 TRENDS TOWARDS WRZ: IMPLICATIONS AND RECOMMENDATIONS

Five locations (OUD: Oudtshoorn, PEW: Port Elizabeth Wo, RIV: Riversdale, ROB: Robertson and WIL: Willowmore), along the southern coast, displayed agreement between either two or three of the seasonality metrics for change tentatively tending towards WRZ conditions during the study

period (Figure 5.47; Table 5.9). The changes detected in seasonality were coupled with an increase in annual rainfall although this was not statistically significant (Figure 5.3), and a predominant increase in rainfall during the winter months (with some statistically significant trends during June, July and August) of the year with mainly decreasing and some increasing trends during the remaining months of the year (Figure 5.6). The trends in rainfall amount during the winter months are relatively consistent with the agreement of trends towards WRZ conditions across the seasonality metrics (Figure 5.47; Table 5.9), however, none of the seasonality trends were statistically significant (Figure 5.46). All of the seasonality score trends were tentatively tending towards stronger WRZ conditions and a greater degree of seasonality, with a possibility of a regime change from YRZ to WRZ conditions by the end of the century for OUD, PEW and RIV (Figure 5.46; Appendix H). All of the trends for the wet season duration quantified using the percentile-based approach were tending towards becoming shorter with the largest trend evident at RIV (-0.56d.yr^{-1}), and it is evident that these trends were mostly due to earlier 10% and 90% dates (Figure 5.46; Appendix G, J). For the onset and cessation dates, the wet season duration was mostly tending towards becoming shorter with the largest trend evident at PEW (-0.39d.yr^{-1}), however, at OUD and WIL trends towards a long wet season duration were quantified (Figure 5.46; Appendix G). In conjunction with the trends towards increased monthly rainfall amount during the winter months (Figure 5.6), it is notable that an increase in the number of rain days was quantified across all of these locations, excluding OUD (Figure 5.46).

Since most of the *p values* were quantified as >0.10 (Figure 5.46), the trends towards increasingly seasonal WRZ conditions should be considered with caution as there is a high possibility that these were detected by chance. It is surprising that the trends towards WRZ conditions demonstrate considerable agreement spatially, across the seasonality metrics and across the monthly rainfall totals (Figure 5.6, 5.46, 5.47). This is because there is a wealth of evidence which demonstrates that the Westerlies are currently and will continue to consequently shift poleward as the Hadley cell continues to widen (Christensen *et al.*, 2007; Biastoch *et al.*, 2009; Engelbrecht *et al.*, 2009; IPCC, 2013, 2018; Mahlalela *et al.*, 2018; Sousa *et al.*, 2018). For South Africa, this would mean a reduction in frontal rainfall during the winter months (Engelbrecht *et al.*, 2009; Mahlalela *et al.*, 2018; Sousa *et al.*, 2018). For the period of 2070-2100, Engelbrecht *et al.* (2009) project a

reduction in both winter rainfall (up to 20%) and annual rainfall (up to 10%) across the southern coast region. Additionally, Lennard and Hegerl (2015) detected a decrease in winter rainfall-bearing circulation types for the period of 1979-2009. To further explore and corroborate these trends toward WRZ conditions, it would be necessary to investigate the changing frequency of all the synoptic circulation systems which bring rainfall to the southern coast (e.g. cold fronts, cut-off lows, ridging high pressure systems, and TTTs; Engelbrecht *et al.*, 2015; See *Chapter 3 Study Region* for a description of these systems), to possibly determine the synoptic drivers behind rainfall seasonality changes (Lennard & Hegerl, 2015). Notably, the results of van Wilgen *et al.* (2016) and du Plessis and Schloms (2017) also oppose the results of this study. van Wilgen *et al.* (2016) quantify a decrease in annual rainfall amount at all locations across the southern coast. At Addo Elephant national park a decrease in SI was quantified, suggesting a reduction in the degree of seasonality with rainfall becoming even more evenly spread throughout the year, whereas at the Garden Route and Bontebok national parks an increase in SI was reported (van Wilgen *et al.*, 2016). du Plessis and Scholms (2017) quantify an increase in the length of the wet season, across numerous weather stations along the southern coast region of the Western Cape, through numerous statistical analyses of monthly rainfall totals for the period of 1900-2014.

Although there is much evidence contradicting the trends quantified along these southern coast locations, there is also evidence demonstrating agreement with these results. Both MacKellar *et al.* (2014) and Kruger and Nxumalo (2017) quantify an increase in annual rainfall along the southern coast. MacKellar *et al.* (2014) and Kruger and Nxumalo (2017) similarly detect an increase in rainfall amount during the winter months, although they also detect an increase in summer rainfall totals. Botai *et al.* (2018) report an increase in PCI along the southern coast for the period of 1998-2015, where this is consistent with the trends towards increasingly seasonal WRZ conditions detected in this study. Dunning *et al.* (2018) project, for the period 2080-2099, a reduction of up to ~8 days in the length of the wet season along the southern coast region due to later onset and earlier cessation dates, which is largely consistent with the trends quantified for the onset and cessation dates and percentile-based approaches. Pascale *et al.* (2016) detect an increase in RE, which is indicative of an increase in the number of dry months along the southern coast.

Indeed, these results reported from different studies using different time frames and methods both contradict and support the results of this section. As a result, it is clear that there is a need for further monitoring across this region. It is interesting that most of the trends quantified using seasonality metrics demonstrated a reduction in seasonality and in the duration of the wet season. In considering this and the consistency both spatially and across the seasonality metrics, it may be suggested that these tentative trends towards WRZ conditions are broadly accurate across OUD, PEW, RIV, ROB and WIL. Given this, the implications of the trends quantified for this region should be considered in general especially if these trends persist. Important to note is that the trends across these locations should still be considered with caution, especially given that these locations were associated with the highest levels of inter-annual variability, particularly for the seasonality scores, and instability regarding the annual rainfall regimes (Figure 5.13 Table 5.8). An increase in the seasonality scores towards WRZ conditions and a reduction in the wet season length would imply a longer dry season which may possibly influence commercial and subsistence rainfed crop (e.g. fruit, vegetables and wheat) and livestock (e.g. cattle and sheep) farming in the region, where longer dry seasons may influence crop yields and land carrying capacities with implications on food security (Thomas *et al.*, 2007; Tadross *et al.*, 2009; Lötter, 2012, 2017; Tongwane & Moeletsi, 2015; Bekele *et al.*, 2017; van Huyssteen *et al.*, 2018; du Preez *et al.*, 2019). Longer dry periods may also influence soil moisture where the increases quantified in annual rainfall totals coupled increasing winter rainfall as well as an increase in rain days, and a shorter wet season may potentially have implications on extreme rainfall tendencies (i.e. drought and flooding) and in turn influence soil erosion as well as desertification in the region (de Luis *et al.*, 2010a; Botai *et al.*, 2018; van Huyssteen *et al.*, 2018). An increased length of dry periods may be detrimental to water resource management both in terms of quality and supply (Mukheibir, 2008; Kusangaya *et al.*, 2014; Botai *et al.*, 2018). Additionally, an increased risk of fire may also be associated with longer dry periods and changing rainfall regimes, where this may be detrimental to both human livelihoods and conservation of the Forest, Fynbos, Succulent Karoo and Albany Thicket, some of which are considered to be the most vulnerable and threatened biomes across South Africa (Elser & Archer, 2018; Kraaij *et al.*, 2018; Finch & Meadows, 2019). Possible mitigation strategies and recommendations may include diversifying crop types to also include more drought resistant

crops, removal of alien invasive species which use up available ground water and are additional sources of biomass fuel for fires, further incorporation of indigenous knowledge, forecasting of seasonal rainfall characteristics, and improved water resource management policies and practices (Tadross *et al.*, 2009; Lötter, 2012, 2017; Zengeni *et al.*, 2016; Kraaij *et al.*, 2018; Knight, 2019; Sutherland & Mazeka, 2019).

6.4.2.3 TRENDS TOWARDS YRZ: IMPLICATIONS AND RECOMMENDATIONS

At the remaining twenty locations, there was agreement between either two or three of the seasonality metrics for change tentatively tending towards YRZ conditions (Figure 5.47; Table 5.9). These locations are concentrated across the southwestern Cape, western coast and eastern coast regions, and were scattered across the eastern interior of the country (Figure 5.47). As a result of these spatial patterns, this section will consider these trends and interpretations separately for the western coast and eastern regions of the country as these regions represent WRZ and SRZ conditions tentatively tending towards YRZ conditions respectively. For the eastern regions of the country, this will also be considered separately for the coastal and interior areas as these regions are split by the Great Escarpment which is a key topographic barrier when considering rainfall. In considering the classification of WRZ or SRZ across these locations, this is where at least two of the four statistical methods agree on the classification (See *Section 6.3*; Figure 6.1; Table 6.1). Under the sections which follow, the implications and recommendations regarding the tentative changes in rainfall seasonality are also discussed.

Southwestern Cape and West Coast

Tentative trends toward YRZ conditions, with agreement between the trends of two or three seasonality metrics, were quantified for most of the WRZ locations (CAG: Cape Agulhas, CTW: Cape Town Wo, CWO: Calvinia Wo, LAW: Langebaanweg AWS, PNO: Port Nolloth, SUT: Sutherland, SWO: Springbok Wo, and VRE: Vredendal) situated within the southwestern Cape, western coast and adjacent inland areas (Figure 5.47; Table 5.9). The agreement between metrics and the spatial consistency across these locations to an extent confirms the tendency to YRZ conditions (Figure 5.47). The agreement of the direction of trends between metrics was mostly evident across for

the seasonality scores and the percentile-based approach (Table 5.9). In considering the percentile-based approach, trends in the 10% and 90% dates were mostly indicative of earlier and later dates respectively (Figure 5.46). Most of the trends for the onset and cessation dates were indicative of an increasing length of the wet season, however, at CAG, CTW and VRE the trends were suggestive of a reduction in the wet season duration (Table 5.9). There were a number of statistically significant trends as well as trends with a very likely probability, given the *p values* <0.10, which are indicative of a reduction in the degree of winter seasonality which suggests that these trends are accurate especially in terms of the direction of change (Appendix G). Statistically significant trends were quantified for CAG, using the seasonality scores, and at LAW as well as PNO, both for an increase in the duration of the wet season (Figure 5.46; Appendix G). Trends with a *p value* quantified as <0.10 include both CAG and CWO, for a very likely possibility of an increase in the duration of the wet season considering the percentile-based approach (Figure 5.46). According to Fitchett and Bamford (2017), a gradual reduction in rainfall seasonality is to be expected prior to a shift from WRZ to SRZ conditions. As such, it is to be expected that the trends across these WRZ locations are indicative of a reduction in the degree of seasonality.

All of the seasonality score trends were indicative of scores tending from negative scores towards zero which is suggestive of a reduction in seasonality and in rainfall amount during the winter months, which would inevitably result in relatively equal monthly rainfall totals throughout the year (Figure 5.41). Similarly, trends for rainfall amount during the winter months were also indicative of a general reduction in winter rainfall, especially given the statistically significant decreasing trends across numerous locations for the months of April, May and September (Figure 5.6). Although, rainfall trends during the winter months (except for June and August) were mostly indicative of reduced rainfall totals, there were notable increases in the number of rain days across both the percentile-based and onset and cessation dates approaches (Figure 5.46). This may suggest a reduction in the general amount of rainfall during rain days. Noteworthy, is that these seasonality trends coincided with a reduction in annual rainfall amount across all of these WRZ locations (except for PNO and SUT), where this was statistically significant for CTW (Figure 5.3).

A reduction in annual rainfall amount across these locations is mostly inconsistent with studies using observed records from weather stations across the southwestern Cape and western coast

regions (MacKellar *et al.*, 2014; van Wilgen *et al.*, 2016; Kruger and Nxumalo, 2017), although for the period of 1985-2016 Botai *et al.* (2017) report reductions in annual rainfall totals across most weather stations located within the Western Cape. This reduction in annual rainfall amount is consistent with the statistically significant reductions of up to 20% projected by Engelbrecht *et al.* (2009). Similarly, trends in seasonal rainfall amount are inconsistent with the monthly rainfall trends quantified for this study. MacKellar *et al.* (2014), Davis *et al.* (2016), and Kruger and Nxumalo (2017) report increasing trends for winter rainfall totals across this region, whereas Grab and Craparo (2011) report reductions in winter rainfall amount across the southwestern Cape. Additionally, Sousa *et al.* (2018) note statistically significant reductions in winter rainfall totals, since 1979, across the southwestern Cape. Interestingly, trends quantified, in previous studies, using seasonality metrics are mostly inconsistent with the results from this current study. Within the Mediterranean region of the Western Cape, du Plessis and Schloms (2017) quantify trends which are indicative of a reduction in the wet season duration. Similarly, the PCI trends presented by Botai *et al.* (2018) are indicative of an increase in the degree of seasonality. Additionally, across a number of weather stations located in the southwestern Cape, Abrahams (2019) mainly demonstrate a reduction in the duration of the wet season, which typically coincides with later onset dates. Most projections for the southwestern Cape and western coast regions are also indicative of increasingly seasonal conditions (Christensen *et al.*, 2007; IPCC, 2013; Pascale *et al.*, 2016; Dunning *et al.*, 2018).

Although the seasonality trends detected across most previous studies disagree with the trends quantified for the southwestern Cape and western coastline, there are some studies which demonstrate agreement. SI trends quantified by van Wilgen *et al.* (2016) for the Agulhas and Table Mountain National Park are indicative of reduced seasonality with a tendency towards YRZ conditions. Li *et al.* (2016) similarly detect a reduction in SI across the southwestern Cape and western coastline. While there are few studies with seasonality trends which are consistent with the results of this study, it is notable that the poleward dynamics of the subtropical high-pressure belt and Westerlies are largely consistent with the tendencies towards reduced winter rainfall (Hewitson & Crane, 2006; Christensen *et al.*, 2007; Engelbrecht *et al.*, 2009; IPCC, 2013, 2018; Mahlalela *et al.*, 2018; Sousa *et al.*, 2018; Burls *et al.*, 2019). With the Hadley Cell expanding and

becoming more intense, and with continued expansion projected until the end of the century, the subtropics and temperate climate belts are as a result projected to deviate poleward (Fyfe, 2003; Christensen *et al.*, 2007; Seidel *et al.*, 2008; Engelbrecht *et al.*, 2009; IPCC, 2013, 2018; Nguyen *et al.*, 2013, 2015; Mahlobo *et al.*, 2018). Over southern Africa this would mean a change in the location (i.e. further south) and intensity of the subtropical high-pressure belt, where during winter this is projected to occur with a considerable southward displacement of the frontal rain bands (Engelbrecht *et al.*, 2009; Mahlalela *et al.*, 2018; Mahlobo *et al.*, 2018; Sousa *et al.*, 2018; Burls *et al.*, 2019). It is thus apparent that these reductions in winter rainfall are consistent with the trends towards YRZ conditions, which may result in relatively even monthly rainfall totals.

It is apparent that there is much disagreement between the rainfall seasonality trends across the WRZ quantified for this study and for previous studies. This highlights a need for continued monitoring of changing rainfall regimes within the WRZ. Although there were few statistically significant trends, there is much agreement in the results of this study both spatially and across the different metrics for which change was quantified (Figure 5.47; Table 5.9). As a result, these trends may be tentatively accepted for the purpose of considering the implications of these trends and for developing adaptation strategies. In considering that the trends to YRZ conditions are most likely to result from a reduction in winter rainfall, then there should be much concern as the implications of this may be devastating. With a dominant signal of a reduction in rainfall amount during the general wet season months coupled with an increasing number of rain days across most locations (Figure 6.5), then extreme heavy rainfall may be less of a concern across the WRZ. This is in agreement with the results of numerous studies (Kruger, 2006; Roy & Rouault, 2013; Lennard & Hegerl, 2015; Kruger & Nxumalo, 2017). Instead the occurrence of drought (i.e. agricultural, meteorological, hydrological and socio-economic drought) conditions may be more prevalent across this region (Botai *et al.*, 2017). Severe drought conditions have already plagued the southwestern Cape region since 2015 (Botai *et al.*, 2017; Sousa *et al.*, 2018; Knight, 2019), where this has already had serious implications on dam water levels, agriculture productivity (e.g. grape farming for wine production, other fruit farming such as apples and pear, livestock agriculture along the western coast), conservation and tourism, among others due to restrictions on water availability and consumption (Grab & Craparo, 2011; Araujo *et al.*, 2016; van Wilgen *et al.*, 2016;

Botai *et al.*, 2017; Prinsloo, 2018; Wolski, 2018). The west coast is already a particularly arid region and reduced frontal rainfall during the winter months is likely to have a profound influence on water resources, livestock farming and biodiversity, among others (Kelso & Vogel, 2007; MacKellar *et al.*, 2007; Davis *et al.*, 2016). For the southwestern Cape and west coast region, it is not a question of whether these trends of reduced winter rainfall will persist. Instead, adaptation plans should already be implemented as drought conditions during the main winter rainfall season have already begun to impact the region considerably (Botai *et al.*, 2017; Sousa *et al.*, 2018; Wolski, 2018; Knight, 2019), and the reduction in winter frontal rainfall is projected to continue with high confidence (Christensen *et al.*, 2007; Engelbrecht *et al.*, 2009; Mahlalela *et al.*, 2018). Possible mitigation strategies in these regions should include grey water reuse and further desalination to provide freshwater where many dams are struggling to keep up with water requirements for agriculture and household use (Botai *et al.*, 2017; Wolski, 2018). Notably, these should not include borehole drilling as a reduction in rainfall during the wet season will influence ground water levels which are not likely to replenish without consistent rainfall during the winter wet season (Botai *et al.*, 2017; Knight, 2019). Additionally, an increase in the prevalence of dry/drought conditions may have considerable implications on wild fire occurrence, where during recent drought years there have already been numerous wild fires within the region which have had considerable implications on the fynbos and succulent karoo biomes as well as urban and agriculture areas (Strydom & Savage, 2016; Elser & Archer, 2018; IPCC, 2018).

East Coast

Concentrated within the Eastern Cape and KwaZulu-Natal, seven locations (CED: Cedara, CMU: Cradock-MUN, ELW: East London Wo, MAN: Mandini, PAD: Paddock, SHA: Shaleburn and UMW: Umtata Wo) classified as SRZ demonstrate agreement between two or three approaches suggesting a tentative shift towards YRZ conditions during the study period (Figure 5.47; Table 5.9). Considering the seasonality scores, it is notable that this regime shift to YRZ conditions may occur by the end of the century (Appendix H). Since there is large spatial agreement within the Eastern Cape and Kwazulu-Natal provinces, then these trends may be tentatively considered as accurate (Figure 5.47), however, only the trend at UMW towards an increasing duration of the

wet season, for the percentile-based approach, was statistically significant (Figure 5.46; Appendix G). All (except for CMU) of the seasonality score trends were tending towards aseasonal, YRZ conditions (Figure 5.41, 5.46). Similarly, all of these locations demonstrated trends towards a longer duration of the wet season for the percentile-based approach, where the largest trend was quantified for UMW (1.07d.yr^{-1}; Figure 5.46). These trends towards a longer wet season coincided with trends towards later 10% and 90%, and an increase in the number of rain days during the wet season was also quantified with a statistically significant increase evident for PAD (Figure 5.46). The onset and cessation dates also demonstrated trends towards later dates which coincided mainly with an increase in the wet season duration across all of the locations, excluding MAN and PAD (Figure 5.46). Increasing trends were mostly quantified for the number of rain days during the wet season, and this was statistically significant for SHA and very likely at CED (Figure 5.46). These seasonality trends were coupled with a reduction in annual rainfall amount (except for CMU), which was statistically significant at CED and MAN (Figure 5.1). In considering the monthly rainfall trends, there were notable reductions across most of the months with numerous locations demonstrating statistically significant trends, however, during January, April, May and July there were instead increasing trends across most of these locations (Figure 5.6). These trends in monthly rainfall amount are broadly consistent with the trends towards YRZ conditions, as increasing trends mainly during the drier months with decreasing trends mainly during the wetter months may result in relatively equal monthly rainfall totals which would be consistent with YRZ conditions. With a reduction in monthly rainfall amount particularly during the wet season and trends mainly towards an increase in the number of rain days, this may possibly suggest that daily rainfall shifted to becoming more evenly spread throughout the wet season. Thus, this may suggest a reduction in the intensity of rainfall events across this region.

Although there is much consistency spatially and between the metrics tested for changes, the trends quantified were mostly statistically insignificant. As such, the trends across these locations (CED, CMU, ELW, MAN, PAD, SHA and UMW) should be considered with caution. Across this region, Engelbrecht *et al.* (2009) project a reduction in annual rainfall totals, and the results from Kruger and Nxumalo (2017) and MacKellar *et al.* (2014) also reveal dominant decreasing trends with a few increasing trends evident. These trends in annual rainfall amount are consistent with

the annual trends quantified for this study. In considering the monthly rainfall trends, it is evident that the results of seasonal rainfall trends quantified by Kruger and Nxumalo (2017) and MacKellar *et al.* (2014) are generally inconsistent, where these are also inconsistent with the monthly rainfall trends quantified for this study. Similarly, the resulting monthly rainfall trends, quantified for this study, are inconsistent with the results reported by Nel (2009) for the eastern Drakensberg region. Interestingly, many studies indicate a tendency towards an increased occurrence of extreme heavy rainfall across the eastern parts of the country, and particularly east of the eastern Escarpment, which is again considerably inconsistent with the results of this study (Mason *et al.*, 1999; Easterling *et al.*, 2000; Groisman *et al.*, 2005; Kruger, 2006; New *et al.*, 2006; Roy & Rouault, 2013; MacKellar *et al.*, 2014; Kruger & Nxumalo, 2017). In considering seasonality trends, it is notable that these are also generally inconsistent with the results of these locations. The trends quantified for this study are broadly consistent with the resulting PCI trends reported by Botai *et al.* (2018) for the period of 1998-2015, where a reduction in PCI was quantified across most of the Eastern Cape. Opposing the trends towards YRZ conditions, Nel (2009) detected relatively strong trends towards increased PCI, with some statistically significant trends, which is indicative of an increase in the degree of seasonality. The projected trends presented by Dunning *et al.* (2018) and Shongwe *et al.* (2009) similarly point towards a reduction in the duration of the wet season across this region. The results of Dunning *et al.* (2018) are indicative of a reduction of between 4-8 days, with statistically significant trends for some areas, by the end of the century. The reduction in the wet season duration evident from Shongwe *et al.* (2009) is as a result of a statistically significant reduction in autumn and spring rainfall totals. Similarly, Pascale *et al.* (2016) project an increase in RE, which is indicative of an increase in the number of dry months implying a reduction in the duration of the wet season. Observed SI trends quantified by Li *et al.* (2016) for the period of 1948-2005 are also indicative of an increase in the degree of seasonality.

Even though there is strong agreement between the seasonality metrics for trends towards YRZ conditions for the eastern coast and adjacent areas, there is considerable disagreement when considering literature. This highlights that the trends across these locations should be considered with much caution and that additional monitoring, over longer temporal periods and with additional weather stations, should take place especially because adaptation plans would not be

the same for different scenarios of rainfall regime changes. With agreement in the results of this study, both spatially and across most of the results of the different metrics regarding rainfall amount and seasonality, these results may tentatively be accepted, and some implications of these changes should be noted. A longer wet season may be seen as beneficial, however, in this regard a longer wet season with reduced rainfall may not necessarily be beneficial. Reduced rainfall during the wet season may result in an increased risk and frequency of drought periods as well as dry spells in general during the wet season (Reason *et al.*, 2005; Usman & Reason, 2004; Tadross *et al.*, 2009; Botai *et al.*, 2017, 2018), where this may have implications on water availability for the predominant sugar cane and subsistence farming within this region as well as household consumption (Botai *et al.*, 2016, 2017; du Preez *et al.*, 2019). Issues with water resources may also be detrimental to tourism (Robinson, 2016; Fitchett *et al.*, 2017a), and continued urban development in the region (Sumner *et al.*, 2001). Reduced wet season rainfall may also have implications on fire frequencies, where Strydom and Savage (2016) quantified an increase in the frequency of fires across KwaZulu-Natal since 2003. The trend of an increased wet season length with reduced rainfall may particularly influence agriculture and water resource management, and thus mitigation strategies and recommendations should include additional rain water harvesting, further incorporation of indigenous knowledge concentrating on soil fertility, moisture and conservation, and improvement of water system infrastructure as well as water resource management and policies (Kahinda *et al.*, 2008; Thomas *et al.*, 2007; Zuma-Netshiukhwi *et al.*, 2013; Zengeni *et al.*, 2016; van Huyssteen *et al.*, 2018; Knight, 2019).

Eastern Interior

Spread across the eastern interior of the country, there were six locations (BET: Bethal, BLW: Bloemfontein Wo, FTN: Frankfort TNK, KWO: Kimberley Wo, MWO: Mafikeng Wo and WTO: Warmbad Towoomba) where the trends in rainfall seasonality were tentatively shifting towards YRZ conditions with agreement across two of the seasonality metrics (Figure 5.47; Table 5.9). These trends were somewhat unexpected given that surrounding locations demonstrated trends tending towards stronger SRZ conditions (Figure 5.47). This highlights that the trends across these locations should be considered with caution as there is low spatial consistency, although

investigation of the seasonality trends for additional weather stations across the regions surrounding these locations may similarly demonstrate a tendency towards YRZ conditions. Indeed these locations could potentially represent areas with local trends and thus should not be disregarded completely. The tentative trends from SRZ to YRZ conditions at these locations appear to have occurred due to a reduction in the positive seasonality scores and an increase in the wet season duration for the percentile-based approach, whereas the wet season duration using the onset and cessation dates was mostly demonstrated to decrease (Figure 5.46; Table 5.9; Appendix G). The trends at these locations were statistically significant at: MWO for a reduction in the positive seasonality scores; BET and FTN for later onset dates; and BLW and KWO for later 90% dates (Figure 5.46; Appendix G). The seasonality trends at these locations mostly coincided with a reduction in the number of rain days (Figure 5.46), which is consistent with a reduction in monthly rainfall amount particularly during the autumn, spring and summer months of the year which coincide with the wet season months across these locations (Figure 5.6). Additionally, these trends towards YRZ conditions also occurred with an overall reduction in annual rainfall amount, where this was only significant at MWO (Figure 5.3).

The reductions in annual rainfall are broadly consistent with previous studies using observational data (Kruger, 2006; MacKellar *et al.*, 2014; Kruger & Nxumalo, 2017) and with projected annual rainfall trends (Engelbrecht *et al.*, 2009). The trends in monthly rainfall across these locations are relatively inconsistent with the trends reported by MacKellar *et al.* (2014) and Kruger and Nxumalo (2017) as these studies detect increasing trends during the summer season. Notably, these studies similarly report reductions in rainfall amount during the spring and autumn months, which is consistent with the results of the locations tending towards YRZ conditions. The seasonality trends toward YRZ conditions are generally inconsistent with previous studies. It is widely reported that rainfall across the interior of South Africa is becoming increasingly seasonal, where this has been detected using observational data and the PCI approach (Botai *et al.*, 2018) as well as the SI metric (Li *et al.*, 2016). Similarly, trends towards increasingly seasonal rainfall have also been projected through a reduction in the duration of the wet season (Dunning *et al.*, 2018) and through an increase in RE coinciding with an increase in the number of dry months (Pascale *et al.*, 2016).

Indeed, there is much disagreement between the results of these locations (i.e. BET, BLW, FTN, KWO, MWO and WTO) and those of previous studies. This, and the relatively low spatial consistency between these locations highlights that these trends are questionable and that it is especially important to continue monitoring the rainfall regimes at these locations, across additional locations and over a longer temporal period. In considering this, and the potential persistence of the trends at these locations, it is important to consider some of the implications on climate sensitive activities at these locations. The implications of a longer wet season with reduced rainfall and fewer rain days during the wet season may particularly involve an increase in the frequency and duration of drought and dry spells (Reason *et al.*, 2005; Tadross *et al.*, 2009; Botai *et al.*, 2016, 2017). This may have devastating implications on, among others, tourism, conservation, soil moisture, agriculture such as forestry, maize and cattle, and urban and rural household water security across these locations which may also have marked implications on continued development (de Luis *et al.*, 2010a; Botai *et al.*, 2016, 2018; Robinson, 2016; van Wilgen *et al.*, 2016; du Preez *et al.*, 2019). Possible mitigation strategies and recommendations may include improved water resource management strategies where it would be especially important to enhance water storage and conservation (Botai *et al.*, 2016, 2017; Knight, 2019). It would also be important to additionally concentrate on forecasting of seasonal rainfall patterns such as wet season rainfall amount and onset dates, especially because maize farming and forestry are activities which both occur in these regions and rely considerably on rainfall patterns (Reason *et al.*, 2005; Tadross *et al.*, 2009; Ratnam *et al.*, 2018).

6.5 LIMITATIONS

Similar to all research projects, this project encountered some limitations. Throughout this chapter, some of the limitations, especially pertaining to the seasonality metrics (See *Section 6.3.1*), associated with the study have already been discussed. Under the sections which follow, some of the main limitations in addressing the overall aim and objectives of this thesis are highlighted and discussed. This study encountered limitations regarding the nature of the rainfall, T_{min} and T_{max} datasets as well as through the statistical analyses. The limitations which were encountered during this study are important to note as these may possibly influence the accuracy

of the results quantified and these may be also used to inform future research which is discussed under *Chapter 7 (Conclusion)*. This section thus explores the limitations which were encountered, highlighting where measures were taken for this study to mitigate these limitations as well as possible measures which may be considered for future research.

6.5.1 DATA LIMITATIONS

Daily rainfall, T_{min} and T_{max} datasets were obtained for 46 weather stations from the SAWS climate database. Since data were collected only from SAWS, an accredited meteorological organisation run by the South African government and a member of the WMO, consistency in these datasets is guaranteed to the user. The datasets from SAWS are ensured to have relatively high accuracy due to the fact numerous quality control processes are undertaken on the meteorological and climate datasets part of the climate database (Dent *et al.*, 1987; Schulze, 2007; Nel, 2007; Dyson, 2009; SAWS, 2019a). However, these datasets are not perfect and numerous limitations in the nature of the rainfall, T_{min} and T_{max} datasets were encountered. Limitations associated with the datasets used for this project may: transpire through the data collection process, be as a result of data gaps and outliers, and be associated with the temporal period as well as the spatial distribution of weather stations.

In considering the limitations associated with data collection, these may occur through human error and faulty equipment. Both human errors and issues with faulty equipment may emerge as either missing data or incorrect data capturing across all the temperature and rainfall datasets. The process undertaken to mitigate human errors, those associated with faulty equipment, and in general any other errors have been captured under *Section 4.3.1* of *Chapter 4 (Data and Methodology)*. Indeed, rain gauge data are often the most used and trusted sources of data on rainfall as these data provide direct and accurate point measurements (Rana *et al.*, 2015). Although considered to have high accuracy, rain gauge measurements do not necessarily represent a 'true rainfall amount' (Schulze, 2007). Inherent errors, not associated with human error and faulty equipment, may transpire due to a number of reasons, for example error in these measurements may result from wind flow where intense winds from convective thunderstorms

may influence the amount of rainfall captured (Schulze, 2007; Rana *et al.*, 2015). For the purpose of the temperature data, mean daily temperature was quantified using T_{min} and T_{max} which were used to quantify mean monthly temperatures. This is a limitation as hourly temperature readings may have provided more accurate values of mean daily temperatures; however, SAWS were not able to provide hourly data for all weather stations and thus to ensure consistency T_{max} and T_{min} measurements were instead used.

Still considering the data collection process, numerous change points were captured using the Pettitt and CUSUM tests, where these were considered in determining the magnitude and direction for trends analyses. Taking note of change points and the trend from the year of change is particularly important for updating management plans for water resource management amongst other activities (Rahmani *et al.*, 2015). These change points may also possibly highlight inhomogeneity in the datasets as the years in which these occurred do not necessarily always correspond, and as a result these may not always have been due to regional atmospheric changes but instead, for example, due to changes in rain gauge exposure from an increase in built up area or instrument changes (Mazvimavi, 2010; Guerreiro *et al.*, 2014; Zarenistanak *et al.*, 2014; Mathbout, 2015). The extent to which data inhomogeneity may have influenced the results is unknown, however, this is not likely to have played a large role in this study as consistency was ensured by only using SAWS datasets (Mathbout, 2015; Rahamani *et al.*, 2015). The point of homogeneity is noted here especially for future studies over smaller spatial scales with a larger collection of weather stations, where further investigation into change points may be particularly important for analyses of synoptic circulation (Mphale *et al.*, 2014), and general homogeneity of the datasets for data quality purposes (Lakhraj-Govender, 2017).

Limitations in the datasets obtained from SAWS also occurred due to data gaps and outliers. Data gaps were captured under *Chapter 4 (Data and Methodology)*. To reduce the impact of data gaps on the accuracy of the results, weather stations were only included if at least 90%, following data cleaning, of data were available for the study period. To reduce the influence of outliers, a data cleaning process was undertaken whereby data values which were outliers were deleted following this process described under *Section 4.3.1* of *Chapter 4 (Data and Methodology)*. Where data were missing or deleted, these remain as omitted data rather than being completed by interpolated

values to ensure that no misleading trends are generated. Interpolated values may be misleading due to intra-annual and inter-annual variability in the data. Missing data values, especially including the months left out of the analyses (Table 4.2 and 4.3), may also lead to misleading trends and are important to note.

The temporal period of the weather stations may also be considered as a data limitation of this research project. In considering the temporal period, a minimum of 30 years was obtained (WMO, 2000), however, a longer period would have been particularly valuable especially given that the focus of this research was on rainfall which is associated with considerable year to year variability. A period longer than 1987-2016 was not possible for the full grid of weather stations due to data gaps prior to 1987 and following 2016. Arguably, although a data limitation, the influence of the relatively short temporal period is a greater issue for statistical analyses and is thus considered further under the next section.

Possibly one of the largest shortcomings of *in situ* rain gauge measurements is the fact that these measurements are unable to provide complete areal coverage as these are location specific (Schulze, 2007; Rana *et al.*, 2015), where this was particularly an issue for the interpolated maps presented throughout *Chapter 5 (Results)*. The spatial gaps across the weather stations only allowed for broad scale spatial patterns to be reflected across the interpolated maps, and where local scale patterns are reflected, these appear to, although do not, reflect outliers, as is apparent for the mean monthly rainfall total for NEL during February and April (Figure 5.5). Across South Africa locations in the Northern Cape and Lowveld with low population densities are particularly underrepresented in the SAWS climate database (Tennant & Hewitson, 2002; Schulze, 2007). In noting the spatial representation of rain gauge measurements, in particular, Lynch *et al.* (2001) highlight the problem of weather stations not being fully representative using six weather stations within 6km and 100m elevation capturing the period of 1954-1999, where trends of different magnitude were detected and localised extreme rainfall events from convective storms were also evident where some locations captured such an extreme event while others did not. As such, there were limitations associated with the spatial distribution of the grid of weather stations selected for this project. On the basis of available weather stations, a choice was made, as discussed under *Section 4.2.1* of *Chapter 4 (Data and Methodology)*, regarding which weather stations to use,

where any choice would have resulted in unavoidable spatial limitations. No measures were needed to overcome the limitations associated with the spatial distribution because a fine scale resolution was not necessary to address the objectives of this research project. Additionally, measures were not needed because the sample weather stations were demonstrated to be representative of the general rainfall characteristics across South Africa, and hence were appropriate to use for this research project.

To overcome the limitations associated with the spatial and temporal distribution of the datasets, future research may benefit from incorporating rainfall data from additional weather stations from other organisations, such as the Agricultural Research Council (ARC). Additionally, precipitation and temperature inputs from reanalysis data and satellite-derived data products may also be incorporated in future research, where the National Oceanic and Atmospheric Administration (NOAA) provide a number of daily and monthly scale data products. However, in saying this, the limitations associated with such data products should be considered before using these products in future research projects.

6.5.2 STATISTICAL LIMITATIONS

This study relied entirely on statistical analyses to generate results, and the data limitations captured in the previous section would have inherently influenced the accuracy of the results quantified from these analyses. Hence, the results obtained from this study should be considered with some caution, but it should be noted that these limitations did not influence achieving any of the study objectives.

There were data gaps in the datasets from the 46 weather stations used in this study. The primary limitation of all statistical analyses and their ability to accurately model and demonstrate patterns arises from gaps in datasets, however, missing data are inevitable in historical studies. Interpolation of the missing values through averaged or modelled values may not result in an identical value of the missing value, and as a result interpolated values could potentially skew the descriptive statistics, time trends or relationships quantified, and any other analyses performed on data throughout this study. For this reason, missing data were omitted and were noted in

Chapter 4 (Data and Methodology). Missing values for these weather stations reduced the *n value* from the maximum number of observations to the number of complete observations. As with inclusion of interpolated values, missing values may also potentially skew any statistical analyses; and had the missing value existed where omitted, a different trend or relationship may have resulted. Concerns regarding missing values were mitigated for all trend analyses through calculation of the *p value*. The *p value* is a measure of statistical significance which determines the probability that the calculated trends and relationships would still hold in the greater dataset (Burt *et al.*, 2009; Underhill & Bradfield, 2009). Besides trend analyses, missing data were problematic for quantification of the annual and monthly rainfall totals and for all of the seasonality metrics. For instance, where missing data coincided with months known to span the timing of onset and cessation dates, and 10% and 90% dates, bias would have existed regarding the dates obtained. Should the missing data have existed different dates may have been quantified. In order to reduce the influence of missing data, years where too little data were present were omitted, especially if months with considerable missing data coincided with months of the beginning, end and during the wet season. Years with more than two months omitted or of missing data were not included in the analyses. This limitation was accounted for by using metrics such as the mean to capture seasonality characteristics.

The time frame of 1987-2016 for this study was relatively short. Although, 30 years were captured, which is suggested by the WMO as a period long enough for trend analysis (WMO, 2000; Arguez & Vose, 2011), this may not be enough to encompass fully any climate variability signal (de Luis *et al.*, 2000, 2011). A longer temporal period, especially for trend analyses, would have potentially yielded different results (de Luis *et al.*, 2000). Additionally, for SRZ weather stations for both the onset and cessation date and percentile-based approaches only 29 years of dates were obtained as the wet season at these locations do not follow the calendar year. Thus, the observed changes quantified for this study should be considered with caution. While for this study a longer temporal period was not necessarily possible and also not essential, future research may, as previously suggested, acquire data from the ARC in addition to data from the SAWS.

In considering the statistical methods used to classify seasonality, it is important to reflect on the limitations associated with these methods. The statistical limitations associated with the

seasonality scores metric, the onset and cessation dates method and the percentile-based approach are discussed under *section 6.3.1.* The limitations associated with the cluster-based approach are not discussed under the aforementioned section. The main limitation associated with this method regards the weather station sample and the scale of analyses. A larger sample of weather stations should improve the strength of the cluster solution. Notably, the strength of the cluster analysis output would greatly improve from using all of the SAWS and ARC weather stations, and with a stronger spatial resolution across the weather stations the YRZ may potentially be clustered (e.g. Favre *et al.*, 2016). Over a monthly scale, variability in daily rainfall is not reflected across the cluster outputs. Although this is a limitation of the cluster output, this highlights that this output should only be considered over a monthly scale. By including CV in the analyses, the cluster outputs reflect monthly variability, which is important given that rainfall is highly variable (Nicholson, 2000). Since the focus for this research was classifying seasonality in part using this cluster-based method, these limitations did not influence achieving the second objective of this research project. However, future research could improve on this method through first clustering weather stations to determine wet and dry seasons on the basis of daily data and then through grouping the outcomes on the basis of wet and dry seasons. By doing this, location specific seasonality can be clustered over a daily scale, which would be valuable with the results of the metrics which define the start and end dates of the wet season (i.e. onset and cessation dates and 10% and 90% dates.

6.6 CONTRIBUTION TO KNOWLEDGE

The details of how this PhD thesis aims to contribute to new knowledge are discussed under *Section 1.1* of *Chapter 1 (Introduction)*, where the main gaps in knowledge and issues in literature were also discussed through a review of the body of literature, under *Chapter 2 (literature Review)*, surrounding the research topic for this thesis. This current section aims to briefly describe how this PhD thesis has in fact contributed to new knowledge for the discipline of climatology across South Africa. This thesis has made a number of contributions to new knowledge, and these surround the development of a standard method to model rainfall seasonality across South Africa and to investigate rainfall seasonality shifts.

Possibly the most important contribution of this research to knowledge surrounds the objective testing of metrics to develop a standard approach to quantify rainfall seasonality across South Africa. This addresses an issue highlighted earlier in this thesis, whereby standard metrics will be particularly important for consistency and comparability of results both spatially and between studies. The standard metrics proposed in this study include the approaches on the relationship between MMR and MMT and the 10% and 90% dates as wet season boundaries, because it was demonstrated that these metrics accurately model the seasonality of rainfall across South Africa. Proposing standard metrics is important to give direction to future research, discussed under *Section 7.3* of *Chapter 7 (Conclusion)*. In testing these metrics, it should be noted that the approaches regarding the seasonality scores, onset and cessation dates, and 10% and 90% dates were for the first time applied to locations spanning the full area of South Africa. As such, the results from these metrics are important and a contribution to knowledge as many of the outputs on the rainfall seasonality characteristics were previously not quantified (e.g. patterns of SRZ, WRZ and YRZ inter-annual variability across the metrics) across the country.

Indeed, there is a lack of research regarding the changes in contemporary rainfall seasonality using observed records. Through investigating how rainfall seasonality may have changed, the results and interpretations thereof provide an important contribution to knowledge. Moreover, the multi-method approach to investigate the agreement in the quantified changes in seasonality was for corroboration purposes, and previously rainfall seasonality changes had not been investigated in this manner. This approach was adopted from palaeoseasonality research where seasonality shifts quantified from fossil pollen records have often been corroborated using diatoms, among other proxies, through a multi-proxy approach (e.g. Norström *et al.*, 2009, 2014; Fitchett *et al.*, 2016, 2017a). Finally, through interpreting the results of the changes in rainfall seasonality in the context of palaeoclimatological research, this study makes another important contribution to knowledge. This is a conceptual contribution, whereby this study contributes to supporting the conceptual palaeoclimate model originally proposed by van Zinderen Bakker (1967), confirming that under anthropogenically induced climate change the spatial extent of the WRZ will continue to reduce, and the SRZ and YRZ are also likely to change in their spatial extent.

6.7 SYNOPSIS

The interpretations and inferences of the results, in the context of current literature as well as the aim and objectives, are presented in this chapter. It is notable that the limitations discussed earlier under *Section 6.5* did not affect the results. In considering addressing all the objectives, it is demonstrated that both the mean annual and monthly rainfall patterns are consistent with literature, both spatially and in magnitude. As such, the sample of weather stations utilised for this research project were demonstrated to be appropriate to address objectives two to four. Additionally, since the annual cycles of rainfall across the sample of weather stations are representative of summer, winter and year-round rainfall regimes, this further highlights the appropriateness of these weather stations.

In objectively testing each of the statistical methods, it is demonstrated that even across the same temporally constrained dataset the classification of rainfall seasonality will always be disputed. This is because of the complexity of the rainfall regimes across South Africa, and the fact that each method inherently defines rainfall seasonality differently. This further emphasises the need for a standard statistical approach to quantify rainfall seasonality, where the seasonality scores approach and the percentile-based approach are suggested as standard approaches which should be applied in future research for the purpose of modelling rainfall seasonality across South Africa. The percentile-based approach with additional quantities (e.g. wet season rainfall amount) provides a complete description of rainfall seasonality over a daily scale, and as such this approach has much societal value for activities such as water resource management. In considering the classification and spatial distribution of rainfall seasonality, the seasonality scores performed best by producing an ideal classification of the YRZ, which is important in further understanding this rainfall zone. In quantifying the mean seasonality through the seasonality scores, this project has also contributed to confirming that the WRZ extent has reduced since the LGM, where this indirectly confirms that the SRZ and YRZ have also changed in their extent. It is also further highlighted that the contemporary WRZ extent will under climate change continue to reduce in size, where it is likely that the WRZ will be replaced by YRZ conditions with reduced rainfall during the winter months.

As a representation of the applicability of these methods, the changes in seasonality were quantified. The trends quantified for the seasonality scores, onset and cessation dates as well as 10% and 90% dates, and the respective wet season duration and number of rain days for these dates were compared to trends quantified for the annual and monthly rainfall totals. The trends across all of the metrics demonstrated high agreement, where there was also high agreement with literature. This highlights that the seasonality metrics are well-suited to quantify change and that the majority of changes quantified were relatively accurate especially in terms of the direction. In noting this, few statistically significant trends were quantified which suggests that there is a high possibility that rainfall seasonality trends may have been quantified by chance and that a longer temporal period is needed to confidently determine the magnitude of change across these trends.

7. CONCLUSION

7.1 INTRODUCTION

Three rainfall regimes (i.e. SRZ, WRZ and YRZ) are known to characterise South Africa, where it is well-known that this complex array of rainfall regimes is a result of the latitudinal location of the country in the subtropical and mid-latitude climatic belts (Chase & Meadows, 2007; Chase *et al.*, 2015, 2017; Fitchett & Bamford, 2017). Much research, since the first known publication in 1938 by Schumann and Hofmeyr, has sought to spatially categorise the rainfall regimes across South Africa (Roffe *et al.*, 2019). Across these attempts to spatially categorise South Africa's rainfall regimes many different methods, with varying degrees of accuracy and usability, have been applied and as a result there is much dispute regarding the spatial distribution of rainfall regimes across the country (Roffe *et al.*, 2019). To address this issue, the first part of this study attempted to determine a standard approach to quantify climatological seasonality. In considering the seasonal characteristics of rainfall across the country, very little research has been undertaken to understand the nature and rate of change using observed meteorological records. The research that has been undertaken is difficult to compare as different seasonality metrics have been applied. As such, the development of a standard climatological seasonality approach also has importance in understanding how rainfall regimes have and may change across South Africa, a country with dire rainfall projections and with a population which is particularly vulnerable to changing rainfall patterns due to a high dependence on the seasonal characteristics of rainfall for agriculture among other activities (Engelbrecht *et al.*, 2009; Tadross *et al.*, 2009; SAWS, 2017; Botai *et al.*, 2018; du Preez *et al.*, 2019). To address this knowledge gap, the second part of this study was intended to investigate and quantify the rate of change of rainfall seasonality for the period of 1987-2016. The results and inferences of the first and second parts of this study are presented in *Chapter 5 (Results)* and *6 (Discussion)*. This chapter presents a synthesis of the work presented in the previous chapters, first by highlighting how and the extent to which the study aim and objectives presented in *Chapter 1 (Introduction)* were achieved. Following this, the avenues for future work are explored, and finally a synopsis of the main findings from this study is provided together with the significance of these.

7.2 ACHIEVEMENT OF STUDY AIM AND OBJECTIVES

The aim and objectives of this study are captured under *Section 1.2* of *Chapter 1 (Introduction)*. The primary aim of this study was to statistically quantify rainfall seasonality and the changes thereof across South Africa. The main objectives developed were for the purpose of addressing this primary aim through contributing to the knowledge gaps highlighted throughout *Chapter 1 (Introduction)* and *Chapter 2 (Literature Review)*. The work to address all the study objectives was undertaken using daily rainfall, and T_{max} and T_{min} for the 30-year period of 1987-2016 from 46 weather stations spread across South Africa. In addressing the objectives of this study, it should be noted that the data and statistical limitations, discussed under *Section 6.5 Chapter 6 (Discussion)*, have not compromised achievement of the study objectives. The objectives of this study are listed below, in the order presented under *Section 1.2* of *Chapter 1 (Introduction)*, with the purpose and process behind these as well as the extent to which these have been achieved.

1. *To investigate the spatiotemporal patterns of rainfall amount for the selection of 46 weather stations over an annual and a monthly scale for the period of 1987-2016.*

This objective required an analysis of the general rainfall characteristics and the changes thereof for each of the selected weather stations for the study period, where the results of this are presented under *Section 5.2* and *5.3* of *Chapter 5 (Results)* as well as *Appendix B*. The details of the methodological process behind this objective was captured under *Section 4.3* of *Chapter 4 (Data and Methodology)*. This objective was achieved through quantifying both the mean and variability in rainfall amount over an annual and a monthly scale. Additionally, the spread of both the annual and monthly rainfall totals were analysed through the five-number summaries. The mean of the annual and monthly rainfall amount for each of the weather stations was mapped in order to investigate the spatial patterns. Linear correlation analysis (viz. direction, magnitude, *r value* and *p value* of temporal trend) of the annual and monthly amounts was used in order to determine whether there had been any progressive change in these variables over the 30-year study period, where these were additionally mapped in order to determine any spatial patterns in the direction and magnitude of the temporal trends. Additionally, change point analysis was

applied to each of the variables across the weather stations to determine variability in the magnitude and direction of trends throughout the study period.

The purpose of these analyses was to determine firstly whether the selected weather stations were representative of the spatial and temporal patterns of annual and monthly rainfall amount, and of the SRZ, WRZ and YRZ rainfall regimes known to exist across South Africa. The discussion regarding these analyses is presented under *Section 6.2* of *Chapter 6 (Discussion)*. In summary, it was concluded that the annual and monthly rainfall amount patterns were consistent with published literature representing closely the true rainfall patterns across the country. Hence, the selected weather stations were determined to be representative of the rainfall regimes across the country which meant that the selected weather stations were appropriate for further analyses required for objectives two to four. Moreover, the annual cycles of rainfall amount were important for a qualitative description of rainfall seasonality, and through that annual cycles of rainfall amount representative of SRZ, WRZ and YRZ conditions were identified under *Section 5.3* of *Chapter 5 (Results)*. Secondly, these analyses were also purposed to determine whether the temporal trends were in agreement with previous literature as well as with the rainfall seasonality trends assessed under objective four. The discussion regarding this was presented under *Section 6.4.2* of *Chapter 6 (Discussion)*. The temporal trends quantified for annual and monthly rainfall amount were both consistent and inconsistent with literature, which is representative of the dispute in published literature regarding temporal trends in rainfall amount (MacKellar *et al.*, 2014; Davis *et al.*, 2016; van Wilgen *et al.*, 2016; Kruger & Nxumalo, 2017). Additionally, there was much agreement between the temporal trends in monthly rainfall amount and the rainfall seasonality metrics. This agreement between these trends was particularly important for corroboration of the rainfall seasonality trends quantified to achieve objective four.

2. *To develop a statistical approach to accurately quantify, characterise and classify the climatological rainfall seasonality of the selection of 46 weather stations using methods, with known application across South Africa, from a diverse range of scientific fields including:*

   a. Cluster analysis of mean monthly rainfall amount and variability (Climatology);

   b. The relationship between mean monthly temperature and rainfall (Palaeoclimatology);

   c. Onset and cessation dates of the wet season (Agroclimatology);

   d. Accumulation of minimum (10%) and maximum (90%) rainfall amount (Agroclimatology).

The published paper presented under *Section 2.2 Chapter 2 (Literature Review)* highlights that the classification of rainfall seasonality across South Africa is disputed across previous published classification attempts using different datasets and methods. This objective was developed in order to address this issue, to determine a seasonality metric or a set of seasonality metrics which may be used as a standard approach to quantify rainfall seasonality across South Africa, and broadly southern Africa, in research following this study. This objective was addressed by applying a selection of seasonality metrics to the datasets of the 46 project weather stations. The justification behind selecting these metrics as well as the methodological process is captured under *Section 4.4* and specifically *Sections 4.4.1*, *4.4.2*, *4.4.3*, *and* *4.4.4* of *Chapter 4 (Data and Methodology)*. The main justification behind these methods is that each method had to some extent been applied across South Africa. Each method also had the ability to statistically distinguish between summer and winter rainfall conditions, which is possibly the most important requirement for a method to model rainfall seasonality characteristics across South Africa (Thackeray & Fitchett, 2016; Fitchett & Bamford, 2017).

The results of the application of each of these methods is presented under *Section 5.4* and more specifically under *Sections 5.4.1*, *5.4.2*, *5.4.3*, *and* *5.4.4* of *Chapter 5 (Results)*. The discussions of these results are presented under *Section 6.3* of *Chapter 6 (Discussion)*, where *Section 6.3.1* was aimed at comparing the methods to determine a standard approach to quantify rainfall seasonality. To determine the best method(s), each approach was assessed on the basis of the methods accuracy, ability to reflect change (assessed under objective four), and the relative value

in terms of application and contribution to completely describing rainfall seasonality. The resulting rainfall seasonality classifications per weather station for each of the methods did not always converge on the same classification, further highlighting the need for a standard approach to quantify and classify rainfall seasonality. The results and discussions behind this objective address the first hypothesis which was developed. As hypothesised, "there is a statistical method that can accurately characterise and classify rainfall seasonality across South Africa". This hypothesis only suggests one method, but both the methods on "the relationship between mean monthly temperature and rainfall" and the "accumulation of minimum (10%) and maximum (90%) rainfall amount" were accurate in their representation of rainfall seasonality, where it was also demonstrated that the results of these methods were broadly consistent with published literature. Thus, the standard method developed draws on these seasonality metrics, where it was also suggested that the method presented by Dunning *et al.* (2016) could be applied given its value to agricultural seasonality. The standard metrics suggested do not present the same rainfall seasonality characteristics due to the different way in which each method defines rainfall seasonality, and thus it was noted that application of these methods is specific to each standard metric. The method on the relationship between mean monthly temperature and rainfall returning seasonality scores was, however, determined as the most accurate, as this method presented the most comprehensive understanding of the YRZ and this method also had relatively no assumptions surrounding it, thus making it a particularly objective seasonality metric to define climatological seasonality. The method on the accumulation of minimum (10%) and maximum (90%) rainfall amount was also selected as a standard approach because it compared well to published literature, it can be used to completely describe rainfall seasonality and one can also obtain much societally relevant information on the seasonal characteristics of rainfall from this approach, however, there were numerous assumptions surrounding this method.

3. *To interrogate and understand the contemporary rainfall seasonality characteristics for the selection of weather stations using the statistical approach developed under objective 2.*

This objective was addressed through quantifying the general rainfall seasonality characteristics obtained from each of the seasonality metrics part of objective two. The results of this objective are presented under *Section 5.4* and more specifically under *Sections 5.4.1*, *5.4.2*, *5.4.3*, *and* *5.4.4* of *Chapter 5 (Results)*. The discussion of these results is presented under *Section 6.3* of *Chapter 6 (Discussion)*. In summary, the different methods provided much information, towards a complete description of rainfall seasonality, where the onset and cessation dates and the percentile-based approach provided the most information on rainfall seasonality. However, it was concluded that climatologically the seasonality scores were the most accurate in quantifying rainfall seasonality because there were relatively no assumptions surrounding quantification of the scores and the seasonality scores provided the best classification of the YRZ. This was because the classification of the YRZ included the transition zone between the SRZ and WRZ as well as the known YRZ locations across the southern coast. It was also demonstrated that all of the methods were suitable in quantifying rainfall seasonality for the SRZ and WRZ. It is also notable that the results of all the seasonality metrics were broadly consistent with literature, especially when considering the mean spatial patterns.

4. *To quantify changes in rainfall seasonality over the period of 1987-2016 for the 46 weather stations.*

This objective required quantification of changes in the rainfall seasonality characteristics for each of the selected weather stations. Linear correlation analysis (viz. direction, magnitude, *r value* and *p value* of temporal trend) as well as change point analysis, described under *Section 4.5* of *Chapter 4 (Data and Methodology)*, was applied to the annual seasonality metrics (viz. seasonality scores, onset and cessation dates and the respective length of the wet season and number of rain days, and 10% and 90% dates and the respective length of the wet season and number of rain days) which were quantified to address objective two. This was to determine whether there were any

progressive changes in rainfall seasonality during the 30-year study period as well as the extent to which the seasonal rainfall characteristics varied, where this was used to address the second hypothesis (i.e. "Rainfall seasonality across South Africa has changed during 1987-2016"). As hypothesised, rainfall seasonality across South Africa changed during the study period, although it is important to note that the seasonal characteristics of rainfall did not change across all of the weather stations. The *p value* was particularly important to determine the probability of change having occurred by chance. The results of the changes in rainfall seasonality are presented under *Section 5.5* of *Chapter 5 (Results)*, where the spatial patterns as well as the agreement of change were particularly important to capture to determine the accuracy of these temporal trends and in part the probability of change having occurred. The discussion regarding the shifts in rainfall seasonality characteristics was captured under *Section 6.4* of *Chapter 6 (Discussion)*. In addition to the numerous seasonality metrics, the annual and monthly temporal trends were also discussed under this section, where this was also for the purpose of corroborating the seasonality trends.

7.3 FUTURE RESEARCH TRAJECTORIES

This study was undertaken to provide a standard approach to quantify and classify rainfall seasonality across South Africa, and to explore how rainfall seasonality may have changed over the period of 1987-2016. The results obtained under *Chapter 5* and discussed under *Chapter 6*, and the literature review broadly highlight that there is a still a need for continued research following this study. The results from this study have considerable value mainly for academic research and some societal value is also noted. In terms of societal value, the results and implications regarding the rainfall seasonality changes may be translated into information, which is accessible to the public of South Africa. The future research trajectories discussed in the paragraphs below are specifically focused on building on from the aim and objectives of this research project, where these avenues for future research surround mainly application of the standard approaches as well as investigation into change and variability of rainfall seasonality across South Africa. It should be noted that even though application for this study was limited to South Africa, future research may also investigate applying both standard approaches to other regions, such as across the remaining countries of southern Africa.

The first and possibly most important avenue for future research surrounds the application of the two standard approaches across southern Africa, where this application should entail academic research endeavors. Application of the seasonality scores may be suitable for any region for now, until further testing, given that this approach worked well in characterising locations with year-round (i.e. aseasonal) rainfall conditions, while the percentile-based approach will work well mainly in regions with a uni-modal wet season. There are many avenues for application, and before some of those avenues are identified it is important to note that some applications may be approach specific and this is important to consider when applying the suggested standard metrics. Numerous avenues for application of the standard metrics exist across southern Africa, where application should include additional climatological and meteorological research and may also involve research regarding climate sensitive activities such as agriculture, conservation, ecosystem services, health care, electricity generation, fishing, tourism, forestry, water resource management, and disaster risk management among others, where this will be important for development and improvement of adaptation strategies. There are numerous applications for these approaches, as the degree of seasonality, commencement and withdrawal of the wet season and the duration, intensity and magnitude of seasonal rainfall influences the timing of key flora and fauna phenological events (e.g. breeding, leaf development and fall, flowering, fruit development; Prevéy *et al.*, 2014; Omondi *et al.*, 2016; Yan *et al.*, 2016; de Araujo *et al.*, 2017; Whitecross *et al.*, 2017), the dynamics of wildlife populations (e.g. Lepage & Llyod, 2004; Senapathi *et al.*, 2011; Brawn *et al.*, 2017; Fitchett *et al.*, 2019) the transmission of malaria (e.g. Briët *et al.*, 2008a,b), the risk of flood and drought (e.g. Beurton & Thieken, 2009; Botai *et al.*, 2016, 2017; Sousa *et al.*, 2018), the risk of soil erosion (de Luis *et al.*, 2010b; Botai *et al.*, 2018), among others.

Although much has been covered regarding the spatial characteristics of rainfall seasonality, the second avenue for future research suggests further investigation into the spatial characteristics of rainfall seasonality. It is highly recommended that the standard approaches suggested under *Section 6.3.1* of *Chapter 6* are applied to all weather stations, which contain rainfall and temperature data, from both the SAWS and ARC climate databases across South Africa, as previously mentioned, as well as for the climate databases for neighbouring countries. This is important for a finer spatial resolution and, as previously noted, reanalysis products and

satellite/gauge-based estimates may also be applied for an improved spatial resolution (see datasets used by Jury, 2013, 2018; Zhang *et al.*, 2013; Dunning *et al.*, 2016; Botai *et al.*, 2018). It is important to first assess the limitations surrounding the spatial and temporal resolution, and accuracy associated with these products before application. An improved spatial resolution may be particularly useful to quantify the average boundary locations of rainfall zones and for investigations focusing on changes and variability in the location of the annual boundary, where it is suggested that the seasonality scores approach be applied for these purposes. Additionally, studies over smaller spatial scales may afford more in-depth analyses and are thus important for an improved understanding of the relationship between geographic location and rainfall seasonality, where studies may focus on for instance the role of locality in terms of position relative to the distribution of land and sea, SSTs, land use/cover, topography in terms of terrain and elevation, and the nature of the underlying terrain (e.g. soil types, soil moisture, etc.) in determining seasonal rainfall characteristics (Taljaard, 1996; Nel, 2009; Pal *et al.*, 2013; Ma & Zhou, 2015). Studies over a smaller scale may also explore, in detail, the implications of changing rainfall regimes to develop location specific plans to improve the capacity to plan, manage and adapt to future rainfall regime changes.

Under *Section 2.3.2.2* of *Chapter 2 (Literature Review)* it is highlighted that there are few published studies which have investigated changes and variability in rainfall seasonality characteristics, and hence a third clear research opportunity involves further investigations on this topic. In terms of the changes in seasonality, as previously mentioned, future studies will benefit from using datasets over longer (>50 years) temporal scales for identification of decadal trends (Schulze *et al.*, 2007), as well as trends over longer time frames in the order of thousands of years (Jones *et al.*, 2009; Nicholson *et al.*, 2018). Since the seasonality scores approach has proven application in the palaeoclimatological record (e.g. Thackeray & Fitchett, 2016), future research may focus on quantifying rainfall seasonality over as long time frames as possible in order to track changes in rainfall seasonality from the late Miocene given that it has been postulated that pronounced seasonality across the southwestern Cape, at least, of southern Africa originated during this period (Sciscio *et al.*, 2013). Such research focusing on developing long temporal scale reconstructions of rainfall seasonality may also consider historical climate datasets (See datasets used by Nicholson,

2000; Kelso & Vogel, 2007; Hannaford *et al.*, 2015; Naidoo, 2016; Nash *et al.*, 2016; Nash, 2017; Picas *et al.*, 2018). By quantifying rainfall seasonality as far back as possible an improved understanding of seasonality fluctuations and even the drivers behind such fluctuations may be gained, and in turn this would be particularly valuable for research regarding adaptation to changes and variability in rainfall seasonality (Fitchett & Bamford, 2017; Nicholson *et al.*, 2018). Additionally, numerous global studies have explored the influence of regional teleconnection forcing mechanisms (e.g. ENSO, Indian Ocean Dipole, Pacific Decadal Oscillation, North Atlantic Oscillation, among others) on rainfall seasonality changes and inter-annual variability patterns (e.g. Sahany *et al.*, 2018; Deng *et al.*, 2019; Zhang *et al.*, 2019). Few studies across southern Africa have explored the influence of ENSO and the SAM, for example, on the seasonal characteristics of rainfall (e.g. Reason *et al.*, 2005; Tadross *et al.*, 2009; Moeletsi *et al.*, 2011). Since the standard approaches were demonstrated to accurately represent inter-annual variability in rainfall seasonality, it is important that this topic be further investigated across the entire country. On the topic of seasonality change, it is also important for further investigation into the synoptic scale forcing as a driver of rainfall seasonality change (Lennard & Hegerl, 2015). Such research may be undertaken using self-organising maps as this is a computationally low intensity technique for representing synoptic types (Engelbrecht *et al.*, 2015; Lennard & Hegerl, 2015). Daily synoptic charts produced by the SAWS may also be used as a way to corroborate results using the self-organising maps technique. For such research, focus can be placed on investigating changes and variability in the frequency of key synoptic scale circulation features, where a first step may be identifying the key synoptic scale circulation types associated with each rainfall zone across southern Africa. Such research would facilitate investigation into the drivers of rainfall seasonality changes, where this may be useful to corroborate trends in seasonality for a more accurate understanding of how rainfall seasonality has changed (Lennard & Hegerl, 2015).

As a fourth avenue it is important to consider the application of both the seasonality scores as well as the percentile-based approach in climate modelling studies, where the focus may be on improving modelling capabilities of RCMs and on developing climate projections and seasonal rainfall forecasts (Camberlin *et al.*, 2009; Shongwe *et al.*, 2015; Ratnam *et al.*, 2018). Such work would be of academic value and it will also be beneficial for studies regarding adaptation to

changing rainfall seasonality patterns, where this will be particularly important to plan for year to year variations in seasonality and in the timing of the wet season. Here application in order to investigate the physical mechanisms underlying variability and changes in rainfall seasonality will also be particularly important (Tadross *et al.*, 2009; Shongwe *et al.*, 2015). Additionally, application of both standard approaches in a single study will be particularly important for corroboration purposes, as it has been for this study, where this may also be useful for projections and predictions on a complete description of rainfall seasonality (Pascale *et al.*, 2016). Important in future research regarding predictions of rainfall seasonality characteristics is communication of findings, especially in southern Africa, for example, where most agricultural activities heavily rely on rainfall. In considering future research regarding seasonal rainfall prediction using the standard approaches suggested in this research, it may be important also to consider the context of agriculture in southern Africa and here it may be necessary to even consider indigenous knowledge systems where short-term traditional forecasts/predictions on rainfall may be merged with science-based rainfall predictions (Zuma-Netshiukhwi *et al.*, 2013).

7.4 SYNOPSIS AND SIGNIFICANCE OF THE STUDY FINDINGS

This study analysed rainfall seasonality using observed rainfall and temperature datasets for the period of 1987-2016 from 46 weather stations which are spread relatively evenly across South Africa. Conducted in two parts, part one of this study focused on developing a standard methodology to accurately quantify rainfall seasonality across the country. Part two of this study drew on the annual seasonality characteristics quantified for part one, where this part focused on investigating changes in the seasonal characteristics of rainfall across each of the study weather stations.

Firstly, four methodologies which quantify rainfall seasonality were objectively tested using the same datasets to determine a standard statistical method which accurately defines rainfall seasonality across South Africa. The methods based on the seasonality scores and the 10% and 90% dates of the wet season were determined to be suitable standard statistical approaches which may be applied across southern Africa. These two methods compared well with published

literature, accurately represented rainfall seasonality and contribute to a complete description of rainfall seasonality. Most important is that these methods were shown to statistically discriminate between the known rainfall zones across South Africa, thus highlighting the applicability of these methods. The significance of these standard methods is highlighted by the fact there is much future research which surrounds the application of these methods, where the avenues for future research were discussed in the previous *Section 7.3*. Since southern Africa is highlighted as being particularly vulnerable to future climate changes (IPCC, 2018), key avenues for future research include the application of these methods to research endeavors surrounding climate modelling and forecasting across southern Africa. Numerous publications have highlighted that incorporating seasonality metrics into climate modeling endeavors is key in assessing the ability of a climate model to simulate current climate conditions and to project future changes (Shongwe *et al.*, 2015; Dunning *et al.*, 2016; Li *et al.*, 2016; Pascale *et al.*, 2016). Moreover, timely and effective adaptation to future rainfall seasonality changes across key economic sectors, such as agriculture and water resource management, requires accurate climate forecasting and projecting ranging from seasonal to decadal scales, and effective communication of these forecasts to key stakeholders which are both affected by and interested in these changes (Ziervogel *et al.*, 2014). Additionally, the method concerning the seasonality scores has applicability in the palaeoenvironmental record (Thackeray & Fitchett, 2016), thus making it a key method which can be used to understand rainfall seasonality beyond the instrumental record. The development and testing of these standard methods are thus a key contribution to knowledge regarding climatological research across South Africa.

The second part of this project involved application of the seasonality metrics to quantify change in the rainfall seasonality characteristics across the selected weather stations. This part of the project represents application of the standard methods, and it also contributes greatly to an understanding of changing rainfall regimes across South Africa which is a topic that has received little attention in published literature. There was relatively high agreement particularly in the direction of change across the project locations, highlighting that these standard methods are accurate in detecting changes in the seasonal characteristics of rainfall. For the most part the changes in seasonality detected for the study period agreed relatively well spatially between the

weather stations and broadly with published literature regarding observed and projected rainfall seasonality changes. The results highlight a high possibility that most of the SRZ locations had experienced an increase in the degree of SRZ seasonality as well as an overall reduction in the length of the wet season particularly due to later start dates for the wet season. Across most of the WRZ locations there was a high likelihood of reduced seasonality and a longer wet season which was linked with a reduction in rainfall amount mostly during the winter months of the year. Across the YRZ locations along the southern coast, an increased WRZ seasonality as well as a reduction in the wet season duration was mostly evident. Although the temporal period was too short to detect many statistically significant trends, the agreement in these changes highlights the need for future research over longer temporal periods as well as across more weather stations to further investigate how the seasonal characteristics of rainfall have changed. Since these changes already demonstrate relatively high agreement, the translation of these results into accessible information for the South African population and government is of importance as these changes may greatly impact agriculture and other economic sectors sensitive to rainfall regimes.

REFERENCES

Abrahams, W. (2019). *Is the rainy season shifting?*. Available at: http://www.csag.uct.ac.za/2019/04/08/is-the-rainy-season-shifting/ (Accessed 1 July 2019).

Ackerly, D.D., Stock, W.D. and Slingsby, J.A. (2014). Geography, climate, and biodiversity?: the history and future of mediterranean-type ecosystems. In Allsopp, N., Colville, J.F. and Verboom, G.A. (eds.). *Fynbos: ecology, evolution, and conservation of a megadiverse region*. Oxford University Press: Oxford.

Adelekan, I.O. and Adegebo, B.O. (2014). Variation in onset and cessation of the rainy season in Ibadan, Nigeria. *Journal of Science Research*, 13: 13-21.

Adikhary, S.K., Yilmaz, A.G. and Muttil, N. (2015). Optimal design of rain gauge network in the Middle Yarra River catchment, Australia. *Hydrological Processes*, 29: 2582-2599.

Akinsanola, A.A. and Ogunjobi, K.O. (2017). Recent homogeneity analysis and long-term spatio-temporal rainfall trends in Nigeria. *Theoretical and Applied Climatology*, 128: 275-289.

Ambrosino, C., Chandler, R.E. and Todd, M.C. (2011). Southern African monthly rainfall variability: An analysis based on generalized linear models. *Journal of Climate*, 24: 4600-4617.

Amekudzi, L.K., Yamba, E.I., Preko, K., Asare, E.O., Aryee, J., Baidu, M. and Codjoe, S.N.A. (2015). Variabilities in rainfall onset, cessation and length of the rainy season for the various agro-ecological zones of Ghana. *Climate*, 3: 416-434.

Araujo, J.A., Abiodun, B.J. and Crespo, O. (2016). Impacts of drought on grape yields in Western Cape, South Africa. *Theoretical and Applied Climatology*, 123: 117-130.

Archer, E., Engelbrecht, F., Hänsler, A., Landman, W., Tadross, M. and Helmschrot, J. (2018). Seasonal prediction and regional climate projections for southern Africa. In Revermann, R., Krewenka, K.M., Schmiedel, U., Olwoch, J.M., Helmschrot, J and Jürgens, N. (eds.). *Climate change and adaptive land management in southern Africa – assessments, changes, challenges, and solutions*. Klaus Hess Publishers: Göttingen.

Arguez, A. and Vose, R.S. (2011). The definition of the standard WMO climate normal: The key to deriving alternative climate normal. *Bulletin of the American Meteorological Society*, 92: 699-704.

Arif, S.N.A.M., Mohsin, M.F.M., Bakar, A.A., Hamdan, A.R. and Abdullah, S.M.S. (2017). Change point analysis: A statistical approach to detect potential abrupt change. *Jurnal Teknologi*, 79: 147-159.

Ati, O.F., Stigter, C.J. and Oladipo, E.O. (2002). A comparison of methods to determine the onset of the growing season in northern Nigeria. *International Journal of Climatology*, 22: 731-742.

Ati, O.F., Muhammed, S.Q. and Ati, M.H. (2008). Variations and trends in annual rainfall amounts and the onset of the rainy season for Kano for 87 years (1916-2002). *Journal of Applied Sciences Research*, 4: 1959-1962.

Awan, J.A., Bae, D.H. and Kim, K.J. (2015). Identification and trend analysis of homogeneous rainfall zones over the East Asia monsoon region. *International Journal of Climatology*, 35: 1422-1433.

Ayoade, J.O. (1970). The seasonal incidence of rainfall. *Weather*, 25: 414-418.

Bargaoui, Z.K. and Chebbi, A. (2009). Comparison of two kriging interpolation methods applied to spatiotemporal rainfall. *Journal of Hydrology*, 365: 56-73.

Bari, S., Hussain, M. and Husna, N.E. (2017). Rainfall variability and seasonality in northern Bangladesh. *Theoretical and Applied Climatology*, 129: 995-1001.

Barrable, A., Meadows, M.E. and Hewitson, B.C. (1998). Environmental reconstruction and climate modelling of the Late Quaternary in the winter rainfall region of the Western Cape, South Africa. *South African Journal of Science,* 98: 611-616.

Beaulieu, C., Chen, J. and Sarmiento, J.L. (2012). Change-point analysis as a tool to detect abrupt climate variations. *Philosophical Transactions of the Royal Society A: Mathematical, Physical and Engineering Sciences*, 370: 1228-1249.

Bekele, F., Korecha, D. and Negatu, L. (2017). Demonstrating effect of rainfall characteristics on wheat yield: Case of Sinana District, south eastern Ethiopia. *Agricultural Sciences*, 8: 371-384.

Bello, N.J. (1998). Evidence of climate change based on rainfall records in Nigeria. *Weather*, 53: 412-418.

Beurton, S. and Thieken, A.H. (2009). Seasonality of floods in Germany. *Hydrological Sciences Journal*, 54: 62-76.

Biastoch, A., Böning, C.W., Schwarzkopf, F.U. and Lutjeharms, J.R.E. (2009). Increase in Agulhas leakage due to poleward shift of Southern Hemisphere Westerlies. *Nature*, 462: 495-499.

Biasutti, M. and Sobel, A.H. (2009). Delayed Sahel rainfall and global seasonal cycle in a warmer climate. *Geophysical Research Letters*, 36: DOI: 10.1029/2009GL041303.

Blamey, R.C., Ramos, A.M., Trigo, R.M., Tomé, R. and Reason, C.J.C. (2018). The influence of atmospheric rivers over the South Atlantic on winter rainfall in South Africa. *Journal of Hydrometeorology*, 19: 127-142.

Blamey, R. and Reason, C.J.C. (2007). Relationships between Antarctic sea-ice and South African winter rainfall. *Climate Research*, 33: 183-193.

Blamey, R.C. and Reason, C.J.C. (2009). Numerical simulation of a mesoscale convective system over the east coast of South Africa. *Tellus A: Dynamic Meteorology and Oceanography*, 61: 17-34.

Blamey, R.C. and Reason, C.J.C. (2013). The role of mesoscale convective complexes in southern Africa summer rainfall. *Journal of Climate*, 26: 1654-1668.

Borchert, R. (1998). Responses of Tropical Trees to Rainfall Seasonality and its Long-Term Changes. In Markham A. (eds.). *Potential Impacts of Climate Change on Tropical Forest Ecosystems.* Springer: Dordrecht.

Botai, C., Botai, J., Muchuru, S. and Ngwana, I. (2015). Hydrometeorological research in South Africa: A review. *Water*, 7: 1580-1594.

Botai, C., Botai, J., Dlamini, L., Zwane, N. and Phaduli, E. (2016). Characteristics of droughts in South Africa: A case study of Free State and North West provinces. *MDPI Water*, 8. DOI: 10.3390/w8100439.

Botai, C., Botai, J., de Wit, J., Ncongwane, K. and Adeola, A. (2017). Drought Characteristics over the Western Cape Province, South Africa. *MDPI Water*, 9. DOI: 10.3390/w9110876.

Botai, C.M., Botai, J.O. and Adeola, A.M. (2018). Spatial distribution of temporal precipitation contrasts in South Africa. *South African Journal of Science*, 114: 70-78.

Boyard-Micheau, J., Camberlin, P., Philippon, N. and Moron, V. (2013). Regional-scale rainy season onset detection: a new approach based on multivariate analysis. *Journal of Climate*, 26: 8916-8928.

Braun, K., Bar-Matthews, M., Ayalon, A., Zilberman, T. and Matthews, A. (2017). Rainfall isotopic variability at the intersection between winter and summer rainfall regimes in coastal South Africa (Mossel Bay, Western Cape Province). *South African Journal of Geology*, 120: 323-340.

Brawn, J. D., Benson, T. J., Stager, M., Sly, N. D. and Tarwater, C.E. (2017) Impacts of changing rainfall regime on the demography of tropical birds. *Nature Climate Change*, 7: 133-136.

Briët, O.J., Vounatsou, P. and Amerasinghe, P.H. (2008a). Malaria seasonality and rainfall seasonality in Sri Lanka are correlated in space. *Geospatial Health*, 2: 183-190.

Briët, O.J., Vounatsou, P., Gunawardena, D.M., Galappaththy, G.N. and Amerasinghe, P.H. (2008b). Temporal correlation between malaria and rainfall in Sri Lanka. *Malaria Journal*, 7. DOI: 10.1186/1475-2875-7-77.

Brito, T.T., Oliveira-Júnior, J.F., Lyra, G.B., Gois, G. and Zeri, M. (2016). Multivariate analysis applied to monthly rainfall over Rio de Janerio state, Brazil. *Meteorology and Atmospheric Physics*, 129: 469-478.

Burls, N.J., Blamey, R.C., Cash, B.A., Swenson, E.T., al Fahad, A., Bopape, M.M., Straus, D.M. and Reason, C.J.C. (2019). The Cape Town "Day Zero" drought and Hadley cell expansion. *Npj Climate and Atmospheric Sciences*. DOI: 10.1038/s41612-019-0084-6.

Burt, J.E., Barber, G.M. and Rigby, D.L. (2009). *Elementary statistics for geographers*. Guilford Press: New York.

Byakatonda, J., Parida, B.P., Kenabatho, P.K. and Moalafhi, D.B. (2019). Prediction of onset and cessation of austral summer rainfall and dry spell frequency analysis in semiarid Botswana. *Theoretical and Applied Climatology*, 135: 101-117.

Camberlin, P. and Diop, M. (2003). Application of daily rainfall principal component analysis to the assessment of the rainy season characteristics in Senegal. *Climate Research*, 23: 159-169.

Camberlin, P., Moron, V., Okoola, R., Philippon, N. and Gitau, W. (2009). Components of the rainy seasons' variability in Equatorial East Africa: onset, cessation, rainfall frequency and intensity. *Theoretical and Applied Climatology*, 98: 237-249.

Cannarozzo, M., Noto, L.V. and Viola, F. (2006). Spatial distribution of rainfall trends in Sicily (1921–2000). *Physics and Chemistry of the Earth,* 31: 1201-1211.

Carr, A.S., Thomas, D.S.G., Bateman, M.D., Meadows, M.E. and Chase, B. (2006). Late Quaternary palaeoenvironments of the winter-rainfall zone of southern Africa: Palynological and sedimentological evidence from the Agulhas Plain. *Palaeogeography, Palaeoclimatology and Palaeoecology,* 239: 147-165.

Chase, B.M. and Meadows, M.E. (2007). Late Quaternary dynamics of southern Africa's winter rainfall zone. *Earth-Science Reviews* 84: 103–138.

Chase, B.M., Scott, L., Meadows, M.E., Gil-Romera, G., Boom, A., Carr, A.S., Reimer, P.J., Truc, L., Valsecchi, V. and Quick, L.J. (2012). Rock hyrax middens: a palaeoenvironmental archive for southern African drylands. *Quaternary Science Reviews*, 56: 107-125.

Chase, B.M., Boom, A., Carr, A.S., Meadows, M.E. and Reimer, P.J. (2013). Holocene climate change in southernmost South Africa: rock hyrax middens record shifts in the southern Westerlies. *Quaternary Science Reviews*, 82: 199-205.

Chase, B.M., Lim, S., Chevalier, M., Boom, A., Carr, A.S., Meadows, M.E. and Reimer, P.J. (2015). Influence of tropical easterlies in southern Africa's winter rainfall zone during the Holocene. *Quaternary Science Reviews* 107: 138–148.

Chase, B.M., Chevalier, M., Boom, A. and Carr, A.S. (2017). The dynamic relationship between temperate and tropical circulation systems across South Africa since the last glacial maximum. *Quaternary Science Reviews*, 174: 54-62.

Chase, B.M. and Quick, L.J. (2018). Influence of Agulhas forcing of Holocene climate change in South Africa's southern Cape. *Quaternary Research*, 90: 303-309.

Cherchi, A., Ambrizzi, T., Behera, S., Freitas, A.C.V., Morioka, Y. and Zhou, T. (2018). The response of subtropical highs to climate change. *Current Climate Change Reports*, 4: 371-382.

Chevalier, M. and Chase, B.M. (2015). Southeast African records reveal a coherent shift from high-to low-latitude forcing mechanisms along the east African margin across last glacial–interglacial transition. *Quaternary Science Reviews*, 125: 117-130.

Chevalier, M. and Chase, B.M. (2016). Determining the drivers of long-term aridity variability: a southern African case study. *Journal of Quaternary Science*, 31: 143-151.

Christensen, J.H., Hewitson, B., Busuioc, A., Chen, A., Gao, X., Held, R., Jones, R., Kolli, R.K., Kwon, W.K., Laprise, R. and Magaña Rueda, V. (2007). Regional climate projections. In IPCC. (eds.). *Climate Change, 2007: The Physical Science Basis. Contribution of Working group I to the Fourth Assessment Report of the Intergovernmental Panel on Climate Change.* University Press: Cambridge.

Chu, H. J., Pan, T. Y., and Liou, J. J. (2012). Change-point detection of long-duration extreme precipitation and the effect on hydrologic design: a case study of south Taiwan. *Stochastic Environmental Research and Risk Assessment*, 26: 1123-1130.

Cockroft, M.J., Wilkinson, M.J. and Tyson, P.D. (1987). The application of a present-day climatic mode to the Late Quaternary in southern Africa. *Climatic Change,* 10: 161-181.

Coetzee, J.A. (1967). Pollen analytical studies in east and southern Africa. *Palaeoecology of Africa*, 3: 1-146.

Combrink, M. (2017). *The Quaternary pollen of Ntsikeni Wetland, KwaZulu-Natal, South Africa*. *MSc Dissertation submitted to the University of the Witwatersrand.*

Cook, B.I. and Buckley, B.M. (2009). Objective determination of monsoon season onset, withdrawal, and length. *Journal of Geophysical Research: Atmospheres*, 114. DOI: 10.1029/2009JD012795.

Cooke, H.B.S. (1946). Some observations on Rainfall distribution in South Africa. *South African Geographical Journal*, 28: 34-38.

Cordova, C.E. (2013). C_3 Poaceae and Restionaceae phytoliths as potential proxies for reconstructing winter rainfall in South Africa. *Quaternary International*, 287: 121-140.

Corporal-Lodangco, I.L. and Leslie, L.M. (2017). Defining Philippine Climate Zones Using Surface and High-Resolution Satellite Data. *Procedia Computer Science*, 114: 324-332.

Cortesi, N., González-Hidalgo, J.C., Brunetti, M. and Martín Vide, J. (2012). Daily precipitation concentration across Europe 1971-2010. *Natural Hazards and Earth System Sciences,* 12: 2799-2810.

Coscarelli, R.A. and Caloiero, T. (2012). Analysis of daily and monthly rainfall concentration in Southern Italy (Calabria region). *Journal of Hydrology*, 416: 145-156.

Cosijn, C. and Tyson, P.D. (1996). Stable discontinuities in the atmosphere over South Africa. *South African Journal of Science*, 92: 381-386.

Coulibaly, M. and Becker, S. (2007). Spatial interpolation of annual precipitation in South Africa-Comparison and evaluation of methods. *Water International*, 32: 494-502.

Cowling, R.M., Cartwright, C.R., Parkington, J.E. and Allsopp, J.C. (1999). Fossil wood charcoal assemblages from Elands Bay Cave, South Africa: implications for Late Quaternary vegetation and climates in the winter-rainfall fynbos biome. *Journal of Biogeography*, 26: 367-378.

Cowling, R.M., Procheş, Ş. and Partridge, T.C. (2009). Explaining the uniqueness of the Cape flora: incorporating geomorphic evolution as a factor for explaining its diversification. *Molecular Phylogenetics and evolution*, 51: 64-74.

Craig, M.H., Kleinschmidt, I., Nawn, J.B., Le Sueur, D. and Sharp, B.L. (2004). Exploring 30 years of malaria case data in KwaZulu-Natal, South Africa: part I. The impact of climatic factors. *Tropical Medicine & International Health*, 9: 1247-1257.

Cramer, M.D. and Hoffman, M.T. (2015). The consequences of precipitation seasonality for Mediterranean-ecosystem vegetation of South Africa. *PloS One*, 10. DOI:10.1371/journal.pone.0144512.

Crétat, J., Richard, Y., Pohl, B., Rouault, M., Reason, C. and Fauchereau, N. (2012). Recurrent daily rainfall patterns over South Africa and associated dynamics during the core of the austral summer. *International Journal of Climatology*, 32: 261-273.

Crétat, J., Pohl, B., Dieppois, B., Berthou, S. and Pergaurd, J. (2019). The Angola low: relationship with southern African rainfall and ENSO. *Climate Dynamics*, 52, 1783-1803.

Dartmouth Flood Observatory. (2018). *Global active archive of large flood events*. Available at: http://www.dartmouth.edu/~floods/Archives/index.html (Accessed: 15 November 2018).

Davis, C.L., Hoffman, T.M. and Roberts, W. (2016). Recent trends in the climate of Namaqualand, a megadiverse arid region of South Africa. *South African Journal of Science*, 112. DOI: 10.17159/sajs.2016/20150217.

Davis, C., Engelbrecht, F., Tadross, M., Wolski, P. and Archer van Garderen, E. (2017). Future climate change over Southern Africa. In Mambo, J. and Faccer, K. (eds.). *South African Risk and Vulnerability Atlas Second Edition Understanding the Social and Environmental Implications of Global Change*. African Sun Media: Stellenbosch.

Dedekind, Z., Engelbrecht, F.A. and Van der Merwe, J. (2016). Model simulations of rainfall over southern Africa and its eastern escarpment. *Water SA*, 42: 129-143.

Dehghan, Z., Eslamian, S.S. and Modarres, R. (2017). Spatial clustering of maximum 24-h rainfall over Urmia Lake Basin by new weighting approaches. *International Journal of Climatology*, 38: 2298-2313.

Demirel, M.C. and Moradkhani, H. (2016). Assessing the impact of CMIP5 climate multi-modeling on estimating the precipitation seasonality and timing. *Climatic Change*, 135: 357-372.

Deng, S., Yang, N., Li, M., Cheng, L., Chen, Z., Chen, Y., Chen, T. and Liu, X. (2019). Rainfall seasonality changes and its possible teleconnections with global climate events in China. *Climate Dynamics*. DOI: 10.1007/s00382-019-04722-3.

de Araujo, H.F., Vieira-Filho, A.H., Barbosa, M.R.D.V., Diniz-Filho, J.A.F. and da Silva, J.M.C. (2017). Passerine phenology in the largest tropical dry forest of South America: effects of climate and resource availability. *Emu-Austral Ornithology*, 117: 78-91.

de Luis, M., Raventós, J., González-Hidalgo, J.C., Sánchez, J.R. and Cortina, J. (2000). Spatial analysis of rainfall trends in the region of Valencia (East Spain). *International Journal of Climatology*, 20: 1451-1469.

de Luis, M., González-Hidalgo, J.C. and Longares, L.A. (2010a). Is rainfall erosivity increasing in the Mediterranean Iberian Peninsula?. *Land Degradation & Development*, 21: 139-144.

de Luis, M., Brunetti, M., Gonzalez-Hidalgo, J.C., Longares, L.A. and Martin-Vide, J. (2010b). Changes in seasonal precipitation in the Iberian Peninsula during 1946–2005. *Global and Planetary Change*, 74: 27-33.

de Luis, M.D., Gonzalez-Hidalgo, J.C., Brunetti, M. and Longares, L.A. (2011). Precipitation concentration changes in Spain 1946–2005. *Natural Hazards and Earth System Sciences*, 11: 1259-1265.

Dent, M.C., Lynch, S.D. and Schulze, R.E. (1987). *Mapping mean annual and other rainfall statistics over southern Africa*. Water Research Commission Report: Pietermaritzburg.

Di Piazza, A., Conti, F.L., Noto, L.V., Viola, F. and La Loggia, G. (2011). Comparative analysis of different techniques for spatial interpolation of rainfall data to create a serially complete monthly time series of precipitation for Sicily, Italy. *International Journal of Applied Earth Observation and Geoinformation*, 13: 396-408.

Dieppois, B., Rouault, M. and New, M. (2015). The impact of ENSO on Southern African rainfall in CMIP5 ocean atmosphere coupled climate models. *Climate Dynamics*, 45: 2425-2442.

Dieppois, B., Pohl, B., Rouault, M., New, M., Lawler, D. and Keenlyside, N. (2016). Interannual to interdecadal variability of winter and summer southern African rainfall, and their teleconnections. *Journal of Geophysical Research: Atmospheres*, 121: 6215-6239.

Dobesch, H., Dumolard, P., & Dyras, I. (2007). *Spatial interpolation for climate data: The use of GIS in climatology and meteorology*. ISTE Ltd: Great Britain.

Dunning, C.M. (2018). Characterising and understanding trends and variability in African rainfall seasonality. *PhD thesis submitted to the University of Reading*.

Dunning, C.M., Black, E.C. and Allan, R.P. (2016). The onset and cessation of seasonal rainfall over Africa. *Journal of Geophysical Research: Atmospheres*, 121: 405-424.

Dunning, C.M., Black, E.C. and Allan, R.P. (2018). Later wet seasons with more intense rainfall over Africa under future climate change. *Journal of Climate*, 31: 9719-9738.

du Plessis, J.A. and Schloms, B. (2017). An investigation into the evidence of seasonal rainfall pattern shifts in the Western Cape, South Africa. *Journal of the South African Institution of Civil Engineering*, 59: 47-55.

du Preez, C.C., Kotzé, E. and van Huyssteen, C.W. (2019). Soils, Agriculture and Food. In Knight, J. and Rogerson, C.M. (eds.). *The Geography of South Africa*. Springer: Switzerland.

Dyer, T.G.J. (1975a). Solar activity and rainfall variation over southern Africa. *South African Journal of Science*, 71: 369-372.

Dyer, T. G. J. (1975b). Secular variation in South African rainfall. *PhD thesis submitted to the University of the Witwatersrand*.

Dyson, L.L. (2009). Heavy daily-rainfall characteristics over the Gauteng Province. *Water SA*, 35: 627-638.

Dyson, L.L. and Van Heerden, J. (2002). A model for the identification of tropical weather systems over South Africa. *Water SA*, 28: 249-258.

Easterling, D.R., Evans, J.L., Groisman, P.Y., Karl, T.R., Kunkel, K.E. and Ambenje, P. (2000). Observed variability and trends in extreme climate events: a brief review. *Bulletin of the American Meteorological Society*, 81: 417-426.

Efron, B. (1982). *The Jackknife, the Bootstrap, and Other Resampling Plans*. Society for Industrial and Applied Mathematics: Philadelphia.

Elagib, N.A. (2011). Changing rainfall, seasonality and erosivity in the hyper-arid zone of Sudan. *Land Degradation & Development*, 22: 505-512.

Ellery, W. N., Grenfell, S. E., Grenfell, M. C., Powell, R., Kotze, D., Marren, P. and Knight, J. (2016). Wetlands in southern Africa. In Knight, J. and Grab, S. (eds.). *Quaternary environmental change in southern Africa: Physical and human dimensions*. Cambridge University Press: Cambridge.

Elser, K.J. and Archer, E. (2018). Southern African Biomes. In Holmes, P.J. and Boardman, J. (eds.). *Southern African Landscapes and Environmental Change*. Routledge: Oxon.

Engelbrecht, C.J. and Engelbrecht, F.A., 2016. Shifts in Köppen-Geiger climate zones over southern Africa in relation to key global temperature goals. *Theoretical and applied climatology*, *123*(1-2), pp.247-261.

Engelbrecht, F.A., McGregor, J.L. and Engelbrecht, C.J. (2009). Dynamics of the Conformal-Cubic Atmospheric Model projected climate-change signal over southern Africa. *International Journal of Climatology*, 29: 1013-1033.

Engelbrecht, F. and Landman, W.A. (2012) Current Climate. In DEA. (eds.). *South African Risk and Vulnerability Atlas*. Government Printer: Pretoria.

Engelbrecht, C.J., Engelbrecht, F.A. and Dyson, L.L. (2013). High-resolution model-projected changes in mid-tropospheric closed-lows and extreme rainfall events over southern Africa. *International Journal of Climatology*, 33: 173-187.

Engelbrecht, C.J., Landman, W.A., Engelbrecht, F.A. and Malherbe, J. (2015). A synoptic decomposition of rainfall over the Cape south coast of South Africa. *Climate Dynamics*, 44: 2589-2607.

Engelbrecht, C.J. and Landman, W.A. (2016). Interannual variability of seasonal rainfall over the Cape south coast of South Africa and synoptic type association. *Climate Dynamics*, 47: 295-313.

Engelbrecht, F.A., Marean, C.W., Cowling, R., Engelbrecht, C., Neumann, F.H., Scott, L., Nkoana, R., O'Neal, D., Fishcer, E., Shook, E., Franklin, J., Thatcher, M., McGregor, J.L., Van Der Merwe, J., Dedekind, Z. and Difford, M. (Under review). Downscaling Last Glacial Maximum climate over southern Africa. *Quaternary Science Reviews.*

Erdin, R., Frei, C. and Künsch, H.R. (2012). Data transformation and uncertainty in geostatistical combination of Radar and rain gauges. *Journal of Hydrometeorology*, 13: 1332-1346.

Evrard, O., Nord, G., Cerdan, O., Souchère, V., Le Bissonnais, Y. and Bonté, P. (2010). Modelling the impact of land use change and rainfall seasonality on sediment export from an agricultural catchment of the northwestern European loess belt. *Agriculture, Ecosystems & Environment*, 138: 83-94.

Ezenwaji, E.E., Nzoiwu, C.P. and Chima, G.N. (2017). Analysis of Precipitation Concentration Index (PCI) for Awka Urban Area, Nigeria. *Hydrology: Current Research*, 8. DOI: 10.4172/2157-7587.1000287.

Faith, J.T., Chase, B.M. and Avery, D.M. (2018). Late Quaternary micromammals and the precipitation history of the southern Cape, South Africa. *Quaternary Research*, 91: 848-860.

Fauchereau, N., Trzaska, S., Rouault, M. and Richard, Y. (2003). Rainfall variability and changes in southern Africa during the 20th century in the global warming context. *Natural Hazards*, 29: 139-154.

Fauchereau, N., Pohl, B., Reason, C.J.C., Rouault, M. and Richard, Y. (2009). Recurrent daily OLR patterns in the Southern Africa/Southwest Indian Ocean region, implications for South African rainfall and teleconnections. *Climate Dynamics*, 32: 575-591.

Favre, A., Hewitson, B., Lennard, C., Cerezo-Mota, R. and Tadross, M. (2013). Cut-off lows in the South Africa region and their contribution to precipitation. *Climate Dynamics*, 41: 2331-2351.

Favre, A., Philippon, N., Pohl, B., Kalognomou, E.A., Lennard, C., Hewitson, B., Nikulin, G., Dosio, A., Panitz, H.J. and Cerezo-Mota, R. (2016). Spatial distribution of precipitation annual cycles over South Africa in 10 CORDEX regional climate model present-day simulations. *Climate Dynamics*, 46: 1799-1818.

Fazel, N., Berndtsson, R., Uvo, C.B., Madani, K. and Kløve, B. (2018). Regionalization of precipitation characteristics in Iran's Lake Urmia basin. *Theoretical and Applied Climatology*, 132: 363-373.

Feng, X., Porporato, A. and Rodriguez-Ilturbe, I. (2013). Changes in rainfall seasonality in the tropics. *Nature Climate Change*, 3: 811-815.

Finch, J.M. and Meadows, M.E. (2019). South African Biomes and Their Changes Over Time. In Knight, J. and Rogerson, C.M. (eds.). *The Geography of South Africa*. Springer: Switzerland.

Finné, M., Norström, E., Risberg, J. and Scott, L. (2010). Siliceous microfossils as late-Quaternary paleo-environmental indicators at Braamhoek wetland, South Africa. *The Holocene*, 20: 747-760.

Fitchett, J.M. (2018). Recent emergence of CAT5 tropical cyclones in the South Indian Ocean. *South African Journal of Science*, 114. DOI: 10.17159/sajs.2018/4426.

Fitchett, J.M. (2019a). The Holocene Climates of South Africa. In Knight, J. and Rogerson, C.M. (eds.). *The Geography of South Africa*. Springer: Switzerland.

Fitchett, J.M. (2019b). *Tropical cyclone Idai: The storm that knew no boundaries*. Available at: http://theconversation.com/tropical-cyclone-idai-the-storm-that-knew-no-boundaries-113931 (Accessed: 24 June 2019).

Fitchett, J.M. (2019c). *Cyclone Kenneth is one of the strongest storms to hit mainland Africa*. Available at: https://www.newscientist.com/article/2200925-cyclone-kenneth-is-one-of-the-strongest-storms-to-hit-mainland-africa/ (Accessed: 24 June 2019).

Fitchett, J.M. and Grab, S.W. (2014). A 66-year tropical cyclone record for south-east Africa: temporal trends in a global context. *International Journal of Climatology*, 34: 3604-3615.

Fitchett, J.M., Grab, S.W., Bamford, M.K. and Mackay, A.W. (2016). A multi-proxy analysis of late Quaternary palaeoenvironments, Sekhokong Range, eastern Lesotho. *Journal of Quaternary Science*, 31: 788-798.

Fitchett, J.M. and Bamford, M.K. (2017). The validity of the Asteraceae: Poaceae fossil pollen ratio in discrimination of the southern African summer-and winter-rainfall zones. *Quaternary Science Reviews*, 160: 85-95.

Fitchett, J.M., Robinson, D. and Hoogendoorn, G. (2017a). Climate suitability for tourism in South Africa. *Journal of Sustainable Tourism*, 25: 851-867.

Fitchett, J.M., Mackay, A.W., Grab, S.W. and Bamford, M.K. (2017b). Holocene climatic variability indicated by a multi-proxy record from southern Africa's highest wetland. *The Holocene*, 27: 638-650.

Fitchett, J.M., Grab, S.W., Bamford, M.K. and Mackay, A.W. (2017c). Late Quaternary research in southern Africa: progress, challenges and future trajectories. *Transactions of the Royal Society of South Africa*, 72: 280-293.

Fitchett, J.M., Grab, S.W. and Portwig, H., 2019. Progressive delays in the timing of sardine migration in the southwest Indian Ocean. *South African Journal of Science*, *115*. DOI: 10.17159/sajs.2019/5887.

Fletcher, M.S. and Moreno, P.I. (2012). Have the Southern Westerlies changed in a zonally symmetric manner over the last 14,000 years? A hemisphere-wide take on a controversial problem. *Quaternary International*, 253: 32-46.

Forestieri, A., Lo Conti, F., Blenkinsop, S., Cannarozzo, M., Fowler, H.J. and Noto, L.V. (2018). Regional frequency analysis of extreme rainfall in Sicily (Italy). *International Journal of Climatology,* 38, 698-716.

Frazier, A.G., Giambelluca, T.W., Diaz, H.F. and Needham, H.L. (2016). Comparison of geostatistical approaches to spatially interpolate month-year rainfall for the Hawaiian Islands. *International Journal of Climatology*, 36: 1459-1470.

Fujita, K. (2008). Effect of precipitation seasonality on climatic sensitivity of glacier mass balance. *Earth and Planetary Science Letters*, 276: 14-19.

Fyfe, J.C. (2003). Extratropical Southern Hemisphere cyclones: Harbingers of climate change?. *Journal of Climate*, 16: 2802-2805.

Gaffney.D.O. (1971). *Seasonal rainfall Zones in Australia Working paper No 141*. Bureau of Meteorology: Australia.

Gasse, F., Chalié, F., Vincens, A., Williams, M.A. and Williamson, D. (2008). Climatic patterns in equatorial and southern Africa from 30,000 to 10,000 years ago reconstructed from terrestrial and near-shore proxy data. *Quaternary Science Reviews*, 27: 2316-2340.

Gillett, N.P., Kell, T.D. and Jones, P.D. (2006). Regional climate impacts of the Southern Annular Mode. *Geophysical Research Letters*, 33. DOI: 10.1029/2006GL027721.

Gillooly, J.F. (1976). Dendroclimatology in South Africa. *South African Forestry Journal*, 98: 64-65.

Gitau, M. (2016). Long-term seasonality of rainfall in the southwest Florida Gulf coastal zone. *Climate Research*, 69: 93-105.

Gocic, M. and Trajkovic, S. (2013). Analysis of changes in meteorological variables using Mann-Kendall and Sen's slope estimator statistical tests in Serbia. *Global and Planetary Change*, 100: 172-182.

Gong, D.Y. and Ho, C.H. (2002). Shift in the summer rainfall over the Yangtze River valley in the late 1970s. *Geophysical Research Letters*, 29. DOI: 10.1029/2001GL014523.

Grab, S.W. (1997). Analysis and characteristics of high altitude air temperature data from northern Lesotho: Implications for cryogeomorphic occurrences. *Geoöko Plus,* 4: 109-118.

Grab, S. and Craparo, A. (2011). Advance of apple and pear tree full bloom dates in response to climate change in the southwestern Cape, South Africa: 1973–2009. *Agricultural and Forest Meteorology*, 151: 406-413.

Grab, S.W. and Knight, J. (2018). Southern African Montane Environments. In Holmes, P.J. and Boardman, J. (eds.). *Southern African Landscape and Environmental Change*. Routledge: Oxon.

Griffith, D.A. and Amrhein. C.G. (1997). *Multivariate Statistics for Geographers*. New Jersey: Prentice-Hall.

Groisman, P.Y., Knight, R.W., Easterling, D.R., Karl, T.R., Hegerl, G.C. and Razuvaev, V.N. (2005). Trends in intense precipitation in the climate record. *Journal of Climate*, 18: 1326-1350.

Guenang, G.M. and Kamga, F.M. (2012). Onset, retreat and length of the rainy season over Cameroon, *Atmospheric Science Letters*, 13: 120-127.

Guerreiro, S.B., Kilsby, C.G. and Serinaldi, F. (2014). Analysis of time variation of rainfall in transnational basins in Iberia: abrupt changes or trends?. *International Journal of Climatology*, 34: 114-133.

Guhathakurta, P. and Saji, E. (2013). Detecting changes in rainfall pattern and seasonality index vis-à-vis increasing water scarcity in Maharashtra. *Journal of Earth System Science*, 122: 639-649.

Hachigonta, S., Reason, C.J.C. and Tadross, M. (2008). An analysis of onset date and rainy season duration over Zambia. *Theoretical and Applied Climatology*, 91: 229-243.

Hahn, A., Schefuß, E., Andò, S., Cawthra, H.C., Frenzel, P., Kugel, M., Meschner, S., Mollenhauer, G. and Zabel, M. (2017). Southern Hemisphere anticyclonic circulation drives oceanic and climatic conditions in late Holocene southernmost Africa. *Climate of the Past*, 13: 649-665.

Hannaford, M.J., Jones, J.M. and Bigg, G.R. (2015). Early-nineteenth-century southern African precipitation reconstructions from ships' logbooks. *The Holocene*, 25: 379-390.

Hare, F.K. (1983). *Climate and Desertification: a revised analysis.* World Climate Program Report No. 44: Geneva, Switzerland.

Harrison, M.S.J. (1984). A generalized classification of South African summer rain-bearing synoptic systems, *Journal of Climatology*, 4: 547-560.

Harrison, M. S. J. (1986). A synoptic climatology of South African rainfall variations. *PhD Thesis submitted to the University of the Witwatersrand.*

Harrison, A. and Petersen, T. (2017). *Land of Thirst: Voices from the drought-stricken Central Karoo*. Available at: https://landofthirst.news24.com/ (Accessed: 24 June 2019).

Hart, N.C.G., Reason, C.J.C. and Fauchereau, N. (2010). Tropical–extratropical interactions over southern Africa: Three cases of heavy summer season rainfall. *Monthly Weather Review*, 138: 2608-2623.

Hart, N.C., Reason, C.J. and Fauchereau, N. (2013). Cloud bands over southern Africa: seasonality, contribution to rainfall variability and modulation by the MJO. *Climate Dynamics*, 41: 1199-1212.

Hattie, J. and Cooksey, R.W. (1984). Procedures for assessing the validities of tests using the "known-groups" method. *Applied Psychological Measurement*, 8: 295-305.

Heine, K. (1982). The main stages of the late Quaternary evolution of the Kalahari region, southern Africa. *Palaeoecology of Africa*, 15: 53-76.

Herbert, A.V. and Harrison, S.P. (2016). Evaluation of a modern-analogue methodology for reconstructing Australian palaeoclimate from pollen. *Review of Palaeobotany and Palynology*, 226: 65-77.

Herrmann, S.M. and Mohr, K.I. (2011). A continental-scale classification of rainfall seasonality regimes in Africa based on gridded precipitation and land surface temperature products. *Journal of Applied Meteorology and Climatology*, 50: 2504-2513.

Hewitson, B.C. and Crane, R.G. (2006). Consensus between GCM climate change projections with empirical downscaling: precipitation downscaling over South Africa. *International Journal of Climatology*, 26: 1315-1337.

Hijmans, R.J., Cameron, S.E., Parra, J.L., Jones, P.G. and Jarvis, A. (2005). Very high resolution interpolated climate surfaces for global land areas. *International Journal of Climatology*, 25: 1965-1978.

Hoerling, M., Hurrell, J., Eischeid, J. and Phillips, A. (2006). Detection and attribution of twentieth-century northern and southern African rainfall change. *Journal of Climate*, 19: 3989-4008.

Hu, Y., Wang, S., Yang, X., Kang, Y., Ning, G. and Du, H. (2019). Impact of winter droughts on air pollution over Southwest China. *Science of The Total Environment*, 664: 724-736.

Huang, J., Islam, A.T., Zhang, F. and Hu, Z. (2017). Spatiotemporal analysis the precipitation extremes affecting rice yield in Jiangsu province, southeast China. *International journal of Biometeorology*, 61: 1863-1872.

Huang, Y., Wang, H., Xiao, W., Chen, L.H., Yan, D.H., Zhou, Y.Y., Jiang, D.C. and Yang, M.Z. (2018). Spatial and Temporal Variability in the Precipitation Concentration in the Upper Reaches of the Hongshui River Basin, Southwestern China. *Advances in Meteorology*, 2018. DOI: 10.1155/2018/4329757.

Hulme, M. (1992). Rainfall changes in Africa: 1931–1960 to 1961–1990. *International Journal of Climatology*, 12: 685-699.

Husak, G.J., Funk, C.C., Michaelsen, J., Magadzire, T. and Goldsberry, K.P. (2013). Developing seasonal rainfall scenarios for food security early warning. *Theoretical and Applied Climatology*, 114: 291-302.

Ilesanmi, O.O. (1972a). An empirical formulation of the onset, advance and retreat of rainfall in Nigeria. *Journal of Tropical Geography*, 34: 17-24.

Ilesanmi, O.O. (1972b). Aspect of the precipitation climatology of the July August rainfall minimum of Southern Nigeria. *Journal of Tropical Geography*, 35: 51-59.

IPCC (2007). *Climate Change 2007: The Physical Science Basis*. Cambridge University Press: Cambridge.

IPCC (2013). *IPCC Fifth Assessment Report: The Physical Science Basis.* Cambridge University Press: Cambridge.

IPCC (2018). *IPCC Special Report: Global Warming of 1.5°C*. World Meteorological Organization: Switzerland.

Johanson, C.M. and Fu, Q. (2009). Hadley cell widening: Model simulations versus observations. *Journal of Climate*, 22: 2713-2725.

Jones, P.D., Briffa, K.R., Osborn, T.J., Lough, J.M., Van Ommen, T.D., Vinther, B.M., Luterbacher, J.W.E.R.Z.F.W., Wahl, E.R., Zwiers, F.W., Mann, M.E. and Schmidt, G.A. (2009). High-resolution palaeoclimatology of the last millennium: a review of current status and future prospects. *The Holocene*, 19: 3-49.

Jury, M.R. (2013). Climate trends in southern Africa. *South African Journal of Science*, 109. DOI: 10.1590/sajs.2013/980.

Jury, M.R. (2018). Climate trends across South Africa since 1980. *Water SA*, 44: 297-307.

Jury, M.R. and Levey, K. (1993). The climatology and characteristics of drought in the Eastern Cape of South Africa. *International Journal of Climatology*, 13: 629-641.

Kabanda, T. and Nenwiini, S. (2016). Impacts of climate variation on the length of the rainfall season: an analysis of spatial patterns in North-East South Africa. *Theoretical and Applied Climatology*, 125: 93-100.

Kahinda, J.M., Lillie, E.S.B., Taigbenu, A.E., Taute, M. and Boroto, R.J. (2008). Developing suitability maps for rainwater harvesting in South Africa. *Physics and Chemistry of the Earth,* 33: 788-799.

Kahla, C. (2019). *Johannesburg weather: Severe thunderstorms and heavy downpours expected*. Available at: https://www.thesouthafrican.com/weathersa/johannesburg-weather-thunderstorms-downpours-localised-flooding/ (Accessed: 24 June 2019).

Kane, R.P. (2009). Periodicities, ENSO effects and trends of some South African rainfall series: an update. *South African Journal of Science*, 105: 199-207.

Kassambara, A. (2017). *Practical guide to cluster analysis in R: unsupervised machine learning*. STHDA.

Kaufman, L. and Rousseeuw, P.J. (2009). *Finding groups in data: an introduction to cluster analysis*. John Wiley & Sons: Hoboken.

Keen, C. S. (1971). Rainfall spectra and the delimitation of rainfall regimes in South Africa. *MSc dissertation submitted to the University of the Witwatersrand*.

Keen, C.S. and Tyson, P.D. (1973). Seasonality of South African rainfall: a note on its regional delimitation using spectral analysis. *Archiv für Meteorologie, Geophysik und Bioklimatologie, Serie B*, 21: 207-214.

Kelso, C. and Vogel, C. (2007). The climate of Namaqualand in the nineteenth century. *Climatic Change*, 83: 357-380.

King, J., Mitchell, S. and Pienaar, H. (2011). Water supply and demand. In King, J. and Pienaar, H. (eds.). *Sustainable use of South Africa's inland waters*. Water Research Commission: Pretoria.

Kisaka, M.O., Mucheru-Muna, M., Ngetich, F.K., Mugwe, J.N., Mugendi, D. and Mairura, F. (2015). Rainfall variability, drought characterization, and efficacy of rainfall data reconstruction: case of Eastern Kenya. *Advances in Meteorology*, 2015. DOI: 10.1155/2015/380404.

Knight, J. (2019). Water Resources in South Africa. In Knight, J. and Rogerson, C.M. (eds.). *The Geography of South Africa*. Springer: Switzerland.

Knight, J. and Holmes, P.J. (2018). Southern African drylands and their unique challenges. In Holmes, P.J. and Boardman, J. (eds.). *Southern African Landscapes and Environmental Change*. Routledge: Oxon.

Knight, J. and Fitchett, J.M. (2019). Climate Change during the late Quaternary in South Africa. In Knight, J. and Rogerson, C.M. (eds.). *The Geography of South Africa*. Springer: Switzerland.

Kniveton, D.R., Layberry, R., Williams, C.J.R. and Peck, M. (2009). Trends in the start of the wet season over Africa. *International Journal of Climatology*, 29: 1216-1225.

Kraaij, T., Baard, J.A., Arndt, J., Vhengani, L. and van Wilgen, B.W. (2018). An assessment of climate, weather, and fuel factors influencing a large, destructive wildfire in the Knysna region, South Africa. *Fire Ecology*, 14. DOI: 10.1186/s42408-018-0001-0.

Kruger, A.C. (2006). Observed trends in daily precipitation indices in South Africa: 1910–2004. *International Journal of Climatology*, 26: 2275-2285.

Kruger, A.C. and Nxumalo, M.P. (2017). Historical rainfall trends in South Africa: 1921–2015. *Water SA*, 43: 285-297.

Kuhlmann, M., Guo, D., Veldtman, R. and Donaldson, J. (2012). Consequences of warming up a hotspot: species range shifts within a centre of bee diversity. *Diversity and Distributions*, 18: 885-897.

Kumi, N. and Abiodun, B.J. (2018). Potential impacts of 1.5° C and 2° C global warming on rainfall onset, cessation and length of rainy season in West Africa. *Environmental Research Letters*, 13. DOI: 10.1088/1748-9326/aab89e.

Kusangaya, S., Warburton, M.L., Van Garderen, E.A. and Jewitt, G.P. (2014). Impacts of climate change on water resources in southern Africa: A review. *Physics and Chemistry of the Earth,* 67: 47-54.

Lakhraj-Govender, R. (2017). An assessment of temperature variability over South Africa. *PhD Thesis submitted to the University of the Witwatersrand.*

Lana, X., Martínez, M.D., Serra, C. and Burgueno, A. (2004). Spatial and temporal variability of the daily rainfall regime in Catalonia (northeastern Spain), 1950–2000. *International Journal of Climatology*, 24: 613-641.

Landman, W.A., Malherbe, J. and Engelbrecht, F. (2017). South Africa's present-day climate. In Mambo, J. and Faccer, K. (eds.). *Understanding the Social and Environmental Implications of Global Change*. Africa Sun Media: Stellenbosch.

Le Roux, K. (2015). *Analysis in variability of summer rainfall for Gauteng from 1985 to 2015*. Honours Research Project. University of the Witwatersrand, Johannesburg.

Lee, S. and Kim, S.U. (2016). Comparison between change point detection methods with synthetic rainfall data and application in South Korea. *KSCE Journal of Civil Engineering*, 20: 1558-1571.

Lee-Thorp, A.M., Rouault, M. and Lutjeharms, J.R.E. (1999). Moisture uptake in the boundary layer above the Agulhas Current: A case study. *Journal of Geophysical Research: Oceans*, 104: 1423-1430.

Lennard, C. (2019). Multi-Scale Drivers of the South African Weather and Climate. In Knight, J. and Rogerson, C.M. (eds.). *The Geography of South Africa*. Springer: Switzerland.

Lennard, C. and Hegerl, G. (2015). Relating changes in synoptic circulation to the surface rainfall response using self-organising maps. *Climate Dynamics*, 44: 861-879.

Lepage, D. and Lloyd, P. (2004). Avian clutch size in relation to rainfall seasonality and stochasticity along an aridity gradient across South Africa. *Ostrich-Journal of African Ornithology*, 75: 259-268.

Leung, J.K. and Law, T.C. (2002). Kriging analysis on Hong Kong rainfall data. *HKIE Transactions*, 9: 26-31.

Leung, L.R. and Gustafson Jr, W.I. (2005). Potential regional climate change and implications to US air quality. *Geophysical Research Letters*, 32. DOI: 10.1029/2005GL022911.

Li, W., Fu, R. and Dickinson, R.E. (2006). Rainfall and its seasonality over the Amazon in the 21st century as assessed by the coupled models for the IPCC AR4. *Journal of Geophysical Research: Atmospheres*, 111. DOI: 10.1029/2005JD006355.

Li, X., Jiang, F., Li, L. and Wang, G. (2011). Spatial and temporal variability of precipitation concentration index, concentration degree and concentration period in Xinjiang, China. *International Journal of Climatology*, 31: 1679-1693.

Li, J. and Heap, A.D. (2014). Spatial interpolation methods applied in the environmental sciences: A review. *Environmental Modelling & Software*, 53, 173-189.

Li, X., Hu, Z.Z., Jiang, X., Li, Y., Gao, Z., Yang, S., Zhu, J. and Jha, B. (2016). Trend and seasonality of land precipitation in observations and CMIP5 model simulations. *International Journal of Climatology*, 36: 3781-3793.

Liebmann, B., Bladé, I., Kiladis, G.N., Carvalho, L.M., B. Senay, G., Allured, D., Leroux, S. and Funk, C. (2012). Seasonality of African precipitation from 1996 to 2009. *Journal of Climate*, 25: 4304-4322.

Lim, S., Chase, B.M., Chevalier, M. and Reimer, P.J. (2016). 50,000 years of vegetation and climate change in the southern Namib Desert, Pella, South Africa. *Palaeogeography, palaeoclimatology, palaeoecology*, 451: 197-209.

Lin, F.R., Wu, N.J. and Tsay, T.K. (2017). Applications of cluster analysis and pattern recognition for typhoon hourly rainfall forecast. *Advances in Meteorology*, 2017. DOI: 10.1155/2017/5019646.

Lindesay, J.A. (1988). South African rainfall, the Southern Oscillation and a Southern Hemisphere semi-annual cycle. *Journal of Climatology*, 8: 17-30.

Lindesay, J.A. and Jury, M.R. (1991). Atmospheric circulation controls and characteristics of a flood event in central South Africa. *Internationa Jjournal of Climatology*, 11: 609-627.

Lipsett, A.S. (2017). Spatio-temporal effects of rainfall on stream/river flow in the Kruger National Park, South Africa. *MSc Dissertation submitted to University of the Witwatersrand.*

Livada, I. and Asimakopoulos, D.N. (2005). Individual seasonality index of rainfall regimes in Greece. *Climate Research*, 28: 155-161.

Lötter, D. (2012). An overview of Agriculture in South Africa. In DEA. (eds.). *South African Risk and Vulnerability Atlas*. Government Printer: Pretoria.

Lötter, D. (2017). Risk and vulnerability in the South African farming sector: Implications for sustainable agriculture and food security. In Mambo, J. and Faccer, K. (eds.). *Understanding the Social and Environmental Implications of Global Change*. Africa Sun Media: Stellenbosch.

Lu, J., Vecchi, G.A. and Reichler, T. (2007). Expansion of the Hadley cell under global warming. *Geophysical Research Letters*, 34. DOI: 10.1029/2006GL028443.

Lumsden, T.G. (2009). Evaluation of potential changes in hydrologically relevant statistics of rainfall in Southern Africa under conditions of climate change. *Water SA*, 35: 649-656.

Luo, X. and Zhang, Y. (2015). Interdecadal change in the seasonality of rainfall variation in South China. *Theoretical and Applied Climatology*, 119. DOI: 10.1007/s00704-013-1088-5.

Ly, S., Charles, C. and Degre, A. (2011). Geostatistical interpolation of daily rainfall at catchment scale: the use of several variogram models in the Ourthe and Ambleve catchments, Belgium. *Hydrology and Earth System Sciences*, 15: 2259-2274.

Lynch, S.D. (2004). *The development of a raster database of annual, monthly and daily rainfall for Southern Africa WRC Report 1156/1/04.* Water Research Commission: Pretoria.

Lynch, S.D., Zulu, J.T., King, K.N. and Knoesen, D.M. (2001). The analysis of 74 years of rainfall recorded by the Irwins on two farms south of Potchefstroom. *Water SA*, 27: 559-564.

Lyra, G.B., Oliveira-Júnior, J.F. and Zeri, M. (2014). Cluster analysis applied to the spatial and temporal variability of monthly rainfall in Alagoas state, Northeast of Brazil. *International Journal of Climatology*, 34: 3546-3558.

Ma, S. and Zhou, T. (2015). Observed trends in the timing of wet and dry season in China and the associated changes in frequency and duration of daily precipitation. *International Journal of Climatology*, 35: 4631-4641.

MacFadyen, S., Zambatis, N., Van Teeffelen, A.J. and Hui, C. (2018). Long-term rainfall regression surfaces for the Kruger National Park, South Africa: a spatio-temporal review of patterns from 1981 to 2015. *International Journal of Climatology*, 38: 2506-2519.

MacKellar, N.C., Hewitson, B.C. and Tadross, M.A. (2007). Namaqualand's climate: recent historical changes and future scenarios. *Journal of Arid Environments*, 70: 604-614.

MacKellar, N., New, M. and Jack, C. (2014). Observed and modelled trends in rainfall and temperature for South Africa: 1960-2010. *South African Journal of Science*, 110. DOI: 10.1590/ sajs.2014/20130353.

Macron, C., Pohl, B., Richard, Y. and Bessafi, M. (2014). How do tropical temperate troughs form and develop over southern Africa?. *Journal of Climate*, 27: 1633-1647.

Mahlalela, P.T., Blamey, R.C. and Reason, C.J.C. (2018). Mechanisms behind early winter rainfall variability in the southwestern Cape, South Africa. *Climate Dynamics*, 53: 21-39.

Mahlobo, D.D., Ndarana, T., Grab, S. and Engelbrecht, F. (2019). Integrated climatology and trends in the subtropical Hadley cell, sunshine duration and cloud cover over South Africa. *International Journal of Climatology*, 39: 1805-1821.

Malherbe, J., Engelbrecht, F.A., Landman, W.A. and Engelbrecht, C.J. (2012). Tropical systems from the southwest Indian Ocean making landfall over the Limpopo River Basin, southern Africa: a historical perspective. *International Journal of Climatology*, 32: 1018-1032.

Manly, B. (2009). *Statistics for environmental science and management*. Chapman & Hall: Florida.

Maraschin, N.M.R. (2016). Faunal distribution in relation to rainfall patterns in the Kalahari Gemsbok National Park. *MSc Dissertation submitted to the University of the Witwatersrand.*

Markham, C. G. (1970). Seasonality of precipitation in the United States. *Annals of the Association of American Geographers*, 60: 593–597.

Marteau, R., Sultan, B., Moron, V., Alhassane, A., Baron, C. and Traoré, S.B. (2011). The onset of the rainy season and farmers' sowing strategy for pearl millet cultivation in Southwest Niger. *Agricultural and Forest Meteorology*, 151: 1356-1369.

Martin-Vide, J. (2004). Spatial distribution of a daily precipitation concentration index in peninsular Spain. *International Journal of Climatology*, 24: 959-971.

Mason, S.J., Waylen, P.R., Mimmack, G.M., Rajaratnam, B. and Harrison, J.M. (1999). Changes in extreme rainfall events in South Africa. *Climatic Change*, 41: 249-257.

Mathbout, S. (2015). Spatial and temporal characteristics of precipitation variability and drought patterns in the eastern Mediterranean. *PhD Thesis submitted to the Universitat de Barcelona*.

Mazvimavi, D., (2010). Investigating changes over time of annual rainfall in Zimbabwe. *Hydrology and Earth System Sciences*, 14: 2671-2679.

McCune, B., Grace, J.B. and Urban, D.L., (2002). *Analysis of ecological communities.* MjM Software Design: Oregon.

McGee, O. S. (1977). The determination of rainfall seasons in South Africa using Markham's technique. *South African Geographer*, 5: 390–396.

Meseguer-Ruiz, O., Ponce-Philimon, P.I., Guijarro, J.A. and Sarricolea, P. (2019). Spatial distribution and trends of different precipitation variability indices based on daily data in Northern Chile between 1966 and 2015. *International Journal of Climatology*. DOI: 10.1002/joc.6089.

Mills, S., Grab, S., Rea, B., Carr, S. and Farrow, A. (2012). Shifting Westerlies and precipitation patterns during the Late Pleistocene in southern Africa determined using glacier reconstruction and mass balance modelling. *Quaternary Science Reviews,* 55: 145-159.

Moeletsi, M.E., Walker, S. and Landman, W.A. (2011). ENSO and implications on rainfall characteristics with reference to maize production in the Free State Province of South Africa. *Physics and Chemistry of the Earth, Parts A/B/C*, 36: 715-726.

Moeletsi, M.E. and Walker, S. (2012). Rainy season characteristics of the Free State Province of South Africa with reference to rain-fed maize production. *Water SA*, 38: 775-782.

Moeletsi, M.E., Moopisa, S.G., Walker, S. and Tsubo, M. (2013). Development of an agroclimatological risk tool for dryland maize production in the Free State Province of South Africa. *Computers and Electronics in Agriculture*, 95: 108-121.

Mphale, K.M., Dash, S.K., Adedoyin, A. and Panda, S.K. (2014). Rainfall regime changes and trends in Botswana Kalahari Transect's late summer precipitation. *Theoretical and Applied Climatology*, 116: 75-91.

Mukheibir, P. (2008). Water resources management strategies for adaptation to climate-induced impacts in South Africa. *Water Resources Management*, 22: 1259-1276.

Munday, C. and Washington, R. (2017). Circulation controls on southern African precipitation in coupled models: The role of the Angola Low. *Journal of Geophysical Research: Atmospheres*, 122: 861-877.

Munday, C. and Washington, R. (2018). Systematic climate model rainfall biases over southern Africa: links to moisture circulation and topography. *Journal of Climate*, 31: 7533-7548.

Mupangwa, W., Walker, S. and Twomlow, S. (2011). Start, end and dry spells of the growing season in semi-arid southern Zimbabwe. *Journal of Arid Environments*, 75: 1097-1104.

Naidoo, R. (2016). A glimpse at the 17th Century Cape Climate of Southern Africa: Documentary Based Evidence from the Jan Van Riebeeck diaries. *MSc Dissertation submitted to the University of the Witwatersrand*.

Nair, A., Joseph, K.A. and Nair, K.S. (2014). Spatio-temporal analysis of rainfall trends over a maritime state (Kerala) of India during the last 100 years. *Atmospheric Environment*, 88: 123-132.

Nandargi, S. and Mulye, S.S. (2012). Relationships between rainy days, mean daily intensity, and seasonal rainfall over the Koyna Catchment during 1961–2005. *The Scientific World Journal*, 2012: 1-10.

Nash, D.J. (2017). Changes in precipitation over southern Africa during recent centuries. *Oxford Research Encyclopedia of Climate Science*. DOI: 10.1093/acrefore/9780190228620.013.539.

Nash, D.J., Pribyl, K., Klein, J., Neukom, R., Endfield, G.H., Adamson, G.C.D. and Kniveton, D.R. (2016). Seasonal rainfall variability in southeast Africa during the nineteenth century reconstructed from documentary sources. *Climatic Change*, 134: 605–619.

Ndarana, T., Bopape, M.J., Waugh, D. and Dyson, L. (2018). The Influence of the Lower Stratosphere on Ridging Atlantic Ocean Anticyclones over South Africa. *Journal of Climate*, 31: 6175-6187.

Nel, W. (2007). On the climate of the Drakensberg: rainfall and surface-temperature attributes, and associated geomorphic effects. *PhD Thesis submitted to the University of Pretoria*.

Nel, W. (2009). Rainfall trends in the KwaZulu-Natal Drakensberg region of South Africa during the twentieth century. *International Journal of Climatology*, 29: 1634-1641.

Neumann, F.H., Botha, G.A. and Scott, L. (2014). 18,000 years of grassland evolution in the summer rainfall region of South Africa: evidence from Mahwaqa Mountain, KwaZulu-Natal. *Vegetation History and Archaeobotany*, 23: 665-681.

Neumann, F.H. and Scott, L. (2018). EM van Zinderen Bakker (1907–2002) and the study of African Quaternary palaeoenvironments. *Quaternary International*, 495: 153-168.

New, M., Hewitson, B., Stephenson, D.B., Tsiga, A., Kruger, A., Manhique, A., Gomez, B., Coelho, C.A., Masisi, D.N., Kululanga, E. and Mbambalala, E. (2006). Evidence of trends in daily climate extremes over southern and west Africa. *Journal of Geophysical Research: Atmospheres*, 111. DOI: 10.1029/2005JD006289.

Ngetich, K.F., Mucheru-Muna, M., Mugwe, J.N., Shisanya, C.A., Diels, J. and Mugendi, D.N. (2014). Length of growing season, rainfall temporal distribution, onset and cessation dates in the Kenyan highlands. *Agricultural and Forest Meteorology*, 188: 24-32.

Nguyen, H., Evans, A., Lucas, C., Smith, I. and Timbal, B. (2013). The Hadley circulation in reanalyses: Climatology, variability, and change. *Journal of Climate*, 26: 3357-3376.

Nguyen, H., Lucas, C., Evans, A., Timbal, B. and Hanson, L. (2015). Expansion of the Southern Hemisphere Hadley cell in response to greenhouse gas forcing. *Journal of Climate*, 28: 8067-8077.

Nicholson, S.E. (2000). The nature of rainfall variability over Africa on time scales of decades to millenia. *Global and Planetary Change*, 26: 137-158.

Nicholson, S.E. (2018). The ITCZ and the seasonal cycle over equatorial Africa. *Bulletin of the American Meteorological Society*, 99: 337-348.

Nicholson, S.E., Funk, C. and Fink, A.H. (2018). Rainfall over the African continent from the 19th through the 21st century. *Global and Planetary Change*, 165: 114-127.

NOAA. (2018). *The Seasons, the Equinox, and the Solstices*. Available at: https://www.weather.gov/cle/seasons (Accessed: 19 March 2019).

Norström, E., Neumann, F.H., Scott, L., Smittenberg, R.H., Holmstrand, H., Lundqvist, S., Snowball, I., Sundqvist, H.S., Risberg, J. and Bamford, M. (2014). Late Quaternary vegetation dynamics and hydro-climate in the Drakensberg, South Africa. *Quaternary Science Reviews*, 105: 48-65.

Norström, E., Scott, L., Partridge, T.C., Risberg, J. and Holmgren, K. (2009). Reconstruction of environmental and climate changes at Braamhoek wetland, eastern escarpment South Africa, during the last 16,000 years with emphasis on the Pleistocene–Holocene transition. *Palaeogeography, Palaeoclimatology, Palaeoecology*, 271: 240-258.

Obroślak, R. and Dorozhynskyy, O. (2017). Selection of a semivariogram model in the study of spatial distribution of soil moisture. *Journal of Water and Land Development*, 35: 161-166.

Odekunle, T.O. (2004). Rainfall and the length of the growing season in Nigeria. *International Journal of Climatology*, 24: 467-479.

Odekunle, T.O. (2006). Determining rainy season onset and retreat over Nigeria from precipitation amount and number of rainy days. *Theoretical and Applied Climatology*, 83: 193-201.

Odekunle, T.O., Balogun, E.E. and Ogunkoya, O.O. (2005). On the prediction of rainfall onset and retreat dates in Nigeria. *Theoretical and Applied Climatology*, 81: 101-112.

Odekunle, T.O. and Adejuwon, S.A. (2007). Assessing changes in the rainfall regime in Nigeria between 1961 and 2004. *GeoJournal*, 70: 145-159.

Oladipo, E.O. and Kyari, J.D. (1993). Fluctuations in the onset, termination and length of the growing season in Northern Nigeria. *Theoretical and Applied Climatology*, 47: 241-250.

Oliver, J. E. (1980). Monthly precipitation distribution: A comparative index. *The Professional Geographer*: 32: 300–309.

Oliver, J. (1984). Delimitation and analysis of homogeneous rainfall regions in the south-eastern Transvaal. *MSc Dissertation submitted Rand Afrikaans University*.

Omondi, S.F., Odee, D.W, Ongamo, G.O., Kanya, J.I. and Khasa, D.P. (2016). Synchrony in leafing, flowering, and fruiting phenology of Senegalia Senegal within Lake Baringo woodland, Kenya: Implication for conservation and tree improvement. *International Journal of Forestry Research*, 2016. DOI: 10.1155/2016/6904834.

Pal, I., Anderson, B.T., Salvucci, G.D. and Gianotti, D.J. (2013). Shifting seasonality and increasing frequency of precipitation in wet and dry seasons across the US. *Geophysical Research Letters*, 40, 4030-4035.

Palaniswami, S. and Muthiah, K. (2018). Change Point Detection and Trend Analysis of Rainfall and Temperature Series over the Vellar River Basin. *Polish Journal of Environmental Studies*, 27: 1673-1681.

Parkington, J., Cartwright, C., Cowling, R.M. and Baxter, A. (2000). Africa: wood charcoal and pollen TS evidence from Elands Bay Cave. *South African Journal of Science*, 96: 543-546.

Pascale, S., Lucarini, V., Feng, X., Porporato, A. and ul Hasson, S. (2015). Analysis of rainfall seasonality from observations and climate models. *Climate Dynamics*, 44: 3281-3301.

Pascale, S., Lucarini, V., Feng, X., Porporato, A. and ul Hasson, S. (2016). Projected changes of rainfall seasonality and dry spells in a high greenhouse gas emissions scenario. *Climate Dynamics*, 46: 1331-1350.

Pettitt, A. (1979). A non-parametric approach to the change-point problem. *Applied Statistics*, 28, 126-135.

Picas, J., Grab, S. and Allan, R. (2019). A 19th century daily surface pressure series for the Southwestern Cape region of South Africa: 1834–1899. *International Journal of Climatology*, 39: 1404-1414.

Phakula, S., Landman, W.A. and Beraki, A.F. (2018). Forecasting seasonal rainfall characteristics and onset months over South Africa. *International Journal of Climatology*, 38: 889-900.

Philippon, N., Rouault, M., Richard, Y. and Favre, A. (2012). The influence of ENSO on winter rainfall in South Africa. *International Journal of Climatology*, 32: 2333-2347.

Pohl, B., Richard, Y. and Fauchereau, N. (2007). Influence of the Madden–Julian oscillation on southern African summer rainfall. *Journal of Climate*, 20: 4227-4242.

Pohl, B., Fauchereau, N., Reason, C.J.C. and Rouault, M. (2010). Relationships between the Antarctic Oscillation, the Madden–Julian Oscillation, and ENSO, and consequences for rainfall analysis. *Journal of Climate*, 23: 238-254.

Pohl, B., Macron, C. and Monerie, P.A. (2017). Fewer rainy days and more extreme rainfall by the end of the century in Southern Africa. *Scientific Reports*, 7. DOI: 10.1038/srep46466.

Pohl, B., Dieppois, B., Crétat, J., Lawler, D. and Rouault, M. (2018). From synoptic to interdecadal variability in Southern African rainfall: toward a unified view across time scales. *Journal of Climate*, 31: 5845-5872.

Polson, D., Hegerl, G.C., Zhang, X. and Osborn, T.J. (2013). Causes of robust seasonal land precipitation changes. *Journal of Climate*, 26: 6679-6697.

Prevéy, J.S. and Seastedt, T.R. (2014). Seasonality of precipitation interacts with exotic species to alter composition and phenology of a semi-arid grassland. *Journal of Ecology*, 102: 1549-1561.

Prinsloo, A.S. (2019). A case study of resource consumption in the sharing economy: Airbnb as tourist accommodation in Cape Town, South Africa. *MSc Dissertation submitted to the University of the Witwatersrand*.

Pryor, S.C. and Schoof, J.T. (2008). Changes in the seasonality of precipitation over the contiguous USA. *Journal of Geophysical Research: Atmospheres*, 113. DOI: 10.1029/2008JD010251.

Quick, L.J., Chase, B.M., Wündsch, M., Kirsten, K.L., Chevalier, M., Mäusbacher, R., Meadows, M.E. and Haberzettl, T. (2018). A high-resolution record of Holocene climate and vegetation dynamics from the southern Cape coast of South Africa: pollen and microcharcoal evidence from Eilandvlei. *Journal of Quaternary Science*, 33: 487-500.

Raes, D., Sithole, A., Makarau, A. and Milford, J. (2004). Evaluation of first planting dates recommended by criteria currently used in Zimbabwe. *Agricultural and Forest Meteorology*, 125: 177-185.

Rahmani, V., Hutchinson, S.L., Harrington Jr, J.A., Hutchinson, J.S. and Anandhi, A. (2015). Analysis of temporal and spatial distribution and change-points for annual precipitation in Kansas, USA. *International Journal of Climatology*, 35: 3879-3887.

Rajah, K., O'Leary, T., Turner, A., Petrakis, G., Leonard, M. and Westra, S. (2014). Changes to the temporal distribution of daily precipitation. *Geophysical Research Letters*, 41: 8887-8894.

Rana, S., McGregor, J. and Renwick, J. (2015). Precipitation seasonality over the Indian subcontinent: An evaluation of gauge, reanalyses, and satellite retrievals. *Journal of Hydrometeorology*, 16: 631-651.

Ratna, S.B., Behera, S., Ratnam, J.V., Takahashi, K. and Yamagata, T. (2013). An index for tropical temperate troughs over southern Africa. *Climate Dynamics*, 41: 421-441.

Ratnam, J.V., Doi, T., Landman, W.A. and Behera, S.K. (2018). Seasonal Forecasting of Onset of Summer Rains over South Africa. *Journal of Applied Meteorology and Climatology*, 57: 2697-2711.

Rau, P., Bourrel, L., Labat, D., Melo, P., Dewitte, B., Frappart, F., Lavado, W. and Felipe, O. (2017). Regionalization of rainfall over the Peruvian Pacific slope and coast. *International Journal of Climatology*, 37: 143-158.

Rauscher, S.A., Seth, A., Liebmann, B., Qian, J.H. and Camargo, S.J. (2007). Regional climate model–simulated timing and character of seasonal rains in South America. *Monthly weather review*, 135: 2642-2657.

Raziei, T. (2017). An analysis of daily and monthly precipitation seasonality and regimes in Iran and the associated changes in 1951–2014. *Theoretical and Applied Climatology*, 134: 913-934.

Raziei, T. (2018). A precipitation regionalization and regime for Iran based on multivariate analysis. *Theoretical and Applied Climatology*, 131: 1429-1448.

Reason, C.J.C. (2001). Subtropical Indian Ocean SST dipole events and southern African rainfall. *Geophysical Research Letters*, 28: 2225-2227.

Reason, C.J.C. (2002). Sensitivity of the southern African circulation to dipole sea-surface temperature patterns in the south Indian Ocean. *International Journal of Climatology*, 22: 377-393.

Reason, C.J.C. and Jury, M.R. (1990). On the generation and propagation of the southern African coastal low. *Quarterly Journal of the Royal Meteorological Society*, 116: 1133-1151.

Reason, C.J.C., Rouault, M., Melice, J.L. and Jagadheesha, D. (2002). Interannual winter rainfall variability in SW South Africa and large scale ocean–atmosphere interactions. *Meteorology and Atmospheric Physics*, 80: 19-29.

Reason, C.J.C., Hachigonta, S. and Phaladi, R.F. (2005). Interannual variability in rainy season characteristics over the Limpopo region of southern Africa. *International Journal of Climatology*, 25: 1835-1853.

Reason, C.J.C. and Jagadheesha, D. (2005). Relationships between South Atlantic SST variability and atmospheric circulation over the South African region during austral winter. *Journal of Climate*, 18: 3339-3355.

Reason, C.J.C. and Rouault, M. (2005). Links between the Antarctic Oscillation and winter rainfall over western South Africa. *Geophysical research letters*, 32. DOI: 10.1029/2005GL022419.

Reason, C.J.C. and Smart, S. (2015). Tropical south east Atlantic warm events and associated rainfall anomalies over southern Africa. *Frontiers in Environmental Science*, 4. DOI: 10.3389/fenvs.2015.00024.

Recha, C.W., Makokha, G.L., Traore, P.S., Shisanya, C., Lodoun, T. and Sako, A. (2012). Determination of seasonal rainfall variability, onset and cessation in semi-arid Tharaka district, Kenya. *Theoretical and Applied Climatology*, 108: 479-494.

Richard, Y., Fauchereau, N., Poccard, I., Rouault, M. and Trzaska, S. (2001). 20th century droughts in southern Africa: spatial and temporal variability, teleconnections with oceanic and atmospheric conditions. *International Journal of Climatology*, 21: 873-885.

Robinson, D.C. (2016). Exploring the value of tourism climate indices for 18 locations in South Africa. *MSc Dissertation submitted to the University of the Witwatersrand*.

Roffe, S.J., Fitchett, J.M. and Curtis, C.J. (2019). Classifying and mapping rainfall seasonality in South Africa: a review. *South African Geographical Journal*, 101, 158-174.

Rouault, M., White, S.A., Reason, C.J.C., Lutjeharms, J.R.E. and Jobard, I. (2002). Ocean–atmosphere interaction in the Agulhas Current region and a South African extreme weather event. *Weather and Forecasting*, 17: 655-669.

Rouault, M. and Richard, Y. (2003). Intensity and spatial extension of drought in South Africa at different time scales. *Water SA*, 29: 489-500.

Roy, S.S. and Rouault, M. (2013). Spatial patterns of seasonal scale trends in extreme hourly precipitation in South Africa. *Applied Geography*, 39: 151-157.

Rutherford, M.C., Mucina, L. and Powrie, L. (2006). Biomes and Bioregions of Southern Africa. In Muncina, L. and Rutherford, M.C. (eds.) *The Vegetation of South Africa, Lesotho and Swaziland*. South African National Biodiversity Institute: Pretoria.

Sahany, S., Mishra, S.K., Pathak, R. and Rajagopalan, B. (2018). Spatiotemporal Variability of Seasonality of Rainfall over India. *Geophysical Research Letters*, 45: 7140-7147.

Salhi, A., Martin-Vide, J., Benhamrouche, A., Benabdelouahab, S., Himi, M., Benabdelouahab, T. and Ponsati, A.C. (2019). Rainfall distribution and trends of the daily precipitation concentration index in northern Morocco: a need for an adaptive environmental policy. *SN Applied Sciences*, 1. DOI: 10.1007/s42452-019-0290-1.

Sangüesa, C., Pizarro, R., Ibañez, A., Pino, J., Rivera, D., García-Chevesich, P. and Ingram, B. (2018). Spatial and temporal analysis of rainfall concentration using the Gini index and PCI. *MDPI Water*, 10. DOI: 10.3390/w10020112.

Saraçli, S., Doğan, N. and Doğan, İ. (2013). Comparison of hierarchical cluster analysis methods by cophenetic correlation. *Journal of Inequalities and Applications*, 2013. DOI: 10.1186/1029-242X-2013-203.

Sarricolea, P., Meseguer-Ruiz, Ó., Serrano-Notivoli, R., Soto, M.V. and Martin-Vide, J. (2019). Trends of daily precipitation concentration in Central-Southern Chile. *Atmospheric Research*, 215: 85-98.

SAWB. (1949). *District rainfall for the union of South Africa (W.B. 6)*. Government Printer: Pretoria.

SAWB. (1957). *Climate of South Africa Part 4 Rainfall Maps (W.B. 22)*. Government Printer: Pretoria.

SAWB. (1960). *Climate of South Africa Part 5 District rainfall (W.B. 23)*. Government Printer: Pretoria.

SAWB. (1965). *Climate of South Africa Part 8 General Survey (W.B. 28)*. Government Printer: Pretoria.

SAWB. (1972). *Climate of South Africa. Part 10, General Survey (W.B. 35)*. Government Printer: Pretoria.

SAWS. (2017). *A Climate change reference Atlas*. Available at: http://www.weathersa.co.za/Documents/Climate/SAWS_CC_REFERENCE_ATLAS_PAGES.pdf (Accessed: 24 June 2019).

SAWS. (2018). *How is rainfall measured?*. Available at: http://www.weathersa.co.za/home/weatherques (Accessed: 1 July 2019).

SAWS. (2019a). *Our Climate Services.* Available at: http://www.weathersa.co.za/home/aboutclimateatsaws (Accessed: 1 July 2019).

SAWS. (2019b). *Overview*. Available at: http://www.weathersa.co.za/home/overview (Accessed: 12 October 2019).

Scholes, B., Driver, A., Biggs, R. and Forsyth, G. (2017). Biodiversity: Natural capital to be wisely used. In Mambo, J. and Faccer, K. (eds.). *Understanding the Social and Environmental Implications of Global Change*. Africa Sun Media: Stellenbosch.

Schumann, T. E. W., & Hofmeyr, W. L. (1938). The partition of a region in rainfall districts: With special reference to South Africa. *Quarterly Journal of the Royal Meteorological Society*, 64: 484–488.

Schulze, R.E. (2007). Rainfall: background. In Schulze, R.E. (eds.). *South African Atlas of Climatology and Agrohydrology WRC Report 1489/1/06*. Water Research Commission: Pretoria.

Schulze, R.E. (2012). *A 2011 Perspective on Climate Change and the South African Water Sector WRC Report TT518/12*. Water Research Commission: Pretoria.

Schulze, R.E. and Kunz, R.P. (1997). Rainfall seasonality. In Schulze, R.E. (eds.). *South African Atlas of Agrohydrology and Climatology WRC report TT82/96*. Water Research Commission: Pretoria.

Schulze, R.E. and Lynch, S.D. (2007). Annual Precipitation. In Schulze, R.E. (eds.). *South African Atlas of Climatology and Agrohydrology WRC Report 1489/1/06*. Water Research Commission: Pretoria.

Schulze, R.E. and Maharaj, M. (2007). Rainfall seasonality. In Schulze, R.E. (eds.). *South African Atlas of Climatology and Agrohydrology WRC Report 1489/1/06*. Water Research Commission: Pretoria.

Sciscio, L., Neumann, F.H., Roberts, D., Tsikos, H., Scott, L. and Bamford, M. (2013). Fluctuations in Miocene climate and sea levels along the southwestern South African coast: inferences from biogeochemistry, palynology and sedimentology. *Palaeontologica Africana*, 48: 2-18.

Scott, L. and Nyakale, M. (2002). Pollen indications of Holocene palaeoenvironments at Florisbad spring in the central Free State, South Africa. *The Holocene*, 12: 497-503.

Scott, L., Marais, E. and Brook, G.A. (2004). Fossil hyrax dung and evidence of Late Pleistocene and Holocene vegetation types in the Namib Desert. *Journal of Quaternary Science: Published for the Quaternary Research Association*, 19: 829-832.

Seidel, D.J., Fu, Q., Randel, W.J. and Reichler, T.J. (2008). Widening of the tropical belt in a changing climate. *Nature Geoscience*, 1: 21-24.

Senapathi, D., Nicoll, M. A., Teplitsky, C., Jones, C.G. and Norris, K. (2011). Climate change and the risks associated with delayed breeding in a tropical wild bird population. *Proceedings of the Royal Society of London B: Biological Sciences*, 278: 3184-3190.

Sene, K.J., Jones, D.A., Meigh, J.R. and Farquharson, F.A.K. (1998). Rainfall and flow variations in the Lesotho Highlands. *International Journal of Climatology*, 18: 329-345.

Sharma, S. and Singh, P.K. (2017). Long Term Spatiotemporal Variability in Rainfall Trends over the State of Jharkhand, India. *MDPI Climate*, 5. DOI: 10.3390/cli5010018.

Shongwe, M.E., Van Oldenborgh, G.J., Van Den Hurk, B.J.J.M., De Boer, B., Coelho, C.A.S. and Van Aalst, M.K. (2009). Projected changes in mean and extreme precipitation in Africa under global warming. Part I: Southern Africa. *Journal of Climate*, 22: 3819-3837.

Shongwe, M.E., Lennard, C., Liebmann, B., Kalognomou, E.A., Ntsangwane, L. and Pinto, I. (2015). An evaluation of CORDEX regional climate models in simulating precipitation over Southern Africa. *Atmospheric Science Letters*, 16: 199-207.

Singh, S.K., Lo, E.Y.M. and Qin, X. (2017). Cluster Analysis of Monthly Precipitation over the Western Maritime Continent under Climate Change. *Climate*, 5. DOI: 10.3390/cli5040084.

Singleton, A.T. and Reason, C.J.C. (2007). Variability in the characteristics of cut-off low pressure systems over subtropical southern Africa. *International Journal of Climatology*, 27: 295-310.

Sobowale, A., Sajo, S.O. and Ayodele, O.E. (2016). Analysis of onset and cessation of rainfall in southwest Nigeria: Food security impact of variability in the length of the growing season. *Hungarian Agricultural Engineering*, 30: 23-30.

Sousa, P.M., Blamey, R.C., Reason, C.J., Ramos, A.M. and Trigo, R.M. (2018). The 'Day Zero' Cape Town drought and the poleward migration of moisture corridors. *Environmental Research Letters*, 13. DOI: 10.1008/1748-9326/aaebc7.

Stager, J.C., Mayewski, P.A., White, J., Chase, B.M., Neumann, F.H., Meadows, M.E., King, C.D. and Dixon, D.A. (2012). Precipitation variability in the winter rainfall zone of South Africa during the last 1400 yr linked to the austral Westerlies. *Climate of the Past*, 8: 877-887.

Stager, J.C., Ryves, D.B., King, C., Madson, J., Hazzard, M., Neumann, F.H. and Maud, R. (2013). Late Holocene precipitation variability in the summer rainfall region of South Africa. *Quaternary Science Reviews*, 67: 105-120.

Statistics South Africa. (2019). *Gross domestic product: First quarter 2019*. Statistical Release P0441. IsIbalo House: Pretoria.

Stern, R.D., Dennett, M.D. and Dale, I.C. (1982). Analysing daily rainfall measurements to give agronomically useful results. I. Direct methods. *Experimental Agriculture*, 18: 223-236.

Stone, A.E. (2014). Last Glacial Maximum conditions in southern Africa: Are we any closer to understanding the climate of this time period?. *Progress in Physical Geography*, 38: 519-542.

Strydom, S. and Savage, M.J. (2016). A spatio-temporal analysis of fires in South Africa. *South African Journal of Science*, 112. DOI: 10.17159/sajs.2016/20150489.

Stuut, J.B.W., Crosta, X., Van der Borg, K. and Schneider, R. (2004). Relationship between Antarctic sea ice and southwest African climate during the late Quaternary. *Geology*, 32: 909-912.

Suepa, T., Qi, J., Lawawirojwong, S. and Messina, J.P. (2016). Understanding spatio-temporal variation of vegetation phenology and rainfall seasonality in the monsoon Southeast Asia. *Environmental Research*, *147*: 621-629.

Sumner, G., Homar, V. and Ramis, C. (2001). Precipitation seasonality in eastern and southern coastal Spain. *International Journal of Climatology*, 21: 219-247.

Sun, W., Zhu, Y., Huang, S. and Guo, C. (2015). Mapping the mean annual precipitation of China using local interpolation techniques. *Theoretical and Applied Climatology*, 119: 171-180.

Sutherland, C. and Mazeka, B. (2019). *Ecosystem Services in South Africa*. In Knight, J. and Rogerson, C.M. (eds.). *The Geography of South Africa*. Springer: Switzerland.

Tadross, M.A., Hewitson, B.C. and Usman, M.T. (2005a). The interannual variability of the onset of the maize growing season over South Africa and Zimbabwe. *Journal of Climate*, 18: 3356-3372.

Tadross, M., Jack, C. and Hewitson, B., (2005b). On RCM-based projections of change in southern African summer climate. *Geophysical Research Letters*, 32. DOI: 10.1029/2005GL24460.

Tadross, M., Suarez, P., Lotsch, A., Hachigonta, S., Mdoka, M., Unganai, L., Lucio, F., Kamdonyo, D. and Muchinda, M. (2007). Changes in growing-season rainfall characteristics and downscaled scenarios of change over southern Africa: implications for growing maize. In *IPCC regional Expert Meeting on Regional Impacts, Adaptation, Vulnerability, and Mitigation, Nadi, Fiji*, 193-204.

Tadross, M., Suarez, P., Lotsch, A., Hachigonta, S., Mdoka, M., Unganai, L., Lucio, F., Kamdonyo, D. and Muchinda, M. (2009). Growing-season rainfall and scenarios of future change in southeast Africa: implications for cultivating maize. *Climate Research*, 40: 147-161.

Tadross, M., Davis, C., Engelbrecht, F., Joubert, A. and Archer van Garderen, E. (2011). Regional scenarios of future climate change over southern Africa. In Davis, C. (eds.). *Climate risk and vulnerability: A handbook for southern Africa First Edition*. Council for Scientific and Industrial Research: Pretoria.

Taljaard, J.J. (1994). *Atmospheric circulation systems, synoptic climatology and weather phenomena of South Africa. Part 1. Controls of the weather and climate of South Africa Technical Paper no 27.* Government Print: Pretoria.

Taljaard, J.J. (1996). *Atmospheric circulation systems, synoptic climatology and weather phenomena of South Africa. Part 6. Rainfall in South Africa Technical Paper no 32*. Government Print: Pretoria.

Taljaard, J. J., & Steyn, P. C. L. (1991). *Relationship between atmospheric circulation and rainfall in the South African region Technical Paper No. 24.* Government Print: Pretoria.

Tamarin-Brodsky, T. and Kaspi, Y. (2017). Enhanced poleward propagation of storms under climate change. *Nature Geoscience*, 10: 908-913.

Tao, Y., Wang, W., Song, S. and Ma, J. (2018). Spatial and Temporal Variations of Precipitation Extremes and Seasonality over China from 1961-2013. *Water*, 10: 7-19.

Tarhule, A. and Woo, M.K. (1998). Changes in rainfall characteristics in northern Nigeria. *International Journal of Climatology*, 18: 1261-1271.

Taylor, W.A. (2000). *Change-point analysis: a powerful new tool for detecting changes*. Available at: https://variation.com/change-point-analysis-a-powerful-new-tool-for-detecting-changes/ (Accessed: 22 November 2018).

Tennant, W.J. and Hewitson, B.C. (2002). Intra-seasonal rainfall characteristics and their importance to the seasonal prediction problem. *International Journal of Climatology*, 22: 1033-1048.

Teodoro, P.E., de Oliveira-Júnior, J.F., Da Cunha, E.R., Correa, C.C.G., Torres, F.E., Bacani, V.M., Gois, G. and Ribeiro, L.P. (2016). Cluster analysis applied to the spatial and temporal variability of monthly rainfall in Mato Grosso do Sul State, Brazil. *Meteorology and Atmospheric Physics*, 128: 197-209.

Thackeray, J.F. (1988). Quantification of climate change during the late Quaternary in southern Africa. *Palaeontology of Africa*, 19: 317-324.

Thackeray, J.F. and Fitchett, J.M. (2016). Rainfall seasonality captured in micromammalian fauna in Late Quaternary contexts, South Africa. *Palaeontologia Africana*, 51: 1-9.

Thambiran, T. and Padayachi, Y. (2017). Air Quality. In Mambo, J. and Faccer, K. (eds.). *Understanding the Social and Environmental Implications of Global Change*. Africa Sun Media: Stellenbosch.

Thomas, D.S.G., Twyman, C., Osbahr, H. and Hewitson B. (2007). Adaptation to climate change and variability: Farmer responses to intra-seasonal precipitation trends in South Africa. *Climate Change*, 83: 301–322.

Thompson, D.W. and Wallace, J.M. (2000). Annular modes in the extratropical circulation. Part I: Month-to-month variability. *Journal of Climate*, 13: 1000-1016.

Tongwane, M.I. and Moeletsi, M.E. (2015). Intra-seasonal rainfall variability during the maize growing season in the northern lowlands of Lesotho. *Theoretical and Applied Climatology*, 120: 575-585.

Truc, L., Chevalier, M., Favier, C., Cheddadi, R., Meadows, M.E., Scott, L., Carr, A.S., Smith, G.F. and Chase, B.M. (2013). Quantification of climate change for the last 20,000 years from Wonderkrater, South Africa: implications for the long-term dynamics of the Intertropical Convergence Zone. *Palaeogeography, Palaeoclimatology, Palaeoecology*, *386*: 575-587.

Tshililo, F.P. (2017). Rainy season characteristics with reference to maize production from the Luvuvhu River Catchment, Limpopo Province, South Africa. *MSc Dissertation submitted to the University of KwaZulu-Natal*.

Turton, A. (2018). Southern African Rivers and Freshwater Resources within the context of the Anthropocene. In Holmes, P.J. and Boardman, J. (eds.). *Southern African Landscapes and Environmental Change*. Routledge: Oxon.

Tyson, P. D. (1977). The enigma of changing world climates. *South African Geographical Journal*, 59: 77–116.

Tyson, P. D. (1978). Rainfall changes over South Africa during the period of the meteorological record. In Werger, M.J.A. (eds.). *Biogeography and ecology of Southern Africa*. The Hague: Australia.

Tyson, P.D. (1981). Atmospheric circulation variations and the occurrence of extended wet and dry spells over southern Africa. *Journal of Climatology*, 1: 115-130.

Tyson, P.D. (1986). *Climate Change and Variability in Southern Africa*. Oxford University Press: Cape Town.

Tyson, P.D., Dyer, T.G. and Mametse, M.N. (1975). Secular changes in South African rainfall: 1880 to 1972. *Quarterly Journal of the Royal Meteorological Society*, 101: 817-833.

Tyson, P.D. and Preston-Whyte, R.A. (2000). *The weather and climate of southern Africa*. Oxford University Press: Cape Town.

Tyson, P.D., Cooper, G.R.J. and McCarthy, T.S. (2002). Millennial to multi-decadal variability in the climate of southern Africa. *International Journal of Climatology*, 22: 1105-1117.

ul Hasson, U., Pascale, S., Lucarini, V. and Böhnerm, J. (2016). Seasonal cycle of precipitation over major river basins in South and Southeast Asia: a review of the CMIP5 climate models data for present climate and future climate projections. *Atmospheric Research*, 180: 42-63.

Unal, Y., Kindap, T. and Karaca, M. (2003). Redefining the climate zones of Turkey using cluster analysis. *International Journal of Climatology*, 23: 1045-1055.

Underhill, L. and Bradfield. (2009). *Introstat*. Cape Town: Juta and Co. Ltd.

Usman, M.T. and Reason, C.J.C. (2004). Dry spell frequencies and their variability over southern Africa. *Climate Research*, 26: 199-211.

Van Der Walt, A.J. and Fitchett, J.M. (Under review). Statistical classification of South African Seasonal Divisions on the Basis of Daily Temperature Data. *South African Journal of Science.*

Van Heerden, J., Terblanche, D.E. and Schulze, G.C. (1988). The southern oscillation and South African summer rainfall. *Journal of Climatology*, 8: 577-597.

van Huyssteen, C.W., du Preez, C.C. and Holmes, P.J. (2018). Agriculture and a changing biophysical environment. In Holmes, P.J. and Boardman, J. (eds.). *Southern African Landscapes and Environmental Change*. Routledge: Oxon.

van Wilgen, N.J., Goodall, V., Holness, S., Chown, S.L. and McGeoch, M.A. (2016). Rising temperatures and changing rainfall patterns in South Africa's national parks. *International Journal of Climatology*, 36: 706-721.

Van Zinderen Bakker, E.M. (1967). Upper Pleistocene stratigraphy and Holocene ecology on the basis of vegetation changes in Sub-Saharan Africa. In Bishop, W.W. and Clark, J.D. (eds.). *Background to Evolution in Africa.* University of Chicago Press: Chicago.

Van Zinderen Bakker, E.M. (1976). The evolution of late Quaternary paleoclimates of Southern Africa. *Palaeoecology of Africa,* 9: 160-202.

Van Zinderen Bakker, E.M. (1983). A late-glacial and post-glacial pollen record from the Namib Desert. *Palaeoecology of Africa*, 16: 421-428.

Vélez, A., Martin-Vide, J., Royé, D. and Santaella, O. (2018). Spatial analysis of daily precipitation concentration in Puerto Rico. *Theoretical and Applied Climatology*, 136: 1347-1355.

Verworn, A. and Haberlandt, U. (2011). Spatial interpolation of hourly rainfall-effect of additional information, variogram inference and storm properties. *Hydrology and Earth System Sciences*, 15: 569-584.

Vyshkvarkova, E. and Voskresenkaya. (2014). Precipitation inequality over Ukraine. *Journal of Scientific Research and Advancements*, 3: 384-396.

Walker, N. D. (1989). Seas surface temperature-rainfall relationships and associated oceanatmosphere coupling mechanisms in the southern African region. *PhD Thesis submitted to the University of Cape Town.*

Walsh, R.P.D. & Lawler, D.M. (1981). Rainfall seasonality: description, spatial patterns and change through time. *Weather* 36: 201-208.

Ward, J.H. (1963). Hierarchical grouping to optimize an objective function. *Journal of the American Statistical Association*, 58: 236-244.

Weiser, J., Baumann, K.H., Hahn, A. and Zabel, M. (2016). Late Holocene paleoceanographic changes off south-western Africa as inferred from coccolithophore assemblages. *Journal of Nannoplankton Research*, 36: 161-171.

Weldon, D. and Reason, C.J.C. (2014). Variability of rainfall characteristics over the South Coast region of South Africa. *Theoretical and Applied Climatology*, 115: 177-185.

Wellington, J. H. (1955). *Southern Africa: A geographical study. Volume 1: Physical Geography*. Cambridge University Press: Cambridge.

Whitecross, M.A., Witkowski, E.T.F. and Archibald, S. (2017). Savanna tree-grass interactions: A phenological investigation of green-up in relation to water availability over three seasons. *South African Journal of Botany*, 108: 29-40.

Wilks, D.S. (1995). *Statistical Methods in the Atmospheric Sciences: An Introduction*. San Diego: Academic Press.

WMO. (2000). *Detecting trends and other changes in hydrological data*. Available at: https://water.usgs.gov/osw/wcp-water/detecting-trend.pdf (Accessed: 6 February 2019).

WMO. (2006). *Guide to Meteorological Instruments and Methods of Observation Preliminary 7th edition WMO-No. 8*. World Meteorological Organization: Geneva.

Wolski, P. (2018). How severe is Cape Town's "Day Zero" drought?. *Significance*, 15: 24-27.

Xu, W., Zou, Y., Zhang, G. and Linderman, M. (2015). A comparison among spatial interpolation techniques for daily rainfall data in Sichuan Province, China. *International Journal of Climatology*, 35: 2898-2907.

Xulu, S., Peerbhay, K., Gebreslasie, M. and Ismail, R. (2018). Drought influence on forest plantations in Zululand, South Africa, using MODIS time series and climate data. *Forests*, 9. DOI: 10.3390/f9090528.

Yan, D., Zhang, X., Yu, Y., Guo, W. and Hanan, N.P. (2016). Characterizing land surface phenology and responses to rainfall in the Sahara desert. *Journal of Geophysical Research: Biogeosciences*, 121: 2243-2260.

Yang, X., Xie, X., Liu, D.L., Ji, F. and Wang, L. (2015). Spatial interpolation of daily rainfall data for local climate impact assessment over greater Sydney region. *Advances in Meteorology*, 2015. DOI: 10.1155/2015/563629.

Yeşilırmak, E. and Atatanır, L. (2016). Spatiotemporal variability of precipitation concentration in western Turkey. *Natural Hazards*, 81: 687-704.

Zarenistanak, M., Dhorde, A.G. and Kripalani, R.H. (2014). Trend analysis and change point detection of annual and seasonal precipitation and temperature series over southwest Iran. *Journal of Earth System Science*, 123: 281-295.

Zengeni, R., Kakembo, V. and Nkongolo, N. (2016). Historical rainfall variability in selected rainfall stations in Eastern Cape, South Africa. *South African Geographical Journal*, 98: 118-137.

Zhang, L.J. and Qian, Y.F. (2003). Annual distribution features of precipitation in China and their interannual variations. *Acta Meteorologica Sinica*, 17: 146-163.

Zhang, Q., Körnich, H. and Holmgren, K. (2013). How well do reanalyses represent the southern African precipitation?. *Climate Dynamics*, 40: 951-962.

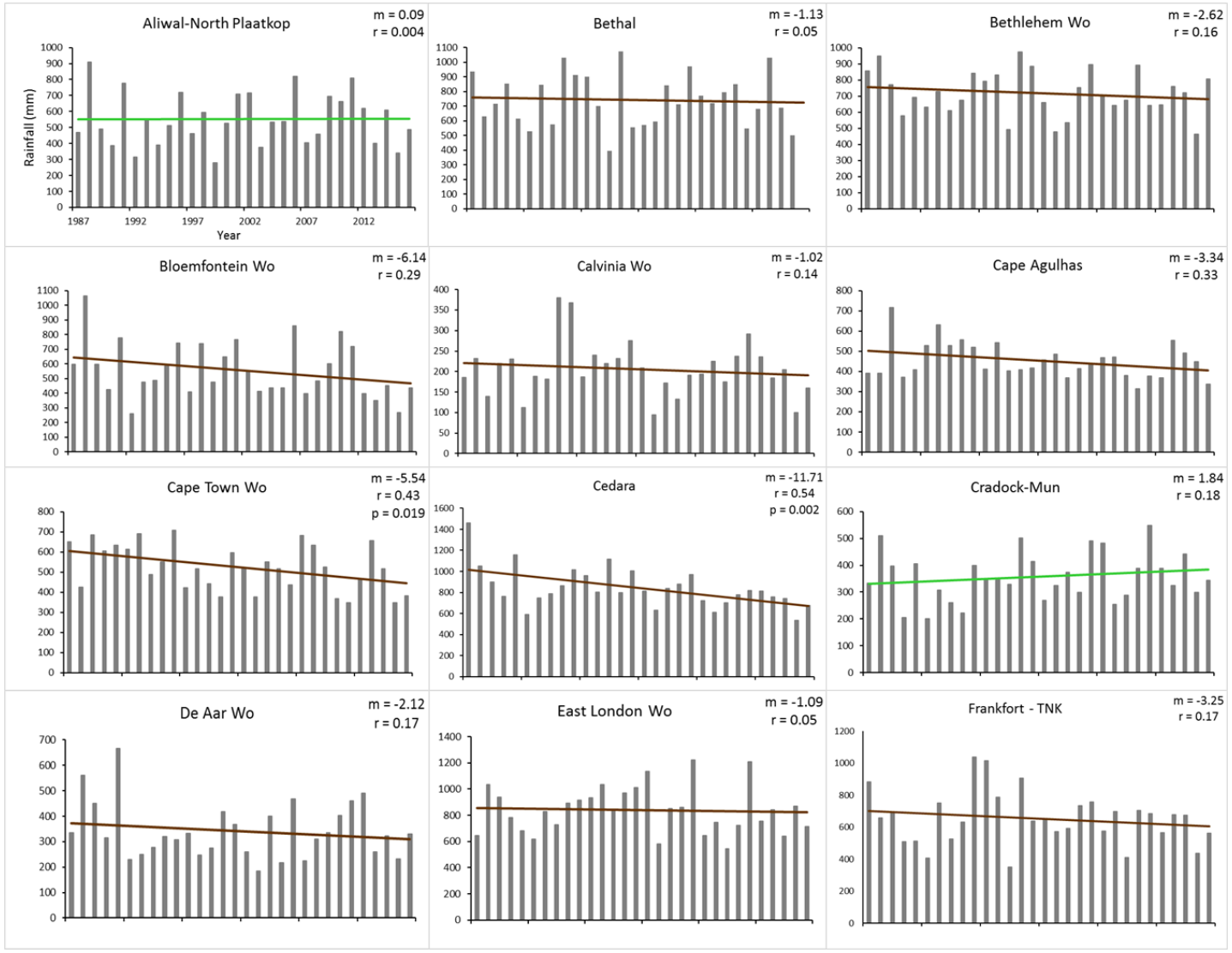
Zhang, K., Yao, Y., Qian, X. and Wang, J. (2019). Various characteristics of precipitation concentration index and its cause analysis in China between 1960 and 2016. *International Journal of Climatology*. DOI: 10.1002/joc.6092.

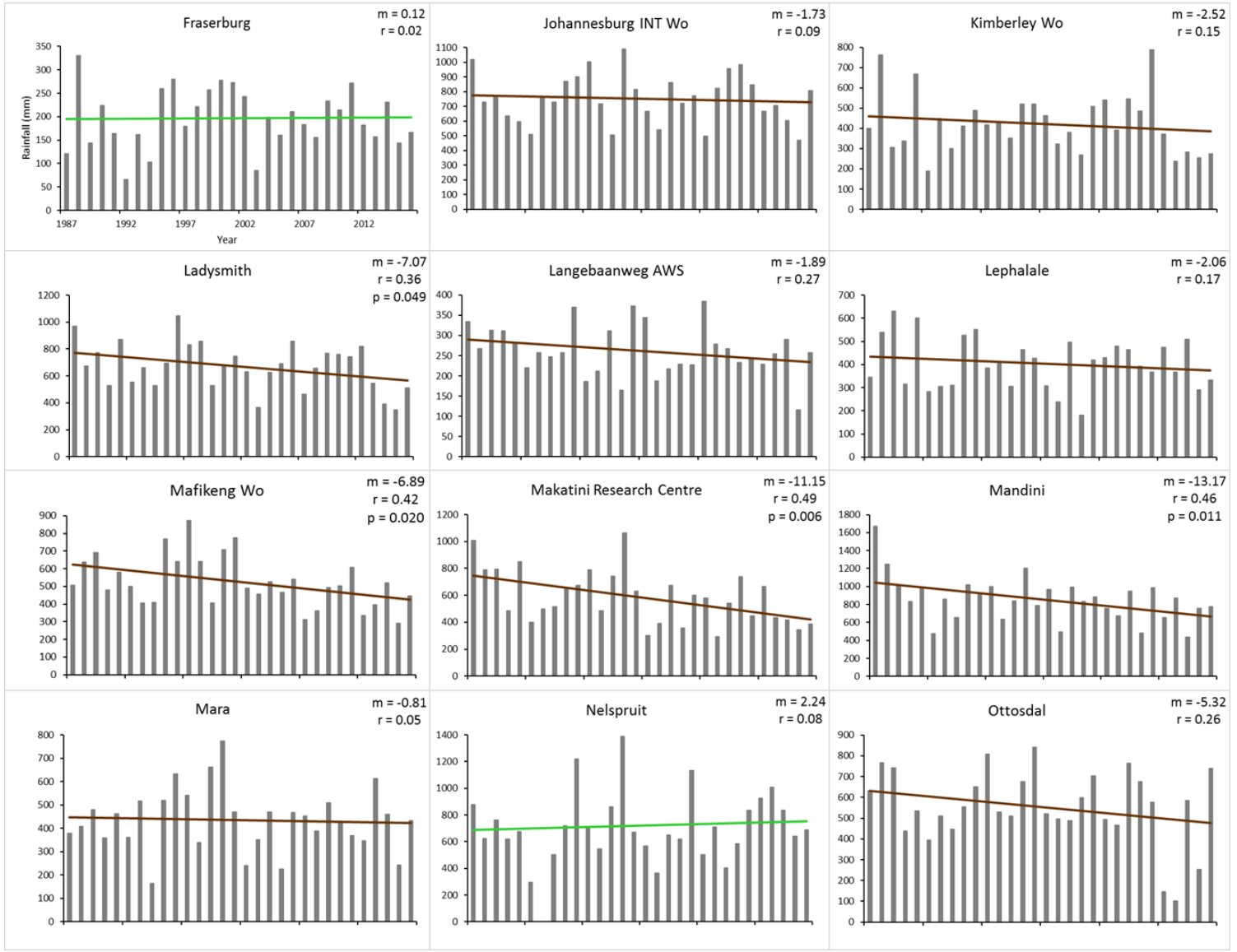
Zhao, W. and Khalil, M.A.K. (1993). The relationship between precipitation and temperature over the contiguous United States. *Journal of Climate*, 6: 1232-1236.

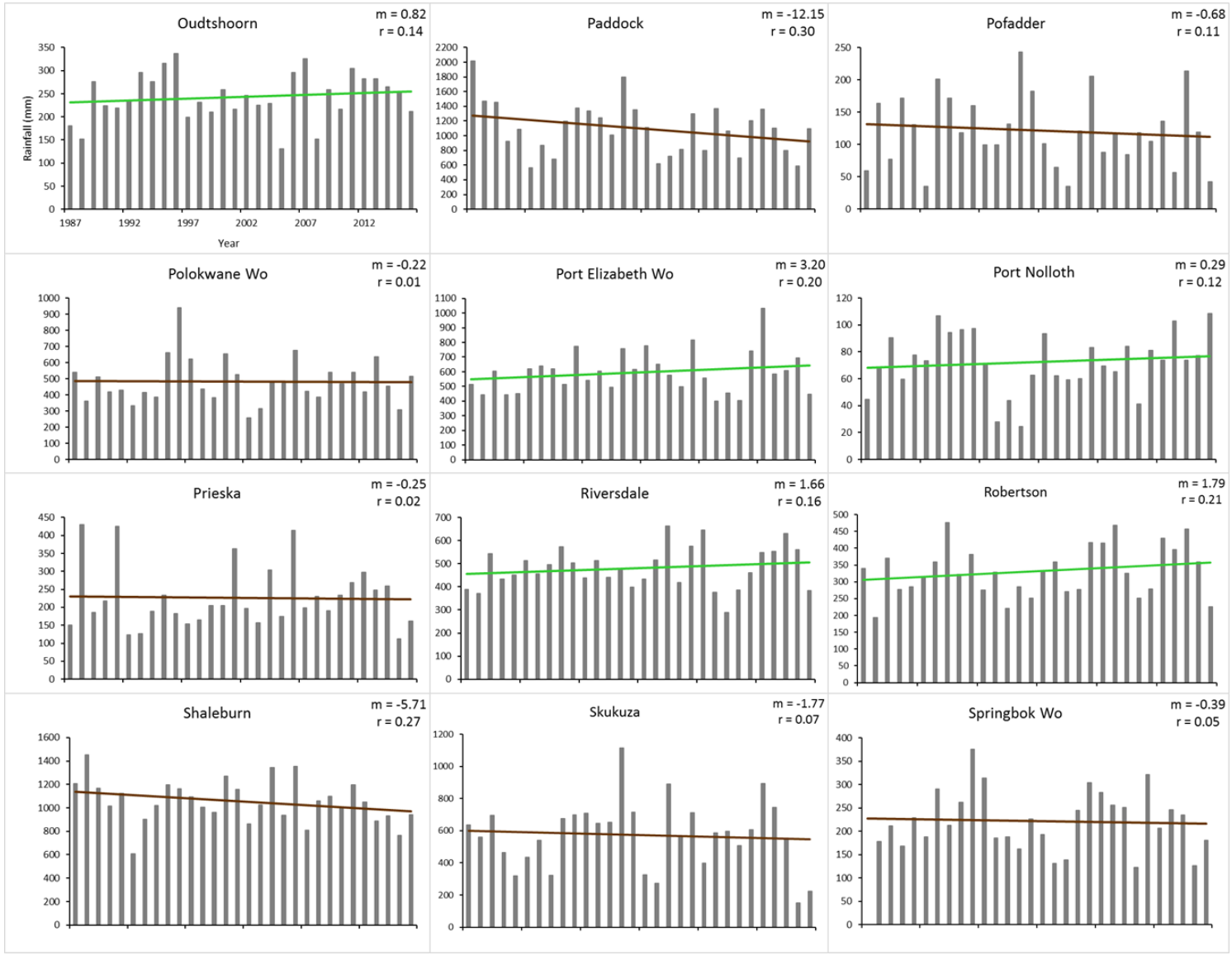
Ziervogel, G., New, M., Archer van Garderen, E., Midgley, G., Taylor, A., Hamann, R., Stuart-Hill, S., Myers, J. and Warburton, M. (2014). Climate change impacts and adaptation in South Africa. *Wiley Interdisciplinary Reviews: Climate Change*, 5: 605-620.

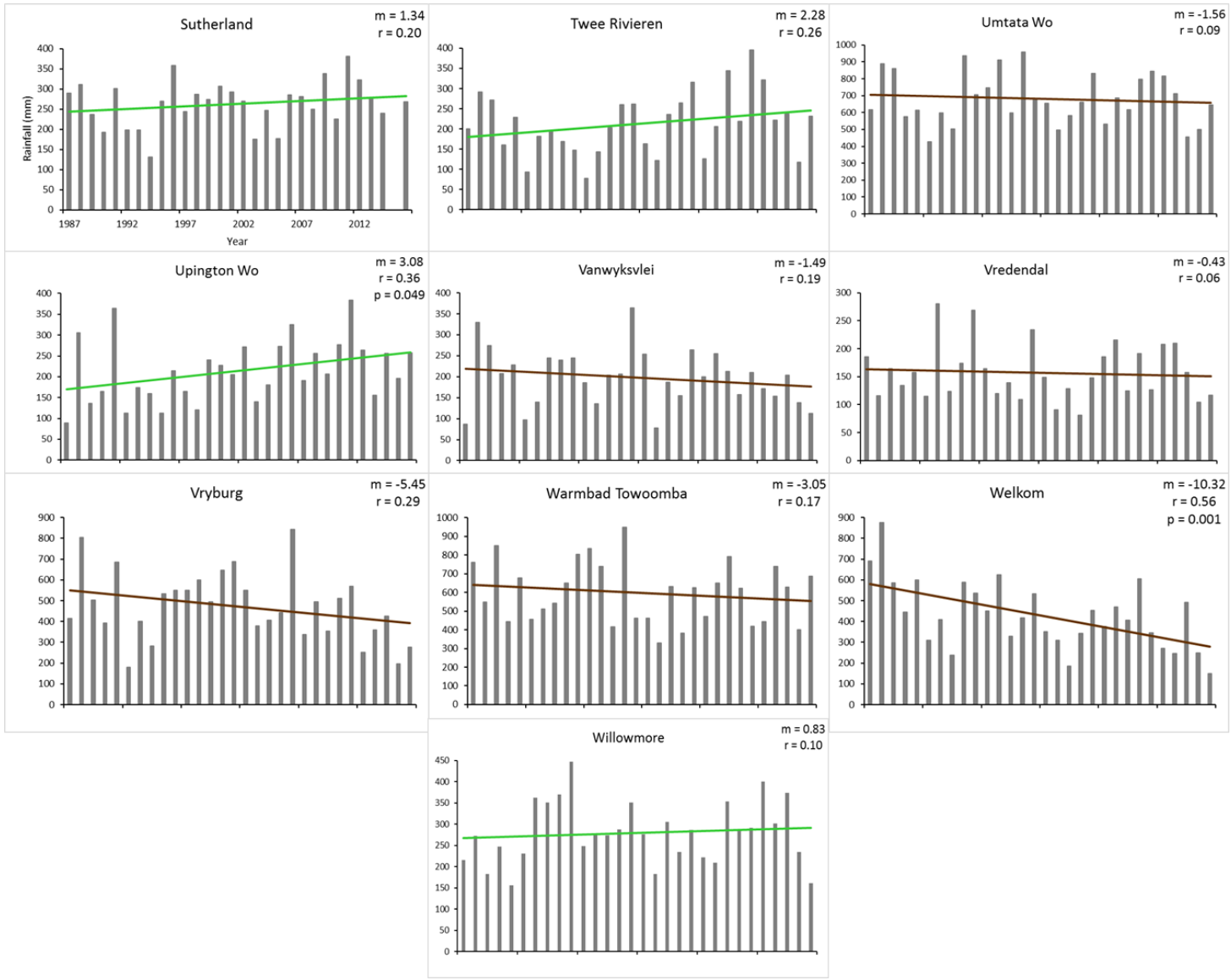
Zuma-Netshiukhwi, G., Stigter, K. and Walker, S. (2013). Use of traditional weather/climate knowledge by farmers in the South-western Free State of South Africa: Agrometeorological learning by scientists. *Atmosphere*, 4: 383-410.

APPENDIX A: BAR CHARTS ANNUAL RAINFALL TOTALS




Fraserburg
m = 0.12
r = 0.02
Rainfall (mm)
Year
Johannesburg INT Wo
m = -1.73
r = 0.09
Kimberley Wo
m = -2.52
r = 0.15
Ladysmith
m = -7.07
r = 0.36
p = 0.049
Langebaanweg AWS
m = -1.89
r = 0.27
Lephalale
m = -2.06
r = 0.17
Mafikeng Wo
m = -6.89
r = 0.42
p = 0.020
Makatini Research Centre
m = -11.15
r = 0.49
p = 0.006
Mandini
m = -13.17
r = 0.46
p = 0.011
Mara
m = -0.81
r = 0.05
Nelspruit
m = 2.24
r = 0.08
Ottosdal
m = -5.32
r = 0.26


Oudtshoorn
m = 0.82
r = 0.14
Rainfall (mm)
Year
Paddock
m = -12.15
r = 0.30
Pofadder
m = -0.68
r = 0.11
Polokwane Wo
m = -0.22
r = 0.01
Port Elizabeth Wo
m = 3.20
r = 0.20
Port Nolloth
m = 0.29
r = 0.12
Prieska
m = -0.25
r = 0.02
Riversdale
m = 1.66
r = 0.16
Robertson
m = 1.79
r = 0.21
Shaleburn
m = -5.71
r = 0.27
Skukuza
m = -1.77
r = 0.07
Springbok Wo
m = -0.39
r = 0.05


Sutherland
m = 1.34
r = 0.20
Rainfall (mm)
Year
Twee Rivieren
m = 2.28
r = 0.26
Umtata Wo
m = -1.56
r = 0.09
Upington Wo
m = 3.08
r = 0.36
p = 0.049
Vanwyksvlei
m = -1.49
r = 0.19
Vredendal
m = -0.43
r = 0.06
Vryburg
m = -5.45
r = 0.29
Warmbad Towoomba
m = -3.05
r = 0.17
Welkom
m = -10.32
r = 0.56
p = 0.001
Willowmore
m = 0.83
r = 0.10

APPENDIX B: MONTHLY RAINFALL STATISTICS

B.1 JANUARY

Location	Mean rainfall (mm)	Range	Coefficient of variation (%)	Sample size (n)	Change over time (mm.yr^{-1})	Strength of trend (r)
Aliwal-North Plaatkop	78.1	192.4	61.5	30	1.47	0.27
Bethal	137.6	342.1	51.2	30	1.36	0.17
Bethlehem Wo	126.5	213.2	48.2	30	2.16	0.32
Bloemfontein Wo	88.5	212.0	64.9	30	-0.10	0.02
Calvinia Wo	9.2	65.1	152.0	30	0.36	0.22
Cape Agulhas	21.2	112.6	130.7	30	0.55	0.17
Cape Town Wo	9.7	60.9	117.8	30	0.10	0.07
Cedara	128.9	188.0	39.4	30	-0.93	0.16
Cradock-Mun	52.8	134.5	60.0	30	1.41	*0.39
De Aar Wo	42.1	146.0	84.7	30	0.79	0.19
East London Wo	88.4	162.3	55.2	30	-0.17	0.03
Frankfort-TNK	111.4	223.8	51.1	30	0.67	0.10
Fraserburg	18.8	86.4	115.2	30	0.54	0.22
Johannesburg INT Wo	139.2	228.2	33.0	30	1.04	0.20
Kimberley Wo	73.6	267.8	77.2	30	1.03	0.16
Ladysmith	123.3	306.0	59.9	30	1.49	0.17
Langerbaanweg AWS	6.0	41.2	146.8	30	0.16	0.15
Lephalale	70.7	168.3	64.6	30	0.40	0.07
Mafikeng Wo	101.4	185.2	50.6	30	-0.93	0.16
Makatini Research Centre	84.2	263.2	80.7	29	-1.87	0.24
Mandini	95.6	227.9	52.3	30	0.18	0.03
Mara	82.5	262.7	81.8	30	1.52	0.20
Nelspruit	113.5	300.0	66.4	30	1.96	0.22
Ottosdal	104.4	282.5	64.0	30	-2.45	0.03
Oudtshoorn	16.1	91.6	120.7	30	0.53	0.24
Paddock	128.0	375.6	58.5	30	0.18	0.02
Pofadder	11.6	42.5	119.0	30	0.59	*0.37
Polokwane Wo	80.7	255.3	71.6	30	-0.95	0.14
Port Elizabeth Wo	32.1	102.6	73.8	30	-0.16	0.06
Port Nolloth	3.7	32.2	201.9	30	0.21	0.25
Prieska	30.7	114.0	87.9	30	0.99	0.32
Riversdale	32.5	188.2	112.8	30	0.82	0.19
Robertson	20.2	172.7	161.2	30	0.94	0.25
Shaleburn	197.3	265.2	27.8	30	0.94	0.15
Skukuza	102.8	313.0	77.9	30	1.59	0.17
Springbok Wo	9.6	56.8	153.7	29	0.56	0.32
Sutherland	12.4	47.0	110.7	30	0.43	0.27
Twee Rivieren	35.6	102.0	87.9	30	1.01	0.28
Umtata Wo	99.8	163.9	39.6	30	1.10	0.24
Upington Wo	37.2	137.7	95.2	30	1.00	0.24
Vanwyksvlei	26.2	105.1	103.6	29	-0.32	0.10
Vredendal	3.0	20.2	149.6	30	0.05	0.10
Vryburg	92.1	253.0	70.7	30	0.31	0.04
Warmbad Towoomba	99.8	295.2	66.1	30	0.98	0.13
Welkom	73.2	187.2	67.6	30	0.80	0.14
Willowmore	24.9	112.8	96.6	30	0.26	0.09

B.2 FEBRUARY

Location	Mean rainfall (mm)	Range	Coefficient of variation (%)	Sample size (n)	Change over time (mm.yr^{-1})	Strength of trend (r)
Aliwal-North Plaatkop	84.9	322.1	71.6	30	-1.04	0.15
Bethal	82.3	254.0	65.2	30	-1.83	0.29
Bethlehem Wo	99.5	201.9	46.4	30	-0.33	0.06
Bloemfontein Wo	94.0	459.3	90.7	30	-2.95	0.31
Calvinia Wo	14.8	83.8	141.2	30	0.11	0.05
Cape Agulhas	17.5	68.4	74.8	30	-0.11	0.07
Cape Town Wo	11.2	38.0	108.6	30	-0.33	0.23
Cedara	107.5	209.5	42.2	30	-2.30	*0.44
Cradock-Mun	55.3	132.4	64.4	30	0.96	0.23
De Aar Wo	59.0	234.2	92.4	30	-1.64	0.26
East London Wo	70.5	152.6	55.5	30	-1.19	0.26
Frankfort-TNK	78.9	229.9	58.9	30	-2.37	*0.44
Fraserburg	27.1	102.8	81.1	30	0.09	0.04
Johannesburg INT Wo	107.1	298.9	64.5	30	-1.60	0.20
Kimberley Wo	73.0	320.1	84.7	30	-1.21	0.17
Ladysmith	99.7	231.6	55.1	30	-2.93	*0.46
Langerbaanweg AWS	5.8	42.8	164.2	30	-0.18	0.16
Lephalale	54.7	182.8	84.0	30	-2.00	*0.38
Mafikeng Wo	83.6	226.0	66.2	30	-1.99	0.31
Makatini Research Centre	80.9	289.5	77.4	30	-1.73	0.24
Mandini	102.9	386.2	76.6	30	-3.36	*0.37
Mara	56.9	315.6	116.8	30	-1.23	0.16
Nelspruit	115.3	372.4	75.7	30	-0.07	0.01
Ottosdal	75.8	213.3	65.4	30	-1.57	0.27
Oudtshoorn	18.4	53.3	75.4	30	0.26	0.16
Paddock	105.7	387.5	86.9	30	-4.86	*0.46
Pofadder	22.0	103.0	113.6	30	0.07	0.03
Polokwane Wo	63.1	328.5	105.2	30	-1.12	0.15
Port Elizabeth Wo	39.1	104.6	63.9	30	0.07	0.02
Port Nolloth	1.9	10.4	136.6	30	0.09	0.29
Prieska	41.8	150.4	88.6	29	-1.28	0.30
Riversdale	31.9	58.9	44.5	30	0.13	0.08
Robertson	14.2	59.1	99.6	30	0.45	0.28
Shaleburn	178.7	293.9	42.0	30	-1.65	0.19
Skukuza	82.1	419.6	113.7	30	-2.09	0.19
Springbok Wo	7.7	62.8	160.3	29	0.13	0.09
Sutherland	22.2	127.6	112.2	30	0.25	0.09
Twee Rivieren	45.4	177.7	103.7	30	0.16	0.03
Umtata Wo	88.4	158.8	45.4	30	-0.25	0.05
Upington Wo	34.8	144.2	106.1	30	0.92	0.21
Vanwyksvlei	29.0	90.6	88.7	30	-0.40	0.14
Vredendal	2.6	9.0	112.3	30	-0.01	0.03
Vryburg	91.8	359	84.4	30	-2.19	0.25
Warmbad Towoomba	80.8	221.6	70.1	30	-2.73	*0.42
Welkom	54.0	192.6	90.0	30	-2.69	*0.48
Willowmore	39.1	125.4	73.9	30	-0.04	0.01

B.3 MARCH

Location	Mean rainfall (mm)	Range	Coefficient of variation (%)	Sample size (n)	Change over time (mm.yr^{-1})	Strength of trend (r)
Aliwal-North Plaatkop	82.3	153.9	50.7	30	0.70	0.15
Bethal	84.5	157.5	52.7	29	-0.49	0.09
Bethlehem Wo	78.2	181.0	52.1	30	-1.33	0.29
Bloemfontein Wo	75.1	134.5	53.9	30	-0.83	0.19
Calvinia Wo	17.4	64.9	103.0	30	-0.37	0.18
Cape Agulhas	26.9	95.1	104.2	30	0.55	0.17
Cape Town Wo	14.5	57.3	102.4	30	-0.02	0.01
Cedara	105.5	179.9	43.7	30	-1.06	0.20
Cradock-Mun	43.8	127.6	55.3	30	0.58	0.21
De Aar Wo	52.1	160.4	68.0	30	-0.49	0.12
East London Wo	84.8	330.1	63.3	30	-0.44	0.07
Frankfort-TNK	85.2	199.5	51.3	30	-0.28	0.06
Fraserburg	30.0	156.1	106.9	30	-0.73	0.20
Johannesburg INT Wo	103.5	312.2	60.4	30	-1.08	0.15
Kimberley Wo	61.3	150.3	67.1	30	-1.14	0.24
Ladysmith	87.6	168.4	47.2	30	-1.45	0.30
Langerbaanweg AWS	6.3	24.3	107.3	30	0.03	0.04
Lephalale	50.9	215.6	90.1	30	0.01	0.002
Mafikeng Wo	64.7	157.8	54.0	30	-0.58	0.14
Makatini Research Centre	65.0	204.3	82.0	30	-1.06	0.17
Mandini	85.3	190.2	65.9	30	-2.24	0.34
Mara	50.1	169.1	90.0	30	-1.02	0.20
Nelspruit	106.2	286.8	59.6	29	0.19	0.03
Ottosdal	70.6	186.2	70.8	30	-1.31	0.23
Oudtshoorn	22.3	70.4	83.0	30	-0.18	0.08
Paddock	117.3	320.3	70.3	30	-3.04	0.32
Pofadder	19.5	66.2	97.5	30	-0.18	0.08
Polokwane Wo	57.8	176.3	63.5	30	-0.01	0.003
Port Elizabeth Wo	46.8	122.4	70.0	30	0.82	0.22
Port Nolloth	2.9	15.2	129.3	30	0.15	0.33
Prieska	38.5	113.2	71.3	30	-0.0004	0.0001
Riversdale	44.2	132.9	70.1	30	0.07	0.02
Robertson	21.5	116.5	116.6	30	-0.34	0.12
Shaleburn	150.5	250.1	41.1	30	-1.02	0.14
Skukuza	70.9	195.8	69.5	30	-0.65	0.11
Springbok Wo	13.7	70.5	126.2	29	0.06	0.03
Sutherland	26.6	111.2	90.1	29	0.12	0.04
Twee Rivieren	35.9	105.0	69.9	30	0.59	0.20
Umtata Wo	89.4	144.7	40.3	30	-0.11	0.03
Upington Wo	43.4	118.8	74.7	30	0.61	0.16
Vanwyksvlei	33.8	116.2	87.5	30	-0.09	0.03
Vredendal	4.7	15.1	99.7	30	-0.03	0.06
Vryburg	65.7	134.4	61.5	30	-0.97	0.21
Warmbad Towoomba	84.6	239.5	72.2	30	0.53	0.07
Welkom	57.5	177.6	73.8	30	-1.94	*0.40
Willowmore	34.1	119.5	73.7	30	1.05	0.36

B.4 APRIL

Location	Mean rainfall (mm)	Range	Coefficient of variation (%)	Sample size (n)	Change over time (mm.yr^{-1})	Strength of trend (r)
Aliwal-North Plaatkop	43.7	102.4	62.9	30	-0.19	0.06
Bethal	38.6	112.5	76.4	29	0.26	0.07
Bethlehem Wo	44.3	113.8	59.7	30	-0.34	0.11
Bloemfontein Wo	42.6	119.3	77.4	30	-0.60	0.16
Calvinia Wo	24.8	77.7	93.1	30	-0.80	0.30
Cape Agulhas	50.1	158.2	82.1	30	-2.31	*0.49
Cape Town Wo	45.9	174.5	81.4	30	-1.60	*0.37
Cedara	48.4	118.2	64.7	30	0.26	0.07
Cradock-Mun	29.4	77.0	68.9	30	-0.58	0.25
De Aar Wo	32.0	94.6	77.8	30	-0.04	0.001
East London Wo	78.1	241.1	68.7	30	2.80	*0.45
Frankfort-TNK	45.8	130.9	73.9	30	-0.08	0.02
Fraserburg	20.5	60.4	93.2	30	-0.17	0.08
Johannesburg INT Wo	40.7	116.9	78.5	30	0.15	0.04
Kimberley Wo	40.6	142.8	80.1	30	-0.50	0.13
Ladysmith	31.8	86.9	79.5	30	-0.04	0.01
Langerbaanweg AWS	21.5	82.7	85.8	30	-0.82	*0.39
Lephalale	26.1	107.2	109.5	30	-0.13	0.04
Mafikeng Wo	43.4	149.5	88.8	30	-0.07	0.01
Makatini Research Centre	37.9	151.7	90.6	30	-0.32	0.08
Mandini	50.9	164.1	83.6	30	0.23	0.05
Mara	21.0	121	135.7	30	0.72	0.22
Nelspruit	52.8	151.2	73.0	29	1.21	0.27
Ottosdal	49.7	154.1	89.2	30	-0.40	0.08
Oudtshoorn	24.6	69.7	74.0	29	-0.28	0.14
Paddock	60.7	192.5	82.3	30	-0.42	0.07
Pofadder	18.5	101.1	145.4	30	-0.72	0.23
Polokwane Wo	30.8	144.4	116.1	30	0.98	0.24
Port Elizabeth Wo	51.9	124.0	57.7	30	0.92	0.27
Port Nolloth	9.3	45.9	129.3	30	-0.34	0.26
Prieska	21.3	85.8	100.5	30	0.17	0.07
Riversdale	50.9	108.5	60.0	30	-1.22	0.35
Robertson	33.9	92.4	70.5	30	-1.07	*0.39
Shaleburn	54.5	104.2	54.2	30	0.56	0.16
Skukuza	39.5	239.4	108.6	30	0.87	0.18
Springbok Wo	18.6	78.9	102.9	29	-0.73	0.32
Sutherland	29.6	81.8	85.5	28	-0.16	0.05
Twee Rivieren	27.1	92.5	100.6	30	0.20	0.06
Umtata Wo	50.8	148.4	69.9	30	0.41	0.10
Upington Wo	20.3	78.6	95.7	30	0.07	0.03
Vanwyksvlei	21.3	102.0	120.3	30	-0.21	0.07
Vredendal	13.0	64.7	105.7	30	-0.63	0.16
Vryburg	38.8	141.2	92.4	30	-0.47	0.11
Warmbad Towoomba	34.6	188.0	113.6	30	1.01	0.22
Welkom	27.0	120.4	111.9	30	-1.55	*0.44
Willowmore	24.7	74.5	87.0	30	-0.92	*0.37

B.5 MAY

Location	Mean rainfall (mm)	Range	Coefficient of variation (%)	Sample size (n)	Change over time (mm.yr^{-1})	Strength of trend (r)
Aliwal-North Plaatkop	18.9	60.2	95.3	30	0.46	0.22
Bethal	13.5	84.3	129.7	29	-0.05	0.03
Bethlehem Wo	17.8	81.3	108.6	30	-0.15	0.07
Bloemfontein Wo	19.3	71.8	113.7	30	0.50	0.21
Calvinia Wo	20.6	71.6	84.9	30	0.40	0.20
Cape Agulhas	52.3	149.5	53.1	30	-1.06	0.33
Cape Town Wo	67.9	127.1	45.4	30	-1.35	*0.38
Cedara	20.5	89.4	98.0	30	-0.18	0.08
Cradock-Mun	13.0	44.8	93.7	30	0.17	0.12
De Aar Wo	18.6	93.0	117.6	30	0.72	0.28
East London Wo	38.6	149.7	98.3	30	0.05	0.01
Frankfort-TNK	17.6	118.8	144.7	30	-0.23	0.08
Fraserburg	11.1	47.4	84.2	30	0.12	0.11
Johannesburg INT Wo	19.3	99.2	130.5	30	0.24	0.08
Kimberley Wo	15.7	81.0	128.2	30	0.56	0.24
Ladysmith	10.5	60.0	147.7	29	0.04	0.02
Langerbaanweg AWS	32.7	78.0	56.0	30	-0.23	0.11
Lephalale	8.7	51.0	157.5	30	0.02	0.01
Mafikeng Wo	19.5	134.7	150.5	30	-0.36	0.11
Makatini Research Centre	19.7	167.3	175.4	30	-0.58	0.15
Mandini	30.8	154.5	114.4	30	-0.44	0.11
Mara	8.6	48.0	146.8	30	-0.04	0.02
Nelspruit	13.2	66.0	123.1	29	0.41	0.22
Ottosdal	15.7	100.2	148.7	30	-0.50	0.18
Oudtshoorn	20.2	59.2	84.3	30	-0.02	0.01
Paddock	34.1	113.0	92.0	30	-0.30	0.08
Pofadder	6.9	44.5	161.3	30	0.06	0.05
Polokwane Wo	10.4	65.0	144.7	30	0.08	0.05
Port Elizabeth Wo	43.6	162.5	98.6	30	0.69	0.14
Port Nolloth	7.3	29.2	97.2	30	0.03	0.04
Prieska	12.2	49.2	131.7	30	0.56	0.30
Riversdale	38.7	88.1	65.4	30	0.14	0.05
Robertson	29.7	63.2	58.1	30	-0.38	0.19
Shaleburn	12.1	42.6	92.3	30	0.07	0.06
Skukuza	8.5	33.7	104.0	30	-0.20	0.19
Springbok Wo	26.5	93.7	100.6	29	-0.28	0.09
Sutherland	27.2	70.9	71.7	29	0.79	0.34
Twee Rivieren	4.6	24.0	151.1	30	0.20	0.25
Umtata Wo	17.6	71.5	92.6	30	0.15	0.08
Upington Wo	9.8	47.0	141.0	30	0.63	*0.39
Vanwyksvlei	12.8	52.0	123.1	30	0.28	0.15
Vredendal	20.5	80.6	96.5	30	-0.19	0.08
Vryburg	16.4	104.0	143.8	30	-0.11	0.04
Warmbad Towoomba	12.5	73.9	141.2	30	-0.16	0.08
Welkom	13.4	54.0	116.6	30	-3.41	0.19
Willowmore	15.6	66.3	107.1	30	-0.07	0.04

B.6 JUNE

Location	Mean rainfall (mm)	Range	Coefficient of variation (%)	Sample size (n)	Change over time (mm.yr^{-1})	Strength of trend (r)
Aliwal-North Plaatkop	18.9	71.2	107.4	30	0.67	0.28
Bethal	9.6	61.8	152.6	29	-0.29	0.16
Bethlehem Wo	13.1	54.8	116.9	30	0.39	0.23
Bloemfontein Wo	13.9	92.8	138.4	30	0.67	*0.34
Calvinia Wo	25.9	56.2	66.5	30	0.51	0.26
Cape Agulhas	61.1	155.2	53.9	30	-0.13	0.03
Cape Town Wo	93.4	204.4	42.5	30	-0.98	0.21
Cedara	12.9	63.4	118.8	30	-0.50	0.28
Cradock-Mun	10.4	42.9	106.5	30	-0.06	0.05
De Aar Wo	16.3	87.4	124.8	30	-0.41	0.18
East London Wo	32.8	195.8	143.1	30	0.62	0.11
Frankfort-TNK	8.9	33.2	117.9	30	0.26	0.22
Fraserburg	6.9	27.5	100.9	29	-0.09	0.11
Johannesburg INT Wo	8.7	53.1	139.5	30	-0.14	0.10
Kimberley Wo	9.4	68.6	151.0	30	0.55	0.34
Ladysmith	8.5	55.8	137.2	30	-0.12	0.09
Langerbaanweg AWS	51.4	128.3	46.2	30	0.07	0.03
Lephalale	4.0	41.6	225.1	30	-0.16	0.15
Mafikeng Wo	5.7	43.8	182.4	30	0.22	0.18
Makatini Research Centre	15.0	52.9	121.9	30	-0.90	*0.42
Mandini	27.6	96.5	103.1	30	-0.34	0.10
Mara	5.3	56.7	203.9	30	-0.30	0.24
Nelspruit	7.5	54.9	171.0	29	-0.49	0.33
Ottosdal	5.6	33.0	164.4	30	0.17	0.16
Oudtshoorn	19.4	43.8	63.0	30	0.64	*0.45
Paddock	44.4	491.4	224.9	30	0.47	0.04
Pofadder	5.2	32.8	142.3	30	0.19	0.22
Polokwane Wo	4.1	23.8	175.0	30	-0.24	0.30
Port Elizabeth Wo	59.9	181.0	83.3	30	0.34	0.06
Port Nolloth	13.3	33.0	75.7	30	0.17	0.15
Prieska	8.3	42.6	142.9	30	-0.03	0.02
Riversdale	37.9	92.3	57.2	30	0.84	0.33
Robertson	40.7	92.7	48.8	30	0.47	0.21
Shaleburn	10.8	54.6	107.0	30	-0.33	0.25
Skukuza	6.6	37.8	156.9	30	-0.53	*0.44
Springbok Wo	39.0	106.6	74.3	29	0.10	0.03
Sutherland	31.9	96.7	71.2	30	0.49	0.19
Twee Rivieren	2.4	27.0	245.2	30	0.21	0.31
Umtata Wo	13.2	137.6	193.6	30	0.04	0.01
Upington Wo	6.1	42.9	180.1	30	0.28	0.23
Vanwyksvlei	10.1	45.0	138.9	30	0.10	0.06
Vredendal	27.0	55.6	59.2	30	0.41	0.22
Vryburg	7.5	52.6	188.1	30	0.43	0.26
Warmbad Towoomba	5.2	33.2	175.1	30	-0.05	0.04
Welkom	6.2	36.4	162.8	29	0.19	0.16
Willowmore	13.8	45.4	89.8	30	0.61	*0.42

B.7 JULY

Location	Mean rainfall (mm)	Range	Coefficient of variation (%)	Sample size (n)	Change over time (mm.yr^{-1})	Strength of trend (r)
Aliwal-North Plaatkop	12.3	71.0	128.5	30	0.72	*0.39
Bethal	3.3	30.1	213.3	29	0.03	0.04
Bethlehem Wo	8.1	74.1	204.9	30	0.19	0.11
Bloemfontein Wo	6.1	34.6	148.2	30	0.09	0.09
Calvinia Wo	24.5	92.8	92.2	30	-0.36	0.14
Cape Agulhas	62.2	150.6	50.9	30	-0.03	0.01
Cape Town Wo	92.7	192.9	49.8	30	-1.36	0.26
Cedara	18.8	135.2	161.3	30	-0.07	0.02
Cradock-Mun	10.4	61.2	127.4	30	0.47	0.31
De Aar Wo	7.9	46.1	125.3	30	-0.01	0.01
East London Wo	37.6	220.8	132.4	30	2.23	*0.39
Frankfort-TNK	5.5	38.8	186.2	30	0.36	0.30
Fraserburg	9.2	37.5	119.5	30	0.29	0.23
Johannesburg INT Wo	1.9	14.5	200.5	30	0.11	0.24
Kimberley Wo	3.3	24.2	169.0	30	-0.07	0.10
Ladysmith	10.6	74.8	173.9	30	0.17	0.08
Langerbaanweg AWS	46.5	105.3	51.1	30	-0.93	0.34
Lephalale	0.9	17.0	329.7	30	-0.04	0.12
Mafikeng Wo	1.6	19.5	277.1	29	0.16	0.31
Makatini Research Centre	8.3	44.3	124.9	30	0.19	0.15
Mandini	46.3	316.7	161.6	30	1.86	0.21
Mara	3.3	53.6	306.9	30	-0.11	0.09
Nelspruit	6.7	29.0	117.6	30	0.14	0.16
Ottosdal	2.0	25.0	261.1	30	0.15	0.24
Oudtshoorn	20.8	75.7	85.0	29	0.43	0.21
Paddock	52.7	371.4	179.1	30	2.69	0.25
Pofadder	5.5	56.5	197.4	30	-0.18	0.15
Polokwane Wo	2.1	28.1	264.2	30	0.01	0.01
Port Elizabeth Wo	49.1	200.4	88.8	30	1.91	*0.38
Port Nolloth	9.8	21.8	68.2	30	-0.15	0.20
Prieska	3.6	30.0	188.2	30	-0.12	0.16
Riversdale	39.9	94.7	58.4	30	0.90	0.33
Robertson	41.8	89.7	57.2	30	0.61	0.22
Shaleburn	14.0	98.9	165.5	30	0.37	0.14
Skukuza	3.5	24.3	141.8	30	0.06	0.11
Springbok Wo	33.6	99.4	72.4	30	-0.20	0.07
Sutherland	24.3	59.1	70.9	30	-0.15	0.08
Twee Rivieren	1.3	27.2	372.5	30	-0.04	0.08
Umtata Wo	16.5	86.2	132.6	30	0.72	0.29
Upington Wo	3.5	34.6	225.5	30	-0.17	0.18
Vanwyksvlei	5.6	50.7	178.8	30	0.04	0.03
Vredendal	28.3	95.6	77.2	30	-0.22	0.09
Vryburg	1.2	8.6	189.9	30	0.01	0.03
Warmbad Towoomba	1.5	22.3	279.6	30	-0.01	0.02
Welkom	4.5	41.6	201.2	30	-0.15	0.14
Willowmore	13.1	69.6	116	30	0.38	0.21

B.8 AUGUST

Location	Mean rainfall (mm)	Range	Coefficient of variation (%)	Sample size (n)	Change over time (mm.yr^{-1})	Strength of trend (r)
Aliwal-North Plaatkop	15.2	145.4	177.0	29	-0.15	0.05
Bethal	11.8	56.5	137.0	29	0.34	0.18
Bethlehem Wo	15.7	77.7	139.4	30	-0.72	0.30
Bloemfontein Wo	11.5	94.3	187.7	30	-0.40	0.17
Calvinia Wo	20.6	47.9	63.1	30	0.22	0.15
Cape Agulhas	50.8	113.0	52.1	30	-0.55	0.18
Cape Town Wo	76.4	138.8	45.3	30	0.43	0.11
Cedara	25.0	90.4	94.9	30	-0.34	0.12
Cradock-Mun	9.8	51.4	128.5	30	0.20	0.14
De Aar Wo	9.9	85.9	191.8	30	0.06	0.03
East London Wo	59.3	463.8	155.4	30	-0.60	0.06
Frankfort-TNK	13.0	61.6	119.6	30	-0.20	0.11
Fraserburg	5.4	40.4	132.9	30	-0.19	0.23
Johannesburg INT Wo	6.3	34.2	134.2	30	-0.09	0.09
Kimberley Wo	6.3	80.8	239.6	30	0.03	0.02
Ladysmith	15.9	73.6	118.8	30	-0.26	0.12
Langerbaanweg AWS	38.6	79.4	55.4	30	0.10	0.04
Lephalale	0.8	11.4	308.0	30	-0.12	*0.42
Mafikeng Wo	3.2	24.0	193.7	30	0.04	0.06
Makatini Research Centre	12.3	63.2	138.6	30	-0.49	0.25
Mandini	32.2	102.7	87.0	30	-0.83	0.26
Mara	0.7	7.6	220.9	30	0.03	0.19
Nelspruit	8.3	41.8	121.2	30	-0.33	0.28
Ottosdal	6.3	54.6	183.5	30	0.03	0.02
Oudtshoorn	20.5	81.4	80.9	30	0.75	*0.39
Paddock	40.9	182.3	110.8	30	-0.64	0.12
Pofadder	3.9	27.0	153.9	30	0.04	0.06
Polokwane Wo	2.9	32.0	241.4	30	-0.24	0.29
Port Elizabeth Wo	65.4	236.3	91.2	30	-0.19	0.03
Port Nolloth	9.4	46.5	100.7	30	0.13	0.12
Prieska	4.8	36.5	206.2	30	-0.02	0.02
Riversdale	38.6	147.9	77.0	30	0.23	0.07
Robertson	35.8	139.1	76.8	30	0.46	0.15
Shaleburn	23.3	77.0	86.5	30	-0.43	0.18
Skukuza	7.2	54.2	157.1	30	-0.54	*0.41
Springbok Wo	30.3	101.0	72.9	30	0.31	0.12
Sutherland	26.0	65.4	65.0	30	0.52	0.26
Twee Rivieren	0.1	3.4	538.5	30	0.01	0.20
Umtata Wo	21.3	98.1	113.8	30	0.32	0.11
Upington Wo	1.1	9.0	169.9	30	0.07	0.33
Vanwyksvlei	3.8	31.4	174.4	30	0.02	0.03
Vredendal	21.9	60.7	65.6	30	0.24	0.15
Vryburg	2.4	36.0	283.2	30	-0.02	0.03
Warmbad Towoomba	3.2	49.3	306.1	30	-0.19	0.17
Welkom	7.5	57.8	181.4	30	-0.27	0.18
Willowmore	18.2	67.5	95.6	30	0.38	0.19

B.9 SEPTEMBER

Location	Mean rainfall (mm)	Range	Coefficient of variation (%)	Sample size (n)	Change over time (mm.yr^{-1})	Strength of trend (r)
Aliwal-North Plaatkop	22.9	110.2	124.3	30	-1.52	*0.46
Bethal	23.5	124.4	138.9	29	-0.78	0.20
Bethlehem Wo	25.1	190.6	146.8	30	-1.14	0.28
Bloemfontein Wo	19.7	188.9	178.8	30	-1.56	*0.39
Calvinia Wo	13.8	70.5	115.6	30	-0.70	*0.38
Cape Agulhas	33.2	70.8	53.8	30	-0.47	0.23
Cape Town Wo	46.2	129.5	65.5	30	-0.38	0.11
Cedara	53.6	554.0	183.4	30	-2.71	0.24
Cradock-Mun	16.4	89.1	138.6	30	-0.59	0.23
De Aar Wo	16.0	86.7	151.2	30	-1.17	*0.42
East London Wo	64.4	203.3	88.7	30	-1.87	0.28
Frankfort-TNK	25.7	147.0	141.4	30	-0.55	0.13
Fraserburg	12.0	56.8	118.5	30	-0.01	0.01
Johannesburg INT Wo	23.7	175.0	159.0	30	-1.07	0.25
Kimberley Wo	13.6	70.0	151.7	30	-0.63	0.27
Ladysmith	25.0	117.8	115.8	30	-0.35	0.10
Langerbaanweg AWS	24.6	56.0	69.7	30	-0.28	0.14
Lephalale	4.5	44.4	215.8	30	-0.28	0.25
Mafikeng Wo	11.2	52.6	140.7	30	-0.31	0.17
Makatini Research Centre	25.1	138.8	135.6	30	-0.49	0.13
Mandini	67.4	645.7	166.5	30	-3.40	0.26
Mara	7.5	54.2	158.9	30	0.27	0.20
Nelspruit	26.9	191.4	149.1	30	0.06	0.01
Ottosdal	18.7	197.0	208.5	30	-1.45	0.32
Oudtshoorn	13.2	69.1	118.9	30	-0.38	0.21
Paddock	100.9	900.5	160.0	30	-4.74	0.25
Pofadder	4.4	25.0	152.4	30	-0.34	*0.44
Polokwane Wo	4.9	23.3	137.9	30	0.03	0.03
Port Elizabeth Wo	48.6	99.3	57.7	30	-0.72	0.22
Port Nolloth	5.6	21.5	110.4	30	-0.08	0.11
Prieska	8.6	92.6	219.9	30	-0.47	0.22
Riversdale	29.6	75.2	59.6	30	-0.20	0.10
Robertson	19.1	38.6	58.4	30	0.05	0.04
Shaleburn	42.7	311.5	131.1	30	-1.17	0.18
Skukuza	16.0	82.6	132.8	30	-0.0002	0.0001
Springbok Wo	17.7	70.6	99.8	30	-0.27	0.13
Sutherland	15.2	78.8	113.7	30	-0.96	*0.48
Twee Rivieren	2.7	22.0	181.4	30	-0.14	0.25
Umtata Wo	36.7	158.6	107.1	30	-0.45	0.10
Upington Wo	4.4	22.7	146.4	30	-0.19	0.26
Vanwyksvlei	8.4	73.7	179.2	30	-0.37	0.21
Vredendal	11.9	40.6	85.4	30	-0.33	0.28
Vryburg	15.7	128.0	174.7	30	-0.88	0.28
Warmbad Towoomba	11.8	71.3	153.8	30	-0.13	0.06
Welkom	14.4	178.9	228.2	30	-1.32	*0.37
Willowmore	11.9	83.0	167.4	30	-0.21	0.09

B.10 OCTOBER

Location	Mean rainfall (mm)	Range	Coefficient of variation (%)	Sample size (n)	Change over time (mm.yr^{-1})	Strength of trend (r)
Aliwal-North Plaatkop	42.3	175.2	103.6	30	-0.59	0.12
Bethal	87.0	311.2	69.5	29	1.09	0.15
Bethlehem Wo	75.9	223.0	73.0	30	-1.20	0.19
Bloemfontein Wo	46.0	215.6	106.1	30	-1.45	0.26
Calvinia Wo	10.5	65.9	155.0	30	-0.48	0.25
Cape Agulhas	32.8	100.2	76.7	30	-0.16	0.06
Cape Town Wo	27.9	97.5	90.8	30	-0.67	0.23
Cedara	85.8	189.2	47.6	30	-0.73	0.15
Cradock-Mun	26.6	106.0	84.7	30	0.55	0.21
De Aar Wo	20.0	176.9	158.6	30	-0.68	0.19
East London Wo	92.0	290.4	75.0	29	-0.30	0.04
Frankfort-TNK	72.0	175.2	64.2	30	-1.74	0.33
Fraserburg	12.0	63.0	140.3	30	-0.04	0.02
Johannesburg INT Wo	68.4	177.3	57.5	30	-0.89	0.20
Kimberley Wo	32.0	160.6	116.2	30	-0.89	0.21
Ladysmith	61.7	171.8	67.0	30	-0.98	0.21
Langerbaanweg AWS	12.9	55.8	104.7	30	-0.24	0.15
Lephalale	30.9	98.5	85.7	30	0.29	0.10
Mafikeng Wo	37.0	134.0	87.4	30	-1.24	0.33
Makatini Research Centre	66.4	151.0	60.9	30	-1.35	0.29
Mandini	95.7	181.2	47.0	30	-1.35	0.26
Mara	36.5	129.4	88.4	30	-0.67	0.18
Nelspruit	53.8	122.0	56.5	30	-0.33	0.10
Ottosdal	46.7	133.2	83.4	30	-1.82	*0.41
Oudtshoorn	25.7	89.4	88.1	30	-0.45	0.17
Paddock	124.3	271.0	55.4	30	-0.26	0.03
Pofadder	6.2	41.2	144.6	30	-0.15	0.15
Polokwane Wo	40.5	101.5	63.6	30	0.18	0.06
Port Elizabeth Wo	58.8	195.0	77.0	30	-0.14	0.03
Port Nolloth	4.5	22.5	115.8	30	-0.10	0.16
Prieska	13.5	114.1	164.3	30	-0.69	0.27
Riversdale	52.4	118.4	72.6	30	0.02	0.01
Robertson	28.3	82.1	86.3	30	0.19	0.07
Shaleburn	81.2	158.7	47.5	30	-0.85	0.19
Skukuza	37.3	85.2	67.0	30	-0.27	0.09
Springbok Wo	9.7	43.5	124.4	30	-0.28	0.20
Sutherland	12.2	63.1	113.3	30	-0.24	0.15
Twee Rivieren	8.8	28.8	101.7	30	0.04	0.04
Umtata Wo	61.8	127.2	51.8	30	-0.14	0.04
Upington Wo	15.3	87.3	134.0	30	0.02	0.01
Vanwyksvlei	10.9	72.5	139.1	30	-0.22	0.12
Vredendal	8.2	30.2	119.9	30	-0.23	0.20
Vryburg	29.2	96.0	98.5	30	-1.18	0.35
Warmbad Towoomba	56.5	133.0	63.1	30	-0.42	0.10
Welkom	38.9	176.6	97.8	30	-1.83	*0.42
Willowmore	17.2	57.8	94.5	30	0.17	0.09

B.11 NOVEMBER

Location	Mean rainfall (mm)	Range	Coefficient of variation (%)	Sample size (n)	Change over time (mm.yr^{-1})	Strength of trend (r)
Aliwal-North Plaatkop	68.9	234.2	76.7	30	-0.85	0.14
Bethal	110.9	230.3	50.8	29	-0.33	0.05
Bethlehem Wo	97.7	245.6	62.7	30	-0.65	0.09
Bloemfontein Wo	67.4	158.2	68.6	30	0.42	0.08
Calvinia Wo	11.2	85.7	176.2	30	-0.21	0.09
Cape Agulhas	27.6	85.6	78.0	30	0.95	*0.38
Cape Town Wo	24.9	84.3	86.3	30	0.84	0.34
Cedara	109.1	240.9	47.3	30	-0.49	0.08
Cradock-Mun	44.7	133.5	74.5	30	-1.36	0.35
De Aar Wo	30.8	92.7	77.4	30	-0.30	0.11
East London Wo	112.1	348.5	73.5	30	-1.40	0.15
Frankfort-TNK	86.8	223.8	63.0	30	-1.16	0.18
Fraserburg	17.8	67.8	118.2	30	0.31	0.13
Johannesburg INT Wo	103.5	210.0	51.6	30	0.19	0.03
Kimberley Wo	39.9	139.4	77.2.0	30	-0.10	0.03
Ladysmith	76.2	180.2	59.8	30	-2.09	*0.40
Langerbaanweg AWS	10.4	35.5	99.7	30	0.28	0.23
Lephalale	61.4	165.8	68.4	30	0.24	0.05
Mafikeng Wo	61.0	209.5	81.0	30	-1.30	0.23
Makatini Research Centre	90.5	200.1	56.7	30	-0.85	0.14
Mandini	124.7	464.4	75.1	30	-2.14	0.20
Mara	81.4	185.4	57.7	30	0.42	0.08
Nelspruit	89.8	219.2	60.1	29	-0.11	0.02
Ottosdal	61.8	107.2	47.6	30	0.03	0.01
Oudtshoorn	22.9	105.5	121.4	30	-0.08	0.02
Paddock	146.9	443.2	67.2	30	-1.38	0.12
Pofadder	7.8	64.6	192.1	30	0.02	0.01
Polokwane Wo	93.1	214.2	47.1	30	-0.15	0.03
Port Elizabeth Wo	56.3	231.2	86.2	30	-0.21	0.04
Port Nolloth	3.1	17.2	146.7	30	0.13	0.25
Prieska	18.1	62.4	106.0	30	-0.31	0.14
Riversdale	50.2	200.9	94.2	30	0.85	0.16
Robertson	27.7	148.4	118.3	30	1.20	0.32
Shaleburn	115.2	233.5	40.8	30	-0.26	0.05
Skukuza	89.5	221.8	66.2	30	0.77	0.11
Springbok Wo	10.9	52.0	124.6	30	0.36	0.23
Sutherland	15.2	88.6	123.8	30	-0.21	0.10
Twee Rivieren	16.7	67.2	104.4	30	-0.38	0.19
Umtata Wo	88.0	188.1	57.6	30	-1.01	0.17
Upington Wo	14.5	82.5	112.8	30	0.03	0.01
Vanwyksvlei	16.2	102.0	148.3	30	-0.21	0.08
Vredendal	7.0	49.4	142.5	30	0.10	0.09
Vryburg	45.2	111.9	72.9	30	0.17	0.04
Warmbad Towoomba	87.4	173.5	52.6	30	-0.58	0.11
Welkom	58.2	138.8	69.1	30	-0.66	0.14
Willowmore	31.8	152.5	111.9	30	-0.21	0.05

B.12 DECEMBER

Location	Mean rainfall (mm)	Range	Coefficient of variation (%)	Sample size (n)	Change over time (mm.yr^{-1})	Strength of trend (r)
Aliwal-North Plaatkop	64.0	152.6	75.5	30	0.30	0.05
Bethal	137.7	189.0	34.6	29	-0.76	0.13
Bethlehem Wo	116.5	248.9	46.9	30	1.15	0.18
Bloemfontein Wo	69.2	154.4	64.4	30	0.63	0.12
Calvinia Wo	12.5	73.9	148.3	30	0.30	0.14
Cape Agulhas	17.4	66.8	98.4	30	-0.55	0.28
Cape Town Wo	13.3	44.4	81.8	30	-0.22	0.17
Cedara	126.8	353.2	54.3	30	-2.68	0.34
Cradock-Mun	43.9	123.6	78.5	30	0.10	0.02
De Aar Wo	36.5	196.6	103.7	30	1.05	0.24
East London Wo	82.9	237.4	69.0	30	-0.41	0.06
Frankfort-TNK	102.7	249.8	55.4	30	2.08	0.32
Fraserburg	23.7	90.0	101.0	30	0.02	0.01
Johannesburg INT Wo	130.1	174.9	37.4	30	1.44	0.26
Kimberley Wo	52.8	160.2	69.9	30	-0.15	0.03
Ladysmith	118.0	267.0	48.6	30	-0.34	0.05
Langerbaanweg AWS	7.0	30.6	102.5	30	-0.08	0.09
Lephalale	90.9	175.1	50.3	30	-0.28	0.05
Mafikeng Wo	92.9	163.4	46.0	30	-0.54	0.11
Makatini Research Centre	79.4	194.2	51.2	29	-1.69	0.36
Mandini	95.2	218.2	50.8	30	-1.34	0.24
Mara	81.7	181.8	54.0	30	-0.43	0.08
Nelspruit	119.2	259.2	52.7	30	1.18	0.16
Ottosdal	96.3	158.8	44.1	30	1.42	0.29
Oudtshoorn	20.9	80.6	105.3	30	-0.33	0.13
Paddock	143.6	366.2	52.5	30	0.16	0.02
Pofadder	8.3	53.7	172.6	30	0.06	0.03
Polokwane Wo	93.9	192.9	50.1	30	1.23	0.23
Port Elizabeth Wo	42.1	176.6	91.1	30	-0.34	0.08
Port Nolloth	1.5	9.0	134.5	30	0.05	0.21
Prieska	27.1	121.2	111.1	29	0.70	0.20
Riversdale	34.2	201.5	114.2	30	-0.89	0.20
Robertson	18.6	62.9	95.4	30	-0.79	*0.39
Shaleburn	170.2	230.4	34.5	30	-2.01	0.30
Skukuza	109.5	187.5	46.7	30	-0.78	0.13
Springbok Wo	4.4	18.8	124.0	30	-0.14	0.22
Sutherland	19.7	86.3	125.2	30	0.09	0.03
Twee Rivieren	32.1	129.2	90.3	30	0.43	0.13
Umtata Wo	98.7	249.1	61.1	30	-2.34	0.34
Upington Wo	20.4	74.0	110.1	30	0.03	0.01
Vanwyksvlei	20.2	87.4	126.6	30	-0.22	0.08
Vredendal	9.3	82.0	198.4	30	0.42	0.20
Vryburg	64.4	125.9	51.3	30	-0.55	0.15
Warmbad Towoomba	118.6	225.7	37.7	30	-1.26	0.24
Welkom	74.5	132.2	53.2	30	-0.58	0.13
Willowmore	35.3	92.4	83.4	30	-0.55	0.16

B.13 SUMMARY OF THE CHANGE POINTS DETECTED FOR MONTHLY RAINFALL

Summary of the change points and trends before and after change point(s) in monthly rainfall for each weather station for the period 1987-2016. Trends with a *p value* of less than 0.05 are significant and are highlighted by an asterisk (*). Only significant change points were captured, and the year reported represents the first year after the change point occurred. Change points are also colour coded, where green represents CUSUM test change points, orange represents Pettitt test change points and grey represents where both tests agreed on the change points.

Location	Change point(s; *p value*)	Trend before and after
	Month: January	
ELW	2012 (0.010)	2.45 (0.37; 0.068); -2.24 (0.19; 0.765)
PEW	1993 (0.025); 2009 (0.049)	1.04 (0.31; 0.549); 0.58 (0.11; 0.688); 1.10 (0.39; 0.345)
	Month: February	
BET	2007 (0.038)	1.93 (0.20; 0.399); -0.29 (0.04; 0.919)
	Month: March	
MAN	1997 (0.030)	-5.02 (0.24; 0.499); 1.92 (0.26; 0.269)
SHA	2008 (0.024)	-2.30 (0.20; 0.386); -7.14 (0.49; 0.179)
VRY	1992 (0.025)	13.72 (0.41; 0.487); -0.47 (0.09; 0.666)
	Month: April	
CAG	2007 (0.017)	-1.55 (0.20; 0.387); -0.08 (0.02; 0.951)
ELW	1995 (0.037)	-2.95 (0.29; 0.479); 1.20 (0.15; 0.519)
FTN	1991 (0.010)	1.21 (0.06; 0.937); 0.42 (0.09; 0.793)
JIW	2014 (0.019)	0.78 (0.18; 0.357); -2.10 (0.20; 0.873)
MWO	1991 (0.0004)	20.8 (0.74; 0.263); 0.34 (0.06; 0.752)
VRE	2008 (0.044)	-0.42 (0.17; 0.451); 0.66 (0.42; 0.258)
WEL	2003 (0.008)	0.36 (0.05; 0.854); -0.49 (0.14; 0.635)
	Month: May	
LAD	1996 (0.040)	-0.10 (0.17; 0.654); -1.72 (0.58; *0.007)
PEW	1996 (0.049)	3.03 (0.72; *0.029); -0.18 (0.02; 0.927)
WTO	1995 (0.030)	0.01 (0.01; 0.986); -1.84 (0.61; *0.002)
	Month: June	
ANP	2008 (0.040)	-0.45 (0.27; 0.243); -6.03 (0.57; 0.111)
OUD	1993 (0.040); 2009 (0.010)	0.93 (0.40; 0.434); 0.61 (0.40; 0.121); -1.35 (0.27; 0.525)
RIV	1993 (0.030); 2005 (0.030)	1.77 (0.27; 0.600); 0.49 (0.18; 0.574); 1.33 (0.20; 0.542)
ROB	1998 (0.030); 2009 (0.020)	0.11 (0.03; 0.941); 1.43 (0.43; 0.183); 2.85 (0.38; 0.357)
VRE	2007 (0.096)	-0.99 (0.40; 0.078); -0.39 (0.08; 0.823)
WIL	2008 (C: 0.040; P: 0.017)	-0.07 (0.05; 0.836); -1.13 (0.25; 0.515)
	Month: August	
CED	2001 (0.007)	-3.05 (0.47; 0.090); -0.80 (0.17; 0.524)
FRA	2004 (0.030)	0.56 (0.33; 0.196); 0.20 (0.31; 0.303)
OUD	2002 (0.025)	0.60 (0.35; 0.199); -1.35 (0.31; 0.262)
RIV	2001 (0.020)	-1.54 (0.34; 0.235); -1.57 (0.20; 0.456)
	Month: September	
MAR	1996 (0.039)	-0.79 (0.45; 0.227); 0.15 (0.07; 0.773)
	Month: October	
OTT	2010 (0.006)	0.24 (0.04; 0.841); 1.93 (0.50; 0.254)
VRY	2004 (0.050)	1.23 (0.19; 0.454); -0.52 (0.13; 0.662)
	Month: November	
SKU	1997 (0.030)	3.85 (0.28; 0.440); -5.64 (0.54; *0.013)
	Month: December	
CED	2002 (0.023)	5.63 (0.29; 0.286); -1.45 (0.25; 0.369)
FRA	1995 (0.024)	-2.33 (0.25; 0.544); -0.61 (0.16; 0.484)
MRC	2008 (0.023)	0.76 (0.13; 0.587); 1.50 (0.14; 0.726)
MAR	1994 (0.038)	7.08 (0.25; 0.593); 1.14 (0.21; 0.345)
SWO	2000 (0.031)	0.39 (0.27; 0.380); 0.18 (0.19; 0.476)

APPENDIX C: CLUSTER ANALYSIS OF MONTHLY RAINFALL, RAIN DAYS AND RESPECTIVE VARIABILITY

C.1: MONTHLY RAINFALL AND VARIABILITY

The cluster analysis validation results for the period of 1987-2016 mean monthly rainfall and monthly CV using Ward's minimum variance algorithm and the squared Eucliedean distance are presented here. This includes the cophenetic correlation coefficient which is 0.6020, and tables of the average silhouette widths. These results are the validation results of the cluster analysis results presented under *section 5.4.1*.The outputs regarding the optimal number of cluster groups are presented below. This consists of the average silhouette width across the tested cluster numbers 2 to 10. The highest average silhouette width is 0.29 for five cluster groups, being the optimal number of cluster groups across the 46 weather stations.

Number of clusters	Average silhouette width
2	0.20
3	0.22
4	0.22
5	**0.29**
6	0.19
7	0.19
8	0.18
9	0.18
10	0.17

The table below presents the validation results, being the average silhouette width, of the monthly rainfall and CV of the cluster groups 1 to 5, to determine the optimal number of season groupings.

Number of clusters	Average silhouette width
Group 1: steppe (subtropical), relatively dry climate	
1	0.25
2	**0.57**
3	0.41
4	0.37
Group 2: wetter temperate climate	
1	0.30
2	**0.58**
3	0.35
4	0.32
Group 3: oceanic, temperate, dry climate	
1	0.21
2	**0.33**
3	0.29
4	0.28
Group 4: oceanic, arid, desert climate	
1	0.21
2	**0.46**
3	0.31
4	0.29
Group 5: arid, desert climate	
1	0.18
2	**0.34**
3	0.24
4	0.20

The table below presents the strength of seasonal clustering for groups 1 to 5, as the cophenetic correlation coefficient.

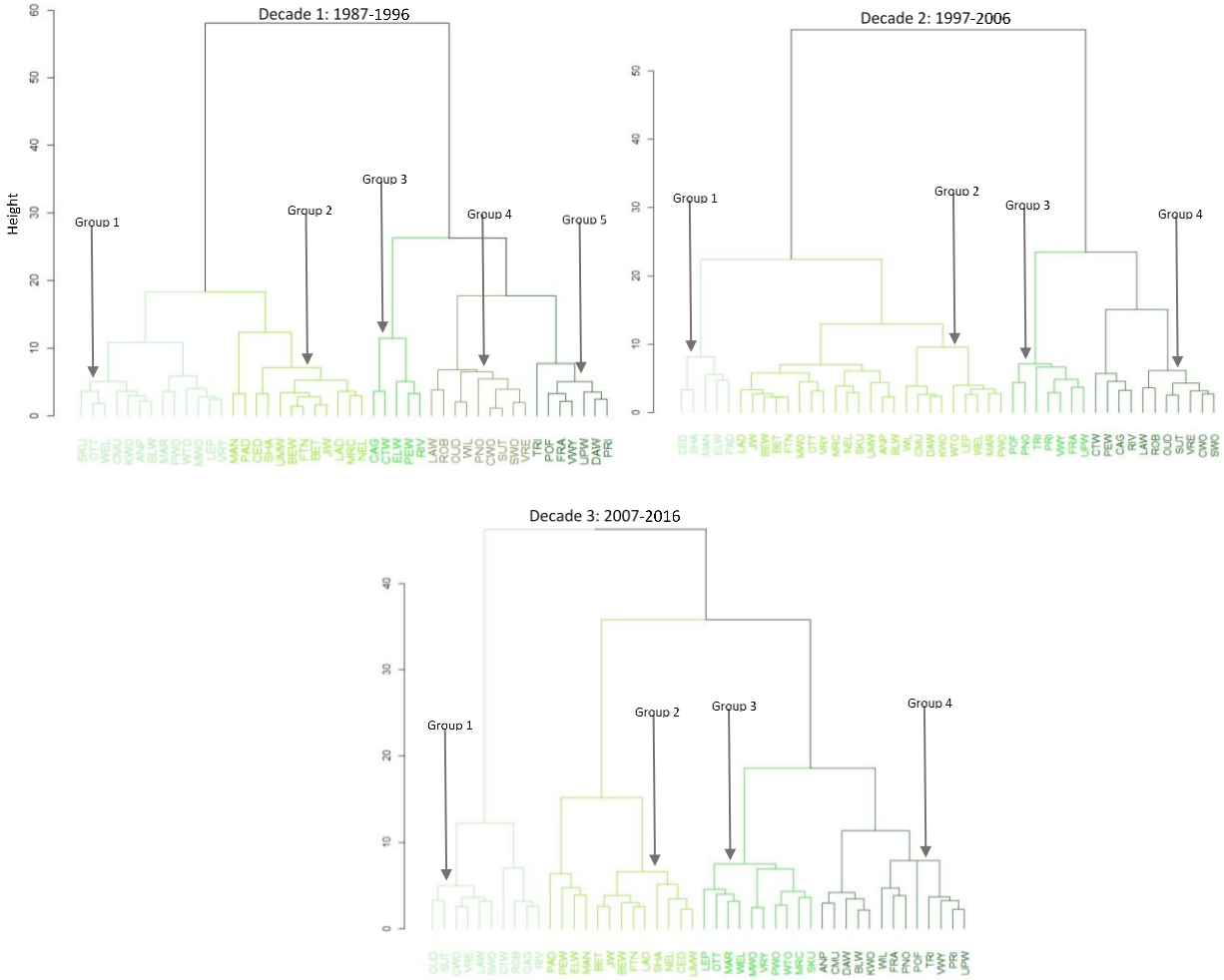
Cluster group	Cophenetic correlation coefficient
1	0.8353
2	0.8762
3	0.6431
4	0.7165
5	0.7079

C.2: DECADAL MONTHLY RAINFALL AND VARIABILITY

This appendix section presents the results of the decadal (i.e. 1987-1996; 1997-2006; 2007-2016) clustering of mean monthly rainfall and CV using the **Ward's minimum variance algorithm and the squared Eucliedean distance**. The results presented include the overall dendrograms for each period with the associated validation results

(i.e. cophenetic correlation coefficient) and the associated spatial distribution of the optimal number of cluster groups per decade. The within group clusters are also presented to demonstrate the seasonal groupings within each of the clusters. This is presented with box plots of each of the main cluster groupings identified in the first dendrograms presented. Finally, the location specific seasonality classifications are also presented for each decade.

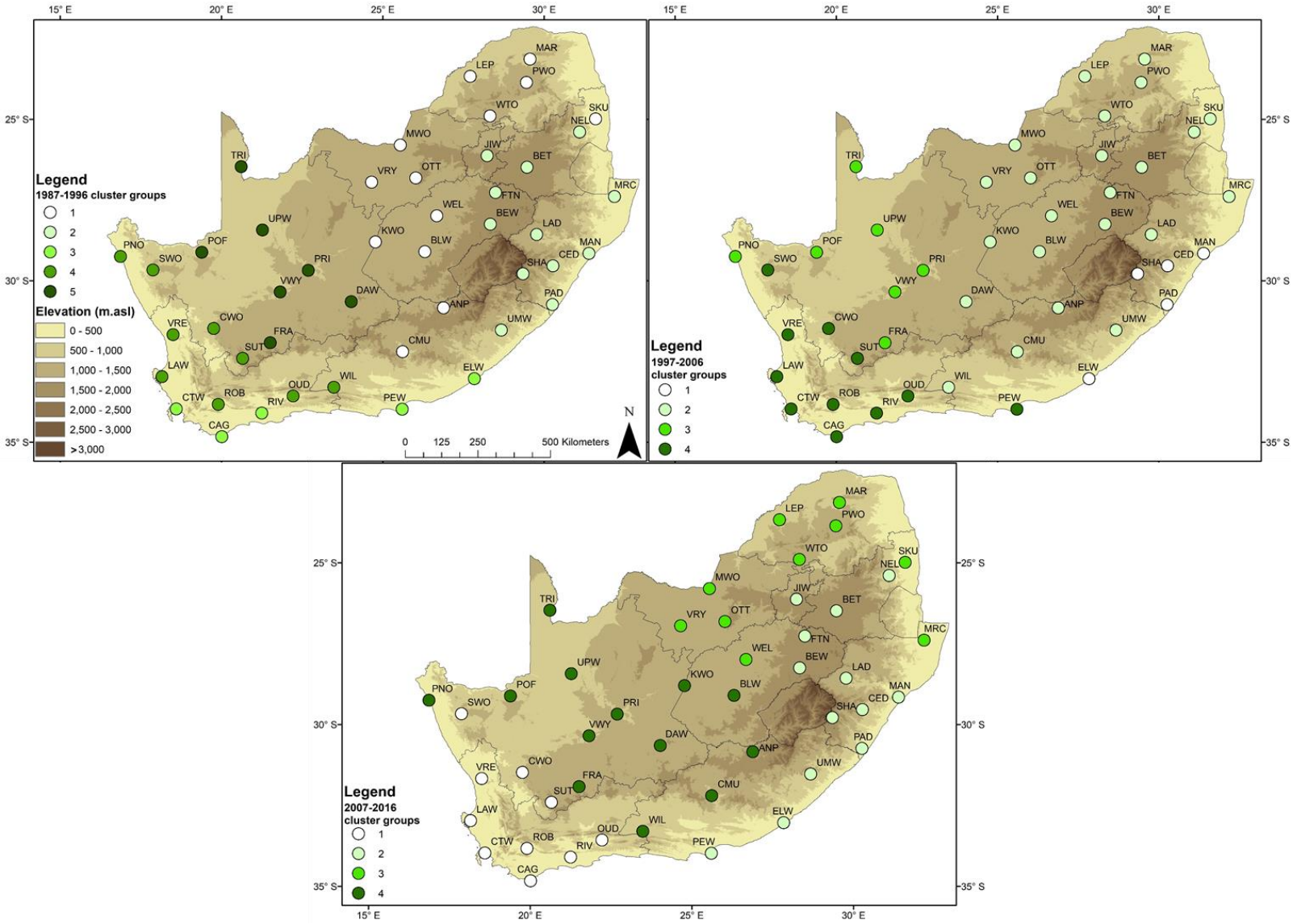
The figure below displays a colour coded dendrogram for each of the three decades of the cluster analysis of mean monthly rain days and associated CV. This figure is colour coded according to the optimal number of cluster groups and is labelled using the weather station codes.



The validation statistics of the decadal cluster analyses are presented below as the overall cophenetic correlation coefficient demonstrating the strength of the cluster solution, and as the average silhouette widths used to determine the optimal number of cluster groups, which was five for decdade one and four for decade two and three

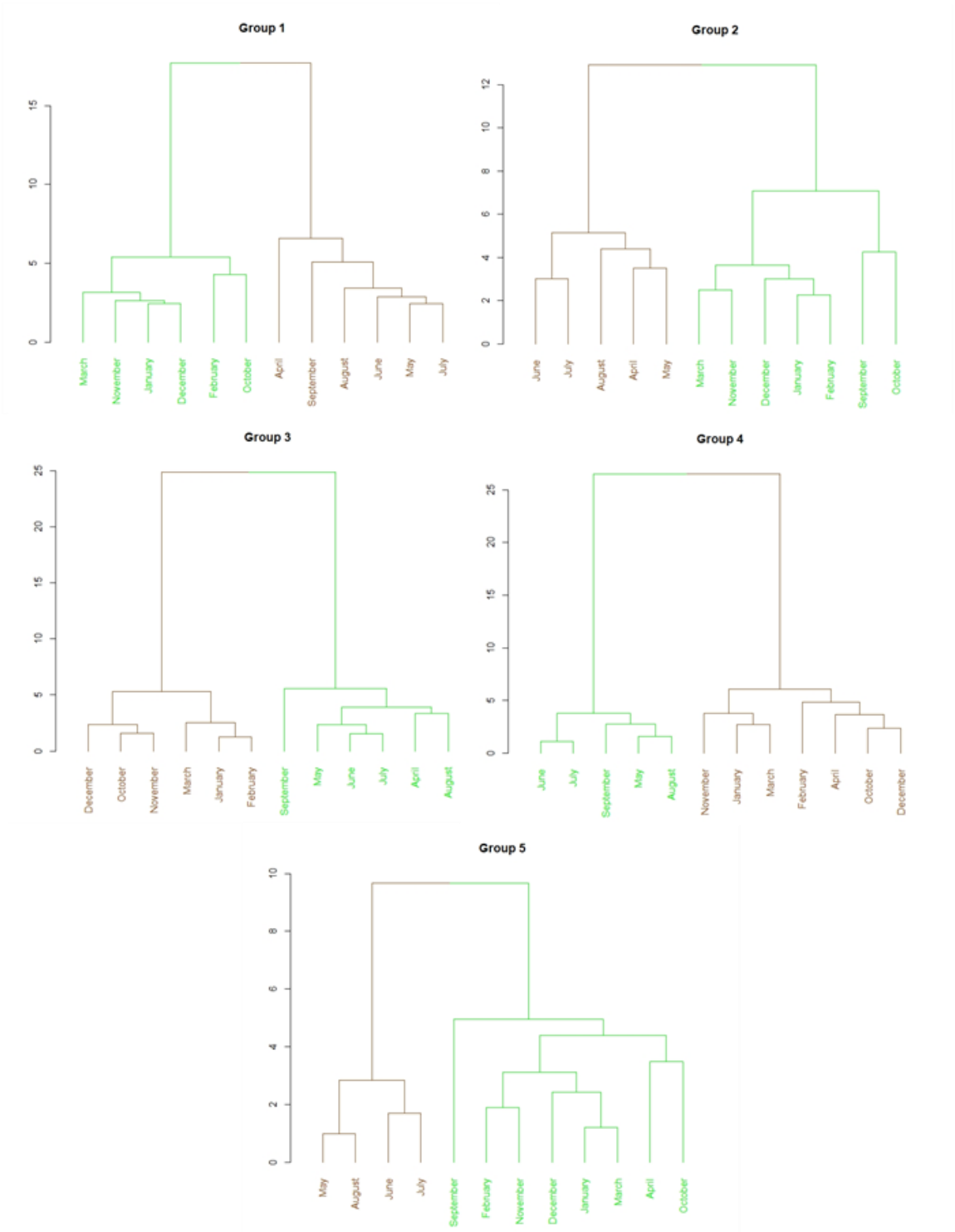
Decade	1: 1987-1996	2: 1997-2006	3: 2007-2016
Cophenetic correlation coefficient	0.5928	0.6444	0.6094
Number of clusters	Average silhouette width	Average silhouette width	Average silhouette width
2	0.19	0.25	0.25
3	0.19	0.27	0.24
4	0.29	**0.29**	**0.27**
5	**0.39**	0.25	0.25
6	0.20	0.17	0.20
7	0.22	0.17	0.18
8	0.23	0.18	0.18
9	0.23	0.19	0.18
10	0.23	0.18	0.18

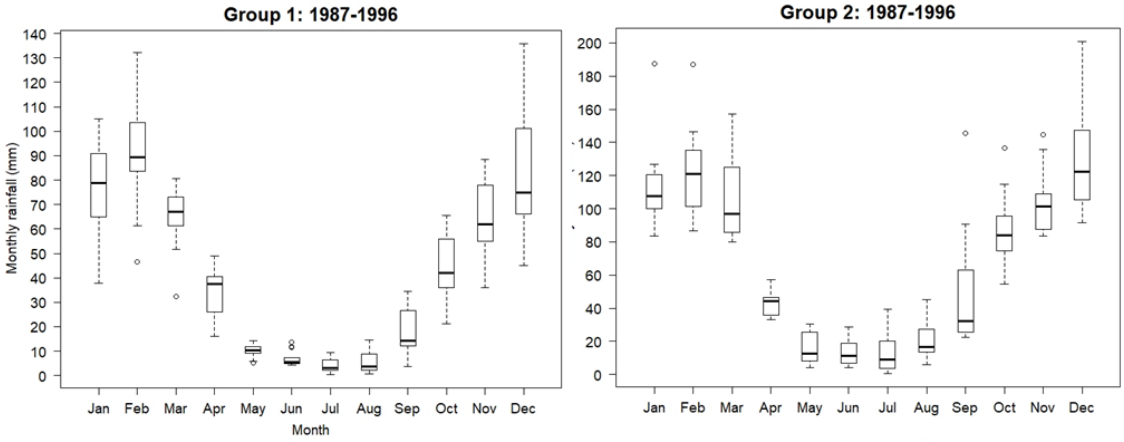
The maps below present the spatial distribution of the cluster groups per decade based on the above dendrograms.



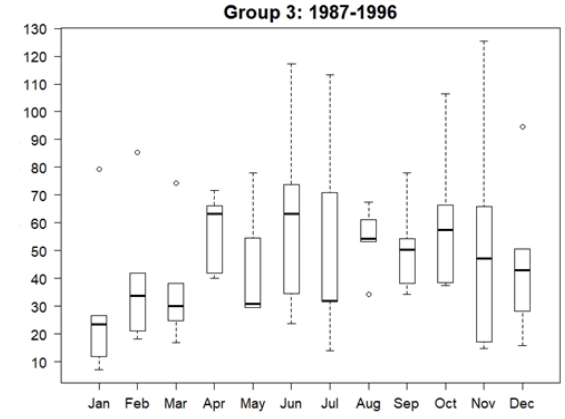
The box plots and withinin group cluster dendrograms are presented below per decade (i.e. 1987-1996; 1997-2006; 2007-2016). The dendrograms below demonstrate the duration of the average wet and dry seasons per cluster group per decade. The boxplots below display the mean monthly rainfall across the weather stations in the respective cluster groups which are marked in the dendrogram above. Circles represent outliers.

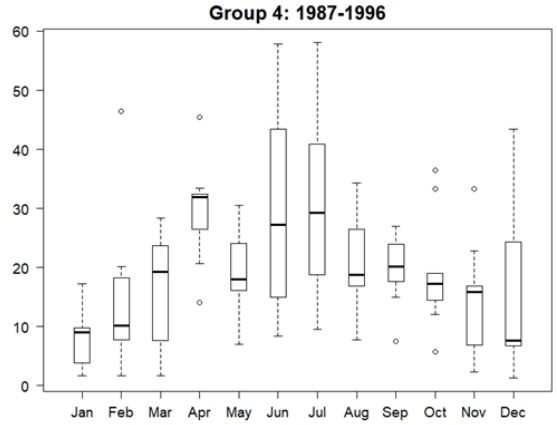
DECADE 1: 1987-1996

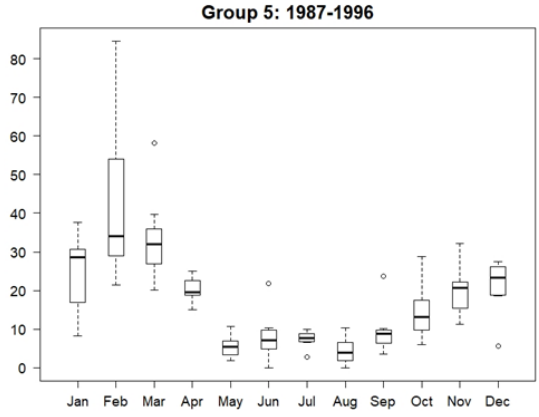



Group 1: 1987-1996
Monthly rainfall (mm)
Month
Jan Feb Mar Apr May Jun Jul Aug Sep Oct Nov Dec

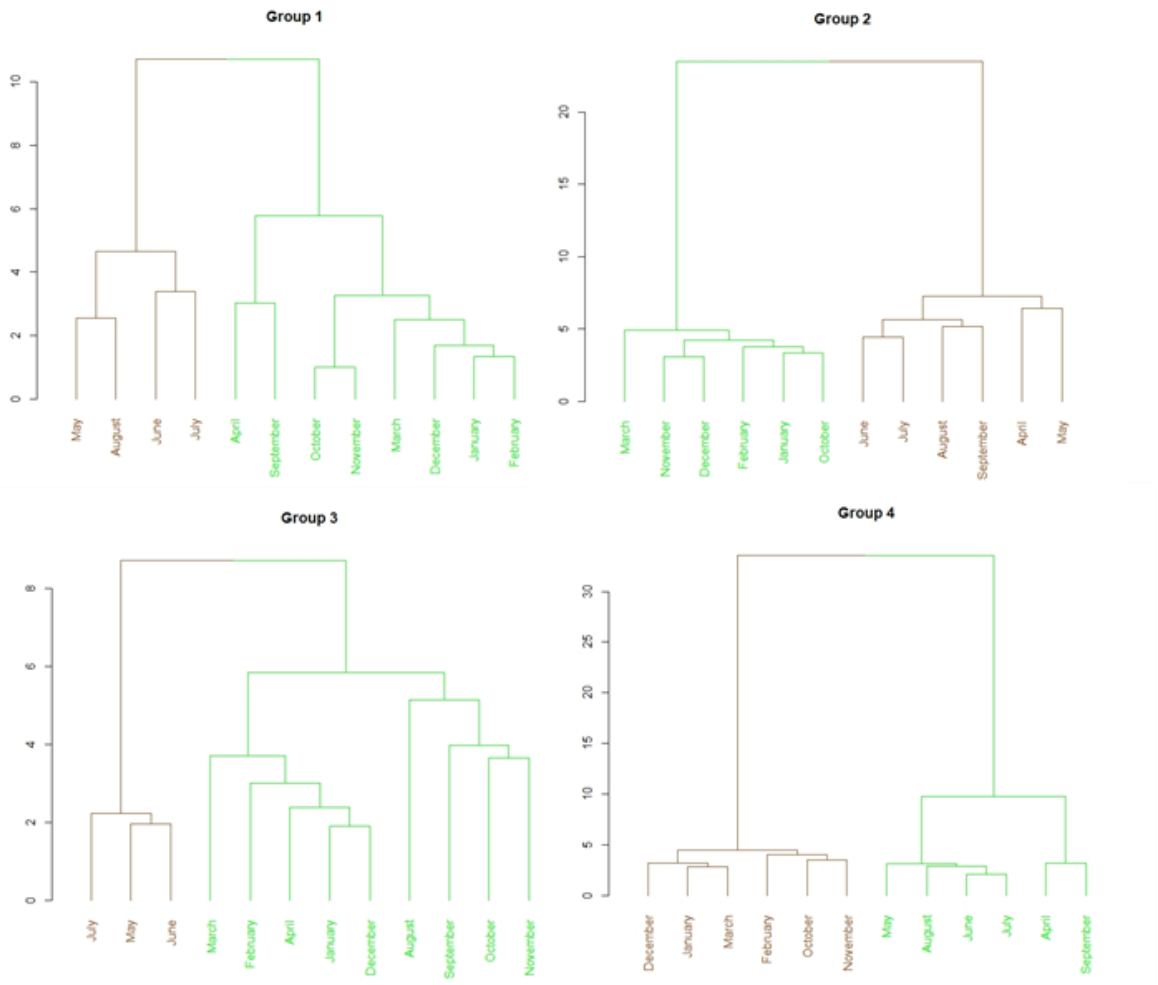
Group 2: 1987-1996
Jan Feb Mar Apr May Jun Jul Aug Sep Oct Nov Dec

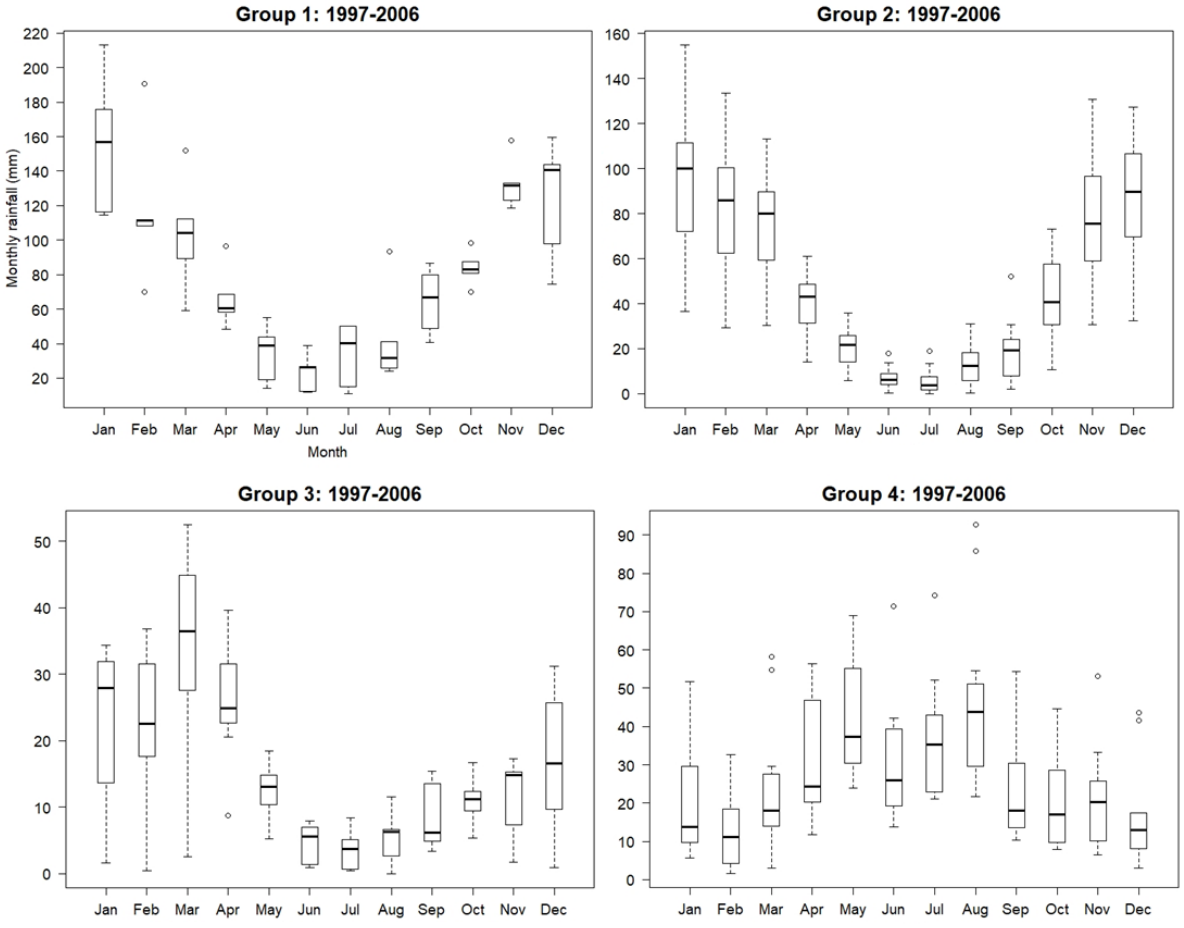

Group 3: 1987-1996
Jan Feb Mar Apr May Jun Jul Aug Sep Oct Nov Dec


Group 4: 1987-1996
Jan Feb Mar Apr May Jun Jul Aug Sep Oct Nov Dec

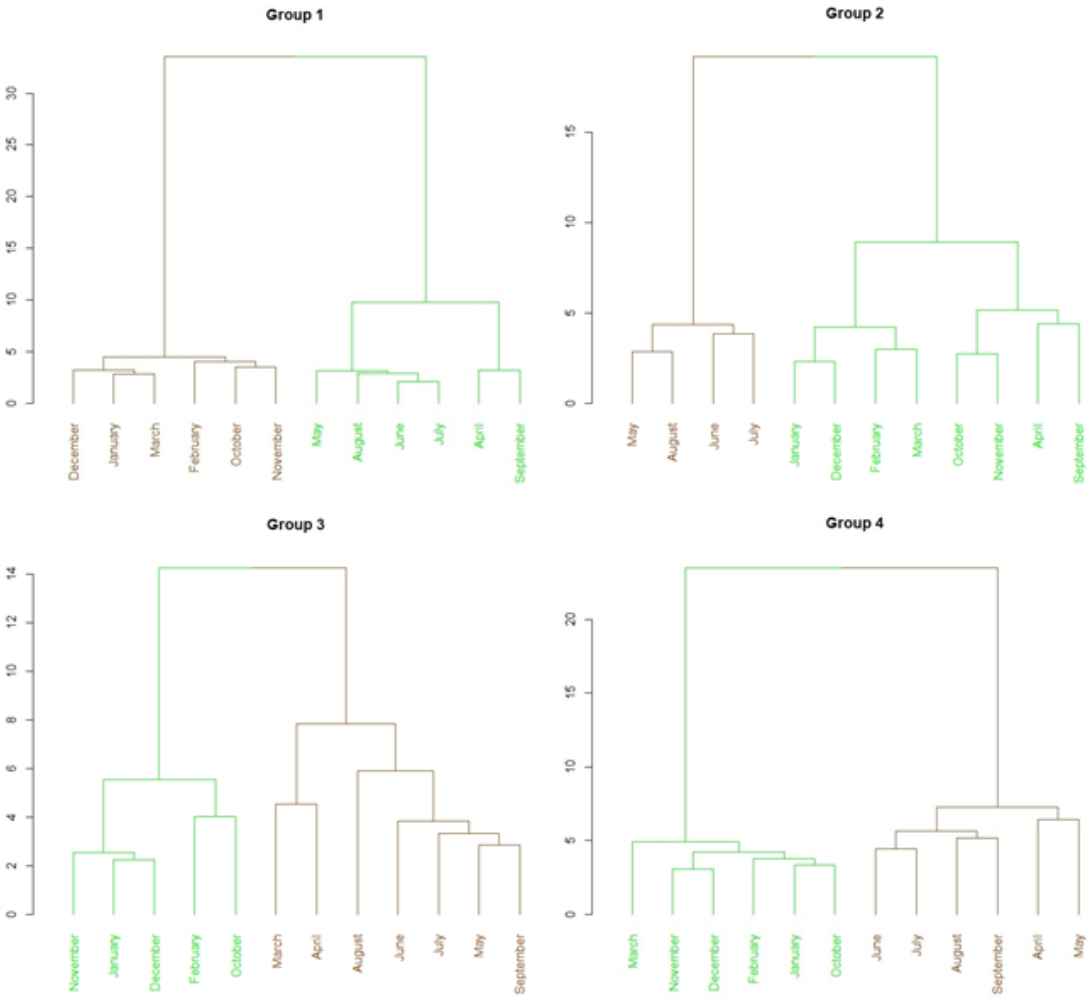

Group 5: 1987-1996
Jan Feb Mar Apr May Jun Jul Aug Sep Oct Nov Dec

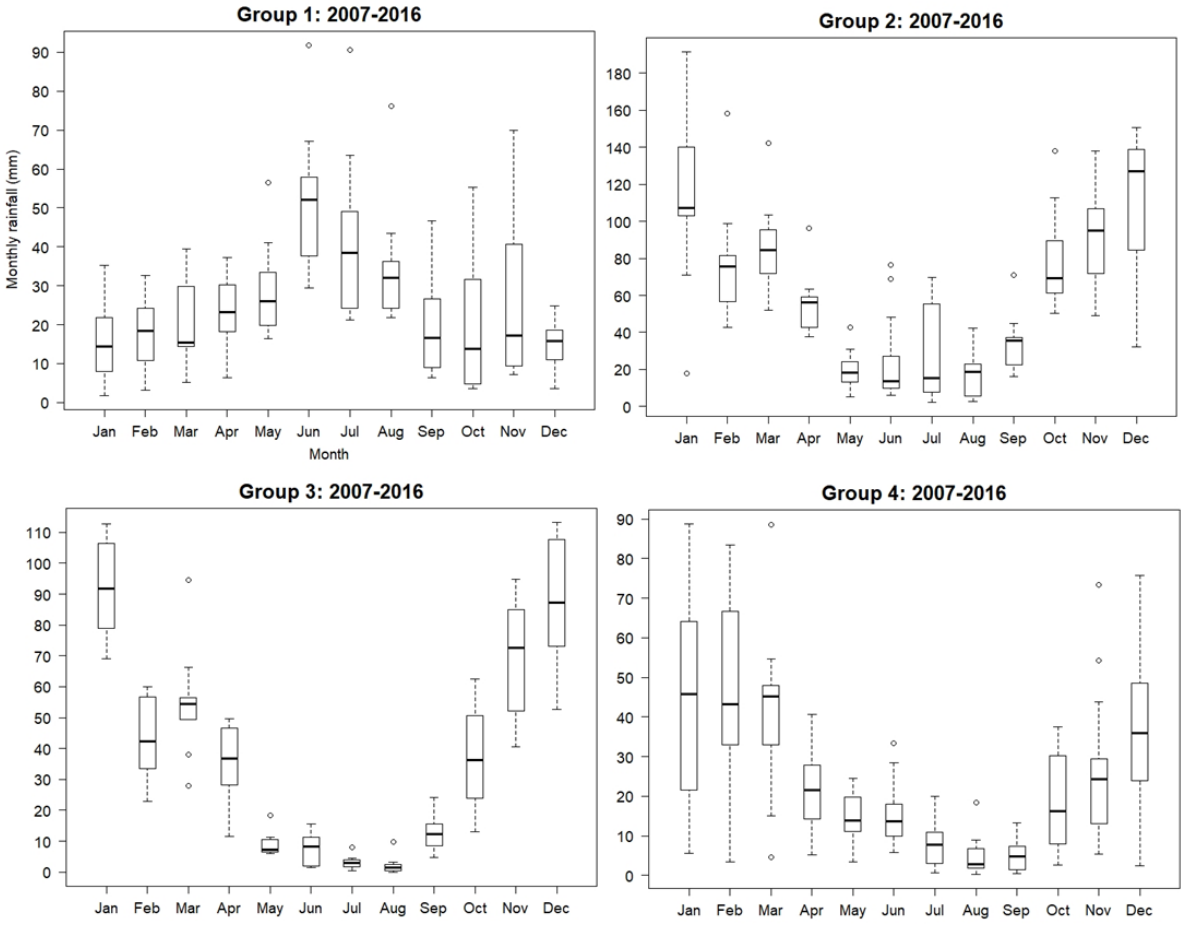
DECADE 2: 1997-2006




Group 1: 1997-2006
Monthly rainfall (mm)
Month
Jan Feb Mar Apr May Jun Jul Aug Sep Oct Nov Dec
Group 2: 1997-2006
Group 3: 1997-2006
Group 4: 1997-2006

DECADE 3: 2007-2016




Group 1: 2007-2016
Monthly rainfall (mm)
Month
Jan Feb Mar Apr May Jun Jul Aug Sep Oct Nov Dec
Group 2: 2007-2016
Jan Feb Mar Apr May Jun Jul Aug Sep Oct Nov Dec
Group 3: 2007-2016
Jan Feb Mar Apr May Jun Jul Aug Sep Oct Nov Dec
Group 4: 2007-2016
Jan Feb Mar Apr May Jun Jul Aug Sep Oct Nov Dec

The tables below present the validation results of the within group seasonal cluster per decade as the overall cophenetic correlation coefficients and as the average silhouette widths.

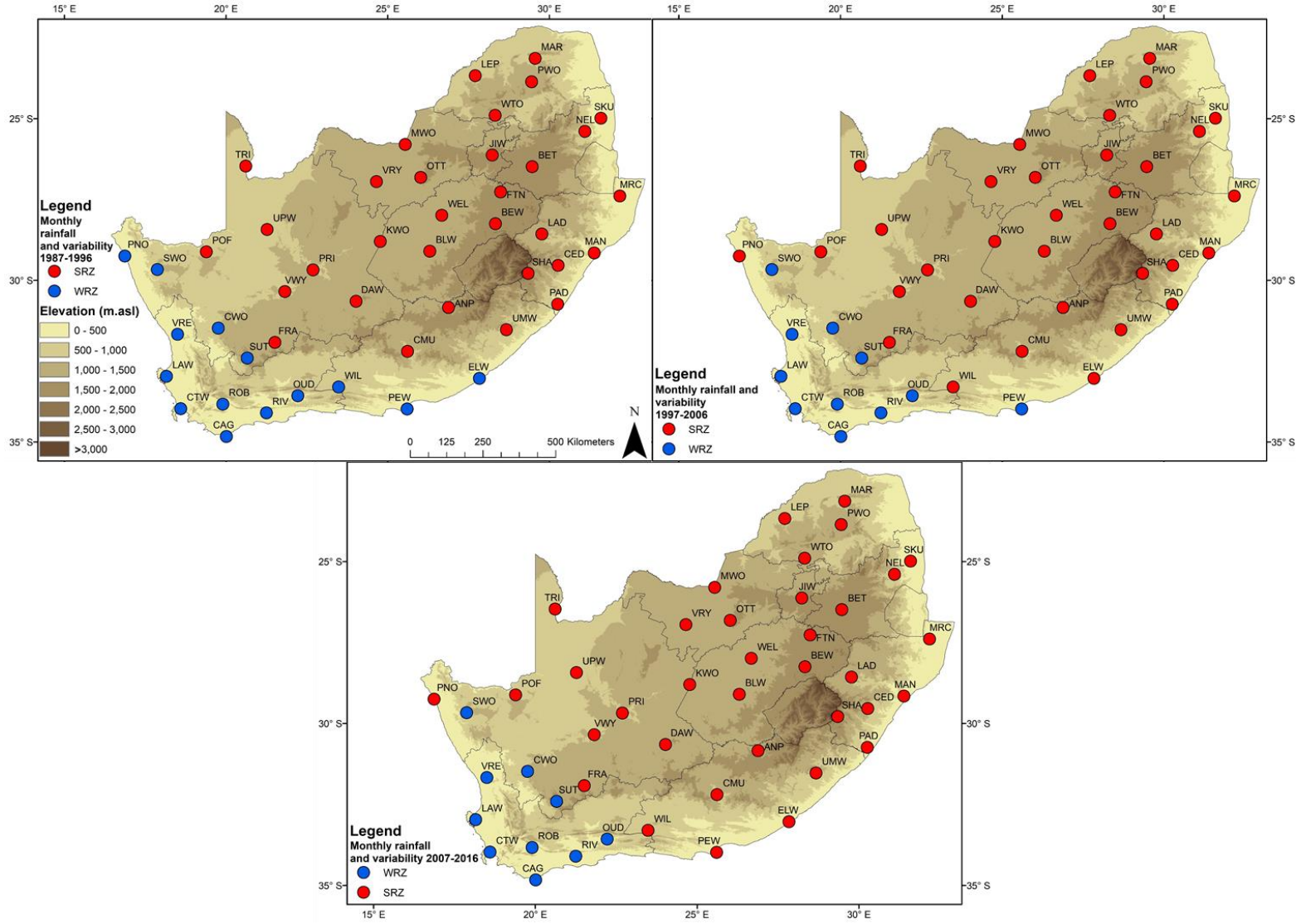
This first table presents the cophenetic correlation coefficient quantifying the strength of the respective cluster solutions associated with the above seasonal dendrograms

	Cophenetic correlation coefficient		
Cluster group	1987-1996	1997-2006	2007-2016
1	0.8548	0.8369	0.8654
2	0.7100	0.8836	0.8064
3	0.8673	0.6075	0.6381
4	0.7940	0.8588	0.6470
5	0.5890	-	-

This second table presents the average silhouette width associated with n cluster groups, to determine the optimal number of seasonal groupings for the seasonal dendrograms presented earlier.

Number of clusters	Average silhouette width 1987-1996	Average silhouette width 1997-2006	Average silhouette width 2007-2016
		Group 1	
1	0.21	0.27	0.30
2	**0.37**	**0.34**	**0.57**
3	0.32	0.29	0.40
4	0.25	0.30	0.40
		Group 2	
1	0.20	0.24	0.24
2	**0.28**	**0.39**	**0.39**
3	0.25	0.29	0.30
4	0.21	0.26	0.25
		Group 3	
1	0.26	0.20	0.18
2	**0.53**	**0.22**	**0.26**
3	0.36	0.20	0.25
4	0.33	0.21	0.23
		Group 4	
1	0.21	0.28	0.15
2	**0.52**	**0.54**	**0.17**
3	0.33	0.45	0.14
4	0.33	0.28	0.15
		Group 5	
1	0.24	-	-
2	**0.29**	-	-
3	0.28	-	-
4	0.24	-	-

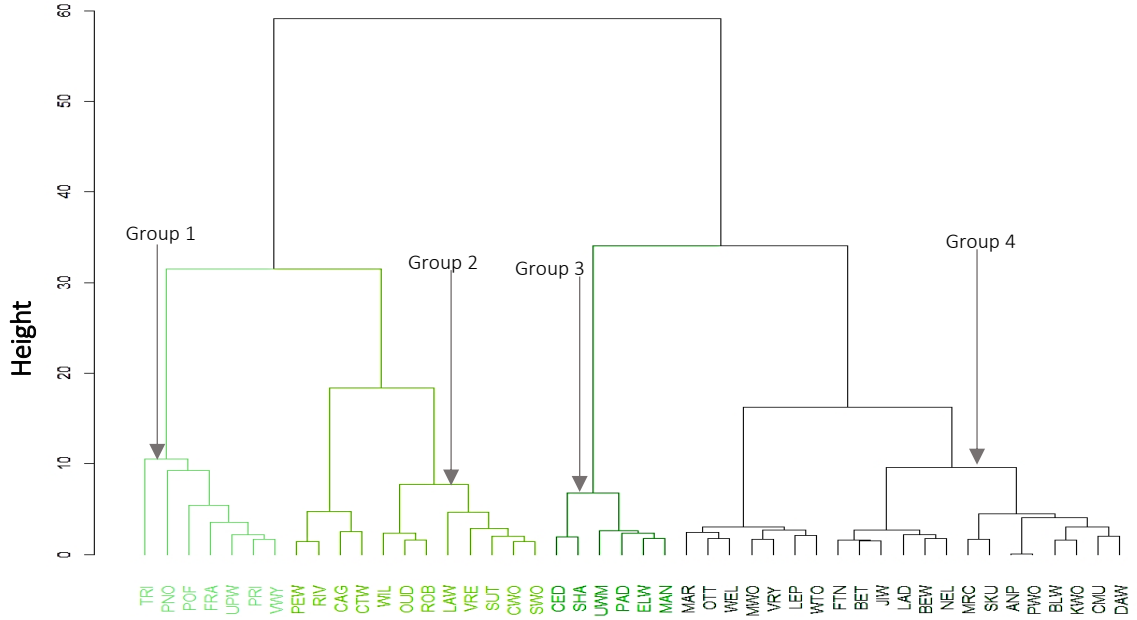
The maps below present the spatial distribution of the SRZ and WRZ based on the timing of the wet and dry seasons reflected by the seasonality of mean monthly rainfall as is demonstrated in the above seasonal dendrograms.



C.3: RAIN DAYS AND VARIABILITY

The cluster analysis results for the period of 1987-2016 of mean monthly rain days and monthly CV using Ward's minimum variance algorithm and the squared Euclidean distance are presented here. This includes the main dendrogram, the validation results (i.e. cophenetic correlation coefficient and average silhouette widths), the spatial distribution of the optimal number of cluster groups, the seasonal groupings per cluster group and associated validation results, and the spatial distribution of the associated seasonality classification.

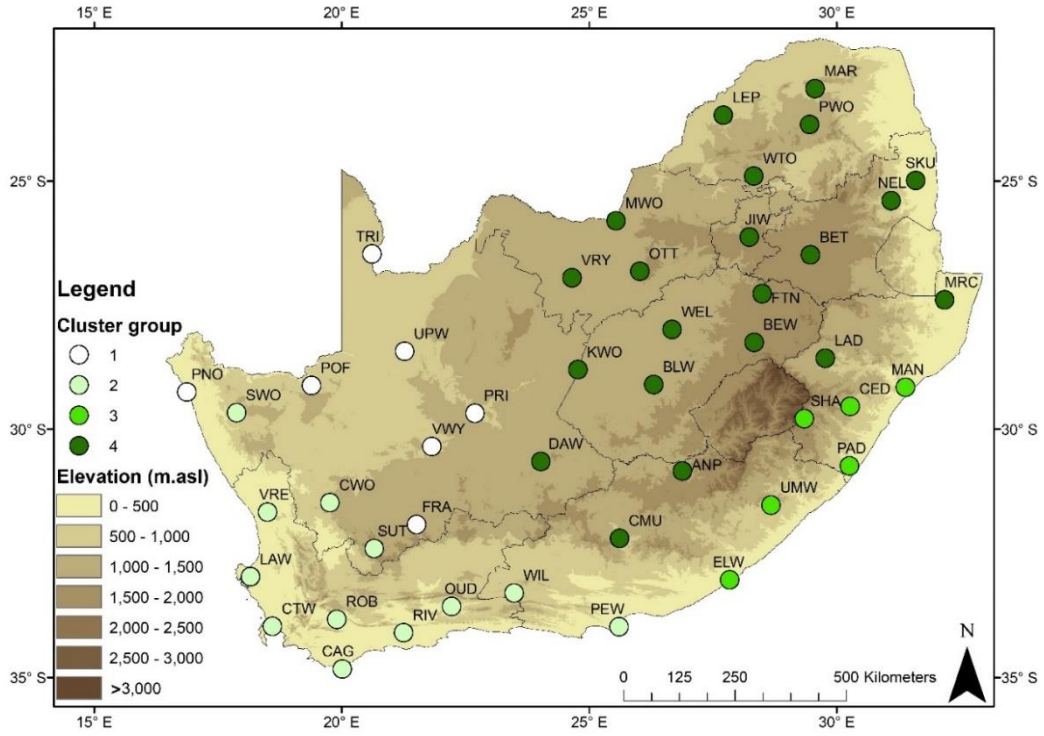
The figure below displays a colour coded dendrogram of the cluster analysis of mean monthly rain days and associated CV. This figure is colour coded according to the optimal number of cluster groups 1 to 4 and is labelled using the weather station codes.



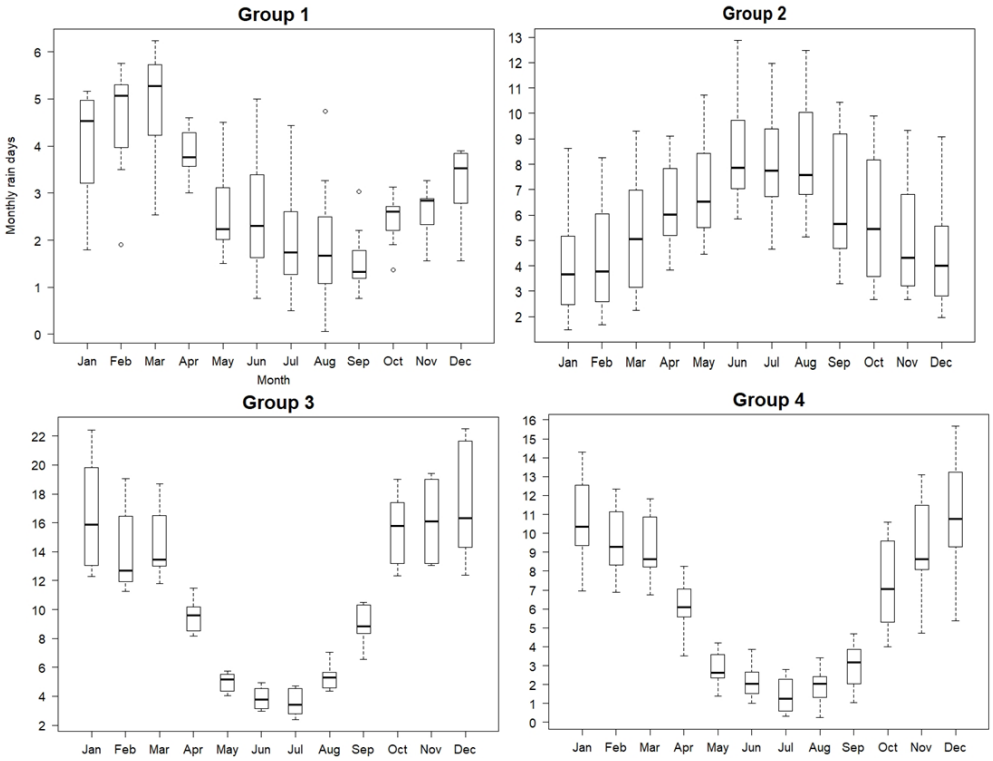
The validation of this cluster analysis process is presented below. Overall, the cophenetic correlation coefficient is 0.6272. Based on the average silhouette widths presented in the table below, four clusters was the optimal number of groups with the highest average silhouette width of 0.37 across the maximum of 10 cluster groups assessed.

Number of clusters	Average silhouette width
2	0.32
3	0.30
4	**0.37**
5	0.35
6	0.32
7	0.32
8	0.31
9	0.32
10	0.32

The map below presents the spatial distribution of the cluster groups 1 to 4, from the dendrogram above.



The boxplots below display the mean monthly rain days across the weather stations in the cluster groups 1 to 4, presented in the previous map. Circles represent outliers.



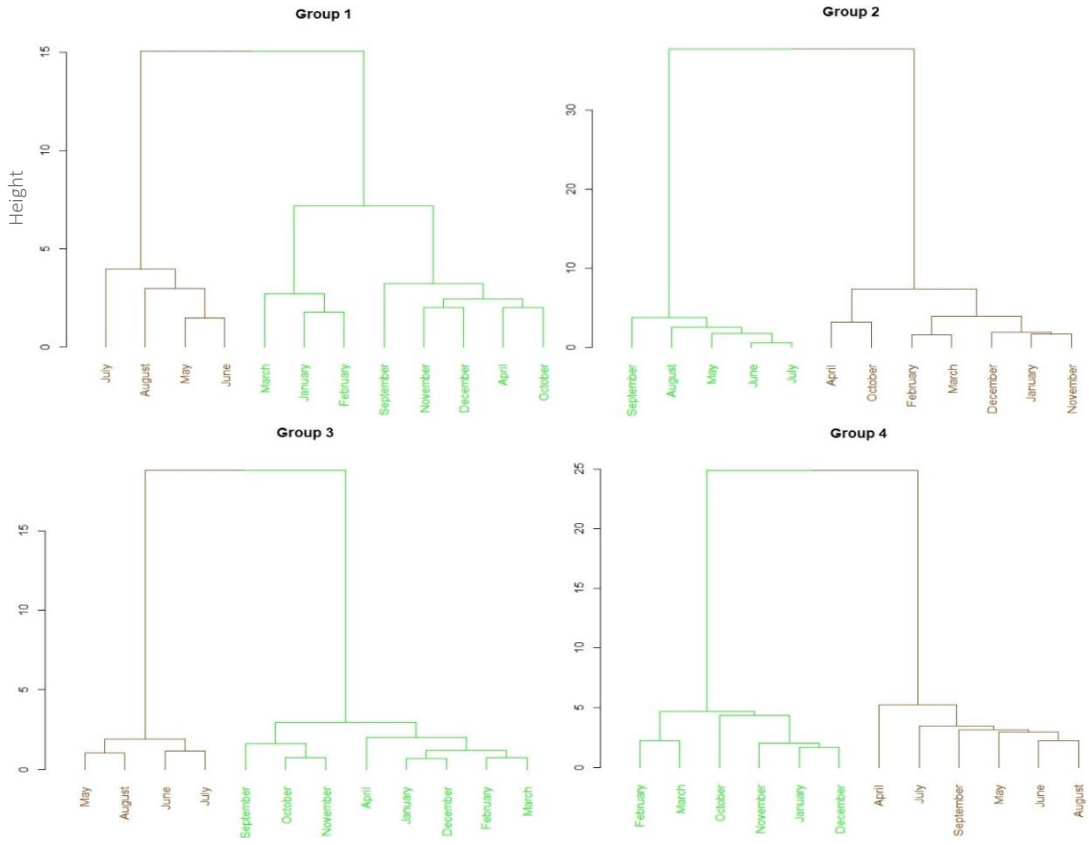
Validation results of the seasonal clustering within each of the groups 1 to 4. This first table presents the cophenetic correlation coefficients of the cluster analysis within each of the cluster groups 1 to 4.

Cluster group	Cophenetic correlation coefficient
1	0.7692
2	0.8932
3	0.9554
4	0.8748

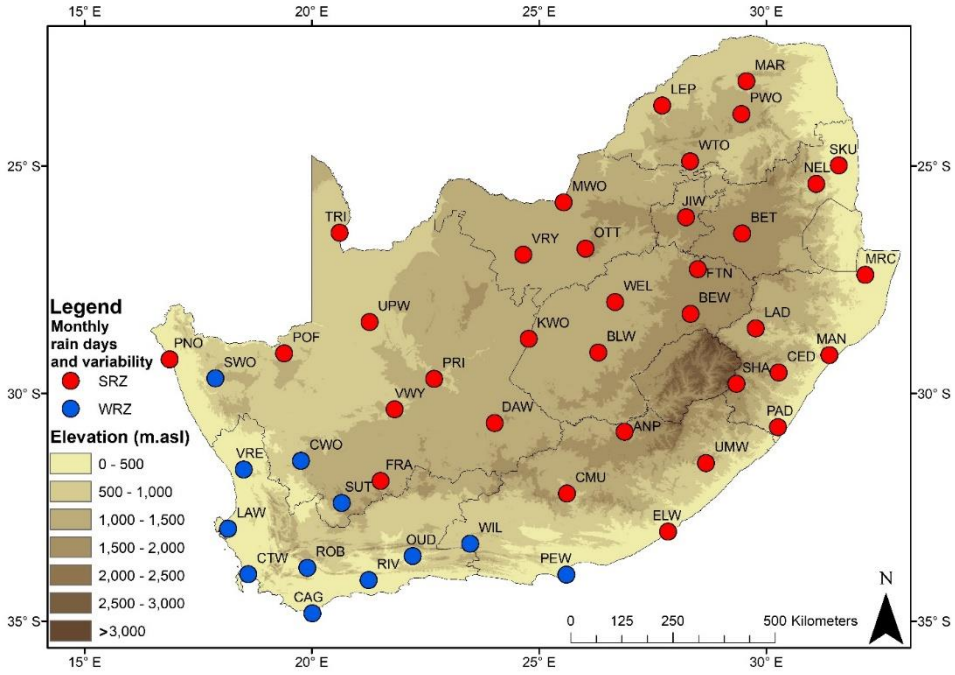
The table below presents the average silhouette widths for a total of one to four groupings within the cluster groups 1 to 4 presented in the above dendrogram and map. Each of the groups 1 to 4 were separated into two main clusters of a wet and a dry season.

Number of clusters	Average silhouette width
Group 1	
1	0.22
2	**0.41**
3	0.34
4	0.28
Group 2	
1	0.30
2	**0.66**
3	0.50
4	0.44
Group 3	
1	0.28
2	**0.70**
3	0.43
4	0.42
Group 4	
1	0.27
2	**0.52**
3	0.35
4	0.24

The figure below displays the dendrograms of the wet and dry season groupings for the rain day cluster groups 1 to 4.



The map below presents the spatial distribution of the SRZ and WRZ based on the timing of the wet and dry seasons reflected by the seasonality of rain days as demonstrated in the above dendrograms.



APPENDIX D: ANNUAL SEASONALITY SCORES

This section contains the annual seasonality scores from all weather stations. Weather stations which contained missing years were indicated by presenting n.

Location	Aliwal-North Plaatkop	Bethal (n = 29)	Bethlehem Wo	Bloemfontein Wo	Calvinia Wo
Year			Annual seasonality score		
1987	0.09	1.02	0.62	0.26	-0.59
1988	0.83	0.73	0.90	0.92	-0.14
1989	0.55	0.98	0.98	0.73	-0.15
1990	0.26	1.45	0.66	0.36	-0.07
1991	0.85	1.11	1.05	0.87	-0.39
1992	0.18	0.97	0.66	0.39	-0.20
1993	0.50	1.44	1.05	0.60	-0.48
1994	0.48	1.25	0.89	0.73	-0.17
1995	0.47	1.59	0.79	0.72	0.003
1996	0.64	1.21	0.61	0.79	-0.67
1997	0.23	0.85	0.35	0.25	-0.40
1998	0.72	1.57	1.60	1.18	0.20
1999	0.65	0.91	0.91	0.68	-0.19
2000	0.54	1.54	1.23	0.86	0.16
2001	0.47	1.02	0.79	0.66	-0.30
2002	0.29	0.89	0.66	0.46	-0.28
2003	0.53	0.85	0.77	0.65	-0.17
2004	0.45	0.95	0.68	0.57	-0.27
2005	0.52	1.69	1.35	0.61	-0.17
2006	0.66	1.37	1.07	0.97	-0.30
2007	0.42	0.96	0.74	0.48	-0.30
2008	0.51	1.36	0.94	0.56	-0.35
2009	0.40	0.91	0.63	0.56	-0.26
2010	0.83	1.34	1.39	1.12	0.21
2011	0.52	0.58	0.61	0.37	0.03
2012	0.35	1.24	0.70	0.35	-0.16
2013	0.77	1.63	1.16	0.84	-0.31
2014	0.97	1.17	1.18	0.69	-0.29
2015	0.12	0.96	0.54	0.10	-0.38
2016	0.19		0.61	0.20	0.0009

Location	Cape Agulhas	Cape Town Wo	Cedara	Cradock-Mun	De Aar Wo	East London Wo
Year			Annual seasonality score			
1987	-0.86	-1.38	0.53	0.08	0.05	0.33
1988	-0.92	-1.14	1.08	0.60	0.32	0.82
1989	-0.95	-1.03	1.30	0.55	0.61	0.002
1990	-0.45	-0.83	1.13	0.26	0.26	0.84
1991	-0.78	-1.28	1.91	0.60	0.45	0.12
1992	-1.12	-1.09	1.53	-0.008	0.02	0.67
1993	-0.97	-1.16	1.75	0.52	0.09	0.41
1994	-0.98	-1.2	1.11	0.52	0.50	1.04
1995	-0.59	-1.03	0.80	0.66	0.50	1.55
1996	-0.96	-1.02	0.73	0.66	0.22	1.13
1997	-1.08	-1.00	0.83	0.43	0.11	-0.06
1998	-0.48	-0.82	1.78	0.85	0.39	1.61
1999	-1.04	-1.35	2.47	0.67	0.32	1.38
2000	-0.65	-1.08	1.43	0.88	0.57	1.67
2001	-1.08	-1.54	1.66	0.44	0.25	1.19
2002	-0.65	-0.72	0.05	0.08	0.01	-0.66
2003	-0.50	-0.67	0.99	0.59	0.34	0.55
2004	-0.74	-1.30	1.04	0.78	0.51	0.36
2005	-0.39	-0.94	2.06	0.74	0.58	1.88
2006	-0.63	-1.01	1.45	0.45	0.22	0.61
2007	-0.63	-1.18	0.83	0.68	0.30	1.45
2008	-0.61	-1.36	1.32	0.52	0.33	1.3
2009	-1.14	-1.34	1.31	0.46	0.28	0.66
2010	-0.59	-0.71	1.72	0.97	0.97	0.07
2011	-0.82	-0.74	0.52	0.73	0.61	-0.68

2012	-0.85	-1.00	0.66	0.17	0.47	-0.20
2013	-0.73	-0.91	0.05	0.71	0.54	1.89
2014	-0.23	-1.12	1.58	0.94	0.35	1.74
2015	-0.51	-0.95	0.97	-0.12	-0.05	-1.01
2016	-0.66	-0.73	0.71	0.45	0.19	-0.05

Location	Frankfort - TNK	Fraserburg	Johannesburg INT Wo	Kimberley Wo	Ladysmith (n = 29)
Year			Annual seasonality score		
1987	0.92	-0.06	1.31	0.47	0.92
1988	0.70	0.37	1.08	0.76	0.68
1989	1.05	0.21	1.06	0.60	1.62
1990	0.73	0.28	1.12	0.45	0.90
1991	0.92	0.06	1.44	0.87	1.77
1992	0.63	-0.06	0.98	0.27	1.21
1993	1.14	0.19	1.67	0.90	1.56
1994	0.81	0.19	1.50	0.57	1.01
1995	0.86	0.28	1.53	0.66	1.58
1996	1.07	-0.06	1.46	0.51	1.07
1997	0.68	-0.04	1.00	0.30	0.44
1998	1.23	0.29	1.62	0.96	1.80
1999	0.76	0.40	0.91	0.57	1.36
2000	1.02	0.34	2.00	0.90	1.24
2001	0.80	-0.04	1.07	0.55	1.11
2002	0.65	0.23	0.97	0.49	0.45
2003	0.36	-0.02	0.93	0.60	
2004	0.76	0.18	1.27	0.54	0.90
2005	1.19	0.24	1.78	0.54	1.48
2006	0.99	-0.03	1.50	0.38	1.37
2007	0.69	0.11	0.72	0.56	0.96
2008	0.96	0.09	1.55	0.58	1.30
2009	0.23	0.25	1.32	0.66	1.23
2010	1.11	0.46	1.75	0.99	1.12
2011	0.48	0.34	1.28	0.62	0.46
2012	0.64	0.28	1.54	0.51	1.56
2013	0.92	0.15	1.35	0.68	1.27
2014	0.98	0.32	1.43	0.50	1.36
2015	0.56	-0.08	0.87	0.24	0.73
2016	0.40	-0.09	1.15	0.41	0.53

Location	Langerbaanweg AWS	Lephalale	Mafikeng Wo	Makatini Research Centre	Mandini	Mara
Year			Annual seasonality score			
1987	-1.01	0.80	0.94	1.18	0.36	1.09
1988	-0.76	1.35	1.16	1.33	1.96	0.68
1989	-0.70	1.45	1.17	1.32	1.26	1.09
1990	-0.58	1.09	1.06	1.11	1.12	1.49
1991	-0.88	1.57	0.98	1.05	1.18	1.19
1992	-0.78	0.86	0.85	1.43	1.36	1.05
1993	-0.90	0.91	1.05	1.23	3.05	1.44
1994	-0.79	1.01	0.99	0.86	0.52	0.74
1995	-0.64	1.14	1.38	0.49	0.15	1.00
1996	-0.54	1.09	1.01	1.46	0.93	0.86
1997	-0.80	0.93	0.81	0.35	0.51	1.25
1998	-0.57	1.10	1.69	1.56	1.68	1.14
1999	-1.18	1.13	0.98	1.54	0.86	1.60
2000	-1.10	1.23	1.41	2.71	2.34	1.49
2001	-1.08	0.84	1.13	1.20	1.76	0.97
2002	-0.52	0.35	0.87	0.44	-0.07	0.75
2003	-0.74	0.66	1.17	0.91	0.56	0.97
2004	-0.79	1.13	1.11	1.41	1.00	1.20
2005	-0.70	0.69	1.19	1.52	2.58	0.84
2006	-1.04	1.09	0.84	1.69	1.35	1.10
2007	-0.63	0.89	0.61	1.05	0.53	0.86
2008	-0.82	1.17	0.68	0.54	1.50	1.36

2009	-0.67	1.10	0.63	0.93	1.89	1.28
2010	-0.40	0.84	1.07	1.80	0.84	0.96
2011	-0.72	0.98	0.87	1.09	-0.50	0.59
2012	-0.75	1.50	0.84	1.50	1.26	1.04
2013	-0.81	1.07	1.18	0.80	1.83	1.46
2014	-0.71	1.25	1.25	1.35	1.06	1.81
2015	-0.50	1.00	0.43	1.42	0.64	0.89
2016	-0.81	1.04	0.58	0.50	-0.33	0.91

Location	Nelspruit (n = 29)	Ottosdal	Oudtshoorn (n = 29)	Paddock	Pofadder	Polokwane Wo
Year			Annual seasonality score			
1987	1.48	0.77	-0.18	-0.47	-0.06	1.14
1988	1.36	0.94	-0.09	2.40	0.18	0.97
1989	1.56	1.13	0.08	1.15	0.19	1.16
1990	2.11	0.82	0.14	0.98	0.06	1.59
1991	1.43	0.99	0.04	1.57	0.09	1.05
1992	1.18	0.75	-0.18	1.04	0.08	1.14
1993		1.07	0.07	1.80	0.19	0.88
1994	1.75	0.90	-0.07	0.84	0.16	1.07
1995	1.95	0.94	0.19	1.05	0.13	1.31
1996	1.95	0.79	0.05	0.81	-0.14	1.35
1997	1.04	0.72	-0.16	0.29	-0.11	1.46
1998	1.98	1.31	0.14	2.63	0.35	1.28
1999	2.07	1.09	0.02	2.23	0.23	1.07
2000	3.54	1.18	0.44	2.97	0.45	1.31
2001	1.59	0.92	-0.05	1.71	0.21	1.11
2002	1.55	0.71	-0.21	0.01	0.11	0.76
2003	1.53	1.02	-0.09	1.01	-0.009	0.88
2004	1.99	0.92	-0.11	0.30	-0.04	1.33
2005	2.24	1.32		2.28	0.14	1.35
2006	2.58	0.93	-0.52	1.87	0.002	1.56
2007	1.61	0.66	0.12	0.94	0.24	0.78
2008	2.00	0.95	-0.14	-0.14	0.14	1.48
2009	1.06	0.72	-0.05	1.27	0.05	1.01
2010	1.20	1.43	-0.06	0.99	0.51	1.00
2011	1.50	1.09	-0.13	-0.41	0.09	0.88
2012	2.90	0.35	-0.24	0.22	0.40	1.46
2013	2.69	0.27	-0.05	1.92	0.09	1.85
2014	2.41	1.11	0.36	1.38	0.37	1.40
2015	1.71	0.33	-0.09	0.81	0.06	0.98
2016	1.56	0.88	-0.19	-0.23	0.16	1.23

Location	Port Elizabeth Wo	Port Nolloth	Prieska	Riversdale	Robertson	Shaleburn	Skukuza
Year			Annual seasonality score				
1987	-0.31	-0.50	0.06	-0.32	-0.54	0.74	0.77
1988	-0.34	-0.60	0.56	-0.21	-0.42	1.56	1.09
1989	-0.44	-0.13	0.44	0.02	-0.28	1.53	1.43
1990	-0.14	-0.48	0.21	-0.01	-0.15	1.19	1.42
1991	-0.24	-0.93	0.47	0.22	-0.23	1.43	0.77
1992	-0.36	-0.58	0.13	-0.15	-0.72	1.21	1.16
1993	-0.42	0.39	-0.001	-0.22	-0.32	1.49	1.24
1994	-0.39	-0.25	0.38	-0.10	-0.13	0.90	0.65
1995	0.36	-0.11	0.41	0.38	-0.08	1.40	1.47
1996	-0.31	-1.64	0.23	0.07	-0.37	0.76	1.06
1997	-0.67	-1.06	0.11	-0.37	-0.57	1.06	1.49
1998	-0.31	0.08	0.53	0.44	-0.04	1.53	1.17
1999	-0.16	-0.73	0.32	0.04	-0.31	1.54	1.34
2000	1.21	-0.10	0.32	0.42	-0.04	1.67	2.20
2001	-0.19	-0.73	0.24	-0.02	-0.48	1.34	1.71
2002	-1.18	-0.60	0.13	-0.34	-0.28	0.74	1.04
2003	-0.28	-0.97	0.31	0.08	-0.12	1.26	0.57
2004	0.21	-0.82	0.40	0.21	-0.24	1.14	1.45
2005	0.97	-0.26	0.28	0.11	-0.12	1.67	1.59

2006	-0.74	-0.66	0.40	-0.71	-0.90	1.61	1.70
2007	-0.05	-0.66	0.31	0.09	-0.31	1.07	0.99
2008	0.16	-0.72	0.11	-0.06	-0.32	1.41	1.76
2009	-0.31	-0.28	0.35	-0.25	-0.37	1.11	1.31
2010	-0.21	-0.15	0.72	-0.33	-0.09	1.26	0.80
2011	-1.16	-0.38	0.42	-0.54	-0.23	0.89	1.30
2012	-0.77	-0.59	0.44	-0.52	-0.66	1.12	1.33
2013	-0.09	-0.63	0.47	-0.20	-0.37	1.69	1.60
2014	-0.13	-0.10	0.35	0.50	0.23	1.57	1.49
2015	-0.63	-0.66	0.03	-0.57	-0.73	0.89	0.68
2016	-0.37	-0.35	0.19	0.24	-0.43	1.00	0.57

Location	Springbok Wo (n = 29)	Sutherland (n = 29)	Twee Rivieren	Umtata Wo	Upington Wo	Vanwyksvlei
Year			Annual seasonality score			
1987		-0.47	0.43	0.64	0.21	0.003
1988	-0.56	0.04	0.65	1.38	0.53	0.47
1989	-0.33	-0.08	0.53	1.21	0.34	0.39
1990	-0.61	0.14	0.51	1.00	0.25	0.19
1991	-0.56	-0.24	0.67	1.19	0.62	0.16
1992	-0.52	-0.22	0.29	1.26	0.36	0.18
1993	-0.60	-0.38	0.53	1.18	0.28	0.12
1994	-0.40	0.15	0.50	0.91	0.34	0.43
1995	-0.53	0.06	0.41	1.53	0.31	0.30
1996	-0.73	-0.33	0.10	1.30	0.14	0.02
1997	-0.92	-0.30	0.19	0.37	0.32	0.06
1998	-0.006	-0.04	0.45	1.90	0.57	0.39
1999	-0.38	0.01	0.51	1.54	0.42	0.45
2000	-0.33	0.24	0.57	1.78	0.48	0.28
2001	-0.59	-0.25	0.53	1.38	0.43	0.14
2002	-0.33	-0.07	0.45	0.20	0.41	0.22
2003	-0.61	-0.11	0.32	0.79	0.33	0.19
2004	-0.51	-0.05	0.43	0.49	0.46	0.30
2005	-0.29	-0.17	0.67	1.87	0.57	0.05
2006	-0.64	-0.30	0.74	0.84	0.60	0.22
2007	-0.65	-0.14	0.46	1.03	0.44	0.38
2008	-0.48	-0.22	0.47	1.16	0.38	0.14
2009	-0.51	-0.06	0.59	0.92	0.53	0.21
2010	-0.40	0.13	0.69	1.42	0.88	0.57
2011	-0.008	0.10	0.62	0.84	0.52	0.27
2012	-0.38	-0.04	0.62	0.57	0.36	0.27
2013	-0.51	-0.12	0.55	1.50	0.42	0.25
2014	-0.53	0.05	0.60	1.55	0.50	0.26
2015	-0.69		0.24	0.57	0.07	-0.15
2016	-0.42	-0.20	0.57	1.10	0.40	0.17

Location	Vredendal	Vryburg	Warmbad Towoomba	Welkom	Willowmore
Year			Annual seasonality score		
1987	-1.01	0.58	1.37	0.60	0.003
1988	-0.42	1.05	1.18	0.89	0.17
1989	-0.59	0.86	1.51	0.99	0.21
1990	-0.29	0.78	1.05	0.65	0.39
1991	-0.68	0.98	1.56	0.91	0.21
1992	-0.60	0.47	0.83	0.27	-0.19
1993	-0.73	0.74	1.44	0.93	0.38
1994	-0.55	0.65	1.23	0.66	0.40
1995	-0.42	0.96	1.17	1.01	0.59
1996	-0.60	0.75	1.24	0.40	0.38
1997	-0.84	0.42	1.12	0.24	0.11
1998	-0.28	1.33	1.65	1.42	0.44
1999	-0.46	0.91	1.08	0.71	0.58
2000	-0.45	0.93	1.48	0.80	0.77
2001	-0.79	0.70	0.84	0.63	0.26
2002	-0.6	0.75	0.79	0.51	-0.15

2003	-0.26	0.83	1.01	0.75	0.28
2004	-0.47	0.61	1.21	0.41	0.34
2005	-0.37	1.07	0.91	0.87	0.46
2006	-0.78	1.07	1.40	0.75	-0.04
2007	-0.43	0.53	0.30	0.39	0.15
2008	-0.84	0.91	1.23	0.79	0.18
2009	-0.79	0.39	1.19	0.52	0.33
2010	-0.31	1.10	1.17	1.25	0.40
2011	-0.56	0.67	0.86	0.08	0.17
2012	-0.24	0.58	1.43	0.65	0.07
2013	-0.76	0.94	1.72	0.74	0.39
2014	-0.45	0.98	1.33	0.90	0.40
2015	-0.76	0.24	1.13	0.28	-0.13
2016	-0.70	0.48	1.11	0.56	0.06

APPENDIX E: ANNUAL ONSET AND CESSATION DATES, LENGTH OF THE WET SEASON AND NUMBER OF RAIN DAYS

The annual onset and cessation dates are colour coded according to which criteria from Table 4.6 produced the latest dates. For the onset dates, orange, purple and brown represent criteria one, two and three respectively. For the cessation dates, blue and green represent criteria one and two respectively. Yellow indicates when two or more criteria agreed on an onset date, and red indicates when both cessation date criteria agreed on a date. ND indicates no date was obtained and thereafter the length of the wet season and number of rain days was left blank.

Aliwal-North Plaatkop				Bethal			
Onset date	Cessation date	Length of wet season	Rain days	Onset date	Cessation date	Length of wet season	Rain days
11-Sep-87	28-Apr-88	231	69	4-Sep-87	9-Apr-88	219	90
7-Sep-88	30-Apr-89	236	78	18-Oct-88	7-Jun-89	233	80
27-Nov-89	29-Apr-90	154	53	25-Oct-89	17-May-90	205	80
6-Dec-90	23-Mar-91	108	41	31-Oct-90	24-Mar-91	145	65
11-Sep-91	1-Apr-92	204	60	11-Dec-91	30-Mar-92	111	43
9-Oct-92	2-May-93	206	55	6-Nov-92	12-Apr-93	158	65
10-Oct-93	13-Mar-94	155	57	2-Oct-93	2-May-94	213	79
13-Nov-94	6-May-95	175	41	5-Nov-94	7-May-95	184	66
24-Sep-95	19-Apr-96	209	79	13-Oct-95	21-Apr-96	192	94
5-Nov-96	1-Jun-97	209	71	23-Oct-96	29-May-97	219	83
10-Jan-98	9-May-98	120	43	9-Sep-97	13-Mar-98	186	78
10-Oct-98	21-Mar-99	163	51	5-Oct-98	23-Mar-99	170	69
17-Dec-99	3-May-00	139	57	11-Dec-99	11-May-00	153	66
22-Sep-00	5-May-01	226	69	28-Oct-00	4-May-01	189	79
22-Sep-01	30-May-02	251	77	20-Sep-01	7-Mar-02	169	53
25-Aug-02	17-May-03	266	60	29-Oct-02	6-Jun-03	221	50
23-Nov-03	21-Apr-04	151	51	22-Oct-03	27-Jul-04	280	75
1-Oct-04	23-Apr-05	205	50	20-Oct-04	26-Mar-05	158	65
24-Oct-05	22-Apr-06	181	64	18-Aug-05	17-Apr-06	243	81
31-Aug-06	26-Apr-07	239	55	10-Aug-06	11-Feb-07	186	49
29-Nov-07	26-Jun-08	211	78	5-Oct-07	23-Mar-08	171	65
15-Nov-08	29-Jun-09	167	85	26-Oct-08	17-Jun-09	235	67
14-Oct-09	14-Jun-10	244	85	10-Aug-09	12-May-10	276	95
12-Nov-10	16-Jun-11	217	126	4-Nov-10	20-Apr-11	168	63
6-Dec-11	26-Jun-12	204	75	23-Aug-11	30-Mar-12	221	46
17-Oct-12	1-Apr-13	167	58	14-Sep-12	20-Apr-13	219	69
23-Nov-13	25-Mar-14	123	46	19-Oct-13	18-Mar-14	151	71
4-Nov-14	3-Apr-15	151	56	18-Aug-14	23-Apr-15	249	62
20-Jan-16	13-May-16	115	41	ND	ND	ND	ND

Bethlehem Wo				Bloemfontein Wo			
Onset date	Cessation date	Length of wet season	Rain days	Onset date	Cessation date	Length of wet season	Rain days
23-Aug-87	24-Apr-88	246	104	23-Aug-87	21-Apr-88	243	96
22-Sep-88	1-May-89	222	95	11-Oct-88	4-May-89	206	95
24-Oct-89	2-May-90	191	92	7-Nov-89	2-May-90	177	69
14-Oct-90	27-Mar-91	165	74	8-Dec-90	26-Mar-91	109	42
17-Oct-91	2-Mar-92	138	52	2-Oct-91	1-Feb-92	123	41
12-Aug-92	17-Apr-93	249	91	9-Nov-92	6-Apr-93	149	37
3-Oct-93	30-Apr-94	210	76	10-Oct-93	2-Apr-94	175	62
6-Nov-94	2-Apr-95	148	57	15-Jan-95	6-May-95	112	36
25-Oct-95	21-Apr-96	180	81	25-Oct-95	18-Apr-96	177	64
26-Sep-96	1-Jun-97	249	116	7-Nov-96	6-Apr-97	151	47
8-Sep-97	2-Apr-98	207	76	31-Dec-97	2-Apr-98	93	38
1-Nov-98	20-May-99	201	77	17-Oct-98	20-May-99	216	58
10-Dec-99	11-May-00	154	69	28-Oct-99	3-May-00	189	66
25-Sep-00	5-May-01	223	94	22-Sep-00	12-May-01	233	63
8-Sep-01	16-Apr-02	221	90	8-Nov-01	30-May-02	204	64
26-Aug-02	23-Mar-03	210	74	25-Aug-02	26-Mar-03	214	59
3-Nov-03	22-Mar-04	141	55	23-Dec-03	4-Apr-04	104	48
29-Nov-04	23-Apr-05	146	68	2-Oct-04	22-Apr-05	203	56
14-Oct-05	30-Apr-06	199	93	15-Oct-05	23-Apr-06	191	69

18-Oct-06	6-Jun-07	232	73	31-Aug-06	18-Apr-07	231	45
4-Oct-07	4-Jun-08	245	84	4-Oct-07	26-May-08	236	78
10-Nov-08	17-Jun-09	220	82	18-Nov-08	21-Feb-09	96	43
4-Nov-09	23-Apr-10	171	77	11-Oct-09	12-May-10	214	82
1-Nov-10	1-May-11	182	86	11-Nov-10	8-Jun-11	210	99
8-Dec-11	23-Jun-12	199	58	6-Dec-11	23-Jun-12	201	52
24-Sep-12	20-Apr-13	209	80	1-Dec-12	31-Mar-13	121	33
25-Oct-13	14-Mar-14	141	68	29-Oct-13	23-Mar-14	146	44
3-Nov-14	25-Apr-15	174	79	7-Nov-14	2-Apr-15	147	43
21-Nov-15	14-May-16	176	54	20-Jan-16	21-May-16	123	26

Calvinia Wo				Cape Agulhas			
Onset date	Cessation date	Length of wet season	Rain days	Onset date	Cessation date	Length of wet season	Rain days
23-Apr-87	26-Sep-87	157	31	22-Apr-87	30-Sep-87	162	64
13-Mar-88	31-Aug-88	172	31	28-Apr-88	16-Oct-88	172	57
ND	ND			20-Mar-89	9-Nov-89	235	87
29-Apr-90	1-Aug-90	95	19	24-Feb-90	1-Aug-90	159	67
ND	ND			28-May-91	29-Oct-91	155	57
ND	ND			12-Apr-92	24-Oct-92	196	78
ND	ND			20-Feb-93	26-Aug-93	188	67
11-Mar-94	1-Aug-94	144	23	24-Apr-94	1-Aug-94	100	36
1-Apr-95	12-Oct-95	195	38	19-Mar-95	29-Nov-95	256	73
9-Jul-96	21-Nov-96	136	41	8-Jun-96	23-Oct-96	138	62
19-Mar-97	1-Aug-97	136	27	7-Apr-97	24-Nov-97	232	81
23-Feb-98	11-Aug-98	170	16	29-Apr-98	23-Nov-98	209	68
ND	ND			24-Apr-99	20-Oct-99	180	62
27-Feb-00	1-Aug-00	157	25	5-Mar-00	31-Aug-00	180	53
5-Apr-01	19-Nov-01	229	65	6-Jul-01	20-Nov-01	138	62
30-May-02	31-Aug-02	94	30	14-Jan-02	3-Oct-02	263	91
ND	ND			22-Mar-03	27-Sep-03	190	58
4-Jun-04	20-Oct-04	139	25	18-Apr-04	29-Oct-04	195	48
ND	ND			10-Apr-05	1-Aug-05	114	31
ND	ND			22-Apr-06	4-Nov-06	197	79
ND	ND			23-May-07	25-Nov-07	187	68
17-Feb-08	31-Aug-08	197	33	12-May-08	13-Nov-08	186	79
ND	ND			12-Jul-09	14-Nov-09	126	50
ND	ND			12-Jun-10	1-Aug-10	51	13
11-Feb-11	1-Aug-11	172	35	23-May-11	31-Aug-11	101	35
4-May-12	20-Aug-12	110	24	11-Jul-12	26-Oct-12	108	57
ND	ND			6-Apr-13	20-Nov-13	229	99
ND	ND			15-Jan-14	31-Aug-14	229	81
ND	ND			25-Mar-15	8-Nov-15	229	52
ND	ND			23-Jul-16	31-Aug-16	40	15

Cape Town Wo				Cedara			
Onset date	Cessation date	Length of wet season	Rain days	Onset date	Cessation date	Length of wet season	Rain days
4-May-87	1-Oct-87	151	65	21-Aug-87	31-May-88	285	158
16-Mar-88	20-Sep-88	189	65	17-Oct-88	23-Apr-89	189	110
21-Mar-89	14-Oct-89	208	81	30-Oct-89	2-Apr-89	155	112
24-Feb-90	11-Aug-90	169	67	19-Aug-90	2-Apr-91	218	120
28-May-91	22-Oct-91	148	63	8-Oct-91	21-Apr-92	204	106
18-Apr-92	29-Oct-92	195	83	20-Dec-92	5-Apr-93	107	53
15-Feb-93	11-Aug-93	178	59	1-Oct-93	29-Apr-94	211	120
26-May-94	1-Aug-94	68	29	22-Aug-94	29-Apr-95	251	110
28-May-95	31-Oct-95	157	63	17-Oct-95	25-May-96	222	120
21-Feb-96	23-Oct-96	246	88	15-Jul-96	28-Apr-97	288	139
13-Apr-97	23-Nov-97	225	69	4-Sep-97	22-Apr-98	231	145
10-May-98	6-Nov-98	181	64	30-Aug-98	27-Mar-99	210	127
24-Apr-99	20-Sep-99	150	55	25-Oct-99	11-May-00	199	108

29-May-00	20-Sep-00	115	48	19-Sep-00	17-Apr-01	211	131
6-May-01	11-Sep-01	129	60	13-Sep-01	18-Apr-02	218	124
22-May-02	5-Oct-02	137	56	27-Jul-02	14-May-03	292	123
23-Mar-03	4-Oct-03	196	64	19-Aug-03	12-Mar-04	207	111
17-Apr-04	29-Oct-04	196	56	11-Sep-04	23-Mar-05	194	111
19-Apr-05	31-Aug-05	135	57	13-Oct-05	2-May-06	202	125
30-Apr-06	21-Aug-06	114	44	18-Aug-06	7-Apr-07	233	135
17-Feb-07	4-Sep-07	200	59	3-Oct-07	28-Apr-08	209	121
29-May-08	12-Nov-08	168	69	12-Nov-08	14-May-09	184	125
15-May-09	13-Nov-09	183	72	10-Aug-09	22-Apr-10	256	146
13-May-10	1-Aug-10	81	24	17-Oct-10	13-May-11	209	135
29-Apr-11	26-Aug-11	120	43	29-Jul-11	31-Mar-12	247	136
7-Apr-12	29-Sep-12	176	72	15-Aug-12	12-May-13	271	152
17-Apr-13	19-Nov-13	217	81	21-Oct-13	2-Apr-14	164	102
27-Mar-14	31-Aug-14	158	55	5-Oct-14	12-Apr-15	190	131
3-Jun-15	1-Aug-15	60	18	30-Jul-15	24-Mar-16	239	118
29-Mar-16	31-Aug-16	156	45				

Cradock-Mun				De Aar Wo			
Onset date	Cessation date	Length of wet season	Rain days	Onset date	Cessation date	Length of wet season	Rain days
28-Sep-87	5-Apr-88	191	43	27-Sep-87	27-Jun-88	275	64
23-Sep-88	27-Apr-89	217	60	22-Sep-88	22-Apr-89	213	46
16-Nov-89	25-Apr-90	161	42	16-Nov-89	27-Jun-90	224	44
6-Dec-90	18-Mar-91	103	31	6-Dec-90	24-Jun-91	201	43
21-Oct-91	11-Jun-92	234	38	3-Oct-91	5-Apr-92	186	39
26-Feb-93	2-May-93	66	16	11-Aug-92	12-Apr-93	245	33
18-Nov-93	13-Mar-94	116	44	14-Oct-93	13-Mar-94	151	49
15-Jan-95	8-Mar-95	53	9	6-Mar-95	7-May-95	63	16
18-Dec-95	1-Feb-96	46	17	13-Dec-95	3-Mar-96	82	28
13-Nov-96	8-Apr-97	147	46	13-Nov-96	27-May-97	196	46
1-Jan-98	25-Apr-98	115	35	ND	ND		
21-Nov-98	23-Mar-99	123	28	27-Nov-98	19-May-99	174	32
19-Nov-99	21-Apr-00	155	52	23-Dec-99	29-Apr-00	129	40
22-Sep-00	16-Apr-01	207	42	22-Sep-00	5-May-01	226	45
21-Sep-01	1-Feb-02	134	30	21-Sep-01	13-Jun-02	266	47
17-Sep-02	3-Mar-03	168	27	26-Aug-02	25-Mar-03	212	37
29-Nov-03	9-Apr-04	133	33	29-Nov-03	4-Apr-04	128	32
1-Oct-04	21-Feb-05	144	21	27-Sep-04	2-Mar-05	157	26
26-Oct-05	3-Mar-06	129	34	9-Jan-06	2-May-06	114	35
23-Dec-06	8-Jun-07	168	39	24-Aug-06	7-Apr-07	227	29
6-Nov-07	11-Apr-08	158	54	3-Nov-07	21-Jun-08	232	51
17-Feb-09	6-Mar-09	18	8	18-Nov-08	29-Apr-09	163	34
2-Nov-09	2-Apr-11	152	42	9-Jan-10	2-Apr-10	84	23
28-Sep-10	23-Mar-11	177	69	26-Nov-10	15-May-11	171	58
10-Oct-11	23-Jun-12	258	65	27-Dec-11	24-Jun-13	181	39
25-Oct-12	31-Mar-13	158	30	24-Oct-12	1-Apr-13	160	30
24-Nov-13	3-Mar-14	100	35	29-Oct-13	20-May-14	204	36
12-Nov-14	30-Jul-15	261	66	16-Aug-14	11-Jun-15	300	45
23-Jan-16	22-Mar-16	60	18	20-Jan-16	14-May-16	116	32

East London Wo				Frankfort-TNK			
Onset date	Cessation date	Length of wet season	Rain days	Onset date	Cessation date	Length of wet season	Rain days
1-Sep-87	28-May-88	271	115	12-Sep-87	17-Mar-88	188	79
27-Aug-88	28-Apr-89	245	99	22-Sep-88	2-May-89	223	70
26-Jul-89	2-Apr-90	251	106	26-Oct-89	29-Apr-90	186	59
28-Aug-90	17-Jun-91	294	94	14-Dec-90	23-Mar-91	100	31
10-Aug-91	20-Apr-92	255	102	17-Oct-91	2-Mar-92	138	45
16-Aug-92	1-Feb-93	170	58	5-Sep-92	17-Apr-93	225	67
16-Aug-93	23-Mar-94	220	91	3-Oct-93	29-Apr-94	209	88

11-Aug-94	31-May-95	294	92	6-Nov-94	7-May-95	183	68
21-Jul-95	12-Apr-96	267	93	14-Oct-95	21-May-96	221	77
10-Oct-96	21-Jun-97	255	118	15-Oct-96	2-Jun-97	231	89
15-Oct-97	2-May-98	200	82	15-Sep-97	15-Mar-98	182	69
7-Aug-98	16-Apr-99	253	93	6-Oct-98	21-May-99	228	86
5-Aug-99	26-May-00	296	126	10-Dec-99	12-May-00	155	62
23-Sep-00	25-Apr-01	215	89	26-Sep-00	2-May-01	219	81
1-Aug-01	15-Apr-02	258	114	21-Sep-01	31-May-02	253	84
25-Jul-02	18-May-03	298	102	13-Aug-02	12-Apr-03	243	83
14-Sep-03	7-Apr-04	207	89	2-Nov-03	11-Apr-04	162	63
22-Jul-04	20-May-05	303	99	27-Nov-04	24-Apr-05	149	56
18-Aug-05	1-Jun-06	288	96	7-Nov-05	12-Apr-06	157	58
11-Aug-06	24-May-07	287	117	5-Nov-06	18-Apr-07	165	41
2-Oct-07	29-Apr-08	211	104	5-Oct-07	24-Mar-08	172	91
25-Aug-08	5-Mar-09	193	79	7-Nov-08	23-Mar-09	137	68
1-Oct-09	17-Jun-10	260	95	16-Jan-10	8-Apr-10	83	42
7-Oct-10	17-Jun-11	254	117	13-Nov-10	13-Jun-11	213	101
3-Oct-11	22-Jun-12	264	106	1-Nov-11	8-Apr-12	160	59
8-Sep-12	11-May-13	246	99	14-Sep-12	25-Apr-13	224	91
27-Oct-13	28-Apr-14	184	77	25-Oct-13	16-Mar-14	143	71
14-Aug-14	6-Jun-15	297	56	19-Oct-14	26-Apr-15	190	96
24-Jul-15	11-May-16	293	104	9-Mar-16	26-Jul-16	140	25

Fraserburg				Johannesburg INT Wo			
Onset date	Cessation date	Length of wet season	Rain days	Onset date	Cessation date	Length of wet season	Rain days
18-Feb-88	12-Mar-88	24	9	12-Sep-87	24-Apr-88	226	107
ND	ND			21-Sep-88	4-Jun-89	257	96
31-Jan-90	21-Apr-90	81	16	15-Oct-89	2-May-90	200	85
ND	ND			16-Oct-90	25-Mar-91	161	68
2-Oct-91	29-Mar-92	180	18	18-Oct-91	2-Mar-92	137	56
ND	ND			6-Nov-92	17-Apr-93	163	64
ND	ND			3-Oct-93	23-Mar-94	172	79
ND	ND			27-Oct-94	6-May-95	192	80
12-Dec-95	2-Mar-96	82	30	13-Oct-95	18-Apr-96	189	83
27-Oct-96	27-May-97	213	30	10-Nov-96	28-May-97	200	81
13-Jan-98	30-Mar-98	77	10	10-Nov-97	26-Feb-98	109	44
25-Sep-98	18-May-99	237	35	13-Oct-98	21-May-99	221	82
5-Oct-99	4-Apr-00	183	44	11-Dec-99	11-May-00	153	67
23-Mar-01	15-Jul-01	115	20	28-Sep-00	11-May-01	226	88
21-Sep-01	29-May-02	251	38	21-Sep-01	31-May-02	253	86
ND	ND			4-Sep-02	2-Apr-03	211	65
ND	ND			19-Oct-03	21-Apr-04	186	64
26-Jan-05	11-Apr-05	76	11	20-Nov-04	2-May-05	164	66
14-Jan-06	5-May-06	112	20	19-Oct-05	27-Mar-06	160	70
ND	ND			31-Oct-06	6-Jun-07	219	64
10-Oct-07	24-May-08	228	43	5-Oct-07	4-May-08	213	83
16-Feb-09	29-Apr-09	73	25	25-Oct-08	11-May-09	199	80
4-Nov-09	13-Mar-10	130	25	22-Oct-09	12-May-10	203	102
18-Dec-10	23-Mar-11	96	28	15-Nov-10	24-Apr-11	161	77
25-Jan-12	30-Mar-12	66	10	10-Oct-11	22-Mar-12	165	72
9-Dec-12	1-Apr-13	114	8	14-Sep-12	20-Apr-12	219	85
4-Jan-14	9-May-14	126	22	25-Oct-13	15-Mar-14	142	72
5-Nov-14	25-Mar-15	141	20	11-Nov-14	26-Mar-15	136	65
21-Jan-16	13-May-16	114	19	12-Sep-15	15-May-16	247	65

Kimberley Wo				Ladysmith			
Onset date	Cessation date	Length of wet season	Rain days	Onset date	Cessation date	Length of wet season	Rain days
11-Sep-87	21-Apr-88	224	73	24-Aug-87	21-Apr-88	242	99
22-Sep-88	4-May-89	225	77	19-Jul-88	2-Apr-89	258	95

12-Feb-90	2-May-90	80	31	1-Nov-89	20-Apr-90	171	85
5-Dec-90	26-Mar-91	112	35	7-Sep-90	2-Apr-91	208	76
18-Oct-91	26-Apr-92	192	42	11-Oct-91	21-Apr-92	194	73
9-Nov-92	26-Feb-93	110	27	5-Sep-92	12-Apr-93	220	67
10-Oct-93	8-Apr-94	181	55	3-Oct-93	30-Apr-94	210	74
16-Jan-95	6-May-95	111	32	5-Nov-94	2-May-95	179	55
12-Dec-95	18-Apr-96	129	40	16-Oct-95	21-Apr-96	189	81
13-Nov-96	27-May-97	196	60	15-Jul-96	12-Jun-97	333	104
1-Jan-98	26-Mar-98	85	31	6-Sep-97	28-May-98	265	84
17-Nov-98	20-May-99	185	41	15-Oct-98	26-Mar-99	163	70
28-Oct-99	22-Apr-00	178	55	28-Oct-99	5-May-00	191	66
22-Sep-00	5-May-01	226	62	26-Sep-00	2-Apr-01	189	62
22-Sep-01	30-May-02	251	54	20-Sep-01	1-Jun-02	255	76
25-Aug-02	21-Mar-03	209	46	26-Jul-02	23-Mar-03	241	64
1-Jan-04	4-Apr-04	95	26	7-Nov-03	1-Apr-04	147	59
2-Oct-04	7-Apr-05	188	40	17-Dec-04	2-Apr-05	107	55
29-Nov-05	30-Apr-06	153	50	18-Aug-05	27-Mar-06	222	79
20-Oct-06	25-Apr-07	188	49	15-Oct-06	7-Apr-07	175	67
5-Oct-07	2-Jun-08	242	73	4-Oct-07	27-Apr-08	207	96
27-Oct-08	26-Feb-09	123	42	10-Nov-08	23-Mar-09	134	72
12-Oct-09	6-Apr-10	177	58	10-Aug-09	7-Apr-10	241	99
12-Dec-10	11-Jun-11	182	80	4-Dec-10	23-Apr-11	141	71
29-Nov-11	23-Jun-12	208	50	2-Aug-11	25-Feb-12	207	74
3-Dec-12	1-Apr-13	120	39	15-Aug-12	22-Apr-13	251	87
3-Dec-13	21-May-14	170	42	26-Oct-13	23-Apr-14	180	77
18-Nov-14	3-Mar-15	106	25	3-Nov-14	23-Mar-15	141	48
21-Jan-16	8-Apr-16	79	19	21-Nov-15	22-Mar-16	123	30

Langebaanweg AWS				Lephalale			
Onset date	Cessation date	Length of wet season	Rain days	Onset date	Cessation date	Length of wet season	Rain days
13-May-87	31-Aug-87	111	36	6-Oct-87	24-Apr-88	202	63
ND	ND			27-Oct-88	7-Jun-89	224	55
22-Apr-89	10-Sep-89	142	45	12-Nov-89	2-May-90	172	42
26-Apr-90	1-Aug-90	98	35	16-Jan-90	29-Mar-91	73	25
21-Jun-91	21-Oct-91	123	44	27-Nov-91	1-Feb-92	67	16
ND	ND			29-Oct-92	1-Feb-93	96	22
13-Apr-93	11-Aug-93	121	37	11-Oct-93	11-Feb-94	124	38
16-Jun-94	1-Aug-94	47	19	20-Nov-94	12-May-95	174	47
13-Jun-95	11-Aug-95	60	23	18-Nov-95	22-Mar-96	126	42
1-Jun-96	25-Sep-96	117	46	31-Oct-96	26-May-97	208	56
27-May-97	1-Aug-97	67	17	27-Nov-97	8-Apr-98	133	31
11-May-98	5-Nov-98	179	45	17-Nov-98	23-Mar-99	127	39
18-Jun-99	11-Sep-99	86	32	14-Nov-99	21-Apr-00	160	43
13-Jul-00	9-Sep-00	59	19	9-Dec-00	3-Mar-01	85	22
13-May-01	5-Sep-01	116	51	8-Nov-01	6-Jun-02	211	39
30-May-02	31-Aug-02	94	34	26-Dec-02	21-Feb-03	58	19
10-Aug-03	1-Sep-03	23	11	17-Jan-04	11-Apr-04	86	30
ND	ND			10-Dec-04	1-Feb-05	54	8
12-Jun-05	31-Aug-05	81	26	13-Nov-05	13-Mar-06	121	43
25-May-06	1-Aug-06	69	22	2-Jan-07	7-Apr-07	96	15
1-May-07	21-Aug-07	113	41	5-Oct-07	16-Mar-08	164	54
20-Jun-08	8-Sep-08	81	36	16-Nov-08	21-Mar-09	126	46
21-Jun-09	14-Nov-09	147	45	21-Oct-09	3-May-10	195	53
ND	ND			8-Nov-10	1-Feb-11	86	31
31-May-11	22-Oct-11	145	41	28-Oct-11	21-Feb-12	117	41
ND	ND			22-Oct-12	20-Apr-13	181	45
3-Jun-13	26-Sep-13	116	49	13-Dec-13	4-Apr-14	113	36
4-Jul-14	12-Nov-14	132	38	9-Dec-14	9-Mar-15	91	29
ND	ND			26-Nov-15	18-Mar-16	114	31
ND	ND						

Mafikeng Wo				Makatini Research Centre			
Onset date	Cessation date	Length of wet season	Rain days	Onset date	Cessation date	Length of wet season	Rain days
12-Sep-87	24-Apr-88	226	79	26-Aug-87	30-Jun-88	310	90
18-Oct-88	4-May-89	199	68	10-Oct-88	4-Jun-89	238	71
29-Dec-89	28-Apr-90	121	34	25-Oct-89	5-Jun-90	224	63
18-Oct-90	17-Jun-91	243	54	12-Oct-90	14-May-91	215	57
27-Sep-91	22-Feb-92	149	47	20-Dec-91	2-Mar-92	74	19
1-Nov-92	17-Apr-93	168	66	20-Nov-92	28-Apr-93	160	30
9-Oct-93	21-Feb-94	136	52	1-Oct-93	30-Mar-94	181	47
14-Dec-94	6-May-95	144	42	19-Oct-94	8-May-95	202	60
26-Oct-95	27-May-96	215	62	13-Oct-95	22-Mar-96	162	62
16-Nov-96	27-May-97	193	74	31-Oct-96	23-Apr-97	175	44
19-Oct-97	2-Apr-98	166	42	11-Aug-97	10-Mar-98	212	65
17-Oct-98	21-May-99	217	57	12-Oct-98	29-Mar-99	169	56
11-Dec-99	3-May-00	145	58	1-Sep-99	1-May-00	244	88
24-Nov-00	2-May-01	160	53	27-Sep-00	26-Jun-01	273	64
27-Sep-01	31-May-02	247	69	20-Sep-01	8-Feb-02	142	40
11-Dec-02	26-Feb-03	78	27	13-Sep-02	2-Apr-03	202	39
28-Oct-03	21-Apr-04	177	48	12-Nov-03	29-Jul-04	261	47
20-Oct-04	22-Apr-05	185	52	30-Nov-04	28-Apr-05	150	26
3-Dec-05	19-Apr-06	138	52	13-Nov-05	23-Apr-06	162	35
24-Dec-06	1-Feb-07	40	11	18-Oct-06	5-Jul-07	261	76
5-Oct-07	18-Mar-08	166	48	8-Oct-07	22-Jun-08	259	70
25-Oct-08	17-Jun-09	236	67	12-Nov-08	7-May-09	177	34
26-Nov-09	2-May-10	158	54	10-Aug-09	27-Apr-10	261	102
25-Nov-10	10-Jun-11	198	70	14-Oct-10	22-Apr-11	191	88
28-Nov-11	21-Mar-12	115	38	28-Oct-11	13-May-12	199	60
9-Dec-12	19-Apr-13	132	40	14-Sep-12	3-Feb-13	143	65
29-Nov-13	23-Mar-14	115	54	26-Oct-13	13-Mar-14	139	51
7-Dec-14	18-Apr-15	133	46	16-Nov-14	30-Mar-15	135	37
13-Sep-15	16-Mar-16	186	44	11-Dec-15	15-May-16	157	39

Mandini				Mara			
Onset date	Cessation date	Length of wet season	Rain days	Onset date	Cessation date	Length of wet season	Rain days
22-Aug-87	5-May-88	258	105	21-Oct-87	30-Jun-88	254	49
18-Jul-88	4-Jun-89	322	106	19-Oct-88	23-Mar-89	156	36
28-Oct-89	29-Apr-90	184	88	31-Oct-89	25-Mar-90	146	47
28-Aug-90	14-May-91	260	104	23-Nov-90	15-May-91	174	46
15-Jul-91	22-Feb-92	223	67	21-Nov-91	2-Feb-92	74	20
7-Oct-92	7-Apr-93	183	71	6-Nov-92	3-Mar-93	118	34
13-Aug-93	18-Mar-94	218	69	1-Dec-93	1-Feb-94	63	17
3-Aug-94	9-May-95	280	109	5-Jan-95	23-May-95	139	33
13-Oct-95	22-Mar-96	162	92	26-Nov-95	24-Jul-96	242	59
15-Jul-96	30-Jun-97	351	142	26-Nov-96	6-Apr-97	132	45
6-Sep-97	16-Apr-98	223	112	17-Oct-97	1-Feb-98	108	29
30-Nov-98	21-May-99	173	72	9-Nov-98	14-Feb-99	98	37
1-Sep-99	31-May-00	274	114	29-Oct-99	11-May-00	196	78
19-Sep-00	5-May-01	229	104	28-Oct-00	3-Mar-01	127	37
13-Sep-01	18-Apr-02	218	86	26-Oct-01	22-Mar-02	148	35
26-Jul-02	25-Mar-03	243	99	15-Dec-02	26-Feb-03	74	16
13-Sep-03	12-Mar-04	182	74	27-Oct-03	1-Apr-04	158	46
4-Aug-04	22-Jun-05	323	102	22-Nov-04	3-Mar-05	102	18
10-Sep-05	10-May-06	243	108	14-Nov-05	2-May-06	170	42
18-Aug-06	30-Jun-07	317	98	1-Dec-06	4-Apr-07	125	23
14-Sep-07	29-Apr-08	229	107	8-Oct-07	2-Mar-08	147	29
20-Sep-08	12-May-09	235	117	9-Nov-08	2-Feb-09	86	25
10-Aug-09	10-Apr-10	244	116	20-Nov-09	4-Apr-10	136	12
13-Oct-10	10-Jun-11	241	89	9-Nov-10	22-Apr-11	165	40
1-Aug-11	1-Apr-12	245	101	25-Oct-11	1-Feb-12	100	30
22-Sep-12	25-Apr-13	216	108	22-Oct-12	21-Apr-13	182	65

29-Sep-13	18-Mar-14	171	89	26-Nov-13	13-Mar-14	108	49
29-Dec-14	12-Apr-15	105	43	17-Dec-14	21-Feb-15	67	23
30-Jul-15	17-May-16	293	91	13-Sep-15	22-Mar-16	192	47

Nelspruit				Ottosdal			
Onset date	Cessation date	Length of wet season	Rain days	Onset date	Cessation date	Length of wet season	Rain days
29-Sep-87	11-Apr-88	196	79	11-Sep-87	24-Apr-88	227	97
3-Sep-88	4-Jun-89	275	81	17-Oct-88	5-May-89	201	77
28-Oct-89	7-Apr-90	162	77	27-Oct-89	28-Apr-90	184	68
12-Oct-90	8-Jun-91	240	59	12-Dec-90	23-Mar-91	102	41
21-Nov-91	15-Apr-92	147	33	2-Oct-91	21-Mar-92	172	49
29-Dec-92	22-Feb-93	56	10	6-Nov-92	17-Apr-93	163	57
30-Aug-93	2-Apr-94	216	78	10-Oct-93	8-Apr-94	181	60
19-Oct-94	6-May-95	200	83	6-Nov-94	2-Apr-95	148	48
9-Nov-95	25-May-96	199	98	25-Oct-95	13-May-96	202	80
25-Oct-96	29-May-97	217	105	1-Nov-96	1-Jun-97	213	83
9-Sep-97	2-Apr-98	206	80	8-Sep-97	30-Mar-98	204	57
19-Sep-98	29-Apr-99	223	80	14-Oct-98	20-May-99	219	62
30-Sep-99	21-Apr-00	205	96	15-Nov-99	3-Apr-00	141	54
27-Sep-00	14-Apr-01	200	72	29-Oct-00	2-May-01	186	54
22-Oct-01	16-Apr-02	177	77	27-Sep-01	13-Mar-02	168	63
6-Oct-02	16-Apr-03	193	73	24-Aug-02	23-Mar-03	212	54
27-Oct-03	11-Apr-04	168	57	27-Oct-03	21-Apr-04	178	50
14-Nov-04	3-Apr-05	141	64	20-Oct-04	23-Apr-05	186	53
7-Nov-05	2-May-06	177	81	29-Nov-05	23-Apr-06	146	52
10-Nov-06	19-Apr-07	161	65	5-Nov-06	5-Jun-07	213	39
4-Oct-07	21-Apr-08	201	79	5-Oct-07	5-Apr-08	184	59
23-Oct-08	9-May-09	199	88	14-Nov-08	15-Jun-09	214	40
20-Feb-09	27-Apr-10	67	44	8-Oct-09	2-May-10	207	57
4-Nov-10	20-Apr-11	168	69	13-Nov-10	26-Apr-11	165	68
28-Sep-11	26-Apr-12	212	98	28-Nov-11	1-Feb-12	66	7
13-Sep-12	15-May-13	245	78	2-Dec-12	1-Feb-13	62	18
27-Oct-13	20-Mar-14	145	78	9-Dec-13	13-Mar-14	95	36
10-Nov-14	17-Apr-15	159	85	8-Nov-14	25-Mar-15	138	53
11-Sep-15	22-Mar-16	194	68	26-Nov-15	15-May-16	172	63

Oudtshoorn				Paddock			
Onset date	Cessation date	Length of wet season	Rain days	Onset date	Cessation date	Length of wet season	Rain days
22-Apr-87	1-Nov-87	193	34	19-Jun-87	11-May-88	328	161
ND	ND			26-Aug-88	23-Apr-89	241	104
22-Mar-89	21-Nov-89	245	58	9-Jul-89	25-Apr-90	291	118
ND	ND			21-Aug-90	13-May-91	266	107
3-Feb-91	1-Nov-91	272	62	8-Sep-91	16-Apr-92	222	110
ND	ND			12-Sep-92	12-Apr-93	213	89
23-Feb-93	1-Nov-93	252	40	26-Sep-93	2-Apr-94	189	89
13-Mar-94	26-Dec-94	289	55	3-Aug-94	13-Apr-95	254	107
5-May-95	31-Dec-95	241	52	12-Oct-95	11-Apr-96	183	93
ND	ND			15-Jul-96	30-May-97	320	141
7-Apr-97	1-Nov-97	209	44	19-Jun-97	22-May-98	338	144
14-Jan-98	21-Dec-98	342	56	14-Aug-98	18-May-99	278	108
ND	ND			10-Sep-99	31-May-00	265	108
24-Jan-00	21-Nov-00	303	38	22-Sep-00	5-May-01	226	115
ND	ND			30-Aug-01	14-Apr-02	228	110
ND	ND			24-Jul-02	19-May-03	300	121
ND	ND			13-Sep-03	1-Apr-04	202	89
ND	ND			3-Aug-04	4-May-05	275	109
ND	ND			5-Oct-05	2-May-06	210	96
ND	ND			29-Aug-06	22-Apr-07	237	118
ND	ND			30-Sep-07	1-May-08	215	107

ND	ND			25-Jun-08	9-May-09	319	129
22-Feb-09	7-Dec-09	289	48	30-Sep-09	23-Apr-10	206	109
4-Mar-10	16-Dec-10	288	58	12-Oct-10	26-May-11	227	104
ND	ND			2-Aug-11	9-Apr-12	252	135
ND	ND			14-Aug-12	12-May-13	272	151
7-Feb-13	1-Nov-13	268	48	25-Oct-13	17-Mar-14	144	93
13-Jan-14	12-Nov-14	304	52	3-Oct-14	14-Apr-15	194	113
30-Mar-15	11-Nov-15	227	35	25-Jul-15	11-May-16	292	135
ND	ND						

Pofadder				Polokwane Wo			
Onset date	Cessation date	Length of wet season	Rain days	Onset date	Cessation date	Length of wet season	Rain days
ND	ND			2-Sep-87	12-Mar-88	193	61
16-Feb-89	22-Apr-89	66	14	20-Oct-88	30-Apr-89	193	50
ND	ND			1-Nov-89	23-Mar-90	143	46
ND	ND			23-Nov-90	25-Mar-91	123	41
ND	ND			21-Nov-91	21-Feb-92	93	23
18-Feb-93	1-May-93	73	13	20-Dec-92	1-Feb-93	44	10
3-Feb-94	6-Mar-94	32	9	12-Nov-93	21-Apr-94	161	40
ND	ND			8-Nov-94	7-May-95	181	58
ND	ND			18-Nov-95	17-Jul-96	243	66
15-Nov-97	27-May-97	194	14	24-Oct-96	13-Mar-97	141	48
ND	ND			10-Oct-97	12-Apr-98	185	42
ND	ND			25-Oct-98	24-Mar-99	151	54
17-Feb-00	1-Apr-00	45	12	20-Nov-99	21-Apr-00	154	59
ND	ND			9-Nov-00	24-Mar-01	136	38
ND	ND			26-Oct-01	1-Feb-02	93	36
ND	ND			21-Dec-02	21-Feb-03	63	14
ND	ND			3-Dec-03	1-Apr-04	121	41
ND	ND			29-Nov-04	13-Mar-05	105	28
26-Jan-06	22-Apr-06	87	7	9-Nov-05	2-Apr-06	145	48
ND	ND			9-Nov-06	5-Apr-07	148	40
ND	ND			5-Oct-07	13-Mar-08	161	49
ND	ND			11-Nov-08	8-May-09	179	51
ND	ND			7-Nov-09	26-Apr-10	171	55
ND	ND			6-Nov-10	19-May-11	195	55
25-Jan-12	11-Feb-12	18	5	25-Oct-11	30-Mar-12	158	45
ND	ND			18-Oct-12	20-Apr-13	185	48
17-Feb-14	24-Mar-14	36	4	30-Oct-13	17-Mar-14	139	48
ND	ND			17-Dec-14	18-Apr-15	123	36
ND	ND			22-Nov-15	22-Mar-16	122	30

Port Elizabeth Wo				Port Nolloth			
Onset date	Cessation date	Length of wet season	Rain days	Onset date	Cessation date	Length of wet season	Rain days
11-Feb-87	22-Dec-87	315	100	ND	ND		
28-Feb-88	11-Nov-88	258	84	ND	ND		
14-Apr-89	23-Nov-89	224	74	ND	ND		
23-Feb-90	1-Nov-90	252	74	ND	ND		
ND	ND			ND	ND		
26-Feb-92	24-Nov-92	273	86	ND	ND		
17-Jan-93	11-Dec-93	329	75	ND	ND		
9-Mar-94	28-Dec-94	295	71	ND	ND		
14-Jan-95	25-Dec-95	346	105	ND	ND		
27-Jan-96	31-Dec-96	340	101	ND	ND		
3-Apr-97	3-Dec-97	245	68	ND	ND		
8-Mar-98	21-Dec-98	289	76	ND	ND		
15-Jan-99	31-Dec-99	351	86	ND	ND		
10-Jan-00	23-Nov-00	319	90	ND	ND		
16-Jan-01	25-Dec-01	344	92	ND	ND		

8-May-02	31-Dec-02	238	80	ND	ND
27-Mar-03	26-Dec-03	275	65	ND	ND
25-Jan-04	31-Dec-04	342	89	ND	ND
7-Feb-05	21-Nov-05	288	73	ND	ND
11-Jan-06	11-Dec-06	335	101	ND	ND
6-Mar-07	25-Dec-07	295	70	ND	ND
21-Apr-08	21-Nov-08	215	50	ND	ND
ND	ND			ND	ND
ND	ND			ND	ND
7-May-11	11-Dec-11	219	77	ND	ND
9-Feb-12	1-Nov-12	267	89	ND	ND
5-Feb-13	4-Dec-13	303	86	ND	ND
9-Mar-14	31-Dec-14	298	96	ND	ND
4-Feb-15	1-Dec-15	301	98	ND	ND
14-Mar-16	21-Nov-16	253	83	ND	ND

Prieska				Riversdale			
Onset date	Cessation date	Length of wet season	Rain days	Onset date	Cessation date	Length of wet season	Rain days
8-Dec-87	22-Mar-88	106	18	19-Apr-87	1-Nov-87	197	54
23-Sep-88	23-Apr-89	213	35	13-Apr-88	1-Nov-88	203	48
10-Feb-90	30-Jun-90	141	22	12-Mar-89	23-Nov-89	257	88
15-Dec-90	19-Jun-91	187	28	24-Feb-90	31-Dec-90	311	82
8-Oct-91	1-Apr-92	177	34	30-Jan-91	8-Dec-91	313	86
ND	ND			14-Feb-92	21-Nov-92	282	97
8-Feb-94	13-Mar-94	34	11	10-Apr-93	4-Dec-93	239	71
1-Apr-95	6-May-95	36	5	10-Feb-94	31-Dec-94	325	98
26-Nov-95	25-Jul-96	243	37	19-Feb-95	31-Dec-95	316	102
13-Nov-96	27-Mar-97	135	23	ND	ND		
21-Feb-97	31-Mar-98	39	8	24-Mar-97	25-Nov-97	247	75
ND	ND			14-Jan-98	21-Dec-98	342	94
9-Dec-99	3-Apr-00	117	34	1-Feb-99	1-Nov-99	274	82
22-Sep-00	4-May-01	225	29	10-Jan-00	21-Nov-00	317	94
ND	ND			20-Mar-01	11-Nov-01	237	66
ND	ND			4-May-02	1-Nov-02	182	52
6-Nov-03	3-Apr-04	150	28	16-Feb-03	1-Nov-03	259	76
ND	ND			1-Apr-04	30-Dec-04	274	67
8-Jan-06	2-May-06	115	34	6-Mar-05	21-Nov-05	261	70
ND	ND			ND	ND		
8-Dec-07	18-Jun-08	194	32	ND	ND		
18-Nov-08	21-Feb-09	96	13	18-Feb-08	21-Nov-08	278	84
11-Jan-10	2-Apr-10	82	22	16-Feb-09	1-Nov-09	259	66
8-Jan-10	10-May-11	123	41	ND	ND		
ND	ND			5-May-11	1-Dec-11	211	74
9-Dec-12	31-Mar-13	113	20	24-Mar-12	1-Nov-12	223	88
11-Dec-13	20-May-14	161	25	11-Feb-13	21-Nov-13	284	81
ND	ND			13-Jan-14	21-Nov-14	313	99
21-Jan-16	9-May-16	110	19	ND	ND		
				ND	ND		

Robertson				Shaleburn			
Onset date	Cessation date	Length of wet season	Rain days	Onset date	Cessation date	Length of wet season	Rain days
22-Apr-87	12-Aug-87	113	22	22-Aug-87	11-Apr-88	234	147
ND	ND			5-Sep-88	22-Apr-89	230	133
22-Apr-89	17-Nov-89	210	55	24-Oct-89	2-May-90	191	114
27-Apr-90	1-Aug-90	97	26	6-Sep-90	24-Mar-91	200	104
30-Jun-91	31-Oct-91	124	33	8-Oct-91	25-Mar-92	170	101
30-May-92	25-Oct-92	149	38	9-Oct-92	12-Apr-93	186	98
10-Apr-93	3-Aug-93	116	35	8-Oct-93	15-Mar-94	159	106

10-Mar-94	21-Oct-94	226	54	3-Aug-94	12-Apr-95	253	111
13-May-95	30-Nov-95	202	38	22-Oct-95	11-Apr-96	173	110
1-Jun-96	21-Nov-96	174	45	5-Nov-96	12-Jun-97	220	122
26-Mar-97	1-Aug-97	129	28	16-Oct-97	22-Apr-98	189	120
30-Apr-98	20-Nov-98	205	32	8-Nov-98	12-Apr-99	156	98
ND	ND			25-Oct-99	26-Apr-00	185	122
10-Mar-00	1-Aug-00	145	31	22-Sep-00	17-Apr-01	208	133
7-Jul-01	31-Aug-01	56	16	8-Sep-01	1-Jun-02	267	142
ND	ND			27-Jul-02	23-Apr-03	271	154
24-Mar-03	25-Aug-03	155	37	3-Nov-03	11-Apr-04	161	110
ND	ND			3-Aug-04	3-Apr-05	244	151
18-Apr-05	12-Nov-05	209	40	18-Aug-05	2-May-06	258	160
17-May-06	31-Aug-06	107	37	24-Aug-06	22-Apr-07	242	158
28-May-07	26-Nov-07	183	36	3-Oct-07	29-Apr-08	210	137
6-Jul-08	14-Nov-08	132	33	26-Sep-08	12-May-09	229	159
23-Apr-09	13-Oct-09	174	34	1-Oct-09	22-Apr-10	204	138
2-Mar-10	25-Oct-10	238	52	13-Oct-10	25-Apr-11	195	146
7-Jun-11	31-Aug-11	86	24	2-Aug-11	5-Apr-12	248	125
14-Jun-12	26-Oct-12	135	55	15-Aug-12	22-Apr-13	251	158
18-Apr-13	19-Nov-13	216	57	26-Oct-13	24-Apr-14	181	120
ND	ND			30-Oct-14	12-Apr-15	165	100
9-Jun-15	30-Sep-15	114	33	30-Jul-15	11-Apr-16	257	127
12-Jun-16	9-Sep-16	90	28				

Skukuza				Springbok Wo			
Onset date	Cessation date	Length of wet season	Rain days	Onset date	Cessation date	Length of wet season	Rain days
2-Sep-87	16-Mar-88	197	71	ND	ND		
8-Sep-88	6-Jun-89	272	60	12-Jun-88	20-Sep-88	101	20
31-Oct-89	29-Apr-90	181	66	22-Apr-89	1-Aug-89	102	13
16-Oct-90	20-Jun-91	248	48	21-Apr-90	1-Aug-90	103	23
22-Nov-91	12-Mar-92	112	21	26-Jun-91	8-Sep-91	75	20
21-Nov-92	28-Apr-93	159	40	15-Jul-92	1-Nov-92	110	17
12-Dec-93	15-Mar-94	94	22	9-Apr-93	1-Aug-93	115	27
21-Oct-94	10-May-95	202	58	19-Apr-94	1-Aug-94	105	14
25-Oct-95	22-May-96	211	81	14-May-95	1-Oct-95	141	24
28-Aug-96	22-Apr-97	238	71	2-Jul-96	9-Nov-96	131	35
17-Oct-97	17-Apr-98	183	56	26-Mar-97	20-Nov-97	240	33
7-Oct-98	29-Apr-99	205	93	ND	ND		
29-Oct-99	11-Apr-00	166	79	ND	ND		
27-Sep-00	2-May-01	218	71	ND	ND		
16-Nov-01	19-Apr-02	155	47	7-Jul-01	5-Sep-01	61	24
7-Nov-02	27-Apr-03	172	44	ND	ND		
14-Sep-03	14-Apr-04	214	66	ND	ND		
11-Sep-04	26-Apr-05	228	59	ND	ND		
7-Nov-05	2-Apr-06	147	64	27-Jan-05	17-Oct-05	264	49
8-Nov-06	3-Mar-07	116	31	25-Apr-06	31-Aug-06	129	33
8-Oct-07	20-Apr-08	196	48	23-May-07	14-Aug-07	84	18
7-Nov-08	8-May-09	183	61	12-Mar-08	8-Sep-08	181	27
18-Nov-09	26-Apr-10	160	44	22-Jun-09	12-Nov-09	144	23
6-Nov-10	5-Apr-11	151	54	ND	ND		
8-Oct-11	31-Mar-12	176	55	13-Jan-11	5-Aug-11	205	36
13-Sep-12	21-Apr-13	221	72	16-Jun-12	1-Dec-12	169	29
27-Oct-13	13-Mar-14	138	51	8-Apr-13	31-Aug-13	146	28
19-Oct-14	1-Feb-15	106	34	6-Jun-14	3-Nov-14	151	23
11-Sep-15	17-Mar-15	189	45	9-Jun-15	1-Aug-15	54	12
				26-Jan-16	2-Aug-16	190	24

Sutherland				Twee Rivieren			
Onset date	Cessation date	Length of wet season	Rain days	Onset date	Cessation date	Length of wet season	Rain days
ND	ND			2-Dec-87	17-Apr-88	138	25
4-Mar-88	9-Dec-88	281	53	26-Dec-88	21-Feb-89	58	13
22-Apr-89	3-Sep-89	135	28	31-Jan-89	21-Apr-90	81	14
ND	ND			9-Dec-90	27-Mar-91	109	16
2-Feb-91	22-Oct-91	263	57	26-Dec-91	17-Mar-92	83	4
ND	ND			ND	ND		
13-Apr-93	1-Aug-93	111	24	30-Jan-94	5-Mar-94	35	13
11-Mar-94	1-Aug-94	144	8	ND	ND		
ND	ND			26-Nov-95	24-Jul-96	242	23
8-Jun-96	29-Nov-96	175	50	ND	ND		
23-May-97	1-Aug-97	71	15	9-Jan-98	27-Mar-98	78	9
1-Mar-98	19-Nov-98	264	30	ND	ND		
ND	ND			16-Dec-99	21-Apr-00	128	29
27-Feb-00	1-Aug-00	157	27	27-Jan-00	30-Apr-01	94	18
ND	ND			ND	ND		
3-Feb-02	31-Aug-02	210	47	ND	ND		
ND	ND			12-Jan-04	8-Apr-04	88	12
10-Apr-04	1-Aug-04	114	11	27-Oct-04	15-Apr-05	171	21
ND	ND			8-Jan-06	21-Apr-06	104	17
6-Feb-06	31-Aug-06	207	36	ND	ND		
ND	ND			24-Dec-07	12-Apr-08	111	25
13-Mar-08	1-Aug-08	142	35	31-Jan-09	3-Mar-09	32	17
14-Mar-09	1-Aug-09	141	46	30-Dec-09	3-Mar-10	64	18
3-Mar-10	20-Dec-10	293	55	30-Dec-11	23-Apr-11	108	44
9-Feb-11	31-Aug-11	204	64	7-Dec-11	1-Apr-12	117	26
4-May-12	23-Dec-12	234	65	20-Dec-12	31-Mar-13	102	19
4-Apr-13	21-Aug-13	140	44	11-Dec-13	2-Apr-14	113	26
ND	ND			27-Mar-15	3-Apr-15	8	5
ND	ND			24-Jan-16	7-Apr-16	75	15
23-Jan-16	1-Aug-16	192	49				

Umtata Wo				Upington Wo			
Onset date	Cessation date	Length of wet season	Rain days	Onset date	Cessation date	Length of wet season	Rain days
21-Sep-87	28-May-88	251	117	10-Mar-88	17-Apr-88	39	9
5-Sep-88	2-May-89	240	105	31-Dec-88	21-Feb-89	53	14
26-Jul-89	1-Apr-90	250	89	ND	ND		
7-Sep-90	24-Mar-91	199	83	19-Jan-91	29-Mar-91	70	19
8-Oct-91	21-Apr-92	197	92	17-Oct-91	27-Feb-92	134	29
10-Dec-92	4-Apr-93	116	42	ND	ND		
1-Oct-93	21-Apr-94	203	88	9-Jan-94	13-Mar-94	64	16
9-Oct-94	28-Apr-95	202	76	ND	ND		
26-Sep-95	22-Mar-96	179	97	24-Jan-96	2-Mar-96	39	10
6-Nov-96	18-Jun-97	225	109	15-Nov-96	26-Mar-97	132	15
26-Nov-97	2-May-98	158	75	ND	ND		
30-Aug-98	26-Mar-99	209	94	ND	ND		
25-Oct-99	11-May-00	200	94	5-Oct-99	21-Apr-00	200	46
22-Sep-00	2-May-01	223	95	ND	ND		
21-Sep-01	30-May-02	252	92	18-Nov-01	21-May-02	185	27
24-Jul-02	2-Apr-03	253	83	ND	ND		
15-Sep-03	4-May-04	233	72	6-Nov-03	22-Mar-04	138	19
3-Aug-04	2-Apr-05	243	60	21-Jan-05	23-Mar-05	62	22
18-Aug-05	22-Apr-06	248	95	8-Jan-06	22-Apr-06	105	26
10-Aug-06	6-Apr-07	240	113	ND	ND		
8-Oct-07	22-Jun-08	259	106	25-Oct-07	18-Jun-08	238	44
18-Nov-08	2-May-09	166	65	ND	ND		
1-Aug-09	22-Apr-10	265	98	11-Oct-09	5-Apr-10	177	31
31-Oct-10	11-Jun-11	224	107	23-Dec-10	8-Jun-11	168	42
2-Aug-11	23-Jun-12	327	109	27-Dec-11	26-Apr-12	122	24

16-Jul-12	12-May-13	301	111	ND	ND		
21-Oct-13	26-Apr-14	188	76	11-Dec-13	3-Mar-14	83	16
3-Oct-14	23-Apr-15	203	68	22-Mar-14	10-Apr-15	20	7
20-Nov-15	21-Apr-16	154	50	20-Jan-16	12-May-16	114	19

Vanwyksvlei				Vredendal			
Onset date	Cessation date	Length of wet season	Rain days	Onset date	Cessation date	Length of wet season	Rain days
23-Feb-88	20-Apr-88	58	18	ND	ND		
27-Dec-88	27-Apr-89	122	28	ND	ND		
ND	ND			ND	ND		
13-Dec-90	18-Jun-91	187	16	ND	ND		
17-Oct-91	29-Mar-92	165	17	ND	ND		
ND	ND			ND	ND		
24-Dec-93	23-Mar-93	90	33	13-Apr-93	1-Aug-93	111	28
ND	ND			ND	ND		
25-Nov-95	24-Jul-96	243	32	ND	ND		
13-Nov-96	27-Mar-97	135	21	ND	ND		
9-Jan-98	30-Mar-98	81	9	28-May-97	1-Aug-97	66	13
6-Feb-99	19-May-99	103	16	ND	ND		
ND	ND			ND	ND		
ND	ND			ND	ND		
23-Sep-01	16-Mar-02	175	30	12-Jul-01	27-Oct-01	108	26
ND	ND			ND	ND		
14-Jan-04	8-Apr-04	86	15	ND	ND		
ND	ND			ND	ND		
25-Jan-06	2-May-06	98	23	ND	ND		
ND	ND			ND	ND		
8-Dec-07	26-Jun-08	202	49	10-Jun-07	2-Aug-07	54	17
29-Nov-08	24-Jun-09	208	34	20-Jun-08	8-Sep-08	81	28
10-Jan-10	3-Mar-10	53	8	ND	ND		
30-Jan-11	18-Mar-11	48	17	ND	ND		
ND	ND			ND	ND		
9-Dec-12	1-Apr-13	114	22	ND	ND		
11-Dec-13	25-Mar-14	105	26	2-Jun-13	3-Sep-13	94	37
ND	ND			ND	ND		
26-Jan-16	9-May-16	105	14	ND	ND		
				ND	ND		

Vryburg				Warmbad Towoomba			
Onset date	Cessation date	Length of wet season	Rain days	Onset date	Cessation date	Length of wet season	Rain days
11-Sep-87	11-Apr-88	214	64	16-Sep-87	24-Apr-88	222	71
19-Oct-88	4-May-89	198	71	9-Sep-88	2-May-89	236	66
8-Jan-90	28-Apr-90	111	38	23-Aug-89	29-Apr-90	250	71
5-Dec-90	17-Jun-91	195	47	4-Dec-90	25-Mar-91	112	53
2-Oct-91	22-Feb-92	144	37	20-Oct-91	24-Mar-92	157	53
29-Jan-93	3-Mar-93	34	13	7-Nov-92	2-Apr-93	147	52
14-Oct-93	15-Apr-94	184	47	11-Oct-93	11-Feb-94	124	46
19-Jan-95	29-Mar-95	70	19	19-Oct-94	12-May-95	206	71
22-Sep-95	12-May-96	234	60	27-Oct-95	18-May-96	205	51
15-Nov-96	12-May-97	179	56	31-Oct-96	26-May-97	208	60
19-Oct-97	2-Apr-98	166	35	13-Oct-97	13-Mar-98	152	47
9-Nov-98	19-May-99	192	47	15-Oct-98	22-May-99	220	60
22-Dec-99	11-May-00	142	42	27-Nov-99	21-Apr-00	147	71
26-Nov-00	3-May-01	159	47	3-Nov-00	1-May-01	180	43
27-Sep-01	31-May-02	247	65	7-Nov-01	31-May-02	206	50
26-Aug-02	23-Mar-03	210	48	3-Sep-02	21-Feb-03	152	32
22-Nov-03	11-Apr-04	142	34	22-Oct-03	23-Mar-04	154	36
29-Nov-04	22-Apr-05	145	45	8-Dec-04	2-May-05	146	26

8-Dec-05	22-Apr-06	136	51	28-Nov-05	2-Apr-06	126	42
4-Nov-06	3-Apr-07	151	26	27-Oct-06	6-Jun-07	223	44
5-Oct-07	3-May-08	212	70	5-Oct-07	1-Apr-08	180	80
19-Nov-08	13-Jun-09	207	47	9-Nov-08	17-Jun-09	221	54
27-Nov-09	12-Apr-10	137	28	29-Oct-09	9-Apr-10	163	60
17-Nov-10	8-Jun-11	204	58	16-Oct-10	23-Apr-11	190	47
13-Dec-11	21-Mar-12	100	24	5-Nov-11	16-Mar-12	133	48
9-Dec-12	19-Apr-13	132	31	15-Sep-12	22-Apr-13	220	75
23-Nov-13	16-Mar-14	114	28	28-Oct-13	23-Mar-14	147	67
2-Nov-14	30-Mar-15	149	50	19-Nov-14	27-Apr-15	160	51
13-Mar-16	8-Apr-16	27	10	13-Sep-15	22-Mar-16	192	64

Welkom				Willowmore			
Onset date	Cessation date	Length of wet season	Rain days	Onset date	Cessation date	Length of wet season	Rain days
23-Aug-87	24-Apr-88	246	89	20-Nov-87	11-Apr-88	144	20
17-Oct-88	2-May-89	198	68	ND	ND		
11-Nov-89	28-Apr-90	169	69	23-Nov-89	22-Apr-90	151	26
12-Dec-90	23-Mar-91	102	47	14-Dec-90	21-Feb-91	70	13
1-Oct-91	2-Mar-92	154	47	29-Oct-91	23-Jul-92	269	39
4-Sep-92	21-Feb-93	171	45	19-Oct-92	25-Feb-93	126	18
10-Oct-93	1-Feb-94	115	44	6-Dec-93	30-Apr-94	146	33
12-Nov-94	6-May-95	176	52	1-Jan-94	8-May-95	128	33
29-Oct-95	8-Jul-96	254	72	23-Dec-95	3-Mar-96	72	20
25-Nov-96	28-Jul-97	246	57	5-Nov-96	27-May-97	204	34
31-Dec-97	2-Apr-98	93	33	27-Mar-97	6-Aug-98	133	19
2-Nov-98	1-Feb-99	92	29	13-Dec-98	12-Mar-99	90	15
10-Dec-99	3-May-00	146	42	31-Dec-99	21-Feb-00	53	11
29-Oct-00	5-May-01	189	63	9-Nov-00	16-Apr-01	159	21
23-Oct-01	10-Apr-02	170	57	4-Nov-01	19-Jul-02	258	42
24-Aug-02	23-Mar-03	212	49	11-Dec-02	25-Mar-03	105	11
19-Nov-03	1-Feb-04	75	20	14-Jan-04	9-Jun-04	148	23
7-Dec-04	14-May-05	159	46	26-Nov-04	17-Apr-05	143	24
29-Nov-05	2-Apr-06	125	44	14-Nov-05	4-Aug-06	264	44
7-Nov-06	1-Feb-07	87	24	ND	ND		
5-Oct-07	23-Mar-08	171	53	1-Dec-07	12-Mar-08	103	27
15-Nov-08	16-Jun-09	214	50	ND	ND		
7-Dec-09	12-Apr-10	127	47	13-Oct-09	16-Jun-10	247	52
24-Oct-10	8-Jun-11	228	59	3-Feb-11	28-Jul-11	176	56
10-Dec-11	1-Feb-12	54	15	31-Jan-12	21-Jul-12	173	40
3-Nov-12	1-Feb-13	91	26	25-Oct-12	2-Apr-13	160	23
29-Oct-13	13-Mar-14	136	46	29-Oct-13	3-Apr-14	157	36
9-Nov-14	2-Apr-15	145	49	25-Sep-14	4-Jun-15	253	39
ND	ND			29-Jan-16	26-Mar-16	58	12

APPENDIX F: ANNUAL 10% AND 90% DATES, LENGTH OF THE WET SEASON AND NUMBER OF RAIN DAYS

This section contains the annual 10% and 90% dates, length of the wet season and number of rain days from all weather stations. Weather stations which contained missing years were indicated by presenting n.

Aliwal-North Plaatkop				Bethal (n = 29)			
10% date	90% date	Length of wet season	Rain days	10% date	90% date	Length of wet season	Rain days
23-Sep-87	15-Apr-88	206	59	27-Sep-87	5-Apr-88	192	78
14-Sep-88	16-Apr-89	215	74	19-Oct-88	16-May-89	210	75
12-Nov-89	3-Jun-90	204	64	2-Nov-89	28-Apr-90	178	73
4-Dec-90	17-Mar-91	104	39	4-Nov-90	4-Mar-91	121	50
2-Oct-91	28-Mar-92	179	54	10-Nov-91	24-Mar-92	136	52
9-Oct-92	12-Apr-93	186	51	30-Oct-92	23-Mar-93	145	64
5-Oct-93	26-Mar-94	173	62	30-Sep-93	14-Mar-94	166	70
13-Nov-94	6-May-95	175	41	8-Nov-94	26-Mar-95	139	54
18-Oct-95	1-Apr-96	167	68	19-Oct-95	14-Mar-96	148	80
13-Oct-96	22-Apr-97	192	71	28-Oct-96	25-May-97	210	77
16-Nov-97	25-Apr-98	161	50	3-Oct-97	19-Feb-98	140	60
10-Oct-98	12-Mar-99	154	49	1-Oct-98	22-Mar-99	173	70
17-Dec-99	29-Apr-00	135	54	21-Dec-99	15-Apr-00	117	55
16-Sep-00	2-May-01	229	71	21-Oct-00	23-Mar-01	154	72
28-Oct-01	10-Apr-02	165	59	25-Oct-01	13-Mar-02	140	52
17-Aug-02	21-Mar-03	217	50	23-Oct-02	13-Apr-03	173	48
30-Oct-03	4-Apr-04	158	54	10-Nov-03	6-Apr-04	149	59
24-Sep-04	4-May-05	223	54	19-Oct-04	15-Mar-05	148	62
30-Oct-05	21-Apr-06	174	61	4-Nov-05	18-Mar-06	135	59
25-Sep-06	17-Apr-07	205	48	24-Aug-06	25-Mar-07	214	51
13-Oct-07	4-May-08	205	80	8-Oct-07	15-Mar-08	160	58
11-Nov-08	21-Jun-09	223	83	6-Nov-08	25-Apr-09	171	57
11-Oct-09	16-Apr-10	188	70	12-Oct-09	5-Apr-10	176	77
16-Nov-10	6-Jun-11	203	118	4-Nov-10	6-Apr-11	154	57
5-Dec-11	21-Jun-12	200	72	1-Oct-11	28-Mar-12	180	41
16-Oct-12	29-Mar-13	165	56	6-Sep-12	3-Apr-13	210	68
16-Nov-13	16-Mar-14	121	46	20-Oct-13	5-Mar-14	137	64
3-Nov-14	2-Jun-15	212	61	12-Oct-14	4-Apr-94	175	54
11-Jan-16	25-Jul-16	197	53	ND	ND		

Bethlehem Wo				Bloemfontein Wo			
10% date	90% date	Length of wet season	Rain days	10% date	90% date	Length of wet season	Rain days
21-Sep-87	13-Mar-88	175	83	8-Sep-87	3-Apr-88	209	82
13-Oct-88	15-Apr-89	185	81	12-Oct-88	21-Apr-89	192	88
2-Nov-89	24-Apr-90	174	86	2-Nov-89	24-Apr-90	174	69
14-Oct-90	18-Mar-91	156	68	5-Dec-90	18-Mar-91	104	40
12-Oct-91	1-Mar-92	142	55	12-Oct-91	19-Feb-92	131	43
30-Aug-92	6-Mar-93	189	78	11-Oct-92	3-Apr-93	175	40
2-Oct-93	1-Mar-94	151	65	2-Oct-93	3-Mar-94	153	59
28-Oct-94	4-Apr-95	159	64	14-Nov-94	2-May-95	170	50
23-Oct-95	5-May-96	196	84	29-Oct-95	4-Apr-96	159	60
22-Oct-96	25-May-97	216	105	7-Nov-96	22-Apr-97	167	49
1-Oct-97	7-Mar-98	158	62	23-Dec-97	26-Mar-98	94	36
28-Oct-98	22-Mar-99	146	62	10-Oct-98	17-May-99	220	58
15-Dec-99	20-Apr-00	128	60	21-Oct-99	3-Apr-00	166	61
3-Oct-00	15-Apr-01	195	83	4-Oct-00	26-Apr-01	205	55
12-Sep-01	9-Apr-02	210	87	21-Oct-01	5-May-02	197	65
28-Aug-02	18-Mar-03	203	67	17-Aug-02	21-Mar-03	217	60
30-Oct-03	4-Apr-04	158	62	3-Nov-03	30-Mar-04	149	56
19-Nov-04	22-Mar-05	124	63	25-Sep-04	18-Apr-05	206	55
19-Oct-05	24-Mar-06	157	77	10-Nov-05	16-Apr-06	158	56
9-Oct-06	14-Apr-07	188	72	23-Aug-06	9-Apr-07	230	43
2-Oct-07	20-Apr-08	202	77	12-Oct-07	24-May-08	226	75

9-Nov-08	5-May-09	178	72	10-Nov-08	5-May-09	177	64
3-Nov-09	29-Mar-10	147	67	12-Oct-09	24-Apr-10	195	74
9-Nov-10	16-Apr-11	159	75	18-Nov-10	6-Jun-11	201	95
22-Nov-11	21-Jun-12	213	63	30-Nov-11	21-Jun-12	205	53
17-Oct-12	19-Apr-13	185	73	25-Oct-12	27-Mar-13	154	38
28-Oct-13	7-Mar-14	131	60	15-Nov-13	14-Mar-14	120	42
1-Nov-14	25-Mar-15	145	70	3-Nov-14	2-Jun-15	212	49
20-Nov-15	24-Jul-16	248	58	20-Nov-15	13-Jun-16	207	36

Calvinia Wo				Cape Agulhas			
10% date	90% date	Length of wet season	Rain days	10% date	90% date	Length of wet season	Rain days
19-Apr-87	21-Sep-87	156	30	13-Apr-87	30-Sep-87	171	69
7-Mar-88	15-Sep-88	193	41	7-Apr-88	31-Oct-88	208	72
1-Mar-89	3-Sep-89	187	41	12-Mar-89	19-Sep-89	192	78
17-Jan-90	9-Jul-90	174	30	20-Feb-90	16-Sep-90	209	87
17-Mar-91	21-Oct-91	219	53	3-Mar-91	21-Oct-91	233	70
18-Feb-92	24-Oct-92	250	40	12-Apr-92	24-Oct-92	196	78
5-Apr-93	20-Aug-93	138	34	20-Feb-93	26-Aug-93	188	67
5-Feb-94	17-Sep-94	225	34	19-Apr-94	23-Dec-94	249	68
27-Feb-95	29-Nov-95	276	57	19-Mar-95	17-Dec-95	274	79
7-Jun-96	8-Nov-96	155	46	15-Apr-96	19-Nov-96	219	82
18-Mar-97	4-Aug-97	140	29	5-Apr-97	15-Nov-97	225	76
20-Feb-98	5-Dec-98	289	45	27-Mar-98	14-Nov-98	233	74
28-Apr-99	21-Dec-99	238	54	7-Apr-99	11-Oct-99	188	66
18-Feb-00	18-Jul-00	152	26	30-Jan-00	26-Sep-00	238	74
23-Mar-01	11-Nov-01	234	65	6-Apr-01	28-Oct-01	206	83
4-Mar-02	30-Sep-02	211	52	11-Jan-02	25-Sep-02	258	89
23-Mar-03	30-Oct-03	222	39	18-Mar-03	25-Oct-03	222	68
1-Apr-04	20-Oct-04	203	35	22-Mar-04	20-Oct-04	213	56
2-Feb-05	22-Aug-05	202	45	28-Jan-05	5-Sep-05	221	54
2-Feb-06	22-Aug-06	202	44	2-Apr-06	3-Nov-06	216	89
3-Apr-07	24-Dec-07	266	38	3-Mar-07	21-Nov-07	264	91
9-Feb-08	31-Aug-08	205	35	2-Apr-08	12-Nov-08	225	91
8-Mar-09	7-Sep-09	184	36	24-Apr-09	26-Oct-09	186	71
22-Feb-10	15-Dec-10	297	45	10-Mar-10	21-Nov-10	257	82
3-Feb-11	23-Aug-11	202	45	2-Apr-11	8-Nov-11	221	75
7-Apr-12	13-Dec-12	251	46	24-Mar-12	19-Oct-12	210	99
1-Apr-13	7-Dec-13	251	50	30-Mar-13	16-Nov-13	232	100
9-Jan-14	2-Nov-14	298	48	7-Jan-14	16-Oct-14	283	101
10-Apr-15	7-Sep-15	151	25	23-Mar-15	1-Nov-15	224	53
20-Jan-16	15-Sep-16	240	31	5-Mar-16	6-Oct-16	216	71

Cape Town Wo				Cedara			
10% date	90% date	Length of wet season	Rain days	10% date	90% date	Length of wet season	Rain days
19-Apr-87	23-Sep-87	158	65	26-Sep-87	14-Mar-88	171	119
5-Apr-88	25-Sep-88	174	61	27-Sep-88	6-Mar-89	161	111
29-Mar-89	8-Oct-89	194	80	30-Oct-89	25-Mar-90	147	106
11-Apr-90	11-Sep-90	154	70	12-Sep-90	10-Mar-91	180	100
19-May-91	18-Oct-91	153	67	8-Oct-91	19-Mar-92	164	96
15-Apr-92	20-Oct-92	189	81	8-Oct-92	15-Mar-93	159	86
5-Apr-93	6-Aug-93	124	52	6-Oct-93	14-Mar-94	160	100
27-Apr-94	17-Sep-94	144	47	28-Sep-94	20-Apr-95	205	104
19-May-95	28-Nov-95	194	70	23-Oct-95	1-Apr-96	162	103
8-Apr-96	21-Oct-96	197	78	8-Jul-96	20-Apr-97	287	138
23-Apr-97	15-Nov-97	207	62	29-Sep-97	26-Mar-98	179	121
22-Apr-98	4-Nov-98	197	72	10-Oct-98	21-Mar-99	163	101
20-Apr-99	12-Sep-99	146	55	14-Nov-99	30-Mar-00	138	82
23-Apr-00	17-Sep-00	148	60	8-Oct-00	11-Apr-01	186	118
4-May-01	23-Sep-01	143	63	12-Sep-01	10-Apr-02	211	120
16-Jan-02	17-Oct-02	275	90	21-Jul-02	13-Apr-03	267	116

22-Mar-03	16-Oct-03	209	69	17-Sep-03	5-Mar-04	171	95
16-Apr-04	20-Oct-04	188	55	25-Sep-04	10-Mar-05	167	100
10-Apr-05	5-Sep-05	149	64	12-Oct-05	11-Apr-06	182	116
22-Apr-06	2-Nov-06	195	62	26-Sep-06	29-Mar-07	185	123
26-Apr-07	22-Oct-07	180	65	5-Oct-07	14-Apr-08	193	115
28-May-08	19-Oct-08	145	64	10-Nov-08	26-Apr-09	168	117
15-May-09	7-Nov-09	177	66	12-Oct-09	20-Mar-10	160	112
4-May-10	8-Nov-10	189	61	28-Oct-10	25-Apr-11	180	120
25-Apr-11	12-Nov-11	202	71	14-Aug-11	30-Mar-12	230	132
7-Apr-12	28-Sep-12	175	71	5-Sep-12	18-Apr-13	226	140
1-Apr-13	15-Nov-13	229	84	20-Oct-13	17-Mar-14	293	95
25-Mar-14	17-Sep-14	177	59	13-Oct-14	19-Mar-15	158	112
25-May-15	1-Nov-15	161	49	16-Sep-15	21-Mar-16	188	107
26-Mar-16	26-Sep-16	185	54				

Cradock-Mun				De Aar Wo			
10% date	90% date	Length of wet season	Rain days	10% date	90% date	Length of wet season	Rain days
22-Sep-87	19-Apr-88	211	48	22-Sep-87	23-Apr-88	215	53
17-Sep-88	27-Apr-89	223	61	13-Sep-88	12-Apr-89	212	43
9-Nov-89	25-Apr-90	168	46	15-Nov-89	20-Jun-90	218	43
29-Nov-90	7-Jun-91	191	42	5-Dec-90	17-Jun-91	185	38
20-Oct-91	11-Jun-92	236	40	26-Sep-91	30-Mar-92	187	40
11-Oct-92	10-Jun-93	243	31	2-Aug-92	2-May-93	274	38
10-Nov-93	7-Mar-94	118	47	6-Oct-93	6-Mar-94	152	50
3-Nov-94	23-Apr-95	172	31	13-Nov-94	5-May-95	174	32
1-Oct-95	28-Mar-96	180	51	19-Nov-95	23-Jul-96	248	57
7-Nov-96	1-May-97	176	55	7-Nov-96	25-May-97	200	48
16-Nov-97	22-Apr-98	158	41	28-Nov-97	6-May-98	160	32
1-Nov-98	5-Jun-99	217	44	10-Oct-98	19-May-99	222	38
14-Nov-99	12-Apr-00	151	54	15-Nov-99	20-Apr-00	158	49
16-Sep-00	16-Apr-01	213	46	16-Sep-00	16-Apr-01	223	41
17-Sep-01	17-Aug-02	335	65	18-Sep-01	12-Jun-02	268	48
2-Nov-02	10-May-03	190	42	18-Aug-02	18-Apr-03	244	46
30-Oct-03	3-Apr-04	157	38	20-Nov-03	3-Apr-04	136	35
25-Sep-04	10-Apr-05	198	30	25-Sep-04	16-Apr-05	204	36
6-Nov-05	1-Aug-06	269	65	31-Dec-05	2-May-06	123	40
15-Oct-06	5-Jun-07	234	49	2-Aug-06	7-Apr-07	249	34
29-Oct-07	4-Apr-08	159	57	26-Oct-07	18-Jun-08	237	54
27-Nov-08	22-Jun-09	208	43	9-Nov-08	19-Jun-09	223	46
26-Oct-09	25-Mar-10	151	44	4-Nov-09	26-Mar-10	143	32
25-Nov-10	6-May-11	163	68	26-Nov-10	5-May-11	161	51
30-Nov-11	7-Jul-12	221	65	25-Dec-11	21-Jun-12	180	38
19-Oct-12	20-Apr-13	184	34	17-Oct-12	31-Mar-13	166	31
15-Nov-13	14-Apr-14	151	46	15-Nov-13	18-May-14	185	34
3-Nov-14	21-Jul-15	261	64	23-Sep-14	2-Jun-15	253	35
18-Oct-15	14-Jun-16	241	52	15-Jan-16	12-May-16	119	33

East London Wo				Frankfort-TNK			
10% date	90% date	Length of wet season	Rain days	10% date	90% date	Length of wet season	Rain days
22-Sep-78	28-May-	250	109	26-Sep-87	11-Mar-88	168	70
27-Aug-88	30-Mar-89	216	90	15-Oct-88	25-Mar-89	162	59
2-Oct-89	24-Mar-90	174	81	25-Oct-89	26-Apr-90	184	58
3-Sep-90	11-May-	251	79	10-Nov-90	17-Mar-91	128	39
17-Aug-91	29-Mar-92	226	93	13-Oct-91	28-Feb-92	139	47
8-Aug-92	3-Apr-93	239	82	8-Oct-92	2-Apr-93	177	63
21-Sep-93	18-Feb-94	151	69	5-Oct-93	28-Mar-94	175	77
12-Aug-94	20-Apr-95	252	83	28-Oct-94	29-Mar-95	153	61
13-Sep-95	29-Mar-96	199	86	29-Oct-95	17-Apr-96	172	65
20-Oct-96	12-Jun-97	236	113	23-Oct-96	25-May-97	215	84
15-Oct-97	2-Apr-98	170	73	10-Sep-97	7-Mar-98	179	68

6-Sep-98	9-Apr-99	216	81	7-Oct-98	22-Mar-99	167	71
28-Jul-99	13-Apr-00	261	117	22-Dec-99	2-May-00	133	52
18-Sep-00	2-Apr-01	197	79	7-Oct-00	5-Apr-01	181	67
5-Aug-01	10-Apr-02	249	110	15-Oct-01	22-May-02	220	81
14-Aug-02	14-Apr-03	244	90	27-Aug-02	6-Jun-03	284	73
14-Sep-03	5-Apr-04	205	88	25-Oct-03	2-Apr-04	161	65
7-Sep-04	11-Apr-05	217	81	5-Nov-04	22-Apr-05	169	63
4-Nov-05	21-May-	199	75	4-Nov-05	26-Mar-06	143	56
20-Aug-06	7-Apr-06	231	102	15-Oct-06	18-Apr-07	186	50
2-Oct-07	29-Apr-07	211	89	3-Oct-07	17-Mar-08	167	87
21-Sep-08	5-Mar-08	166	76	5-Nov-08	14-Mar-09	130	67
28-Sep-09	29-Apr-10	214	87	8-Jan-10	16-Apr-10	99	52
14-Oct-10	10-Jun-11	240	111	26-Nov-10	26-Apr-11	152	83
7-Jul-11	31-Mar-12	269	92	29-Oct-11	30-Mar-12	154	60
6-Sep-12	22-Apr-13	229	97	6-Sep-12	19-Apr-13	226	92
21-Oct-13	25-Apr-14	187	78	27-Oct-13	5-Mar-14	130	61
30-Aug-14	5-Jun-15	280	53	12-Oct-14	26-Mar-15	166	84
22-Jul-15	19-Apr-16	273	99	14-Oct-15	25-Jul-16	286	59

	Fraserburg				Johannesburg INT Wo		
10% date	90% date	Length of wet season	Rain days	10% date	90% date	Length of wet season	Rain days
12-Nov-87	17-Apr-88	158	22	26-Sep-87	12-Mar-88	169	92
7-Nov-88	20-Apr-89	165	32	17-Oct-88	30-Apr-89	196	86
17-Jan-90	21-May-90	125	20	2-Nov-89	25-Apr-90	175	76
5-Dec-90	17-Jun-91	195	14	1-Nov-90	17-Mar-91	137	62
26-Sep-91	6-Jul-92	285	28	16-Oct-91	29-Feb-92	137	56
28-Jan-93	30-Aug-93	215	24	2-Nov-92	22-Mar-93	141	60
8-Nov-93	20-Jun-94	225	28	5-Oct-93	3-Mar-94	150	69
26-Dec-94	20-Aug-95	238	35	28-Oct-94	8-Apr-95	163	70
19-Nov-95	25-Jul-96	250	37	29-Oct-95	13-Mar-96	137	67
18-Oct-96	8-Jun-97	234	35	14-Nov-96	24-May-97	192	75
5-Jan-98	5-Aug-98	213	20	24-Oct-97	19-Feb-98	119	46
16-Sep-98	12-May-99	239	34	25-Oct-98	22-Apr-99	180	71
20-Oct-99	1-Apr-00	165	42	12-Dec-99	26-Mar-00	106	53
11-Feb-01	18-Jul-01	158	29	20-Oct-00	30-Apr-01	193	75
15-Sep-01	29-May-02	257	41	12-Sep-01	8-Apr-02	209	80
10-Dec-02	22-May-03	164	16	26-Oct-02	20-Mar-03	146	55
5-Jan-04	6-Jun-04	154	21	19-Oct-03	6-Apr-04	171	61
22-Dec-04	14-May-05	144	20	27-Nov-04	3-Apr-05	128	59
11-Nov-05	14-Jul-06	246	36	5-Nov-05	20-Mar-06	136	61
17-Oct-06	26-Jun-07	263	39	27-Oct-06	18-Apr-07	174	64
1-Oct-07	18-Jun-08	262	48	8-Oct-07	1-Apr-08	177	71
9-Dec-08	19-Jun-09	193	38	8-Nov-08	18-Mar-09	131	64
11-Oct-09	10-Mar-10	151	29	30-Oct-09	7-Apr-10	160	84
15-Dec-10	24-May-11	161	44	15-Nov-10	6-Apr-11	143	66
1-Dec-11	13-May-12	165	26	29-Oct-11	9-Mar-12	133	64
1-Dec-12	2-Jun-13	184	16	15-Sep-12	19-Apr-13	217	83
2-Dec-13	9-May-14	159	28	21-Oct-13	5-Mar-14	136	63
2-Nov-14	30-Aug-15	302	46	15-Nov-14	21-Mar-15	127	59
6-Nov-15	17-Aug-16	286	43	16-Nov-15	14-May-16	181	57

	Kimberley Wo				Ladysmith		
10% date	90% date	Length of wet season	Rain days	10% date	90% date	Length of wet season	Rain days
29-Sep-87	4-Apr-88	189	59	3-Sep-87	13-Mar-88	193	89
14-Sep-88	28-Apr-89	227	76	11-Oct-88	21-Mar-89	162	82
8-Dec-89	24-Apr-90	138	47	2-Nov-89	12-Apr-90	162	82
5-Dec-90	18-Mar-91	104	33	18-Oct-90	18-Mar-91	152	68
13-Oct-91	29-Mar-92	169	38	12-Oct-91	2-Mar-92	143	63
31-Oct-92	20-Feb-93	113	31	1-Nov-92	29-Mar-93	149	54
6-Oct-93	20-Mar-94	166	53	2-Oct-93	22-Mar-94	172	64

5-Dec-94	29-Mar-95	115	34	28-Oct-94	29-Mar-95	153	50
1-Nov-95	17-Apr-96	169	49	16-Nov-95	15-Mar-96	121	67
7-Nov-96	6-May-97	181	57	24-Sep-96	25-May-97	244	92
31-Dec-97	26-Mar-98	86	32	2-Oct-97	11-Apr-98	192	74
9-Oct-98	12-May-99	216	40	15-Nov-98	12-Mar-99	118	58
21-Oct-99	24-Mar-00	156	47	10-Nov-99	2-May-00	175	62
16-Sep-00	27-Apr-01	224	59	7-Oct-00	23-Mar-01	168	57
15-Oct-01	23-Apr-02	191	47	12-Sep-01	22-Mar-02	192	69
17-Aug-02	20-Mar-03	216	46	14-Aug-02	19-Mar-03	218	61
23-Oct-03	4-Apr-04	165	35	4-Nov-03	23-Mar-04	141	57
24-Sep-04	6-Apr-05	195	41	22-Oct-04	20-Mar-05	150	70
29-Nov-05	21-Apr-06	144	47	7-Oct-05	20-Mar-06	165	70
11-Oct-06	17-Apr-07	189	48	2-Oct-06	4-Mar-07	154	69
1-Oct-07	3-May-08	216	69	5-Oct-07	30-Mar-08	178	87
9-Nov-08	8-Apr-09	151	46	11-Nov-08	9-Mar-09	119	63
12-Oct-09	31-Mar-10	171	55	12-Oct-09	4-Apr-10	175	81
14-Dec-10	11-May-11	149	70	3-Dec-10	2-Apr-11	121	58
29-Nov-11	21-Jun-12	206	48	30-Sep-11	16-Mar-12	169	67
25-Oct-12	29-Mar-13	156	46	5-Sep-12	19-Apr-13	227	84
26-Nov-13	9-May-14	165	40	26-Oct-13	9-Mar-14	135	63
11-Nov-14	2-Jun-15	204	42	16-Oct-14	14-Mar-15	150	48
20-Nov-15	12-May-16	175	37	24-Oct-15	16-Mar-16	145	35

Langebaanweg AWS				Lephalale			
10% date	90% date	Length of wet season	Rain days	10% date	90% date	Length of wet season	Rain days
19-Apr-87	24-Sep-87	159	54	6-Nov-87	23-Mar-88	139	54
6-Apr-88	15-Sep-88	163	55	19-Oct-88	26-Apr-89	190	51
30-Mar-89	17-Sep-89	172	52	3-Nov-89	1-Apr-90	150	40
21-Apr-90	9-Aug-90	111	40	2-Dec-90	21-Mar-91	110	31
24-May-91	18-Oct-91	148	50	20-Nov-91	15-Feb-92	88	21
26-Apr-92	22-Oct-92	180	59	28-Oct-92	29-Mar-93	153	36
12-Apr-93	22-Aug-93	133	39	24-Oct-93	25-Feb-94	125	39
19-Apr-94	17-Sep-94	152	37	16-Nov-94	28-Apr-95	164	46
29-Mar-95	12-Oct-95	198	56	19-Nov-95	13-Mar-96	116	41
11-Mar-96	10-Oct-96	214	62	8-Nov-96	20-Mar-97	133	45
5-Apr-97	15-Nov-97	225	44	10-Nov-97	8-Apr-98	150	38
5-May-98	2-Nov-98	182	48	18-Nov-98	13-Mar-99	116	34
2-May-99	10-Sep-99	132	42	9-Nov-99	14-Apr-00	158	43
25-May-00	23-Sep-00	122	34	30-Nov-00	2-May-01	154	34
4-May-01	16-Oct-01	166	64	8-Nov-01	31-May-02	205	37
16-Jan-02	2-Oct-02	260	72	8-Oct-02	23-Mar-03	167	34
3-May-03	14-Oct-03	165	39	14-Dec-03	5-Apr-04	114	37
15-Apr-04	20-Oct-04	189	42	13-Nov-04	2-Apr-05	141	32
10-Apr-05	25-Aug-05	138	43	27-Nov-05	21-Mar-06	115	42
16-May-06	30-Oct-06	168	50	12-Nov-06	7-Apr-07	147	29
26-Apr-07	4-Nov-07	193	62	5-Oct-07	12-Mar-08	160	50
21-May-08	2-Oct-08	135	64	13-Nov-08	12-Mar-09	120	44
14-May-09	8-Nov-09	179	59	4-Nov-09	3-May-10	181	52
7-Mar-10	20-Nov-10	259	63	31-Oct-10	23-Jan-11	85	33
2-May-11	30-Oct-11	182	56	28-Oct-11	13-Feb-12	109	41
7-Apr-12	26-Sep-12	173	69	23-Oct-12	3-Apr-13	163	41
16-Apr-13	19-Sep-13	157	62	10-Dec-13	27-Mar-14	108	36
7-Feb-14	3-Nov-14	270	70	12-Nov-14	26-Mar-15	135	43
13-Feb-15	29-Sep-15	229	51	27-Oct-15	9-Mar-16	135	32
1-Apr-16	15-Sep-16	168	53				

Mafikeng Wo				Makatini Research Centre			
10% date	90% date	Length of wet season	Rain days	10% date	90% date	Length of wet season	Rain days
6-Nov-87	4-Apr-88	151	64	25-Sep-87	14-Mar-88	172	69
19-Oct-88	22-Apr-89	186	62	10-Oct-88	13-May-89	216	64

11-Nov-89	25-Apr-90	166	44	21-Oct-89	20-Apr-90	182	60
23-Nov-90	24-Mar-91	122	46	14-Nov-90	13-May-89	181	48
26-Sep-91	20-Mar-92	177	50	10-Oct-91	2-Mar-92	145	31
1-Nov-92	22-Mar-93	142	60	11-Nov-92	27-Apr-93	168	35
7-Oct-93	7-Feb-94	124	46	2-Oct-93	30-Mar-94	180	46
8-Dec-94	29-Mar-95	112	33	13-Oct-94	3-May-95	203	61
3-Nov-95	17-Apr-96	167	51	23-Oct-95	12-Mar-96	142	55
16-Nov-96	23-May-97	189	71	23-Oct-96	26-May-97	216	50
13-Oct-97	27-Mar-98	166	43	9-Sep-97	22-Feb-98	167	57
16-Oct-98	11-Apr-99	178	46	14-Oct-98	23-Mar-99	161	52
10-Dec-99	30-Mar-00	112	51	24-Oct-99	28-Mar-00	157	69
25-Nov-00	25-Apr-01	152	46	10-Oct-00	30-Apr-01	203	57
23-Oct-01	23-May-02	213	63	8-Oct-01	12-Feb-02	128	40
26-Oct-02	19-Feb-03	117	41	7-Oct-02	3-Jun-03	240	43
20-Oct-03	4-Apr-04	168	47	12-Nov-03	6-Apr-04	147	39
20-Nov-04	7-Apr-05	139	47	27-Oct-04	21-Mar-05	146	27
5-Dec-05	9-Apr-06	126	47	5-Nov-05	12-Apr-06	159	34
18-Oct-06	18-Apr-07	183	53	17-Oct-06	19-Apr-07	185	60
1-Oct-07	2-Apr-08	185	55	7-Oct-07	20-Apr-08	197	61
12-Nov-08	8-Jun-09	209	56	1-Nov-08	3-May-09	184	40
4-Nov-09	23-Apr-10	171	57	25-Sep-09	4-Apr-10	192	89
1-Dec-10	23-Apr-11	144	60	14-Oct-10	25-Mar-11	163	75
19-Nov-11	16-Mar-12	119	43	28-Oct-11	31-Mar-12	156	55
1-Dec-12	18-Apr-13	139	42	6-Sep-12	26-Mar-13	202	79
1-Dec-13	11-Mar-14	101	49	28-Oct-13	8-Mar-14	132	48
2-Nov-14	18-Apr-15	168	53	15-Oct-14	30-Mar-15	167	50
4-Sep-15	13-May-16	253	57	28-Oct-15	9-May-16	195	51

Mandini				Mara			
10% date	90% date	Length of wet season	Rain days	10% date	90% date	Length of wet season	Rain days
26-Sep-87	8-Mar-88	165	81	13-Oct-87	28-Jun-88	260	49
28-Apr-88	20-Mar-89	205	83	18-Oct-88	15-Mar-89	149	37
30-Oct-89	6-Apr-90	159	80	22-Oct-89	20-Mar-90	150	47
30-Aug-90	24-Mar-91	207	95	20-Nov-90	24-Mar-91	125	40
26-Jul-91	18-Feb-92	208	65	12-Nov-91	2-Feb-92	83	26
4-Oct-92	29-Mar-93	177	71	13-Nov-92	4-Feb-93	84	20
24-Sep-93	9-Mar-94	167	56	12-Nov-93	22-Jan-94	72	22
12-Oct-94	17-Jun-95	249	95	10-Dec-94	29-Apr-95	141	30
14-Oct-95	4-Mar-96	143	85	21-Nov-95	19-May-96	181	54
8-Jul-96	29-May-97	326	138	21-Nov-96	19-Mar-97	119	38
8-Sep-97	27-Mar-98	201	102	8-Oct-97	16-Feb-98	132	34
25-Sep-98	16-May-99	234	98	8-Nov-98	4-Mar-99	117	42
28-Sep-99	11-May-00	227	101	25-Oct-99	31-Mar-00	159	71
20-Oct-00	18-Mar-01	150	69	3-Nov-00	20-Apr-01	169	49
12-Sep-01	27-Mar-02	197	80	7-Nov-01	22-Mar-02	136	34
19-Jul-02	19-Mar-03	244	99	5-Nov-02	23-Mar-03	139	26
13-Sep-03	11-Mar-04	181	73	26-Oct-03	21-Mar-04	148	43
25-Aug-04	11-Mar-05	199	79	12-Oct-04	27-Mar-05	167	30
20-Oct-05	30-Apr-06	193	89	6-Nov-05	28-Mar-06	143	41
25-Aug-06	2-Jun-07	282	90	16-Nov-06	22-Apr-07	158	30
2-Oct-07	21-Apr-08	203	97	29-Sep-07	28-Feb-08	153	36
2-Oct-08	20-Apr-09	201	104	8-Nov-08	30-Jan-09	84	24
19-Aug-09	1-Apr-10	226	112	19-Nov-09	4-Apr-10	137	13
13-Oct-10	12-May-11	212	80	6-Nov-10	21-Apr-11	167	40
26-Jul-11	27-Mar-12	246	100	18-Oct-11	18-Jan-12	93	32
17-Oct-12	26-Mar-13	161	86	22-Oct-12	4-Apr-13	165	58
27-Sep-13	9-Mar-14	164	85	18-Nov-13	8-Mar-14	111	51
8-Oct-14	4-Apr-15	179	85	14-Nov-14	28-Mar-15	135	48
21-Jul-15	8-May-16	293	96	14-Oct-15	15-May-16	215	54

Nelspruit				Ottosdal			
10% date	90% date	Length of wet season	Rain days	10% date	90% date	Length of wet season	Rain days
30-Sep-87	12-Mar-88	165	72	17-Sep-87	4-Apr-88	201	89
1-Sep-88	30-Apr-89	242	78	20-Oct-88	29-Apr-89	192	73
2-Nov-89	24-Mar-90	143	67	6-Nov-89	25-Apr-90	171	62
1-Nov-90	11-May-91	192	52	18-Nov-90	15-Mar-91	118	46
13-Nov-91	22-Mar-92	131	31	25-Sep-91	18-Mar-92	176	50
1-Oct-92	22-Feb-93	145	15	4-Nov-92	28-Mar-93	145	54
25-Sep-93	31-Mar-94	188	76	6-Oct-93	8-Mar-94	154	58
14-Oct-94	21-Apr-95	190	76	12-Nov-94	29-Mar-95	138	48
18-Nov-95	24-Mar-96	128	75	29-Oct-95	17-Apr-96	172	74
23-Oct-96	20-Apr-97	180	97	15-Nov-96	7-May-97	174	74
8-Sep-97	25-Mar-98	199	80	9-Sep-97	15-Mar-98	188	52
8-Oct-98	23-Mar-99	167	62	15-Oct-98	7-May-99	205	54
19-Nov-99	4-Apr-00	138	77	20-Nov-99	27-Mar-00	129	51
2-Nov-00	11-Apr-01	161	56	24-Oct-00	30-Apr-01	189	56
25-Oct-01	10-Apr-02	168	72	15-Oct-01	6-Mar-02	143	59
6-Oct-02	20-Feb-03	138	61	27-Aug-02	9-Mar-03	195	51
22-Nov-03	6-Apr-04	137	47	19-Oct-03	4-Apr-04	169	50
12-Nov-04	22-Mar-05	131	60	28-Nov-04	7-Apr-05	131	45
22-Nov-05	11-Apr-06	141	70	30-Nov-05	11-Apr-06	133	45
26-Oct-06	12-Apr-07	169	67	6-Oct-06	25-Apr-07	202	44
25-Oct-07	8-Apr-08	167	65	27-Sep-07	22-Mar-08	178	58
3-Nov-08	17-Mar-09	135	71	13-Nov-08	5-May-09	174	37
13-Feb-09	24-Apr-10	71	48	4-Oct-09	30-Mar-10	178	50
31-Oct-10	14-Apr-11	166	65	24-Nov-10	15-Apr-11	143	58
3-Oct-11	16-Mar-12	166	83	20-Nov-11	27-Dec-12	38	9
7-Sep-12	3-Apr-13	209	75	16-Nov-12	25-Dec-13	40	23
27-Oct-13	9-Mar-14	134	72	9-Dec-13	11-Mar-14	93	35
10-Nov-14	9-Apr-15	151	82	3-Nov-14	18-Apr-15	167	63
15-Oct-15	6-Apr-16	175	64	20-Nov-15	13-May-16	176	62

Oudtshoorn				Paddock			
10% date	90% date	Length of wet season	Rain days	10% date	90% date	Length of wet season	Rain days
27-Feb-87	30-Sep-87	216	38	21-Sep-87	8-Mar-88	170	109
12-Mar-88	19-Dec-88	283	56	27-Aug-88	15-Apr-89	232	100
13-Mar-89	15-Nov-89	248	58	19-Oct-89	25-Mar-90	158	87
3-Feb-90	14-Oct-90	254	57	29-Aug-90	24-Mar-91	208	98
26-Jan-91	3-Dec-91	312	66	19-Sep-91	28-Feb-92	163	92
12-Feb-92	24-Oct-92	256	40	22-Sep-92	14-Mar-93	174	73
14-Feb-93	8-Nov-93	268	44	22-Sep-93	3-Mar-94	163	79
7-Mar-94	23-Dec-94	292	55	17-Aug-94	9-Apr-95	241	103
18-Mar-95	23-Dec-95	281	62	18-Sep-95	3-Mar-96	201	90
2-Mar-96	21-Nov-96	265	64	8-Jul-96	21-Mar-97	257	114
17-Mar-97	26-Oct-97	224	49	12-Jun-97	14-Apr-98	307	136
6-Jan-98	14-Dec-98	343	58	6-Sep-98	23-Mar-99	199	94
9-Apr-99	22-Dec-99	258	48	25-Oct-99	4-Apr-00	163	78
24-Jan-00	12-Nov-00	294	39	19-Sep-00	23-Apr-01	217	110
23-Mar-01	19-Nov-01	242	50	12-Sep-01	12-Feb-02	154	88
28-Feb-02	21-Dec-02	297	55	19-Jul-02	20-Mar-03	245	108
22-Mar-03	16-Oct-03	209	41	12-Sep-03	11-Mar-04	182	83
21-Feb-04	20-Oct-04	243	41	27-Jul-04	14-Mar-05	231	96
2-Feb-05	12-Nov-05	284	33	5-Oct-05	23-Apr-06	201	93
28-Mar-06	16-Sep-06	173	59	3-Sep-06	29-Mar-07	208	110
4-Mar-07	25-Dec-07	297	60	30-Sep-07	13-Apr-08	197	95
10-Feb-08	8-Oct-08	242	48	17-Jun-08	1-Mar-09	258	108
15-Feb-09	7-Dec-09	296	49	27-Sep-09	2-Mar-10	157	95
23-Feb-10	15-Dec-10	296	60	13-Oct-10	7-May-11	207	97
3-Feb-11	20-Nov-11	291	62	10-Jun-11	24-Mar-12	289	137
16-Mar-12	22-Oct-12	221	65	17-Aug-12	31-Mar-13	237	138
29-Jan-13	26-Oct-13	271	50	18-Oct-13	4-Mar-14	138	87

7-Jan-14	3-Nov-14	301	55	28-Sep-14	4-Apr-15	189	112
23-Mar-15	1-Nov-15	224	38	25-Jul-15	18-Apr-16	269	125
19-Feb-16	16-Sep-16	211	53				

Pofadder				Polokwane Wo			
10% date	90% date	Length of wet season	Rain days	10% date	90% date	Length of wet season	Rain days
22-Sep-87	21-Aug-88	335	31	28-Sep-87	10-Mar-88	165	55
9-Dec-88	21-Apr-89	134	25	20-Oct-88	22-Apr-89	185	46
5-Feb-90	20-May-90	105	11	22-Oct-89	25-Mar-90	155	49
10-Dec-90	8-Jun-91	181	20	20-Nov-90	21-Mar-91	122	41
24-Sep-91	26-Mar-92	185	18	15-Nov-91	1-Mar-92	108	28
9-Feb-93	23-Apr-93	74	14	2-Nov-92	17-Apr-93	167	40
19-Jan-94	24-Jun-94	160	21	24-Oct-93	30-Mar-94	158	43
13-Jan-95	21-Jul-95	190	23	10-Nov-94	27-Apr-95	169	53
23-Sep-95	24-Jul-96	306	28	21-Nov-95	13-May-96	175	52
6-Nov-96	26-May-97	202	16	23-Oct-96	9-Mar-97	138	47
5-Jan-98	5-Aug-98	213	15	1-Oct-97	11-Mar-98	162	41
16-Sep-98	7-May-99	234	20	25-Oct-98	15-Mar-99	142	48
1-Dec-99	25-Mar-00	116	31	22-Nov-99	15-Apr-00	146	55
26-Feb-01	7-Jul-01	132	14	30-Oct-00	9-Apr-01	162	44
27-Oct-01	22-Aug-02	300	16	31-Oct-01	25-Feb-02	118	41
8-Sep-02	13-Aug-03	340	10	30-Oct-02	23-Mar-03	145	24
17-Sep-03	8-Apr-04	205	8	24-Nov-03	22-Mar-04	120	45
20-Oct-04	14-May-05	207	14	23-Nov-04	11-Mar-05	109	30
11-Nov-05	21-Aug-06	284	19	19-Nov-05	27-Mar-06	129	47
25-Jan-07	6-Jun-07	133	8	2-Nov-06	29-Mar-07	148	40
29-Nov-07	18-Jun-08	203	33	5-Oct-07	12-Mar-08	160	48
1-Dec-08	11-Jul-09	223	27	11-Nov-08	7-May-09	178	50
9-Jan-10	6-Mar-10	57	12	4-Nov-09	20-Apr-10	168	53
31-Dec-10	7-Jun-11	159	26	6-Nov-10	16-Apr-11	162	48
16-Jan-12	25-Apr-12	101	15	18-Oct-11	12-Mar-12	147	42
1-Dec-12	1-Jun-13	183	17	19-Oct-12	14-Apr-13	178	46
23-Dec-13	4-Jun-14	164	27	10-Nov-13	17-Mar-14	128	45
2-Nov-14	9-Jun-15	220	23	8-Dec-14	16-Apr-15	130	40
19-Jan-16	8-May-16	111	9	14-Oct-15	18-Mar-16	157	38

Port Elizabeth Wo				Port Nolloth			
10% date	90% date	Length of wet season	Rain days	10% date	90% date	Length of wet season	Rain days
9-Feb-87	26-Nov-87	291	92	3-Apr-87	22-Sep-87	173	17
26-Feb-88	3-Nov-88	252	82	27-May-88	15-Sep-88	112	19
29-Mar-89	15-Nov-89	232	74	12-Apr-89	1-Oct-90	173	23
20-Feb-90	30-Oct-90	253	77	19-Apr-90	11-Jul-90	84	13
15-Feb-91	20-Nov-91	279	79	22-Apr-91	20-Oct-91	182	27
27-Feb-92	12-Nov-92	260	80	9-Apr-92	31-Oct-92	206	22
20-Feb-93	3-Dec-93	287	66	5-Apr-93	11-Jul-93	98	11
1-Mar-94	24-Dec-94	299	74	19-Apr-94	15-Sep-94	150	12
14-Feb-95	30-Nov-95	290	87	13-Jan-95	25-Sep-95	256	18
2-Mar-96	24-Nov-96	268	80	7-Jun-96	7-Nov-96	154	21
25-Mar-97	26-Oct-97	216	64	18-Mar-97	15-Nov-97	243	19
1-Mar-98	18-Nov-98	263	67	23-Mar-98	4-Dec-98	257	13
1-Feb-99	14-Nov-99	287	69	19-May-99	26-Sep-99	131	12
11-Jan-00	12-Nov-00	307	86	10-Jun-00	12-Nov-00	156	6
14-Jan-01	26-Nov-01	317	83	5-Apr-01	18-Sep-01	167	23
6-May-02	13-Nov-02	192	74	1-Apr-02	8-Sep-02	161	21
23-Mar-03	16-Oct-03	208	53	25-May-03	12-Oct-03	141	14
24-Jan-04	22-Dec-04	334	87	16-Apr-04	20-Oct-04	188	14
21-Jan-05	12-Nov-05	296	74	5-Mar-05	17-Oct-05	227	18
4-Feb-06	4-Oct-06	243	78	16-Apr-06	14-Aug-06	121	15
4-Mar-07	26-Nov-07	268	64	26-Apr-07	21-Nov-07	210	31
10-Feb-08	13-Nov-08	278	69	10-Apr-08	26-Oct-08	200	48

28-Feb-09	25-Oct-09	240	69	24-Mar-09	8-Nov-09	230	52
1-Mar-10	15-Dec-10	290	82	21-Jan-10	3-Oct-10	256	55
16-Apr-11	23-Nov-11	222	78	27-Apr-11	19-Nov-11	207	53
23-Feb-12	20-Oct-12	241	82	29-Mar-12	28-Sep-12	184	49
10-Feb-13	17-Nov-13	281	78	27-Mar-13	19-Sep-13	177	50
8-Mar-14	2-Dec-14	270	88	6-Jan-14	4-Aug-14	211	41
14-Feb-15	1-Nov-15	261	85	2-Jun-15	1-Dec-15	183	48
5-Mar-16	9-Nov-16	250	85	21-Jan-16	22-Nov-16	307	62

Prieska				Riversdale			
10% date	90% date	Length of wet season	Rain days	10% date	90% date	Length of wet season	Rain days
12-Nov-87	12-Mar-88	122	23	14-Feb-87	1-Oct-87	230	64
14-Sep-88	13-Apr-89	212	31	5-Mar-88	18-Nov-88	259	64
2-Feb-89	28-Jun-90	147	25	1-Mar-89	15-Nov-89	260	88
6-Dec-90	16-Jun-91	193	28	21-Feb-90	23-Nov-90	276	73
26-Sep-91	27-Mar-92	184	34	26-Jan-91	3-Dec-91	312	84
27-Aug-92	18-Jul-93	326	20	11-Feb-92	1-Nov-92	265	90
11-Oct-93	4-Mar-94	145	37	3-Mar-93	2-Dec-93	275	77
13-Nov-94	5-May-95	174	26	11-Feb-94	23-Dec-94	316	94
18-Nov-95	23-Jul-96	249	40	15-Feb-95	6-Dec-95	295	89
17-Nov-96	6-May-97	181	30	14-Feb-96	21-Nov-96	282	74
15-Jan-97	27-Mar-98	72	12	19-Mar-97	16-Nov-97	243	71
19-Dec-98	18-May-99	151	20	6-Jan-98	15-Dec-98	344	92
2-Dec-99	2-Apr-00	123	34	1-Feb-99	24-Oct-99	266	80
16-Sep-00	27-Apr-01	224	27	1-Jan-00	17-Nov-00	322	95
18-Sep-01	21-May-02	246	41	16-Mar-01	3-Nov-01	233	68
17-Aug-02	12-Apr-03	239	25	6-Feb-02	8-Nov-02	276	79
30-Oct-03	2-Apr-04	156	28	8-Feb-03	15-Oct-03	250	71
25-Sep-04	22-Jun-05	271	35	21-Mar-04	22-Dec-04	277	66
31-Dec-05	17-Apr-06	108	31	28-Jan-05	3-Nov-05	280	73
21-Aug-06	19-Apr-07	242	23	16-Mar-06	16-Oct-06	215	77
31-Oct-07	18-Jun-08	232	35	4-Mar-07	26-Nov-07	268	84
9-Nov-08	23-Apr-09	166	24	11-Feb-08	13-Nov-08	277	88
7-Dec-09	26-Mar-10	110	26	14-Feb-09	14-Nov-09	274	71
31-Dec-10	4-May-11	125	41	10-Mar-10	28-Nov-10	264	86
25-Dec-11	26-Apr-12	124	29	17-Feb-11	22-Nov-11	279	88
30-Nov-12	31-Mar-13	122	23	15-Mar-12	20-Oct-12	220	85
8-Dec-13	19-May-14	163	26	8-Mar-13	15-Nov-13	253	72
8-Aug-14	2-Jun-15	299	26	6-Jan-14	3-Nov-14	302	97
19-Jan-15	8-May-16	111	20	4-Mar-15	1-Nov-15	243	84
				13-Jan-16	6-Oct-16	268	96

Robertson				Shaleburn			
10% date	90% date	Length of wet season	Rain days	10% date	90% date	Length of wet season	Rain days
14-Apr-87	24-Sep-87	164	39	27-Sep-87	16-Mar-88	172	116
25-Apr-88	18-Dec-88	238	44	11-Oct-88	20-Mar-89	161	114
23-Mar-89	27-Oct-89	219	56	2-Nov-89	27-Mar-90	146	95
6-Mar-90	16-Dec-90	286	54	18-Oct-90	11-Mar-91	145	83
26-Jan-91	29-Oct-91	277	65	11-Oct-91	18-Mar-92	160	94
27-Apr-92	20-Oct-92	177	40	10-Oct-92	4-Apr-93	177	95
20-Feb-93	1-Dec-93	285	66	20-Oct-93	2-Mar-94	134	88
6-Mar-94	23-Dec-94	293	62	8-Oct-94	4-Apr-95	179	96
19-Mar-95	17-Dec-95	274	61	11-Nov-95	15-Mar-96	126	90
2-Mar-96	15-Nov-96	259	51	21-Sep-96	28-Mar-97	189	122
19-Mar-97	26-Oct-97	222	42	14-Oct-97	25-Mar-98	163	111
17-Mar-98	14-Dec-98	273	44	27-Oct-98	12-Mar-99	137	93
20-Apr-99	23-Dec-99	248	44	10-Nov-99	30-Mar-00	142	99
24-Jan-00	24-Oct-00	275	59	20-Sep-00	1-Apr-01	194	122
31-Mar-01	27-Oct-01	211	55	12-Oct-01	9-Mar-02	149	106
30-Jan-02	13-Nov-02	288	66	6-Sep-02	25-Mar-03	201	127

15-Jan-03	25-Aug-03	223	46	5-Nov-03	29-Mar-04	146	101
1-Mar-04	17-Nov-04	262	35	17-Oct-04	15-Mar-05	150	123
19-Jan-05	12-Nov-05	298	54	18-Oct-05	11-Apr-06	176	131
29-Apr-06	2-Oct-06	157	47	26-Sep-06	11-Mar-07	167	120
26-Apr-07	2-Dec-07	221	46	5-Oct-07	30-Mar-08	178	122
2-Apr-08	12-Nov-08	225	48	9-Nov-08	6-Apr-09	149	113
24-Feb-09	26-Oct-09	245	40	5-Oct-09	24-Mar-10	171	119
24-Feb-10	21-Nov-10	271	59	9-Nov-10	7-Apr-11	150	120
10-Feb-11	20-Nov-11	284	61	15-Sep-11	30-Mar-12	198	113
30-Mar-12	17-Oct-12	202	70	13-Sep-12	29-Mar-13	198	138
2-Apr-13	15-Nov-13	228	59	15-Nov-13	9-Mar-14	115	86
6-Jan-14	3-Nov-14	302	79	1-Nov-14	17-Mar-15	137	83
26-Mar-15	30-Sep-15	189	47	17-Sep-15	12-Mar-16	178	104
25-Jan-16	9-Sep-16	229	52				

Skukuza				Springbok Wo (n = 29)			
10% date	90% date	Length of wet season	Rain days	10% date	90% date	Length of wet season	Rain days
27-Sep-87	9-Mar-88	165	59	ND	ND		
13-Oct-88	22-Mar-89	161	44	20-Apr-88	2-Nov-88	197	37
25-Oct-89	28-Mar-90	155	58	1-Mar-89	3-Sep-89	187	32
8-Oct-90	25-Mar-91	169	43	20-Apr-90	17-Jul-90	89	21
13-Nov-91	2-Mar-92	111	26	5-Apr-91	14-Oct-91	193	45
13-Nov-92	30-Mar-93	138	42	30-Mar-92	24-Oct-92	209	31
11-Nov-93	31-Mar-94	141	33	20-Mar-93	3-Aug-93	137	31
14-Oct-94	28-Apr-95	197	54	5-Feb-94	27-Sep-94	235	29
9-Nov-95	1-Apr-96	145	67	5-May-95	24-Oct-95	173	33
13-Nov-96	4-Apr-97	143	56	31-May-96	8-Nov-96	162	41
9-Oct-97	22-Feb-98	137	52	26-Mar-97	15-Nov-97	235	31
15-Oct-98	17-Mar-99	154	77	27-Mar-98	1-Nov-98	220	26
19-Nov-99	19-Mar-00	122	65	17-Apr-99	20-Oct-99	187	33
2-Nov-00	13-Apr-01	163	56	18-Feb-00	11-Nov-00	268	29
9-Nov-01	7-Mar-02	119	43	6-Apr-01	31-Aug-01	148	37
30-Oct-02	14-May-03	197	52	28-Feb-02	9-Sep-02	194	37
5-Nov-03	6-Apr-04	154	55	25-May-03	25-Aug-03	93	13
27-Oct-04	3-Mar-05	128	41	9-Apr-04	20-Oct-04	195	22
6-Nov-05	20-Mar-06	135	62	18-Jan-05	17-Oct-05	273	51
4-Nov-06	4-Apr-07	152	41	16-Apr-06	21-Aug-06	128	34
10-Oct-07	7-Apr-08	181	45	26-Apr-07	23-Aug-07	120	24
8-Nov-08	1-Mar-09	114	49	5-Mar-08	14-Sep-08	194	34
19-Nov-09	19-Apr-10	152	38	23-Apr-09	8-Nov-09	200	35
6-Nov-10	3-Apr-11	149	52	22-Feb-10	20-Sep-10	211	27
28-Oct-11	30-Mar-12	155	49	5-Jan-11	22-Aug-11	230	41
12-Oct-12	17-Mar-13	157	58	25-Apr-12	30-Nov-12	220	36
21-Oct-13	5-Mar-14	136	47	30-Mar-13	19-Sep-13	174	35
16-Oct-14	31-Mar-15	167	44	23-Mar-14	2-Nov-14	225	38
5-Sep-15	6-Apr-16	215	50	2-Jun-15	30-Aug-15	90	18
				21-Jan-16	26-Sep-16	250	31

Sutherland (n = 29)				Twee Rivieren			
10% date	90% date	Length of wet season	Rain days	10% date	90% date	Length of wet season	Rain days
25-Feb-87	19-Sep-87	207	33	8-Oct-87	15-Apr-88	191	30
4-Mar-88	9-Dec-88	281	53	12-Dec-88	21-Mar-89	100	22
7-Feb-89	5-Dec-89	211	54	22-Jan-90	20-Apr-90	89	16
3-Feb-90	17-Jul-90	165	27	3-Dec-90	23-Mar-91	111	18
25-Jan-91	14-Oct-91	263	53	7-Nov-91	17-Mar-92	132	10
26-Mar-92	1-Nov-92	221	45	31-Dec-92	24-Apr-93	115	14
5-Apr-93	20-Oct-93	199	40	10-Nov-93	1-Mar-94	112	25
12-Feb-94	17-Sep-94	218	14	14-Nov-94	28-Mar-95	135	11
7-Mar-95	17-Dec-95	286	51	19-Nov-95	24-Jul-96	249	26
30-May-96	20-Nov-96	175	52	7-Nov-96	22-May-97	197	22

18-Mar-97	16-Nov-97	244	34	3-Jan-98	27-Mar-98	84	11
20-Feb-98	19-Nov-98	273	32	16-Sep-98	14-May-99	241	17
30-Mar-99	22-Dec-99	268	53	14-Dec-99	19-Apr-00	128	29
18-Feb-00	2-Sep-00	198	32	27-Nov-00	30-Apr-01	155	21
23-Mar-01	17-Nov-01	240	41	8-Nov-01	23-Apr-02	167	19
27-Jan-02	1-Nov-02	279	55	1-Nov-02	12-Apr-03	163	18
1-Apr-03	21-Nov-03	235	30	30-Oct-03	1-Apr-04	155	19
20-Feb-04	17-Nov-04	272	31	19-Oct-04	6-Apr-05	170	20
20-Jan-05	24-Sep-05	248	44	30-Dec-05	15-Apr-06	107	18
1-Feb-06	22-Aug-06	203	37	16-Nov-06	21-Apr-07	157	23
24-Apr-07	24-Dec-07	245	64	31-Oct-07	23-May-08	206	42
6-Mar-08	2-Oct-08	211	56	28-Nov-08	22-Apr-09	146	33
24-Feb-09	26-Oct-09	245	65	3-Oct-09	11-Mar-10	160	26
22-Feb-10	16-Dec-10	298	54	30-Dec-10	22-Apr-11	114	50
3-Feb-11	23-Aug-11	202	67	5-Dec-11	20-Apr-12	138	30
25-Mar-12	14-Dec-12	265	77	30-Nov-12	31-Mar-13	122	23
9-Feb-13	24-Oct-13	258	66	7-Dec-13	13-Apr-14	128	32
7-Jan-14	2-Nov-14	300	69	31-Oct-14	1-Apr-15	153	31
ND	ND			20-Jan-16	7-Apr-16	79	19
22-Jan-16	17-Aug-16	209	55				

Umtata Wo				Upington Wo			
10% date	90% date	Length of wet season	Rain days	10% date	90% date	Length of wet season	Rain days
25-Sep-87	5-Apr-88	194	103	28-Nov-87	17-Apr-88	142	27
22-Oct-88	15-Apr-89	176	83	6-Nov-88	14-Apr-89	160	40
15-Oct-89	24-Mar-90	161	76	15-Nov-89	20-Jun-90	218	30
31-Aug-90	19-Mar-91	201	82	11-Dec-90	26-Mar-91	106	20
8-Oct-91	21-Mar-92	166	79	26-Sep-91	27-Mar-92	184	36
7-Oct-92	3-Apr-93	179	66	10-Oct-92	18-Jul-93	282	28
13-Oct-93	9-Mar-94	148	68	22-Oct-93	11-Apr-94	172	32
21-Oct-94	10-Apr-95	172	68	13-Nov-94	29-Mar-95	137	18
18-Oct-95	8-Mar-96	143	81	4-Dec-95	5-Jul-96	215	25
5-Nov-96	11-Jun-97	219	106	6-Nov-96	26-Mar-97	141	17
15-Oct-97	26-Mar-98	163	81	15-Jan-98	27-Mar-98	72	10
2-Oct-98	21-Mar-99	171	82	9-Nov-98	16-May-99	189	21
25-Oct-99	17-Apr-00	176	85	2-Oct-99	25-Mar-00	176	37
10-Oct-00	23-Mar-01	165	75	12-Oct-00	26-Apr-01	197	23
7-Oct-01	5-Apr-02	181	78	12-Nov-01	21-May-02	191	30
21-Jul-02	23-Mar-03	246	82	1-Nov-02	12-Apr-03	163	26
13-Sep-03	19-Mar-04	189	69	28-Oct-03	20-Mar-04	145	21
6-Sep-04	27-Mar-05	203	53	20-Oct-04	14-May-05	207	30
20-Oct-05	17-Apr-06	180	82	30-Dec-05	21-Apr-06	113	30
15-Aug-06	14-Mar-07	212	106	15-Nov-06	17-Apr-07	154	17
17-Oct-07	3-May-08	200	85	8-Oct-07	17-Jun-08	254	45
5-Oct-08	20-Apr-09	198	75	1-Dec-08	23-Apr-09	144	22
1-Oct-09	17-Apr-10	199	81	3-Oct-09	5-Apr-10	185	32
4-Nov-10	6-May-11	184	98	25-Nov-10	5-May-11	162	42
2-Oct-11	31-Mar-12	182	83	25-Dec-11	20-Jun-12	179	30
7-Aug-12	20-Apr-13	257	104	3-Nov-12	31-Mar-13	149	26
20-Oct-13	1-Apr-14	164	69	9-Dec-13	19-May-14	162	29
1-Oct-14	4-Apr-15	186	64	3-Nov-14	26-Jun-15	236	26
17-Sep-15	4-Apr-16	201	67	17-Jan-16	9-May-16	114	20

Vanwyksvlei				Vredendal			
10% date	90% date	Length of wet season	Rain days	10% date	90% date	Length of wet season	Rain days
22-Sep-87	20-Apr-88	212	36	19-Apr-87	22-Sep-87	157	37
18-Dec-88	20-Apr-89	124	29	21-Apr-88	25-Sep-88	158	34
8-Feb-90	27-Jun-90	140	18	12-Mar-89	18-Sep-89	191	47
4-Dec-90	17-Jun-91	196	19	12-Apr-90	17-Jul-90	97	26
26-Sep-91	29-Mar-92	186	21	30-May-91	21-Oct-91	145	40

10-Oct-92	27-Jun-93	261	17	1-May-92	24-Oct-92	177	28
16-Dec-93	20-Mar-94	95	34	5-Apr-93	3-Aug-93	121	36
3-Nov-94	5-Aug-95	276	26	20-Apr-94	17-Sep-94	151	26
31-Oct-95	23-Jul-96	267	37	28-Mar-95	30-Oct-95	217	39
6-Nov-96	26-May-97	202	29	18-Apr-96	16-Nov-96	213	51
5-Jan-98	21-Apr-98	107	12	19-May-97	15-Nov-97	181	29
1-Nov-98	17-May-99	198	24	5-May-98	14-Dec-98	224	33
20-Oct-99	20-Apr-00	184	33	17-Apr-99	26-Sep-99	163	34
16-Sep-00	27-Apr-01	224	30	18-Apr-00	12-Sep-00	148	22
17-Sep-01	11-Jun-02	268	43	4-May-01	25-Oct-01	175	39
1-Nov-02	18-Apr-03	169	23	1-Apr-02	1-Sep-02	162	38
30-Oct-03	2-Apr-04	156	22	17-Apr-03	29-Oct-03	196	31
20-Oct-04	22-Jun-05	246	28	5-Jan-04	20-Oct-04	290	38
6-Jan-06	18-May-06	133	30	6-Apr-05	24-Sep-05	172	34
13-Oct-06	19-Apr-07	189	27	1-May-06	22-Aug-06	114	33
29-Nov-07	18-Jun-08	203	48	26-Apr-07	15-Dec-07	234	51
21-Nov-08	20-Jun-09	212	33	31-May-08	8-Sep-08	129	50
4-Oct-09	3-Mar-10	151	20	16-May-09	19-Aug-09	96	30
31-Dec-10	24-May-11	145	40	10-May-10	16-Dec-10	221	34
12-Jan-12	13-Jul-12	184	26	2-May-11	4-Nov-11	187	48
30-Nov-12	2-Jun-13	185	27	24-May-12	24-Dec-12	215	62
7-Dec-13	8-May-14	153	35	17-Apr-13	19-Sep-13	156	50
28-Oct-14	26-Jun-15	242	24	23-Mar-14	3-Nov-14	226	56
20-Jan-16	8-May-16	110	17	31-May-15	25-Aug-15	87	34
				22-Apr-16	11-Sep-16	143	45

Vryburg				Warmbad Towoomba			
10% date	90% date	Length of wet season	Rain days	10% date	90% date	Length of wet season	Rain days
21-Sep-87	22-Mar-88	184	58	27-Sep-87	26-Mar-88	182	63
19-Oct-88	15-Apr-89	179	61	12-Oct-88	21-Apr-89	192	61
7-Dec-89	22-Apr-90	137	46	2-Nov-89	28-Mar-90	147	55
5-Dec-90	18-Mar-91	104	40	22-Nov-90	15-Mar-91	114	49
27-Sep-91	28-Mar-92	184	45	16-Oct-91	24-Mar-92	161	54
31-Oct-92	27-Apr-93	179	43	1-Nov-92	1-Mar-93	121	47
20-Oct-93	5-Mar-94	137	40	6-Oct-93	7-Feb-94	125	47
9-Dec-94	29-Mar-95	111	30	23-Oct-94	27-Apr-95	187	66
17-Oct-95	29-Apr-96	196	54	8-Nov-95	13-Mar-96	127	47
16-Nov-96	22-Apr-97	158	54	17-Nov-96	20-Apr-97	155	48
14-Oct-97	26-Mar-98	164	35	12-Oct-97	8-Mar-98	148	45
8-Nov-98	7-May-99	181	42	15-Oct-98	23-Mar-99	160	52
8-Dec-99	14-Apr-00	129	46	9-Dec-99	4-Apr-00	118	58
22-Nov-00	30-Apr-01	160	47	2-Nov-00	29-Apr-01	179	42
20-Sep-01	9-Mar-02	171	50	25-Oct-01	12-Apr-02	170	51
8-Oct-02	19-Mar-03	163	44	27-Aug-02	16-Feb-03	174	37
13-Nov-03	6-Apr-04	146	37	25-Nov-03	20-Mar-04	117	32
1-Dec-04	6-Apr-05	127	39	11-Nov-04	3-Apr-05	144	26
19-Dec-05	11-Apr-06	114	47	20-Nov-05	18-Mar-06	119	39
27-Oct-06	17-Apr-07	173	33	18-Oct-06	5-Jun-07	231	44
26-Sep-07	2-May-08	220	71	8-Oct-07	16-Mar-08	161	67
19-Nov-08	8-Jun-09	202	44	8-Nov-08	18-Apr-09	131	45
19-Nov-09	5-Apr-10	138	30	29-Oct-09	3-Apr-10	157	56
24-Nov-10	9-May-11	167	51	27-Oct-10	16-Apr-11	172	38
10-Dec-11	21-Mar-12	103	25	28-Oct-11	11-Mar-12	136	49
16-Nov-12	26-Mar-13	131	33	9-Oct-12	3-Apr-13	177	67
19-Nov-13	11-Mar-14	113	29	28-Oct-13	9-Mar-14	133	62
2-Nov-14	11-Apr-15	161	52	14-Nov-14	9-Apr-15	147	47
14-Oct-15	20-Apr-16	190	51	26-Oct-15	6-Apr-16	164	65

Welkom				Willowmore			
10% date	90% date	Length of wet season	Rain days	10% date	90% date	Length of wet season	Rain days
21-Sep-87	4-Apr-88	197	75	12-Nov-87	7-Aug-88	270	41
13-Oct-88	26-Apr-89	196	69	15-Dec-88	21-Jun-89	189	36
7-Nov-89	25-Apr-90	170	70	14-Nov-89	20-May-90	188	37
4-Dec-90	19-Mar-91	106	49	29-Nov-90	2-Aug-91	247	42
26-Sep-91	1-Mar-92	158	49	28-Oct-91	15-Aug-92	293	45
9-Oct-92	30-Mar-93	173	56	15-Oct-92	23-Sep-93	344	50
6-Oct-93	14-Mar-94	160	58	3-Dec-93	7-Aug-94	248	52
3-Nov-94	29-Mar-95	147	46	23-Dec-94	20-Aug-95	241	45
29-Oct-95	5-May-96	190	65	22-Nov-95	4-Aug-96	257	52
8-Nov-96	25-May-97	199	58	6-Nov-96	26-May-97	202	32
11-Nov-97	27-Mar-98	137	40	23-Dec-97	5-Aug-98	226	31
1-Nov-98	8-May-99	189	46	19-Nov-98	1-Jul-99	225	33
3-Dec-99	1-May-00	151	43	22-Dec-99	2-Apr-00	103	21
20-Oct-00	23-Apr-01	186	59	6-Nov-00	8-Jul-01	245	37
21-Oct-01	9-Apr-02	171	58	3-Nov-01	18-Aug-02	289	49
26-Aug-02	19-Mar-03	206	44	11-Dec-02	25-May-03	166	20
10-Oct-03	21-Mar-04	164	55	29-Oct-03	7-Jun-04	223	30
28-Nov-04	23-Apr-05	147	50	19-Nov-04	11-Apr-05	144	24
20-Nov-05	24-Mar-06	125	45	12-Nov-05	2-Aug-06	264	44
22-Aug-06	5-Jun-07	288	61	7-Oct-06	26-Jun-07	263	29
1-Oct-07	17-Mar-08	169	54	22-Nov-07	7-Jul-08	229	56
7-Nov-08	8-Jun-09	214	51	19-Dec-08	24-Jun-09	188	47
18-Nov-09	5-Apr-10	139	50	11-Oct-09	7-Jun-10	240	48
8-Nov-10	9-May-11	183	50	15-Dec-10	24-Jul-11	222	70
22-Nov-11	23-Jan-12	63	20	21-Jan-12	15-Jul-12	177	41
25-Oct-12	18-Jan-13	86	25	18-Oct-12	2-Jun-13	228	32
15-Nov-13	5-Mar-14	111	39	15-Nov-13	24-Sep-14	314	65
2-Nov-14	24-Apr-15	174	53	11-Nov-14	31-Aug-15	294	48
21-Sep-15	16-Mar-16	178	38	30-Dec-15	17-Aug-16	232	48

APPENDIX G: INDIVIDUAL WEATHER STATION SEASONALTY SHIFTS AND CHANGE POINTS

Summary of the trends and change points for each method for each weather station for the period 1987-2016. Method one (M1) represents the seasonality scores. Method two (M2) represents the onset (O) and cessation (C) dates, length of the wet season (L) and number of rain days (R). Method three (M3) represents the 10% (T) and 90% (N) dates, length of the wet season (L) and number of rain days (R). Trends with a *p value* of less than 0.05 are significant and are highlighted by an asterisk (*). Only significant change points are captured, and the year reported represents the first year after the change point occurred. Change points are also colour coded, where green represents CUSUM test change points, orange represents Pettitt test change points and grey represents where both tests agreed on the change points. L for the change points represents the later change point selected where both tests produced different change points. For the trends and change points N/A represents those which were not calculated, which is only represented at PNO.

Weather station code and method	Trend rate (M1: yr^{-1}, M2 and 3: $d.yr^{-1}$)	Trend (*r* and *p value*)	Change point(s; *p value*)	Rate (*r* and *p value*) before and after change point(s; M1: $.yr^{-1}$, M2 and 3: $d.yr^{-1}$)
ANP:				
Method 1	0.0013	0.05; 0.784	None	-
Method 2	O: 1.40	0.31; 0.105	None	-
	C: 1.07	0.30; 0.116	2008 (0.040); 2013 (0.040)	0.83 (0.23; 0.309); -1.30 (0.29; 0.574); 13.80 (0.79; 0.111)
	L: -0.54	0.10; 0.589	None	-
	R: 0.35	0.17; 0.385	None	-
Method 3	T: 1.16	0.31; 0.096	None	-
	N: 1.61	0.42; *0.025	None	-
	L: 0.45	0.12; 0.521	None	-
	R: 0.42	0.23; 0.230	None	-
BET:				
Method 1	0.0013	0.04; 0.845	None	-
Method 2	O: -1.67	0.41; *0.030	2005 (0.049)	0.16 (0.03; 0.900); 1.70 (0.15; 0.677)
	C: -0.42	0.10; 0.622	None	-
	L: 1.26	0.26; 0.188	None	-
	R: -0.43	0.26; 0.179	None	-
Method 3	T: -0.63	0.23; 0.245	None	-
	N: -0.34	0.13; 0.505	None	-
	L: 0.29	0.09; 0.661	None	-
	R: -0.44	0.35; 0.070	None	-
BEW:				
Method 1	0.0013	0.04; 0.844	None	-
Method 2	O: 1.59	0.44; *0.017	None	-
	C: 0.88	0.27; 0.156	None	-
	L: -0.72	0.17; 0.365	None	-
	R: -0.56	0.31; 0.098	None	-
Method 3	T: 1.11	0.39; *0.039	None	-
	N: 1.48	0.38; *0.040	None	-
	L: 0.36	0.10; 0.593	None	-
	R: -0.38	0.29; 0.122	None	-
BLW:				
Method 1	-0.0052	0.17; 0.360	None	-
Method 2	O: 0.88	0.19; 0.312	None	-
	C: 0.77	0.21; 0.270	None	-
	L: -0.12	0.02; 0.912	None	-
	R: -0.51	0.22; 0.246	None	-
Method 3	T: 0.58	0.17; 0.378	None	-
	N: 1.76	0.50; *0.006	None	-
	L: 1.18	0.28; 0.141	None	-
	R: -0.27	0.15; 0.429	None	-
CAG:				
Method 1	0.0119	0.38; *0.036	None	-

Method 2	O: 1.39	0.25; 0.179	None	-
	C: -0.03	0.01; 0.975	None	-
	L: -1.43	0.22; 0.237	None	-
	R: -0.59	0.25; 0.177	None	-
Method 3	T: -0.53	0.16; 0.385	None	-
	N: 0.49	0.16; 0.412	None	-
	L: 1.02	0.34; 0.070	None	-
	R: 0.32	0.22; 0.235	2006 (0.050)	-0.47 (0.28; 0.239); -1.25 (0.27; 0.415)
CED:				
Method 1	-0.0119	0.19; 0.329	None	-
Method 2	O: -0.82	0.18; 0.269	None	-
	C: -0.40	0.17; 0.984	None	-
	L: 0.43	0.09; 0.299	None	-
	R: 0.57	0.25; 0.072	None	-
Method 3	T: -0.88	0.21; 0.284	None	-
	N: 0.55	0.30; 0.113	1995 (0.040)	0.36 (0.12; 0.791); -0.38 (0.17; 0.461)
	L: 1.43	0.31; 0.102	None	-
	R: 0.49	0.30; 0.111	None	-
CMU:				
Method 1	0.0046	0.15; 0.449	None	-
Method 2	O: 0.04	0.01; 0.971	None	-
	C: 0.39	0.08; 0.676	None	-
	L: 0.35	0.12; 0.801	None	-
	R: 0.23	0.12; 0.534	None	-
Method 3	T: 0.68	0.26; 0.180	None	-
	N: 1.08	0.22; 0.244	None	-
	L: 0.40	0.08; 0.697	None	-
	R: 0.33	0.26; 0.175	None	-
CTW:				
Method 1	0.0074	0.28; 0.130	None	-
Method 2	O: 0.59	0.16; 0.298	None	-
	C: -0.62	0.15; 0.722	None	-
	L: -1.21	0.24; 0.264	None	-
	R: -0.70	0.34; *0.040	None	-
Method 3	T: 0.09	0.03; 0.869	None	-
	N: 0.82	0.28; 0.137	None	-
	L: 0.73	0.21; 0.265	None	-
	R: -0.16	0.14; 0.455	None	-
CWO:				
Method 1	0.0040	0.17; 0.373	None	-
Method 2	O: -0.81	0.07; 0.713	None	-
	C: -0.37	0.15; 0.793	None	-
	L: 0.22	0.04; 0.873	None	-
	R: 0.14	0.09; 0.742	None	-
Method 3	T: -0.64	0.21; 0.376	None	-
	N: 1.13	0.17; 0.276	None	-
	L: 1.77	0.34; 0.069	None	-
	R: 0.02	0.02; 0.924	None	-
DAW:				
Method 1	0.0041	0.16; 0.391	None	-
Method 2	O: 0.76	0.13; 0.518	None	-
	C: -0.03	0.01; 0.967	None	-

	L: -0.80	0.12; 0.555	None	-
	R: -0.28	0.23; 0.243	None	-
Method 3	T: 1.37	0.28; 0.146	None	-
	N: 0.25	0.07; 0.735	None	-
	L: -1.12	0.22; 0.252	None	-
	R: -0.30	0.33; 0.077	None	-
ELW:				
Method 1	-0.0086	0.09; 0.615	None	-
Method 2	O: 0.92	0.27; 0.158	None	-
	C: 1.09	0.27; 0.150	None	-
	L: 0.17	0.04; 0.847	None	-
	R: -0.21	0.11; 0.576	None	-
Method 3	T: -0.05	0.01; 0.946	None	-
	N: 0.70	0.22; 0.249	None	-
	L: 0.74	0.19; 0.323	None	-
	R: -0.09	0.05; 0.780	None	-
FRA:				
Method 1	0.0004	0.02; 0.917	None	-
Method 2	O: 0.25	0.04; 0.869	None	-
	C: 0.23	0.06; 0.804	None	-
	L: -0.02	0.003; 0.990	None	-
	R: -0.01	0.01; 0.961	None	-
Method 3	T: -0.50	0.11; 0.580	None	-
	N: 0.15	0.03; 0.882	None	-
	L: 0.65	0.11; 0.570	None	-
	R: 0.41	0.36; 0.055	None	-
FTN:				
Method 1	-0.0082	0.29; 0.126	None	-
Method 2	O: 1.85	0.37; *0.045	None	-
	C: 0.67	0.18; 0.343	None	-
	L: -1.18	0.24; 0.218	None	-
	R: 0.09	0.04; 0.843	None	-
Method 3	T: 0.44	0.13; 0.487	None	-
	N: 1.00	0.27; 0.161	None	-
	L: 0.56	0.11; 0.555	None	-
	R: 0.43	0.28; 0.137	None	-
JIW:				
Method 1	0.0016	0.04; 0.813	None	-
Method 2	O: 0.17	0.06; 0.742	None	-
	C: -0.04	0.01; 0.946	None	-
	L: -0.22	0.05; 0.793	None	-
	R: -0.27	0.17; 0.373	None	-
Method 3	T: 0.38	0.17; 0.392	None	-
	N: 0.22	0.08; 0.673	None	-
	L: -0.17	0.05; 0.797	None	-
	R: -0.28	0.22; 0.253	None	-
KWO:				
Method 1	-0.0033	0.15; 0.425	None	-
Method 2	O: 0.58	0.11; 0.549	None	-
	C: -0.29	0.07; 0.700	None	-
	L: -0.40	0.07; 0.735	None	-
	R: -0.23	0.12; 0.535	None	-

Method 3	T: 0.54	0.14; 0.454	None	-
	N: 1.47	0.49; *0.007	None	-
	L: 0.93	0.22; 0.260	None	-
	R: -0.02	0.01; 0.941	None	-
LAD:				
Method 1	-0.0070	0.17; 0.389	None	-
Method 2	O: 1.23	0.25; 0.199	None	-
	C: -0.90	0.33; 0.083	None	-
	L: -2.12	0.36; 0.054	None	-
	R: -0.67	0.35; 0.065	None	-
Method 3	T: 0.11	0.04; 0.839	None	-
	N: -0.21	0.10; 0.600	None	-
	L: -0.33	0.09; 0.642	None	-
	R: -0.46	0.30; 0.119	None	-
LAW:				
Method 1	0.0041	0.19; 0.307	None	-
Method 2	O: 1.38	0.39; 0.067	None	-
	C: 1.72	0.41; *0.049	None	-
	L: 0.34	0.07; 0.745	None	-
	R: 0.14	0.09; 0.671	None	-
Method 3	T: -0.73	0.21; 0.272	None	-
	N: 0.89	0.31; 0.101	None	-
	L: 1.62	0.36; *0.048	None	-
	R: 0.45	0.38; *0.039	2007 (0.040)	-0.16 (0.09; 0.702); -0.65 (0.31; 0.378)
LEP:				
Method 1	-0.0028	0.10; 0.612	None	-
Method 2	O: 0.37	0.11; 0.560	None	-
	C: -0.92	0.21; 0.272	None	-
	L: -1.29	0.22; 0.246	None	-
	R: -0.20	0.12; 0.524	None	-
Method 3	T: -0.07	0.04; 0.848	None	-
	N: -0.44	0.14; 0.455	None	-
	L: -0.37	0.11; 0.569	None	-
	R: -0.06	0.06; 0.738	None	-
MAN:				
Method 1	-0.0165	0.18; 0.350	None	-
Method 2	O: 0.93	0.20; 0.301	None	-
	C: -0.05	0.01; 0.944	None	-
	L: -0.86	0.13; 0.488	None	-
	R: -0.08	0.03; 0.856	None	-
Method 3	T: -0.22	0.06; 0.768	1996 (0.020)	2.80 (0.26; 0.500); 0.54 (0.10; 0.685)
	N: 0.70	0.19; 0.312	None	-
	L: 0.91	0.18; 0.357	None	-
	R: 0.41	0.22; 0.251	None	-
MAR:				
Method 1	0.0009	0.03; 0.889	None	-
Method 2	O: -0.31	0.11; 0.565	None	-
	C: -1.33	0.26; 0.175	None	-
	L: -0.97	0.17; 0.373	None	-
	R: -0.14	0.08; 0.686	None	-
Method 3	T: -0.21	0.11; 0.578	None	-
	N: -0.06	0.01; 0.945	None	-

	L: 0.15	0.03; 0.872	None	-
	R: 0.17	0.11; 0.554	None	-
MRC:				
Method 1	-0.0020	0.04; 0.847	None	-
Method 2	O: 0.55	0.14; 0.467	None	-
	C: -0.71	0.14; 0.471	None	-
	L: -1.27	0.20; 0.285	None	-
	R: -0.06	0.03; 0.891	None	-
Method 3	T: 0.01	0.006; 0.974	None	-
	N: -0.25	0.08; 0.690	None	-
	L: -0.27	0.08; 0.665	1992 (0.038); 2007(0.032)	-0.70 (0.05; 0.953); -0.46 (0.07; 0.817); -2.16 (0.29; 0.087)
	R: 0.20	0.12; 0.547	None	-
MWO:				
Method 1	-0.0112	0.37; *0.047	None	-
Method 2	O: 0.95	0.26; 0.175	None	-
	C: -0.65	0.16; 0.421	None	-
	L: -1.60	0.28; 0.140	None	-
	R: -0.48	0.28; 0.143	None	-
Method 3	T: 0.16	0.05; 0.778	None	-
	N: 0.64	0.21; 0.277	None	-
	L: 0.48	0.12; 0.549	None	-
	R: -0.04	0.04; 0.836	None	-
NEL:				
Method 1	0.0200	0.24; 0.750	None	-
Method 2	O: 0.50	0.12; 0.544	None	-
	C: -0.45	0.17; 0.388	None	-
	L: -0.95	0.18; 0.359	None	-
	R: 0.31	0.13; 0.486	None	-
Method 3	T: 0.90	0.25; 0.199	None	-
	N: -0.05	0.02; 0.900	2012 (0.036)	0.18 (0.07; 0.757); 4.80 (0.55; 0.303)
	L: -0.95	0.25; 0.185	None	-
	R: 0.32	0.17; 0.381	None	-
OTT:				
Method 1	-0.0068	0.22; 0.243	None	-
Method 2	O: 1.30	0.40; *0.037	None	-
	C: -0.61	0.16; 0.401	None	-
	L: -1.88	0.37; *0.049	None	-
	R: -1.10	0.52; *0.004	None	-
Method 3	T: 1.05	0.33; 0.078	None	-
	N: -0.73	0.19; 0.333	None	-
	L: -1.77	0.38; *0.047	None	-
	R: -0.94	0.52; *0.004	2003 (0.040)	-0.98 (0.36; 0.191); -0.26 (0.07; 0.805)
OUD:				
Method 1	-0.0030	0.16; 0.407	None	-
Method 2	O: -1.28	0.35; 0.217	None	-
	C: 0.01	0.01; 0.983	None	-
	L: 1.29	0.31; 0.276	None	-
	R: -0.08	0.09; 0.758	None	-
Method 3	T: -0.27	0.10; 0.595	None	-
	N: -0.73	0.21; 0.259	None	-
	L: -0.45	0.11; 0.577	None	-
	R: -0.01	0.01; 0.962	None	-

PAD:				
Method 1	-0.0200	0.20; 0.300	None	-
Method 2	O: 1.17	0.27; 0.153	None	-
	C: -0.11	0.05; 0.805	None	-
	L: -1.28	0.23; 0.240	None	-
	R: 0.19	0.09; 0.660	None	-
Method 3	T: -0.63	0.14; 0.476	None	-
	N: 0.36	0.15; 0.428	None	-
	L: 0.99	0.19; 0.313	None	-
	R: 0.74	0.37; *0.049	None	-
PEW:				
Method 1	-0.0038	0.07; 0.725	None	-
Method 2	O: 0.39	0.10; 0.631	None	-
	C: 0.007	0.003; 0.988	None	-
	L: -0.39	0.08; 0.687	None	-
	R: 0.03	0.02; 0.914	None	-
Method 3	T: 0.09	0.03; 0.872	None	-
	N: -0.26	0.12; 0.512	None	-
	L: -0.35	0.09; 0.620	None	-
	R: 0.05	0.05; 0.798	None	-
PNO:				
Method 1	0.0006	0.01; 0.946	None	-
Method 2	O: N/A	N/A	N/A	N/A
	C: N/A	N/A	N/A	N/A
	L: N/A	N/A	N/A	N/A
	R: N/A	N/A	N/A	N/A
Method 3	T: -1.36	0.29; 0.117	None	-
	N: 1.24	0.28; 0.137	None	-
	L: 2.59	0.45; *0.014	None	-
	R: 1.41	0.75; *<0.0001	2007 (C & P: p < 0.0001)	-0.22 (0.25; 0.290); 1.24 (0.45; 0.189)
POF:				
Method 1	0.0044	0.25; 0.188	None	-
Method 2	O: -2.13	0.20; 0.637	None	-
	C: -1.80	0.49; 0.214	None	-
	L: -1.89	0.31; 0.451	None	-
	R: -0.39	0.89; *0.003	None	-
Method 3	T: 0.65	0.11; 0.571	None	-
	N: -0.50	0.09; 0.646	None	-
	L: -1.15	0.13; 0.495	None	-
	R: -0.10	0.12; 0.545	None	-
PRI:				
Method 1	0.0018	0.09; 0.617	None	-
Method 2	O: 0.45	0.08; 0.721	None	-
	C: -0.36	0.08; 0.722	None	-
	L: -0.81	0.12; 0.599	None	-
	R: 0.06	0.05; 0.826	None	-
Method 3	T: 0.63	0.11; 0.580	None	-
	N: -0.14	0.03; 0.869	None	-
	L: -0.77	0.10; 0.593	None	-
	R: -0.04	0.04; 0.824	None	-
PWO:				
Method 1	0.0036	0.12; 0.520	None	-

Method 2	O: 0.44	0.16; 0.411	None	-
	C: 0.40	0.10; 0.605	None	-
	L: -0.04	0.01; 0.964	None	-
	R: -0.04	0.02; 0.902	None	-
Method 3	T: 0.31	0.15; 0.424	None	-
	N: 0.13	0.05; 0.784	None	-
	L: -0.19	0.08; 0.698	None	-
	R: -0.08	0.09; 0.630	None	-
RIV:				
Method 1	-0.0053	0.15; 0.427	None	-
Method 2	O: -0.45	0.11; 0.607	None	-
	C: -0.55	0.22; 0.305	1999 (0.049)	3.54 (0.57; 0.065); 0.41 (0.13; 0.681)
	L: -0.10	0.02; 0.926	None	-
	R: 0.17	0.09; 0.659	None	-
Method 3	T: -0.02	0.008; 0.969	None	-
	N: -0.57	0.24; 0.196	None	-
	L: -0.56	0.17; 0.381	None	-
	R: 0.30	0.26; 0.158	None	-
ROB:				
Method 1	-0.0006	0.02; 0.906	None	-
Method 2	O: 0.90	0.21; 0.309	None	-
	C: 0.65	0.13; 0.524	None	-
	L: -0.25	0.04; 0.835	None	-
	R: 0.14	0.11; 0.591	None	-
Method 3	T: -0.93	0.24; 0.198	None	-
	N: -1.08	0.31; 0.097	None	-
	L: -0.15	0.03; 0.866	None	-
	R: 0.23	0.19; 0.314	None	-
SHA:				
Method 1	-0.0015	0.04; 0.843	None	-
Method 2	O: -0.59	0.15; 0.448	None	-
	C: 0.33	0.16; 0.418	None	-
	L: 0.92	0.22; 0.258	None	-
	R: 0.93	0.38; *0.040	2001 (C: < 0.0001; P: 0.008)	-1.19 (0.32; 0.284); -1.28 (0.33; 0.212)
Method 3	T: -0.11	0.05; 0.808	None	-
	N: 0.15	0.12; 0.536	None	-
	L: 0.25	0.09; 0.627	None	-
	R: 0.53	0.29; 0.127	2001 (< 0.0001)	-0.18 (0.06; 0.849); -1.21 (0.38; 0.144)
SKU:				
Method 1	0.0019	0.04; 0.826	None	-
Method 2	O: -0.10	0.03; 0.875	None	-
	C: -1.50	0.44; *0.017	None	-
	L: -1.40	0.27; 0.149	None	-
	R: -0.23	0.12; 0.546	None	-
Method 3	T: -0.18	0.09; 0.645	2012 (0.040)	0.68 (0.34; 0.099); -11.9 (0.73; 0.272)
	N: 0.18	0.09; 0.657	None	-
	L: 0.36	0.13; 0.513	None	-
	R: -0.03	0.03; 0.892	None	-
SUT:				
Method 1	0.0030	0.16; 0.404	None	-
Method 2	O: -1.01	0.23; 0.348	None	-
	C: -0.78	0.12; 0.615	None	-

	L: 0.16	0.02; 0.896	None	-
	R: 0.74	0.35; 0.117	2009 (0.050)	-0.49 (0.20; 0.516); -0.59 (0.16; 0.760)
Method 3	T: -0.14	0.03; 0.856	None	-
	N: 0.26	0.05; 0.783	None	-
	L: 0.40	0.09; 0.650	None	-
	R: 0.81	0.49; *0.007	2007 (C: 0.020; P: 0.0004)	-0.25 (0.13; 0.586); -0.81 (0.74; 0.517)
SWO:				
Method 1	0.0030	0.13; 0.507	None	-
Method 2	O: -1.59	0.28; 0.206	None	-
	C: 0.27	0.06; 0.785	None	-
	L: 1.86	0.33; 0.138	None	-
	R: 0.20	0.23; 0.310	None	-
Method 3	T: -0.60	0.13; 0.493	None	-
	N: -0.03	0.01; 0.973	None	-
	L: 0.57	0.10; 0.618	None	-
	R: -0.03	0.03; 0.864	None	-
TRI:				
Method 1	0.0034	0.20; 0.292	None	-
Method 2	O: 0.64	0.19; 0.384	None	-
	C: -0.17	0.05; 0.821	None	-
	L: -0.85	0.16; 0.472	None	-
	R: 0.23	0.25; 0.263	None	-
Method 3	T: 0.14	0.04; 0.848	None	-
	N: -0.003	0.001; 0.996	None	-
	L: -0.15	0.03; 0.881	None	-
	R: 0.50	0.47; *0.010	L: 2008 (0.020)	0.02 (0.02; 0.923); -1.88 (0.55; 0.129)
UMW:				
Method 1	-0.0040	0.08; 0.665	None	-
Method 2	O: -0.67	0.18; 0.356	None	-
	C: 0.39	0.18; 0.359	None	-
	L: 1.07	0.21; 0.285	2001 (0.050)	-3.85 (0.40; 0.172); -1.95 (0.21; 0.441)
	R: -0.25	0.11; 0.562	None	-
Method 3	T: -0.62	0.20; 0.286	None	-
	N: 0.50	0.21; 0.265	None	-
	L: 1.11	0.37; *0.048	2003 (0.019)	-0.49 (0.11; 0.693); -1.38 (0.23; 0.427)
	R: -0.10	0.06; 0.747	None	-
UPW:				
Method 1	0.0040	0.22; 0.234	None	-
Method 2	O: -0.14	0.03; 0.913	None	-
	C: 1.72	0.47; *0.045	None	-
	L: 1.84	0.28; 0.254	1997 (0.040)	0.71 (0.06; 0.910); -3.93 (0.39; 0.186)
	R: 0.30	0.24; 0.329	2000 (0.040)	0.03 (0.01; 0.975); -1.09 (0.48; 0.114)
Method 3	T: 0.72	0.20; 0.291	None	-
	N: 0.65	0.16; 0.417	None	-
	L: -0.08	0.01; 0.939	1999 (0.026)	-3.50 (0.20; 0.554); -0.98 (0.14; 0.575)
	R: 0.03	0.03; 0.858	None	-
VRE:				
Method 1	0.0007	0.03; 0.867	2006 (0.020)	B: 0.012 (0.33; 0.163); A: 0.003(0.06; 0.870)
Method 2	O: 2.05	0.51; 0.301	None	-
	C: 1.17	0.26; 0.626	None	-
	L: -0.88	0.29; 0.581	None	-
	R: 0.51	0.44; 0.378	None	-
Method 3	T: 0.46	0.15; 0.437	None	-

	N: 0.76	0.16; 0.391	None	-
	L: 0.30	0.06; 0.768	None	-
	R: 0.47	0.426; *0.019	None	-
VRY:				
Method 1	-0.0047	0.17; 0.383	None	-
Method 2	O: 1.16	0.23; 0.238	None	-
	C: -0.17	0.05; 0.793	None	-
	L: -1.34	0.21; 0.274	None	-
	R: -0.52	0.27; 0.153	None	-
Method 3	T: 0.56	0.18; 0.349	None	-
	N: 0.31	0.12; 0.526	None	-
	L: -0.26	0.07; 0.720	None	-
	R: -0.29	0.24; 0.215	None	-
VWY:				
Method 1	-0.0012	0.07; 0.726	None	-
Method 2	O: 0.41	0.10; 0.698	None	-
	C: -0.56	0.12; 0.621	None	-
	L: -0.96	0.15; 0.531	None	-
	R: 0.03	0.02; 0.927	None	-
Method 3	T: 0.82	0.17; 0.368	None	-
	N: 0.21	0.05; 0.812	None	-
	L: -0.61	0.10; 0.597	None	-
	R: 0.13	0.13; 0.490	None	-
WEL:				
Method 1	-0.0061	0.18; 0.337	None	-
Method 2	O: 1.09	0.28; 0.157	None	-
	C: -0.93	0.16; 0.430	None	-
	L: -2.02	0.30; 0.121	None	-
	R: -0.96	0.48; *0.009	None	-
Method 3	T: 0.25	0.08; 0.679	None	-
	N: -0.65	0.17; 0.391	None	-
	L: -0.91	0.18; 0.349	None	-
	R: -0.86	0.60; *0.001	None	-
WIL:				
Method 1	-0.0023	0.09; 0.640	None	-
Method 2	O: -0.01	0.002; 0.991	None	-
	C: 1.30	0.20; 0.335	None	-
	L: 1.33	0.18; 0.390	None	-
	R: 0.49	0.33; 0.100	None	-
Method 3	T: 0.16	0.05; 0.783	None	-
	N: -0.005	0.001; 0.996	None	-
	L: -0.17	0.03; 0.883	None	-
	R: 0.31	0.22; 0.245	2008 (0.020)	-0.76 (0.45; *0.046); -0.55 (0.13; 0.740)
WTO:				
Method 1	-0.0041	0.12; 0.524	None	-
Method 2	O: 0.54	0.17; 0.389	None	-
	C: -0.09	0.02; 0.900	None	-
	L: -0.64	0.14; 0.454	None	-
	R: -0.15	0.10; 0.614	2001 (0.030); 2008 (0.040)	-0.49 (0.20; 0.514); -0.68 (0.18; 0.699); -0.52 (0.12; 0.759)
Method 3	T: 0.23	0.09; 0.629	None	-
	N: 0.32	0.12; 0.552	None	-
	L: 0.09	0.03; 0.892	None	-
	R: -0.07	0.05; 0.781	None	-

APPENDIX H: DETAILS ON THE SEASONALITY SCORE SHIFTS

Summary of the seasonality score shifts during the study period, and details on the direction of change and regime change year. Each location is colour coded according to the classification given under *Section 5.4.2*, where red, blue and yellow represent SRZ, WRZ and YRZ respectively. Significant changes are denoted using asterisk (*) next to the location code. The values of 1987 and 2016 were calculated using the total period seasonality score as the midpoint of the study period (i.e. 2001) and the rate of change. These values were used to construct *Figure 5.41*. Any rainfall zone changes were calculated through extended regression analysis and were captured by the year of occurrence, which is the first year of a new rainfall zone, and none reported here represents where the seasonality score changes tended further into the respective rainfall zone. Highlighted using grey are regime changes during the study period. Change points were captured and denoted using (CP) and were considered for the calculations of 1987 and 2016.

Location	Seasonality score (2001)	Rate of change (seasonality score.yr^{-1})	1987	2016	Change description	Rainfall zone change year
ANP	0.48	0.0013	0.46	0.50	SRZ	None
BET	1.09	0.0013	1.07	1.11	SRZ	None
BEW	0.82	0.0013	0.80	0.84	SRZ	None
BLW	0.58	-0.0052	0.66	0.51	YRZ	2056
CAG (*)	-0.75	0.0131	-0.95	-0.55	YRZ	2035
CED	0.88	-0.0119	1.06	0.70	YRZ	2050
CMU	0.50	0.0046	0.43	0.57	SRZ	None
CTW	-1.04	0.0074	-1.16	-0.93	YRZ	2102
CWO	-0.21	0.0040	-0.27	-0.15	SRZ	2131
DAW	0.32	0.0041	0.26	0.38	SRZ	1995
ELW	0.59	-0.0086	0.72	0.46	YRZ	2035
FRA	0.15	0.0004	0.15	0.16	SRZ	2379
FTN	0.77	-0.0082	0.90	0.65	YRZ	2059
JIW	1.24	0.0016	1.21	1.26	SRZ	None
KWO	0.56	-0.0033	0.61	0.51	YRZ	2082
LAD	0.99	-0.0070	1.10	0.89	YRZ	2100
LAW	-0.74	0.0041	-0.80	-0.68	YRZ	2108
LEP	0.96	-0.0028	1.00	0.92	YRZ	2235
MAN	0.93	-0.0165	1.18	0.68	YRZ	2039
MAR	1.03	0.0009	1.02	1.04	SRZ	None
MRC	1.08	-0.0020	1.11	1.05	YRZ	2389
MWO (*)	0.93	-0.0112	1.10	0.76	YRZ	2057
NEL	1.59	0.0200	1.29	1.89	SRZ	None
OTT	0.82	-0.0068	0.92	0.72	YRZ	2077
OUD	-0.05	-0.0030	-0.01	-0.10	WRZ	2086
PAD	0.81	-0.0200	1.11	0.51	YRZ	2027
PEW	-0.27	-0.0038	-0.22	-0.33	WRZ	2007
PNO	-0.37	0.0006	-0.38	-0.36	YRZ	2112
POF	0.13	0.0044	0.07	0.20	SRZ	2040
PRI	0.30	0.0018	0.27	0.33	SRZ	2000
PWO	1.14	0.0036	1.09	1.20	SRZ	None
RIV	-0.08	-0.0053	0.002	-0.16	WRZ	2044
ROB	-0.33	-0.0006	-0.32	-0.34	WRZ	None
SHA	1.21	-0.0015	1.23	1.19	YRZ	2605
SKU	1.13	0.0019	1.10	1.16	SRZ	None
SUT	-0.10	0.0030	-0.15	-0.06	SRZ	2136
SWO	-0.50	0.0030	-0.55	-0.46	YRZ	2067
TRI	0.49	0.0034	0.44	0.54	SRZ	None
UMW	1.02	-0.0040	1.08	0.96	YRZ	2180
UPW	0.40	0.0040	0.34	0.46	SRZ	None
VRE (CP: 2006)	-0.55	0.012; 0.0003	-0.66	-0.57	YRZ	2090
VRY	0.73	-0.0047	0.80	0.66	YRZ	2092
VWY	0.22	-0.0012	0.24	0.20	WRZ	2441
WEL	0.63	-0.0061	0.72	0.54	YRZ	2055
WIL	0.23	-0.0023	0.26	0.19	WRZ	2233
WTO	1.09	-0.0041	1.15	1.03	YRZ	2194

APPENDIX I: DETAILS ON THE ONSET AND CESSATION DATE SHIFTS

Summary of the onset and cessation date shifts during the study period, and details on the direction of change and regime change year. Each location is colour coded according to the classification given under *Section 5.4.3*. ND represents no dates obtained. Significant changes are denoted using asterisk (*) next to the location code. The values of 1987 and 2016 were calculated using the mean onset and cessation dates as the midpoint of the study period (i.e. 2001) and the rate of change. These values were used to construct *Figures 5.42* and *5.43*. Dates above (below) 365 represent onset or cessation dates moving to the next (previous) calendar year. Any regime changes were captured by the year of occurrence, which is the first year of the regime change. These regime changes represent when the solstice which characterises the wet season may potentially not occur during the season, and this is captured for later (earlier) onset (cessation) dates. For earlier (later) onset (cessation) dates, the year which was captured represents the year in which the solstice from the opposite season may occur during the wet season. Highlighted using grey are regime changes during the study period. Change points were captured and denoted using CP (i.e. the year from which the change occurred) and were considered for the calculations of 1987 and 2016.

I.1 ONSET DATES

Location	Mean onset date (2001)	Rate of change ($d.yr^{-1}$)	1987	Date	2016	Date	Change description	Regime change year
ANP	301	1.40	280	7-Oct	322	18-Nov	Later onset	2041
BET (* and CP: 2005)	281	0.16; 1.70	279	6-Oct	299	26-Oct	Later onset	2050
BEW (*)	289	1.59	265	22-Sep	313	9-Nov	Later onset	2044
BLW	305	0.88	292	19-Oct	318	14-Nov	Later onset	2060
CAG	113	1.39	92	2-Apr	134	14-May	Later onset	2044
CED	260	-0.82	272	29-Sep	248	5-Sep	Earlier onset	2108
CMU	320	0.04	319	15-Nov	321	17-Nov	Later onset	2914
CTW	110	0.59	101	11-Apr	119	29-Apr	Later onset	2107
CWO	98	-0.81	110	20-Apr	86	27-Mar	Earlier onset	2134
DAW	309	0.76	298	25-Oct	320	16-Nov	Later onset	2064
ELW	240	0.92	226	14-Aug	254	11-Sep	Later onset	2128
FRA	347	0.25	343	9-Dec	351	17-Dec	Later onset	2039
FTN (*)	298	1.85	270	27-Sep	326	22-Nov	Later onset	2033
JIW	290	0.17	287	14-Oct	293	20-Oct	Later onset	2393
KWO	316	0.58	307	3-Nov	325	21-Nov	Later onset	2071
LAD	272	1.23	254	11-Sep	290	17-Oct	Later onset	2071
LAW	153	1.38	132	12-May	174	23-Jun	Later onset	2016
LEP	323	0.37	317	13-Nov	329	25-Nov	Later onset	2092
MAN	250	0.93	236	24-Aug	264	21-Sep	Later onset	2116
MAR	314	-0.31	319	15-Nov	309	5-Nov	Earlier onset	2458
MRC	289	0.55	281	8-Oct	297	24-Oct	Later onset	2124
MWO	311	0.95	297	24-Sep	325	21-Nov	Later onset	2050
NEL	293	0.50	286	13-Oct	301	28-Oct	Later onset	2128
OTT (*)	301	1.26	282	9-Oct	320	16-Nov	Later onset	2046
OUD	62	-1.28	81	22-Mar	43	12-Feb	Earlier onset	2057
PAD	237	1.17	219	7-Aug	255	12-Sep	Later onset	2104
PEW	55	0.39	49	18-Feb	61	2-Mar	Later onset	2303
PNO	ND	ND	ND	ND	ND	ND	ND	ND
POF	394	-2.13	426	2-Mar	362	28-Dec	Earlier onset	2019
PRI	350	0.45	343	9-Dec	357	23-Dec	Later onset	2016
PWO	312	0.44	305	1-Nov	319	15-Nov	Later onset	2103
RIV	63	-0.45	70	11-Mar	56	25-Feb	Earlier onset	2160
ROB	127	0.90	114	24-Apr	141	21-May	Later onset	2052
SHA	264	-0.59	273	30-Sep	255	12-Sep	Earlier onset	2157
SKU	291	-0.10	293	20-Oct	290	17-Oct	Earlier onset	3187
SUT	77	-1.01	92	2-Apr	62	3-Mar	Earlier onset	2086
SWO	123	-1.59	147	27-May	99	9-Apr	Earlier onset	2084
TRI	366	0.64	356	22-Dec	376	11-Jan	Later onset	2268
UMW	265	-0.67	275	2-Oct	255	12-Sep	Earlier onset	2140
UPW	353	-0.14	355	21-Dec	351	17-Dec	Earlier onset	3291
VRE	155	2.05	124	4-May	186	5-Jul	Later onset	2010
VRY	321	1.16	304	31-Oct	338	4-Dec	Later onset	2032
VWY	356	0.41	350	16-Dec	362	28-Dec	Later onset	2003
WEL	307	1.09	291	18-Oct	323	19-Nov	Later onset	2047
WIL	339	-0.01	339	5-Dec	339	5-Dec	Earlier onset	18652
WTO	295	0.54	287	14-Oct	303	30-Oct	Later onset	2115

I.2 CESSATION DATES

Location	Mean cessation date (2001)	Rate of change (d.yr^{-1})	1987	Date	2016	Date	Change description	Regime change year
ANP (CP: 2008;2013)	124	0.83; -1.30;	112	22-Apr	166	6-May	Later cessation	2017
BET	112	-0.42	118	28-Apr	106	16-Apr	Earlier cessation	2291
BEW	117	0.88	104	14-Apr	130	10-May	Later cessation	2063
BLW	111	0.77	99	9-Apr	123	3-May	Later cessation	2080
CAG	283	-0.03	283	10-Oct	283	10-Oct	Earlier cessation	2249
CED	111	-0.40	117	27-Apr	105	15-Apr	Earlier cessation	2303
CMU	97	0.39	91	1-Apr	103	13-Apr	Later cessation	2193
CTW	269	-0.62	278	5-Oct	260	17-Sep	Earlier cessation	2202
CWO	250	-0.37	256	13-Sep	244	1-Sep	Earlier cessation	2214
DAW	124	-0.03	124	4-May	124	4-May	Earlier cessation	6451
ELW	127	1.09	111	21-Apr	143	23-May	Later cessation	2042
FRA	110	0.23	107	17-Apr	113	23-Apr	Later cessation	2269
FTN	114	0.67	104	14-Apr	124	4-May	Later cessation	2087
JIW	113	-0.04	114	24-Apr	112	22-Apr	Earlier cessation	5064
KWO	112	-0.29	116	26-Apr	108	18-Apr	Earlier cessation	2420
LAD	105	-0.90	119	29-Apr	92	2-Apr	Earlier cessation	2129
LAW (*)	254	1.72	228	16-Aug	280	7-Oct	Later cessation	2061
LEP	87	-0.92	101	11-Apr	73	14-Mar	Earlier cessation	2106
MAN	119	-0.05	120	30-Apr	118	28-Apr	Earlier cessation	4571
MAR	85	-1.33	105	15-Apr	65	6-Mar	Earlier cessation	2073
MRC	118	-0.71	129	9-May	107	17-Apr	Earlier cessation	2181
MWO	110	-0.65	120	30-Apr	100	10-Apr	Earlier cessation	2185
NEL	112	-0.45	119	29-Apr	105	15-Apr	Earlier cessation	2271
OTT	105	-0.61	114	24-Apr	96	6-Apr	Earlier cessation	2189
OUD	327	0.01	327	23-Nov	327	23-Nov	Later cessation	4951
PAD	119	-0.11	121	1-May	117	27-Apr	Earlier cessation	3170
PEW	343	0.01	343	9-Dec	343	9-Dec	Later cessation	3251
PNO	ND	ND	ND	ND	ND	ND	ND	ND
POF	97	-1.80	124	4-May	70	11-Mar	Earlier cessation	2061
PRI	117	-0.36	122	2-May	112	22-Apr	Earlier cessation	2353
PWO	93	0.40	87	28-Mar	99	9-Apr	Later cessation	2198
RIV (CP: 1999)	329	3.54; 0.41	282	9-Oct	335	1-Dec	Later cessation	2066
ROB	278	0.65	268	25-Sep	288	15-Oct	Later cessation	2121
SHA	110	0.33	105	15-Apr	115	25-Apr	Later cessation	2188
SKU (*)	105	-1.50	128	8-May	83	24-Mar	Earlier cessation	2078
SUT	259	-0.78	271	28-Sep	247	4-Sep	Earlier cessation	2114
SWO	259	0.27	255	12-Sep	263	20-Sep	Later cessation	2359
TRI	97	-0.17	100	10-Apr	94	4-Apr	Earlier cessation	2628
UMW	120	0.39	114	24-Apr	126	6-May	Later cessation	2134
UPW (*)	99	1.72	73	14-Mar	125	5-May	Later cessation	2034
VRE	240	1.17	222	10-Aug	258	15-Sep	Later cessation	2100
VRY	111	-0.17	114	24-Apr	108	18-Apr	Earlier cessation	2710
VWY	115	-0.56	123	3-May	107	17-Apr	Earlier cessation	2224
WEL	96	-0.93	110	20-Apr	82	23-Mar	Earlier cessation	2115
WIL	126	1.30	107	17-Apr	146	26-May	Later cessation	2036
WTO	108	-0.09	109	19-Apr	107	17-Apr	Earlier cessation	3296

APPENDIX J: DETAILS ON THE 10% AND 90% DATE SHIFTS

Summary of the 10% and 90% date shifts during the study period, and details on the direction of change and regime change year. Each location is colour coded according to the classification given under *Section 5.4.4*. Significant changes are denoted using asterisk (*) next to the location. The values of 1987 and 2016 were calculated using the mean 10% and 90% dates as the midpoint of the study period (i.e. 2001) and the rate of change. These values were used to construct *Figures 5.44* and *5.45*. Dates above (below) 365 represent 10% or 90% dates moving to the next (previous) calendar year. Any regime changes were captured by the year of occurrence, which is the first year of the regime change. These regime changes represent when the solstice which characterises the wet season may potentially not occur during the season, and this is captured for later (earlier) 10% (90%) dates. For earlier (later) 10% (90%) dates, the year which was captured represents the year in which the solstice from the opposite season may occur during the wet season. Highlighted using grey are regime changes during the study period. Change points were captured and denoted using CP (i.e. the year from which the change occurred) and were considered for the calculations of 1987 and 2016.

J.1 10% DATES

Location	10% date (2001)	Rate of change ($d.yr^{-1}$)	1987	Date	2016	Date	Change description	Regime change year
ANP	298	1.16	281	8-Oct	315	11-Nov	Later 10%	2052
BET	293	-0.63	302	29-Oct	284	11-Oct	Earlier 10%	2193
BEW (*)	293	1.11	276	3-Oct	310	6-Nov	Later 10%	2059
BLW	297	0.58	288	15-Oct	306	2-Nov	Later 10%	2104
CAG	76	-0.53	84	25-Mar	68	9-Mar	Earlier 10%	2161
CED	267	-0.88	280	7-Oct	254	11-Sep	Earlier 10%	2109
CMU	300	0.68	290	17-Oct	310	6-Nov	Later 10%	2085
CTW	107	0.09	106	16-Apr	108	18-Apr	Later 10%	2729
CWO	67	-0.64	77	18-Mar	57	26-Feb	Earlier 10%	2119
DAW	297	1.37	276	3-Oct	318	14-Nov	Later 10%	2045
ELW	251	-0.05	252	9-Sep	250	7-Sep	Earlier 10%	3572
FRA	325	-0.50	333	29-Nov	318	14-Nov	Earlier 10%	5052
FTN	294	0.44	287	14-Oct	301	28-Oct	Later 10%	2144
JIW	300	0.38	294	21-Oct	306	2-Nov	Later 10%	2150
KWO	302	0.54	294	21-Oct	310	6-Nov	Later 10%	2102
LAD	287	0.11	285	12-Oct	289	16-Oct	Later 10%	2633
LAW	103	-0.73	114	24-Apr	92	2-Apr	Earlier 10%	2154
LEP	313	-0.07	314	10-Nov	312	8-Nov	Earlier 10%	4009
MAN (CP: 1996)	257	2.80; 0.54	226	14-Aug	265	22-Sep	Later 10%	2186
MAR	307	-0.21	310	6-Nov	304	31-Oct	Earlier 10%	2642
MRC	290	0.01	290	17-Oct	290	17-Oct	Later 10%	8551
MWO	308	0.16	306	2-Nov	310	6-Nov	Later 10%	2298
NEL	298	0.90	285	12-Oct	312	8-Nov	Later 10%	2066
OTT	301	1.05	285	12-Oct	317	13-Nov	Later 10%	2054
OUD	55	-0.27	59	28-Feb	51	20-Feb	Earlier 10%	2237
PAD	244	-0.63	253	10-Sep	235	23-Aug	Earlier 10%	2115
PEW	55	0.09	54	23-Feb	56	25-Feb	Later 10%	3307
PNO	97	-1.36	117	27-Apr	77	18-Mar	Earlier 10%	2079
POF	336	0.65	326	22-Nov	346	12-Dec	Later 10%	2033
PRI	311	0.63	302	29-Oct	320	16-Nov	Later 10%	2074
PWO	306	0.31	301	28-Oct	311	7-Nov	Later 10%	2164
RIV	48	-0.02	48	17-Feb	48	17-Feb	Earlier 10%	4831
ROB	68	-0.93	82	23-Mar	54	23-Feb	Earlier 10%	2084
SHA	287	-0.11	289	16-Oct	285	12-Oct	Earlier 10%	3042
SKU (CP: 2012)	300	0.68; -11.90	290	26-Oct	259	16-Sep	Earlier 10%	2024
SUT	62	-0.14	64	5-Mar	60	1-Mar	Earlier 10%	2505
SWO	87	-0.60	96	6-Apr	78	19-Mar	Earlier 10%	2161
TRI	327	0.14	325	21-Nov	329	25-Nov	Later 10%	2212
UMW	275	-0.62	284	11-Oct	266	23-Sep	Earlier 10%	2167
UPW	317	0.72	306	2-Nov	328	24-Nov	Later 10%	2056
VRE	111	0.46	104	14-Apr	118	28-Apr	Later 10%	2135
VRY	310	0.56	302	29-Oct	318	14-Nov	Later 10%	2085
VWY	320	0.82	308	4-Nov	332	28-Nov	Later 10%	2046
WEL	298	0.25	294	21-Oct	302	29-Oct	Later 10%	2235
WIL	326	0.16	324	20-Nov	328	24-Nov	Later 10%	2192
WTO	300	0.23	297	24-Oct	303	30-Oct	Later 10%	2247

J.2 90% DATES

Location	90% date (2001)	Rate of change ($d.yr^{-1}$)	1987	Date	2016	Date	Change description	Regime change year
ANP (*)	115	1.61	91	1-Apr	140	20-May	Later 90%	2037
BET	89	-0.34	94	4-Apr	84	25-Mar	Earlier 90%	2291
BEW (*)	110	1.48	88	29-Mar	132	12-May	Later 90%	2043
BLW (*)	109	1.76	83	24-Mar	135	15-May	Later 90%	2037
CAG	298	0.49	291	18-Oct	305	1-Nov	Later 90%	2119
CED (CP: 1995)	88	0.36; -0.38	87	28-Mar	82	23-Mar	Earlier 90%	2240
CMU	133	1.08	117	27-Apr	149	29-May	Later 90%	2037
CTW	285	0.82	273	30-Sep	297	24-Oct	Later 90%	2087
CWO	280	1.13	263	20-Sep	297	24-Oct	Later 90%	2068
DAW	128	0.25	124	4-May	132	12-May	Later 90%	2175
ELW	108	0.70	98	8-Apr	119	29-Apr	Later 90%	2092
FRA	164	0.15	162	11-Jun	166	15-Jun	Later 90%	2051
FTN	101	1.00	86	27-Mar	116	26-May	Later 90%	2072
JIW	91	0.22	88	29-Mar	94	4-Apr	Later 90%	2367
KWO (*)	106	1.47	84	25-Mar	128	8-May	Later 90%	2046
LAD	85	-0.21	88	29-Mar	82	23-Mar	Earlier 90%	2451
LAW	279	0.89	266	23-Sep	292	19-Oct	Later 90%	2287
LEP	86	-0.44	93	3-Apr	79	20-Mar	Earlier 90%	2219
MAN	98	0.70	88	29-Mar	109	19-Apr	Later 90%	2106
MAR	82	-0.06	83	24-Mar	81	22-Mar	Earlier 90%	3531
MRC	99	-0.25	103	13-Apr	95	5-Apr	Earlier 90%	2435
MWO	100	0.64	90	31-Mar	110	20-Apr	Later 90%	2113
NEL (CP: 2012)	92	0.18; 4.80	89	30-Mar	113	23-Apr	Later 90%	2029
OTT	90	-0.73	101	11-Apr	79	20-Mar	Earlier 90%	2136
OUD	317	-0.73	328	24-Nov	306	2-Nov	Earlier 90%	2201
PAD	85	0.36	80	21-Mar	90	31-Mar	Later 90%	2242
PEW	320	-0.26	324	20-Nov	316	12-Nov	Earlier 90%	2573
PNO	281	1.24	262	19-Sep	300	27-Oct	Later 90%	2062
POF	158	-0.50	166	15-Jun	151	31-May	Earlier 90%	2334
PRI	124	-0.14	126	6-May	122	2-May	Earlier 90%	2955
PWO	89	0.13	87	28-Mar	91	1-Apr	Later 90%	2636
RIV	317	-0.57	326	22-Nov	308	4-Nov	Earlier 90%	2257
ROB	311	-1.08	327	23-Nov	295	22-Oct	Earlier 90%	2131
SHA	82	0.15	80	21-Mar	84	25-Mar	Later 90%	2598
SKU	86	0.18	83	24-Mar	89	30-Mar	Later 90%	2476
SUT	296	0.26	292	19-Oct	300	27-Oct	Later 90%	2230
SWO	273	-0.03	273	30-Sep	273	30-Sep	Earlier 10%	11385
TRI	106	-0.003	106	16-May	106	16-May	Earlier 10%	40168
UMW	95	0.50	88	29-Mar	103	13-Apr	Later 90%	2154
UPW	121	0.65	111	21-Apr	131	11-May	Later 90%	2079
VRE	281	0.76	270	27-Sep	292	19-Oct	Later 90%	2100
VRY	100	0.31	95	5-Apr	105	15-Apr	Later 90%	2232
VWY	140	0.21	137	17-May	143	23-May	Later 90%	2151
WEL	97	-0.65	107	17-Apr	87	28-Mar	Earlier 90%	2165
WIL	192	-0.01	192	11-Jul	192	11-Jul	Earlier 10%	3952
WTO	88	0.32	83	24-Mar	93	3-Apr	Later 90%	2262